15825

NASA CR-66840

CASE FILE COPY

N69-40036

# METEOROID PENETRATION DETECTOR DEVELOPMENT PROGRAM

FINAL SUMMARY REPORT
VOLUME I

By Sidney L. Russak, Rufus O. Moses
Del Gray, and Russell L. McCord

Distribution of this report is provided in the interest of information exchange. Responsibility for the contents resides in the author or organization that prepared it.

Prepared under Contract No. NAS1-7043 by
MARTIN MARIETTA CORPORATION
Denver, Colorado

for

NATIONAL AERONAUTICS AND SPACE ADMINISTRATION

# FOREWORD

This document is submitted in accordance with the requirements of paragraph 5.8 of NAS1-7043, Contract Statement of Work L-7138A, Exhibit A.

The work pertaining to development of meteoroid detectors is included in this volume. Volume II comprises the investigation performed on thermal control coatings for the MPPD program.

CONTENTS


| | Page |
|---|---|
| INTRODUCTION | 1 |
| SUMMARY | 3 |
| Design Development Phase | 8 |
| Manufacturing and Testing Phase | 10 |
| DETECTOR DESIGN AND DEVELOPMENT | 14 |
| Engineering Objectives | 15 |
| Design Progressing | 15 |
| Preliminary design and development | 17 |
| Design Development phase | 55 |
| Manufacturing and Test phase | 78 |
| Design Support Studies | 86 |
| Detector material selection studies | 86 |
| Detector pressurization gas | 89 |
| Detector pressurization level | 91 |
| Dual detector puncture simulation test | 93 |
| Stiffness evaluation tests | 95 |
| Subsize detector design tests | 102 |
| PROCESS DEVELOPMENT AND FABRICATION | 121 |
| Preliminary Design and Development Phase | 121 |
| Process development | 121 |
| Tooling | 132 |
| Detail fabrication and assembly | 140 |
| Design and Development Phase | 140 |
| Process development | 140 |
| Tooling | 141 |
| Detail fabrication and assembly | 146 |
| Manufacturing and Test Phase | 146 |
| Process development | 146 |
| Tooling | 149 |
| Detail fabrication and assembly | 149 |
| MPPD TESTING | 152 |
| Preliminary Design Evaluation Testing | 157 |
| Subsize design evaluation test | 158 |
| Full-size evaluation testing | 164 |
| Special design evaluation test | 180 |
| Design Development Evaluation Testing | 184 |
| Detector design development evaluation testing | 188 |
| Detector design development test results | 195 |
| Special materials test | 198 |
| Production Testing | 201 |
| Pressure switches | 202 |
| Detector/panels | 229 |
| Switch transfer pressure | 245 |

Test Program Evaluation . . . . . 281
Test documentation . . . . . 281
Test criteria . . . . . 284
Switch contact resistance . . . . . 287
Test tooling development . . . . . 290
RELIABILITY AND QUALITY
Summary of Deliverable Contract End Items for the MPPD Program . . . . . 297
Corrosion Resistant Steel Sheet Selection . . . . . 298
Nondestructive Testing Methods . . . . . 299
Ultrasonic inspection technique . . . . . 300
Infrared inspection technique . . . . . 302
Radiographic inspection techniques . . . . . 302
CONCLUSIONS . . . . . 302
APPENDIX A -- DOCUMENTATION . . . . . 305
APPENDIX B -- ENGINEERING DRAWING IDENTIFICATION AND NUMERICAL DRAWING INDEX . . . . . 319
APPENDIX C -- FAILURE HISTORIES . . . . . 333
Pressure Actuated Switch MRB and Failure History . . . 334
Summary of Switch Functional Parameters . . . . . 339
B1A Detector Panel Failure Reports . . . . . 342
C1 Detector Panel Failure Reports . . . . . 345
D2A Detector Failure Reports . . . . . 345
D3A Detector Failure Reports . . . . . 346
E1A Detector Failure Reports . . . . . 347
E3A Detector Failure Reports . . . . . 348
F1A Detector Panel Failure Reports . . . . . 349
Failure Report Trend Analysis . . . . . 354
REFERENCES . . . . . 358

Figure

1 Pressure Expand Square Array . . . . . 20
2 Preform Square Array . . . . . 20
3 Parallel Seam Labyrinth Detector . . . . . 22
4 Concentric Pillow Array . . . . . 23
5 Spotwelded Hexagonal Array . . . . . 24
6 Seam Welded Hexagonal Array . . . . . 25
7 Spotwelded Spacing (Square Pattern), Material 21-6-9 Stainless Annealed . . . . . 27
8 Detector Pillow Cavity vs. Expansion Pressure . . . 28
9 Spotwelded Hexagonal Cell Size vs. Thickness, 21-6-9 Stainless Steel . . . . . 28
10 Detector Assembly, D3A . . . . . 38
11 Servonic Instruments Incorporated Switch Configuration . . . . . 42

| | | |
|---|---|---|
| 12 | Carleton Controls Corporation Switch Configuration | 43 |
| 13 | Switch Support "Volcano" | 45 |
| 14 | Carleton Switch Installation | 46 |
| 15 | Switch Support Gusset (Thin Gage Target) | 47 |
| 16 | B1 Full-Size Panel Showing Switch Gusset, 12x40-in., 21-6-9 Stainless Steel | 47 |
| 17 | Alternative Switch Support (Thin Gage Target) | 49 |
| 18 | Switch Installation for B and F Configurations | 50 |
| 19 | Commercial Mounts Evaluation | 51 |
| 20 | MPDD Mounting Frame | 52 |
| 21 | Mounting Configuration No. 4 | 54 |
| 22 | Mounting Configuration No. 5 | 56 |
| 23 | Selected Mount | 57 |
| 24 | Bumper Sheet Assembly | 59 |
| 25 | Bumper Installation F1A | 60 |
| 26 | Detector Fill Tube Installations | 62 |
| 27 | Improved Switch Installation | 63 |
| 28 | F1A Original Bumper Support | 64 |
| 29 | F1A Modified Bumper Support | 66 |
| 30 | Switch Support Assembly | 67 |
| 31 | Pressure Switch (Pressure Side | 69 |
| 32 | Pressure Switch (Back Side) | 70 |
| 33 | Configuration F1A Load Distribution | 72 |
| 34 | Design Loads for 40x12-in. Panels | 73 |
| 35 | Design Loads for 40x49-in. Panels (49-in. Side) | 74 |
| 36 | Design Loads for 40x49-in. Panels (40-in. Side) | 75 |
| 37 | Servonic Switches | 80 |
| 38 | Switch Cup Assembly | 81 |
| 39 | Serpentine Pressure Tube | 84 |
| 40 | Four-Loop Serpentine Pressure Tube | 84 |
| 41 | Six-Loop Serpentine Reworked Configuration | 85 |
| 42 | Panel Fitting Modification | 85 |
| 43 | Test Schematic and Procedure for Puncture Simulation Test | 94 |
| 44 | Effective Thickness vs. Pillow Height | 96 |
| 45 | Effective Panel Thickness vs. Panel Frequency | 99 |
| 46 | Stiffness (Effective Thickness) vs. Pillow Height | 100 |
| 47 | Effective Panel Thickness vs. Panel Frequency | 101 |
| 48 | Configuration B Test Specimens | 104 |
| 49 | Configuration C Test Specimens | 104 |
| 50 | Configuration D Test Specimens | 105 |
| 51 | Configuration E Test Specimens | 107 |
| 52 | Configuration F Test Specimens | 107 |
| 53 | Pressure Loading Warpage | |

54 Configuration C Test Specimen . . . . . 119
55 Configuration E Test Specimens . . . . . 119
56 Braze Joints Used in MPDD Program . . . . . 126
57 Explosive Forming Setup . . . . . 128
58 Chem-Milled Process Comparisons . . . . . 129
59 Three-Ply Weld Showing "Dog-Bone" Appearance . . . 131
60 Foil Reel Rack . . . . . 133
61 Chem-Milling Template on A-Frame Handling Truck . . 133
62 Vinyl Spot Welding Template, 12x40-in. . . . . 134
63 Vinyl Spot Welding Template, 40x49-in. . . . . 134
64 Spot Welding Showing Table and Frame Holding Target Sheets and Vinyl Template . . . . . 135
65 Seam Welding Table . . . . . 135
66 Pressure Switch "Volcano" Form Die Sets . . . . . 136
67 Forming of Pressure Switch "Volcano" . . . . . 136
68 Final Step in Forming of "Volcano" . . . . . 137
69 Integrally Mounted Dummy Pressure Switch . . . . . 137
70 Switch Cup Forming Tool . . . . . 138
71 Restraint Fixture . . . . . 138
72 Switch Welding Tool . . . . . 139
73 Preformed Target Sheet Showing Plastic Separator . . . . . 142
74 Pressure Switch Block-Off Tool . . . . . 143
75 Squeeze Die Installed on Bliss Press . . . . . 143
76 Accelerated Life Cycle Fixture, First Module . . . 144
77 12x40-in. Detector and Mount Drill Template . . . . 145
78 12x40-in. Cleaning and Handling Fixture . . . . . 145
79 F1A Drill Assembly Fixture . . . . . 150
80 S-IVB Subsize Panel Forming Tool (Disassembled) . . 151
81 S-IVB Subsize Panel Forming Tool (Assembled) . . . 151
82 Pressure Cycling Test Setup . . . . . 159
83 Pressure Cycling Tool . . . . . 160
84 Experimental Setup . . . . . 163
85 Subsize Stiffness Evaluation Test Setup . . . . . 165
86 Proof Pressure Test Setup . . . . . 167
87 Leak Test Setup . . . . . 168
88 Residual Gas Analysis Test Setup . . . . . 170
89 Accelerometer and Strain Gage Locations, Stiffness Evaluation Test . . . . . 172
90 Vibration Test Setup Photograph . . . . . 173
91 Vibration Test Setup . . . . . 174
92 Vibration Test Setup for F Configuration Panel . . 175
93 Angle Mounting Evaluation Test Setup . . . . . 176
94 Bumper Sheet Deflection Evaluation Test Setup . . . 177
95 Acoustic Test Setup, F Configuration . . . . . 178
96 Thermal Test, Radiant Heat, Mount Evaluation . . . 181

97 Thermal Test, $LN_2$ Cooling, Mount Evaluation . . . . 182
98 Switch Monitoring Diagram . . . . . 185
99 Pressure Switch Vibration and Shock Test Setup . . 186
100 Switch Monitoring Test Setup . . . . . 189
101 Functional Test Setup, Contact Resistance . . . . . 190
102 40x12-in. Panel Vibration Test Setup . . . . . 193
103 40x49-in. Detector Vibration Test Setup . . . . . 194
104 Acoustic Test Setup, 40x12-in. Panel . . . . . 196
105 Solar Cell Contamination Test Setup, Front View . . 199
106 Solar Cell Contamination Test Setup, Back View . . 200
107 Functional Test Tool for Pressure Switches and Panel/Detector . . . . . 203
108 Helium Leak Test Setup . . . . . 204
109 Helium Leak Test Diagram . . . . . 205
110 Vibration Test Setup Sketch . . . . . 206
111 Random Vibration Spectrum, Pressure Switch FAT . . 207
112 Sinewave Vibration Specification, Pressure Switch FAT . . . . . 208
113 Sawtooth Shock Pulse Specification, Pressure Switch FAT . . . . . 210
114 Shock Response Spectrum, Pressure Switch FAT . . . 211
115 Sustained Acceleration Test Setup Sketch . . . . . 213
116 Sustained Acceleration Test Setup . . . . . 214
117 Switch Qualification . . . . . 216
118 Random Vibration Spectrum, Pressure Switch Qualification . . . . . 217
119 Acoustic Test Spectrum, Pressure Switch Qualification . . . . . 218
120 Pressure Switch Thermal Vacuum Soak Test Setup before Switch Installation . . . . . 219
121 Overall Test Setup, Pressure Switch Thermal Vacuum Soak . . . . . 219
122 Overall Test Setup, Pressure Switch ALC Test . . . 222
123 Closeup of Hot and Cold Baths, Pressure Switch ALC Test . . . . . 223
124 Pressure Switch ALC Control and Power Rack . . . . 223
125 Pressure Switch Instrumentation Sketch, ALC Test . . . . . 224
126 Typical Temperature Cycle, Pressure Switch ALC . . 228
127 Leak Test Setup, Helium . . . . . 230
128 Leak Test Setup, RGA . . . . . 230
129 Photo of RGA Leak Test Setup . . . . . 232
130 Vibration Test Setup, 40x49-in. Detector, FAT . . . 233
131 Vibration Test Setup, 40x12-in. Panel, FAT . . . . 234
132 Random Vibration Criteria, Detector/Panel FAT . . . 235
133 Control and Instrumentation Equipment, Dynamics Detector/Panel FAT . . . . . 236

134 X-Axis Vibration and Shock Test Setup, 40x49-in. Detector . . . . . 236
135 Y-Axis Vibration and Shock Test Setup, 40x49-in. Detector . . . . . 237
136 Z-Axis Vibration and Shock Test Setup, 40x49-in. Detector . . . . . 237
137 Thermal Cycling and ALC Control Console . . . . . 240
138 Block Diagram, Thermal Cycling Test . . . . . 241
139 Top View of Damage to F1A, S/N 0000105 . . . . . 244
140 Bottom View of Overall Splice Area, F1A, S/N 0000105 . . . . . 244
141 Closeup of Top View of Damage to F1A, S/N 0000105 . . . . . 244
142 Sinewave Vibration Specification, Detector/Panel Qual . . . . . 247
143 Random Vibration Spectrum, Detector/Panel Qual . . 248
144 Shock Response Spectrum, Detector/Panel Qual . . . 249
145 Sawtooth Pulse Specification, Detector/Panel Qual . . . . . 250
146 Acoustic Spectrum, Detector/Panel Qual . . . . . 251
147 Acoustic Facility Control and Analysis Consoles . . 252
148 Acoustic Facility Recording Consoles . . . . . 252
149 Typical Test Setup . . . . . 252
150 Infrared Lamp Array for 40x49-in. Detector . . . . 254
151 Sketch of Test Setup, Thermal Vacuum Soak . . . . . 255
152 Installation of D2A Dual Detector . . . . . 256
153 Test Holding Fixture Shown Suspended from Chamber Lid . . . . . 257
154 Loading Operations . . . . . 258
155 Post-Thermal Vacuum Soak Test Examination of B1A Panel, S/N 0000101 . . . . . 266
156 Temperature History Summary . . . . . 269
157 Overall View, ALC Test Setup . . . . . 272
158 40x40-in. Detector Setup . . . . . 273
159 Typical 12x40-in. Panel Setup . . . . . 274
160 Typical 12x40-in. Current Conduction Fingers . . . 275
161 Typical 40x49-in. Current Conduction Fingers . . . 276
162 Typical Temperature Cycle, 325°F, -100°F Requirement . . . . . 279
163 Typical Temperature Cycle, 325°F, -50°F Requirement . . . . . 279
164 Typical Temperature Cycle, 325°F, -20°F Requirement . . . . . 280
165 Leak and Stress Area, F1A, S/N 0000103A . . . . . 280
166 Leak and Stress Area, F1A, S/N 0000111 . . . . . 281
167 Machined Weldment Vibration Fixture . . . . . 292

168 40x49-in. Configuration, In-Plane Axis . . . . . 293
169 12x40-in. Configuration, In-Plane Axis . . . . . 293
170 40x49-in. Configuration, Out-of-Plane Axis . . . . 294
171 12x49-in. Configuration, Out-of-Plane Axis . . . . 294
172 Pentane Evaluation Fixture . . . . . 296
173 Full-Size Pentane Fixture . . . . . 296
174 Ultrasonic Inspection of 0.016-in. Welding Samples . . . . . 301
175 Ultrasonic Inspection of Welds on Full-Size Panel, Transducer Assembly . . . . . 301
176 Chart Recorder Used for Ultrasonic Inspection of Welds on Full-Size Panel . . . . . 301

Table

1 Schedule of Required Detectors and Panels . . . . . 16
2 Original Complement of MPDD Detector Designs . . . 18
3 MPDD Complement of Designs . . . . . 19
4 MPDD Configuration Rejections . . . . . 32
5 Configuration Comparison, 40x49-in. Detectors . . . 33
6 Data Comparison Technique . . . . . 34
7 Weighting Factor Determination . . . . . 34
8 Selection of Configuration D1 . . . . . 36
9 Recommended Designs and Basic Differences . . . . . 37
10 PDD Phase Detector Mount Design (40x49-in. Panels) . . . . . 76
11 Present Detector Mount Design (Interchangeable) . . 77
12 Data Tabulation, Sinusoidal Vibration Tests of Five 18x18-in. Panel Configurations . . . . . 97
13 Spotweld Strength, 0.008-in. Gage 21-6-9 . . . . . 108
14 Spotweld Strength, 0.027-in. Gage 21-6-9 . . . . . 109
15 Reliability Pressure Test Summary . . . . . 116
16 Target Areas and Efficiencies . . . . . 120
17 Reliability Test Data . . . . . 122
18 Configuration Reliability and Margins . . . . . 124
19 Pressure Switch Transfer Pressure Shift . . . . . 226
20 Detector/Panel Thermal Cycling Temperature Limits . . . . . 238
21 Test History, Flight Assurance Test Program . . . . 242
22 Chronological Summary of Qualification Testing . . 259
23 Summary of Switch Contact Resistance Measurements Obtained During Qualification Testing . . . . . 341
24 Carlton Controls Pressure-Actuated Switch Component . . . . . 355
25 MPPD Assemblies . . . . . 357

# METEROID PENETRATION DETECTOR DEVELOPMENT PROGRAM

## FINAL SUMMARY REPORT

## VOLUME I

By Sidney L. Russak, Rufus O. Moses, Del Gray
and Russel L. McCord
Martin Marietta Corporation

## INTRODUCTION

The Meteoroid Penetration Detector Development (MPDD) program objective was to develop and qualify penetration detectors for use in long-term earth-orbital or deep-space missions. The detectors developed on this program were an extension of the concept of the smaller detectors successfully flown on the NASA-LRC S-55 series of satellites and Lunar Orbiters. Both NASA and Martin Marietta, under contract to NASA, studied the scaling up of penetration detectors from the size used in the aforementioned programs. These studies and the experimental work that followed indicated that large, flat, pressurized detectors that offered an advantage in target area efficiency over the cylindrical detectors could be made. One cylindrical detector configuration was, however, called for in the MPDD program. Stainless steel was specified as the MPDD target material to provide continuity with the data obtained on the S-55 satellite program. Detector thicknesses were specified extending from 0.002 in. up to 0.042 in. The thinnest gage afforded continuity with the thin foil data of the S-55s and Lunar Orbiters. The heavier gage detectors were, however, of primary interest because they would measure the penetration hazard at thicknesses more meaningful to actual space vehicles and eliminate the great uncertainty existing in the extrapolation of thin foil data to spacecraft structural thicknesses.

At the initiation of the MPDD program, the intent of the program was to develop meteoroid detectors to be flown on the advance meteoroid project (AMP) satellite. The detectors were to be developed in two sizes (40 by 49 in. and 40 by 12 in.), which could be fitted interchangeably into a mounting bay of the spacecraft, and in the material gages stated above. The program was subsequently expanded to include a wide application of detector configurations capable of flying on other missions, such as

"piggy-back" experiments on other spacecraft, with a minimum of additional qualification for changes in detector size and/or thickness.

A variety of detector configurations were specified to increase the utility of the developed hardware. These comprised a family of detectors that could be flown on varied missions and included varieties to be flown on open spacecraft (and subject to puncture from either side), or on spacecraft providing protection to one side of the detector. The basic pressurized detector configuration is composed of two facing sheets of target material of equivalent thickness and uses an integral pressure switch for sensing detector puncture. For this configuration, both surfaces could be exposed to the meteoroid environment with the detector mounted in an open framework. A variation of these detectors is made up of three-plies, the middle ply acting as a common bulkhead forming two pressure chambers. Each chamber has its own pressure switch. The direction of arrival of the penetrating projectile can then be grossly determined. Another variation was intended to be mounted so that one side only would be exposed to the meteoroid environment. The unexposed side is made thinner than the target side of the detector. A bumper-detector configuration made use of a thin foil "bumper" on the 0.002-in. flat detector panel. The "bumper" could be adjusted to various standoff distances from the target sheet. This configuration when compared with data from the S-55 program will evaluate the efficiency of a double-wall structure in resisting meteoroid penetration.

All detectors designed, built, and tested during this program were fabricated of a relatively new corrosion resistant steel alloy, Armco 21-6-9 alloy. This material combines very high strength in the annealed condition with high ductility and good weldability. The material performed admirably, permitting detectors to withstand all the test environments.

Ten detector configurations were initially investigated on the MPDD program. These are described in table 1 on page 16 of this report. Seven of these configurations were carried through to completion and qualification testing.

Only a limited number of detectors were built for delivery at the end of the program. It was anticipated that a subsequent procurement might be initiated for the large number of detectors that would be needed on a meteoroid spacecraft. To facilitate this subsequent procurement, a comprehensive Production Plan was prepared covering all aspects of procurement, fabrication, testing, and inspection of the detectors to facilitate competitive bid.

## SUMMARY

The Meteoroid Penetration Detector Development (MPDD) program to design, develop, fabricate, and test meteoroid detectors was organized into three phases. The first eight months of the program comprised the Preliminary Design and Development Phase. The tasks during this period included the selection of candidate components and materials, design and analysis of detectors, establishment of candidate fabrication techniques, and the fabrication and testing of both subsize and full-size candidate detectors for each of 10 configurations described in table 1 to determine their characteristics. Candidate detectors for each of these configurations were designed, built, and tested both in subsize and full size to assist in final detector selection and evaluation. Detector configurations were selected from four joining processes, three cavity forming processes, and numerous cavity designs as described in table 2.

Of the joining processes considered, solder was quickly dropped when it became apparent that solders could not meet the strength requirements at the upper detector temperature limit. The relative success with resistance welding as the joining process and the relative lack of success with fluxless inert gas furnace brazing led to the elimination of further work in brazing except for the thinnest gage "F" configuration. Brazing development was carried on in that configuration in a high temperature vacuum furnace acquired shortly after the start of the second phase. Welding proved to be a very effective and reliable method for fabrication of detectors, both in spot and seam welding. However, welding the thin foil "F" configuration presented a special problem that resistance welders of the latest designs available at the Martin Marietta Corporation could not solve. Following a survey of the welding industry, a new type of resistance spot welder was acquired for that specific configuration. This welder proved to be suitable for the "F" configuration and satisfactorily joined the 2 mil target sheets to the 16 mil core.

Cavity formation was achieved by three methods, namely preforming of target sheets, pressure expansion of joined detector target sheets, and chem-milling. It was discovered that chem-milling could not maintain the required target sheet thickness tolerances and was eliminated except for the core sheet of the three-ply configurations (D2 and E2). The first preforming specimens were made with individual punch and die sets. This proved the technique feasible. Modified welding electrodes had

to be developed to fit within the shape of the "dimpled" preformed target sheets. When the requirements of this technique were established, the preforming of target sheets was shifted to use of a dimpled die and use of either a hydraulic press or explosive forming. Toward the end of this phase of the program, full-size target sheets for the three-ply configurations were preformed using a machined die and explosive forming. This technique was very successful and possibly could have been used for all the gages of steel in the program. However, the high-yield strength of the 21-6-9 stainless steel limited the gages that would be preformed full size in the 150-ton hydraulic press acquired for use in the MPDD program.

Most of the experimental designs were pressure-expanded after joining. This cavity formation technique was quite successful and provided a built-in check of the strength of the joints. The technique involves joining the two target sheets together so they are pressure tight, and then introducing pressure between the two sheets to expand them into the desired cavity. This technique proved to provide a good check of the detector joints, in that approximately three times detector proof pressure was required to provide the desired cavity. Joints that withstood this pressure without failing rarely gave problems later; and the joints had adequate strength to withstand this pressure reliably.

The joint patterns included squares, triangles, circles, hexagons, and labyrinth patterns. Some of the patterns were made both in interrupted seamwelds as well as spot welds. The detector edges were sealed by seam welding. Several hundred subsize detectors were built and tested using combinations of the above-described forming and joining methods. These specimens were pressure cycled to develop engineering data for design of full-size detectors.

Joint strengths used for design of the joint pattern were based on existing MIL-HDBK-5 values and the fabrication of subsize detectors commenced as soon as welding schedules were established that gave joints with strength at least equal to handbook values. For brazing, we developed our own "allowables" appropriate to this specific application. Braze joint strengths were lower than weld strengths and inconsistent. After experience was gained with resistance welds, it was established that the MIL-HDBK-S weld strength values were very conservative, at least for the 21-6-9 stainless steel used in the MPDD program. Static peel strengths as high as an order of magnitude greater than MIL-HDBK-5 were obtained. This fact assured feasiblity of

pressure expansion of detectors without joint support or failure. Subsize test specimen pressure cycling also demonstrated that the handbook spot weld values were conservative even for fatigue. A number of experiments were conducted to find the relationship between joint strength as loaded in handbook shear and tension tests and as loaded in meteoroid detectors. The actual strengths obtained, being greater than handbook values, permitted designs to be modified by increasing the joint spacing and decreasing the number of joints. This yielded a small but useful increase in target area and a small saving in detector fabrication time. Some initial experiments were conducted showing that the single joint was not the only basis for increasing spacing of joints however. The geometry of the pressure formed cell, as well as the ratio of forming pressure, were important factors. This latter point was confirmed by an experimental program to evaluate the pressure-strain relation of joints in detectors. That program was a successful counterpart to the analytical computer program used to determine strain at the joints. These constrained joint spacing increases to between 10 and 20% of the original spacing.

Attempts were made to analyze the meteoroid detector as a pressure cell to determine pressure induced stresses, and to analyze detectors for loads induced by the launch phase environment of flight. For the former, the individual joints and the area around the joint were programed on a computer. These analyses of spotweld joint loadings for margin of safety data were unsuccessful because the measurement of the pressure cell shape near the joint could not be made accurately and the symmetrical idealization used in the computer program was erroneous. After numerous unsuccessful attempts at analysis, NASA agreed to accept experimental pressure cycle survival data in lieu of analytical data on design safety margins. Problems were also encountered with computations of detector loads due to flight launch environments. The answers achieved were only approximate because of assumptions of homogeneity of the detector as a structural entity. These analyses were also dropped in favor of empirical tests.

In parallel with detector target development, a pressure switch was developed for use on MPDD detectors. This was the most important component used in the program. Two vendors with very different concepts were selected to design and fabricate switches for development use. Switches were procured from both vendors and were tested. One configuration was carried forward into the detector final design. Designs were initiated for mounting the pressure switch in the detectors. For the heavier gage detectors (16 mil and over) the pressure switch was mounted integrally in

the detector by welding. For lighter gage detectors, the pressure switch was mounted remotely on a bracket attached to the detector.

At the start of the program, it was thought that an existing flexible vibration isolator could be procured for use as the mount between the detectors and the spacecraft. Vibration tests conducted during the first month showed that the isolator would not survive the specified environment. Rigid mount studies were then started, and these produced a dozen designs; two were selected for fabrication and testing. One of these required a redesign of the detectors to provide a right angle flange at each edge. These designs were successfully fabricated. However, because of their complexity and weight, a simpler, lighter arrangement was studied. A simple aluminum angle was tested that could be mounted directly to the detectors and did not require a flange to be formed on the detector edges. Oversize holes and Teflon tape accommodated the detector thermal expansion and carried the out-of-plane loads. A slot and matching shoulder bolt at the middle of each edge carried the in-plane loads and also provided for thermal expansion and contraction. Following the successful demonstration of this concept in vibration testing and in a simple thermal test, studies were begun: (1) to design an optimum angle mount for each detector configuration; (2) to design a set of mounts for the program that would provide maximum interchangeability of detectors in the spacecraft and have commonality of use among the different detector configurations. The latter approach was selected by NASA-LRC.

An experimental program was undertaken to determine the relationship between joint pattern and cavity height as it affected detector stiffness, and to determine the desirability of detector stiffness as it affected detector and mount loads. The program showed that stiffness was related to cavity height, but joint patterns that formed large cells did not necessarily result in stiffer panels. This program showed the superiority of simple square joint patterns. Square patterned detectors were also proved to be more stable structurally. Subsequent tests showed that mount loading increased with detector stiffness, so that there was no advantage in using stiffness as a design criterion. As a result of this discovery, large cell configurations such as the hexagon were dropped.

Studies and tests on surface finish of stainless steel and modification of the as-received finish were performed during this phase. This included hand polishing, electropolishing, and vapor honing of specimens of stainless steel and measuring the values of absorptance and emittance before and after modification.

The experiments in vapor honing stainless steel proved the capability to vary absorptance and emittance within the limits specified by NASA. These experiments were successful and led to the procurement of a vapor honing machine for use on the program.

The introduction of Armco 21-6-9 stainless steel into the MPDD program was a significant event of this phase. This is a relatively new stainless steel on the market, having an annealed strength more than double the annealed strength of 304L, an elongation over 40%, and ready weldability. Its use contributed to the success of the program.

Toward the end of the Preliminary Design and Development Phase, a large number of acceptable candidate detector designs existed. Designs at this point were mostly of the square array, but also included triangles, hexagons, and parallel seams. It was decided to conduct an additional subsize experimental program to quantitatively rank the candidates. The results of these experiments eliminated some of the candidate designs and also obviated the need to carry multiple design alternatives in full size to the Preliminary Design Review. The selection originally planned for that review was thereby made earlier and more logically using quantitative data from these subsize detectors. This was particularly true because the testing to be performed on full-size detectors during this phase of the MPDD program was very limited, and of a go/no-go nature only. A number of full-size detectors were built and tested early in the program. However, fabrication of full-size detectors was stopped for some period while the above subsize detector fabrication and experiments were conducted.

The first phase of the program ended with the establishment of designs to be further developed and tested in the second phase. These were all square, spotwelded patterns, pressure expanded, except the three-ply D2 and E2 configurations, which were preformed. All detectors except the "B" and "F" configurations have pressure switches welded directly into the target sheets. This could not be done on the thinner configurations. On those configurations switches were mounted on a bracket at one corner of the detector and connected to the detector cavity with a stainless steel tube. Some process development work was to be continued on brazing and diffusion bonding for possible alternatives for resistance welding of the "F" configuration.

## Design Development Phase

During the three-month Design Development Phase, Martin Marietta continued development of and completely constructed and tested the detector designs approved by NASA-LRC at the Preliminary Design Review. The development test program was essentially an early version of the qualification test program to be conducted later. Test levels were the same as qualification levels. Development tests included a 21 344 pressure cycle test not in the qualification program, but did not have the 30-day thermal vacuum soak qualification test.

Most of the detector designs carried forth into this phase were fairly well established and presented few problems. However, fabrication problems were encountered with the "B" and "F" configurations. Considerable difficulty was experienced in welding detectors in these two thin gages, particularly in welding the 2 mil target sheets to the 16 mil core sheet for the "F" detector. This detector panel had more than 3000 spot welds in the target area. The ability to make this many consistently strong, leak-free spot welds in the three plies was considerably improved using the new welding machine procured in the previous phase. However, failures were still too prevalent, even using peel sheets overlaying the target sheets, a newly developed technique. A variety of experiments were conducted to improve the welding of this configuration. From these experiments, three factors were found to improve the welds. These were increasing the rate of electrode set down, elimination of the second half cycle of weld current, and special control of the surface resistance of the stainless steel sheets. The significance of the last factor was recognized after a new batch of the thicker gages of stainless steel produced some welds with expelled metal. These "spits" were not structurally significant in the thicker gages, but would burn through 0.002-in. material, producing leaks. A standard cleaning procedure was developed that eliminated any uncertainty in the surface resistance of the material as received from the mill. Corollary experiments indicated that the best condition for welding the three-ply "F" materials was a low resistance, and a special cleaning procedure was developed and implemented. Proper adjustment and control of these factors enabled the three-ply configuration to be successfully welded with consistent strong leak-free results.

In addition to improving the welds for the "F" configuration, producibility was improved by redesigning the panel in halves, and splicing the halves together after fabrication. Thus, a leaking

detector half could be replaced by a new detector by removing a line of rivets. Previously, a leak in either half resulted in scrapping of the entire panel.

A problem with both the "B" and "F" configurations concerned leaks in the "plumbing" joining the remote pressure switches to the target sheets. The leak problem was solved by changing the design of the tube fitting into the target sheet and changing the process of attaching the switch cups to their brackets from fusion to resistance welding. Also modified during this phase was the pressure switch mounting bracket for the "B" and "F" detector panels. This modification added provisions for a cantilever extension on the switch bracket. The extension provided a bumper support member for switch brackets used on the "F" detector. The effect of this modification was to permit interchangeability of all 40- by 12-in. detectors on their mounts.

A problem common to all detectors was leakage through the seamwelding in the completed detectors. This leakage was found to be located at the last corner crossover of the seam welds in the edges of the detector. The cause was determined to be shunting of the weld current from the seam weld wheels through the previous (oncoming) seam weld. The problem was cured by overspotwelding the last weld crossover after completion of the seam welds, thereby sealing the leak.

A problem peculiar to the three-ply "D2A" and "E2A" detectors pertained to straightness of the edges of the detector after completion. These two configurations were fabricated from explosively preformed target sheets. The preformed sheets were slightly warped by the forming operation and resulted in warped specimens after joining. A sheet metal shrinking die was used very successfully to straighten these edges.

Other miscellaneous changes made during this phase included changing mount attachment hardware from castle nuts with cotter pins to self-locking nuts. A new torquing procedure was prepared for installing these nuts.

A special thermal vacuum material test showed that outgassing from Teflon tape adhesive and potting compound used on the detectors would not degrade solar cell performance.

At the end of the Design Development Phase the successful designs were baselined for use in the Manufacturing and Test Phase. Approval by NASA-LRC of the "F" and "B" configurations was conditioned on their successful completion of development testing.

This occurred a few months after the beginning of the final phase. The pressure switch qualification test program had started and was approximately half complete. These pressure switches successfully completed the component flight assurance test program before beginning the qualification testing.

The first draft of the Production Plan was prepared and submitted to NASA-LRS during this phase.

## Manufacturing and Testing Phase

The final, or Manufacturing and Test Phase of the program comprised the manufacture of detectors to designs approved at the Design Development Review, and the testing of these detectors in accordance with the Integrated Test Plan (prepared during the first phases) through Flight Assurance, Qualification, and Accelerated Life Cycle tests. Development testing of the "B" and "F" configurations and qualification testing of the pressure switches were still open items at the beginning of this period. These two detector configurations completed development testing early in the final phase, and were then subjected like the others to Flight Assurance, Qualification, and Accelerated Life Cycle testing. The Carleton pressure switch passed qualification, but the Servonic switch developed leaks through the glass seals early in the thermal vacuum soak test. It was subsequently dropped from the program.

All pressure switches used during this phase of the program were flight assurance tested and then installed in detector assemblies. All detectors were then, in turn, flight assurance tested. From this point the detectors were directed either to Qualification Testing, Accelerated Life Cycle testing, or delivery. Specimens delivered to NASA-LRC received no testing beyond flight assurance testing. The results of Flight Assurance testing, Qualification, and Accelerated Life Cycle testing is summarized below.

Forty-one specimens were subjected to flight assurance testing; thirty-five of these passed. Four specimens initially failed flight assurance testing, were repaired, and subsequently passed. Failures during flight assurance testing were of the following nature:

1) Three ring weld leaks in the pressure target sheet to the transfer fitting joining the target sheet to the pressure tube leading to the pressure switch. This leak was in the circular ring weld joining the fitting to the target sheet;

2) One leak in the fusion weld joining the pressure switch to its mounting pressure cup;

3) Two pressure switch diaphragms leaked;

4) One seam weld leaked.

Twelve specimens were subjected to qualification testing. Ten specimens passed qualification testing and these represented specimens of all configurations carried through into the final phase of the program. These were the B1A, C1, D2A, D3A, E1A, E3A, and the F1A configurations. Two specimens failed and were removed from testing. All of the failures in qualification test were in the B1A and F1A detectors, and were associated with the remotely mounted switch. One switch cup developed a crack. The other failures were in the joints of the pressure tube joining the switch cup to the target sheet.

Three specimens of the pressure switch were subjected separately to accelerated life cycle testing, consisting of 21 344 temperature cycles between the high and low temperature limits of near-earth orbit.

One specimen of each of the large detector configurations (E1A, D3A, E3A) except D2A, and two specimens of the small detectors (B1A, C1, F1A) were exposed to 21 344 cycles of accelerated life cycle testing between the temperature limits of 325 and -100°F. The D2A detector was designated for interplanetary space flight and, therefore, was exempted from accelerated life cycle testing. Of the six configurations exposed to accelerated life cycle testing three configurations passed. These were the C1, E1A, and E3A. One of the two B1A detector specimens passed and one failed. The two F1A and the D3A failed. All of these failures were really categorized as test induced failures rather than true specimen failures except for the B1A. The B1A detector ended the test with a random failure when one of its two microswitches in the pressure switch stuck. It would not transfer. The cause of failure could not be determined nor duplicated. The switch was removed, inspected and then reinstalled. It then functioned properly. The D3A failed by fatigue at the edges clamped by the electric heating bus bar. Here dissimilar metals (aluminum and stainless steel) were clamped rigidly together while

cycling through accelerated life cycle thermal cycles and the test specimen failed by combined thermal and pressure stresses. The F1A detectors failed by a similar test condition problem. It is concluded that all of the detectors that failed during this test could probably survive actual space flight, or even accelerated life cycle tests with test fixture modifications.

Several accelerated life cycle test fixture concepts were evaluated and discarded during this phase. The approach finally selected used a liquid nitrogen spray to cool the detectors, and resistive heating to heat the detectors. This made use of the internal resistance of the detectors to a low-voltage, high-amperage current to heat them. This approach enabled the detectors to be mounted in a box and be alternately heated and cooled in place. It represented a breakthrough in simplicity over other approaches considered. However, much development was necessary before the fixtures using this concept were to operate satisfactorily.

A separate accelerated life cycle test of pressure switches was undertaken during the final phase of the program. Because of the construction of the switch it was not possible to conduct this as part of the detector accelerated life cycle test. A liquid immersion test was conceived to cycle all parts of the switch through the temperature extremes in approximately 10 minutes. Glycerin heated and thermostatically controlled by both a hot-plate and immersion heater provided the hot bath. Ethyl alcohol cooled by liquid carbon dioxide was used for the cold bath. The switches under test were cycled between the two baths under control of thermocouples embedded in one of the switches. Three switches were tested. Two of these were within performance specifications after final cleaning at completion of the required 21 344 test cycles. The third was found to be out of specification at the completion of test. This specimen had been disassembled during test and is believed to have been misadjusted at reassembly. Moving the adjustment by one increment (0.002 in.) brought this specimen back within specification.

During the final phase of the program, two new tasks were started. The first comprised design, fabrication, and testing of subsize specimens of MPDD detectors curved to be mounted on the outside of an S-IVB stage. The second task was to develop and test radiation resistant thermal coatings.

The final version of the Production Plan using a new format for the flow charts was prepared and submitted to NASA-LRC and subsequently approved.

All documents prepared and submitted under this contract are listed in Appendix A, the engineering drawings are identified in Appendix B, and testing failure histories are listed in Appendix C.

## DETECTOR DESIGN AND DEVELOPMENT

The engineering approach to establishing the detector design for the MPDD program was to evaluate anticipated problem areas and unknown design constraints using studies and analyses, where applicable, and using subsize specimen tests where appropriate. Studies and analyses performed in support of detector designs were as follows:

1) Pressure switch minimum operating levels and minimum size;

2) Detector pressurization levels;

3) Detector pressurization gas;

4) Detector mount studies;

5) Target area efficiency comparison;

6) Switch support studies;

7) Detector material selection studies;

8) Mount interchangeability studies;

9) Mount standardization studies.

Subsize tests performed in support of detector development were:

1) Subsize detector pressure expansion tests;

2) Subsize detector pressure cycle tests;

3) Braze, spotweld, and seamweld subsize development specimens;

4) Dual detector puncture simulation tests;

5) Subsize vibration testing (stiffness evaluation);

6) Surface finish tests;

7) Joint strength evaluation tests;

8) Reliability specimen tests.

Full size detector specimens were tested to determine experimentally the actual loads on the detector mounts and to determine amplification factors for vibration inputs levels as they affect the vibration loads in the detector and on the pressure switches. Those studies and tests of interest are described in this chapter.

## Engineering Objectives

The initial engineering objective of the MPDD program was to develop meteoroid penetration detectors for flight on an advance meteoroid project (AMP) spacecraft. These objectives were later expanded to include a wide variety of detectors capable of flying on other missions such as "piggy-back" experiments on other spacecraft. These detectors shall be capable of withstanding the prelaunch and launch environment associated with the spacecraft booster and the environment of near-earth orbit and deep-space flight thereafter. The test environments to prove this capability are defined in the Testing chapter presented later.

The detectors developed under this program represent a continuation of pressurized-cell detector concept developed at NASA-LRC for the S-55 series of spacecraft. These detectors comprise a pressure vessel fabricated of penetration target material. The detector incorporates a pressure switch responding to the internal pressure of the detector. The penetration is detected by loss of internal pressure after puncture of the target material. Pressure switch contact transfer provides the record of the puncture to the data gathering subsystem on board the spacecraft.

The MPDD contract required that detectors be designed of stainless steel target material of the sizes and configurations defined in table 1. These detectors are required to have leak integrity so that they will not leak down to switch trip pressure in 100 years. Their anticipated space flight life span was a minimum of two years.

## Design Progression

The engineering design of the MPDD detectors was accomplished in three phases as follows:

1) Preliminary Design and Development (PDD Phase) - The PDD phase of the contract required selection of candidate components and materials, performance of design and analysis, establishment of candidate fabrication techniques

TABLE 1.- SCHEDULE OF REQUIRED DETECTORS AND PANELS

| Detector designation | Stainless steel thickness, in. | Description and configuration | Approximate detector dimensions, in. (see figs. 2 and 3) | | |
|---|---|---|---|---|---|
| | | | Length | Width | Diameter |
| A | 0.002 | Cylindrical or semicylindrical detector | 9.8 | - - | 2.5 |
| B | 0.008 | Flat chamber detector panel | 40.0 | 12.0 | - - |
| C | 0.016 | Flat chamber detector panel | 40.0 | 12.0 | - - |
| D1 | 0.027 | Flat chamber detector | 49.0 | 40.0 | - - |
| D2 | 0.027 | Dual flat chamber detectors separated by minimum 0.012-in.-thick stainless steel or equivalent divider | 49.0 | 40.0 | - - |
| D3 | 0.027<br>Opposite side thickness to be determined by contractor (0.016) | Flat chamber detector with test material thickness on one side only and opposite side thickness optimum for minimum weight and reliability | 49.0 | 40.0 | - - |
| E1 | 0.042 | Flat chamber detector | 49.0 | 40.0 | - - |
| E2 | 0.042 | Dual flat chamber detectors separated by minimum 0.018-in.-thick stainless steel or equivalent divider | 49.0 | 40.0 | - - |
| E3 | 0.042<br>Opposite side thickness to be determined by contractor (0.020) | Flat chamber detector with test material thickness on one side only and opposite side thickness optimum for minimum weight and reliability | 49.0 | 40.0 | - - |
| F | 0.001<br>0.002 | Bumper detector panel | 40.0 | 12.0 | - - |

and fabrication and testing of both subsize and full-size candidate detectors to determine their characteristics.

2) Design Development (DD Phase) - The DD phase required continued development of detector designs selected at the end of the PDD phase. Detector designs developed and fabricated during this phase were to include the pressure actuated switch subsystem and the detector and panel mounts selected at the Preliminary Design Review.

3) Manufacturing and Test (M&T Phase) - This phase required manufacturing and testing of detector and panel designs selected at the end of the DD phase. Although this phase was directed primarily at manufacture of hardware for qualification testing of detectors and for delivery, the designs finalized during this period included certain modifications and improvements resulting from the Design Development Review.

Preliminary design and development.-

Detector cavity design development: The preliminary design and development phase was initiated with the intent of performing as much detector development work in subsize specimens as possible. The work would then be expanded to include full-size detectors after initial elimination of inferior designs in subsize work. The subsize designs were characterized by three cavity formation methods, four joining processes, and various target sheet designs as defined in table 2. The complement of designs initially considered are shown in table 3. This table indicates the combinations of forming methods, joining processes, and cavity designs evaluated. In this table the prefix letter designates the target material thickness (from table 1) of the designated detector.

Some of the pressure cavities actually developed and evaluated in the PDD phase are shown in figure 1 thru figure 6. Figure 1 depicts a cavity formed by spotwelding together two target sheets with a square array of spot welds, seamwelding the borders for pressure retention, and then pressure expanding the volume between the two sheets. The resulting cavity is a natural quilted-pillow shape that the target sheets assume during pressure expansion.

Figure 2 shows a preformed square pattern with seam-welded edges and spotwelded field attachment. The flat-sided cavity is produced by forming the target sheets into a flat bottom die. Initially, it was not known whether the pressure-expanded designs would be successful in all configurations, particularly the three-

TABLE 2.- ORIGINAL COMPLEMENT OF MPDD DETECTOR DESIGNS

| Cavity formation | Joining processes | Target sheet cavity designs |
|---|---|---|
| 1. Pressure expand<br>2. Preform<br>3. Chem-mill | 1. Spotweld<br>2. Seamweld<br>3. Braze<br>4. Solder | Spotweld<br>1. Square array<br>2. Hexagon array, one spot at each corner<br>3. Hexagon array, multiple spots per side<br>4. Triangular array<br>5. Concentric circular pillows<br><br>Seamweld<br>1. Parallel seam cell (air mattress)<br>2. Hexagon cell<br>3. Cylindrical detector<br><br>Braze<br>Essentially the same candidates as spotweld plus cylinder<br><br>Solder<br>Cylindrical detector |

TABLE 3.- MPDD COMPLEMENT OF DESIGNS

| Designation | Detector configuration |
|---|---|
| Cylindrical detector | |
| A1 | Seam weld longitudinal seam, arc weld end caps |
| A2 | Seam weld longitudinal seam, braze end caps |
| A3 | Seam weld longitudinal seam, solder end caps |
| Flat detectors | |
| B1 | Spot weld field joints, square array, pressure expand |
| B1A | Spot weld field joints, concentric circle array, pressure expand |
| B2 | Seam weld field joints, parallel seam weld labyrinth, pressure expand |
| B3 | Braze field joints, preform or chem mill square array |
| B4 | Spot weld field joint, six spot hexagonal array, pressure expand |
| C1 | Spot weld field joint, square array, pressure expand |
| C1A | Spot weld field joint, hexagonal array, multiple spots per side, pressure expand |
| C1B | Spot weld field joint, triangular array, pressure expand |
| C2-01 | Seam weld field joints, hexagonal array, 5 in. hex. cell, pressure expand |
| C2-02 | Seam weld field joints, parallel seam weld labyrinth, pressure expand |
| C3A | Braze field joints, square array, chem mill target sheet |
| C3B | Braze field joints, preform square array |
| C4 | Spot weld field joints, six spot hexagonal array, pressure expand |
| D1A | Spot weld field joints, square array, pressure expand |
| D1B | Spot weld field joints, preform square array |
| D1C | Braze field joints, preform square array |
| D2A | Spot weld field joint, preform target sheet, square array |
| D2B | Spot weld field joint, chem mill core sheet, square array |
| D2C | Braze field joint, chem mill core sheet, square array |
| D3A | Spot weld field joint, square array, pressure expand |
| D3B | Spot weld field joint, preform square array |
| D3C | Braze field joint, square array, pressure expand |
| E1A | Spot weld field joint, square array, pressure expand |
| E1B | Spot weld field joint, preform square array |
| E1C | Braze field joint, preform or chem mill square array |
| E1C-01 | Spot weld field joint, triangular array, pressure expand |
| E2A1 | Spot weld field pattern, preform core sheets |
| E2A2 | Braze field pattern, preform core sheets |
| E2A4 | Seam weld field pattern, preform parallel seam (labyrinth) target sheet |
| E2B | Spot weld field pattern, chem mill core sheet, square array |
| E2C | Spot weld field pattern, preform square array |
| E2D | Spot weld field pattern, chem mill core sheet, square array, dish preform target sheets |
| E3A | Spot weld field pattern, square array, pressure expand |
| E3B | Spot weld field pattern, preform square array (thin side only) |
| E3C | Braze field pattern, preform square array (thin side only) |
| F1A | Spot weld field pattern, square array, pressure expand |
| F1B | Seam weld field pattern, parallel seam weld (labyrinth) pressure expand |
| F2 | Braze field pattern, chem mill core sheet, square array |
| F4 | Spot weld field pattern, external square pattern overlay pillow support frame |

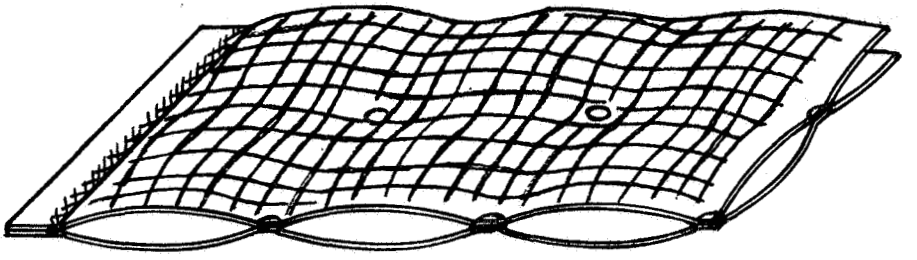

Figure 1.- Pressure Expand Square Array

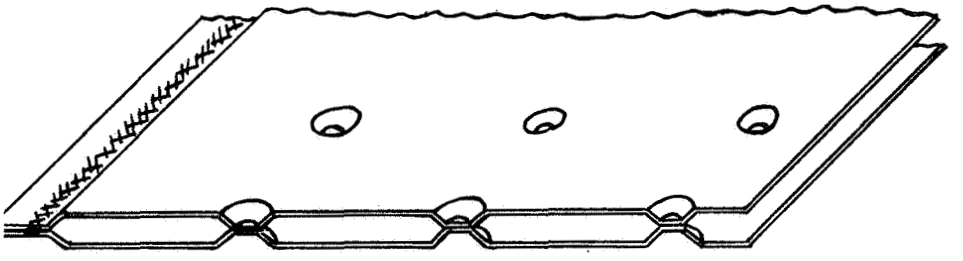

Figure 2.- Preform Square Array

ply E2 and D2 configurations. Thus, this design was conceived.

Figure 3 represents a configuration characterized by seam-welding of the field of the detector as well as the border. The configuration consists of an "labyrinth" design using long, narrow pillows interrupted only by interconnect air passages between pillows. This design proved poor from a pressure cycling capability.

Figure 4 represents a design concept using concentric continuous pressure pillows. This configuration is spotwelded in the field of the target sheet and seamwelded along the border. It was thought that this design would eliminate problems associated with discontinuities of long, parallel pressure cells like those of figure 3.

Figures 5 and 6 represent hexagonal cell designs using spot-welded and seamwelded pressure cells in the field of the detector. These cell designs lend themselves to fabrication of large pressure cells without overloading the welded joints.

The detector pressure cavity design efforts were initially directed to development of successful cavity configurations by both empirical and analytical methods. Attempts were made to analyze the detector pressure cells for stresses due to internal pressure, and the entire detector for loads induced by vibration and acoustic environments. Considerable effort was expended attempting to mathematically model the actual pressure cavity shape and to analyze this shape for pressure-induced stresses. The problem was programed into existing pressure-vessel stress-analysis computer programs. These computer programs, however, failed to produce usable answers in spite of several revisions to the programs. The problem does not lend itself to analysis. A decision was subsequently made to abandon attempts to stress analyze the detectors, and rely on empirical test data instead.

The loads analyses for evaluating detector loads induced by vibration and acoustic inputs to the detectors were based on the assumption that the detector was a homogeneous plate, and produced good output loads. However, these loads had to be converted into detector stresses. The same problem associated with the pressure cell analysis appeared here. The shape of the detector pressure cell had to be known precisely, and the detector loads converted into stresses induced into this particular shape. This proved extremely difficult. Consequently both types of analyses were abandoned, and reliance placed on empirical test results.

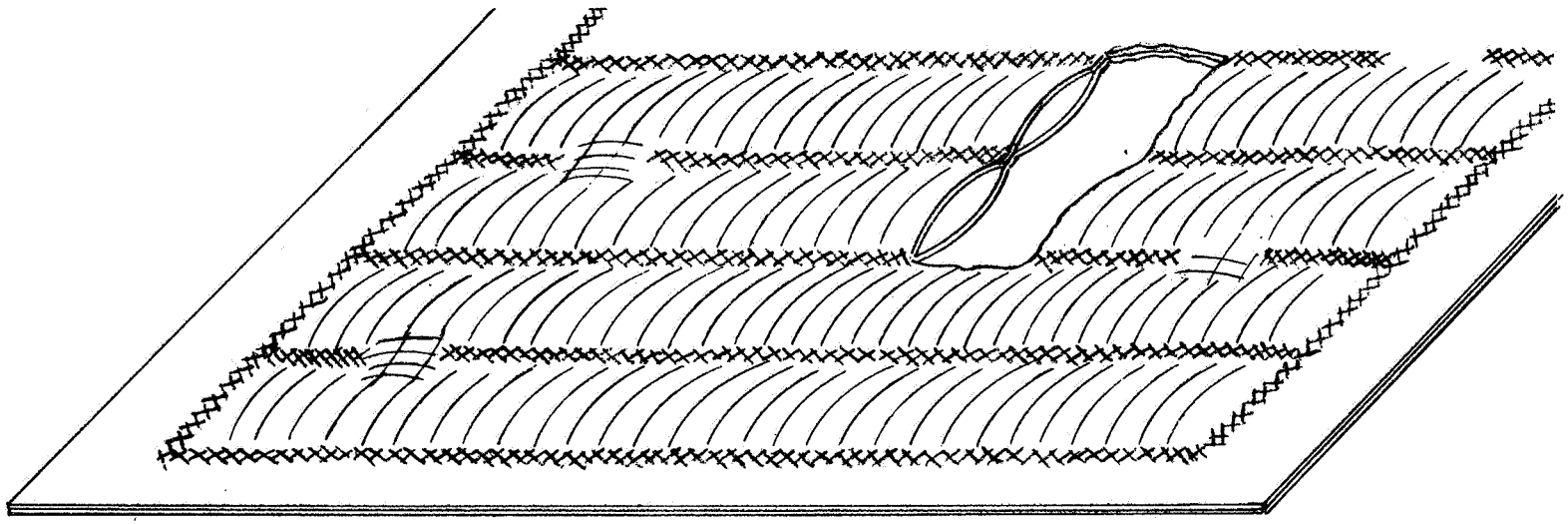

Figure 3.- Parallel Seam Labyrinth Detector

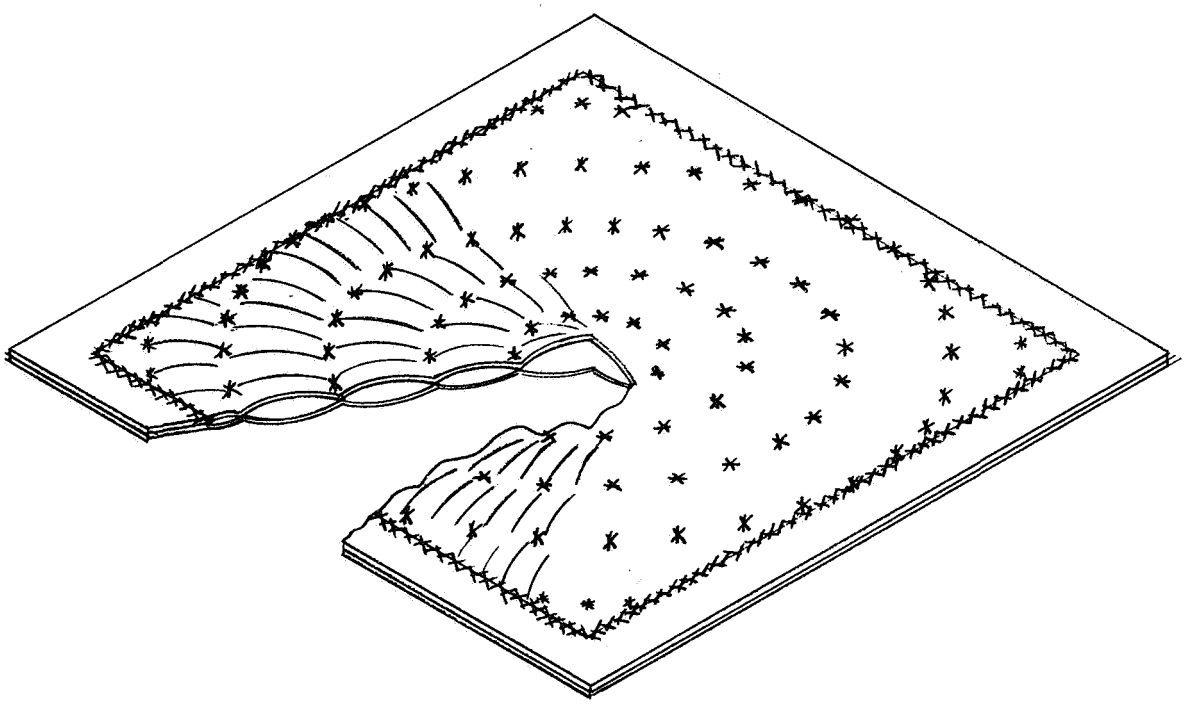

Figure 4.- Concentric Pillow Array

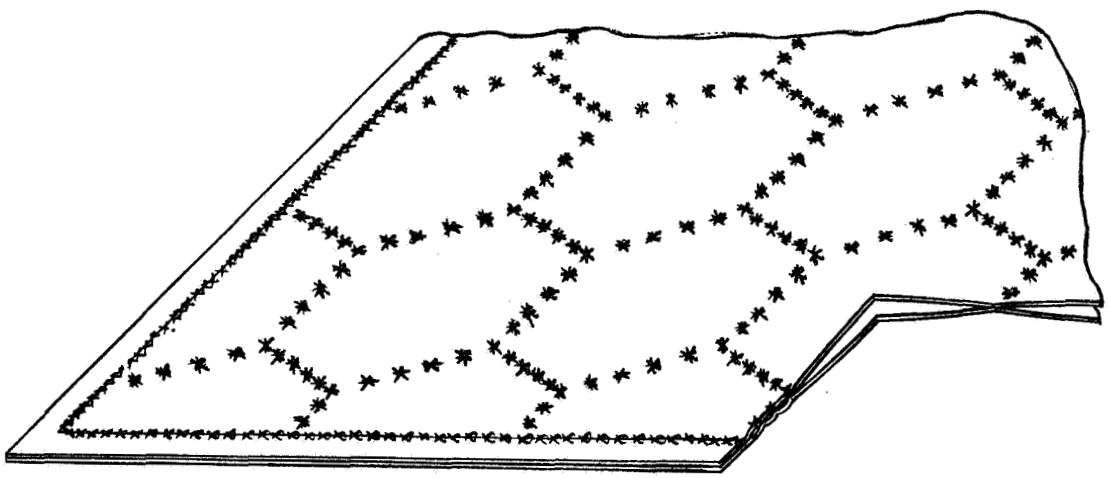

Figure 5.- Spotwelded Hexagonal Array

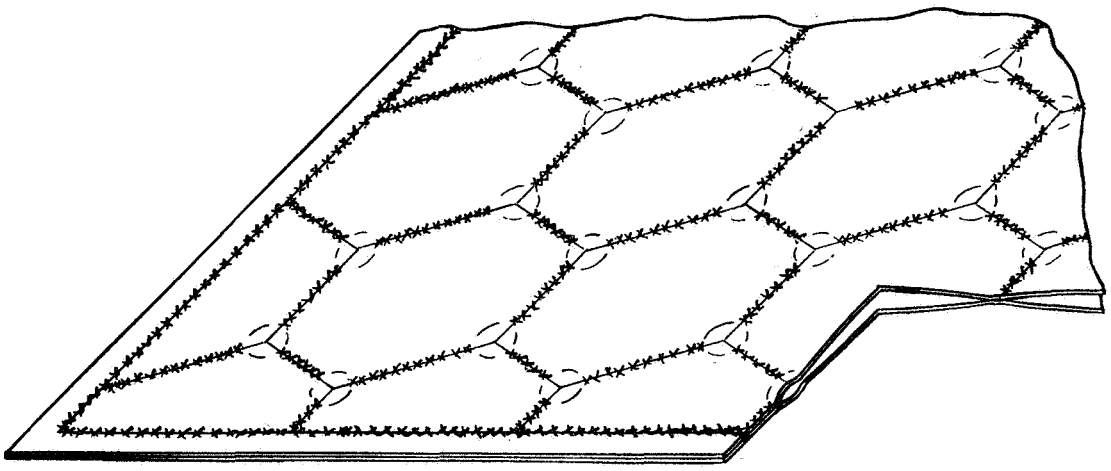

Figure 6.- Seamwelded Hexagonal Array

The design of the test cavity configurations evaluated during this phase were based on keeping the joint loads and the membrane stresses low in the pressure pillow. MIL-HDBK-5 values were used initially for weld allowables for pressure cell pattern design. The pressure cell for a square pattern detector was sized as described in the following paragraphs.

The square pattern joint spacing was based on the tension load capability of the joint for an internal panel pressure of 67 psig (detector ultimate pressure).

$$\text{Spacing} = \left(\frac{\text{Joint Tension Allowable}}{67.0}\right)^{1/2}$$

Panels and detectors having flat plate cells such as preformed detectors and the center sheet of dual detectors were analyzed by the method in Seely and Smith Text Advanced Mechanics of Materials (ref. 1). The equation:

$$\sigma = 2/9 \quad (A^2/t^2)w$$

w = internal pressure,

a = spacing of joints,

t = sheet thickness.

This spacing along with the initial spot spacing allowable by MIL-HDBK-5 spot weld allowables is shown in figure 7. The membrane stress in the pressure pillow was evaluated at the center of the pillows by computing the radius of curvature and assuming that the curvature at the center was spherical (actually not quite true). The curvature was calculated using pressure expansion data from expansion tests such as that depicted in figure 8. The membrane stress is then computed from the formula:

$$f = \frac{pr}{2t}$$

A stress level of 15 000 psi (thusly computed) proved to be a good indicator for test survival for square pattern pressure cells. Other pressure cell shapes were evaluated in a similar manner. Data for spotwelded hexagonal cells is shown in figure 9.

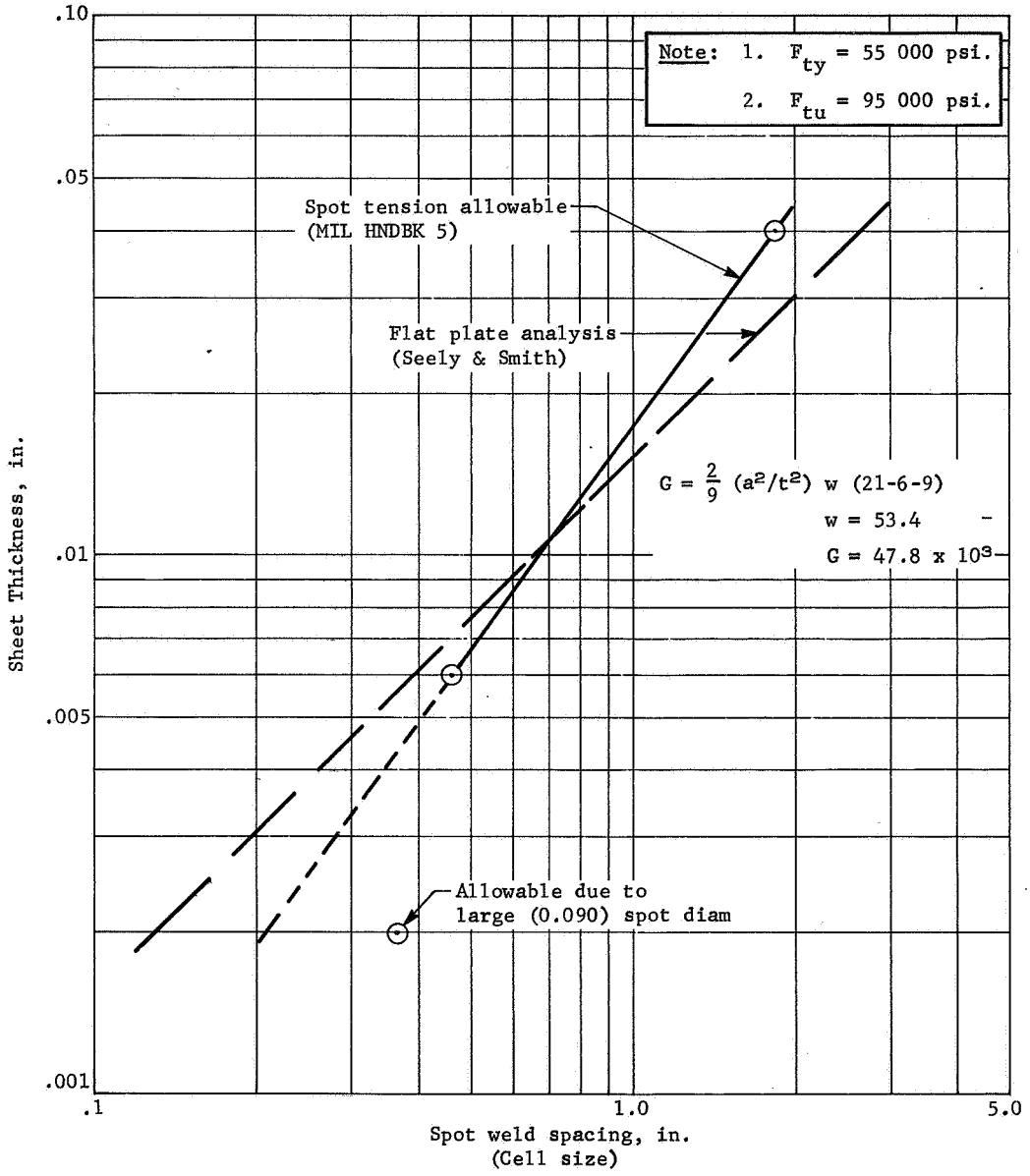


Figure 7.- Spotweld Spacing (Square Pattern), Material 21-6-9 Stainless Annealed

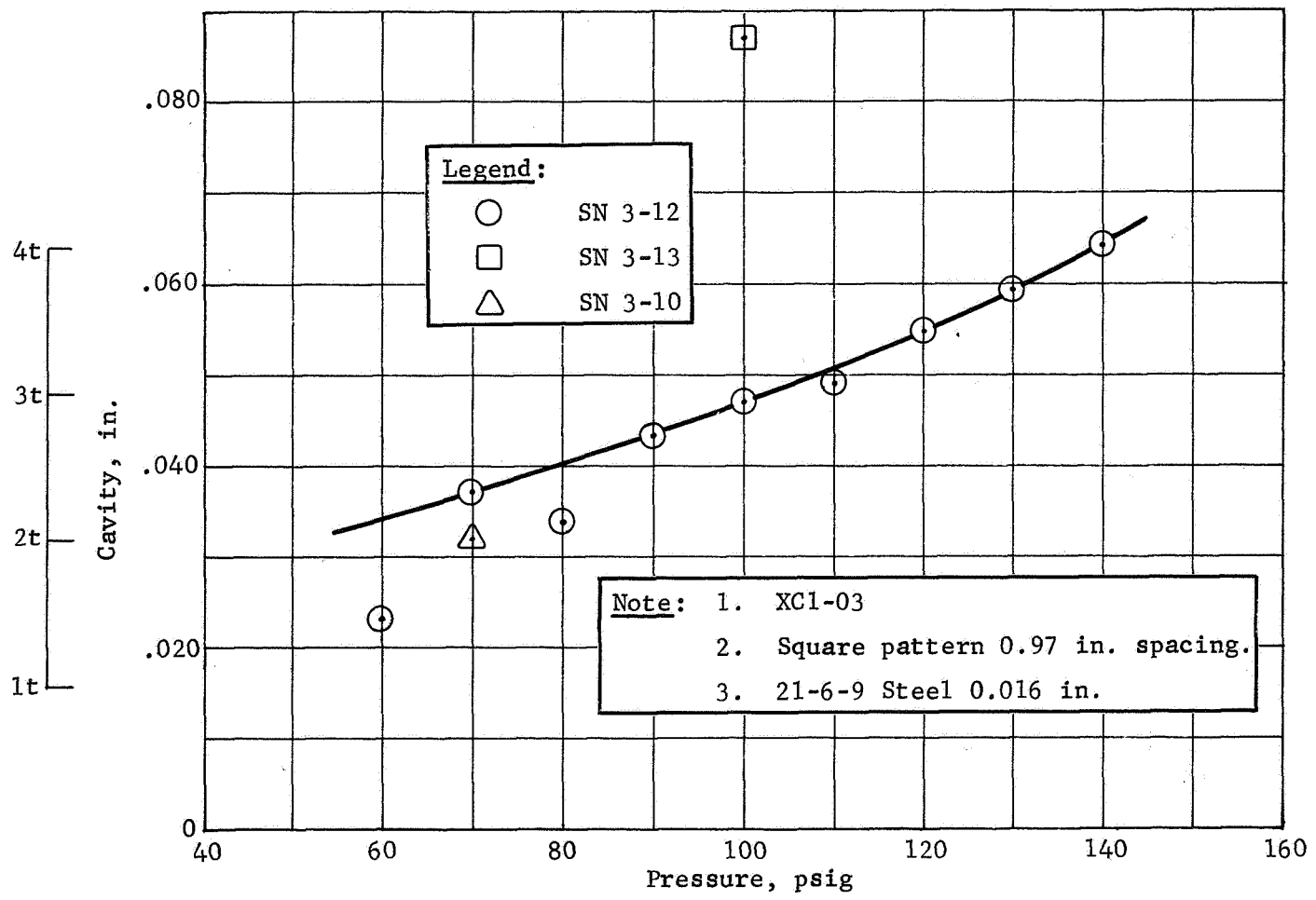


Figure 8.- Detector Pillow Cavity vs Expansion Pressure

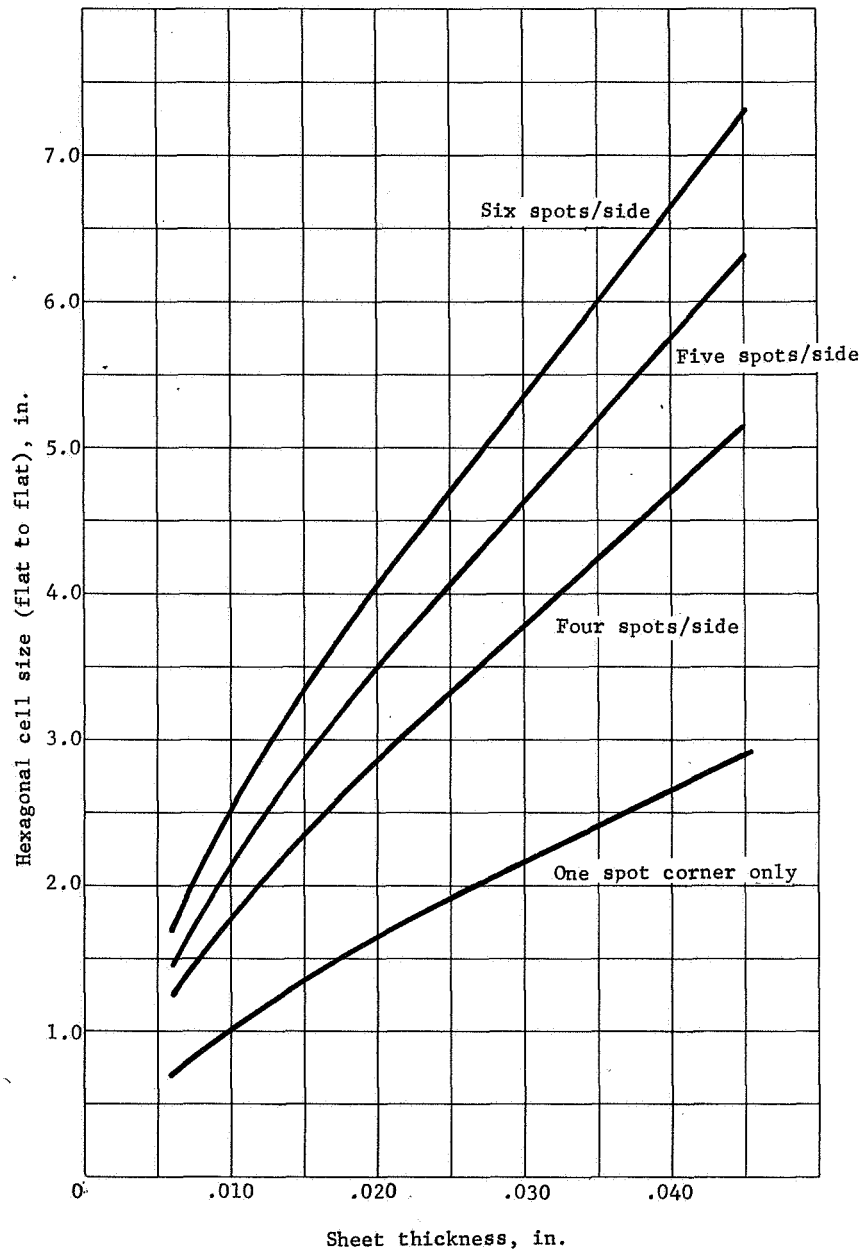


Figure 9.- Spotwelded Hexagonal Cell Size vs Thickness, 21-6-9 Stainless Steel

The results of these subsize evaluations are presented and discussed later in this chapter.

Full-size detector designs were developed and evaluated in parallel with subsize detector design and test. Both subsize and full-size test results were evaluated for selection of final designs to be continued during the subsequent Design Development phase. Four levels of screening the design were used to select the configurations. At the first level the design had to produce good, high-strength, reliable joints suitable to withstand expansion and/or proof pressure, as applicable. At the second design level the given configuration and its attachment joints were required to withstand 80 000 pressure cycles over the expected normal range of detector pressures in orbit. These pressures were initially calculated to be 14 psia at the cold side of the near-earth orbit and 39 psia on the sun side of the orbit for an initial charge pressure of 27.4 psia. The high pressure of 39 psia was arbitrarily increased by 10% to 43 psia (and later to 49 psia) to account for the anticipated reduced strength of the parent material at sun side temperatures of orbit. The selection of 80 000 cycles for test represents roughly four times the required number of pressure cycles for life cycle testing of the final detector. This number was considered an adequate margin.

The third design level consisted of vibration testing of full-size detectors to one sinewave sweep through the environment specified in the Statement of Work. These three design selection levels resulted in selection or elimination of the candidate designs. The surviving designs still were not ranked quantitatively. Consequently, a final design level was initiated. This consisted of pressure cycle testing of subsize test specimens to determine cycle-strength reliability margin. These specimens were pressure cycled for 21 344 cycles, between the limits of 14 psig and 49 psig, and then burst. From the absolute value and scatter of the burst pressure data the reliability of the specimens to survive additional pressure cycles was determined. This provided quantitative ranking data.

Full size and intermediate size (18 by 18 in.) detectors were built and tested to determine the merits of increased stiffness of the detectors to assist in resisting vibration and acoustic loads. These detectors were instrumented with accelerometers (and with strain gages in the case of the full-size detector) and vibrated to determine characteristics of the detectors at various pressure cell cavity heights. These tests indicated there was little or no merit in stiffness increase in the detectors. This fact was responsible for discontinuing development of large pressure cell detectors.

Table 4 shows the configurations rejected by the various design evaluations. Eventually, all brazed specimen configurations were discontinued because of the slow progress of development of brazing of joints, and erratic repeatability and dependability of braze strength. Configuration "A" detectors were also eventually discontinued with NASA concurrence because they presented little advantage over the half-cylinder detectors developed for the S-55 program.

The final selection of detectors for further development in the design development phase was made on a numerical selection basis. Table 5 shows the parameters that were compared between various candidate configurations of the large 40 x 49-in. detectors. Similar data were also prepared for the 40 x 12-in. detectors. The area shown is the effective target area available for meteoroid penetration. Panel weight includes the weight of the detectors, switches, switch covers, wire covers, mounts, and mounting hardware. Forming pressure reliability, life cycle reliability and strength safety margin data were obtained from a subsize reliability test program described in a later chapter. The relative cost data are shown as a ratio of the subject panel cost to the cost of a configuration D1A-01 panel.

To compare various detector configurations the basic parameters such as area, weight, reliability, etc, were normalized to permit the calculations of a figure of merit for each configuration. The values of each parameter for all candidate configurations of a given family of detectors were summed individually. The percent of the total number for each configuration then represents an approach coefficient for that parameter. For parameters such as cost where a low number is the most desirable, the reciprocal of the value was summed. Such comparison data are typified by table 6.

Finally, weighting factors were applied to the basic detector parameters for comparison of detectors; as shown in table 7. The weighting factors to be applied to each parameter were determined by use of mathematical decision plot. This is a subjective method whereby successive sets of two parameters are compared. Whichever parameter is judged the most important of the two is assigned a value of "1" and the other given a "0". After all parameters are compared one against the other the point total for each separate parameter is tallied, and the total points for all parameters are figured. The percent of the total number of points, represented by each parameter, is then calculated and this percentage becomes the parameter weighting factor.

TABLE 4.- MPDD CONFIGURATION REJECTIONS

| | |
|---|---|
| **Prescreen rejections** | |
| C3A, and E1C (alt.) | |
| | Chem milling of target sheets not within required target sheet thickness tolerance |
| E2A1, and E2A2 | |
| | No obvious means of producing satisfactory preformed core |
| **Joint strength screen rejections** | |
| A3 | Soft solder strength inadequate at elevated temperatures |
| C3B, D1C, D2C, D3C, E1C, and F2 | |
| | Braze joint development not commensurate with program progress |
| **Vibration screen rejections** | |
| C2-01, and C1A | |
| | Stiffness afforded by large hexagonal seam welded cell not required, nor desirable |
| **Pressure cycle and burst test rejections** | |
| B2 | Specimens performance erratic during pressure forming |
| C1A | Specimens failed during pressure cycling |
| C2-02 | Seam weld failures at end of seam weld during pressure cycle |
| F1B | Seam weld failures along middle of seam welds |

TABLE 5.- CONFIGURATION COMPARISON, 40x49-in. DETECTORS

| Configuration | No. of spots | Area, in.$^2$ | Area eff, % | Weight, lb | Area/wt, in.$^2$/lb | Forming Pressure Reliability | Life Cycle Reliability | Strength safety margin | Relative cost/pnl |
|---|---|---|---|---|---|---|---|---|---|
| D1A-01 | 1044 | 3611.5 | 92.1 | 32.4 | 111.8 | $.9^{18}85$ | $.9^{22}$ | 5.08 | 1.00 |
| D1A-02 | 594 | 3628.7 | 92.6 | 32.4 | 112.5 | $.9^{9}$ | $.9^{25}$ | 3.05 | .94 |
| D1B-01 | 918 | 3528.2 | 90.0 | 32.4 | 109.2 | NA | $.9^{23}$ | 4.66 | 1.08 |
| D2A-01 | 2000 | 3480.0 | 88.8 | 41.8 | 83.2 | NA | .9944 | 4.28 | 1.50 |
| D2B-01 | 920 | 3479.3 | 88.7 | 49.0 | 71.0 | NA | .902 | 4.54 | 1.49 |
| D3A-02 | 1540 | 1793.3 | 91.5 | 26.2 | 68.4 | .99985 | $.9^{9}547$ | 3.86 | 1.08 |
| D3B-01 | 2180 | 1747.7 | 89.1 | 26.2 | 61.6 | NA | $.9^{22}88$ | 4.03 | 1.18 |
| E1A-01 | 500 | 3612.0 | 92.2 | 49.4 | 73.4 | $.9^{35}$ | $.9^{60}$ | 6.25 | 1.00 |
| E1A-02 | 252 | 3625.8 | 92.6 | 49.4 | 73.7 | $.9^{20}$ | $.9^{70}$ | 2.95 | .96 |
| E1B-01 | 415 | 3569.0 | 91.2 | 49.4 | 72.5 | NA | .99874 | 3.72 | 1.06 |
| E1C-01 | 520 | 3611.0 | 92.2 | 49.4 | 73.4 | $.9^{55}$ | $.9^{86}$ | 6.16 | 1.00 |
| E1C-02 | 220 | 3627.4 | 92.6 | 49.4 | 73.7 | $.9^{9}287$ | $.9^{35}$ | 3.04 | .96 |
| E2C-01 | 980 | 3485.4 | 88.9 | 61.1 | 57.0 | NA | $.9^{11}314$ | 4.53 | 1.59 |
| E2D-01 | 414 | 3551.3 | 90.6 | 67.4 | 52.6 | NA | .0032 | 2.34 | 1.59 |
| E3A-02 | 980 | 1804.6 | 92.1 | 37.1 | 48.6 | $.9^{8}583$ | $.9^{17}$ | 4.49 | 1.14 |
| E3B-01 | 1386 | 1752.7 | 89.4 | 37.1 | 47.2 | NA | 0 | 4.03 | 1.32 |

TABLE 6.- DATA COMPARISON TECHNIQUE

| Normalized data | | | | |
|---|---|---|---|---|
| Area | | | | |
| D1A-01 | 3611.5 | 3611.5/10768.4 = 0.335 | | |
| D1A-02 | 3628.7 | 3628.7/10768.4 = 0.337 | | |
| D1B-01 | 3528.2 | 3528.2/10768.4 = 0.328 | | |
| | 10768.4 | | 1.000 | |
| Cost | | | | |
| D1A-01 | 1.0 | 1/1.0 = | 1.00 | 1.00/2.99 = 0.335 |
| D1A-02 | .942 | 1/.942 = | 1.06 | 1.06/2.99 = 0.355 |
| D1B-01 | 1.08 | 1/1.08 = | 0.93 | .93/2.99 = 0.310 |
| | | | 2.99 | 1.000 |
| Weighted data | | | | |
| Area | | | | |
| D1A-01 | 0.355 X 0.267 = 0.0895 | | | |
| D1A-02 | 0.337 X 0.267 = 0.0900 | | | |
| D1B-01 | 0.328 X 0.267 = 0.0875 | | | |

TABLE 7.- WEIGHTING FACTOR DETERMINATION

| Parameter | Choice tally | Total | Emphasis coefficient |
|---|---|---|---|
| Panel area | 1 0 1 1 1 | 4 | 0.267 |
| Panel weight | 0 0 1 1 1 | 3 | 0.200 |
| Probability of surviving 21 344 pressure cycles | 1 1 1 1 1 | 5 | 0.333 |
| Probability of surviving forming pressure | 0 0 0 1 1 | 2 | 0.133 |
| Manufacturing complexity | 0 0 0 0 0 | 0 | 0 |
| Manufacturing cost | 0 0 0 0 1 | 1 | 0.067 |
| | | 15 | |

Selection of the detector from the D1 series of candidates is shown in table 8.

The normalized data -- approach coefficients -- and weighted data for each candidate configuration of the D1 family of detectors is shown. The absolute values of each of the parameters can be seen on table 8. The following can be concluded:

1) The area efficiency of configurations D1A-01 and D1A-02 are superior to D1B-01;

2) The weight of all of the configurations are equal;

3) The reliability of all of the configurations exceeds program goals;

4) Two figures of merit are shown, one including the forming pressure survivability parameter and one excluding the parameter, since configuration D1B is not pressure expanded;

5) Configuration D1A-02 is the superior design.

Selection of detectors in the other categories was made on the same basis. The recommended configurations for DD phase are listed in table 9. The open-spacing designs represent configurations having joints loaded more highly than is permitted by MIL-HDBK-5. These higher loaded joint configurations are in keeping with the strength of spotweld joints as developed on the MPDD program. A drawing of one of the preliminary design and development phase detectors is shown in figure 10.

Pressure switch development: Pressure actuated switch design development was initiated in parallel with development of the detector cavity design studies.

The electrical characteristics of the pressure switch subsystem were established by NASA-LRC at the beginning of the program as follows:

1) The unit should have a double-pole, double-throw contact arrangement;

2) Contacts should be rated at 1 A continuous;

3) Contact resistance should not exceed 50 milliohms at 100 μA (subsequently changed to 100 milliohms at 0.5A and 200 milliohms at 100 μA, with NASA concurrence);

TABLE 8.- SELECTION OF CONFIGURATION D1

| | Normalized data | | | Weighted data | | |
|---|---|---|---|---|---|---|
| | D1A-01 | D1A-02 | D1B-01 | D1A-01 | D1A-02 | D1B-01 |
| Area | 0.335 | 0.337 | 0.328 | 0.0895 | 0.0900 | 0.0875 |
| Weight | 0.333 | 0.333 | 0.333 | 0.0666 | 0.0666 | 0.0666 |
| Life cycle reliability | 0.333 | 0.333 | 0.333 | 0.1000 | 0.1000 | 0.1000 |
| Form pressure survivability | 0.500 | 0.500 | - - - | 0.0665 | 0.0665 | - - - |
| Manufacturing cost | 0.335 | 0.355 | 0.310 | 0.0221 | 0.0234 | 0.0245 |
| Figure of merit | 1.836 | 1.858 | 1.304 | 0.3446 | 0.3465 | 0.2786 |
| Figure of merit | 1.336 | 1.358 | 1.304 | 0.2782 | 0.2800 | 0.2786 |
| | Square array pressure expand std spacing | Square array pressure expand open spacing | Square array preform | | | |

TABLE 9.- RECOMMENDED DESIGNS AND BASIC DIFFERENCES

| | | |
|---|---|---|
| B1A | - | Spot welded field joints, square array, pressure expanded |
| C1 | - | Spot welded field joints, square array, open spacing (1.1 in.), pressure expanded |
| D2A | - | Spot welded field joints, preform both target sheets (0.94 in. spacing) |
| D3A | - | Spot welded field joints, square array, open spacing (1.1 in.), pressure expanded |
| E1A | - | Spot welded field joints, square array, open spacing (2.64 in.), pressure expanded |
| E3A | - | Spot welded field joints, square array, open spacing (1.32 in.), pressure expanded |
| F1A | - | Spot welded field joints, square array, pressure expanded |

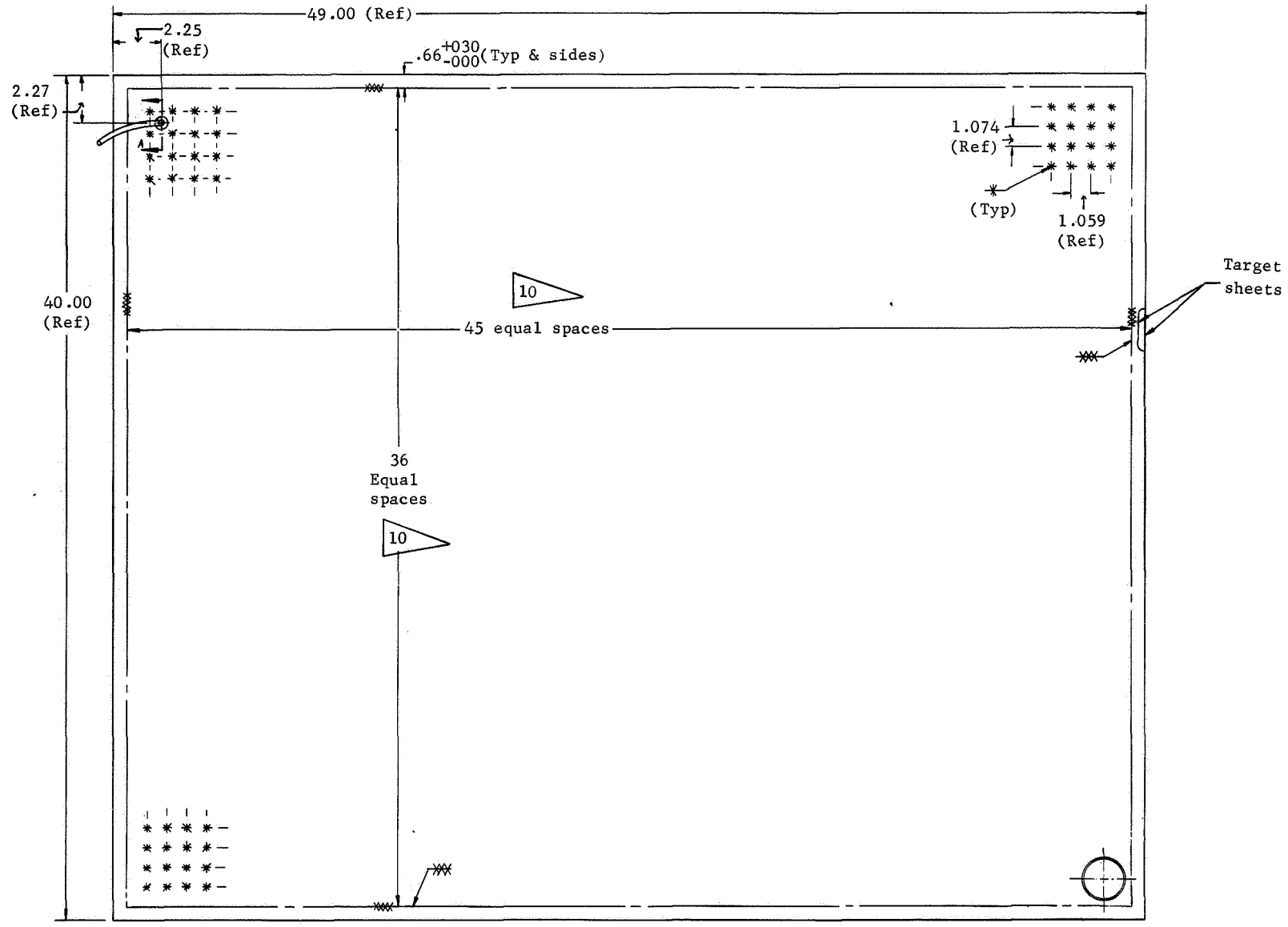


Figure 10.- Detector Assembly, D3A

4) Switch insulation should not be less than 100 MΩ at 600 V rms.

It was desired that the pressure actuated switch be of minimum size to minimize the meteoroid detector sensitive area shaded by the switch and weight added to the detector. From a detector standpoint, the switch should operate at minimum practical pressure to minimize pressure stresses in the detector itself.

The following companies were contacted to determine the feasibility of building a pressure switch to meet this requirement of the MPDD program:

1) Servonic Instruments, Inc., Costa Mesa, California;

2) Consolidated Controls Corp., Bethel, Connecticut;

3) Sigmanetics, Inc., Parsippany, New Jersey;

4) The Bristol Company, Waterbury, Connecticut;

5) Custom Components Switches, Chatsworth, California;

6) Carleton Controls Corp., East Aurora, New York.

The desired switch characteristics and requirements were discussed with potential switch subsystem vendors to determine how these requirements could best be met. As a result of these discussions it was determined that a switch could be built with maximum dimensions of 1.50 in. diameter and 1.00 in. depth, using a snap-through design for the pressure switch. The snap-through feature would eliminate the potential problem of "teasing" of electrical contacts near the trip pressure of the switch. It was further determined that a design goal maximum weight of 5 ounces for the switch subsystem would be realistic. Minimum switch trip pressure was established to be approximately 3 psi for a unit that would withstand booster launch vibration with reasonable assurance that the switch would not trip. The switch trip (and reverse trip) pressure range was subsequently established at 6 $\pm$ 2.5 psi, a range considered achievable by the switch vendors.

Early studies and experiments with pressure switch mounting schemes indicated that the switch should be mounted to the detector as near as possible at the center of gravity of the switch. The high level of environmental input vibration to the detector plus amplification of these levels by the MPDD detector panels

indicated that cantilever mounting of pressure switches was less than desirable, if not impractical. Consequently, the requirement was added that the pressure switch assembly have a circumferential flange to attach the pressure switch to the detector. The resulting switch design provides for the mounting flange to be located close to the center of gravity and have a wide attachment footprint for accommodating environmental dynamic loads. This flange permits welding of the units into the MPDD detectors to provide a gas-tight joint, and the web of the flange provides a thermal standoff to prevent welding heat from reaching and damaging the sensitive internal switch parts. The present specification requirements for the switch subsystem are defined in reference 2.

Two vendors were chosen for pressure switch subsystem development to assure development of at least one acceptable design. Contracts were let with Carleton Controls Corporation of East Aurora, New York, and Servonic Instrument, Inc. of Costa Mesa, California.

The Servonic Instruments Incorporated (SII) pressure switch assembly was one of the two designs chosen for development for the MPDD program. This configuration was chosen for development because its design features were different than the other candidates and appeared simple and reliable. These features are:

1) Integral electric contacts of the switch were immersed in the pressurizing media of the detector on which the switch assembly would be used. Thus, as long as the detector maintained pressure, the electric contacts are not subjected to ionization and arc-over problems;

2) The electric contacts were directly linked to a simple driving mechanism consisting of two Belleville spring diaphragms welded back-to-back to form a pressure-sensitive capsule. This pressure capsule has the feature of snapping cleanly through from one position to the other upon reaching switch-trip pressure. The contacts are thus not "teased" at or near trip pressure for increasing or decreasing pressure changes;

3) The back-to-back Belleville-spring pressure capsule bottoms out on itself with increasing pressure applied to the pressure port. This feature permits the pressure capsule to stand high external over-pressures. In test this pressure capsule has withstood pressures as high as 750 psi without changing switch point characteristics.

The SII internal configuration is shown in figure 11. As can be seen from the figure, the entire internal cavity of the switch (with the exception or the pressure-capsule interior) is immersed in the pressurizing medium. The internal pressure of the switch assembly (and also the detector) can be checked simply by applying a back pressure to the interior of the pressure capsule, thereby acting against the capsule external pressure to trip the switch. This provides a handy method for checking pressurization of detectors.

The disadvantage of this configuration lies in the numerous glass-bead hermetic seals for electric feedthrough connections from the internal switch contacts. These seals represent potential leak paths. The SII configuration performed well, initially, and was developed during the preliminary design phase of the MPDD program.

The Carleton Controls Corporation (CCC) pressure switch assembly was chosen as the second design for development for the MPDD program. This configuration represented a conventional approach to a pressure switch design. The features of this configuration are:

1) Use of proved hermetically-sealed microswitches. Two single-pole double-throw microswitches provide redundant activation indication although both microswitches are actuated by a common striker plate;

2) Use of a pressure diaphragm backed up by a Belleville spring provides a snap-through action to the electric contacts. The diaphragm and Belleville spring snap through cleanly from one position to the other when the pressure traverses through the trip pressure range, causing the striker plate to strike (or release from) the microswitch actuator arms. The microswitches in turn are snap through devices. No electric contact "teasing" is possible with this configuration at or near trip pressures;

3) Only one leak path exists for this design. Pressure can leak only through the diaphragm weld (assuming the parent metal itself does not leak).

This design functioned well in test and had generally lower contact resistance than the Servonic switch. The internal configuration of the Carleton switch assembly is shown in figure 12. The stainless steel pressure diaphragm of 0.002-in. thick material

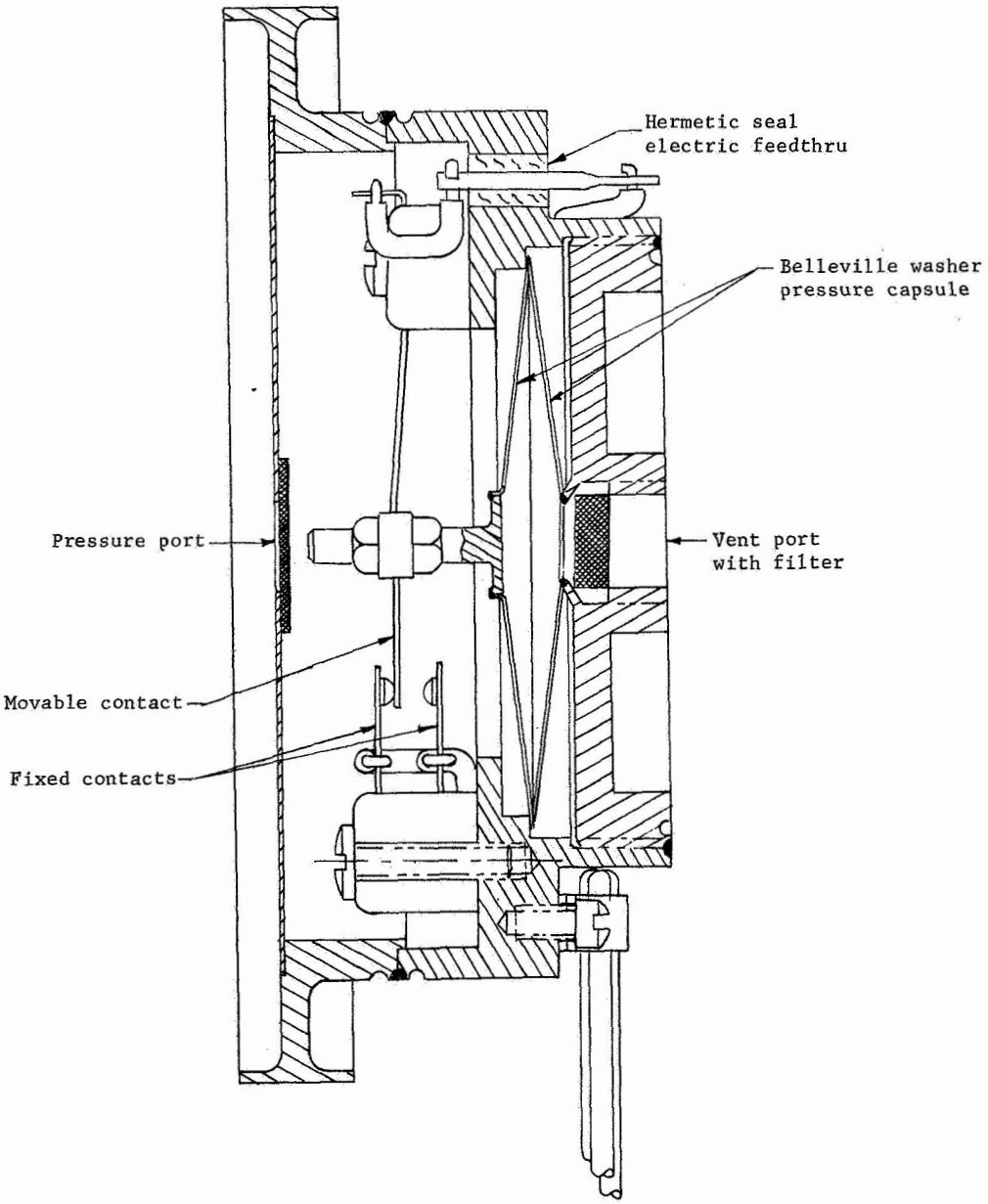


Figure 11.- Servonic Instrument Incorporated Switch Configuration

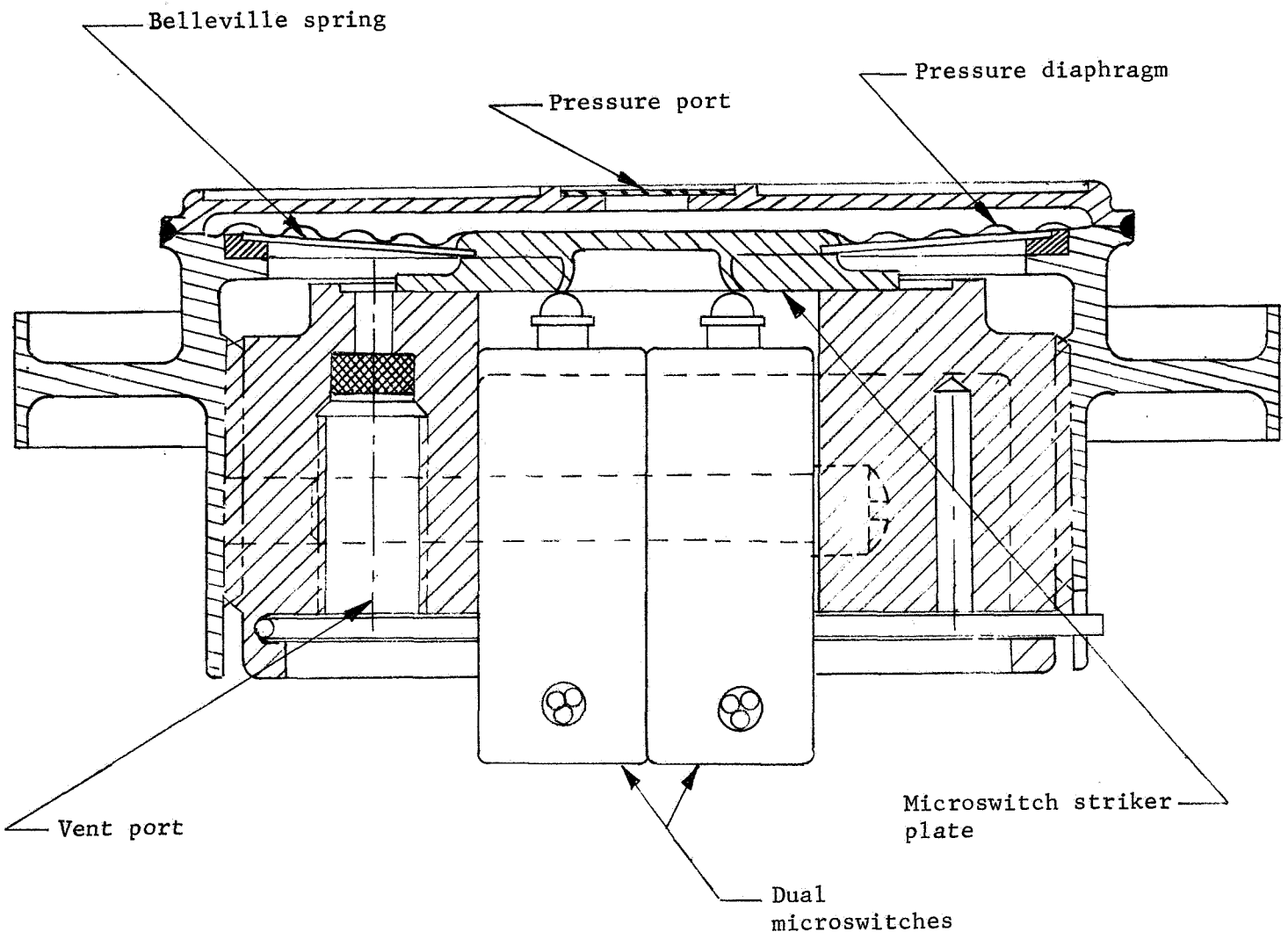


Figure 12.- Carleton Controls Corporation Switch Configuration

backed up by a Belleville spring can be seen in the figure. The center of the Belleville spring contains an aluminum striker plate that pushes against the actuator arms of the microswitches to actuate the microswitch contacts. The two microswitches are attached to a threaded switch holder, providing adjustment of the microswitches in the main body of the switch assembly. This switch assembly, like the Servonic configuration, has a vent port to permit checking the detector internal pressure by applying overpressure through the vent. This procedure has not been quite as satisfactory for the Carleton switch because of the pressure leakage through the threads of the switch holder.

Pressure switch mount: Pressure switch mount development proceeded along two parallel paths. The pressure switch mounting concept for heavy gage (over 16 mil) detectors permitted direct mounting of the switch into the detector itself. The lighter gage detectors would not permit this approach, and required remote mounting of the pressure switch assembly. Both mounting concepts were evaluated during the preliminary design and development phase.

The heavy gage detector switch mount concept was developed during the early months of the program and proved successful from its inception. The concept involves forming a drawn cup "volcano" integral in the target sheet of the detector, as shown in figure 13. The pressure switch is then pressed into the volcano and fusion welded to join the lip of the pressure switch mounting flange to the lip of the volcano. A positive, leaktight pressure seal results from this installation. The initial design used a pressurizing fill tube brazed into the bottom radius of the volcano for pressurizing the detector after installing the switch assembly. This tube was pinched off, sealed, and wrapped around the volcano. A fill tube protector was installed over the fill tube and a switch-terminal shield installed over the pressure switch to protect these items from puncture by meteoroids. The installed switch installation is shown in figure 14.

The thin gage detectors proved to be less easy to provide with a simple pressure switch mount. The first design concept pursued was an attempt to copy the desirable features of the switch mount for the heavy gage detectors. This approach involved providing a triangular 16-mil doubler plate (gusset) on the detector. This gusset was seam welded to the upper target sheet for pressure integrity, and provided an integral volcano for mounting the pressure switch. A raised flange across the diagonal edge transmitted switch vibration loads over to the edge of the detector panel. This configuration is shown in figures 15 and 16. This design was inefficient because it blanketed too large an area of the target sheet; it was therefore discarded.

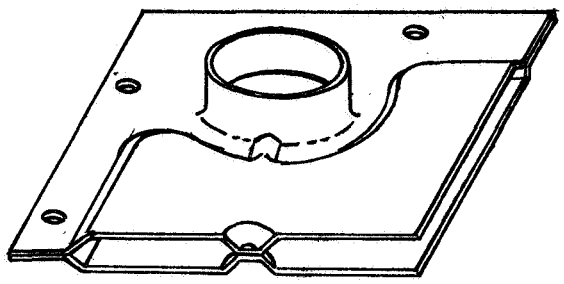

Figure 13.- Switch Support "Volcano"

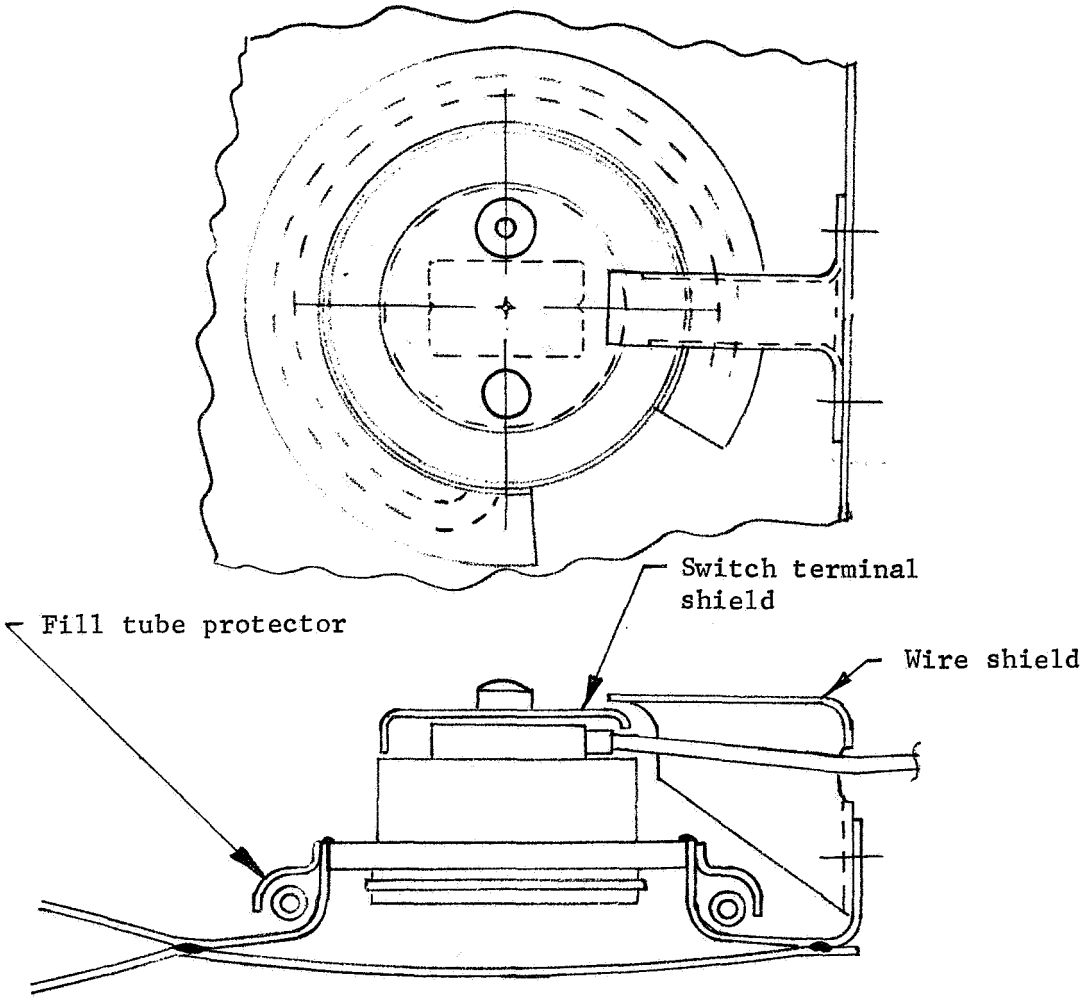


Figure 14.- Carleton Switch Installation

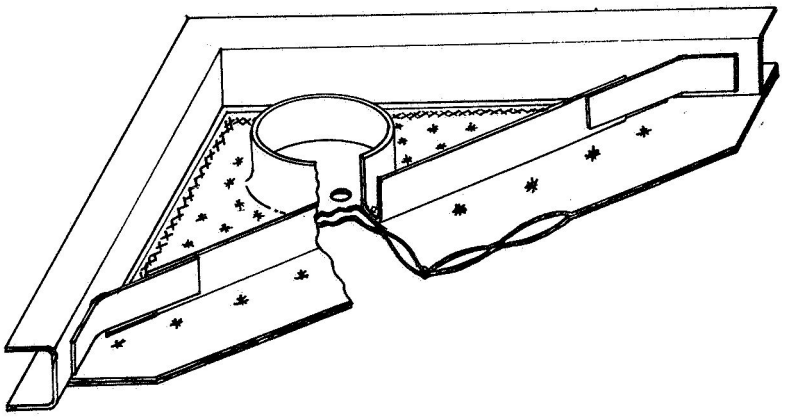

Figure 15.- Switch Support Gusset
(Thin Gage Target)

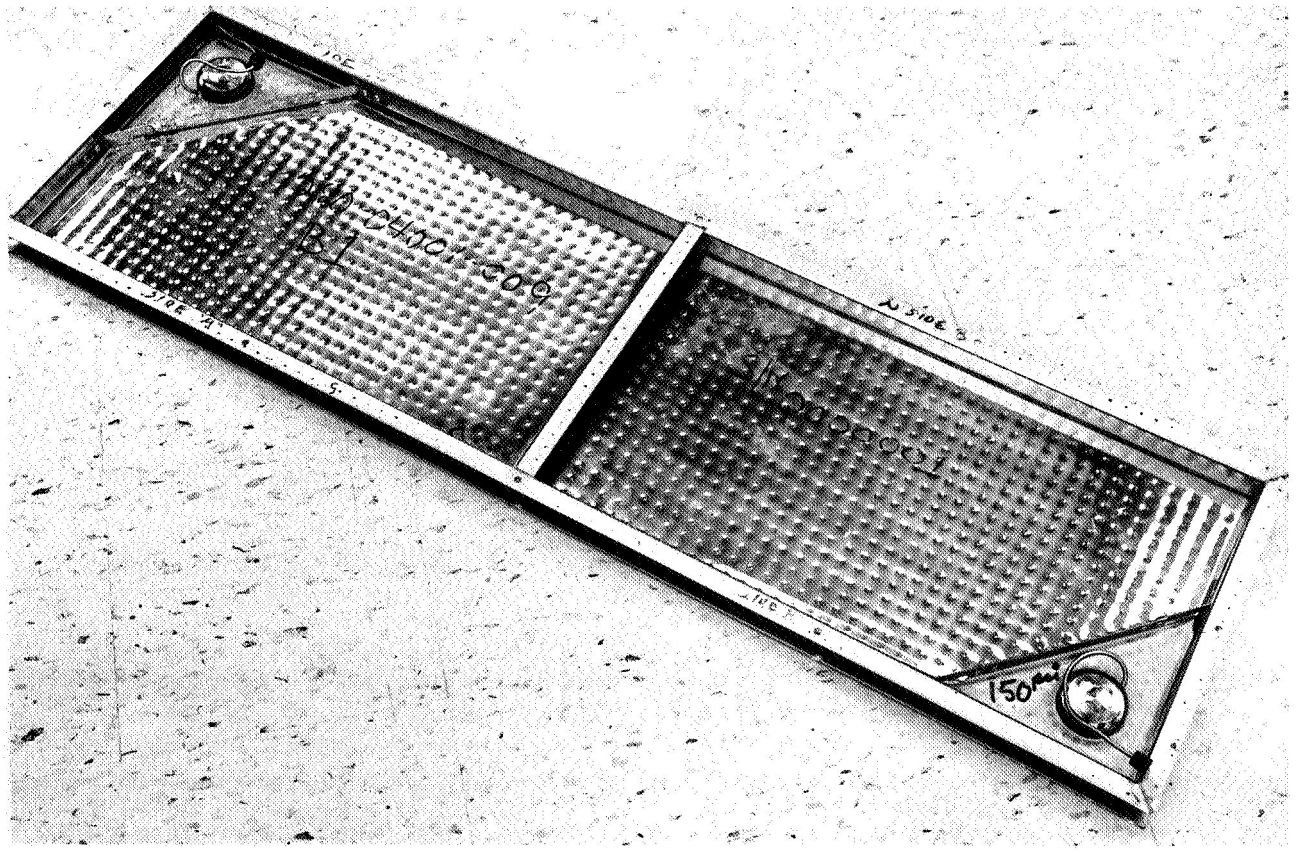

Figure 16.- B1 Full-Size Panel Showing Switch Gusset,
12x40 in., 21-6-9 Stainless Steel

The second design approach is shown in figure 17. This concept provided for mounting of the pressure switch in a pressure cup remote from the detector, with a pressure tube joining the cup to the detector. This approach was heavy and also covered more of the target sheet than desired.

The third configuration generated during the PDD phase is shown in figure 18. This configuration also mounts the pressure switch remotely from the detector. It differs from the second configuration in that the pressure switch is mounted at right angles to the detector to minimize the shadowing of the detector. The pressure switch is welded into a pressure cup, which is in turn supported by a corner-mounted bracket. A pressure tube joins the switch-mounting-pressure-cup to the detector. A flanged tube fitting welded to the upper target sheet with an annular resistance weld (ring-weld) provides a leaktight pressure connection to the detector pressure cavity. The pressure switch is protected from meteoroids by a switch cover and a flange on the bracket.

Detector mount design: The detectors designed, built, and tested by Martin Marietta before the MPDD program had problems in surviving vibration testing. Several of the detectors failed because of fatigue of the parent metal around the spot welds. Consequently, early mount studies were centered around the use of vibration isolators. The original vibration input level specified by NASA had an input amplitude of 0.3-in. at the low frequency end of the spectrum. A good vibration isolator could have a vibration "Q" factor at resonance as low as 5. The vibration isolator could therefore experience vibration amplitudes as great as 1.5 in. A survey of available vibration isolators indicated that suitable isolators could not be found. A test of two cable-type commercial isolators was made, however, to evaluate isolator response to the specified test environment. These isolators are shown mounted for test on a vibration fixture in figure 19. This test resulted in mechanical rupture of the isolators. It appeared that there was no commercially available isolator suitable for the MPDD program. Consequently, detector mount attention was redirected to hard-mounting the detector with emphasis on mount approaches that would alleviate the detector loads.

The first detector mount designed for MPDD detectors is shown in figure 20. This mount consisted of a continuous "C" channel rigidly attached to the detector. This mount would provide continuous and uniform support for the detector without discontinuities or structural-impedance mismatch except at the corners. Structural dynamics analysts suggested that this approach might assist in

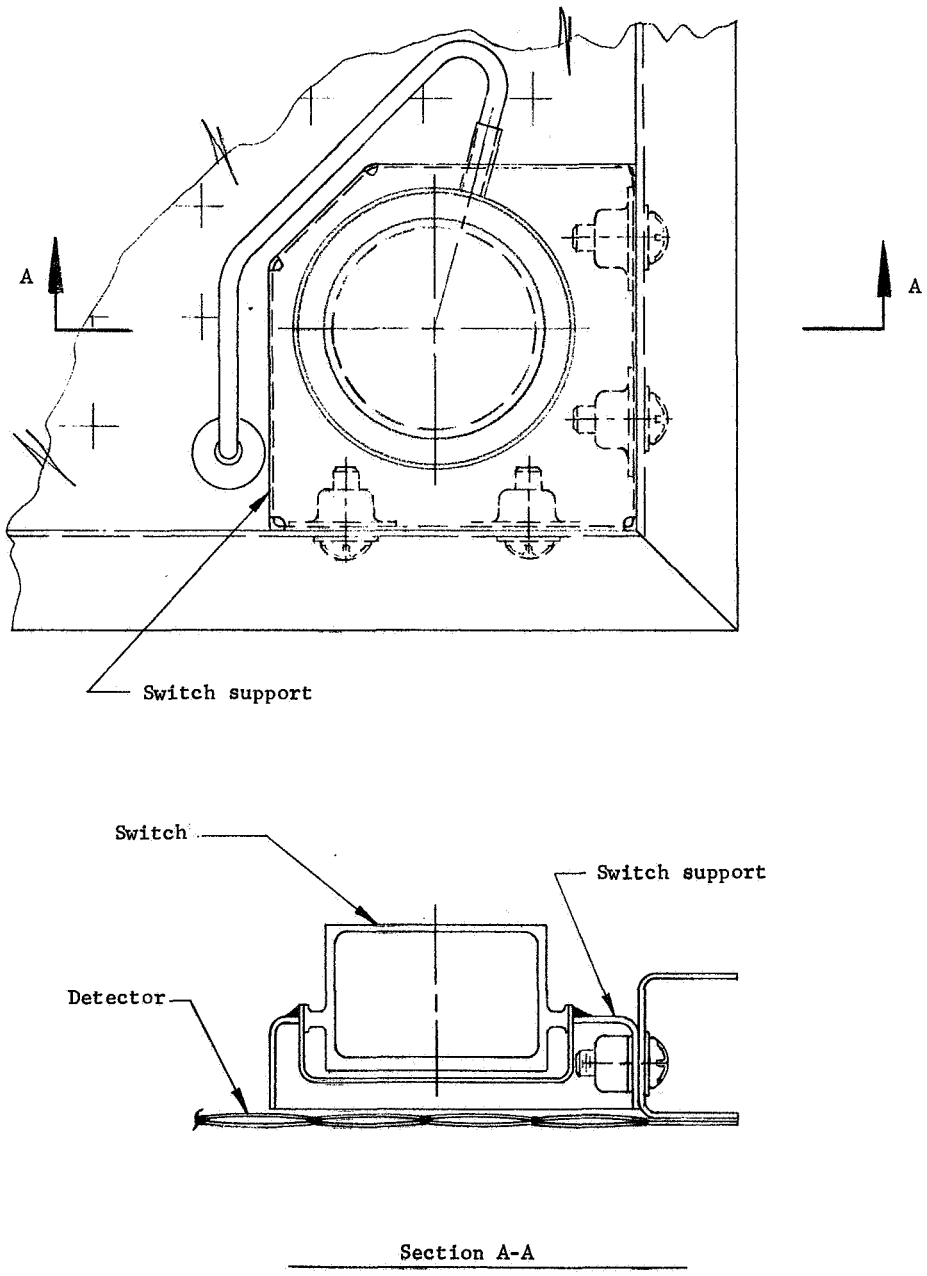


Figure 17.- Alternative Switch Support (Thin Gage Target)

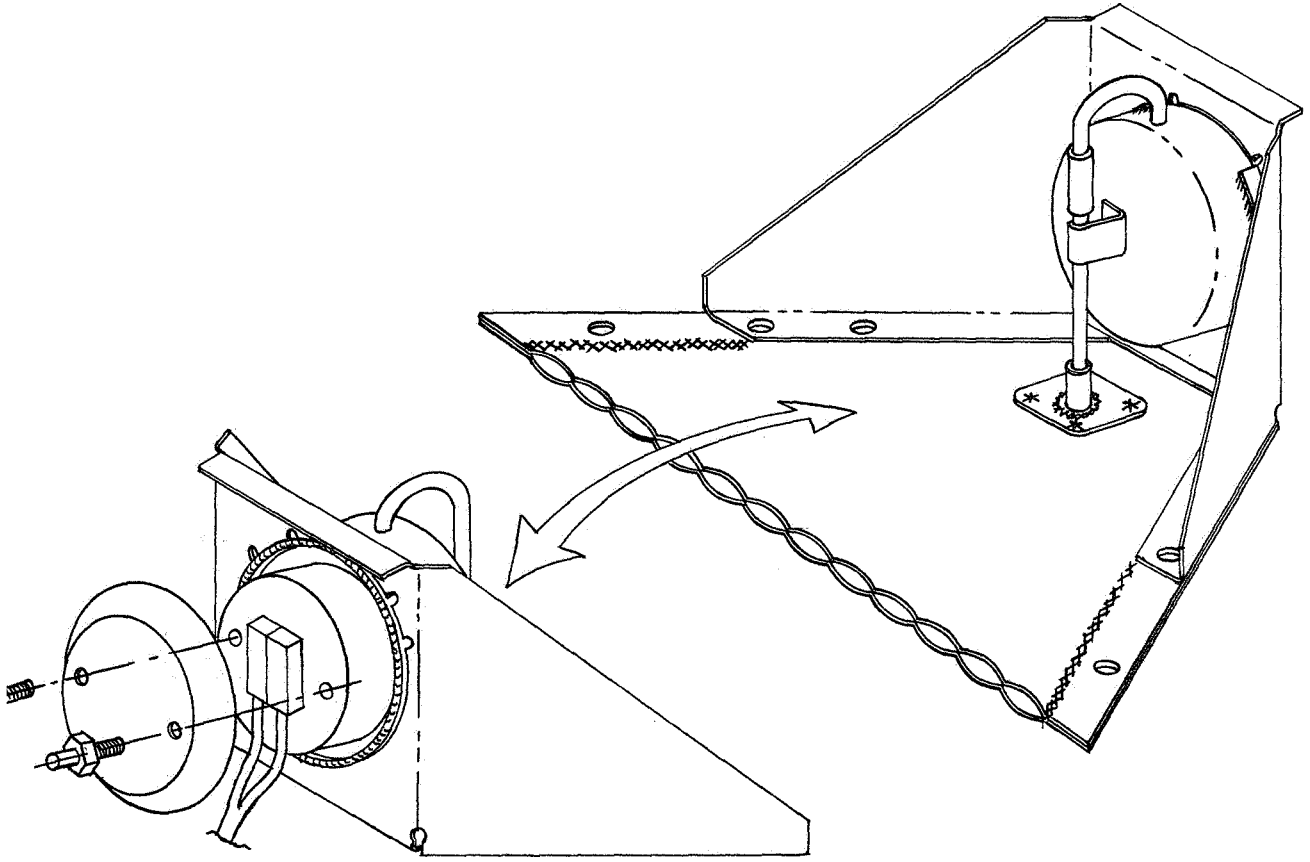

Figure 18.- Switch Installation for B and F Configurations

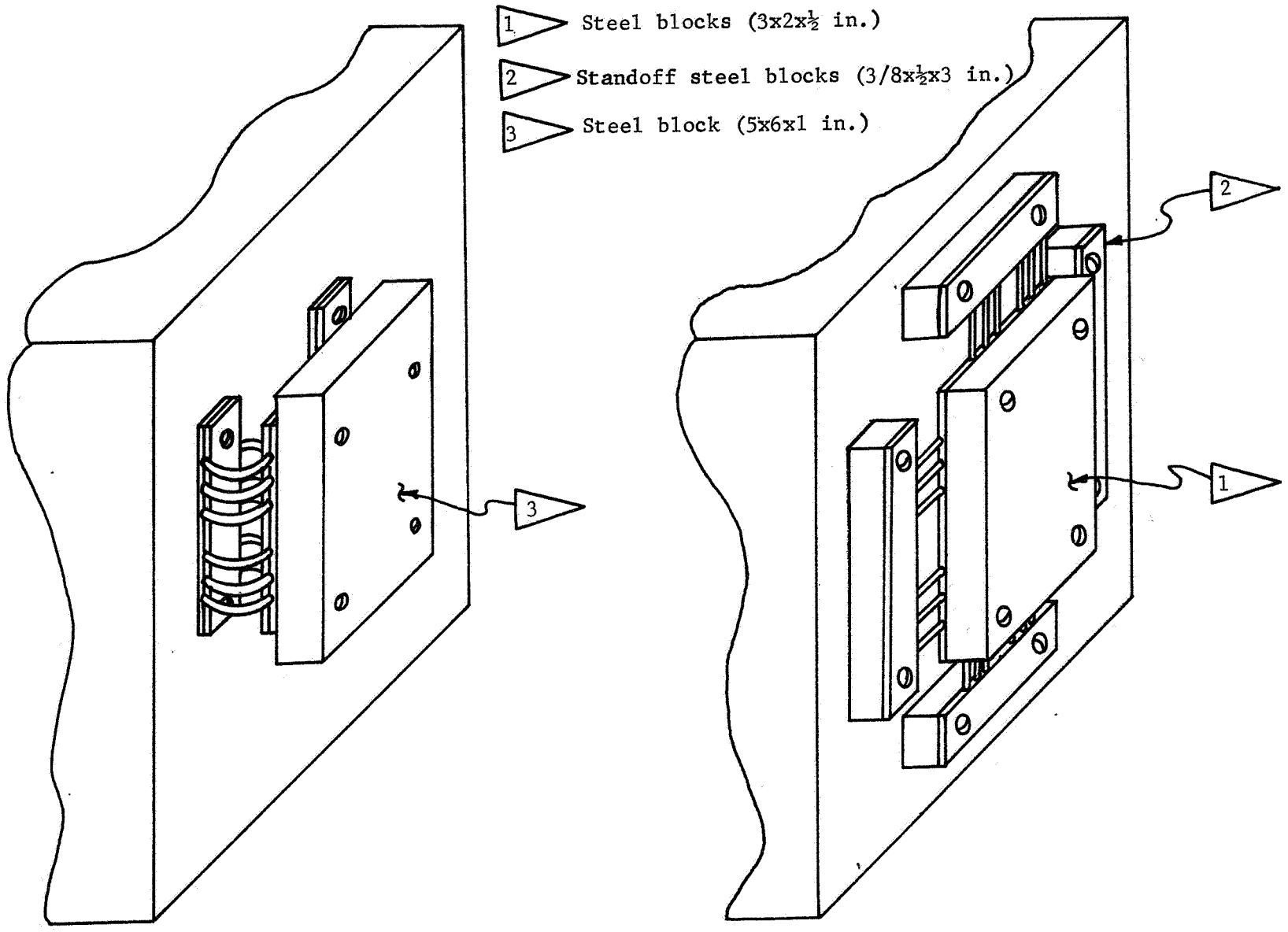


Figure 19.- Commercial Mounts Evaluation

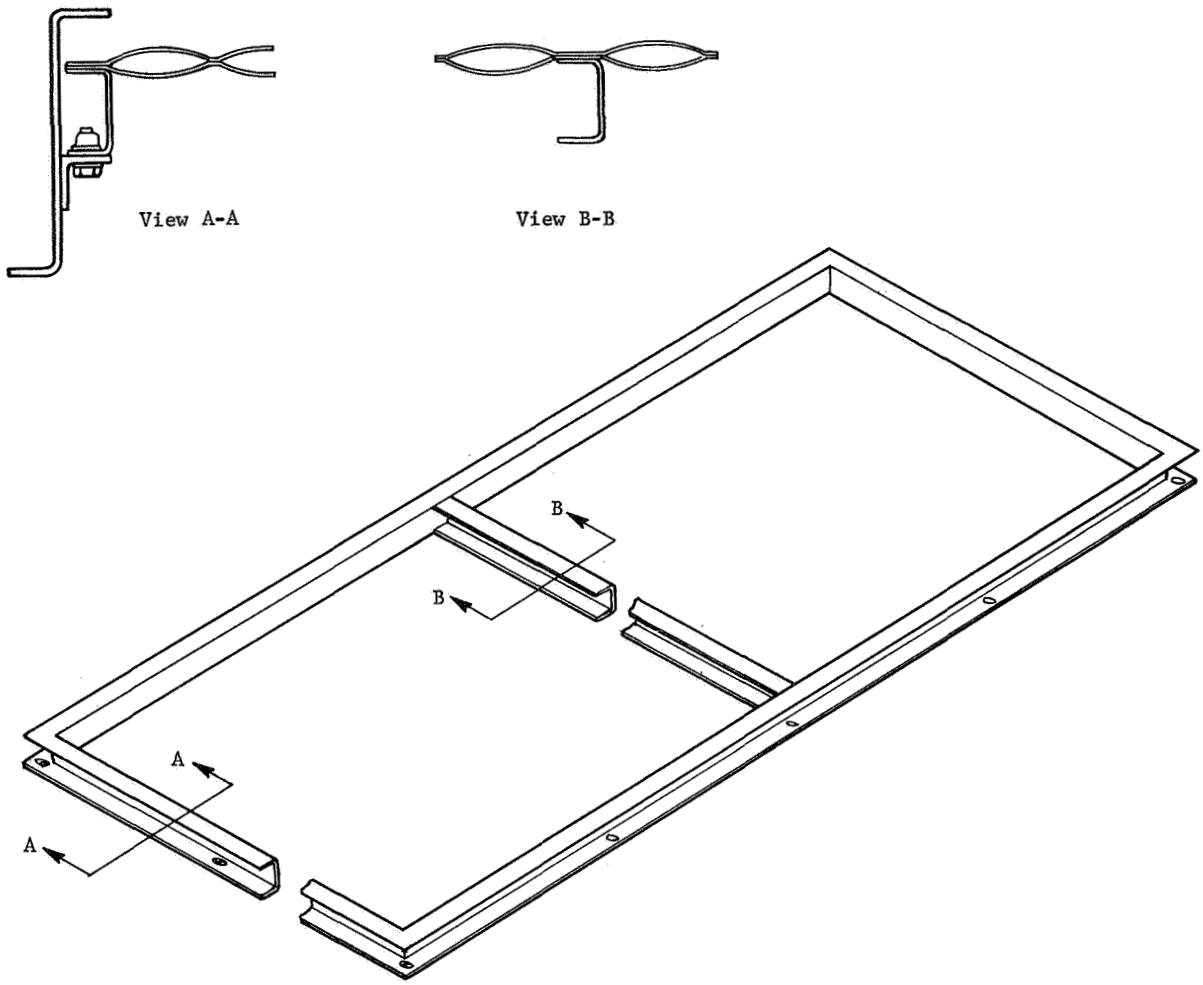


Figure 20.- MPDD Mounting Frame

reducing vibration loads experienced by the detector and enhance the detector's chances of surviving vibration testing. This mount, if successful, would be lightened by adding holes in the web and chem-milling the outer flange to match the loads measured in the mount channel. This mounting concept was discussed with NASA during an early design review. NASA personnel felt that the presence of the channel could preclude valid load data obtained during vibration. It was also felt that this approach would not produce an optimized mounting concept, particularly since an evaluation of thermal expansion affects was not considered. It was suggested that other mounting concepts be evaluated.

A study was made to determine the relative thermal expansion of the detectors with respect to the spacecraft. The results of these studies indicated that for an aluminum spacecraft and stainless steel detectors the relative thermal expansion could be as large as shown:

| Detector edge length, in. | Relative expansion, in. |
|---|---|
| 49 | 0.101 |
| 40 | 0.082 |
| 12 | 0.025 |

Detector mount studies were then initiated to determine suitable designs to cope with the anticipated loads and thermal expansion. Approximately 12 mounting concepts were evaluated during the PDD phase of the program. These studies developed into three basic concepts with variations in each group. Figures 21 thru 23 show the basic concepts considered.

Figure 21 shows a concept using flexing spring fingers supporting the detector. The main view of this figure is a composite of one large detector (40x49 in.) with part of the view cut away to show four of the small (40x12 in.) detectors. (Four of the small detectors can be installed in a detector bay in place of one large detector.) Each centerline ray in the main view represents the location at the panel edge of a panel support mount spring. Sections A-A and C-C on the figure show the configuration of these support spring fingers. The fingers flex to permit thermal growth of the detector, but are otherwise stiff to carry detector loads. The disadvantage of this approach lies in the fact that each spring along an edge is different, and installation of detectors is relatively complex.

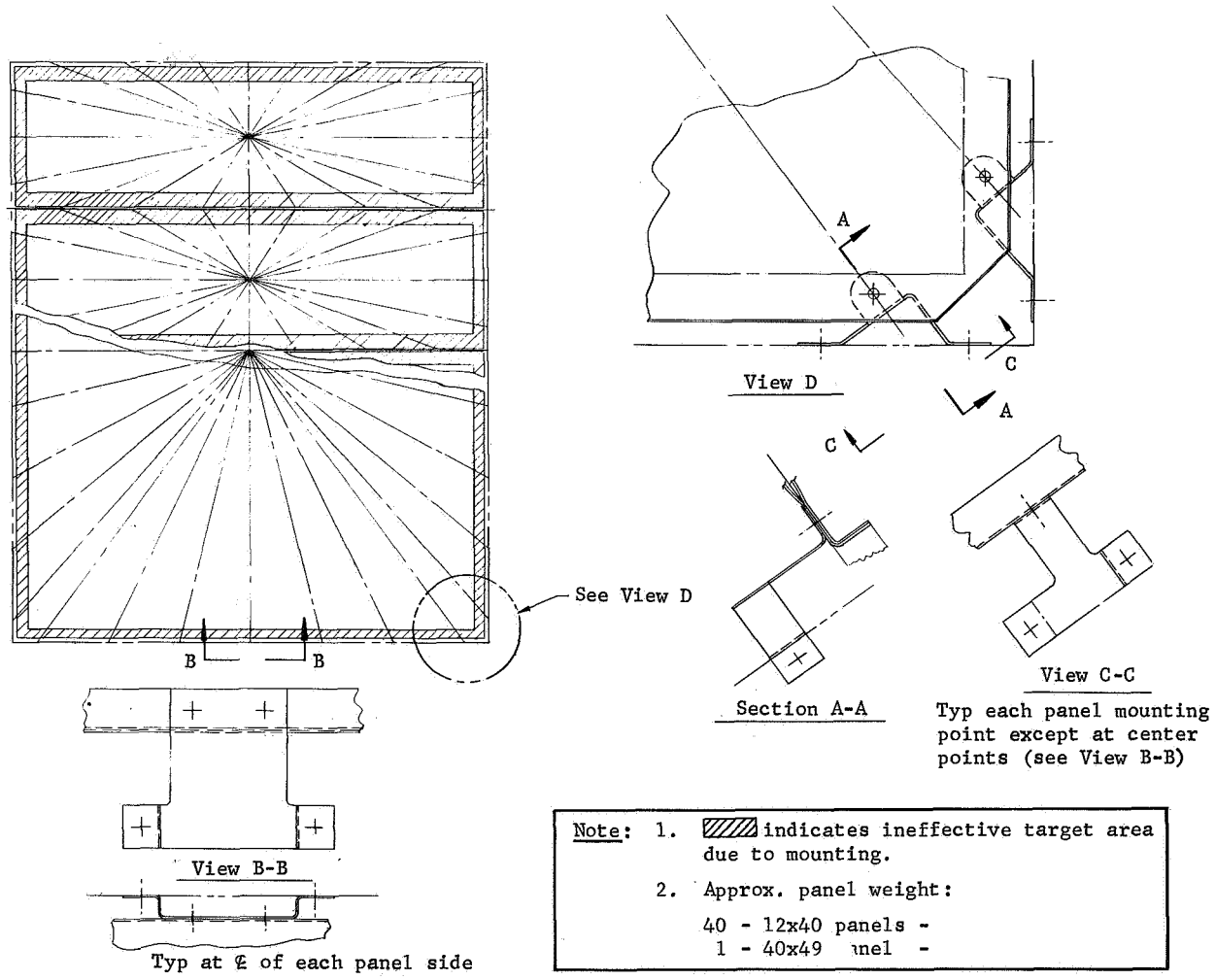


Note: 1. ▨ indicates ineffective target area due to mounting.

2. Approx. panel weight:

40 - 12x40 panels -
1 - 40x49 panel -

Figure 21.- Mounting Configuration No. 4

Figure 22 shows a mount concept using rotating links. The support links are seen in view B-B on the drawing. These links rotate to permit detector expansion along the edge and flex to permit expansion at right angles to the rotational axis. Out-of-plane detector loads are carried as axial loads in the links. In-plane loads are carried by four flex plates, one at the center of each detector edge. These flex plates are hard points for carrying in-plane detector loads in the plane of each flex plate. These plates, like the rotating links flex to provide for detector thermal growth. The disadvantage of this configuration lies in the numerous parts and difficulty in installation.

Figure 23 shows a mount concept using sliding components. This concept was eventually chosen as the one to be developed. The mount consists of bent angles (or extrusions) of aluminum that are bolted or riveted directly to the mounting-bay walls of the spacecraft, providing a flat shelf for the detector to rest on. The detector is attached to these angles by bolts as shown. All of the bolt holes in the detector and the mating holes in the mount angle are oversize except for those in the center of each edge. These holes, being oversize for the attachment bolts, provide for relative thermal expansion between the spacecraft and the detectors. Four "hard-point" bolts are provided at the center of each detector edge. These consist of flat-sided bolts riding in radial slots in the detector edge and fitting tightly in holes in the mount angles. They provide for thermal expansion of the detectors radially (in the direction of the slots), and by virtue of the snug fit of the slab sides of the bolt in the slot, react detector in-plane loads perpendicular to the slot. All bolts accept out-of-plane loads from the detector. Teflon tape on both sides of the detector and under the mount angle provides for low friction sliding during relative thermal expansion between the detector and the spacecraft.

All configurations were studied to select the proper mount. Weight tradeoff studies were performed along with complexity and cost studies. The configuration selected appeared to be the best compromise and was the simplest and lowest cost.

Design Development phase.- The Design Development (DD) phase of the MPDD program was designated for continuing development of the detector designs produced during the Preliminary Design and Development phase. During the earlier phase detector pressure cavity development work was completed, and designs were developed for pressure switches, pressure-switch mounts, and detector mounts. Completion of the entire detector system involving mating of the pressure switch and its mount to the detector, the detector to its spacecraft mount, and the "F" detector bumper sheets to the

**Weights**

| | | |
|---|---|---|
| Springs | = | 1.47 |
| Bolts | = | 1.01 |
| Washers | = | .48 |
| Nuts | = | .28 |
| Rivets | = | .01 |
| Pins | = | .83 |
| Plates | = | .08 |
| Added flange | = | 3.37 |
| | | 7.53 lb |

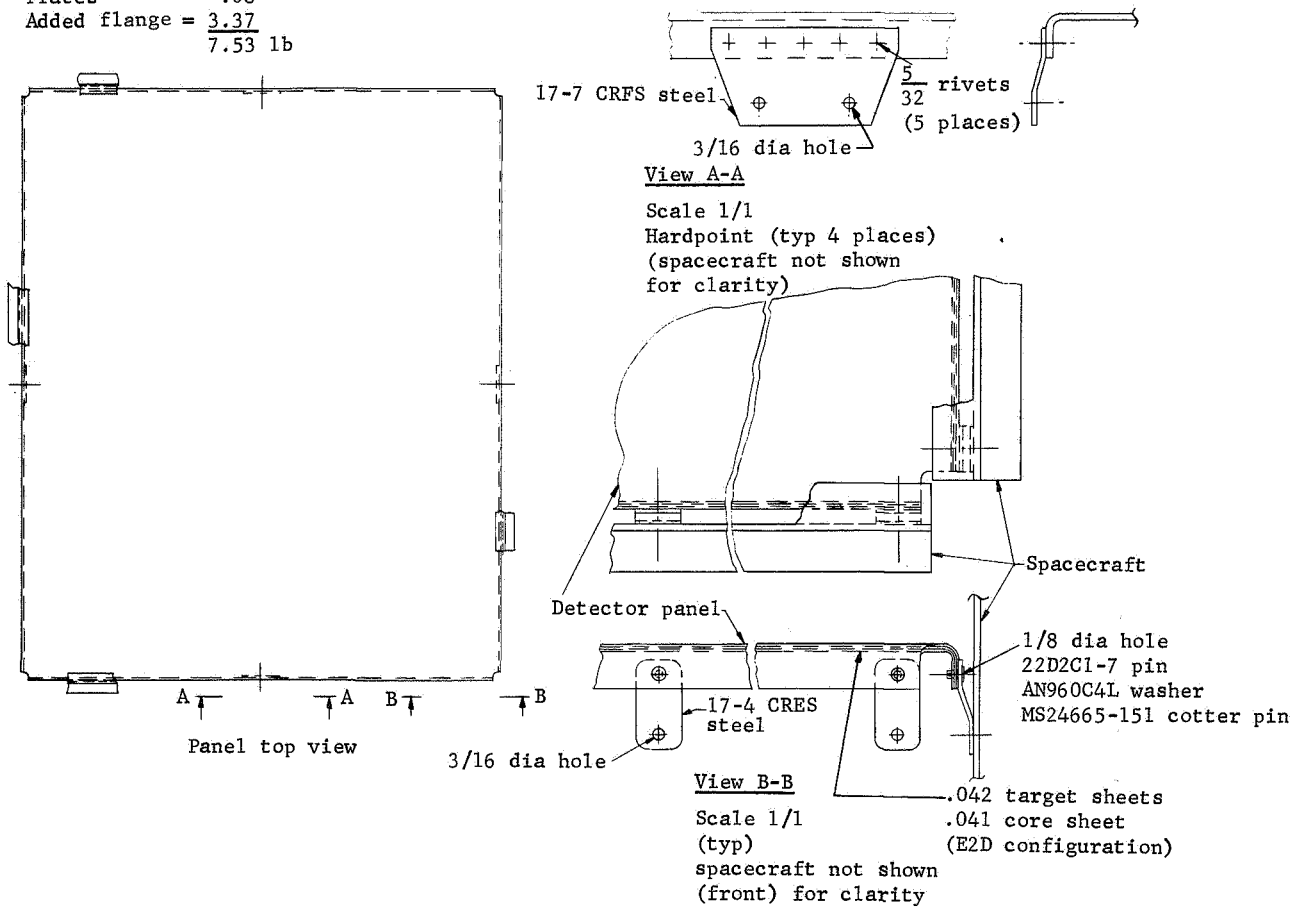


Figure 22.- Mounting Configuration No. 5

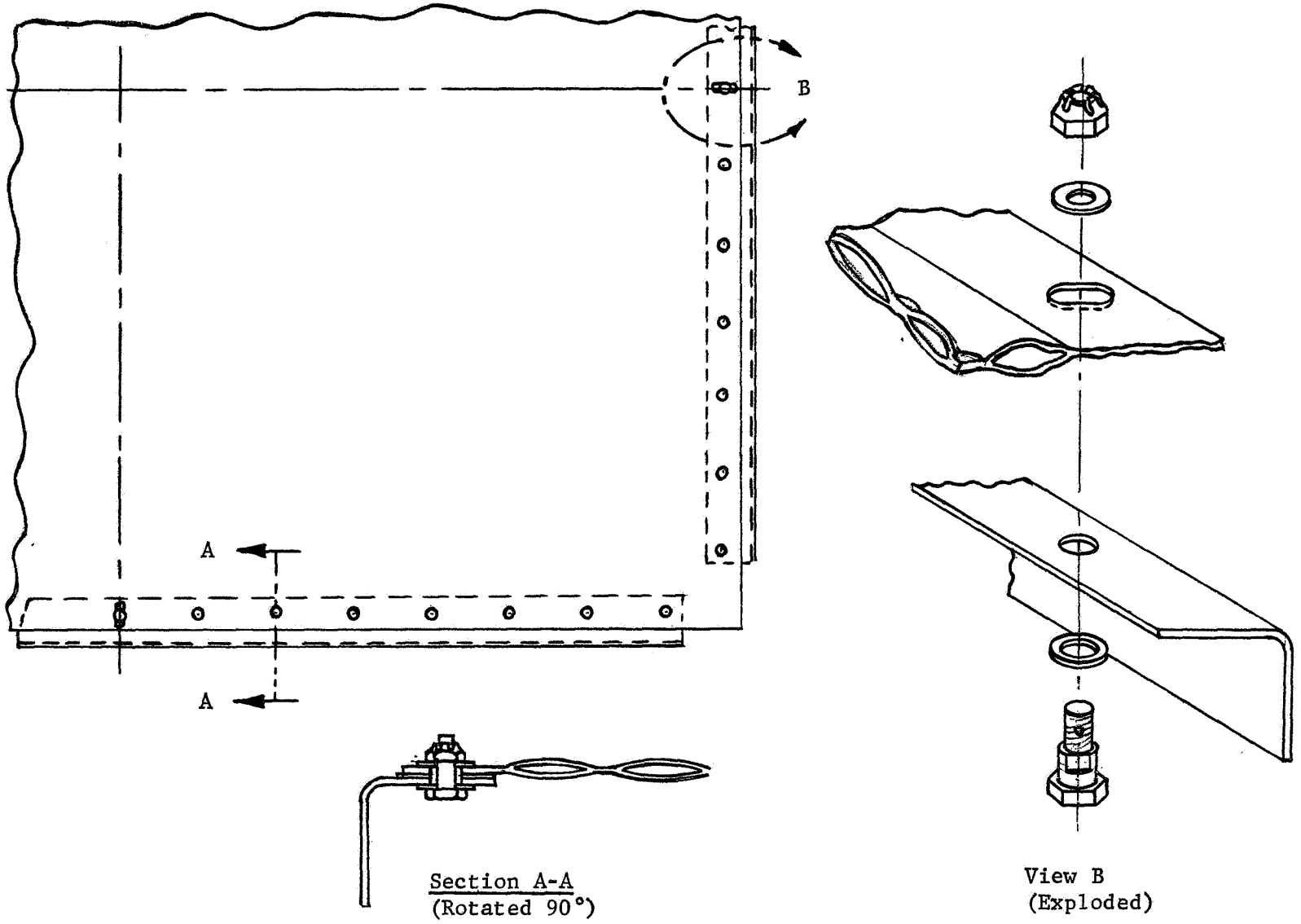


Figure 23.- Selected Mount

basic detector still was not accomplished. This engineering development work was accomplished in the DD phase. In addition, detector components were changed and improved during this phase. This work is described herein.

Detector bumper support: The detector bumper for the "F" configuration detector was required by specification to be a 1-mil-thick stainless steel sheet, and be adjustable from 0.25 to 1.50 in. away from the detector. Studies were initiated during the PDD phase and completed during the DD phase on supporting the bumper sheet on the detector. It was concluded that the best way to support it was to hold it in tension in the desired position, provided that the bumper would not hit the detector during vibration tests. It did not appear practical to make the bumper rigid and self supporting by adding flanges. The chosen concept proved successful and the design remained relatively unchanged through the program. The bumper sheet design shown in figure 24, consists of a sheet of 0.001-in.-thick 21-6-9 stainless steel sheet reinforced by 0.008-in.-thick doublers at the corners. The doublers provide for introduction of the supporting spring loads and distributing of these loads into the thin bumper sheet. The bumper sheet corners are trimmed back to provide clearance for the supporting springs and brackets.

Figure 25 shows the installation of the bumper sheets on the detector. The detector is supported on four corners by brackets, two of which are the pressure switch brackets. These brackets extend above and below the detector to mount a bumper sheet on each side, and have holes to provide incremental adjustment of the bumper location. Coil springs acting on clevis pins through these adjustment holes provide the necessary tension to position and support the bumper sheets.

This configuration was vibration tested to see if the bumper sheets would be damaged or present undesirable characteristics. For these tests the bumper sheets were positioned in the closest position to the detector target sheet. No damage was incurred in the test, nor were any problems evident. The design successfully met the test requirements.

Pressure switch mount development: The pressure switch mounting concepts developed during the PDD phase proved to be satisfactory. However, improvement changes were made in these configurations as the MPDD detector designs were further developed during the DD phase. These changes are described below for the heavy and light gage detectors.

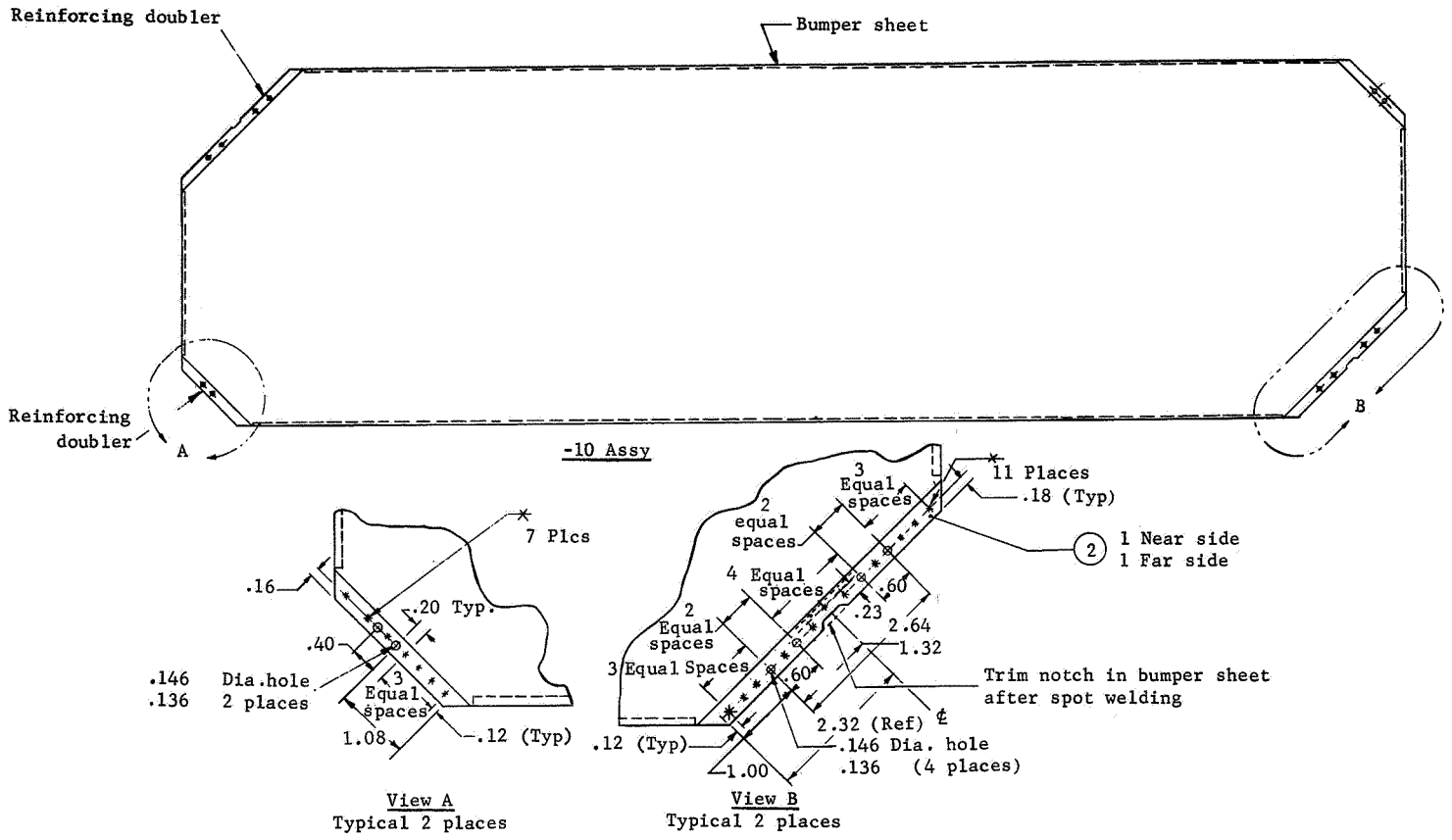


Figure 24.- Bumper Sheet Assembly

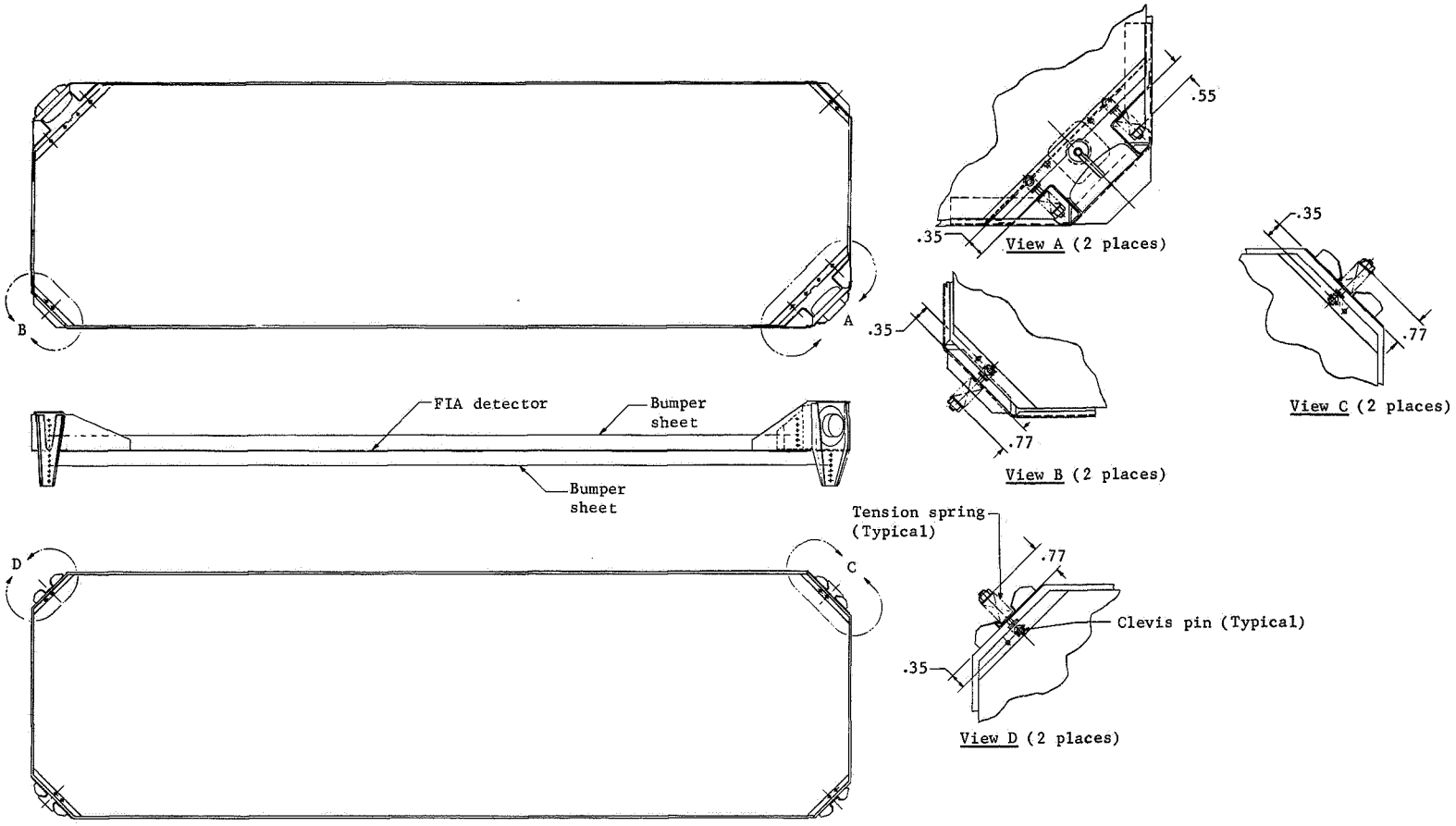


Figure 25.- Bumper Installation FIA

For the heavy gage detector switch mount the basic concept of mounting the pressure switch in a formed cup "volcano" in the detector target sheet proved completely satisfactory. No problems were encountered with switches mounted in this manner. The welded joint was leaktight and troublefree. The fill tube arrangement for pressurizing the detector, however, was changed to eliminate potential problems. The pressure fill tube was hand brazed in the base of the volcano. This posed a potential problem of changing the local surface finish characteristics of the target sheet. This area was spot welded subsequently to join the two target sheets; and differences in surface finish could produce welding problems. A second reason for changing the design was to eliminate the use of tack-soldering of the end of the tube after wrapping the tube around the volcano. Corrosive fluxes used with solder proved to be a potential problem.

As a result of design improvement studies the fill tube was moved away from the volcano and located remote from the switch installation. A special ring-weld technique was developed to attach a fill tube adapter to the detector target sheet as shown in figure 26. This fitting provided a durable attachment for the pressure fill tube. A fill tube protector cap protected the fill tube from meteoroid puncture. This cap was installed after final pressure fill and sealing of the detector.

In removing the fill tube from the volcano, the fill tube protector was also removed (see fig. 14). This left the upper portion of the volcano unprotected from meteoroid puncture. The formed material of the volcano was thinner than the rest of the target sheet. A volcano protector strap was welded around the volcano to protect it from puncture by meteoroids. This strap is shown in figure 27 along with the hollow bolt fitting attaching the switch terminal shield to the pressure switch. This fitting is used to check the internal pressure of the detector by applying a back pressure to the switch vent port. This drives the switch diaphragm against the internal pressure of the detector to trip the switch.

For the light-gage-detector, early studies of supporting the bumper sheet on the "F" detector resulted in providing a bumper-sheet support bracket below and above the detector. The upper bumper sheet support bracket for two corners of the detector was the pressure-switch support bracket. This configuration is shown in figure 28. During detector mount evaluation studies, it became apparent that the lower bracket interfered with detector mount. As a result the selected detector mount was shortened to clear this bracket. This was not a problem as it pertained to

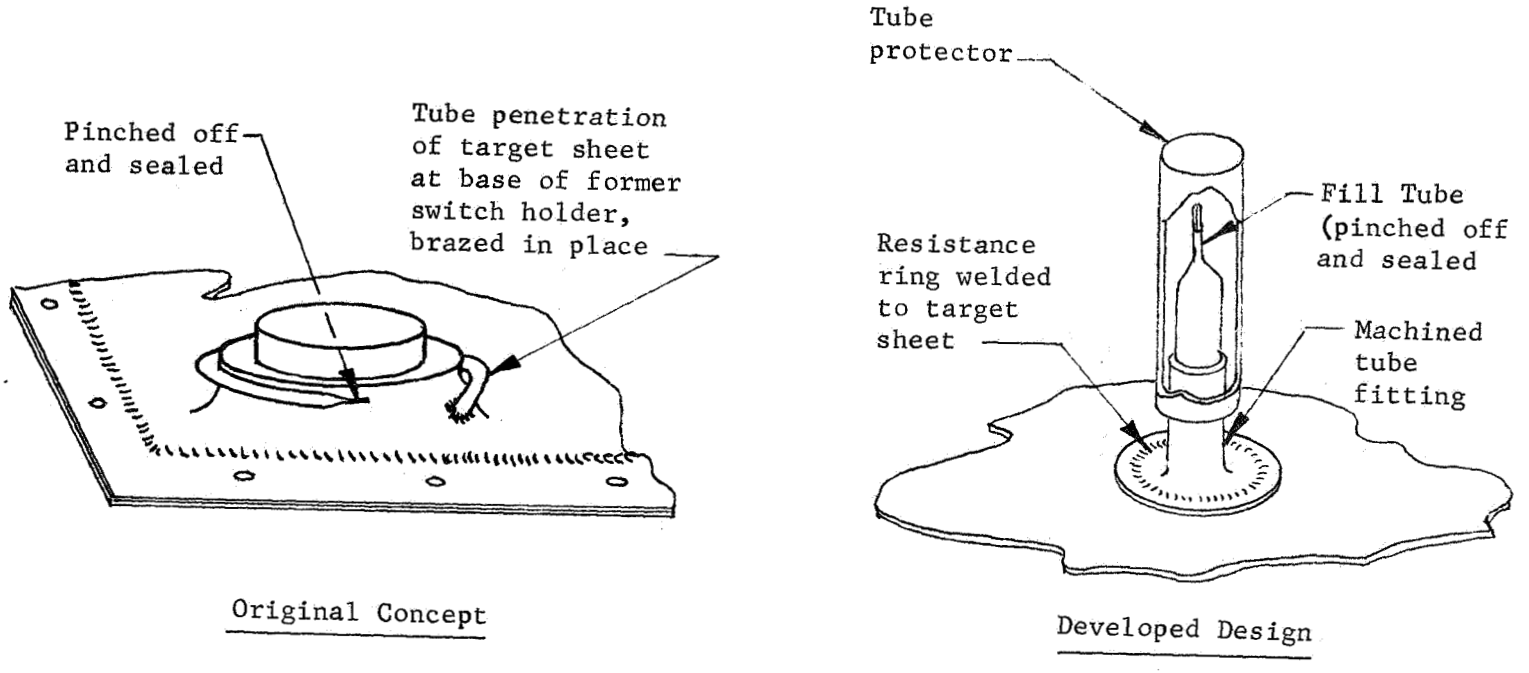


Figure 26.- Detector Fill Tube Installations

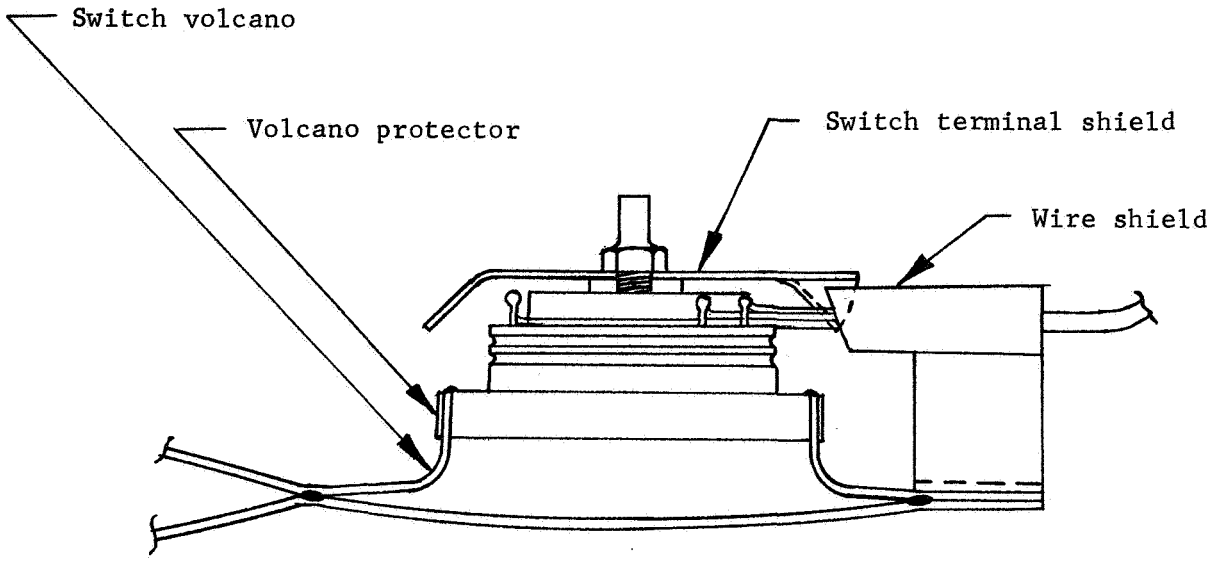


Figure 27.- Improved Switch Installation

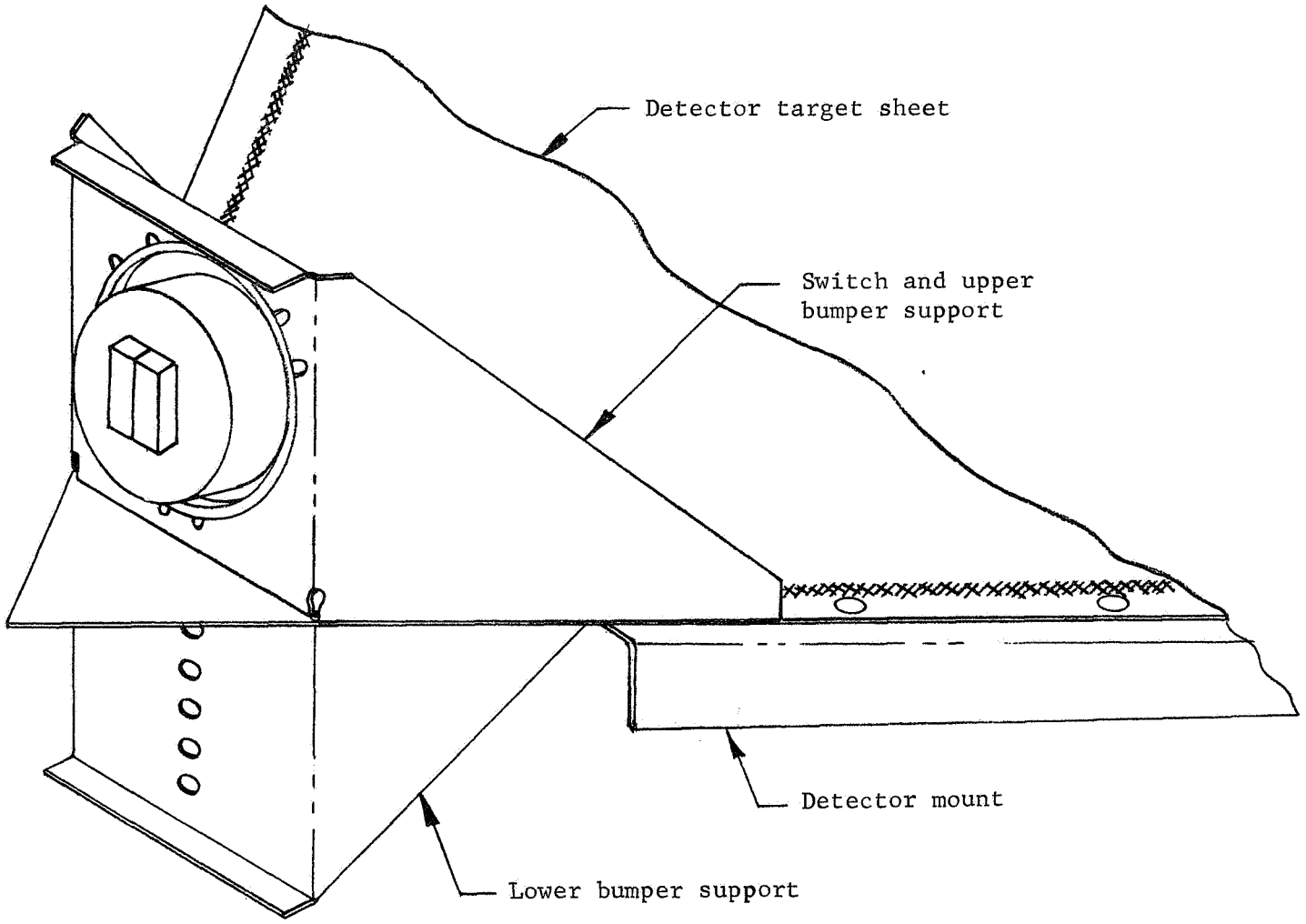


Figure 28.- F1A Original Bumper Support

the "F" configuration detector, but caused the "F" detector mount to be different than the other 40x12-in. detectors. To provide mount interchangeability between all of the small detectors the lower bracket was modified. The final design resulted in the pressure switch bracket being redesigned to support the lower bumper sheet as well as the top sheet. This was accomplished, as shown in figure 29, by adding a cantilevered extension to the switch bracket. The cantilevered extension eliminated the interference with the extended detector mount and permitted mount interchangeability with other detectors.

The switch mount for the "F" detector panel is also usable on the "B" detector panels. However, the "B" configuration does not require a bumper support bracket. The final design of the switch support bracket is shown in figure 30. The bracket is usable directly for the "B" and has predrilled holes for attaching the additional top and bottom bumper-sheet supporting bracketry with rivets. This final bracket design used a lighter gage of material than its predecessors, and had additional flanged reinforcement of bracket free edges.

Pressure switch changes: Pressure switch design was established during the PDD phase of the program and development was completed at the end of this phase. The need for several changes in the switch design was recognized and changes were initiated during the PDD phase. These changes, in general, did not occur until the DD phase. They are reported herein.

The maximum weight of the pressure switch was established by specification not to exceed 5.0 oz. Both vendors produced switch designs well within the specification weight value. The switches weighed approximately 3.5 oz. Both vendors' products, however, still appeared to be capable of weight reduction. Therefore, during this period with consultation inputs from the vendors the pressure switch Procurement Drawing PD7100075 was changed to decrease the maximum allowable weight of the switch from 5.0 oz to 2.7 oz. Both switch vendors modified their designs to incorporate this change. Lightweight hardware was fabricated and delivered to Martin Marietta. The Carleton switch weighed 2.56 oz and the Servonic switch weighed 2.50 oz. Both weights include the required wire pigtails.

Other changes included the addition of particle filters on both the pressure and vent ports of the switches to prevent contaminating particles from entering the switch, and modification of wire routing clips on the switch assemblies.

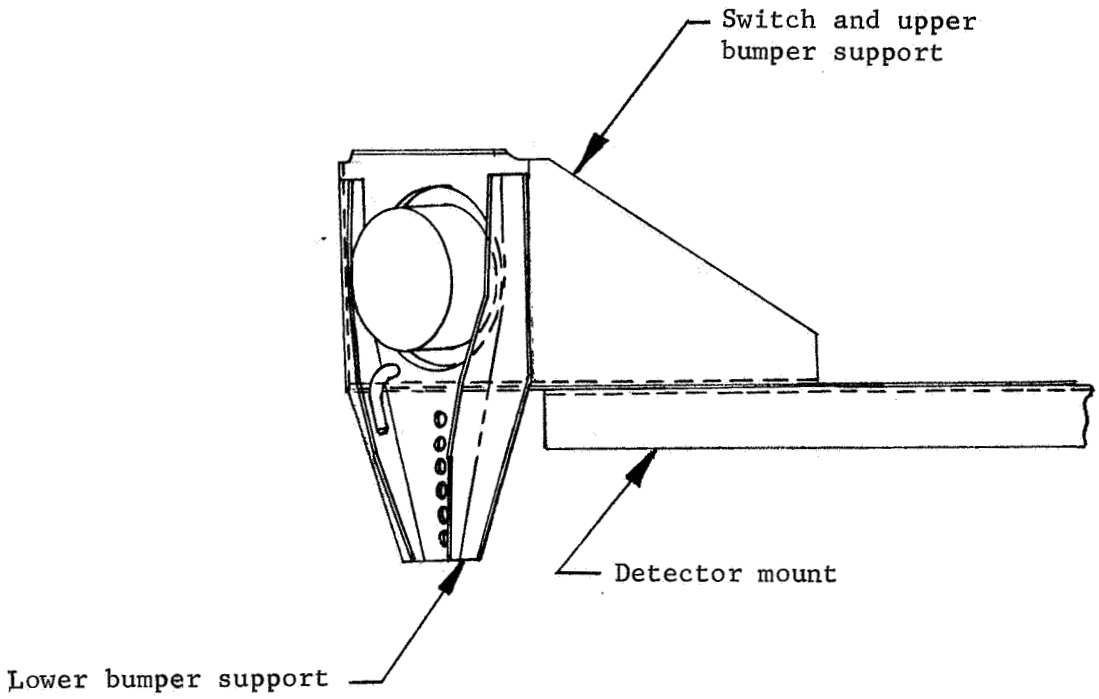


Figure 29.- F1A Modified Bumper Support

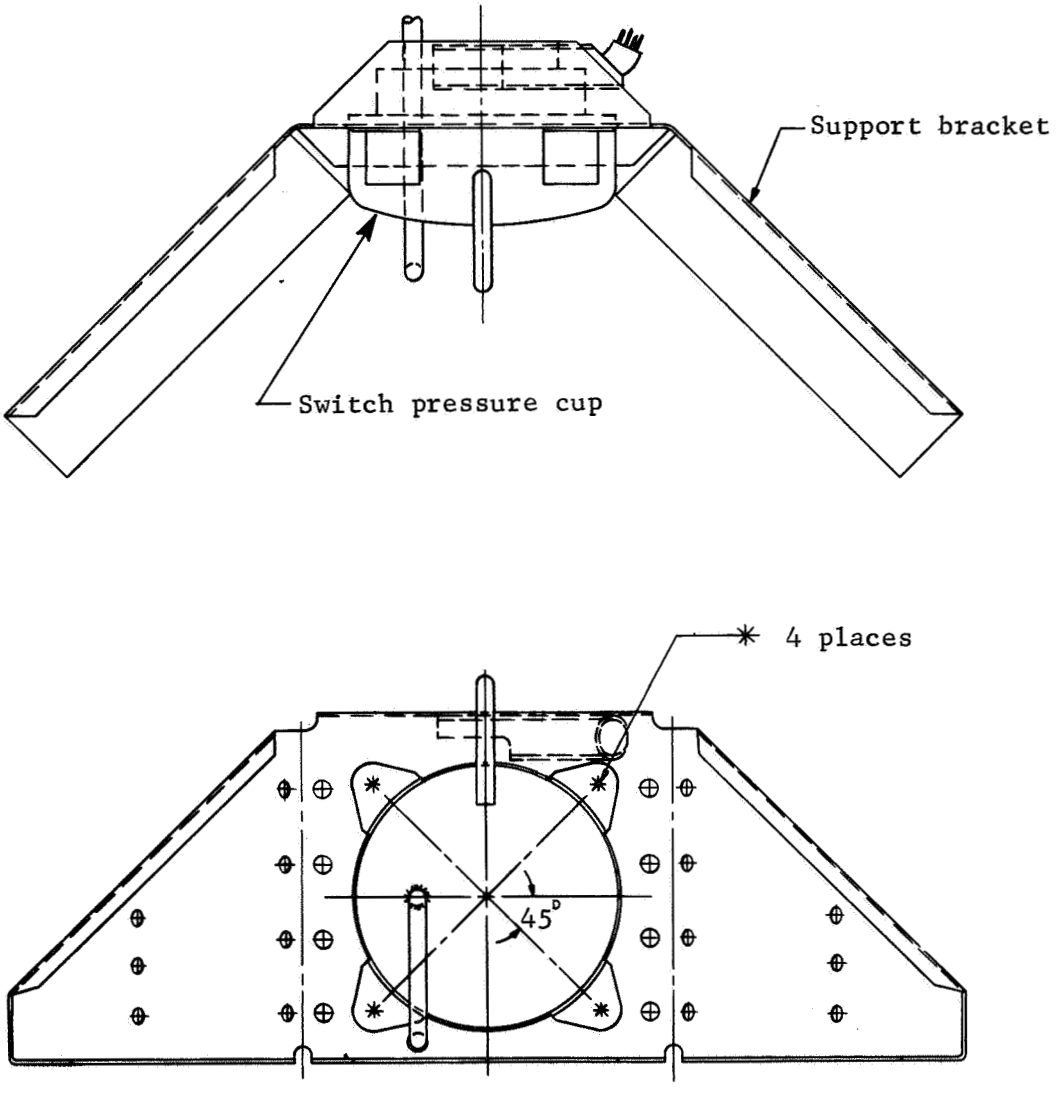


Figure 30.- Switch Support Assembly

One of the switches received for engineering evaluation tests was vibrated at 100 g through the frequency range of 20 to 2000 cps to determine whether the switch would stand higher vibration levels than are defined in the switch procurement specification. The reason for performing this test is that the exact level of vibration that the switch will see in service as mounted in detectors might not be known before switch development testing will be completed. Some confidence was desired that the switches would stand a higher vibration level. The specimen tested passed this test with no contact chatter or bounce and without leaking. After the switch designs were lightened, they were retested. One each of the Carleton and Servonic switches were subjected to three-axis sinusoidal vibration tests at an input level of 100 g (from 70 Hz to 2000 Hz) to determine the switch survivability at high vibration levels. Both of the switches survived these tests and exhibited the same switch points after the test as before. However, some contact chatter occurred during the test. The Servonic switch displayed a greater tendency to chatter than did the Carleton switch. The switches were dissected after the test to determine if any physical damage could be detected. No damage was noted. Both vendors made switch modifications to alleviate the contact chatter problem. These modifications helped, but did not eliminate chatter. Subsequently, during Flight Assurance Testing of the Carleton and Servonic switches, sinusoidal vibration, random vibration, and shock tests were performed. Both switches experienced contact chatter during the 66 g sinusoidal tests and the 30 grms random vibration tests. Contact transfer tests were within specification limits after these tests.

Since no damage was incurred by switch contact chatter during any of the tests, and contact chatter did not appear to be a problem during boost phase of actual flight, the specification for the switch was changed. Contact chatter was permitted in test provided the switch showed no change in functional or electrical characteristics after chattering.

The configuration of the final switches by Servonics and Carleton are shown in figures 31 and 32.

Detector mount development: The angle-mount design concept selected during the PDD phase was maintained through the remainder of the program with only minor changes. During the DD phase of the program the loads in the mount were determined. Analytical evaluation of loads proved quite difficult. The NASA specified vibratory and acoustic test requirements cover a frequency range that excites the detector in many resonant vibration modes. Several of these modes, in turn, have a different level of input

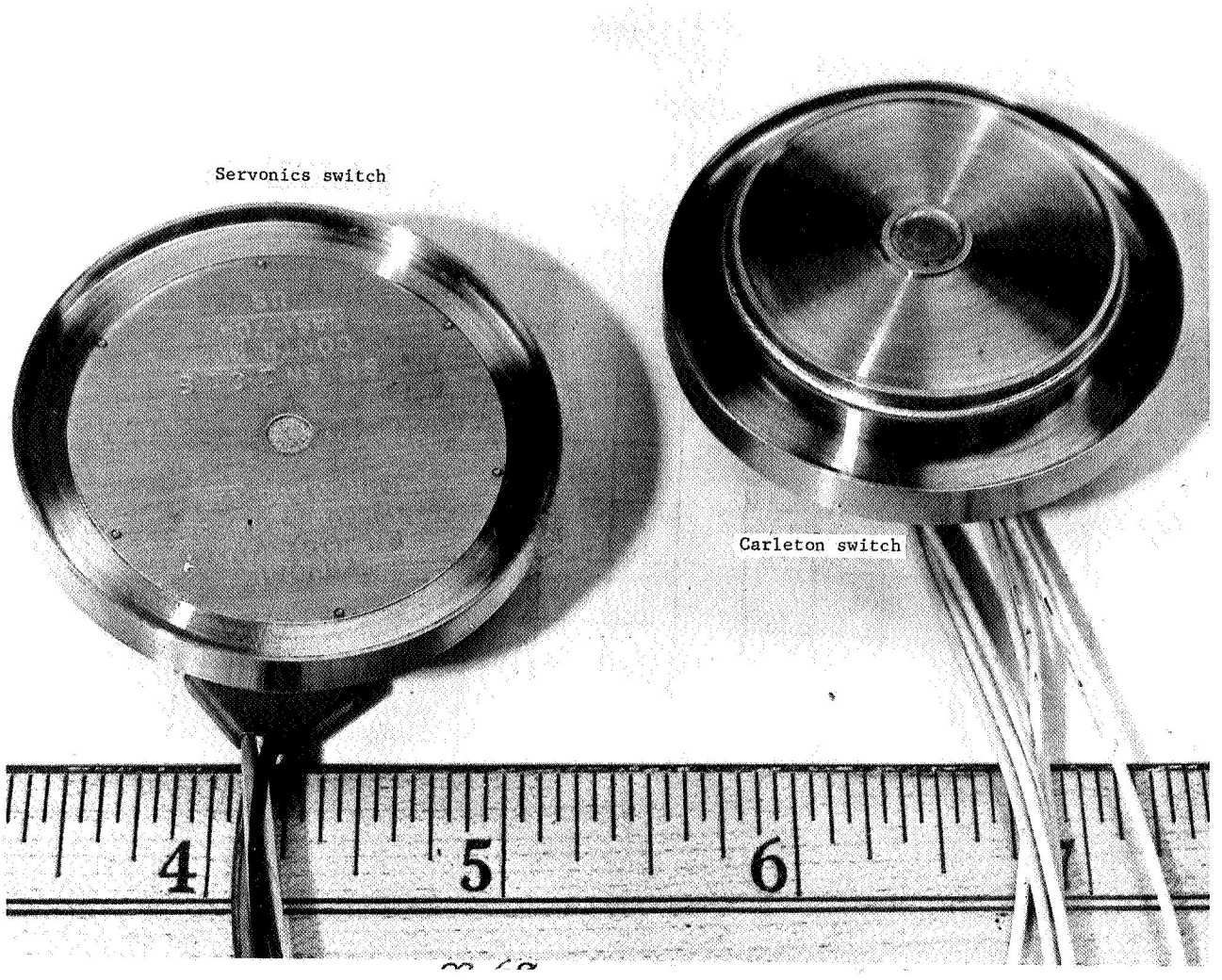


Figure 31.- Pressure Switch (Pressure Side)

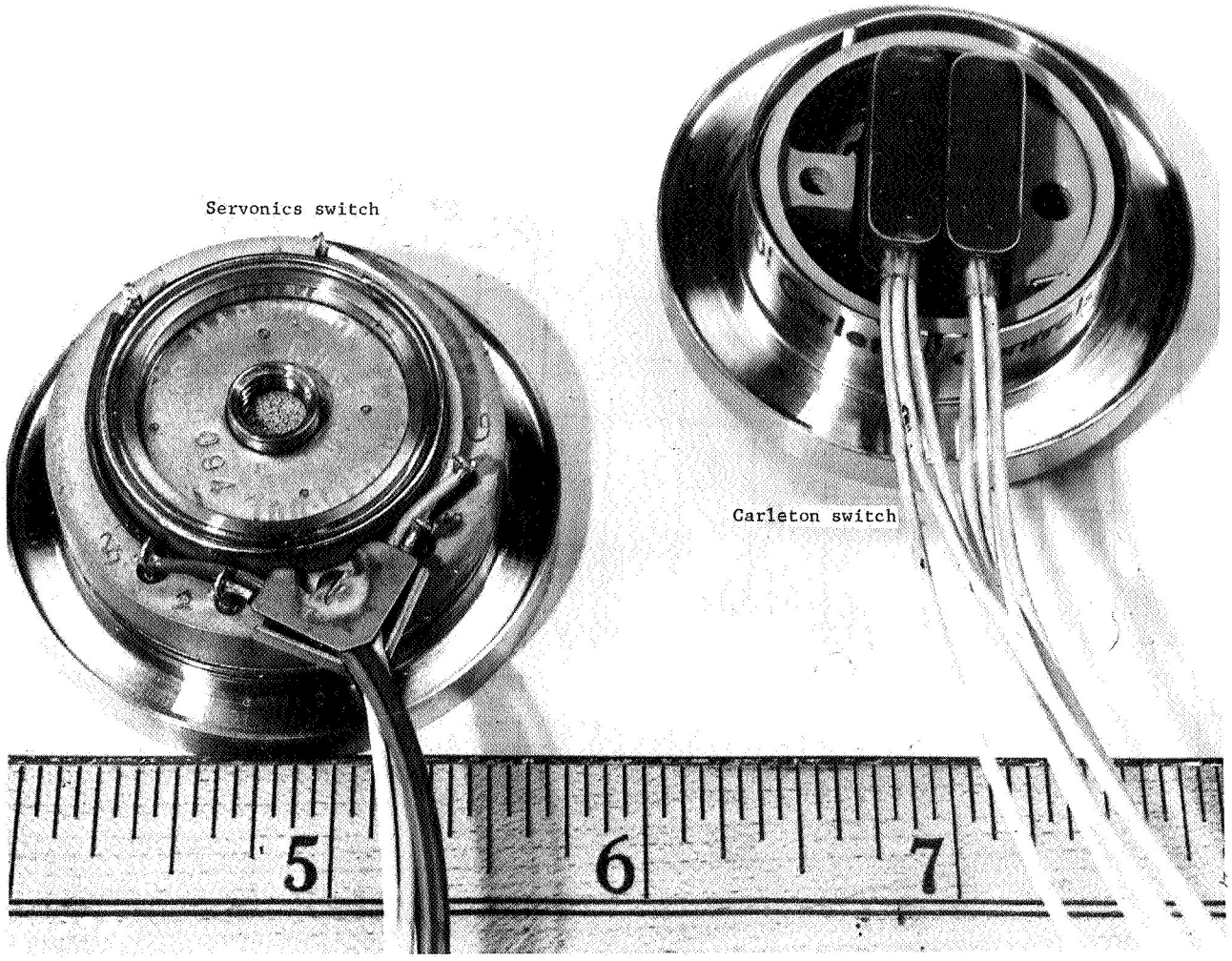


Figure 32.- Pressure Switch (Back Side)

excitation to the detector. These problems plus the fact that, for simplifying the analysis, the detector must be treated as a homogenous structure (which it is not), eventually lead to the abandonment of analytical evaluation of loads. Loads evaluation was then directed to empirical approaches. Mounting angles were instrumented with strain gages near each attachment bolt, and the gages calibrated by application of incremental loads. The test detector was then installed on the mount angles and subjected to the NASA specified sinusoidal and random vibration inputs. The sinusoidal vibration proved to be the most critical. The reduced data from these tests are shown in figure 33. A number of resonant modes are apparent in the figure. The loads in the mount do vary considerably from one mode to the next, as might be expected.

The loads evaluation test was performed on the F1A detector panel, in the 40x12-in. size category, and on the E1A detector, in the 40 x 49-in. size category. The loads data derived from these tests were ratioed mathematically to obtain loads for the remaining detectors. The loads data used for design of the mount angles are shown in figures 34, 35, and 36. These data were used to determine the mount-angle material gage and to determine the bolt spacing for attaching the detectors to the mounts.

The first approach to making the detector mount design final was to minimize the total weight of all detector systems as installed on the spacecraft. This required tradeoff studies varying the number of fasteners to determine the minimum combined weight of the mounts and the fasteners. The results of this study are shown in table 10 for the large 40x49-in. detectors. This design approach resulted in three different material gages of mount angles being used, and the three different bolt spacings. This approach was not conducive to providing interchangeability of detectors on the spacecraft.

The final design for mounts for MPDD detectors was directed toward minimum weight consistent with interchangeability. This was based on using one gage mount angle suitable for all detectors in a given size class (40x49 in. or 40x12 in.), but not providing interchangeability between detector size classes. Again tradeoff studies were performed to evaluate hole spacing required for different detectors to determine what common bolt spacing could be used. For this analysis, 0.050-in. mount angles were used for the large detectors and 0.025-in. mount angles were used for the small detectors; both were of 7075 T6 aluminum alloy. The results of this study are shown in table 11. The chosen bolt spacing for the large panels, for example, was 1.20 in. along the long (49 in.) side and 1.06 in. along the short (40 in.) side. The mount angles

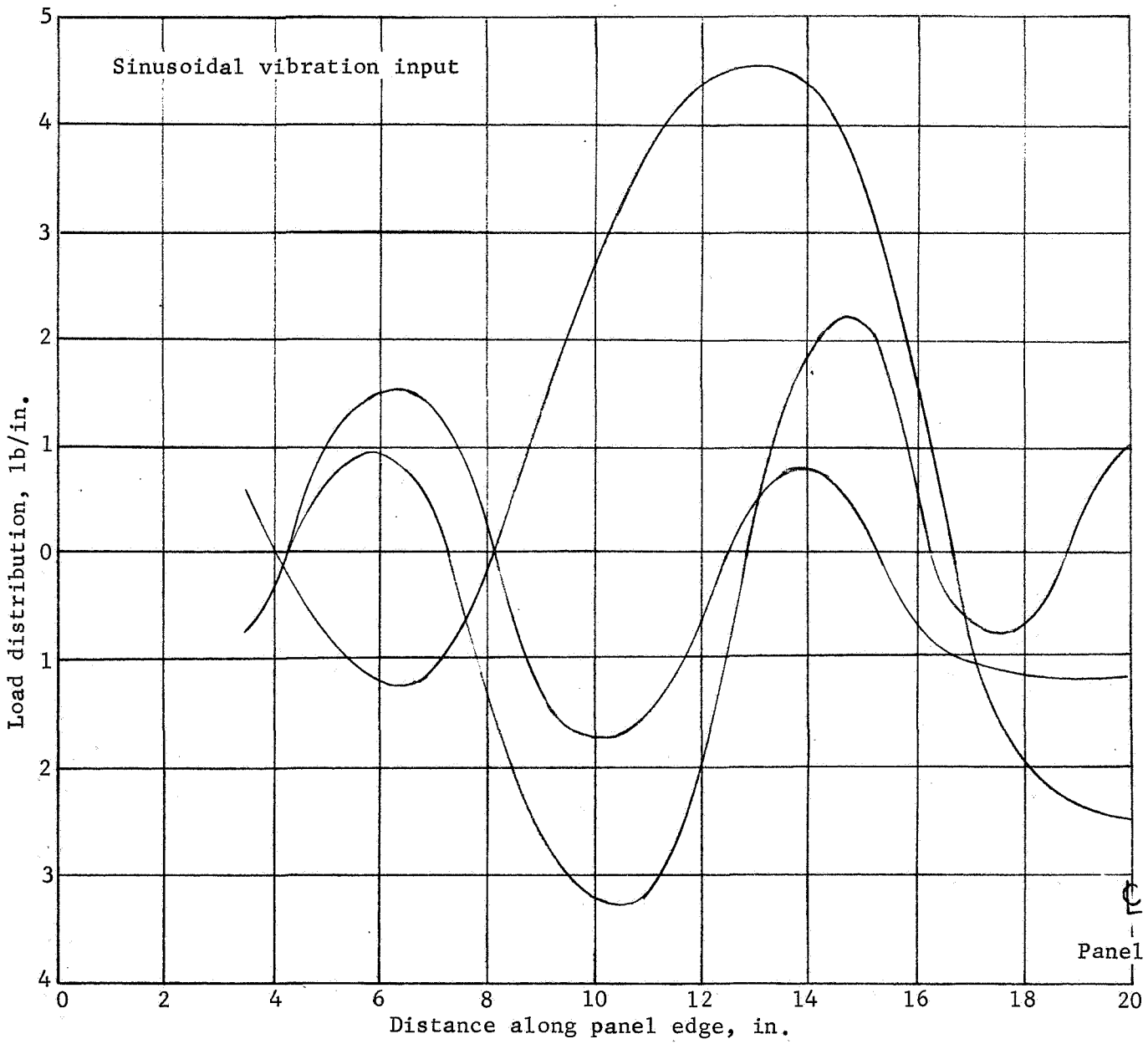


Figure 33.- Configuration FIA Load Distribution

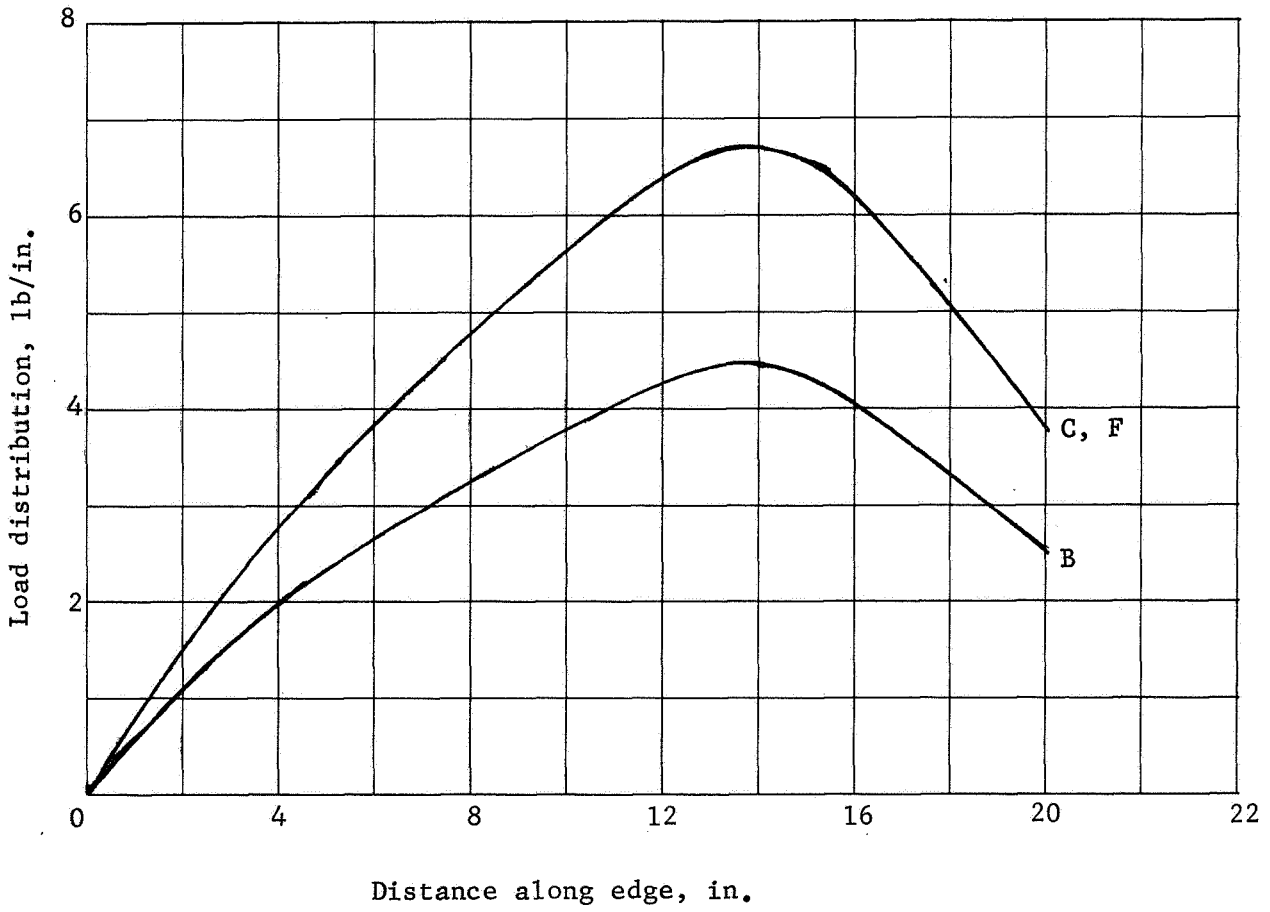


Figure 34.- Design Loads for 40 x 12 in. Panels

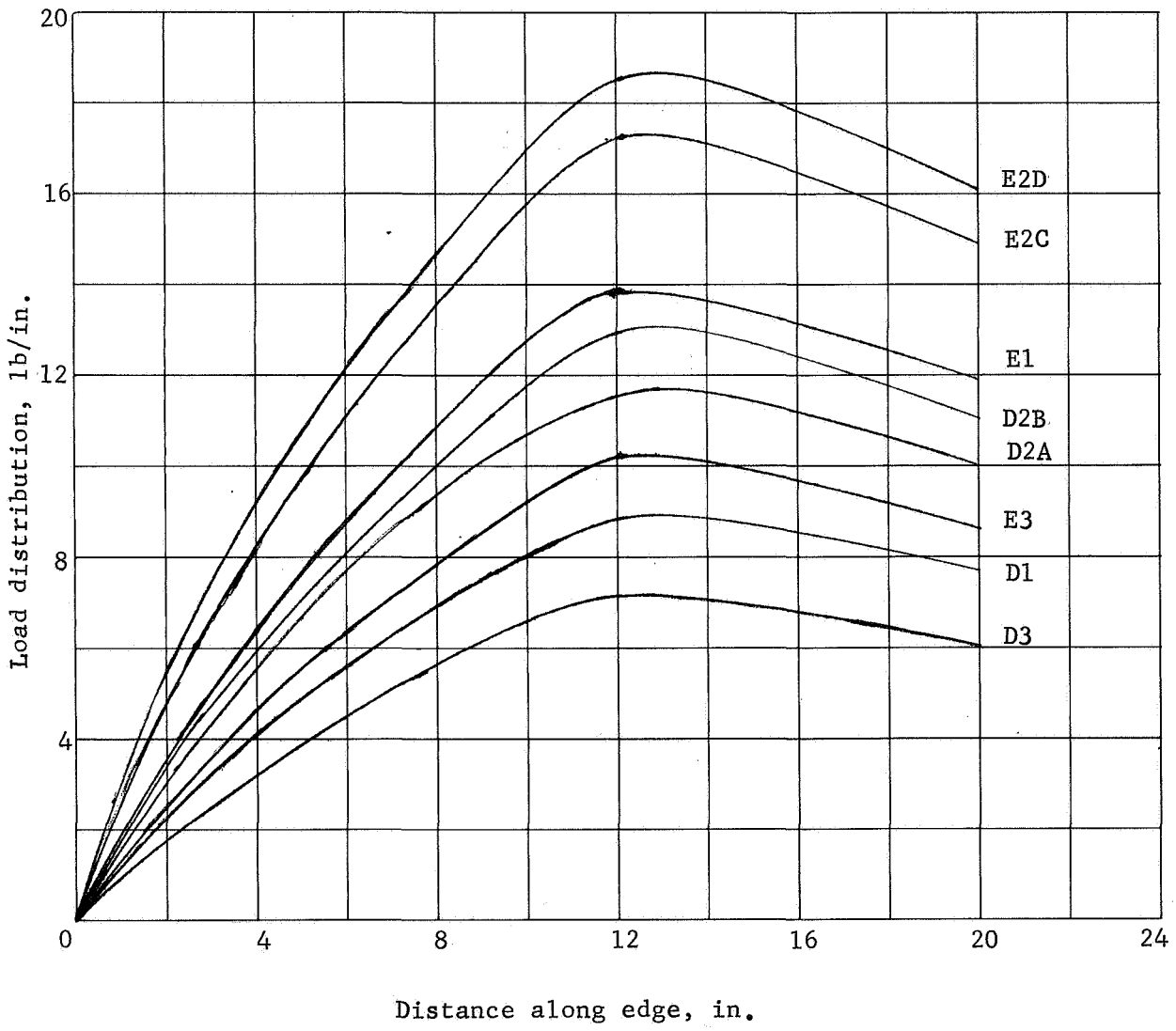


Figure 35.- Design Loads for 40 x 49 in. Panels (49-in. Side)

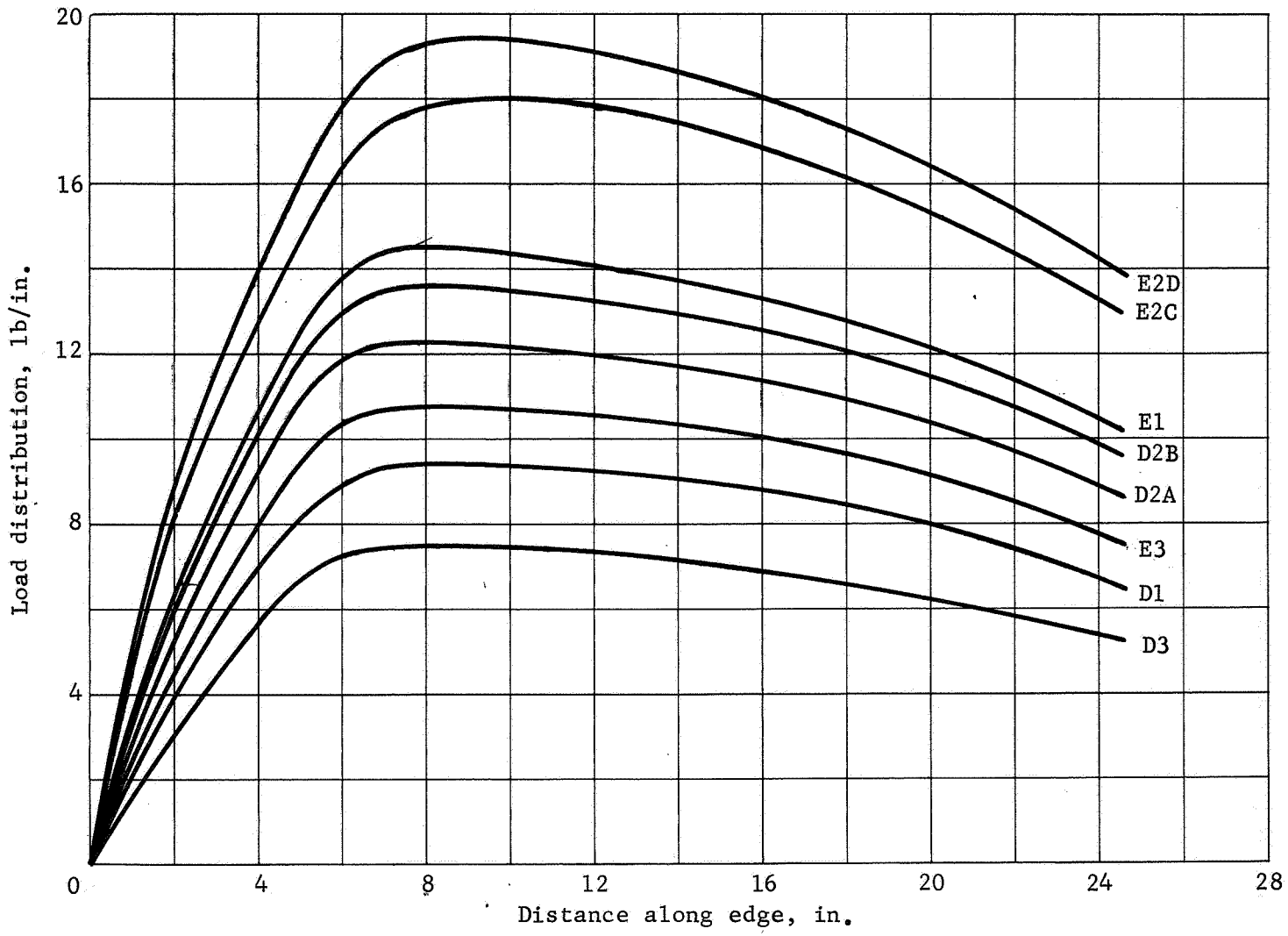


Figure 36.- Design Loads for 40 x 49 in. Panels (40-in. Side)

TABLE 10.- PDD PHASE DETECTOR MOUNT DESIGN (40x49-in. PANELS)

| Panel | Design load, lb/in. | Angle thickness, in. | | Bolt spacing, in. | |
|---|---|---|---|---|---|
| | | Minimum required | Used | Maximum | Used |
| E2C | 18.0 | 0.0425 | 0.050 | 2.78 | 2.75<br>2.57 |
| E1A | 14.6 | 0.038 | 0.040 | 2.19 | 2.00<br>2.00 |
| D2A | 12.3 | 0.035 | 0.040 | 2.60 | 2.44<br>2.57 |
| E3A | 10.8 | 0.033 | 0.040 | 2.96 | 2.75<br>2.57 |
| D1A | 9.5 | 0.031 | 0.032 | 2.14 | 2.00<br>2.00 |
| D3A | 7.5 | 0.0275 | 0.032 | 2.70 | 2.44<br>2.57 |

TABLE 11.- PRESENT DETECTOR MOUNT DESIGN (INTERCHANGEABLE)

| Panel | Design load, lb/in. | Angle thickness, in. | Maximum bolt spacing, in. | Spacing used |
|---|---|---|---|---|
| B1A | 4.5 | 0.025 | 2.00 | 1.95/1.61 |
| C1 | 6.7 | 0.025 | 2.46 | 1.95/1.61 |
| D1A | 9.5 | 0.050 | 3.66 | 3.60/3.18 |
| D2A | 12.3 | 0.050 | 4.05 | 3.60/3.18 |
| D3A | 7.5 | 0.050 | 3.96 | 3.60/3.18 |
| E1A | 14.6 | 0.050 | 3.42 | 2.40/2.12 |
| E2C | 18.0 | 0.050 | 2.78 | 2.40/2.12 |
| E3A | 10.8 | 0.050 | 3.83 | 3.60/3.18 |
| F1A | 4.5 | 0.025 | 2.00 | 1.95/1.61 |

all have this hole spacing. The detector, on the other hand, has bolt hole spacing compatible with loads in the particular detector configuration. These holes line up with every second or every third hole in the detector mount angle. Therefore, any detector can be used interchangeably with any other on the detector mount.

A secondary design item in selecting the final mount design was the design of the fastener attaching the detector to the mount. The loads in any given bolt are fairly low. Almost any fastener that could be put in the hole would carry the mount load (with the exception of the four hard-point bolts). The critical components from a loads consideration are the mount angles and the detector itself. Studies were performed to determine the best fastener to use, and a literature survey made of existing fastener components. The chosen fastener was an aluminum bolt with a self-locking stainless steel nut. An aluminum nut would also have sufficed, except that an aluminum nut with a self-locking feature binds and galls the aluminum bolt. Castellated nuts with cotter pins were not desirable. NASA specified a preference not to use any fastener smaller than 3/16-in. because smaller sized bolts are easily snapped off. Installation tests performed on the aluminum bolts with the stainless steel nuts showed an installation torque of 8.4 in./lb average to overcome locking friction and a twist-off torque of 61.6 in./lb average. Since the nuts are tightened very little past friction torque levels the ratio of friction to snap-off torque is satisfactory.

Detector design development: Detectors selected at the end of the DD phase are defined by drawings itemized in Appendix B.

Manufacturing and Test phase.- The design of MPDD detectors was well established at the beginning of the manufacturing and test (M&T) phase. There was a high confidence level in the ability of the detectors to successfully pass qualification testing. However, a few problems did occur during this phase that required corrective engineering action. These are discussed below.

Servonic switch deletion: The Servonic Instrument's pressure switch failed to pass qualification testing. Since the end of qualification testing of the pressure switches occurred early in the M&T phase, both pressure switch designs were carried forward into this phase. Up to this point in time engineering drawings had reflected "either/or" configurations permitting detectors to be built using either Carleton or Servonic pressure switches. After failure of the Servonic configuration the engineering drawings were revised to delete the detector configurations using this switch. The Servonic switch design was very rugged mechanically,

and was quite simple and straightforward in its design. In early development tests the switch had performed fairly well. The switch mechanical and electrical characteristics were acceptable. However, the electric leads were carried through the switch pressure case by hermetically-sealed glass-insulated feed-through connectors. These hermetic seals were troublesome and leaked on the qualification specimen. Discussions with Servonics indicated that they had received a bad batch of glass seals. Servonic Instrument, Inc. volunteered to redesign the seal slightly and resubmit new switches for qualification. This was done. The new switch, however, failed qualification by leaking through the hermetic seals.

In redesigning the seals Servonic had enlarged the case slightly making it more difficult to test and to install than the earlier model. The two are shown for comparison in figure 37.

Switch mount changes: The "F" and "B" configuration detector panels used four small clips for attachment of the pressure switch mounting cup to the switch support bracket. The attachment of these clips to the pressure switch cup was more of a problem than was anticipated. Initially, the clips were designed as an integral part of the switch support bracket and were to be soldered to the switch pressure cup after sliding the cup into the bracket (reference fig. 18). However, soldering was very difficult to accomplish on 21-6-9 corrosive flux. Corrosion after soldering, plus the low strength of solder at high temperature, resulted in dropping this approach.

The second design still maintained the attachment clips as part of the mounting bracket but changed processes from soldering to fusion welding. In this case the poor fit of the clips to the pressure cup after pressing in the cup resulted in a difficult weld with poor access for welding. The success ratio of these welds was poor with occasional pressure leaks through the weld resulting.

The final design removed the clips from the mounting bracket and fabricated them as separate parts. These were then spotwelded onto the switch pressure cup before welding the pressure switch into the cup. Finally, the cup with the clips attached was slid into the mounting bracket and the clip ears spotwelded onto the switch support bracket. The final design showing attachment of the ears to the pressure cup is shown in figure 38.

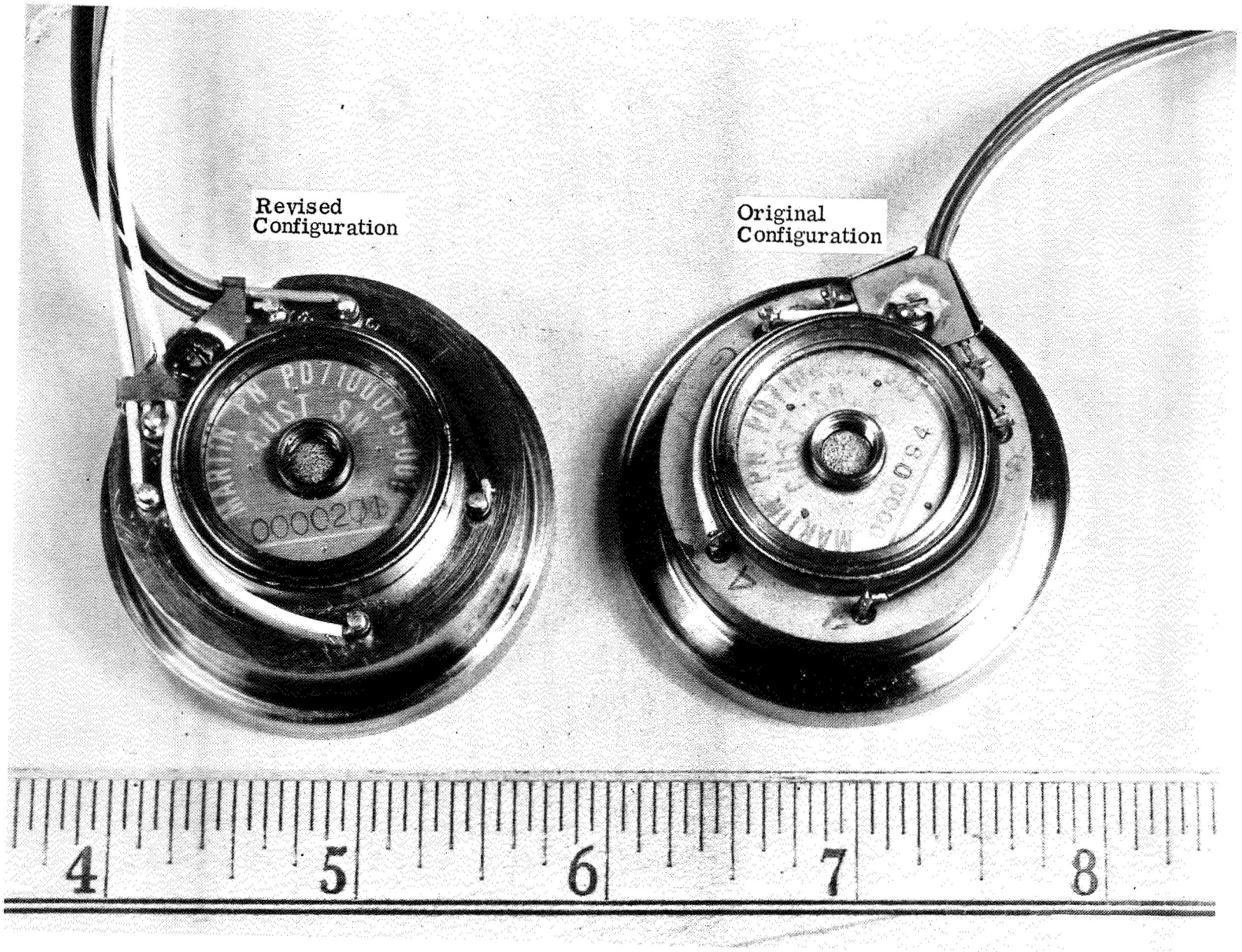


Figure 37.- Servonic Switches

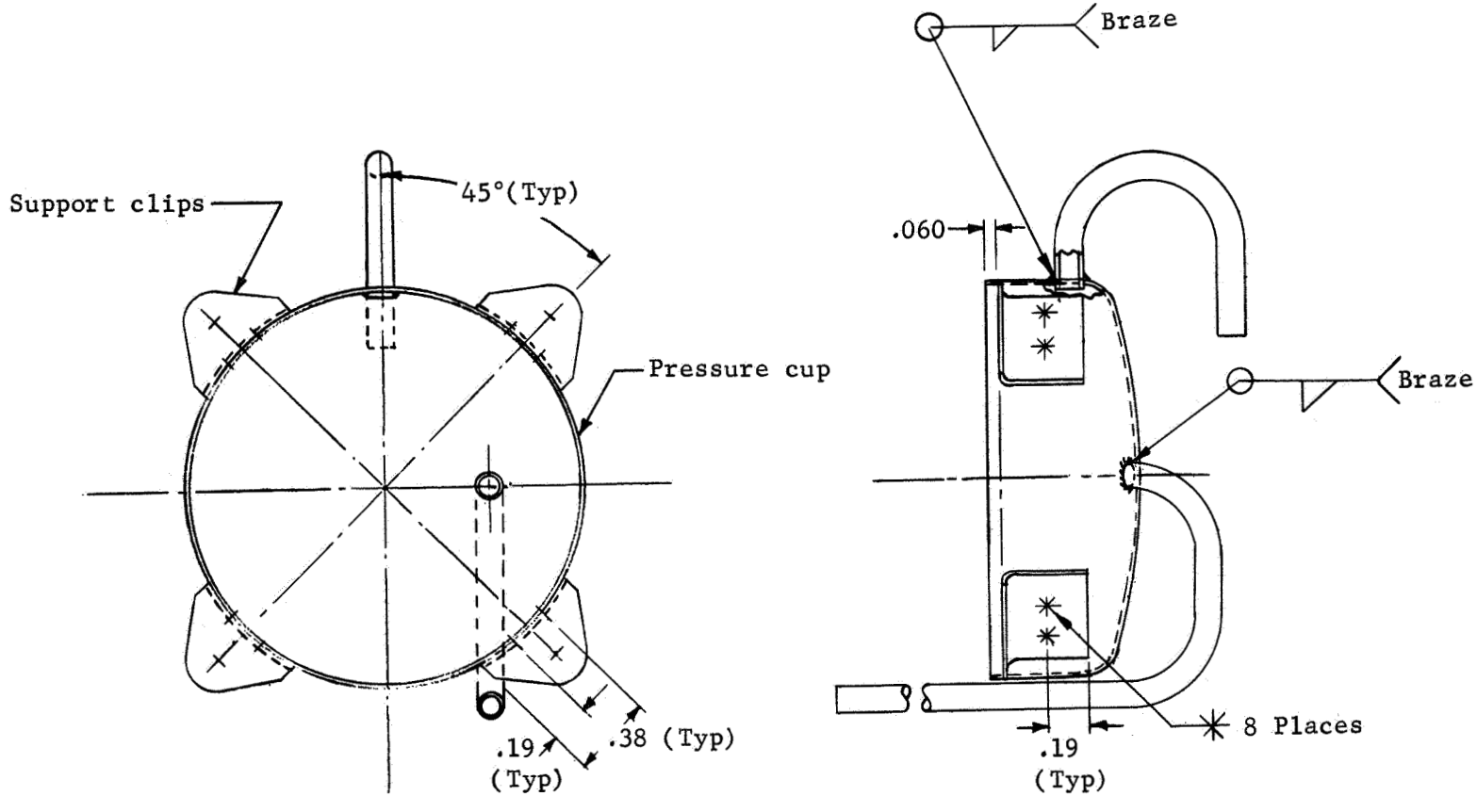


Figure 38.- Switch Cup Assembly

"F" configuration detector modification: The F1A detector panel consists of two detectors, each of which have approximately 1600 spot welds in the pressure cavity area of the target sheet. Initially, this detector panel was designed and fabricated in one piece, with the pressure cavities of the two detectors separated by a seam weld down the center of the panel. This configuration represents the lightest way to build this panel, but requires over 3000 individual spot welds without producing any potential leaks. Welding the three-ply F1A detector in the material gage combination of 0.002 to 0.016 to 0.002 in. is quite touchy at best, and several detectors were produced with a few faulty spot welds. To eliminate scrapping a good detector half because of a faulty detector on the other end of the panel, the detector was redesigned. The present design calls for fabricating the detector halves as separate subassemblies and then splicing these subassemblies together after they have been pressure expanded and leak tested. A butt joint using a splice strap on either side is riveted together with aluminum rivets. If at any time during manufacture of flight assurance testing a failure should occur, the bad half can be removed and a good half reinstalled. This design approach has proved to be of value in reducing replacement detector fabrication cost.

Interconnect tube modification: This basic design of the gas transfer interconnect system on the B1A detector panel is shown in figure 18. The system used on the F1A bumper panel is identical to the B1A system. Subsequent to detector assembly and during various phases of leak test, helium leaks were detected in some of the tube-to-switch cup braze joint. The joints showed evidence of fatigue cracking, either through the braze metal or in the 21-6-9 CRES switch cup material. Finally a B1A panel fitting that attached this tube to the target material fractured at the joint during acoustic tests.

Examination of the various failures indicated that excessive bending loads were being introduced into both the panel fitting joint and the switch cup joint. This condition was created by the independent movement of the switch support assembly relative to the panel and the resulting load interaction along the axis of the tube. This condition, coupled with any preloading of joints caused by misalignment and welding-induced stresses, lead to joint failures. Under the combination of these adverse factors, the interconnect tube design becomes marginal.

Various methods of relieving this load were investigated, within the constraints of the space-available envelope between the bumper and the switch bracket of the F1A bumper panel.

A configuration was selected and developed as shown in figure 39. The serpentine energy-absorbing tube design was based on the use of 0.065-in. O.D. x 0.009-in. wall 304 CRES tube. The proposed design was dynamically analyzed for the worst test condition (acoustics), loads were determined, and structural analyses performed. These analyses showed that the serpentine tube design would withstand the test environment. The design was based on tube development in both four- and six-loop configurations. The four-loop configuration was applied to a new switch cup assembly on a B1A panel, shown in figure 40. (Note that the four-loop tube was joined to the base of the cup as an optimized approach to the design.) The six-loop configuration was applied as a rework to existing B1A and F1A panels, shown in figure 41. In this case the small tube was interconnected to the existing tube on the top of the switch cup.

The tube stock acquired in the "as-drawn" condition was vacuum annealed to 1/2 H condition and formed on mandrels. Where required for detector rework, tapered adapters were made to provide an interference fit between the small serpentine tube and existing tubes and fittings. Joints were made by controlled brazing to eliminate braze or flux transfer into tube openings.

The design was confirmed through acoustic tests on both design applications.

Panel fitting modification: The original design of the tube interconnect panel fitting is shown in figure 42(a). The design was predicated on a resistance ring weld capability developed during the preliminary design phase of the program for application to B1A and F1A panels. The barrel of the fitting was counterbored to receive the tube, with an orifice exposed to the panel pressure cavity. The base of the fitting was designed to accommodate a 3/8 in.-diameter ring weld and four spot welds at each corner to retain spot weld spacing continuity in the panel.

The fitting was difficult to manufacture because the large base flexed in machining, resulting in excessive variation in thickness across the area. This variation produced erratic resistance spot weld quality. Furthermore, the pressure and heat involved in the ring welding process forced the corners away from the panel target material creating residual stresses in the part when spot welded.

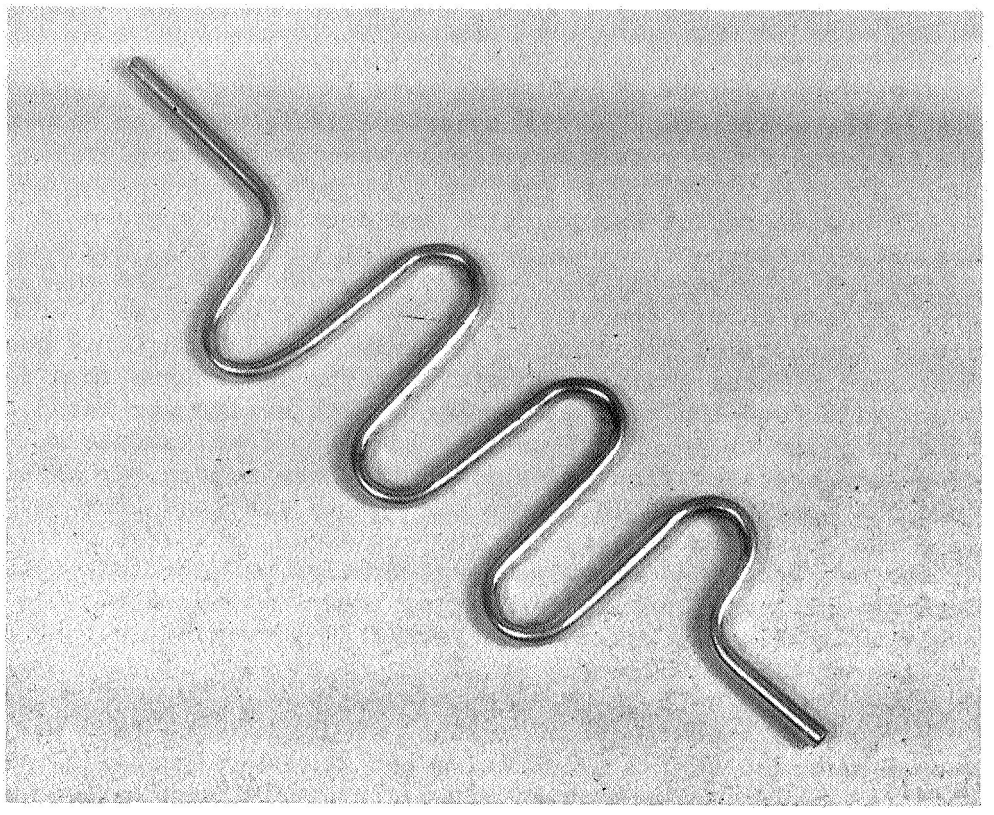

Figure 39.- Serpentine Pressure Tube

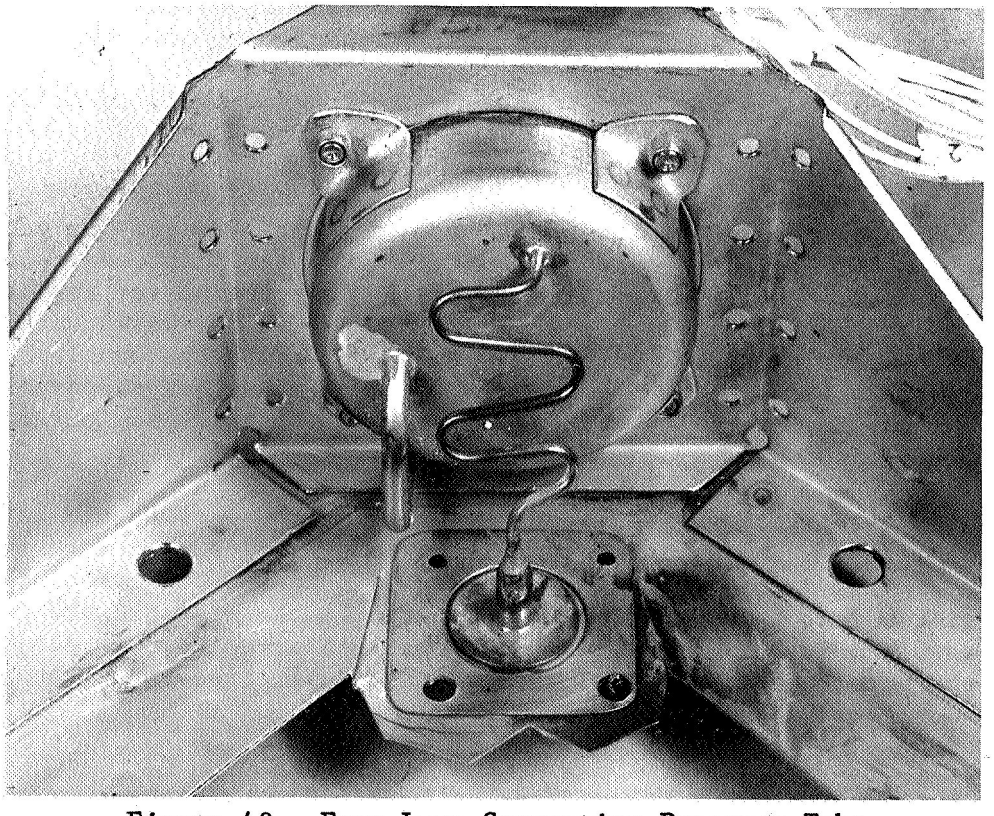

Figure 40.- Four-Loop Serpentine Pressure Tube

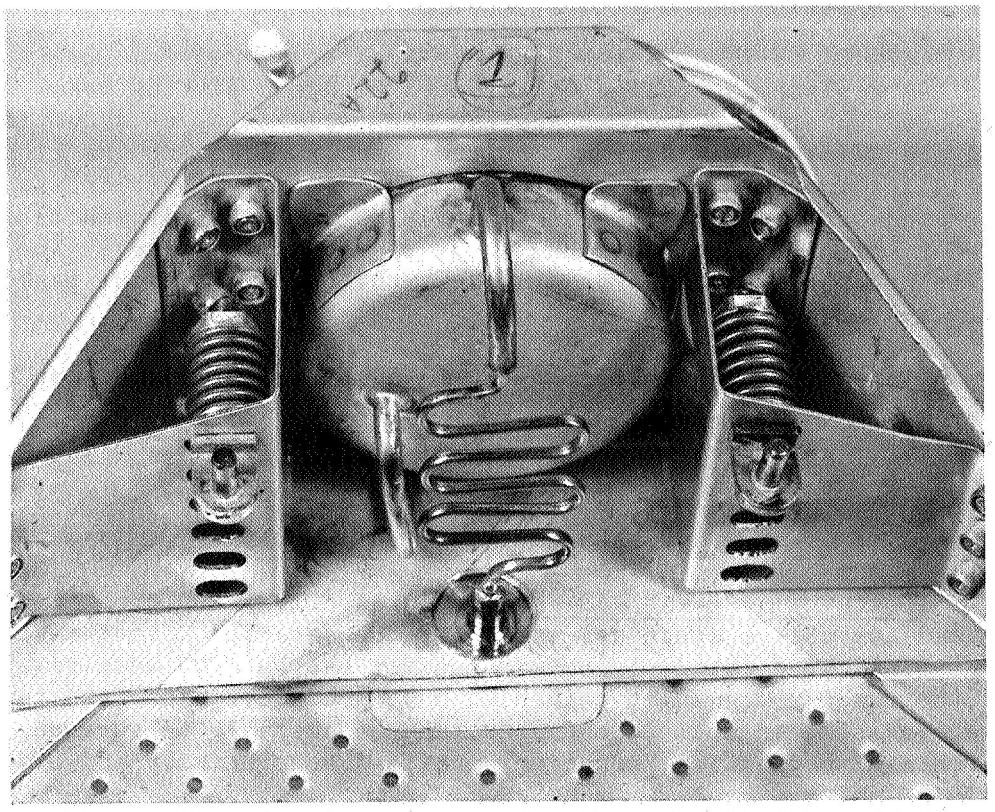

Figure 41.- Six-Loop Serpentine Reworked Configuration

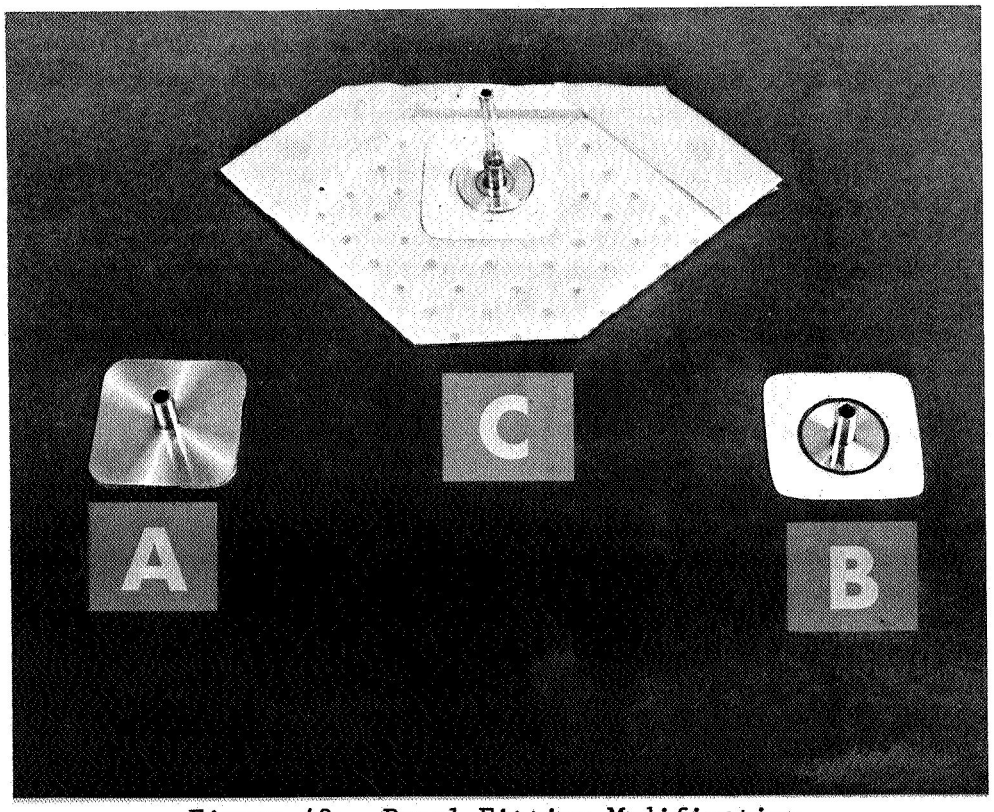


Figure 42.- Panel Fitting Modification

A replacement design was created with the fitting base reduced in area to accommodate the ring weld only, as shown in figure 42(b). This design permitted better access to the ring weld for inspection and leak testing. A separate doubler was created from fixed thickness 21-6-9 CRES sheet to circumscribe the fitting base and to pick up the required spot welds. The fitting-doubler details are shown installed on a typical panel in figure 42(c).

This design has shown that good flatness tolerances can be achieved and maintained, resulting in greatly improved resistance spot welding control.

## Design Support Studies

Detector material selection studies.- The MPDD program designated the use of stainless steel for the detector target test material. The materials considered for use on MPDD were required to be readily formable, weldable, have good corrosion resistance, be available in foil thicknesses, and be amenable to surface treatment capable of producing specified absorptivity and emissivity values.

Various 300 series stainless steel alloys were investigated and used for Martin Marietta-sponsored meteoroid detector development. These alloys included Types 301, 302, 304, and 321 in the annealed and work-hardened condition. Tests on specimens built under this early development program resulted in the selection of the annealed condition for all of these steels because of the marked resistance to fatigue under cyclic loading. From this group of steels, Type 304L was selected as a candidate for use in the Preliminary Design and Development Phase because of its lower percentage of carbide precipitates, good welding properties, high corrosion resistance, and availability in the various sheet and foil thicknesses required for the program. This steel was acquired under Specification QQ-S-766C for fabrication and test of detector subsize test hardware.

Unfortunately the first shipment of 304L steel was metallurgically dirty, revealing the presence of excessive sulfide inclusions (stringers). A metallurgical evaluation of the material confirmed that stringers transversed the thickness of the sheets and foil. Though the material conformed to the cleanliness requirements of Specification QQ-S-766C, it was determined that this condition could impair resistance weld repeatability and create the possibility of helium leakage in detector panels,

particularly in the thinner (0.002 in.) gages. It was also determined that it would be difficult and uneconomical to segregate 304L rolling stock to produce foil thickness with the desired microstructure.

At this time, it was also determined that 304L annealed material did not have a high enough guaranteed yield strength to meet the contract design requirements for the cylindrical detector, Configuration "A". Use of roll hardened steel was impractical because furnace brazing (one of the candidate joining processes) would tend to anneal the material to the lower strength.

With industry assistance, stainless steels were reviewed to determine a suitable replacement for the 304L. Armco stainless steel, 21-6-9 was selected from this review, as the candidate material. It had good cleanliness (freedom from stringers), workability, and high strength in the annealed condition. Because there were no government or industry specifications in existence to cover this material, a workable specification was negotiated with the supplier, identified as Martin Marietta Corporation Material Specification STM 1216. The specification, in addition to constraints on inclusions and intergranular corrosion producing precipitated carbides, established the following minimum mechanical properties for the annealed condition:

| Condition | Test condition | $F_{tu}$, psi (minimum) | $F_{ty}$, psi at 0.2% offset (minimum) | Percent elongation in 2 in. (minimum) Thickness, in. | | |
|---|---|---|---|---|---|---|
| | | | | 0.007 & under | 0.008 to 0.015 | 0.016 & over |
| A (annealed) | As-received | 100 000 | 55 000 | 15 | 35 | 40 |

The material was acquired in thicknesses of 0.001, 0.002, 0.008, 0.016, 0.020, 0.027, and 0.042 in., and tested and evaluated to determine its characteristics. The strength results of this evaluation are shown in the following tabulation.

| Thickness, in. | Tensile ultimate, psi | Tensile yield, 0.2% offset, psi | Elongation in 2 in., % |
|---|---|---|---|
| .042 | 112 400 | 64 300 | 43.5 |
| .027 | 114 300 | 68 200 | 43.5 |
| .020 | 116 000 | 69 300 | 43.5 |
| .016 | 115 600 | 69 800 | 42.5 |
| .008 | 123 400 | 77 300 | 41.5 |
| .002 | 119 000 | 68 500 | 32.5 |
| .001 | 118 300 | 75 400 | 22.0 |

Shear and tensile tests conducted on resistance spot and seam welded specimens showed good nugget formation and penetration comparable to nuggets formed in 304L. These tests also showed a very high degree of weld repeatability from sheet to sheet in all thickness ranges used in the program. The material was found to be adaptable to fusion welding, including heli-arc, tungsten inert gas, and gas welding. The material was also found to be compatible with the 300 series stainless steels in joining by welding.

The alloy demonstrated good brazing characteristics. Various brazing processes, including vacuum furnace, hydrogen blanketed furnace, and flux torch brazing were applied to the material. Comparative tests between Type 304 CRES and 21-6-9 CRES showed that the braze wetting angle in the latter was increased by approximately 7%.

The material as fabricated in test specimens demonstrated a higher degree of resistance to fatigue than comparable specimens fabricated from Type 304L. During the Martin Marietta-sponsored advanced development of resistance welded flat detectors, fatigue failure occurred in the Type 304 series material adjacent to the spot welds when subjected to the vibration and acoustic environments. In comparable tests with similar designs, the 21-6-9 alloy remained free from fatigue failures.

This material was acquired for and used in the fabrication of all revised subsize test specimens and development of full-size detector hardware. Inspection and tests of the received material showed compliance with the specification.

Detector pressurization gas.- The MPDD meteoroid detector design requirements are based on an anticipated lifetime of two years in a space environment. The detector is required to have low leakage so that the internal pressure will not leak down to switch trip pressure in 100 years. From pressure expansion data developed on the program it was determined that the smallest-internal-volume detector, had an internal volume of 6.2 cu in. Knowing this volume, studies were performed to determine the allowable gas leakage rate, and what gas or gases should be used in the detector. Calculations for allowable leakage rate were based on the following:

1) It was assumed that the pressure switch would trip at the upper limit of the pressure switch trip tolerance ($6.0 \pm 2.5$ psig), or 8.5 psi;

2) The amount of pressurization gas that could be permitted to be lost in 100 years would permit the internal pressure to decay from the normal pressure at -250°F (10.7 psia) down to switch trip pressure of 8.5 psi.

This leakage gas volume is:

$$V_e = \frac{10.7 - 8.5 \text{ psi}}{10.7 \text{ psi}} \times 6.2 \text{ in.}^3 \times 16.4 \text{ cc/in.}^3 =$$

21 cc at -250°F and 10.7 psi

Corrected to standard conditions this volume becomes:

$$V_e = 21 \times \frac{460 + 60^\circ\text{F}}{460 - 250^\circ\text{F}} \times \frac{10.7 \text{ psi}}{14.7 \text{ psi}} = 38 \text{ cc}$$

Allowable leakage rate is determined to be 38 cc per 100 years, or $1.2 \times 10^{-8}$ scc/sec.

With the allowable leakage rate determined, it was desired to know what gas or gases would be optimum for pressurization of MPDD detectors. It was desired that the selected gas be readily detectable and measurable for leak detection, and that it be a slow leaking gas for pressure retention. Analyses were performed using the Poiseuille and Knudsen equations for flow rate determination and corresponding hole size correlation. If a leak path

does develop large enough to permit free molecular flow of the gas, the flow rate can be theoretically calculated from Poiseuille's equation:

$$Q = \frac{\pi a^4}{8 \eta L} \quad \frac{\overline{P} \triangle P}{P} \tag{1}$$

Where:

$Q$ = volume flow rate, $cm^3/sec$,

$a$ = capillary radius, cm,

$\eta$ = coefficient of viscosity, poise,

$L$ = capillary length, cm,

$P$ = pressure drop across capillary length, $dynes/cm^2$,

$\overline{P}$ = mean pressure across the capillary, $dynes/cm^2$,

$P$ = pressure at the capillary inlet, $dynes/cm^2$.

$$Q = \xi \, 4/3 \sqrt{\frac{2 \pi RT}{M}} \left(\frac{a^3}{L}\right)\left(\frac{\triangle P}{P}\right) \tag{2}$$

where:

$R$ = universal gas constant, $8.31 \times 10^7$ ergs/mole/$^oK$,

$T$ = temperature, $^oK$,

$M$ = molecular weight,

$\xi$ = constant (Adzumi constant) = 0.66.

Computations using equations (1) and (2) result in hole sizes as follows for the detector to leak down to switch trip pressure in 100 years:

Equation 1 = 1750 Å radius;

Equation 2 - 856 Å radius;

Comparing helium, argon, hydrogen, nitrogen, and oxygen gases, it can be shown that molecular diameters of all these gases lie between 2.34 Å and 3.15 Å, all of which are small compared to the allowable leakage hole diameter. Likewise, the viscosity of all these gases lies between 0.00874 and 0.02217 centipoises. Referring to equations (1) and (2) it can be seen that little is gained in using a heavy gas or a mixture of gases for the pressurization medium. It was concluded that the best choice for the pressurizing media is 100% helium, since this gas provides the best leak detection capability. A more detailed report of pressurization gas selection is presented in reference 3.

The present pressurization procedure for MPDD detectors requires purging of the interior of the detectors of unwanted gases before final helium filling. This was accomplished as follows:

1) Pump down the interior of the detector to a vacuum of one torr to remove unwanted gases and/or moisture;

2) Repressurize the interior of the detector with helium to a level of 20 psia;

3) Repeat the pumpdown of 1) above;

4) Pressurize to the final pressure level (27.4 psia) with helium and seal the detector.

This procedure should produce a helium fill which is 99.999% helium fill gas, a level which is better than the purity level of procured gas itself.

Detector pressurization level.- So that the MPDD detectors are able to maintain pressure integrity for several years of space flight, it is desirable to keep the stress level of the meteoroid detectors as low as practical. For near-earth orbit applications the detectors may experience as many as 20 000 thermal cycles as the spacecraft goes from the sunlit side of the earth to the dark side. The detectors may experience temperature extremes as great as +325°F to -100°F during these cycles, resulting in cyclical internal pressures and corresponding metal fatigue stresses. The approach taken to minimize these fatigue

stresses is to keep the detector internal pressure as low as is practical.

The pressurization level of the detectors is based on maintaining a pressure level just slightly above the detector pressure switch trip level while the spacecraft is on the launch pad before launch. The internal pressure level is based on the following assumptions:

1) Switch may trip at maximum tolerance of pressure tripping range (8.5 psig max);

2) Detector switch may not be permitted to trip on the launch pad;

3) Ambient sea level pressure may rise as high as 15.0 psi (barometric);

4) Ambient temperature may drop as low as $0^{o}F$.

The required detector charge pressure then becomes (at $75^{o}F$):

$$Pc = (15.0 + 8.5 \text{ psi}) \times \frac{459.7 + 75^{o}F}{459.7 + 0^{o}F} = 27.3 \text{ psia}$$

to meet the above assumptions.

Actual charge pressure used on the MPDD program for deliverable hardware was $27.4 \pm 0.1$ psia at $70^{o} \pm 5^{o}F$. Flight pressures for near-earth orbit then become:

Maximum pressure at $325^{o}F$ =

$$P_{max} = 27.5 \times \frac{459.7 + 325}{459.7 + 65} = 41.1 \text{ psia.}$$

Minimum pressure at $-100^{o}F$ =

$$P_{min} = 27.3 \times \frac{459.7 - 100}{459.7 + 75} = 18.3 \text{ psia.}$$

Flight pressures for interplanetary missions become:

Maximum pressure at +350°F =

$$P_{max} = 27.5 \times \frac{459.7 + 350}{459.7 + 65} = 42.4 \text{ psia.}$$

Minimum pressure at -250°F =

$$P_{min} = 27.3 \times \frac{459.7 - 250^{\circ}F}{459.7 + 75} = 10.7 \text{ psia.}$$

## Engineering Design Support Tests

A number of design-evaluation tests were performed in support of MPDD engineering design. These tests were performed to develop design data for use in design of full size detectors. Several of the tests are described herein.

Dual detector puncture simulation test.- The dual detectors designed for the MPDD program consisted of back-to-back pressure cavities with a common separator wall between them. The common wall in all cases consisted of a flat sheet supported, for pressure loads, by the cavity cell joints. As long as the detectors have pressure on both sides of the common wall, the wall remains in the center of the two cavities. However, if one side becomes punctured by a meteoroid, than the separator wall is exposed to the full pressure of the unpunctured detector. A simple test was devised to determine if the separator wall would deflect enough to affect the pressure in the unpunctured detector. The test setup is shown in figure 43. For this test a small subsize detector test specimen was used. A mercury manometer and suitable valves for pressurizing and depressurizing the detector was attached to each pressure cavity as shown. The test was performed to simulate the case of interplanetary flight at -250°F. For this case the detector internal pressure would be at approximately 10.7 psi, only 2.2 psi from the maximum switch trip pressure of 8.5 psi. The test results indicated that after pressurizing both sides to 10.7 psi and simulating puncture (venting) of one side, the pressure dropped less than 10% (less than 1 psi) in the pressurized side. This test was repeated on three configurations with similar results. It was concluded that no problem exists in separator wall deflection.

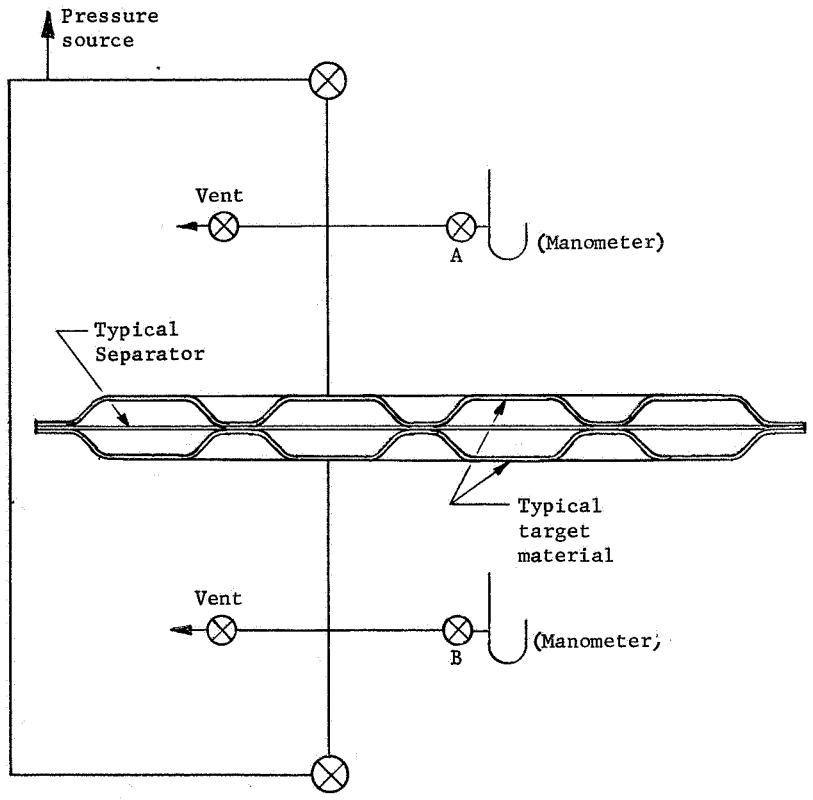


Step 1 Pressurize simultaneously through Ports A and B to 10.7 psig, equal to minimum operating pressure at -250°F.

Step 2 Dump through Port B to ambient pressure.

Step 3 Record pressure drop through Port A in inches of Hg, converted to psig.

Step 4 Pressurize simultaneously through Ports A and B to 42.7 psig, equal to maximum operating pressure at 350°F.

Step 5 Dump through Port B to ambient pressure.

Step 6 Record pressure drop through Port A in inches of Hg, converted to psig.

Step 7 Repressurize simultaneously through Ports A and B to 10.2 psig, equal to minimum operating pressure at -250°F.

Step 8 Dump through Port A to ambient pressure.

Step 9 Record pressure drop through Port B in inches of Hg, converted to psig.

Figure 43.- Test Schematic and Procedure for Puncture Simulation Test

Stiffness evaluation tests.- During the early development of MPDD detectors questions arose as to the merits of stiffness in detector design. There was concern as to whether stiffness in detectors had merit in assisting detectors to survive the boost phase environment of flight (vibration and acoustic). Also a second question was raised. If stiffness did in fact have merit, what was the best detector cavity design to achieve maximum stiffness. To answer both of these questions a test program was initiated. This program evaluated relative stiffness potential of various detector configurations and the extent to which the stiffness can be varied in a given design by varying pillow height. The evaluation was accomplished by fabricating small 18 in square specimens in the desired designs using spot welded field joints and seam welded edges and vibrating these specimens to determine the fundamental resonant frequency of each specimen. The relative stiffness was determined from the resonant frequency.

The specimens used for the test comparison were all of 0.016 in. gage 21-6-9 steel and of designs as follows:

1) A square array specimen having a spot spacing of 1.44 in. (XC1-06);

2) Same as 1) except for 2.88 in. spacing (XC1-07);

3) A hexagonal cell array having one spot weld at each corner and having a dimension across the flats of the hexagon of 1.75 in. (XC1-09);

4) Same as 3) except for a dimension of 3.48 in. across the flats (XC1-08);

5) A hexagonal cell array having six spot welds per side (including corner joints) and a dimension of 3.48 in. across the flats of the hexagon (XC1-05).

The test was conducted by mounting the specimen under evaluation to the vibration fixture, pressure-expanding the specimen to a small pillow height, and then vibrating the specimen. The frequency was swept slowly until the first mode resonance was determined. The resonant frequency and the pillow height corresponding to that frequency was noted. This test was then repeated, expanding the specimen to different increasing pillow heights. The results of the various specimens tested are shown in figure 44 and tabulated in table 12. The effective thickness of the specimens as shown in figure 44 and table 12 is derived from MacDuff and Felgar design nomographs. The effective thickness

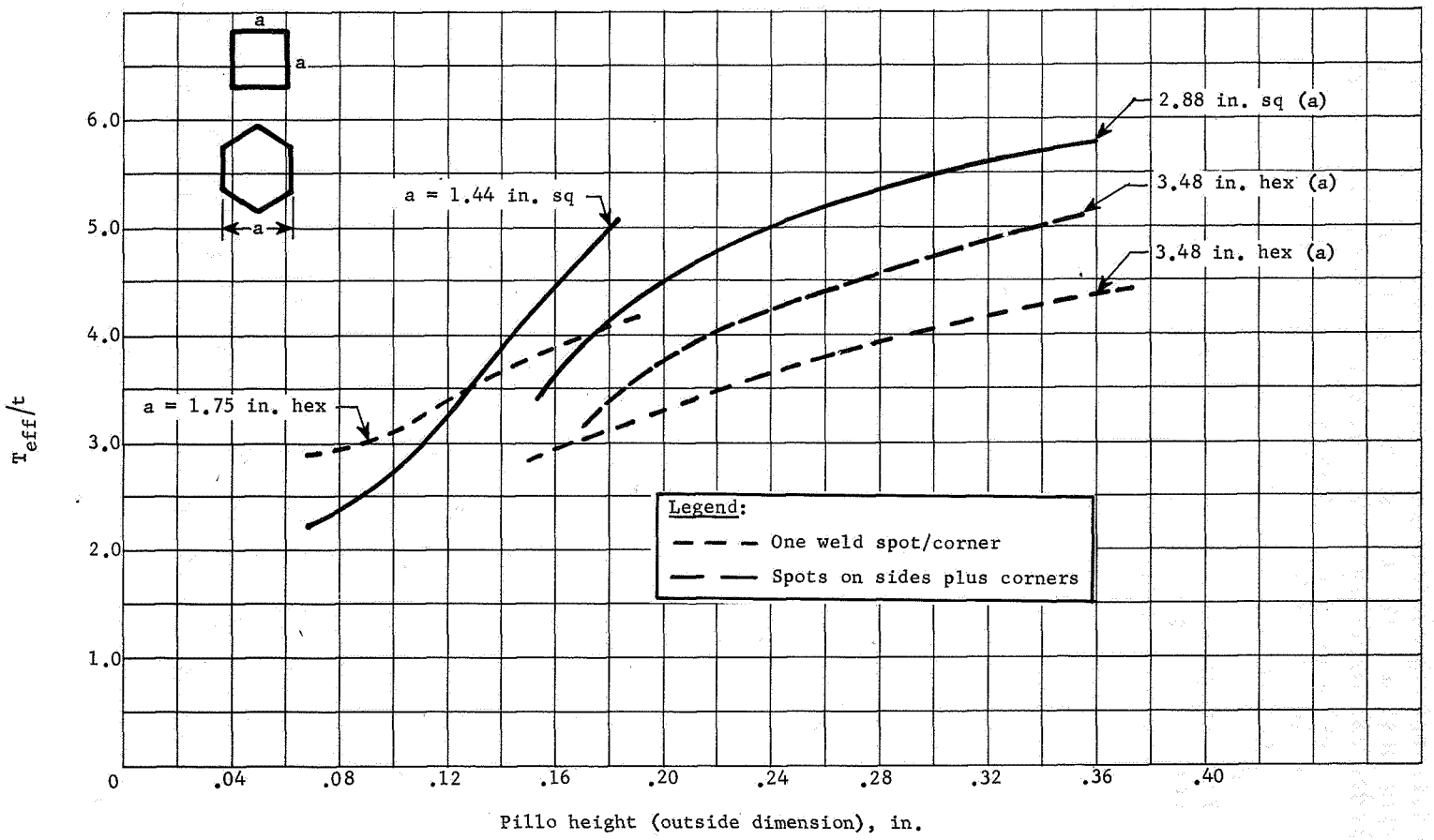


Figure 44.- Effective Thickness vs Pillo Height

TABLE 12.- DATA TABULATION,
SINUSOIDAL VIBRATION TESTS OF FIVE 18x18-in. PANEL CONFIGURATIONS

| $f_n$ Hz | Input accel, mV | Output accel, V | Q $\frac{\text{Output}}{\text{Input}}$ | Panel press, psig | Pillow height (outside/outside), in. | Effective thickness, in. |
|---|---|---|---|---|---|---|
| Test 1, Panel XC1-06, S/N 01, 1.44-in., sq | | | | | | |
| 39 | 210 | 6.2 | 29.55 | 5 | 0.068 | 0.035 |
| 55 | 210 | 10.0 | 47.6 | 19 | 0.1035 | 0.044 |
| 99 | 210 | 8.6 | 41.0 | 55 | 0.149 | 0.065 |
| 118 | 210 | 8.6 | 41.0 | 70 | 0.1655 | 0.073 |
| 136 | 210 | 7.7 | 36.65 | 85 | 0.1825 | 0.080 |
| Test 2, Panel XC1-07, S/N 01, 2.88-in., sq (washer/rivets) | | | | | | |
| 77 | 210 | 4.5 | 21.4 | 5 | 0.1535 | 0.054 |
| 110 | 210 | 5.8 | 27.6 | 12.25 | 0.1965 | 0.070 |
| 124 | 210 | 6.1 | 29.0 | 18 | 0.2295 | 0.077 |
| 135 | 210 | 6.25 | 29.8 | 22 | 0.252 | 0.080 |
| 145 | 210 | 6.8 | 32.4 | 26 | 0.281 | 0.085 |
| 157 | 210 | 6.8 | 32.4 | 32 | 0.3195 | 0.089 |
| 166 | 210 | 7.0 | 33.4 | 38 | 0.360 | 0.092 |
| Test 3, Panel XC1-05, S/N 01, 3.48-in., hex | | | | | | |
| 64 | 210 | 4.7 | 22.4 | 20 | 0.1725 | 0.049 |
| 88 | 210 | 6.8 | 32.4 | 30 | 0.199 | 0.060 |
| 96 | 210 | 7.4 | 35.2 | 38 | 0.218 | 0.064 |
| 105 | 210 | 7.6 | 36.2 | 50 | 0.244 | 0.067 |
| 111 | 210 | 7.4 | 35.2 | 60 | 0.2625 | 0.0695 |
| 120 | 210 | 7.8 | 37.2 | 75 | 0.2985 | 0.073 |
| 133 | 210 | 8.0 | 38.1 | 90 | 0.325 | 0.978 |
| 142 | 210 | 8.7 | 41.5 | 105 | 0.356 | 0.081 |
| Test 4, Panel XC1-08, S/N 01, 3.48-in. hex (1 spot per corner) | | | | | | |
| 50 | 210 | 4.7 | 22.4 | 5 | 0.151 | 0.0455 |
| 81 | 210 | 7.0 | 33.3 | 15 | 0.231 | 0.0565 |
| 97 | 210 | 7.5 | 35.7 | 25 | 0.299 | 0.064 |
| 114 | 210 | 5.2 | 24.8 | 35 | 0.374 | 0.0705 |
| Test 5, Panel XC1-09, S/N 01, 1.75-in. hex (1 spot per corner) | | | | | | |
| 59 | 210 | 6.8 | 32.4 | 15 | 0.071 | 0.046 |
| 64 | 210 | 6.2 | 29.5 | 30 | 0.0955 | 0.0485 |
| 71 | 210 | 6.6 | 31.4 | 45 | 0.114 | 0.052 |
| 81 | 210 | 7.5 | 35.7 | 60 | 0.1325 | 0.0565 |
| 88 | 210 | 6.8 | 32.4 | 75 | 0.1515 | 0.060 |
| 94 | 210 | 6.4 | 30.5 | 90 | 0.170 | 0.062 |
| 103 | 210 | 6.9 | 32.8 | 106 | 0.189 | 0.066 |

is the equivalent thickness of a synthetic solid plate having the same mass as that of the two 0.016 in.-thick steel target sheets that would vibrate at the same fundamental frequency as the actual detector under test. A plot derived from MacDuff and Felgar nomographs is shown in figure 45 for 18x18 in. square plates. From this figure the effective thickness of the specimen for stiffness comparisons were derived.

It can be seen from figure 44 that, for a given pillow height, the small square array is stiffer than the large square, the small hexagon array is stiffer than the large hexagon, and square arrays are stiffer than hexagonal arrays.

The data shown in figure 44 are for specimens that were vibrated while containing the pressure required to establish the pressure-expanded pillow height. To determine if pressure contributes to stiffness, the same test was repeated with identical specimens. This was accomplished by expanding the specimens to different pillow heights, backing off on the internal pressure to 12 psig after each expansion, and vibrating the specimens to again determine the fundamental frequency. Figure 46 is typical of the results of this testing. The pillow height is that measured at 12 psig after expanding at higher pressures. These data do not produce the smooth curves of the first part of the test, but do show the same trends. Stiffness increases with pillow height.

As a result of the tests described above, it was established that detector stiffness does increase with increasing pillow height for a given cell size and shape. It was desired at this point to acquire data quickly that would indicate how stiffness of a detector affected loads in the detector itself and its mount. Detector E1A (40x49 in. 0.042 mil) having a "C" channel peripheral support had been previously vibration tested with a substantial amount of strain gaging. These test data yielded considerable stress information on the detector and on the mount. It was decided to expand this specimen to a higher pillow height and vibration test it again. This was done. The stiffness effective thickness of the detector was 2.62 for the first vibration test and 3.57 for the second test as shown in figure 47. The test results showed that the bending moment in the "C" channel between mounting bolts increased with increased detector stiffness. The bending moment increased from approximately 5700 psi at lower detector stiffness to 8500 psi at higher detector stiffness. The load in the "C" channel at the attachment bolts increased correspondingly from 27 000 psi to 67 000 psi.

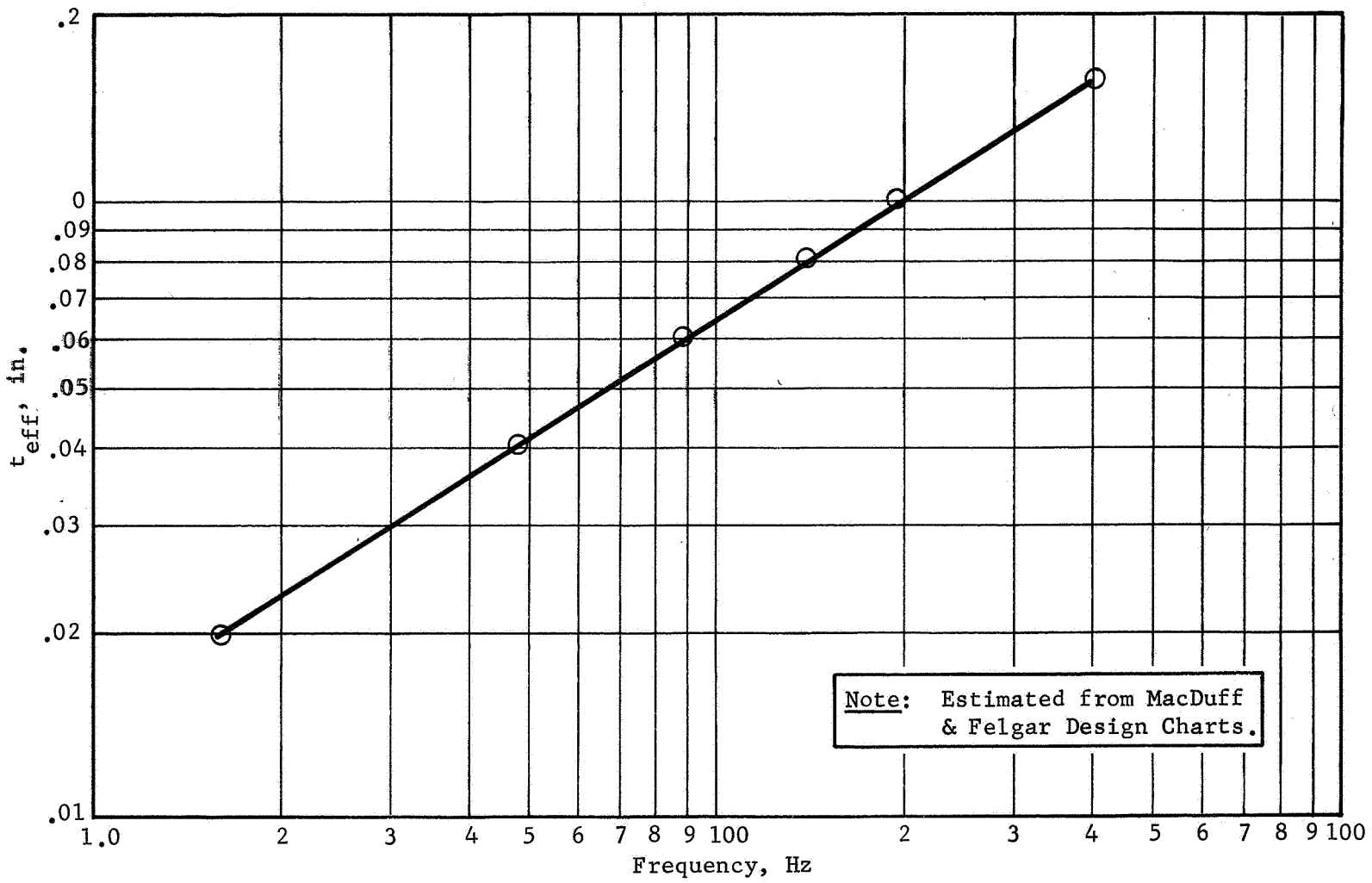


Figure 45.- Effective Panel Thickness vs Panel Frequency

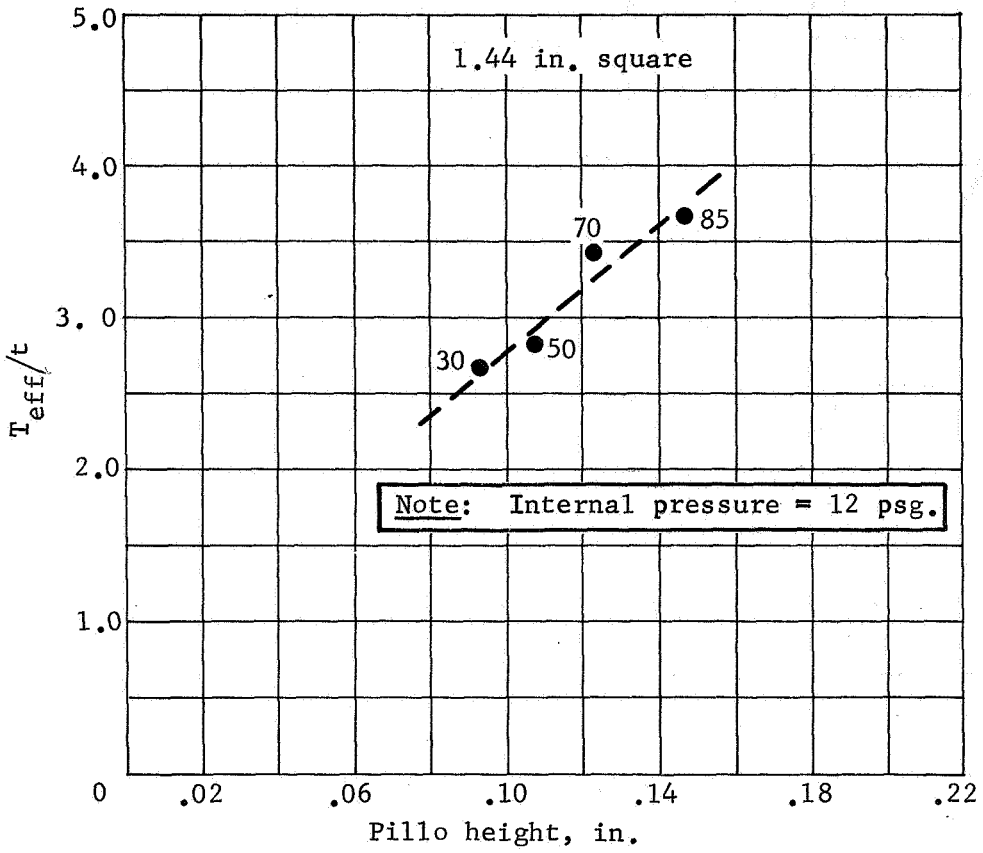


Figure 46.- Stiffness (Effective Thickness) vs Pillow Height

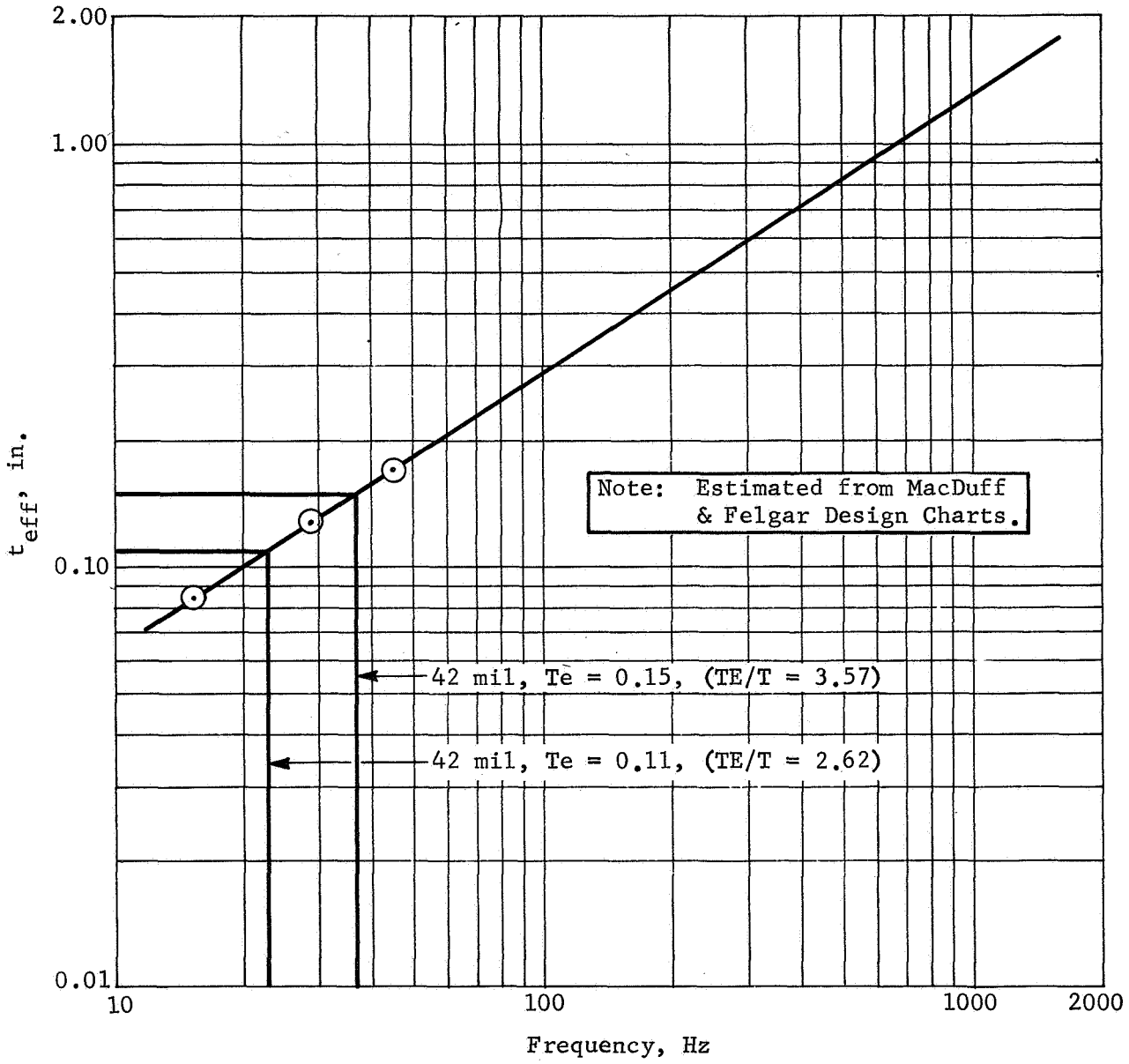


Figure 47.- Effective Panel Thickness vs Panel Frequency

The detector itself underwent stress changes as follows as a result of increased stiffness:

1) Stresses in the center of the detector increased from 10 000 psi to 14 000;

2) Stresses at various points between the center and the edge reduced (typically 9500 psi down to 5800, and increased (typically 8000 psi to 9000 psi);

3) Stresses at the edge increased considerably (from 14 000 psi up to 29 000 psi on the long edge and 13 000 to 52 000 on the short edge).

It was concluded that the merits of increased stiffness were not clear cut, and detector designs should be governed by other more critical design constraints.

Subsize detector design tests.- The primary objectives of subsize testing was to produce empirical data to assist detector design and to verify preliminary design approaches, material selection, and fabrication processes. Specifically, these data were to be used to develop pressure cavity designs for pressurization and mechanical forming, to establish candidate pressure cell geometry, develop joint attachment strength and fatigue criteria resulting from pressure cycling, and to define the processes and techniques to be used in joining.

The subsize test results and correlated investigations were used as the basis for screening and selection of candidate designs for continued development.

The following outputs were obtained from this program:

1) Confirmation of structural analysis and basic design approach;

2) Establishment of joint strength for use in design, as subjected to static loading induced by internal pressures;

3) Determination of the degree of resistance to fatigue when the joints and parent material of the design was subjected to cyclic internal pressures representative of pressure changes expected in the space thermal environment;

4) Determination of the effects of static and cyclic pressure on the stability of the detector designs;

5) Development of static pressure levels and procedures for expansion of flat pressure vessel cells and the relation of such pressures to cell profiles;

6) Study of the effects of static and cyclic pressures on varied cell geometries and the development of comparative data for use in design selection;

7) Evaluation of the effects of static and cyclic pressures on preformed target material and flat sheet design applications;

8) Confirmation of the stability of flat separator sheets of dual detectors when subjected to delta pressures.

Subsize test designs: A detailed description of each subsize detector design is presented and test results are discussed in program progress reports written earlier in this program. In general, the designs were developed in the following groups.

Designation "B" series, 0.008/0.008 in. targets. Eleven designs were developed with variations in cavity geometry and joint spacing. Typical "B" test specimens are shown in figure 48.

Designation "C" series, 0.016/0.016 in. targets. Ten designs were developed with variations in cavity geometries, joint spacing, and joining processes. A typical "C" test specimen is shown in figure 49.

Designation "D" series with combinations of two-ply 0.027/0.027 in. targets, three-ply 0.027 in. target/0.016-in. separator/0.027 in. target, and two-ply 0.027 in. target/0.016 in. backup. Fourteen designs were developed in this category with variations in cavity geometries, joint spacing, and joint processes. Typical "D" test specimens are shown in figure 50.

Designation "E" series with combinations of two-ply 0.042/0.042 in. targets, three-ply 0.042 in. target/0.020 in. separator/0.042 in. target, and two-ply 0.042 in. target/0.020 in. backup. Nine designs were developed in this category with variations in cavity geometries, joint spacing, and joint processes. Typical "E" test specimens are shown in figure 51.

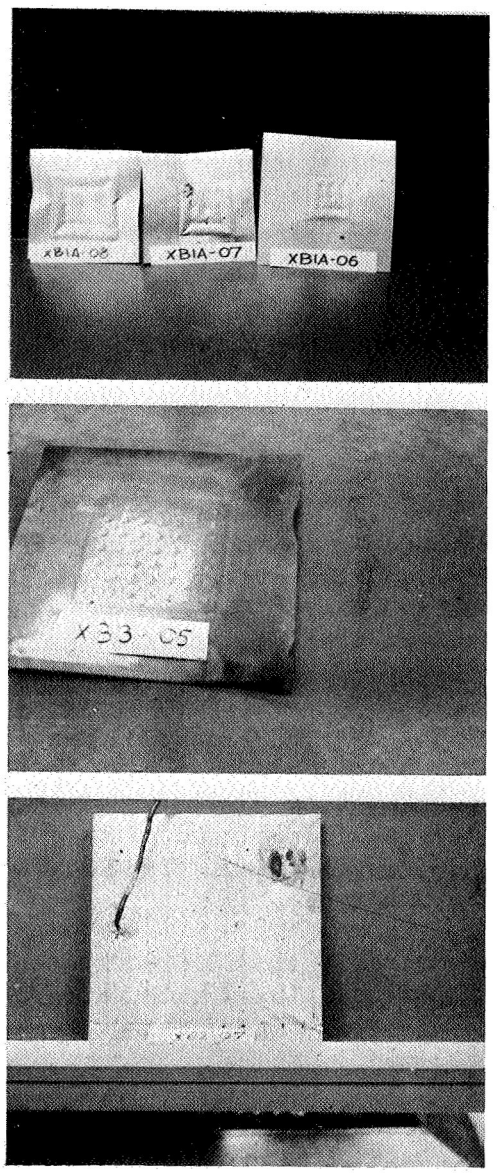


Figure 48.- Configuration B Test Specimens

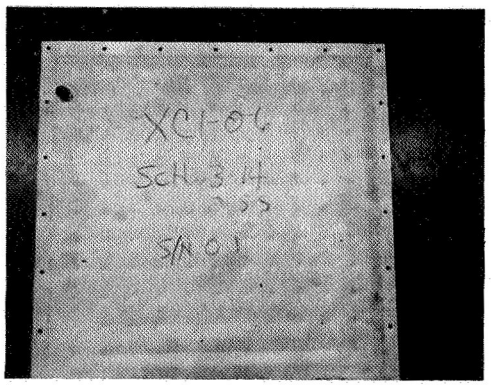

Figure 49.- Configuration C Test Specimen

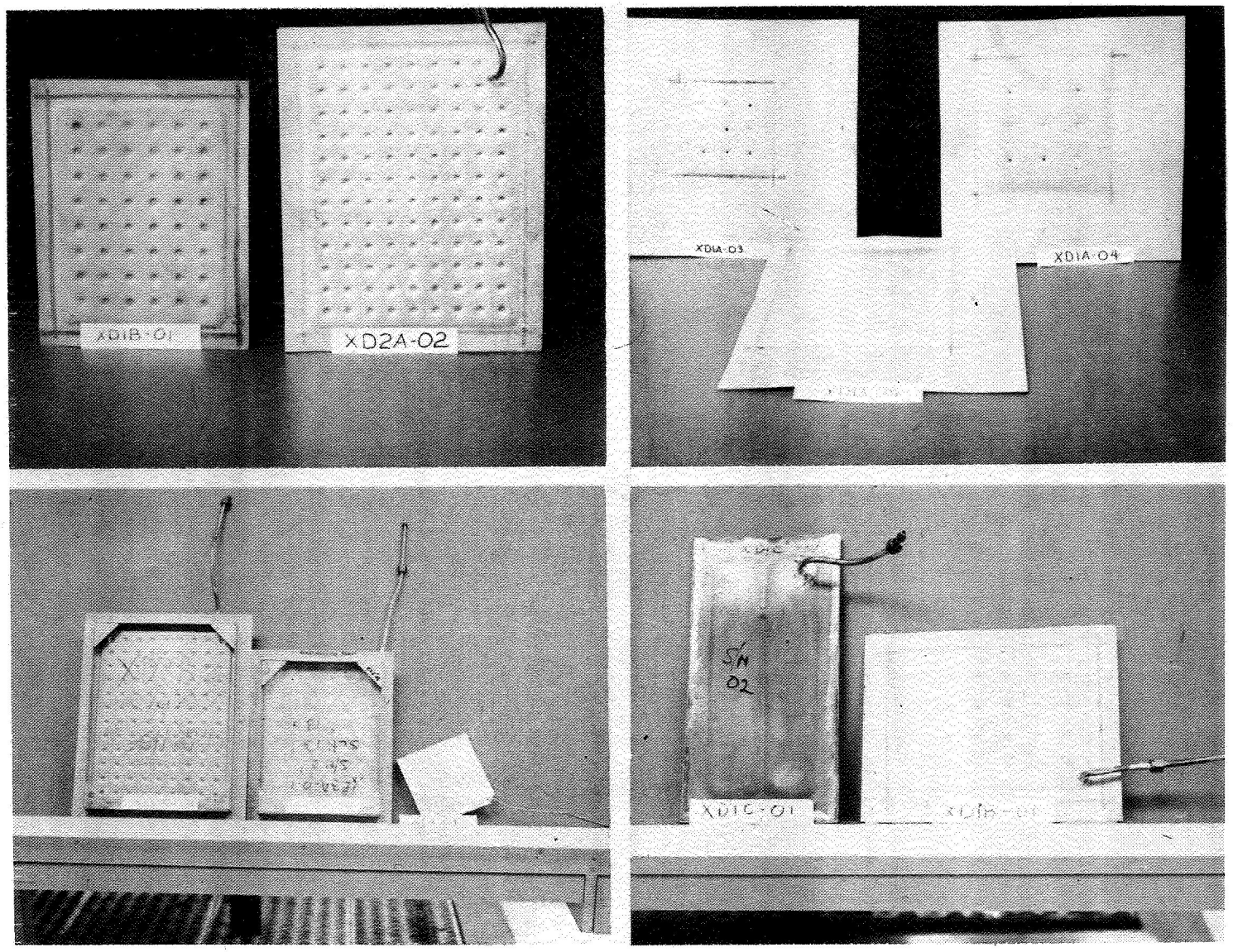


Figure 50.- Configuration D Test Specimens

Designation "F" series with two 0.002 in. targets attached to a 0.016 in. core. Nine designs were developed in this category with variations in cavity geometries, joint spacing, joint processes, and techniques. Typical "F" test specimens are shown in figure 52.

Test pressures: Static expansion pressures applied to subsize test specimens were varied incrementally to achieve forming profiles versus pressure in each specific combination of thicknesses of materials. For preformed pressure cavity specimens a uniform 53.4 psig was used for proof. For cyclic pressures, a range of 14 to 49 psig was used. The development of pressure levels were discussed earlier in this report.

Joint strength evaluation: The original welded joint spacing used on subsize designs were based on the spot weld tensile allowables permitted in MIL-HDBK-5. (These allowables are 25% of specified shear values for nickel steel alloys.) As a result of this constraint, joint spacing was conservative, somewhat reducing the effective target efficiency and increasing the number of joints for a given target sheet area.

An investigation was made into the feasibility of increasing the spot weld spacing by increasing the load in the joints. Information furnished by Wright-Patterson Air Force Base indicated that typical values for tensile pull specimens run between 50% to 75% of shear values, and in all cases above 25% of shear values. Because of scatter in developed data, the lower limit was used for design limits in MIL-HDBK-5.

To evaluate typical tensile values on 21-6-9 CRES, a series of spot welded subsize test specimens were burst tested and the data related to tension pull and shear pull coupon test data. The results of this test appear in tables 13 and 14. These tests were performed on 0.008 and 0.027 in. material, representative of the range of thicknesses planned for design.

The test data on pull strips bore out the fact that tension pull values exceed 25% of shear pull values. Tension-to-shear ratios were 0.77 in the 0.008 in. gage and 0.57 in the 0.027 in. gage steel. Note that the scatter in the shear pull specimens is considerably less than in the tension pull tests. Also, the tension pull specimens agree fairly closely with the burst tension values in the close spacing versions of the burst specimens.

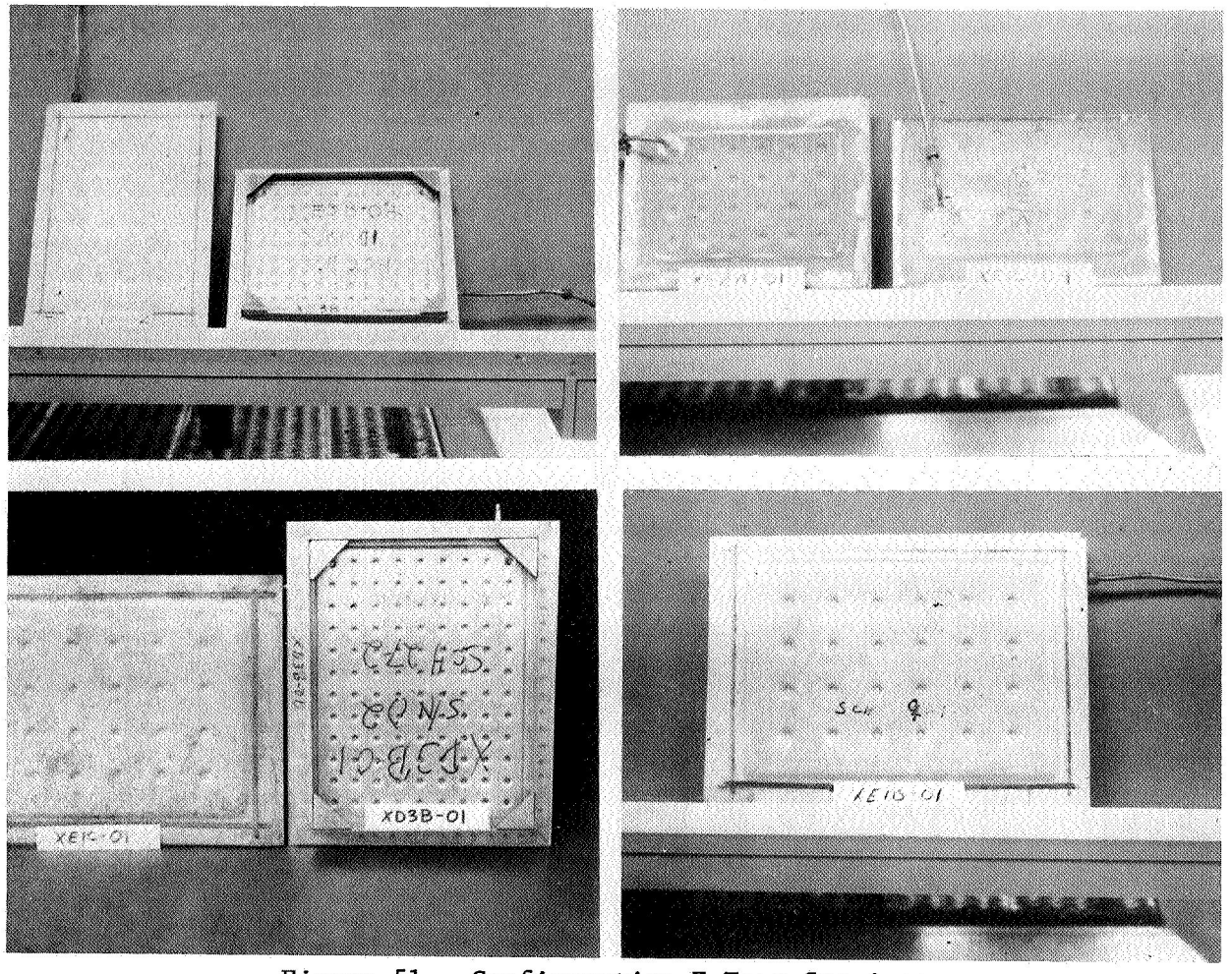


Figure 51.- Configuration E Test Specimens

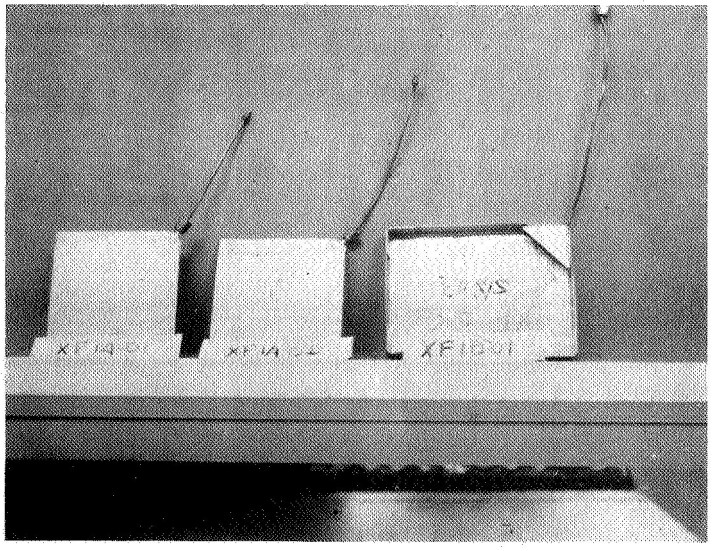

Figure 52.- Configuration F Test Specimen

TABLE 13.- SPOT WELD STRENGTH, 0.008-in. GAGE 21-6-9

| Tension full test, lb | Shear pull test, lb | Burst specimen test, lb | |
|---|---|---|---|
| 205 | 283 | | 191 |
| 215 | 263 | 0.56 spacing | 222 |
| 188 | 272 | | 172 |
| 195 | 268 | | 201 average |
| 230 | 255 | | |
| 205 | 259 | | |
| 205 | 272 | | 224 |
| 165 | 268 | 0.79 spacing | 193 |
| 228 | 250 | | 181 |
| 221 | 278 | | 199 average |
| 205 average | 263 | | |
| | 273 | | |
| | 267 | | 169 |
| | 277 | 0.97 spacing | 132 |
| | 263 | | 141 |
| | 274 | | 147 average |
| | 264 | | |
| | 276 | | |
| | 269 | | |
| | 259 | | |
| | 274 | | |
| | 260 | | |
| | 276 | | |
| | 280 | | |
| | 262 | | |
| | 264 Average | | |
| MIL-HDBK-5 allowable in 0.008-in. gage = 22 lb | | | |

TABLE 14.- SPOT WELD STRENGTH, 0.027-in. GAGE 21-6-9

| Tension pull test, lb | Shear pull test, lb | Burst specimen test, lb | |
|---|---|---|---|
| 680 | 1155 | 1.30 spacing | 523 |
| 634 | 1140 | | 710 |
| 632 | 1175 | | 794 |
| 714 | 1120 | | 684 |
| 671 | 1180 | | 710 |
| 711 | 1165 | | 684 average |
| 743 | 1195 | | |
| 539 | 1250 | | |
| 738 | 1210 | 1.84 spacing | 693 |
| 655 | 1195 | | 778 |
| 672 average | 1150 | | 727 |
| | 1155 | | 693 |
| | 1174 average | | 710 |
| | | | 720 average |
| | | 2.25 spacing | 760 |
| | | | 785 |
| | | | 733 |
| | | | 683 |
| | | | 760 |
| | | | 740 average |
| MIL-HDBK-5 allowable in 0.027-in. gage = 120 lb | | | |

Based on the data derived from the foregoing tests, a series of 0.008 in. and 0.027 in. subsize specimens were designed and pressure cycle tested. The designs for each thickness was predicated on joint spacing of 1.0, 1.5 and 2.0 times that permitted by MIL-HDBK-5 allowables. The results of these tests are shown in tables 13 and 14.

It was concluded from the test results that in the thicker gages of target material, welded joints could be opened up to the limit of 1.5 times the value derived from MIL-HDBK-5. However, the spot weld spacing in the thinner materials should remain consistent with the handbook requirements.

Pressure cavity profile development: Preliminary test data derived from initial cycling testing in the subsize program clearly indicated that the fatigue life of the welded joints were dependent on the degree of bending in the material of the pressure cell adjacent to the spotweld. It was evident that the material adjacent to each joint had to be formed so that it assumed more nearly membrane loading, and minimized bending loading. For pressure-expanded specimens, cavity cells were developed to radii consistent with the detector ultimate pressure of 67 psi. Cavity expanding pressures were incrementally applied to achieve the cavity membrane radii producing stress levels of 15 000, 22 500, and 30 000 psi at ultimate pressure for each thickness-to-joint spacing combination. Test results indicated that, without exception, the profile developed on the basis of the 15 000 psi value best withstood the application of 14 to 49 psig pressure cycling.

It was concluded from these tests that all designs, regardless of material thickness combinations or joint spacing, should have cells developed such that the membrane stress of the material in the cell did not exceed 15 000 psi.

Detector joint geometry evaluation: There were five basic joint geometries used in subsize design, some of which were carried over from design approaches conceived by NASA-LRC and/or Martin Marietta during advanced studies. These geometries fall into the following groups:

1) Square or nearly square spot weld arrangement, forming a square pressure cavity;

2) The arrangement of spot welded joints to form a hexagonal cell. This approach was varied to use six corner spotweld joints, six corner welds with intermediate welds

along the hexagonal sides, and cavity peripheral seam welds interrupted to provide gas passages;

3) Pressure cavities formed by parallel seam welds with interruptions to provide gas transfer passages;

4) Spot welded joints arranged in concentric circular cavities;

5) Spot welded joints arranged to form triangular cavities.

Subsize test specimens were built and tested. The test results applicable to geometry evaluation are summarized below:

1) Square spot weld joint arrangements provided for more uniform development of pressure cell cavities and evenness for pressure expansion across the specimens. The arrangement also provided for a balanced pressure vessel system resulting in detector stability and higher resistance to fatigue failures under cyclic pressure loading;

2) Hexagonal patterns showed instability under static or cyclic pressure loading. The pressure cell profiles formed by pressure expansion did not develop in an uniform manner within individual cells or between cells. The unpredictable creasing effects at welded joints restrained the natural membrane profile of cells formed under pressure, resulting in increased bending stresses of the material under pressure cycling load. The degree of warpage resulting from pressure loading is shown in figure 53;

3) Test specimens having cavities formed by parallel seam welds in general failed to survive the pressure cycle tests. The failures resulted from the following conditions:

   - Instability of the specimens in the transverse direction of the cell length, resulting in warpage,

   - Seamweld termination failures as the result of erratic and excessive loads introduced into the joints;

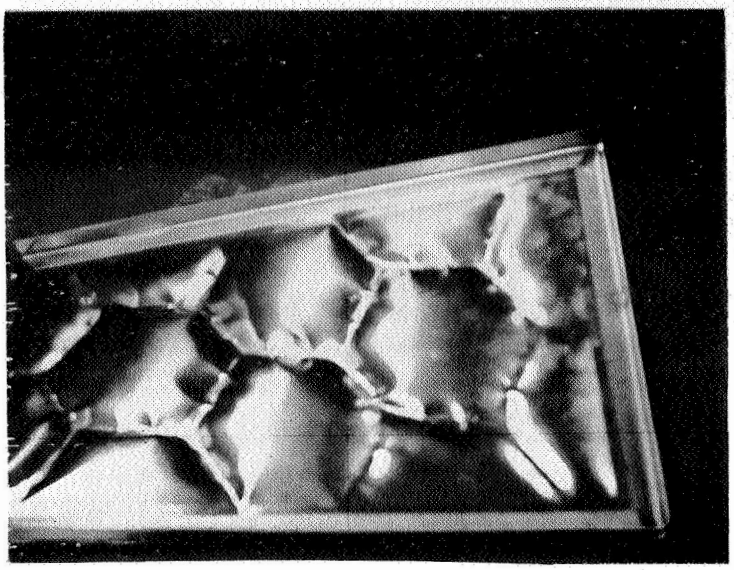

Figure 53.- Pressure Loading Warpage

4) The specimens having concentric spot weld arrangements showed a high degree of instability during cycle testing, resulting in early joint failures. It was also found that excessive pressure (300 psig or up) would be required to expand the cavities to acceptable levels;

5) The triangular cell specimens passed cyclic pressure tests, and maintained good out-of-plane stability. However, creasing was evident at the apex of the triangle.

The following conclusions were derived from this phase of subsize design, development, and tests:

1) Detectors having square spot weld joint arrays demonstrated high strength, good fatigue resistance, and marked stability under static and cyclic pressure loads. These designs were suitable for continued development;

2) The detectors having hexagonal patterns of joint attachments showed reasonably good individual cavity joint strength. However, because of the unpredictable creasing and cavity distortion induced by static and cyclic pressure loading, detector stability was questionable. These designs were suitable for further limited development;

3) Detectors having cavities formed by parallel seam welds demonstrated a high degree of dynamic instability during cyclic loading. This condition induced erratic loading at seam weld terminations. Continued development was required to ascertain all facets of the behavior of the detector under pressure loads;

4) The detector design having concentric circular joint arrangements were eliminated for continued development. the out-of-plane instability of the panel, requirements for excessive forming pressures and low resistance to fatigue to cycle pressures made this design too marginal;

5) The triangular pattern of joint arrangements for detectors showed high joint strength, reasonably good panel stability and good resistance to fatigue under cyclic pressure loads. These designs were suitable for continued development.

In summary, the pressure cavity geometries that passed this phase of the subsize test program were subjected to continued

development, test, and evaluation under the Reliability Pressure Test phase of the program, discussed later in this report.

Methods of pressure cavity development: Two methods were developed to form pressure cavities in the target material of the subsize test specimens -- preformed cavities and pressure-expanded cavities.

The preformed cavity of the target sheet was explosive-formed (but could have been press formed) into a female die having a geometrically defined cavity depth and weld position indentations. The target sheet boundary was formed in plane with the weld indentations. The parts thus formed were consistent with the design requirements for thin out and cavity configuration. This method of forming was limited to 0.027- and 0.042-in.-thick material for this program.

The application of pressure to completely welded specimen assemblies formed the cavity shape. The cavities were formed at discrete forming pressures selected to achieve the desired cavity profiles. The pressures required to form cavities in all thicknesses of material was in excess of 53.4 psig proof. This applied pressure has no deleterious effect on the joints or material of the specimens.

It was concluded that preforming target sheets by explosive forming was practical and suitable for design. However, it was found to be less economical than pressure forming. It was also found to be appropriate for use where the cavity volume is limited by closely spaced joints and where thinner sheets were combined with thicker target material.

The pressure expansion method of forming cavities proved to be practical, economical, and suitable for design applications. It was apparent that this forming technique imparted work hardening of the material adjacent to the joints, increasing the resistance to static and cyclic fatigue pressure failures.

Reliability pressure tests: The reliability pressure test phase of subsize development was conceived as a final design evaluation screen for weld joint geometries and for selection of full-size final designs. The results of this test phase were also used to determine the optimum joint spacing, cavity behavior under load, panel stability, and weld strength repeatability across groups of similar test specimens. In all, the program developed a measurement of reliability of design and processes to assure a high confidence in design applications to full-size detectors.

A description of designs created for this test, numbers of specimens, test applications, and results are shown in table 15.

Test specimens built for the C1A detector panel design (0.016 in./0.016 in.) combination, hexagonal joint arrangement are shown in figure 54. Test specimens built for the E1A detector design (0.042 in./0.042 in.) combination, square joint arrangement are shown in figure 55. These test specimen configurations are typical of these used for this test phase. The joint patterns developed in this phase of the program were projected to the anticipated design configurations to determine the effects of meteoroid penetration efficiencies. The results of this study are reflected in table 16.

The results of these tests and studies other than reliability evaluation are summarized below:

1) Designs with square spot welded array spaced up to 1.5 x basic (MIL-HDBK-5) developed allowables in the heavier materials (0.016, 0.027, and 0.042 in.) demonstrated good joint strength, resistance to fatigue, and good panel stability. Designs using 2.0 x basic allowables for spacing were marginal. The designs with thinner materials (0.002 and 0.008 in.) demonstrated the same characteristics as those having heavier material when using basic developed allowables, but did not lend themselves to increased joint loads. The application of this joint array to one-sided detectors (0.027 in./0.016 in. and 0.002 in./0.020 in.) demonstrated the same characteristics as balanced (same gage) target sheet combinations, with the exception that the cavity profiles formed in the thinner material under expansion pressures. The target efficiencies for this joint design ranged from 82.2% to 92.6% in thickness combinations using 0.0042-, 0.027-, 0.016-, and 0.008-in. material. For 0.002 in. combinations this efficiency range was 78.4%.

2) Designs with varied configurations of hexagonal joint patterns exhibited instability in individual pressure cavities resulting in panel warpage. This condition developed through pressure expansion with the boundaries constrained and cyclic pressure applications. The condition exerted erratic loads on individual joints causing premature failures. The problem was overcome by adding continuous stiffening members to the specimens. The target efficiencies for this joint design ranged between 82.1% and 82.3% in 0.008 in. and 0.016 in. material thickness combinations.

TABLE 15.- RELIABILITY PRESSURE TEST SUMMARY

| Drawing design | Configuration, (all dimensions are inches) | Specimen size, in. | Specimen number | Cavity development PFM-preform cavity PX-pressure expand, psig | Cycle test, 14-49.3 psig | Burst pressure, psig | Test results |
|---|---|---|---|---|---|---|---|
| [illegible]-01 | Balanced, 2 targets 0.008/0.008 square array, 0.56 spacing spot welded field, seam welded border | 4.12x4.12 | S/N 01 | 150 PX | 21 633 | 450 | Positive |
| | | | S/N 02 | 150 PX | 21 633 | 470 | Positive |
| | | | S/N 03 | 150 PX | 21 426 | 300 | Positive |
| | | | S/N 04 | 150 PX | 21 633 | 550 | Positive |
| | | | S/N 05 | 150 PX | 21 426 | 345 | Positive |
| | | | S/N 06 | 150 PX | 21 633 | 470 | Positive |
| | | | S/N 07 | 150 PX | 21 633 | 450 | Positive |
| | | | S/N 08 | 150 PX | 21 633 | 405 | Positive |
| | | | S/N 09 | 150 PX | 21 633 | 480 | Positive |
| | | | S/N 10 | 150 PX | 21 633 | 495 | Positive |
| B2-01 | Balanced, 2 targets 0.008/0.008 parallel cavities, 0.96 spacing, 0.50 transfer, all seam welded | 12.0x6.12 | S/N 01 | 90 PX | 8 880 | | Failed in cycle test |
| | | | S/N 02 | 90 PX | | | Failed during pressure expansion |
| | | | S/N 03 | 90 PX | 6 501 | | Failed in cycle test |
| | | | S/N 04 | 90 PX | 19 000 | | Failed in cycle test |
| | | | S/N 05 | 90 PX | | | Failed during pressure expansion |
| | | | S/N 06 | 90 PX | 21 860 | | Failed in cycle test |
| | | | S/N 07 | 90 PX | 6 501 | | Failed in cycle test |
| | | | S/N 08 | 90 PX | 6 502 | | Failed in cycle test |
| | | | S/N 09 | 90 PX | 6 502 | | Failed in cycle test |
| | | | S/N 10 | 90 PX | 8 880 | | Failed in cycle test |
| B4-01 | Balanced, 2 targets 0.008/0.008 point hexagonal array, 0.82 across flats, spot welded field, seam welded border | 3.78x5.48 | S/N 01 | 90 PX | 20 715 | | Failed in cycle test |
| | | | S/N 02 | 90 PX | 15 654 | | Failed in cycle test |
| | | | S/N 03 | 90 PX | 20 715 | | Failed in cycle test |
| | | | S/N 04 | 90 PX | 15 654 | | Failed in cycle test |
| | | | S/N 05 | 90 PX | 18 930 | | Failed in cycle test |
| | | | S/N 06 | 90 PX | | 196 | Verified reqm't for border stiffeners |
| | | | S/N 07 | 90 PX | | 504 | Verified reqm't for border stiffeners |
| | | | S/N 08 | 90 PX | | 375 | Verified reqm't for border stiffeners |
| | | | S/N 09 | 90 PX | | 131 | Verified reqm't for border stiffeners |
| | | | S/N 10 | 90 PX | | 206 | Verified reqm't for border stiffeners |
| B4-01A | Balanced, 2 targets, 0.008/0.008 hexagonal array, 0.82 across flats, spot welded field, seam welded border, with boundary stiffener | 3.78x5.48 | S/N 01 | 160 PX | 21 344 | 370 | Positive |
| | | | S/N 02 | 160 PX | 21 344 | 195 | Damaged specimen |
| | | | S/N 03 | 160 PX | 21 344 | 353 | Positive |
| | | | S/N 04 | 160 PX | 21 344 | 382 | Positive |
| | | | S/N 05 | 160 PX | 21 344 | 375 | Positive |
| | | | | Boundary restrained | | | |
| C1-01 | Balanced, 2 targets 0.016/0.016 square array, 0.91 spacing, spot welded field, seam welded border | 6.8x6.8 | S/N 01 | 170 PX | 21 344 | 400 | Positive |
| | | | S/N 02 | 170 PX | 21 344 | 350 | Positive |
| | | | S/N 03 | 170 PX | 21 344 | 365 | Positive |
| | | | S/N 04 | 170 PX | 21 344 | 365 | Positive |
| | | | S/N 05 | 170 PX | 21 344 | 375 | Positive |
| C1-02 | Balanced, 2 targets .016/.016 square array, 1.1 spacing, spot welded field, seam welded border | 6.8x6.8 | S/N 01 | 140 PX (0.112-in.) | 21 344 | 395 | Positive |
| | | | S/N 02 | 135 PX (0.110-in.) | 21 344 | 257 | Positive |
| | | | S/N 03 | 135 PX (0.111-in.) | 21 344 | 259 | Positive |
| | | | S/N 04 | 150 PX (0.114-in.) | 21 344 | 274 | Positive |
| | | | S/N 05 | 140 PX (0.113-in.) | 21 344 | 234 | Positive |
| C1A-01 | Balanced, 2 targets .016/.016 hexagonal multi-spot, 3.48 across flats, spacing .40, spot welded field, seam welded border | 12.9x12.4 | S/N 01 | 20 PX | | | Gas pressurization tube joint failed |
| | | | S/N 02 | 125 PX | 10 756 | | Cracked adjacent to border seam weld |
| | | | S/N 03 | 125 PX | 22 163 | 82 | |
| | | | S/N 04 | 125 PX | 19 836 | | Cracked adjacent to border seam weld |
| | | | S/N 05 | 125 PX | 21 344 | 92 | |

TABLE 15.- RELIABILITY PRESSURE TEST SUMMARY - continued

| Drawing design | Configuration (all dimensions are inches) | Specimen size, in. | Specimen number | Cavity development PFM-preform cavity PX-pressure expand, psig | Cycle test 14-49.3 psig | Burst pressure, psig | Test results |
|---|---|---|---|---|---|---|---|
| C1A-02 | Balanced, 2 targets .016/.016 hexagonal multi-spot, 3.48 across flats, .50 spacing, spot welded field, seam welded border | 14.2x11.7 | S/N 01 | 125 PX | 18 984 | | Parent mtl failure adjacent to weld nugget |
| | | | S/N 02 | 125 PX | 18 984 | | Parent mtl failure adjacent to weld nugget |
| | | | S/N 03 | 125 PX | 18 648 | | Parent mtl failure adjacent to weld nugget |
| | | | S/N 04 | 125 PX | 8 396 | | Parent mtl failure adjacent to weld nugget |
| | | | S/N 05 | 125 PX | 20 225 | | |
| C1B-01 | Triangular pattern, 1.00 in. between spot welds in field, seam welded border | 10.3x7.38 | S/N 01 | 130 PX | 21 355 | 325 | Positive |
| | | | S/N 02 | 110 PX | 21 355 | 333 | Positive |
| | | | S/N 03 | 110 PX | 21 355 | 344 | Positive |
| | | | S/N 04 | 100 PX | 21 355 | 345 | Positive |
| | | | S/N 05 | 100 PX | 21 355 | 345 | Positive |
| C2-01 | Balanced, 2 targets .016/.016 parallel cavities, 1.88 spacing, 1.40 transfer cavity, spot weld seam terminations, remainder seam welded | 12.0x10.7 | S/N 01 | 155 PX | 9 318 | | Failed at seam terminations |
| | | | S/N 02 | 155 PX | 3 525 | | Failed at seam terminations |
| | | | S/N 03 | 155 PX | 3 525 | | Failed at seam terminations |
| | | | S/N 04 | 155 PX | 9 318 | | Failed at seam terminations |
| | | | S/N 05 | 155 PX | 3 408 | | Failed at seam terminations |
| | | | S/N 06 | 155 PX | 6 696 | | Failed at seam terminations |
| | | | S/N 07 | 155 PX | 6 696 | | Failed at seam terminations |
| | | | S/N 08 | 155 PX | 6 696 | | Failed at seam terminations |
| | | | S/N 09 | 155 PX | 6 696 | | Failed at seam terminations |
| | | | S/N 10 | 155 PX | 6 696 | | Failed at seam terminations |
| D1A-01 | Balanced, 2 targets .027/.027 square array, 1.36 spacing, spot welded field, seam welded border | 8.2x8.2 | S/N 01 | 160 PX | 21 378 | 325 | Positive |
| | | | S/N 02 | 160 PX | 21 378 | 345 | Positive |
| | | | S/N 03 | 160 PX | 21 378 | 360 | Positive |
| | | | S/N 04 | 160 PX | 21 378 | 330 | Positive |
| | | | S/N 05 | 160 PX | 21 378 | 340 | Positive |
| D1A-02 | Balanced, 2 targets .027/.027 square array, 1.73 spacing, spot welded field, seam welded border | 8.2x8.2 | S/N 01 | 135 PX | 21 828 | 210 | Positive |
| | | | S/N 02 | 100 PX | 21 828 | 396 | Positive |
| | | | S/N 03 | 135 PX | 21 433 | 210 | Positive |
| | | | S/N 04 | 100 PX | 21 433 | 198 | Positive |
| | | | S/N 05 | 135 PX | 21 433 | 213 | Positive |
| D1B-01 | Balanced, 2 targets .027/.027 square array, 1.30 spacing, spot welded field, seam welded border | 11.0x8.5 | S/N 01 | PFM | 21 770 | 326 | Positive |
| | | | S/N 02 | PFM | 21 770 | 360 | Positive |
| | | | S/N 03 | PFM | 21 770 | 344 | Positive |
| | | | S/N 04 | PFM | 21 770 | 364 | Positive |
| | | | S/N 05 | PFM | 21 770 | 327 | Positive |
| D2A-02 | Dual, 2 targets and one separator .027/.016/.027 square array, .94 spacing, spot welded field, seam welded border | 13.8x11.0 | S/N 01 | PFM targets | N/A | 462 | Failed, spot weld delamination |
| | | | S/N 02 | PFM targets | N/A | 675 | Positive |
| | | | S/N 03 | PFM targets | N/A | 530 | Positive |
| | | | S/N 04 | PFM targets | N/A | 695 | Positive |
| | | | S/N 05 | PFM targets | N/A | 685 | Positive |
| D2B-01 | Dual, 2 targets .027/.027 and one separator .020 chem-milled from .100, square array, 1.29 spacing, spot welded field, seam welded border | 6.48x6.48 | S/N 01 | Chem-mill separator | N/A | 376 | Positive |
| | | | S/N 02 | Chem-mill separator | N/A | 404 | Positive |
| | | | S/N 03 | Chem-mill separator | N/A | 330 | Positive |
| | | | S/N 04 | Chem-mill separator | N/A | 297 | Positive |
| | | | S/N 05 | Chem-mill separator | N/A | 423 | Positive |
| D3A-02 | One sided, one target .027, one backup .016, square array, 1.1 spacing, spot welded field, seam welded border | 6.8x6.8 | S/N 01 | 105 PX (.040 Cavity) | 25 291 | 267 | Positive |
| | | | S/N 02 | 105 PX (.040 Cavity) | 25 291 | 177 | Positive |
| | | | S/N 03 | 105 PX (.041 Cavity) | 25 291 | 277 | Positive |
| | | | S/N 04 | 115 PX (.039 Cavity) | 25 291 | 249 | Positive |
| | | | S/N 05 | 115 PX (.041 Cavity) | 25 291 | 296 | Positive |
| D3B-01 | One sided, one target .027, one backup .016, square array, .94 spacing, spot welded field seams welded border | 13.8x12.2 | S/N 01 | PFM backup | 25 291 | 299 | Positive |
| | | | S/N 02 | PFM backup | 25 291 | 294 | Positive |
| | | | S/N 03 | PFM backup | 25 291 | 301 | Positive |
| | | | S/N 04 | PFM backup | 25 291 | 315 | Positive |
| | | | S/N 05 | PFM backup | 25 291 | 306 | Positive |
| E1A-01 | Balanced, 2 targets .042/.042 square array, 1.86 spacing, spot welded field, seam welded border | 8.7x8.7 | S/N 01 | 185 PX | 21 426 | 410 | Positive |
| | | | S/N 02 | 185 PX | 21 426 | 430 | Positive |
| | | | S/N 03 | 185 PX | 21 426 | 419 | Positive |
| | | | S/N 04 | 185 PX | 21 426 | 419 | Positive |
| | | | S/N 05 | 185 PX | 21 344 | 429 | Positive |

TABLE 15.- RELIABILITY PRESSURE TEST SUMMARY - concluded

| Drawing design | Configuration (all dimensions are inches) | Specimen size, in. | Specimen number | Cavity development PFM-preform cavity PX-pressure expand, psig | Cycle test, 14-49.3 psig | Burst pressure, psig | Test results |
|---|---|---|---|---|---|---|---|
| E1A-02 | Balanced, 2 targets .042/.042 square array, 2.64 spacing, spot welded field, seam welded border | 11.8x11.8 | S/N 01 | 150 PX (0.181 cavity) | 21 344 | 200 | Positive |
| | | | S/N 02 | 150 PX (0.180 cavity) | 21 344 | 200 | Positive |
| | | | S/N 03 | 150 PX (0.181 cavity) | 21 344 | 195 | Positive |
| | | | S/N 04 | 150 PX (0.183 cavity) | 21 344 | 197 | Positive |
| | | | S/N 05 | 150 PX (0.179 cavity) | 21 344 | 201 | Positive |
| E1B-01 | Balanced, 2 targets .042/.042 square array, 1.90 spacing, spot welded field, seam welded border | 15.3x11.5 | S/N 01 | PFM 2 targets | 45 645 | 277 | Positive |
| | | | S/N 02 | PFM 2 targets | 45 645 | 265 | Positive |
| | | | S/N 03 | PFM 2 targets | 45 645 | 219 | Positive |
| | | | S/N 04 | PFM 2 targets | 12 940 | | Metal failed adjacent to spot weld |
| | | | S/N 05 | PFM 2 targets | 45 645 | 279 | Positive |
| E1C-01 | Balanced, 2 targets .042/.042 equilateral triangular array, 2.08 spacing, spot welding field, seam welded border | 9.6x8.5 | S/N 01 | 175 PX | 21 344 | 384 | Positive |
| | | | S/N 02 | 175 PX | 21 344 | 389 | Positive |
| | | | S/N 03 | 175 PX | 21 344 | 378 | Positive |
| | | | S/N 04 | 175 PX | 21 344 | 381 | Positive |
| | | | S/N 05 | 175 PX | 21 344 | 377 | Positive |
| E1C-02 | Balanced, 2 targets .042/.042 equilateral triangular array, 2.94 spacing, spot welded field, seam welded border | 11.5x10.1 | S/N 01 | 100 PX (0.120 cavity) | 21 344 | 194 | Excessive reduction in burst strength |
| | | | S/N 02 | 100 PX (0.134 cavity) | 21 344 | 195 | Excessive reduction in burst strength |
| | | | S/N 03 | 100 PX (0.124 cavity) | 21 344 | 184 | Excessive reduction in burst strength |
| | | | S/N 04 | 100 PX (0.121 cavity) | 21 344 | 195 | Excessive reduction in burst strength |
| | | | S/N 05 | 100 PX (0.131 cavity) | 21 344 | 192 | Excessive reduction in burst strength |
| E2C-01 | Dual, 2 targets .042/.042 and one separator .020, square array, 1.3 spacing, spot welded field, seam welded border | 11.06x8.5 | S/N 01 | PFM targets | N/A | 675 | Positive |
| | | | S/N 02 | PFM targets | N/A | 600 | Positive |
| | | | S/N 03 | PFM targets | N/A | 700 | Positive |
| | | | S/N 04 | PFM targets | N/A | 600 | Positive |
| | | | S/N 05 | PFM targets | N/A | 700 | Positive |
| E2D-01 | Dual, 2 targets .042/.042 and one separator .041 chem-milled from .125, square array, 1.84 spacing, spot welded field, seam welded border | 8.4x8.4 | S/N 01 | Chem-mill separator | N/A | 165 | Relatively low burst strength |
| | | | S/N 02 | Chem-mill separator | N/A | 140 | Relatively low burst strength |
| | | | S/N 03 | Chem-mill separator | N/A | 185 | Relatively low burst strength |
| | | | S/N 04 | Chem-mill separator | N/A | 215 | Relatively low burst strength |
| | | | S/N 05 | Chem-mill separator | N/A | 206 | Relatively low burst strength |
| E3A-02 | One sided, one target .042, one backup .020, square array, 1.32 spacing, spot welded field, seam welded border | 7.9x7.9 | S/N 01 | 140 PX (0.047 cavity) | 21 344 | 307 | Positive |
| | | | S/N 02 | 140 PX (0.045 cavity) | 21 614 | 336 | Positive |
| | | | S/N 03 | 140 PX | 21 614 | 294 | Positive |
| | | | S/N 04 | 135 PX (0.046 cavity) | 21 614 | 306 | Positive |
| | | | S/N 05 | 135 PX (0.046 cavity) | 21 614 | 325 | Positive |
| E3B-02 | One sided, one target .042, one backup .020, square array, .94 spacing, spot welded field, seam welded border | 12.2x11.0 | S/N 01 | PFM backup | 21 344 | 409 | |
| | | | S/N 02 | PFM backup | | | Failed. Forming crack in metal |
| | | | S/N 03 | PFM backup | 21 344 | 350 | |
| | | | S/N 04 | PFM backup | | | Failed. Forming crack in metal |
| | | | S/N 05 | PFM backup | 21 344 | 367 | |
| F1A-01 | Balanced, 2 targets .002, one core .016, square array, .37 spacing, spot welded field, seam welded border | 6.5x4.8 | S/N 01 | 150 PX (0.037 cavity) | 21 344 | 270 | Positive |
| | | | S/N 02 | 150 PX (0.037 cavity) | 21 344 | 290 | Positive |
| | | | S/N 03 | 150 PX (0.047 cavity) | 21 344 | 375 | Positive |
| | | | S/N 04 | 150 PX (0.041 cavity) | 21 344 | 335 | Positive |
| | | | S/N 05 | 150 PX (0.035 cavity) | 21 344 | 365 | Positive |
| | | | S/N 06 | 150 PX (0.036 cavity) | 21 344 | 375 | Positive |
| | | | S/N 07 | 150 PX (0.036 cavity) | 21 344 | 260 | Positive |
| | | | S/N 08 | 150 PX | 21 344 | 225 | Positive |
| | | | S/N 09 | 150 PX (0.037 cavity) | 21 344 | 265 | Positive |
| | | | S/N 10 | 150 PX (0.035 cavity) | 21 344 | 325 | Positive |
| F1B-01 | Balanced, 2 targets .002, one core .016, parallel cavities, .50 spacing, .37 transfer cavities, spot welded seam terminations, remainder seam welded | 6.5x4.8 | S/N 01 | 150 PX (0.018 cavity) | 21 344 | 170 | Positive |
| | | | S/N 02 | 150 PX (0.026 cavity) | 21 344 | 172 | Positive |
| | | | S/N 03 | 150 PX (0.025 cavity) | 21 344 | 236 | Positive |
| | | | S/N 04 | 140 PX (0.025 cavity) | | | Seam weld leaked at 140 psig |
| | | | S/N 05 | 150 PX (0.027 cavity) | | | Seam weld leaked at 150 psig |
| | | | S/N 06 | 150 PX (0.027 cavity) | | | Seam weld leaked at 150 psig |
| | | | S/N 07 | 120 PX (0.023 cavity) | | | Seam weld leaked at 120 psig |
| | | | S/N 08 | 150 PX (0.027 cavity) | 21 320 | | Seam weld leaked during cycle test |
| | | | S/N 09 | 150 PX (0.030 cavity) | 21 344 | 196 | Positive |
| | | | S/N 10 | 150 PX (0.025 cavity) | 21 344 | 146 | Positive |

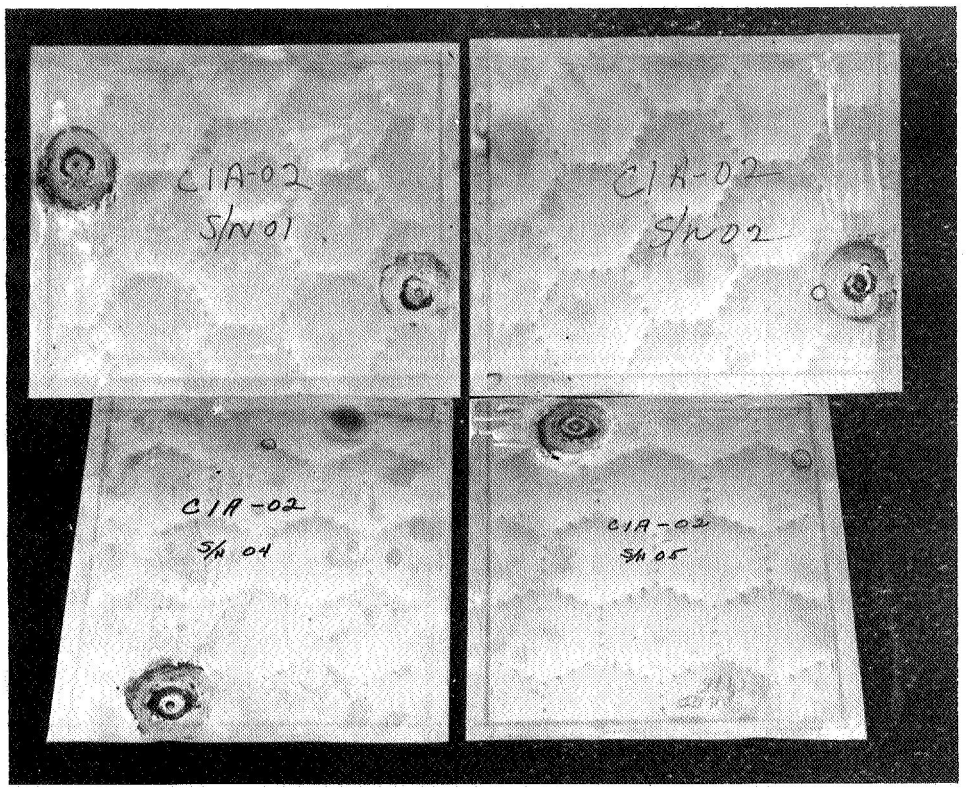


Figure 54.- Configuration C Test Specimen

Figure 55.- Configuration E Test Specimens

TABLE 16.- TARGET AREAS AND EFFICIENCIES

| Configuration | Total area available, in.$^2$ (a) | Effective target area, in.$^2$ (b) | Area efficiency, % |
|---|---|---|---|
| B1 -01 | 960 | 788.9 | 82.2 |
| B2 -01 | 960 | 773.4 | 80.5 |
| B4 -01 | 960 | 790.4 | 82.3 |
| C1 -01 | 960 | 791.4 | 82.4 |
| C1 -02 | 960 | 795.0 | 82.8 |
| C1A-01 | 960 | 789.4 | 82.3 |
| C1A-02 | 960 | 792.3 | 82.1 |
| C1B-01 | 960 | 791.4 | 82.4 |
| C2 -01 | 960 | 760.6 | 79.3 |
| D1A-01 | 3920 | 3611.1 | 92.1 |
| D1A-02 | 3920 | 3628.7 | 92.6 |
| D1B-01 | 3920 | 3528.2 | 90.0 |
| D2A-02 | 3920 | 3480.0 | 88.8 |
| D2B-01 | 3920 | 3479.3 | 88.7 |
| D3A-02 | 1960 | 1793.3 | 91.5 |
| D3B-01 | 1960 | 1747.7 | 89.1 |
| E1A-01 | 3920 | 3612.0 | 92.2 |
| E1A-02 | 3920 | 3625.8 | 92.6 |
| E1B-01 | 3920 | 3569.0 | 91.2 |
| E1C-01 | 3920 | 3611.0 | 92.2 |
| E1C-02 | 3920 | 3627.4 | 92.6 |
| E2C-01 | 3920 | 3485.4 | 88.9 |
| E2D-01 | 3920 | 3551.3 | 90.6 |
| E3A-02 | 1960 | 1804.6 | 92.1 |
| E3B-02 | 1960 | 1752.7 | 89.4 |
| F1A-01 | 960 | 752.2 | 78.4 |
| F1B-01 | 960 | 636.5 | 66.4 |

(a) Areas based on envelope dimensions specified in the Statement of Work.

(b) The areas shown are net, and reflect the reduction of the total area by field joint areas, boundary and switch areas.

3) Designs with parallel seam welded cavities consistently failed static and cyclic pressure loads. It was found that the specimens distorted from pressure pulsing motions under cyclic pressures, introducing excessive and unpredictable loads on seam weld terminations at the gas transfer passages. Detectors having this style joint design had an area efficiency range of 79.3% to 80.5%.

4) The designs having spot welded joints arranged in triangular patterns based on 1.0 x developed allowables passed all phases of the cyclic and static pressure tests. However, the joint spacing based on 1.5 x developed allowables in the 0.042 in./0.042 in. material combination showed a marked reduction in burst strength after being subjected to cyclic pressures. The target area efficiency for this joint design ranged from 82.4% to 92.6%.

Reliability evaluation: Based on the results of the tests, a reliability analysis was performed on each of the designs. The analysis of the B1 standard spacing design is shown in table 17. This table typically reflects the methods used in analyzing all of the designs.

The results of this evaluation is summarized in table 18. The life cycle reliability data shown in the table is identical with the probability of surviving ultimate design allowable. The ultimate values were established after the specimens were pressure cycled.

## PROCESS DEVELOPMENT AND FABRICATION

### Preliminary Design and Development Phase

Process development.- The earliest subsize detector specimens were made up in resistance welded pressure-expanded designs. Spot weld schedules were quickly developed that met the handbook strength requirements used in design. Corresponding data were not available for resistance seam welds and some simple specimens were developed to corroborate seam weld strength projections made by Engineering. Welding of the three unequal plies of the "F" configuration particularly without the "peel" sheet gave less than satisfactory results early in the program and remained an open development item for some time after the end of the first and second phases.

TABLE 17.- RELIABILITY TEST DATA

Configuration: B1 STD Spacing 0.008 x 0.008-in. square array spotweld pressure expand 0.56 spacing 21 344 cycles

| Sample | Pressure, psi | Spot spacing | Spot loading, lb (Xi) |
|---|---|---|---|
| 1 | 450 | .56 | 141.12 |
| 2 | 470 | .56 | 147.39 |
| 3 | 550 | .56 | 172.48 |
| 4 | 470 | .56 | 147.39 |
| 5 | 450 | .56 | 141.12 |
| 6 | 406 | .56 | 127.01 |
| 7 | 480 | .56 | 150.53 |
| 8 | 495 | .56 | 155.23 |
| | | | = 1182.27 |

$\bar{X}$ = 147.78

S = 12.2

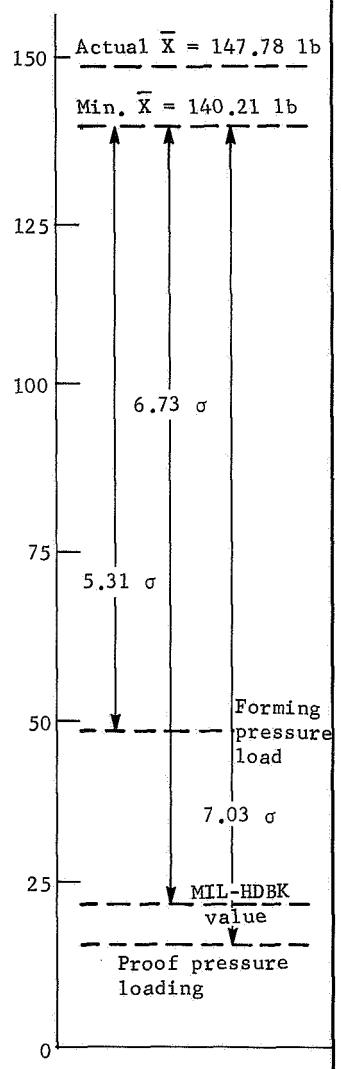


L = Minimum spot weld

Allowable MIL-HDBK-5 (22 lb)

Safety margin (50% confidence) = $\frac{\bar{X}-L}{S} = \frac{147.78-22}{12.2}$ = 10.31 STD Deviation of safety margin

Minimum strength average (95% confidence level)

$\bar{X}$ = 140.21

Maximum STD deviation (95% confidence level)

= 17.56

Strength safety margin (95% confidence level)

S.M. = 6.73

Probability of surviving proof pressure (53.4 psi or 16.75 lb)

Pa = .999 999 999 318 (single detector)

Pa = .999 999 998 636 (dual detector)

Probability of surviving ultimate design allowable (22 lb)

Pa = .999 999 999 440 (single detector)

Pa = .999 999 998 88 (dual detector)

Probability of surviving forming pressure (150 psi or 47.04 lb)

Pa = .999 963 (single detector)

Pa = .999 927 (dual detector)

Configuration: B1 STD spacing

| Sample | Xi | $(Xi-\bar{X})$ | $(Xi-\bar{X})^2$ |
|---|---|---|---|
| 1 | 141.12 | - 6.66 | 44.36 |
| 2 | 147.39 | - .39 | .15 |
| 3 | 172.48 | 24.70 | 610.09 |
| 4 | 147.39 | - .39 | .15 |
| 5 | 141.12 | - 6.66 | 44.36 |
| 6 | 127.01 | -20.77 | 431.39 |
| 7 | 150.53 | 2.75 | 7.56 |
| 8 | 155.23 | 7.45 | 55.50 |
| | | | 1193.56 |

$S = \frac{(Xi-\bar{X})^2}{n}$

S = 149.2

S = 12.2

TABLE 17.- RELIABILITY TEST DATA - Concluded

$$\bar{X} = \sum_{i=1}^{8} \frac{Xi}{n} = \frac{1182.27}{8} = 147.78$$

STD Error of the mean

$$\bar{X} = \frac{S}{n-1} = \frac{12.2}{2.65} = 4.60$$

STD error of the STD deviation

$$S = \frac{S}{2(n-1)} = \frac{12.2}{3.74} = 3.26$$

Minimum strength average @ 95% confidence level

$$A = \bar{X} - 1.645\ (4.60) = 147.78 - 7.57 = 140.21$$

Maximum STD deviation @ 95% confidence level

$$B = S + 1.645\ (3.26) = 12.2 + 5.36 = 17.56$$

Strength safety margin @ 95% confidence level

$$S.M. = \frac{140.21-22}{17.56} = \frac{118.21}{17.56} = 6.73$$

The B1 detector configuration would have 660 spot welds.

Probability of surviving proof pressure

$$R_T = R = (.999\ 999\ 999\ 998\ 966)^{660}$$

$$R = 1-(.000\ 000\ 000\ 001\ 034)^{660}$$

$$R = .999\ 999\ 999\ 318 \text{ (single detector)}$$

$$R = .999\ 999\ 998\ 636 \text{ (dual detector)}$$

Probability of surviving ultimate design allowable (22 lb)

$$R_T = R = (.999\ 999\ 999\ 991\ 517)^{660}$$

$$R = 1-(.000\ 000\ 000\ 008\ 483)\ 660$$

$$R = .999\ 999\ 999\ 440 \text{ (single detector)}$$

$$R = .999\ 999\ 998\ 88 \text{ (dual detector)}$$

Probability of surviving forming pressure (47.04 lb)

$$R_T = R = (.999\ 999\ 945\ 2)^{660}$$

$$R = .999\ 963 \text{ (single detector)}$$

$$R = .999\ 927 \text{ (dual detector)}$$

TABLE 18.- CONFIGURATION RELIABILITY AND MARGINS

| Configuration | Forming pressure reliability | Life cycle reliability | Strength safety margin |
|---|---|---|---|
| B1 -01 | $.9^{4}27$ | $.9^{8}88$ | 6.36 |
| B2 -01 | 0 | 0 | ---- |
| B4 -01 | $.9^{9}3$ | $.9^{12}85$ | 4.64 |
| C1 -01 | $.9^{9}856$ | $.9^{25}58$ | 4.98 |
| C1 -02 | .99738 | $.9^{11}8$ | 3.62 |
| C1A-02 | 0 | 0 | ---- |
| C1A-02 | 0 | 0 | ---- |
| C1B-01 | $.9^{20}$ | $.9^{58}$ | 4.85 |
| C2 -01 | 0 | 0 | ---- |
| D1A-01 | $.9^{18}85$ | $.9^{22}$ | 5.08 |
| D1A-02 | $.9^{9}$ | $.9^{25}$ | 3.05 |
| D1B-01 | NA | $.9^{23}$ | 4.66 |
| D2A-02 | NA | .9944 | 4.28 |
| D2B-01 | NA | .902 | 4.54 |
| D3A-02 | .99985 | $.9^{9}547$ | 3.86 |
| D3B-01 | NA | $.9^{22}88$ | 4.03 |
| E1A-01 | .935 | .960 | 6.25 |
| E1A-02 | .920 | .970 | 2.95 |
| E1B-01 | NA | .99874 | 3.72 |
| E1C-01 | $.9^{55}$ | $.9^{86}$ | 6.16 |
| E1C-02 | $.9^{9}287$ | $.9^{35}$ | 3.04 |
| E2C-01 | NA | $.9^{11}314$ | 4.53 |
| E2D-01 | NA | .0032 | 2.34 |
| E3A-02 | $.9^{8}583$ | $.9^{17}$ | 4.49 |
| E3B-01 | NA | 0 | 4.03 |
| F1A-01 | ---- | .544 | 4.35 |
| F1B-01 | 0 | 0 | ---- |

The brazing process initially selected called for a hydrogen atmosphere at approximately 2000°F with an 82% gold-18% nickel filler alloy. This alloy was selected for high strength, and a minimal tendency to attack and dissolve the base metal during the brazing operation. Also, it wet and filled the capillary joint interface even though the surface oxide reduction is marginal. The procedure that was effective used 0.002- to 0.004-in.-thick brazing alloy shim tabs on each preformed node as shown in figure 56. The placement was assured by small capacitor discharge spot welds. Elongated tabs (strips) were also placed around the periphery of the panel. The two halves of the panel were assembled and held into relative alignment by jigging or by jig-spot welding. One or more of the assemblies was placed in a high temperature muffle purged with flowing argon for 10 minutes, followed by a purge of hydrogen. With hydrogen flowing, the sealed muffle was then introduced to a brazing furnace, and the temperature stabilized at the brazing temperature. Early experiments included brazing temperatures in the range 1750° to 2100°F, for 5 to 40 minutes. Only designs using chem-milled core sheets or preformed target sheets were considered for brazing. These provided a node upon which the braze alloy could be placed, and minimized the need for "stop-off" to restrict flow of the molten alloy.

Early problems with the process have included composition control of the hydrogen, and time-temperature control of sufficient precision to prevent excessive aggression (dissolving) of 0.002-in. stainless steel target sheets by the brazing alloy at the brazing temperature. Braze joint strengths were sufficiently encouraging to continue experimentation.

More than anticipated difficulty was encountered in resistance welding preformed sheets. It was necessary to develop a preformed node geometry that was compatible with weld electrode geometries, and also to allow some clearance between the side of the node and the sides of the electrodes. Allowing for electrode-to-node clearance, and avoiding the incorporation of an electrode whose cone angle was so steep as to cause "mushrooming", the resistance welding nugget became a rather small proportion of the total area available at the base of the node pedestal.

Target sheet preforming process development was also more time consuming than anticipated, primarily because of the necessity to optimize the geometry of the preformed node. Steep sides on the node were desired to obtain maximum moment of inertia for the vibration environment. However, steep sides

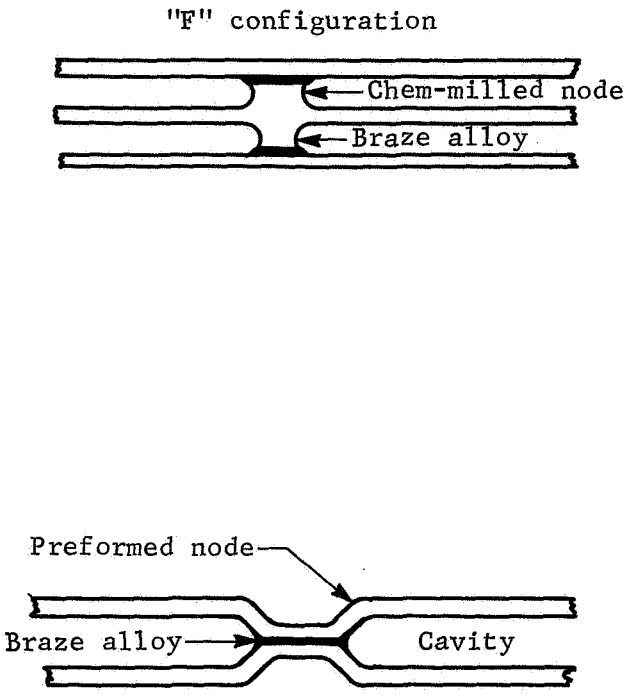


Figure 56.- Brazed Joints used in MPDD Program

were difficult to form because of high strain requirements. These sides also made it difficult to resistance spot weld at the base of the node. Thus, compromises were necessary. However, successful procedures were developed using a single die and explosive forming as shown in figure 57. After placing the blank over the die, the cavity between the die and the blank is sealed. A sheet explosive is then placed on a cardboard standoff approximately 6 in. above the die. The die and explosive are then lowered under 24 in. of water, and the explosive is detonated. With this procedure the explosive and water act as a fluid pressure media to emboss the blank onto the die. In subsequent forming experiments, a block of rubber, pushed downward by a press was substituted for the explosive. Dies for this process were made by conventional machining and by chem-milling. Both processes appear to be satisfactory. The node cross section can be more precisely controlled by conventional machining, while the tolerances on node spacing can be held tighter with chem-milling.

Chem-milling procedures were developed for 304 stainless steel, 21-6-9 stainless steel, and for low alloy hardenable steels for explosive forming dies. The only material that gave appreciable difficulty was the 21-6-9, because no experience existed with this material. Chem-milling solutions must be "balanced" to obtain uniform etching rates for each new material. Early experiments resulted in local erosions as shown in the top specimen of figure 58. However, by adjusting the solution and by experimenting with the geometry of immersion of the part in the bath -- the latter is important in that it controls the path of hydrogen bubbles which are given off by the reaction -- the much improved geometry control shown in the lower specimen of figure 58 was obtained.

As part of the task to develop processes to vary the absorptivity ($\alpha$) and emissivity ($\epsilon$) these properties were measured early in the phase for a number of specimens of 304L stainless steel. Samples were obtained from Armco Steel, Rodney Metals, and Republic Steel, as well as hand polished samples from NASA-LRC. Tests were also conducted early in the program to verify that the Spadone Vapor Hone would be useful in modifying $\alpha$ and $\epsilon$. The dull finish Armco 21-6-9 received from Rodney Metals and the Esco Corporation had higher $\alpha$ values than the Armco sample card, indicating some difference because of the different alloy or texture of the rolls or cleaning etchant. Most of the experiments performed early in the program were directed toward raising both $\alpha$ and $\epsilon$ to reduce the value of $\alpha / \epsilon$. This required a much larger percentage increase in $\epsilon$. This was done because

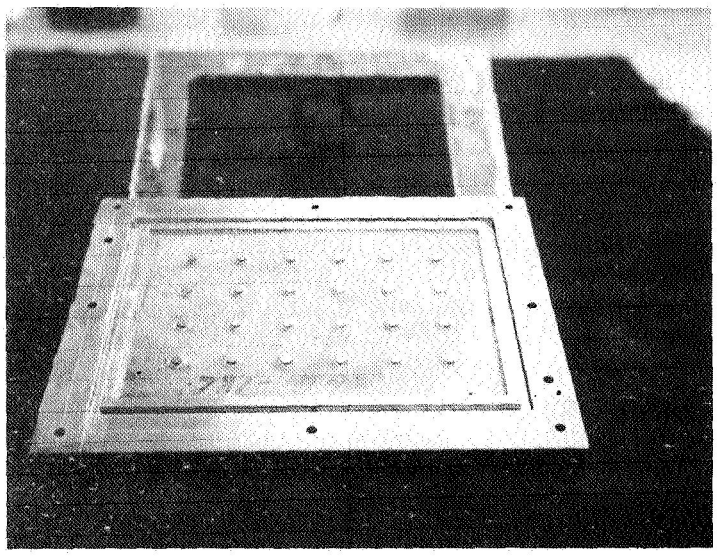

(a) Die Face with Raised "Nodes" and Edges. "O" Ring Groove Seals Blank-Die Cavity, which is Evacuated

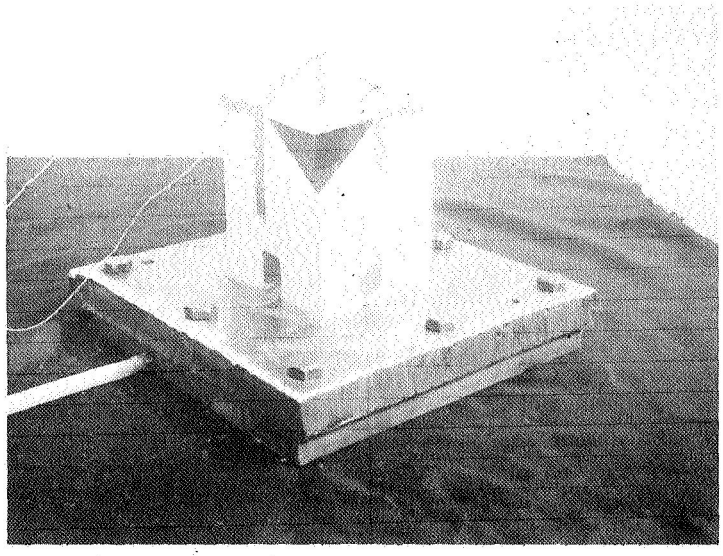

(b) Ready for Shot, Showing Vacuum Line, Holddown Frame, Card-Board "Stand-Off", Sheet Explosive and Electric Cap.

Figure 57.- Explosive Forming Setup

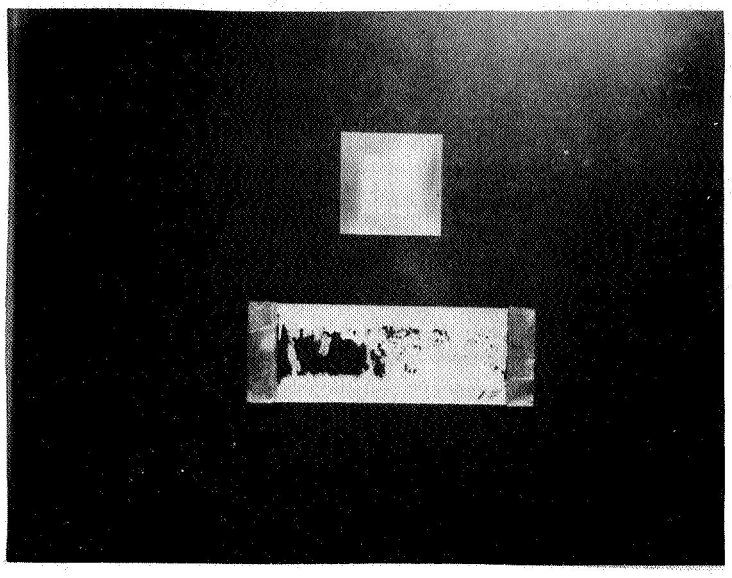

Figure 58.- Chem-Milled Process Comparisons

the material as-received had a value of $\alpha / \epsilon$ very close to the maximum goal set for the program.

The experiments were primarily vapor honing, i.e., impinging a slurry of water and aluminum oxide grit at various air and water pressure combinations exposure times and grit sizes. Electropolishing was also shown to be useful for raising the $\alpha / \epsilon$ value. Some data were also obtained on the effect of heating on $\alpha / \epsilon$. Hand polishing had little effect in changing the as-received values of $\alpha$ and $\epsilon$.

During the last half of the first phase there was much emphasis on the determination of the statistical distribution of weld strengths at selected machine settings, for each thickness combination. Comparisons of shear test and peel test specimens (single pull tension) showed that peel test specimens optimize at lower welding heats than shear specimens. The ratio of shear-to-peel strength is a factor which can range up to 15:1 in some materials. The standard deviation of peel specimens is larger than equivalent shear specimens. This characteristic behavior is indicative of a system very sensitive to process variables. The data was used to revise weld machine settings so that small perturbations in parameter settings would not result in inferior welds.

Welding machine certifications were also performed at this time. Some progress was made in the weld process development for the 0.002 to 0.016 to 0.002-in. sandwich used in the "F" configuration detectors. The peel sheet enhanced our ability to obtain consistently strong welds and its use was recognized by NASA-LRC. During this period the welds that had a "dog-bone" shape in cross section, as seen in figure 59, produced higher and more consistent strength results than the classical rectangular nugget for this configuration.

Brazing development in the latter half of the first phase was limited to the "F" configuration as a possible backup to resistance welding development in that configuration. The results were mixed. Progress was made in reducing erosion of the stainless steel by using less braze alloy and by refining the time temperature cycle of the process. Specimens were made that had high strength joints which, when tested to failure, failed in the parent metal rather than in the braze. The specimens, however, were still highly oxidized in appearance and had inconsistent survival times in pressure cycling (fatigue) tests.

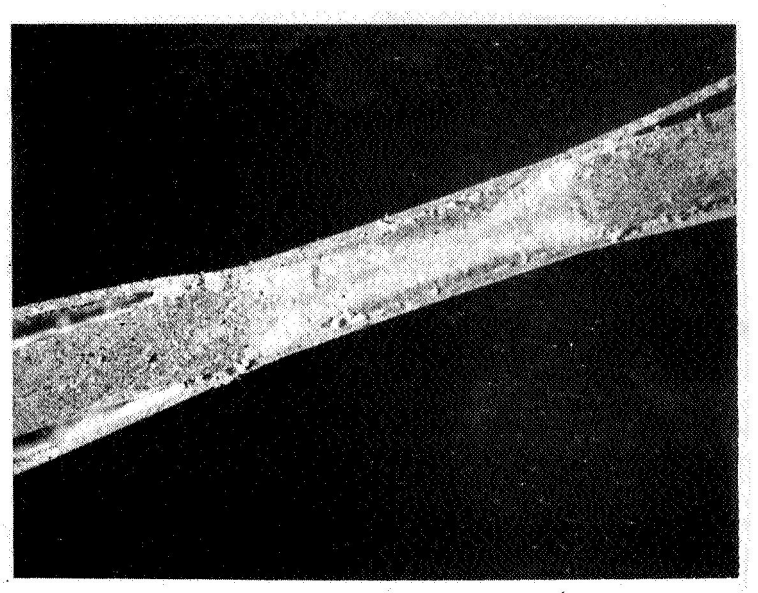

Figure 59.- Three-Play Weld showing "Dog-Bone" Appearance

Tooling.- Early tooling requirements consisted of a large number of polypropolene templates drilled out in the detector joint patterns. These were used to guide the welding electrodes to the specified patterns for both spot and seam welded subsize detectors. Material handling tools were also made early in the program. Plastic-lined plywood box racks were made up to handle the 0.001, 0.002, 0.008, and 0.016-in. coils of stainless steel. One of these is shown in figure 60. Figure 61 shows one of the A-frame trucks made for moving full-size detector details. A template for chem-milling the joint pattern of one of the full-size detector configurations is shown on the truck. Metal frame forms with clamps were made up in the two basic detector sizes to hold the detector details during spot welding and subsequent edge drilling. As the candidate full-size designs were released, polypropolene templates were made up with the joint pattern array to guide weld locations. Figures 62 and 63 show a 12x40 in. and a 40x49 in. template, respectively. These templates were clamped together in the metal frames together with the stainless steel target sheet details, as shown in figure 64. The entire assembly is rolled on a special table (also in fig. 64) to facilitate the large number of welding operations. Seam welding of the detector edges was done subsequent to welding the pattern in the target field. A special table with nylon rollers shown in figure 65 was used for seam welding. Tooling also supported Engineering Test in the fabrication of part of the pressure cycle test fixture.

Some specialized forming tools were made during this phase. Die sets to form the flange or "volcano" in the target sheets into which the pressure switch would be welded are shown in figure 66. Figures 67 and 68 show two steps in the forming operation. During this phase "dummy" pressure switches were used to simulate the mass of the real pressure switches. These were made at Martin Marietta. Figure 69 shows a dummy switch welded into the formed target sheet volcano. A special forming tool was also made for the remotely mounted pressure switch as designed for configurations "B" and "F" late in the first phase. This tool and the formed cup are shown in figure 70. Two piece frames were also made up to restrain the detectors from warping during pressure expansion. These were held in a 150-ton hydraulic platen press during the pressurization. Figure 71 shows a restraining frame with a 12x40-in. detector. An automatic welding tool was designed and built to weld pressure switches into either the raised volcano flange or the formed cup depending on the detector configuration. This tool is shown on figure 72.

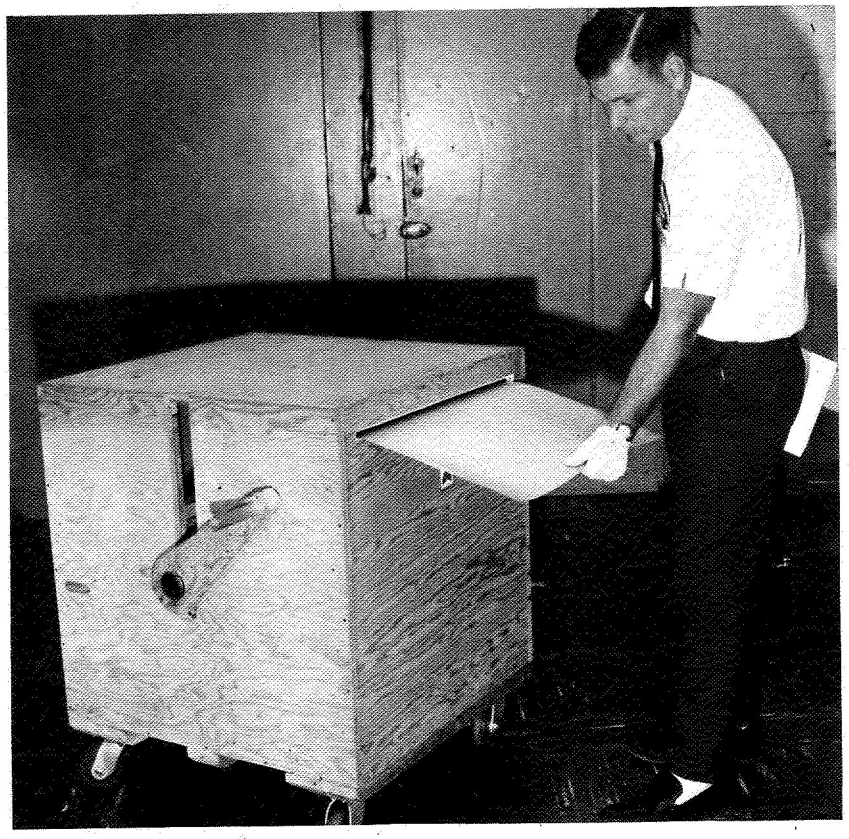

Figure 60.- Foil Reel Rack

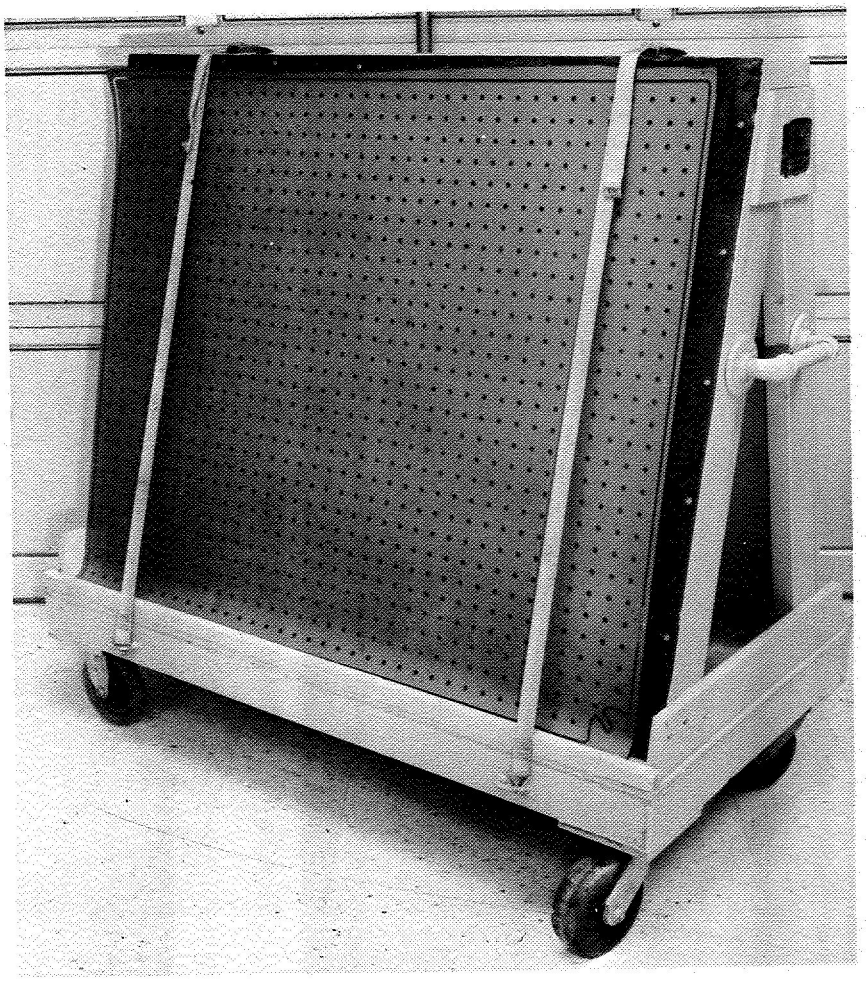

Figure 61.- Chem-Milling Template on A-Frame Handling Truck

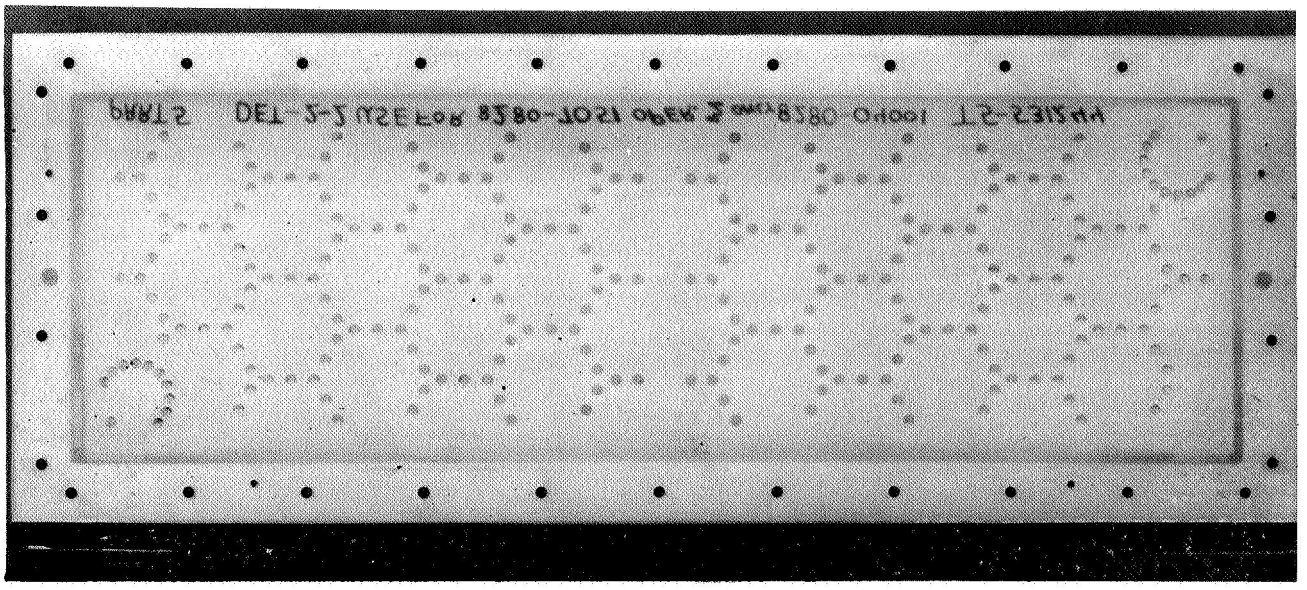

Figure 62.- Vinyl Spot Welding Template, 12x40 in.

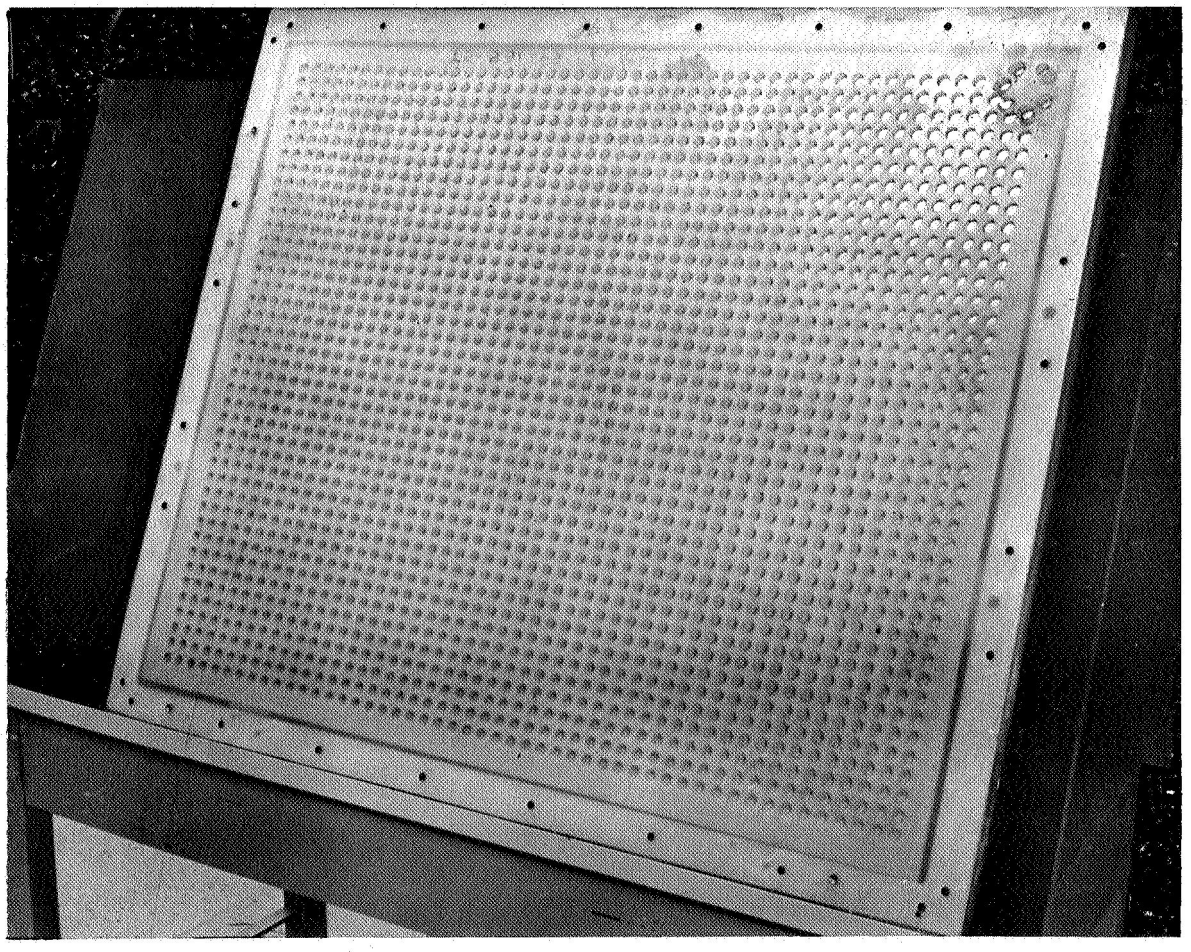

Figure 63.- Vinyl Spot Welding Template, 40x49 in.

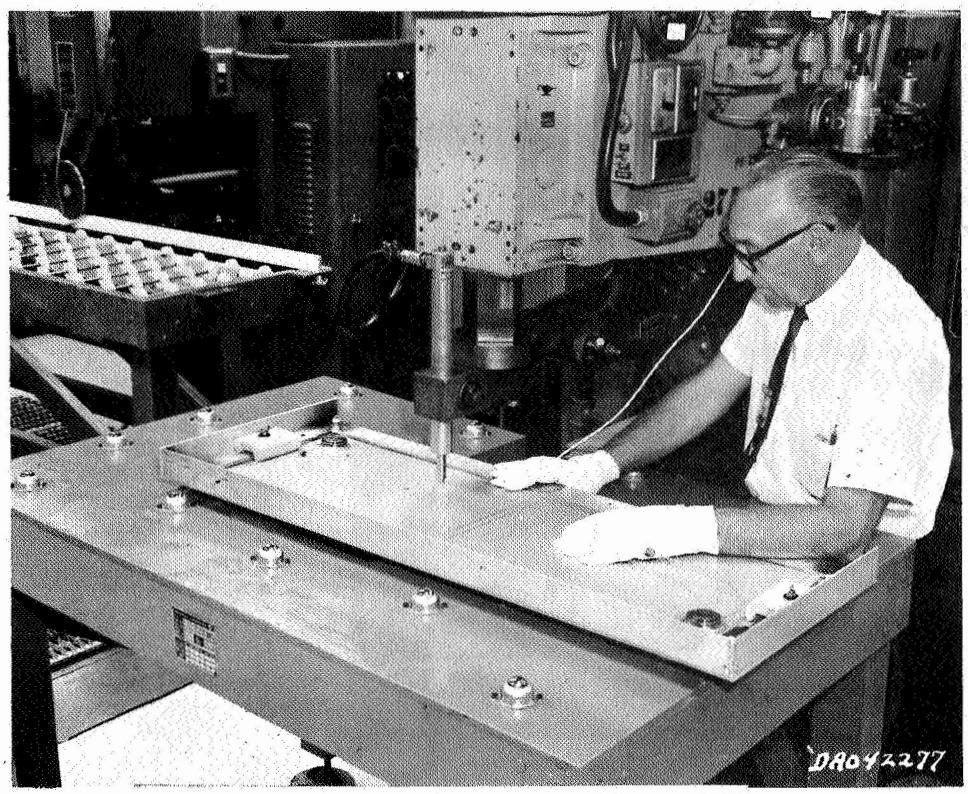


Figure 64.- Spot Welding Showing Table and Frame Holding Target Sheets and Vinyl Template

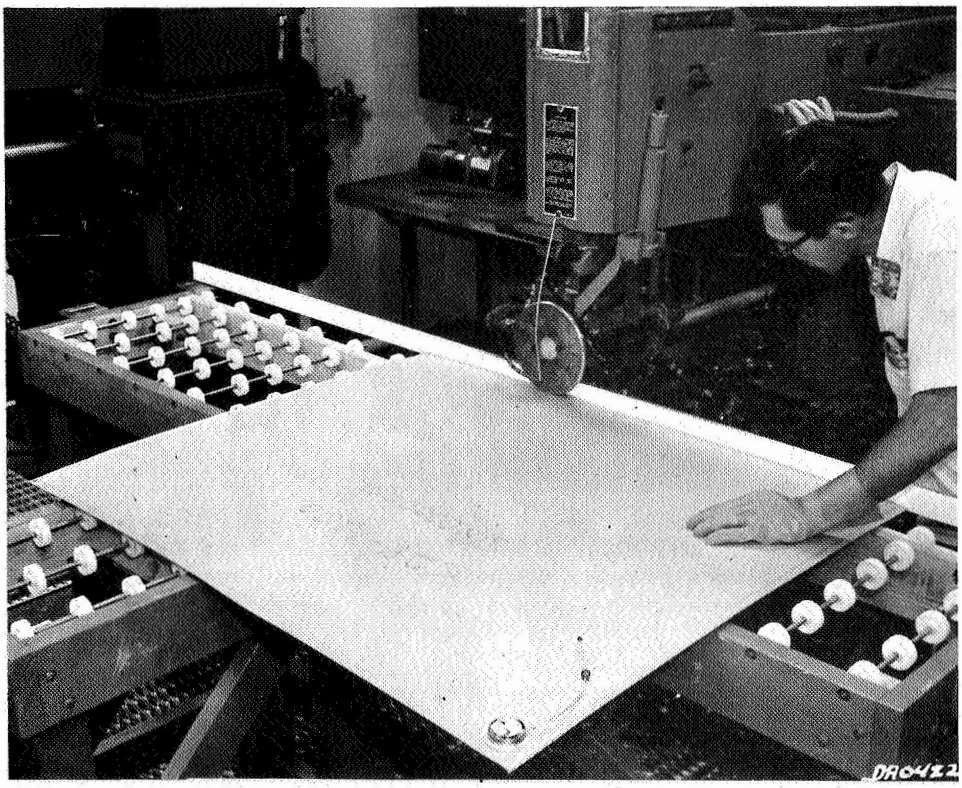

Figure 65.- Seam Welding Table

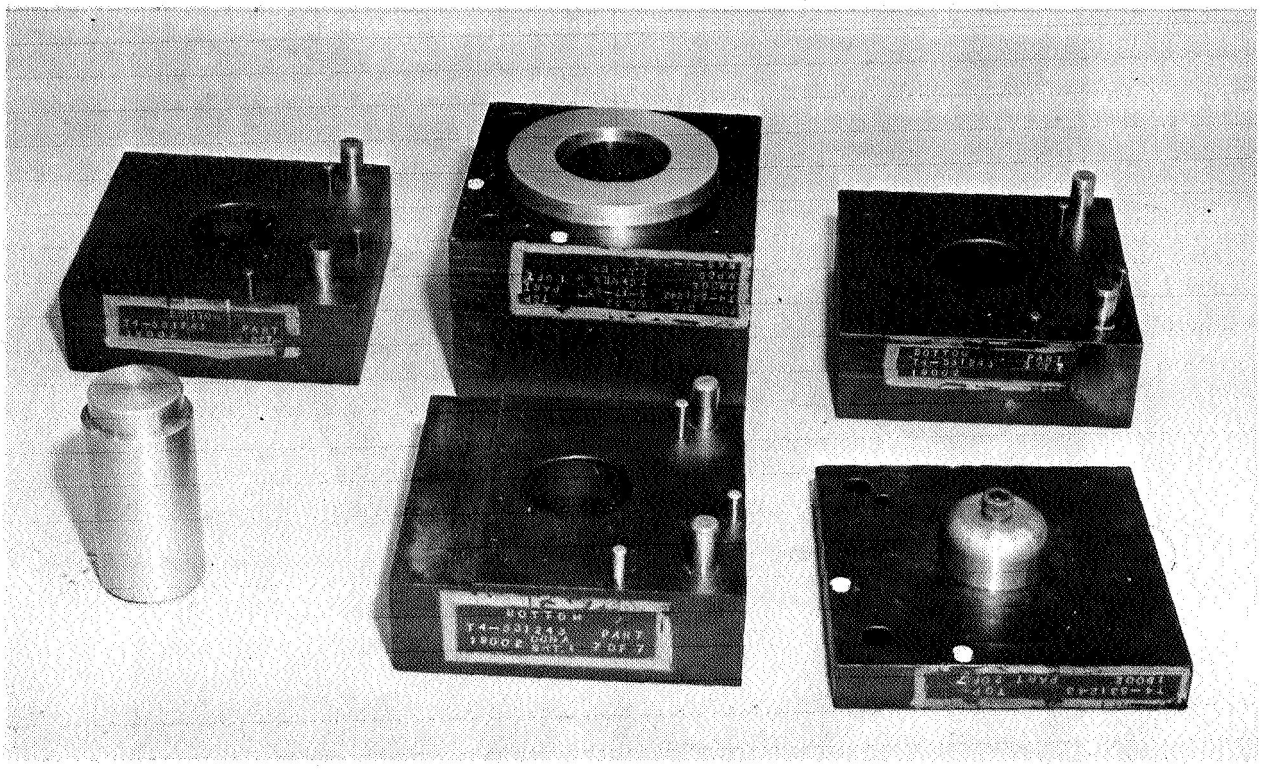

Figure 66.- Pressure Switch "Volcano" Form Die Sets

Figure 67.- Forming of Pressure Switch "Volcano"

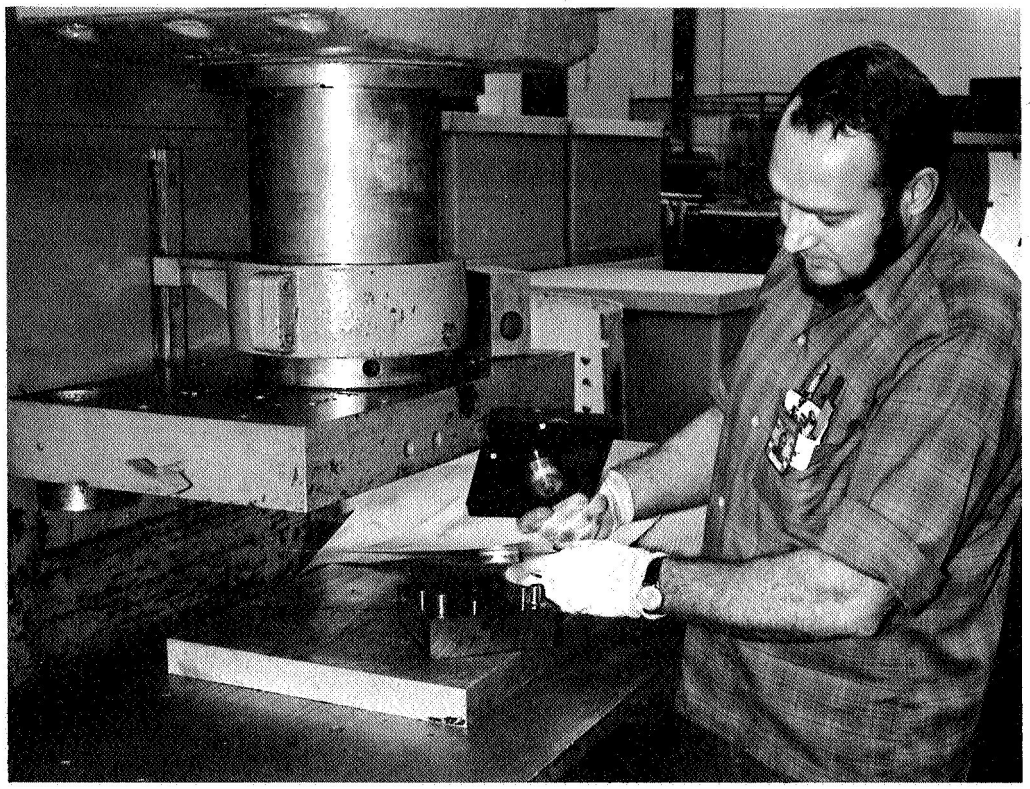

Figure 68.- Final Step in Forming of "Volcano"

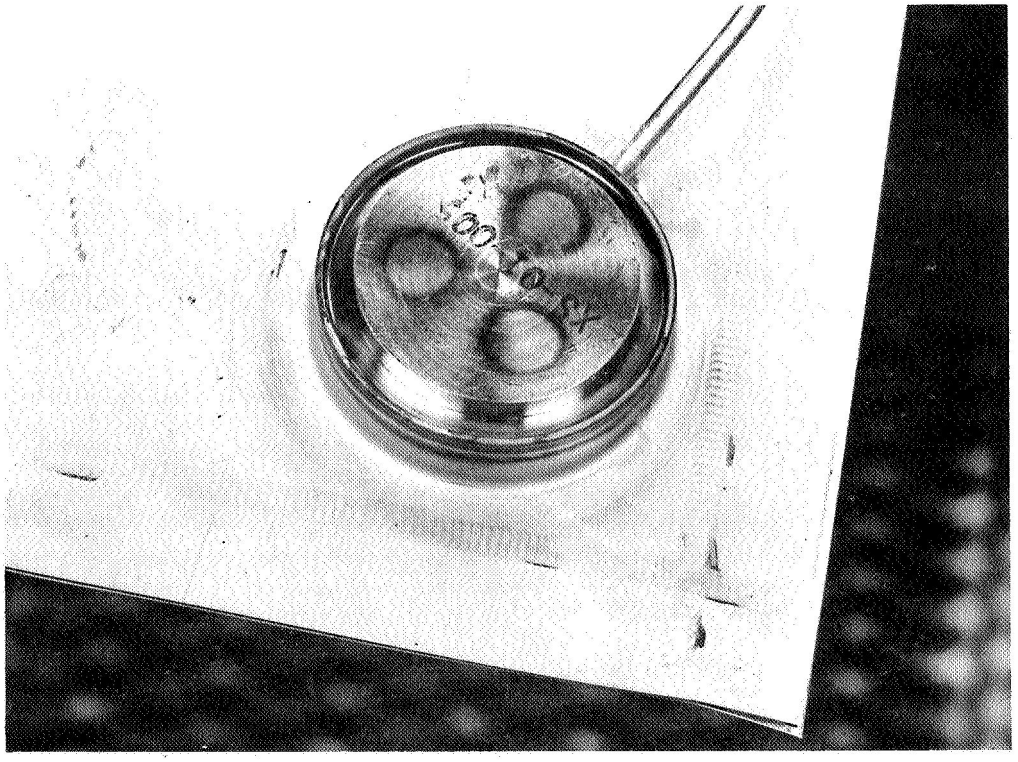

Figure 69.- Integrally Mounted Dummy Pressure Switch

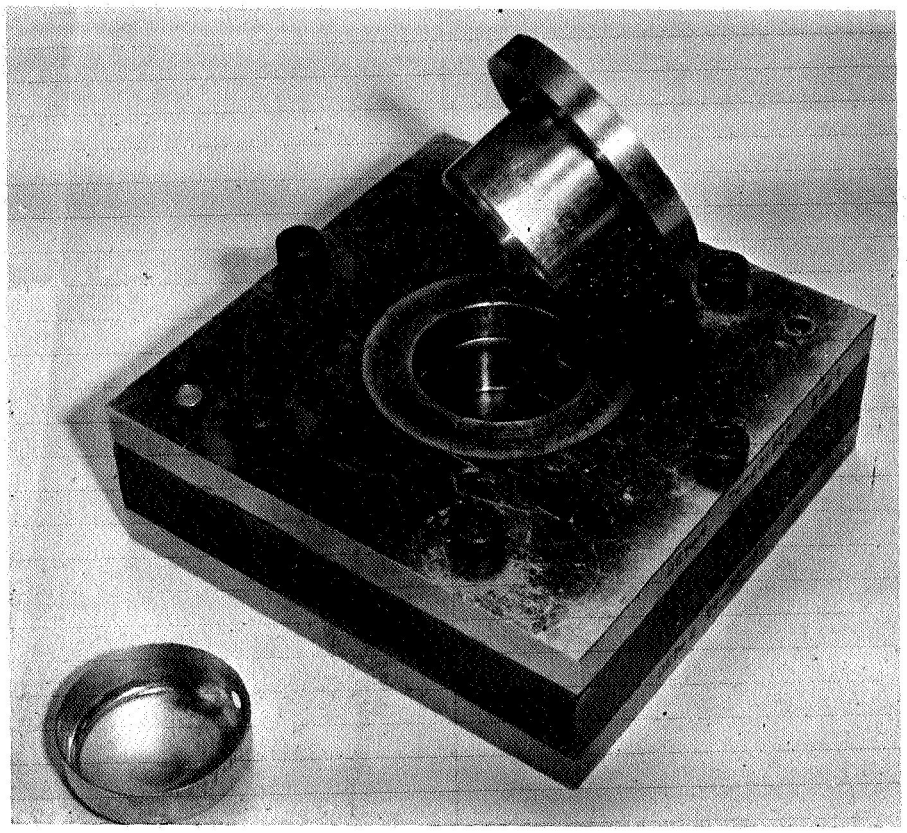

Figure 70.- Switch Cup Forming Tool

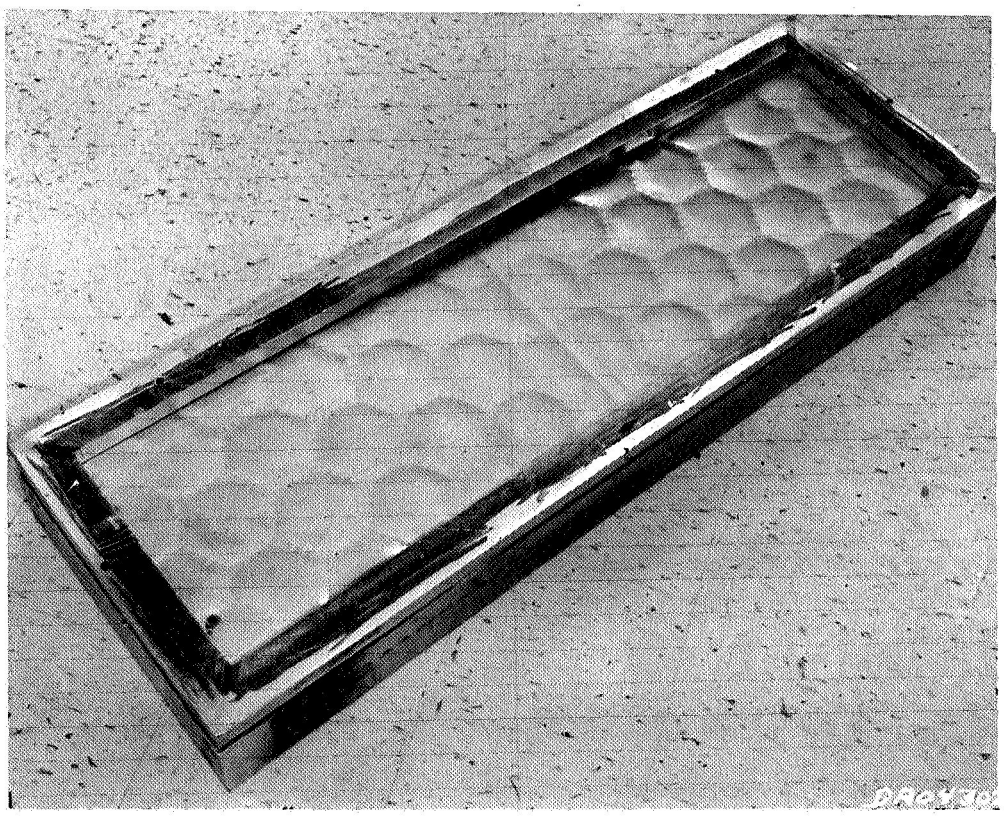

Figure 71.- Restraint Fixture

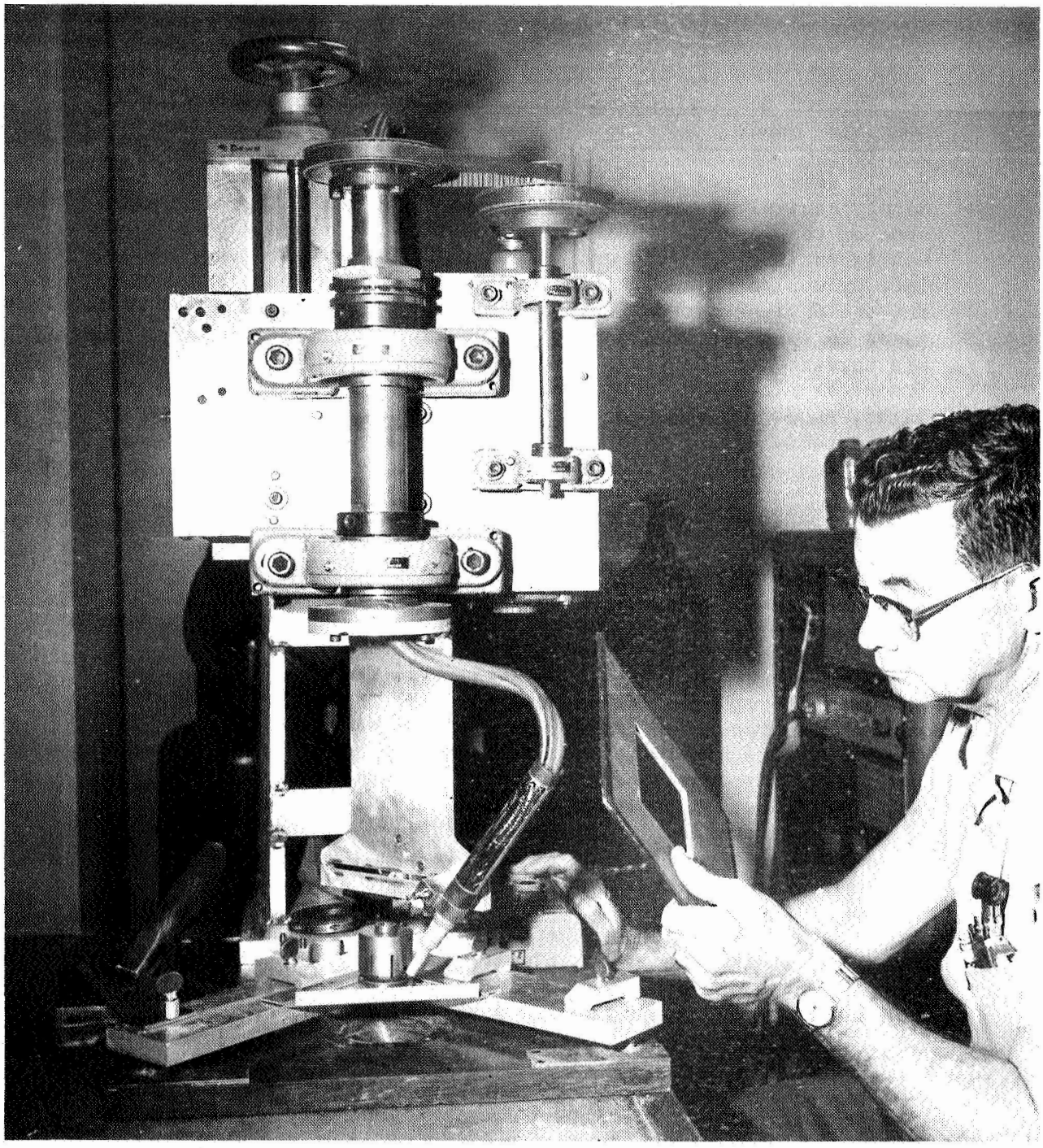

Figure 72.- Switch Welding Tool

During the Preliminary Design and Development Phase over 60 tools were fabricated including those for the cylindrical "A" configuration, which was eliminated before the phase ended.

Detail fabrication and assembly.- During the first phase over five hundred subsize detectors were fabricated. Approximately two dozen full-size detectors were completely assembled. Detail fabrication and partial assembly was made on an approximately equivalent number of full-size detectors. These included some of the "A" configuration, which was eliminated, and some configurations with integral mount flanges that were made obsolete by design changes. Production plan drafts were formulated for the designs carried to final assembly. The adequacy of these plans in turn was verified by the ability to fabricate and assemble hardware to the plans as written. Although the dull finish stainless steel was surprisingly sensitive to handling and tool marks, no particular problems were encountered in fabrication and assembly during this phase.

## Design Development Phase

Process development.- Surface finish modification experiments were concluded during this phase. They showed that vapor honing could produce an absorptivity-to-emissivity ratio approaching the goal of 1.62, but with lower than the goal values of $\alpha$ and $\epsilon$ of 0.65 and 0.40, respectively. The experiments also showed that vapor honing was not thickness sensitive and did not remove measurable amounts of material. A separate report, MDS-10010, Surface Finish Report, was prepared covering the work on this task. Process development work in brazing continued with some participation from the Baltimore Division of the Martin Marietta Corporation. Excessive alloy flow and target sheet wrinkling was reduced by modifying the specimen orientation and the braze cycle. Some encouraging pressure cycle test data were obtained on these specimens. Further specimen fabrication was deferred to await the installation and availability of a large vacuum furnace in our facility. During this period successful diffusion bonds were made, but the specimens were metallurgically degraded and had low peel strength.

A resistance spot welding machine with special features useful to welding the three-ply "F" configuration was installed during this phase. Initial results were not very encouraging because of the phenomenon of tiny marginally welded regions occurring immediately adjacent to the weld spot. These would tear out during pressurization and produce leaks in the detector.

Changes to the welding electrode geometry eliminated this defect. During this phase an overspot weld process was developed for eliminating small leaks in seam welded corners. The shunting of weld current as the wheels crossed over the first seam was the likely cause of the leak causing discontinuity. The overspot was successfully developed, rather than change the seam weld parameters that were optimum in all other respects. The use of a peel sheet in seam welding the edges of the "F" configuration was decided during this phase. A peel sheet over the seam weld had the same advantage here as when used in spot welding; it allowed the heat to be increased to obtain a stronger joint without producing molten metal expulsions at the surface.

Tooling.- Machined dies for explosive forming of the "D2" and "E2" configurations were completed and target sheets were successfully formed. The die with a thin sheet of plastic film over it is shown in the explosive forming fixture in figure 73. The interchangeable corners which allow one die to be used for both target sheets may also be seen in the photograph.

Detectors manufactured in the first phase used dummy pressure switches welded in place before pressure expansion. The real pressure switches could not be exposed to the forming pressures and were to be welded into the detectors after this operation. Therefore, removable sealing tools were required to close the hole to be used for the switch during pressure forming. One of these tools is shown on figure 74. Stretching of the metal in explosive forming left an excess of metal at the edges, resulting in waviness of the edge. This condition made seam welding of the edges difficult since the two plies were not in intimate contact. The edges were successfully straightened using dies made for the Titan program (fig. 75). Compressing of the edge "shrank" the excess material left during explosive forming.

During the last half of the first phase design of the full-size accelerated life cycle test fixture was completed. The first full-size module planned for use in a check out test in the vacuum chamber was fabricated during the Design Development Phase. This module is shown in figure 76. One of the quartz heating lamp banks is shown at the top of the picture with the detector holding frame in front. The cable mechanism for lowering the detector frame into the cold bath is also visible. Coils to carry liquid nitrogen are located in each of the tandem tank sections below the heating lamps. Metal templates for match drilling of the detectors and mounts were made during this phase. Figure 77 shows one of these templates. Special neoprene-coated screen separators were made to handle batches of target core and bumper sheet material

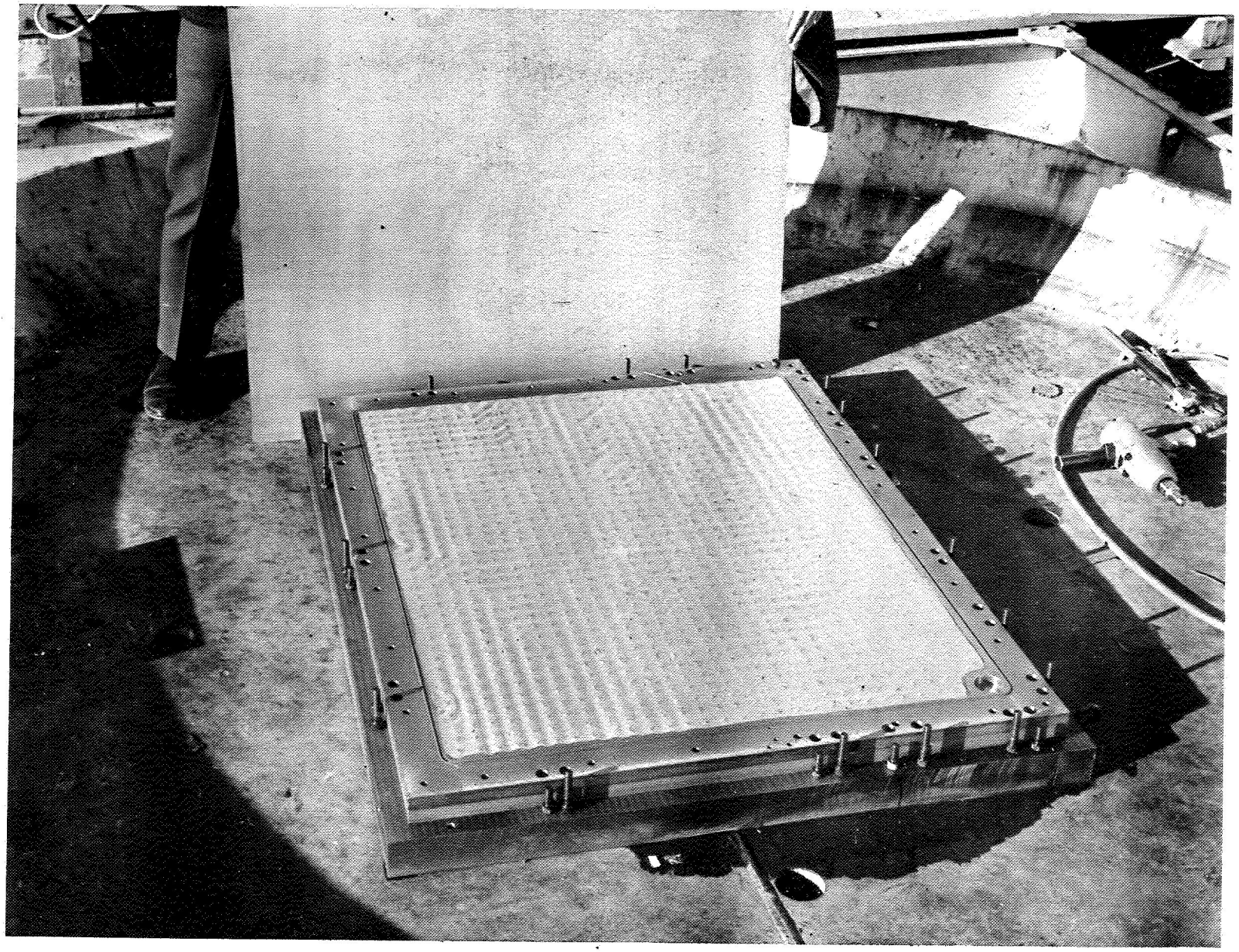

Figure 73.- Preformed Target Sheet Showing Plastic Separator

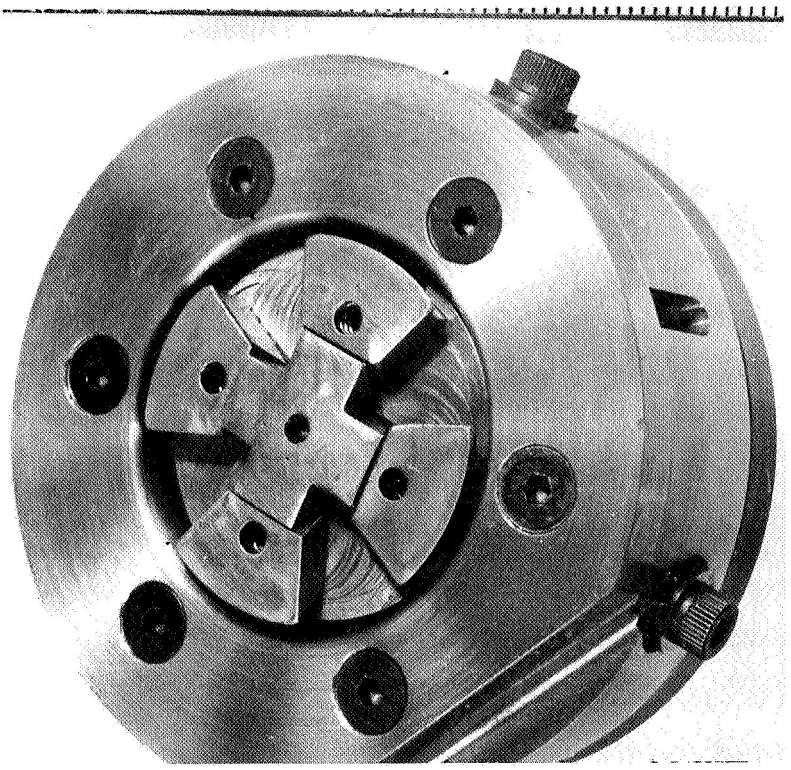

Figure 74.- Pressure Switch Block Off Tool

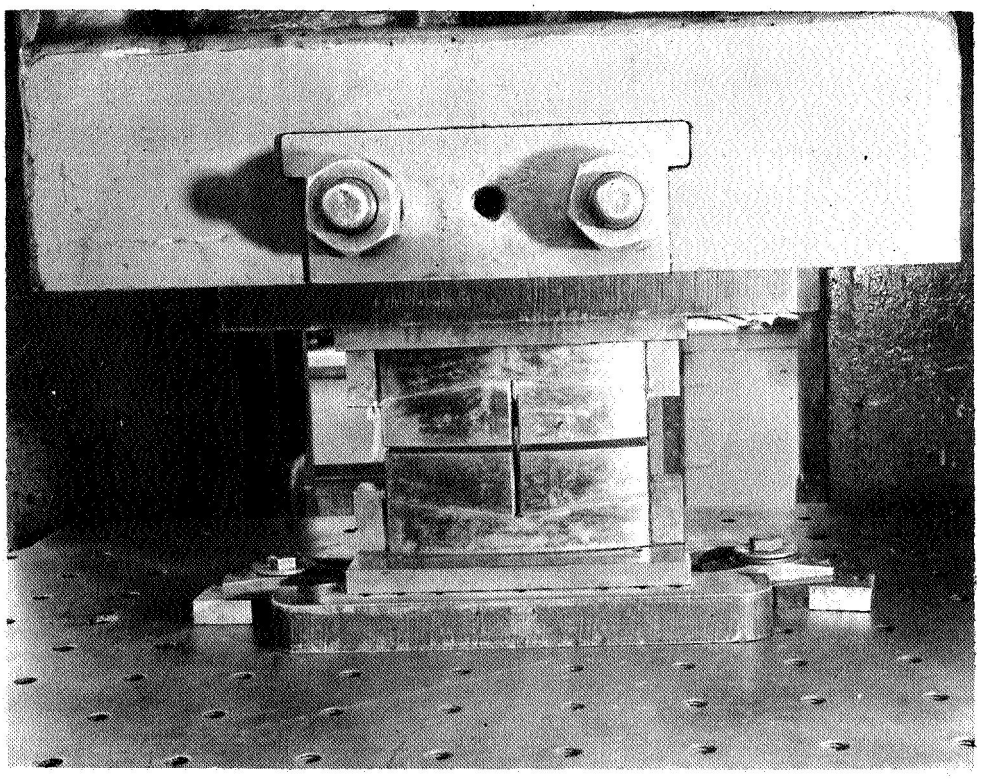

Figure 75.- Squeeze Die Installed on Bliss Press

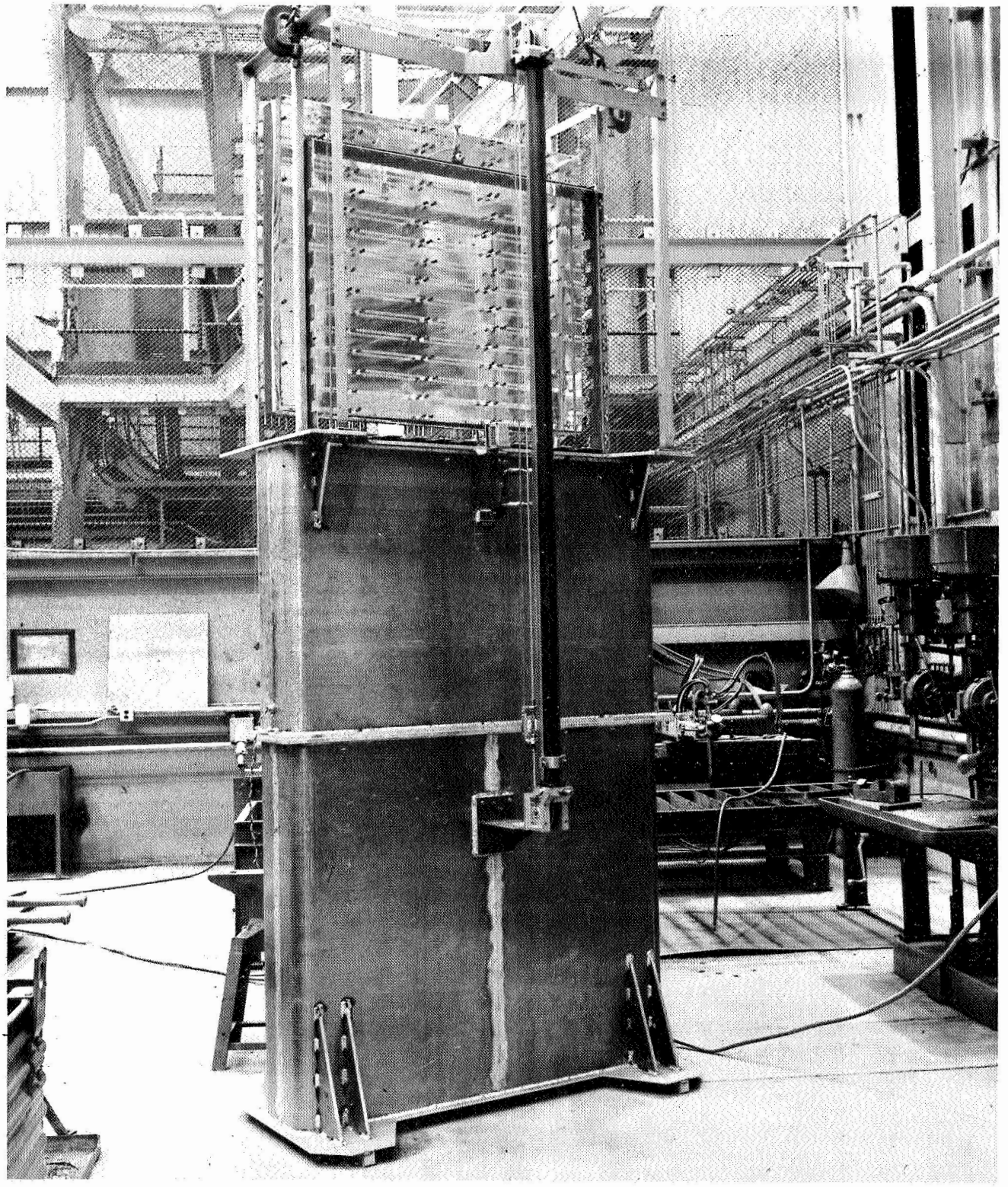

Figure 76.- Accelerated Life Cycle Fixture, First Module

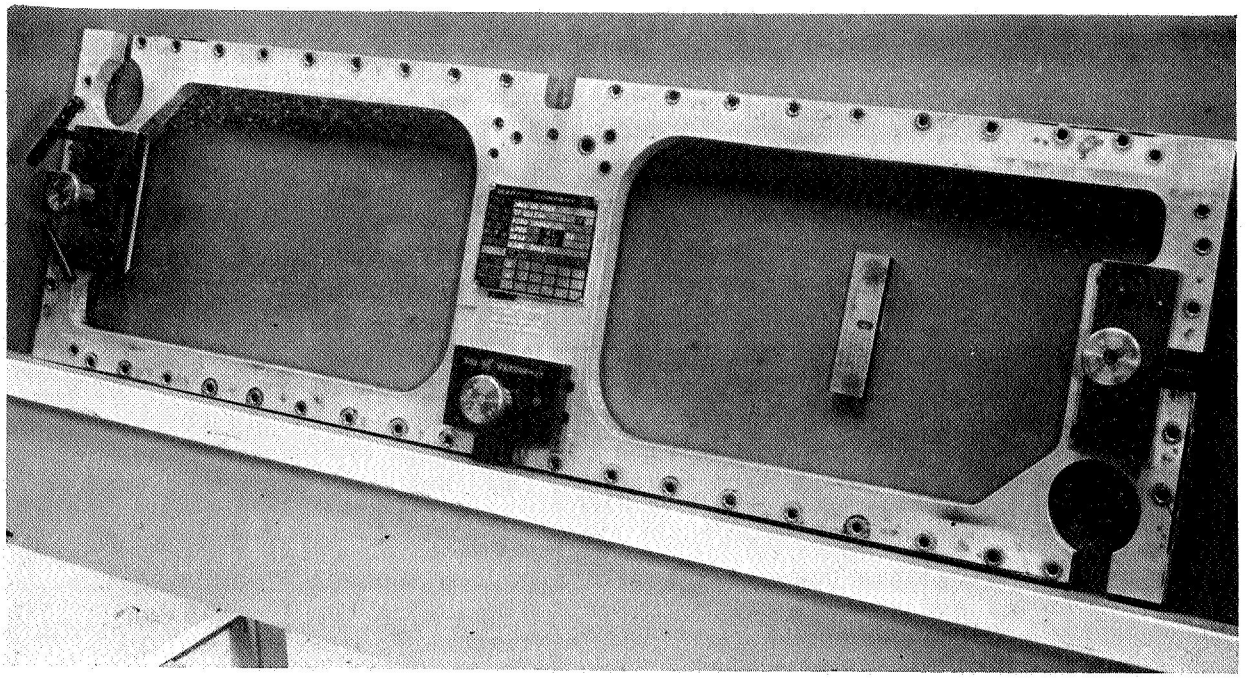

Figure 77.- 12x40-in. Detector and Mount Drill Template

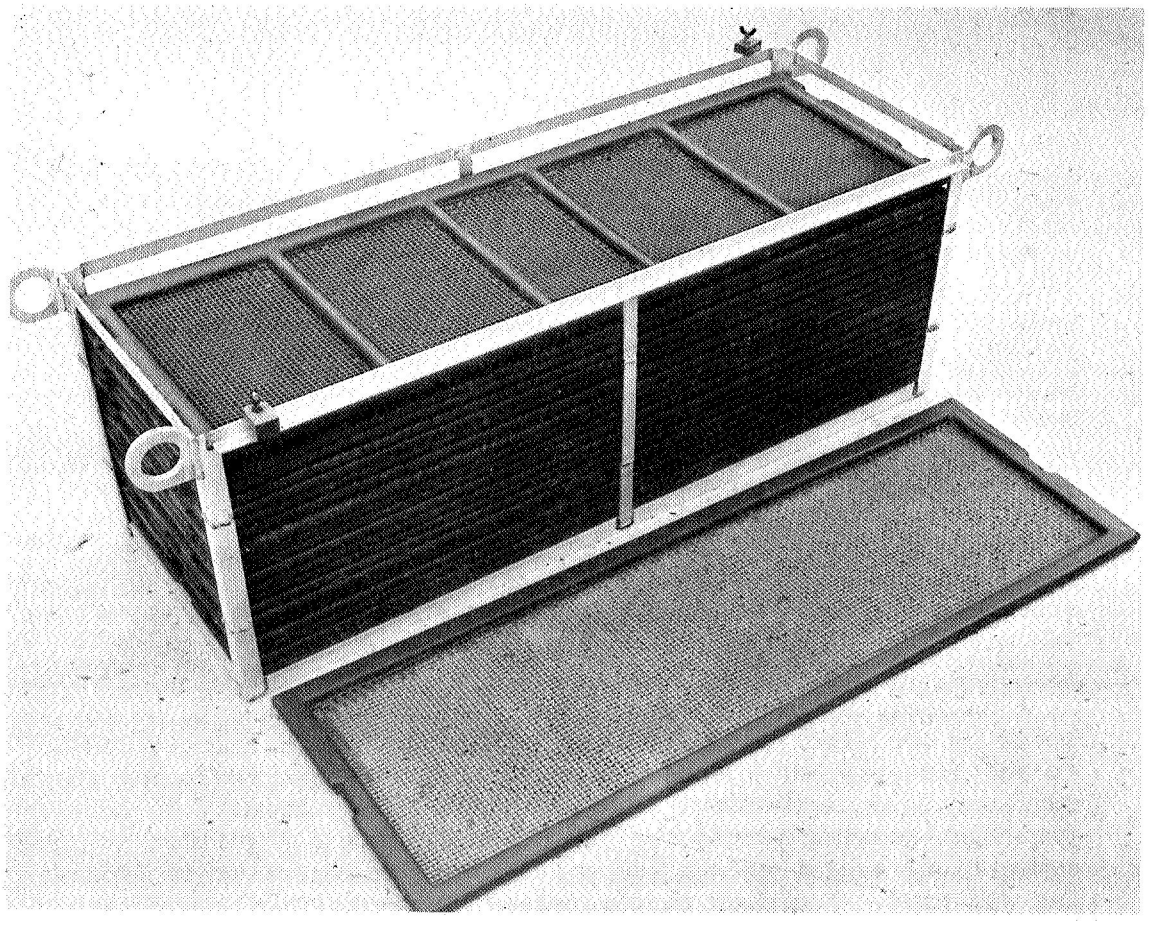

Figure 78.- 12x40-in. Cleaning and Handling Fixture

in the cleaning and passivating sequences. These were located in a frame that held the sheets securely during these operations. Figure 78 shows this fixture comprising the frame and screens.

Detail fabrication and assembly.- Eighteen full-size detectors were fabricated during the Design Development Phase. Data were gathered on the fabrication and tooling requirements of each configuration. The "F" configuration had approximately three times the number of fabrication operations as the simpler configurations. The "B" and preformed "E2" and "D2" were next in fabrication complexity.

During this phase all the fabrication Process Plans were reviewed and updated before their inclusion in the Production Plan submitted to NASA-LRC. At the request of NASA-LRC the Process Plans for each configuration were augmented by detailed flow charts made directly from these plans. This facilitates studying the manufacturing inspection and testing operations for efficiency of the flow.

## Manufacturing and Test Phase

Process development.- Welding process development comprised routine certifications of some of the material combinations not certified during the second phase. These were primarily specialized welds in the pressure switch and bumper sheet brackets of the "F" and "B" configurations. The other and major area of weld process development was for spot welding target sheets for the "F" panels. None of the five "F" panels made for development testing was successful in all the tests. An extensive experimental program was started to determine what caused the metal expulsions or "spits" during welding that produced leaks in the detectors and to eliminate the causes. Diagnostic measurements of a large number of weld operations led to the discovery that spits always occurred during the second half of the cycle of weld, which was the second energy pulse. A half-cycle weld schedule was then developed that gave joints of good strength and greatly reduced the frequency of spitting.

An important second factor in spitting was found to be the speed of the electrode descent. A small rap of the electrodes to the five-ply panel caused a slight coining that conformed the surfaces to one another. This increases the uniformity of current flux passing across the nugget area, giving a uniform symmetrical nugget growth and solidification important in avoiding spitting. Too much rap decreases electrical resistance and the weld size.

Experiments also disclosed low material surface resistance as a third factor. Weldability was improved by replacing the passivation operation with a pickling process, as well as limiting the time between this cleaning and welding to 12 days. This inhibits molten metal formation at the 0.002 to 0.016-in. interface and enhances the diffusion bond zone around the nugget at the interface. The resulting joint showed uniform high strength. Approximately 100 000 welds have been made with the new weld process without any spits occurring. All three aforementioned process changes combined have allowed a standard for electrode dressing as rarely as every 100 welds. In practice, 547 welds were made before dressing the electrodes without spits. This was considered to be an important side benefit of the new welding process. This work is discussed in detail in a separate report, MDS-10018, Resistance Welding Technology Developments for the MPDD F1A configuration.

At this time NASA-LRC suggested several experiments to determine if changes to the finish, thickness, or material of the peel sheet would result in improvements. Generally, the 2, 4, and 8 mil, whether dull or polished 21-6-9 or 304 material, when welded to the 0.002-in. target would not peel off. The standard 1-mil-thick 21-6-9 polished peel sheet did peel off and the nugget had the customary penetration. In this "dog-bone" weld, the nugget obtained with that peel sheet had a narrower center and a smaller cross sectional area. A smaller cast volume (lower energy input) was also advantageous in reducing the spit frequency.

Experiments were also run changing peel sheets on seam welding. These showed that materials thinner than 8 mils tended to stick to the target, sometimes severely. Also, unless the surface of the 8-mil peel sheet had been polished, it would stick. The nugget penetrated the 2-mil target sheet satisfactorily.

Early in the last phase experiments were begun to develop repair techniques, particularly for the "F" configuration, where one bad weld of 3000 could cause the entire panel to be scrapped. One specimen used solder repairs. This developed a large number of leaks because of the stress corrosion precipitated by solder flux. The problem was solved by eliminating the use of solder on any hardware. Further assurance against stress corrosion was obtained by using deionized water to cool panels and wheels of both seam welders.

Repair test specimens were made by vacuum brazing patches over the leak point with nickel-gold alloy. It was indicated that these joints were starved. Additional braze repair experiments will be performed using a larger quantity of braze alloy.

One oven braze repair was fabricated using silver braze alloy, however, because of the detrimental effect to the vacuum oven by silver deposit, this repair was made in a retort oven and the resulting oxide coating precluded proper melting. A number of plastic and epoxy repair patches were also tried but were unsuccessful. With the development of the new spot weld process further work on repair techniques was halted.

Welding inconsistencies were found when using a new shipment of 21-6-9 material. These inconsistencies were solved by the addition of a modified cleaning process that reduced the material to a condition where it welds without spitting using the certified welding schedules. The high and variable resistance of the new material was assumed to be the source of trouble. The absolute value of resistance and its variability were reduced by pickling in nitric and hydrofluoric acid. The material was passivated and baked at 275°F. Both of these processes increase the resistance uniformly to a few hundred micro-ohms at which value welding to the previously established settings could be done reliably. This work is reported in MDS-10016, Technical Resolution of MPDD Finish Welding Problem.

The final set of "F" subsize braze specimens was fabricated for tests during this period. Three nine-spot specimens were brazed with nickel-gold alloy in the new vacuum furnace and were forwarded for testing. These specimens developed leaks before completing the pressure cycling test. Following the successful development of a new improved spot welding schedule for the "F" configuration, the backup brazing development effort was discontinued.

One unanticipated difficulty that occurred late in the second phase was eliminated in the final phase. The "F" and "B" configurations used a different fill tube fitting than the other detectors. This fitting had a large square base to pick up spot welds through to a backup plate on the opposite target sheet. The fitting itself was ring welded to only one target face. It was not possible to machine the thin large base to the tight tolerance, parallelism, and finish necessary to obtain a good leak-free ring weld. The leaks were minute and usually developed after the detector had been fabricated. At that point it was not possible to go over the ring weld. The problem was solved

by using a standard round fill tube fitting within a separate square washer to pick up the supporting spot welds. The tight tolerance in thickness, parallelism, and finish essential to a sealing ring weld, were obtained with relative ease in the round-based fitting.

A new process development task was the establishment of spot and seam weld schedules for three new 21-6-9 stainless steel thickness combinations being considered for detectors flown piggy-back on the outside of a Saturn stage.

The final task was the development of a fill tube pinchoff and seal process. This used a spot welder to flatten the tube and form a diffusion bond that acted as a temporary seal until the end of the tube was fusion welded. A weld schedule and special offset weld electrodes were developed for this operation. Process development personnel also contributed to major sections of the specifications prepared by Engineering for the MPDD contract. This effort was performed in all phases culminating in a major review and update in the last phase before submittal of the final version of the Production Plan.

Tooling.- A number of new tools were made for the modified "F" configuration. These tools allowed each detector half to be fabricated separately and then spliced together. Figure 79 shows the assembly fixture for drilling the detectors for the riveted splice. A special tool was also designed and built to permit the pressure expansion of detectors into a slightly curved shape equivalent to the curvature of the Saturn S-IVB. This is shown on figures 80 and 81. Flat unpressurized detectors were put in between the curved plates. The tool was then assembled and clamped in a hydraulic press. The detectors were then pressurized and with a proper allowance for springback they retained the desired curvature after removal from the tool.

Detail fabrication and assembly.- Effort during this period consisted of fabrication and assembly of the detectors for the various test programs and for delivery to NASA-LRC. A single batch build was selected for each configuration because this offered the lowest costs. Detail fabrication was fairly routine. Except for configuration "F" the designs were essentially identical to those built in the second phase. Fabrication performance was somewhat better than projected from cost data gathered during the building of detectors for the second phase.

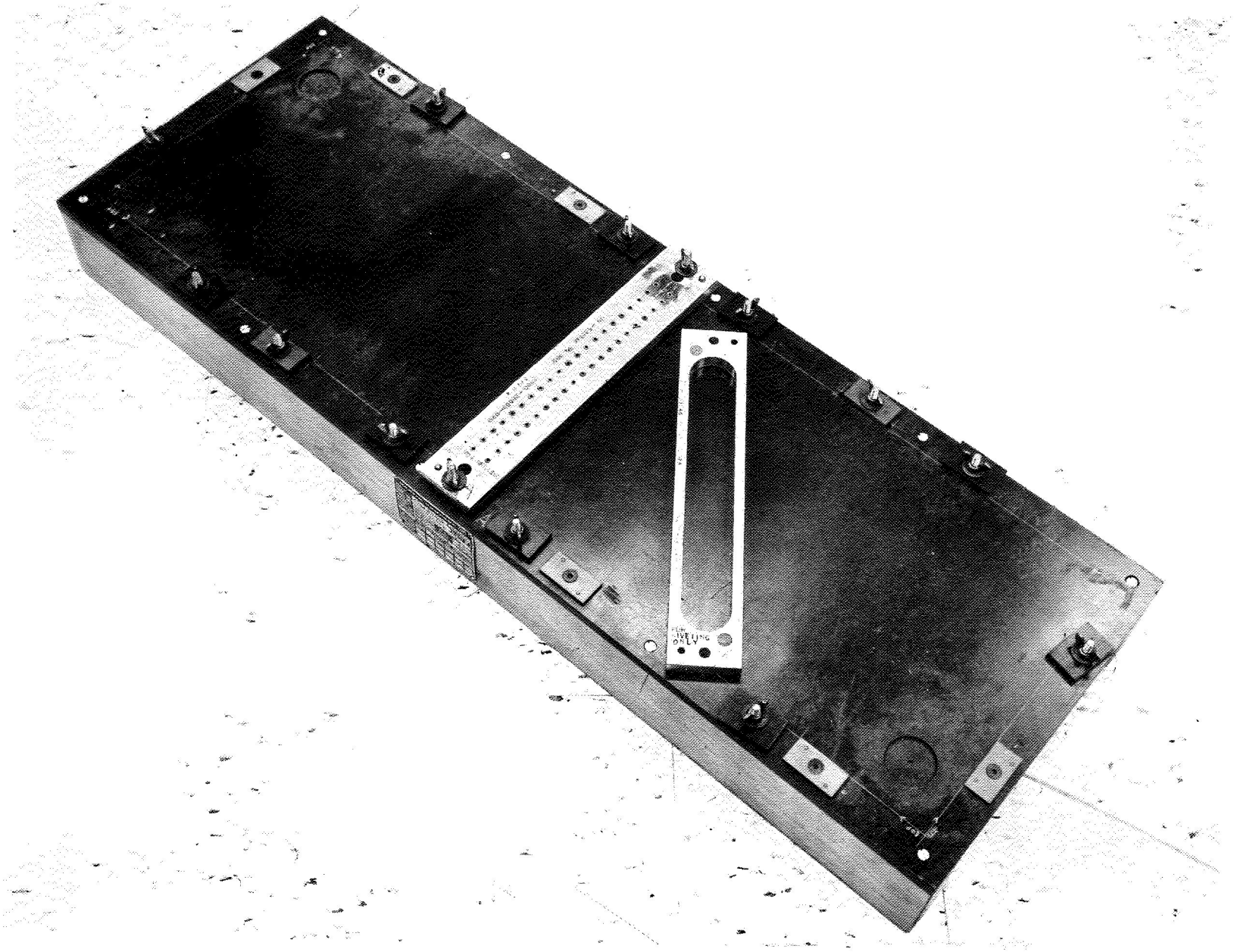

Figure 79.- F1A Drill Assembly Fixture

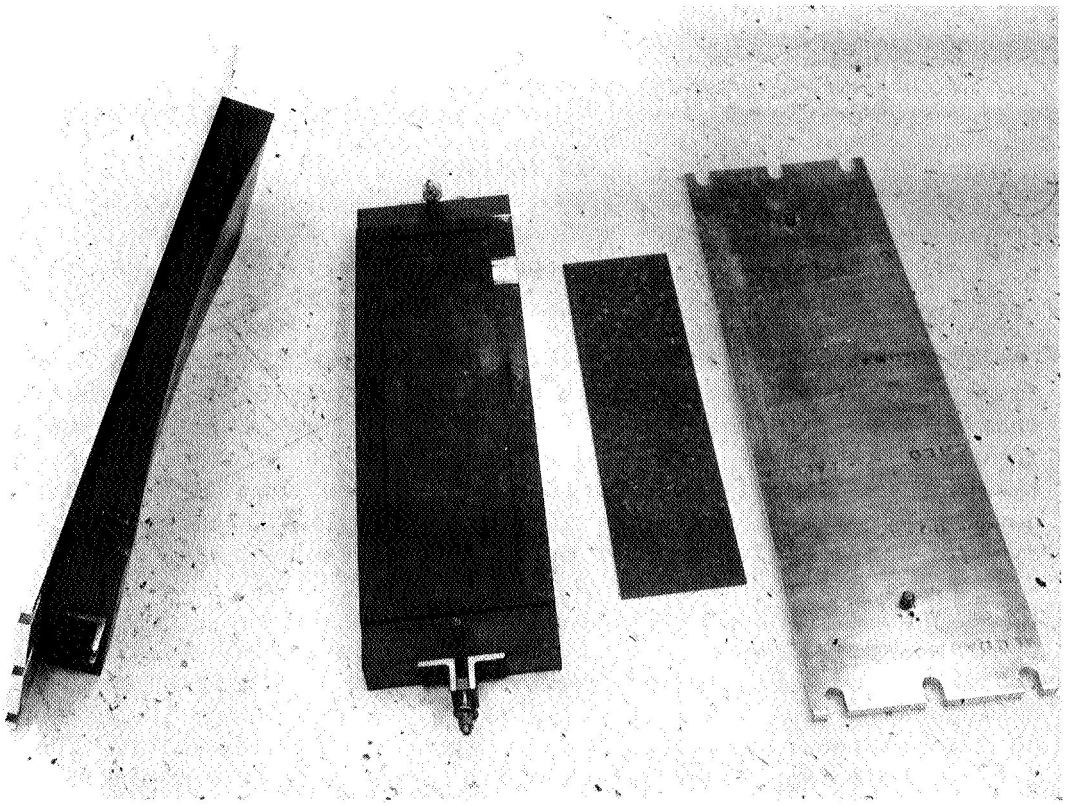

Figure 80.- S-IVB Subsize Panel Forming Tool (Disassembled)

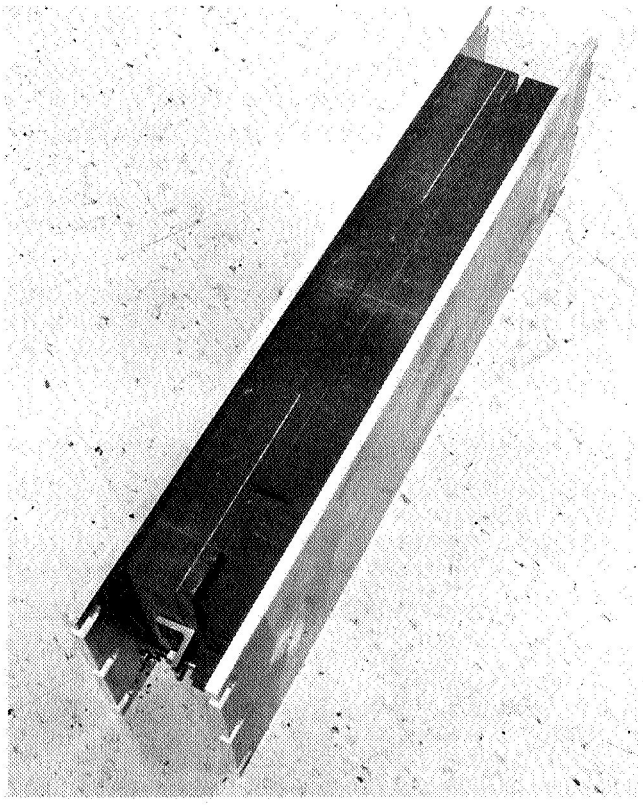

Figure 81.- S-IVB Subsize Panel Forming Tool (Assembled)

## MPDD TESTING

The testing program in support of the MPDD Program was performed in three distinct phases with varying objectives. The first phase of testing occurred during the Preliminary Design and Development Phase. This testing basically was directed to assess design and process survival in the area of critical environments that did not lend themselves to satisfactory analytical evaluation. Therefore empirical data were gathered to more accurately select those initial configurations that would be pursued during final development. As a result of this gross design evaluation other dynamic characteristics that appeared to present design problems were noted and investigated.

The second phase of testing occurred during the Design Development Phase of the program. Again the basic objective to assess design and process survival capability. This testing was expanded to include total functional and environmental evaluations. These tests were accomplished at full qualification levels to further enhance success probability during the final phase of the testing program.

The third and final phase of testing occurred during the Manufacturing and Testing Phase of the program and was oriented along the lines of a pilot production type of test program. This testing included a flight assurance test program, a qualification test program, and a special accelerated life cycling test program. The testing was generally accomplished on a go-no/go basis. However, as a result of empirical test data, limited configuration improvements were incorporated. Results and types of testing accomplished in the three phases are summarized in this chapter. If detailed information, such as actual test data or testing techniques, are required by the reader, these can be obtained in the following documents.

Preliminary Design Evaluation Testing:

1) MPDD Preliminary Development Test for B1, 8280-04001 - OP500, dated 05/26/67

2) MPDD Preliminary Development Test for B1A, 8280-04051 - OP500, dated 06/20/67

3) MPDD Preliminary Development Test for B2, 8280-05001 - OP500, dated 06/20/67

4) MPDD Preliminary Development Test for B3, 8280-06001 - OP500, dated 06/20/67

5) MPDD Preliminary Development Test for C1, 8280-07001 - OP500, dated 06/06/67

6) MPDD Preliminary Development Test for C1A, 8280-07051 - OP500, dated 06/07/67

7) MPDD Preliminary Development Test for C2, 8280-08001 - OP500, dated 06/20/67

8) MPDD Preliminary Development Test for C3B, 8280-09001 - OP500, dated 06/20/67

9) MPDD Preliminary Development Test for D1A, 8280-10001 - OP500, dated 06/07/67

10) MPDD Preliminary Development Test for D1B, 8280-11001 - OP500, dated 06/07/67

11) MPDD Preliminary Development Test for D1C, 8280-12001 - OP500, dated 06/20/67

12) MPDD Preliminary Development Test for D2A, 8280-13001 - OP500, dated 06/20/67

13) MPDD Preliminary Development Test for D2B, 8280-14001 - OP500, dated 06/20/67

14) MPDD Preliminary Development Test for D2C, 8280-15001 - OP500, dated 06/20/67

15) MPDD Preliminary Development Test for D3A, 8280-16001 - OP500, dated 06/12/67

16) MPDD Preliminary Development Test for D3B, 8280-17001 - OP500, dated 06/20/67

17) MPDD Preliminary Development Test for D3C, 8280-18001 - OP500, dated 06/20/67

18) MPDD Preliminary Development Test for E1A, 8280-19001 - OP500, dated 06/12/67

19) MPDD Preliminary Development Test for E1B, 8280-20001 - OP500, dated 06/20/67

20) MPDD Preliminary Development Test for E1C, 8280-21001 - OP500, dated 06/20/67

21) MPDD Preliminary Development Test for E2A2, 8280-22001 - OP500, dated 06/20/67

22) MPDD Preliminary Development Test for E2D, 8280-23001 - OP500, dated 06/20/67

23) MPDD Preliminary Development Test for E2C, 8280-24001 - OP500, dated 06/20/67

24) MPDD Preliminary Development Test for E3A, 8280-25001 - OP500, dated 06/20/67

25) MPDD Preliminary Development Test for E3B, 8280-26001 - OP500, dated 06/20/67

26) MPDD Preliminary Development Test for F2, 8280-27001 - OP500, dated 06/20/67

27) MPDD Preliminary Development Test for F1A, 8280-28001 - OP500, dated 06/20/67

28) MPDD Preliminary Development Test for F1B, 8280-29001 - OP500, dated 06/20/67

29) Testing Report of Configuration "B" PDD Detector Effort

30) Testing Report of Configuration "C" PDD Detector Effort

31) Testing Report of Configuration "D1" PDD Detector Effort, dated 10/19/67

32) Testing Report of Configurations "D2" and "D3" Detector Effort, dated 11/17/67

33) Testing Report of Configuration "E1" PDD Detector Effort.

34) Testing Report of Configurations "E2" and "E3" PDD Detector Effort, dated 11/17/67

35) Testing Report of Configuration "F" PDD Detector Effort, dated 11/16/67

36) Test Report of Aeroflex Helical Cable Isolator C3-HB410-12 and 6 Strand Ladder Isolator

37) 18 x 18 Subsize Stiffness Evaluation Test Report

38) MDS-10029 Strain Evaluation Analysis Report, dated 10/23/67

Design Evaluation Testing:

1) MDS-10001, Development Test Plan, dated 10/26/67

2) MPDD Design Development Test for B1A, 8280-04051 - OP510, dated 11/13/67

3) MPDD Design Development Test for BA, 8280-06051 - OP510, dated 11/13/67

4) MPDD Design Development Test for C1, 8280-07061 - OP510, dated 11/13/67

5) MPDD Design Development Test for C1B, 8280-07071 - OP510, dated 11/13/67

6) MPDD Design Development Test for D1A, 8280-10051 - OP510, dated 11/13/67

7) MPDD Design Development Test for D2A, 8280-13001 - OP510, dated 11/13/67

8) MPDD Design Development Test for D3A, 8280-16051 - OP510, dated 11/13/67

9) MPDD Design Development Test for E1A, 8280-19051 - OP510, dated 11/13/67

10) MPDD Design Development Test for E2C, 8280-24051 - OP510, dated 11/13/67

11) MPDD Design Development Test for E3A, 8280-25001 - OP510, dated 11/13/67

12) MPDD Design Development Test for F1A, 8280-28001 - OP510, dated 11/13/67

13) MPDD Design Development Test for F1B, 8280-29001 - OP510, dated 11/13/67

14) MPDD, B1A Panel Design Development Test Report, dated 08/16/68

15) MPDD, C1 Panel Design Development Test Report, dated 03/13/68

16) MPDD, D1A Detector Design Development Test Report, dated 02/20/68

17) MPDD, D2A Dual Detector Design Development Test Report, dated 03/14/68

18) MPDD, D3A, Detector Design Development Test Report, dated 02/21/68

19) MPDD, E1A Detector Design Development Test Report, dated 02/29/68

20) MPDD, E2C Dual Detector Design Development Test Report, dated 02/23/68

21) MPDD, E3A Detector Design Development Test Report, dated 02/22/68

22) MPDD, F1A Panel Design Development Test Report, dated 08/22/68

23) MDS-10015, Solar Cell Contamination Test Report, dated 09/23/68

Production Evaluation Testing:

1) MDS-10003, Integrated Test Plan, PCN-2, dated 03/06/69

2) PD7100075-OP520, Flight Assurance Test, Master Procedure - Pressure Switch, PCN-6, dated 03/12/68

3) PD7100075-OP530, Qualification Test, Master Procedure - Pressure Switch, PCN-1, dated 03/05/68

4) PD7100075-OP550, Accelerated Life Cycle Test, Master Procedure - MPDD Pressure Switch, dated 03/15/69

5) Pressure Switch Flight Assurance Test Reports, PD7100075-OP520 Associated Data Packages

6) Qualification Test Report, PD7100075-OP530, Pressure Switch, dated 07/23/68

7) Accelerated Life Cycle Test Report, PD7100075-OP550, Pressure Switch

8) Flight Assurance Test, Master Procedure Meteoroid Detector/Panel - OP520, PCN-4, dated 03/06/69

9) Qualification Test, Master Procedure Meteoroid Detector/Panel - OP530, PCN-2, dated 03/06/69

10) Accelerated Life Cycle Test, Master Procedure Meteoroid Detector/Panel - OP540, PCN-1, 06/27/69

11) Flight Assurance Test Report, Meteoroid Penetration Detector Development - OP520, dated 07/31/69

12) Qualification Test Report, Meteoroid Penetration Detector Development - OP530, dated 07/31/69

13) Accelerated Life Cycle Test Reports, Meteoroid Penetration Detector Development - OP540

## Preliminary Design Evaluation Testing

The Preliminary Design Evaluation Testing program was developed to evaluate those environments critical to the anticipated designs and processes that were used in fabrication of the preliminary meteoroid detectors. This program was accomplished in three distinct areas: (1) subsize design evaluation test;

(2) full-size design evaluation test; and (3) special design testing. The primary objectives in each of these areas are delineated in the following paragraphs.

Subsize design evaluation test.- The primary objective of this testing was one of design and fabrication process survival when subsize specimens were exposed to pressure excursions generated by near-earth orbital mission thermal environments. Secondary objectives were assessment of survival by varying such design characteristics a cell spacing and geometry, cell heights, detector stiffness, and forming pressures.

Subsize pressure cycling test: The subsize pressure cycling test was accomplished on specimens of the program designated detector configurations. This test primarily evaluated parent metal fatigue in the area of spot weld nodes and peripheral seam welds. These specimens were further used to determine the most suitable spot spacing and expansion heights. Additional benefits derived from this testing were the accumulation of reliability data and assessment of residual material strength. The residual strength was obtained by bursting several specimens that had not been pressure cycled, and then bursting other specimens of the same configuration after being exposed to pressure cycling.

The test setup (figs. 82 and 83) simulated the detector internal pressure excursion anticipated during a near-earth orbital mission. These excursions are the result of the thermal environment experience when an orbiting spacecraft enters or exits the earth shadow. The initial test conditions were established as a go-no/go fatigue test where the specimens were exposed to sufficient pressure cycles to simulate four operational lifetimes. The second test conditions were to expose other specimens to a single expected lifetime of pressure cycles, and then pressurize them to burst levels to assess residual strength. Test criteria during these test were: (1) pressure excursions of 14.0 psig to 49.3 psig; (2) initial cycle duration of 80 000 cycles; and (3) second cycle duration of 21 344 cycles. A summary of the individual configuration pressure cycle test results is presented in the following paragraphs.

Fifty-eight subsize "B" configuration specimens were subjected to pressure cycling. Of this number, 15 were pressurized to burst after completion of 21 344 cycles. Of the remaining 43 specimens, 29 failed during pressure cycling.

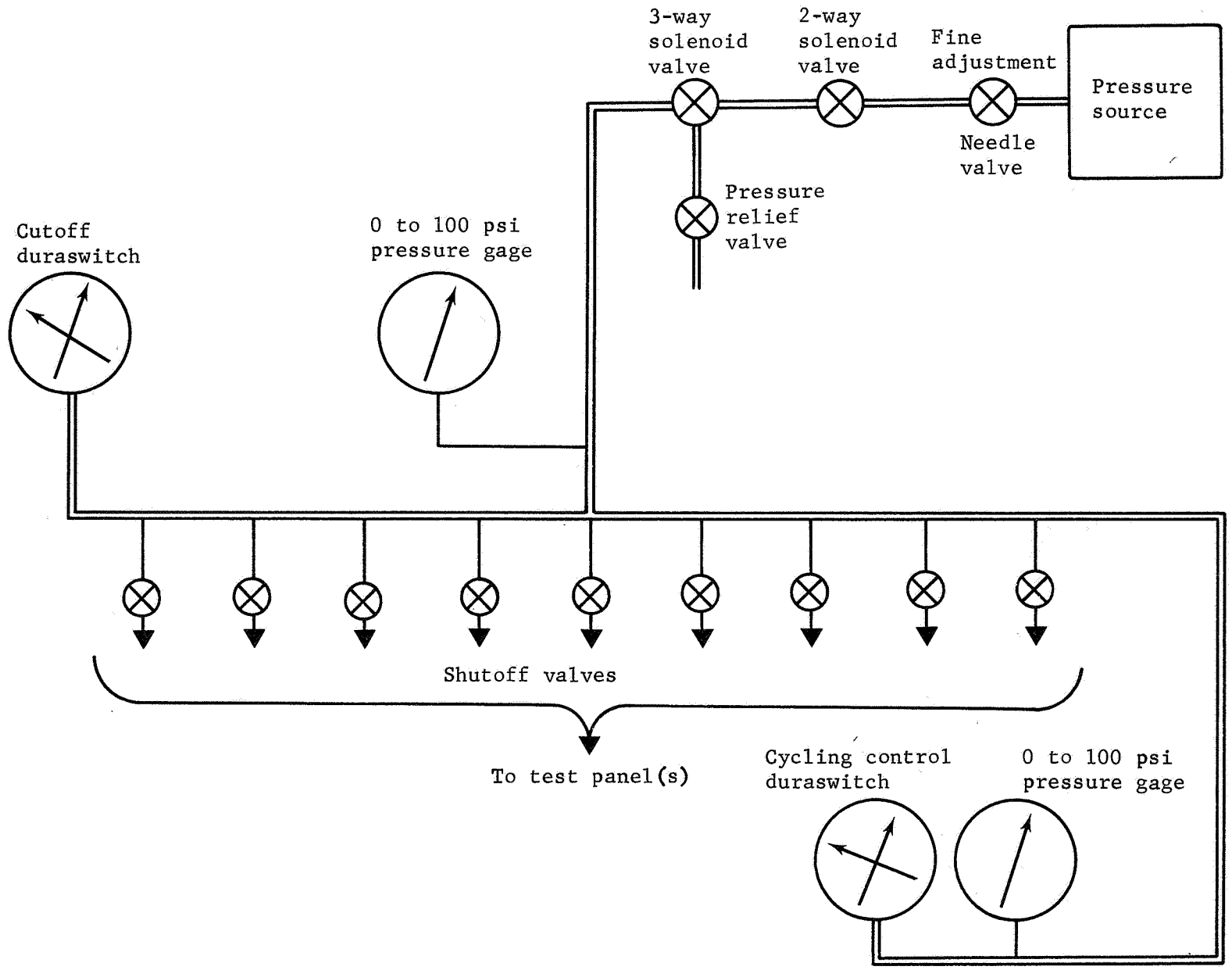


Figure 82.- Pressure Cycling Test Setup

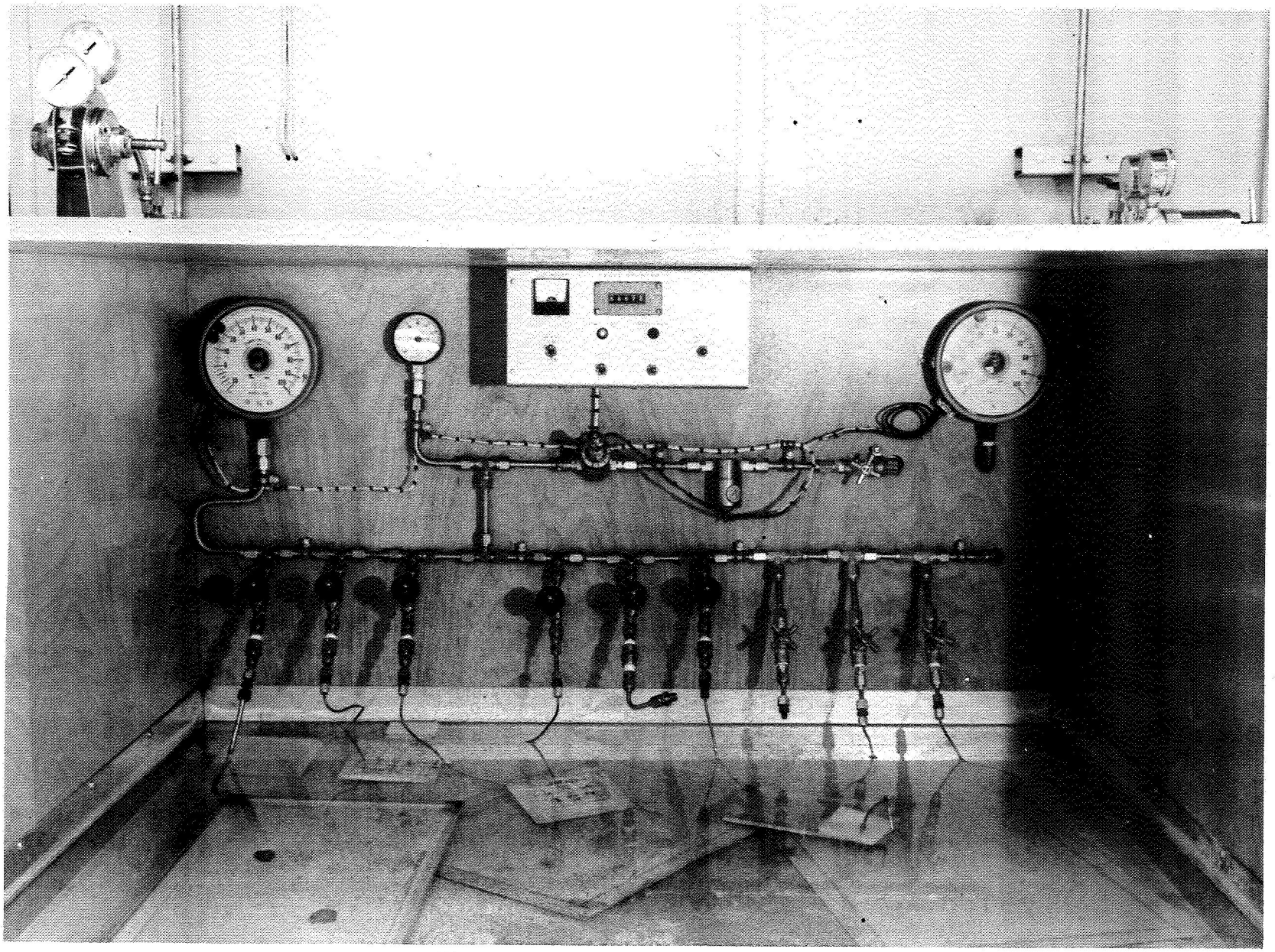

Figure 83.- Pressure Cycling Tool

Forty-nine subsize "C" configuration specimens were subjected to pressure cycling. Nineteen of these specimens were cycled to 60 000 cycles or failure. The remaining 30 specimens were cycled to 21 344 cycles or failure and then burst. Of the 19 items, six failed pressure cycling. Of the 30 items, 18 failed pressure cycling.

Thirty-four subsize "D1" configuration specimens were subjected to pressure cycling. Of this number, 15 items were pressurized to burst after completion of 21 344 cycles. Of the remaining 19 specimens, 3 failed during pressure cycling.

Twenty-one "D3" subsize configuration specimens were subjected to pressure cycling. Eleven of these specimens were cycled to 60 000 cycles or to failure. Of these 11 items, two failed pressure cycling. Ten "D3" specimens were subjected to 21 344 cycles or to failure and then burst. All ten of these items passed pressure cycling. An additional ten "D2" specimens were subjected to burst pressure only.

Thirty-seven subsize "E1" specimens were subjected to pressure cycling. Of this number, 25 were pressurized to burst after completion of 21 344 cycles. One of the 25 specimens failed during pressure cycling. Of the remaining 12 specimens, three failed during pressure cycling. All of these specimens were fabricated of 304 stainless steel, a material that was replaced by 21-6-9 stainless steel.

Twenty-four "E3" subsize specimens were subjected to pressure cycling. Fourteen of these specimens were cycled to 60 000 cycles or to failure. Of these 14 items, two items failed pressure cycling. Ten of these items were cycled to 21 344 cycles or to failure and the burst. Of these ten items, two failed pressure cycling. An additional ten "E2" specimens were subjected to burst pressure only.

Forty-four subsize "F" configuration specimens were subjected to pressure cycling. Of this number, 23 items were subjected to a cycling and burst test of 21 344 cycles. Of these 23, eight items failed cycling testing. Of the remaining 21 specimens, 12 failed during pressure cycling.

Stress evaluation test: A subsize experimental stress investigation test was performed to assess the structural behavior of a pressure-formed detector configuration. The objectives of this test were to: (1) determine what the pressure-strain relation was at significant specimen locations; (2)

evaluate elastic stress range subsequent to pressure forming; and (3) obtain an estimate of the total strain developed during pressure forming operations. The test objectives were accomplished using a subsize detector with strain gage instrumentation.

The test setup (fig. 84) for the initial evaluation consisted of instrumenting the specimen that had been pressure formed to 140 psig. Strain gages were applied with no pressure in the panel. Strain readings were then recorded during pressure application incrementally to 160 psig. A second panel was tested to demonstrate that pillow heights developed by incremental pressure steps are the same as those for one pressurization from zero to the forming pressure. The pressure forming test used a small photoetch grid but provided no additional quantitative strain data, other than indicating no extensive regions of large permanent strain during pressure forming.

This test yielded the following summary results:

1) Pressure forming causes yielding and permanent deformation that is somewhat uniform at all locations on the panel;

2) The largest value of permanent set occurs adjacent to the spot weld in a radial direction;

3) Increased forming pressures reduce strain at pressures less than the forming pressure because of an improvement in pillow shape;

4) Stresses due to pressure 1/2 of the forming pressure are completely elastic, except for the material adjacent to the spot weld;

5) Stresses at proof pressure of 54 psig are less than 40 000 psi for the entire specimen;

6) Pillow forming in one pressure application is identical to incremental application in the forming process.

Stiffness evaluation test: The stiffness evaluation test on the 18x18-in. subsize MPDD detectors had several primary objectives. These objectives were to evaluate the effects on target sheet and peripheral loading, as well as the change in the fundamental mode and first and second harmonics when design parameters were changed on the test specimens. During the test cell height, cell spacing, and cell geometry were varied. The

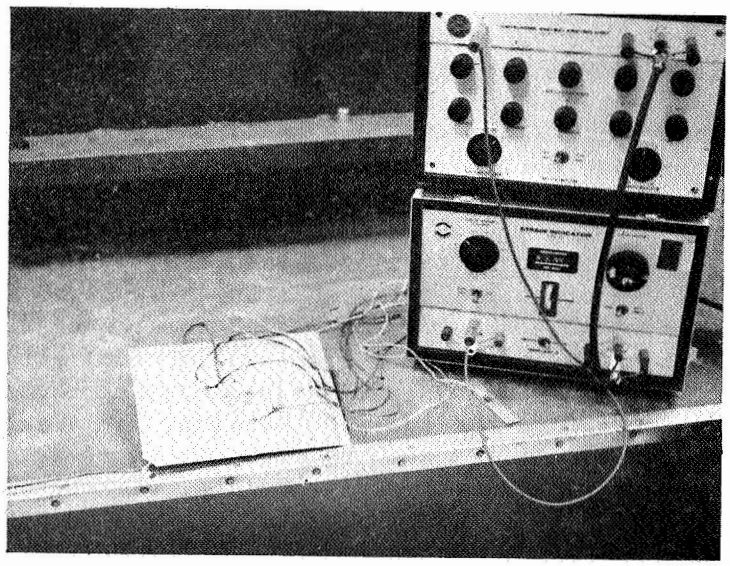

Figure 84.- Experimental Setup

specimens were exposed to sinusoidal vibration testing and the aforementioned effects measured.

The test was set up (fig. 85) with the test fixture and test specimen mounted on a vibration exciter with the control accelerometer mounted on the bottom side of the vibration fixture directly under one of the test specimen mounting points. The monitor accelerometer was mounted in the center of the test specimen. The test conditions used during this test were an exciter input of: (1) frequency, 5 thru 2000 Hz; (2) amplitude, 0.3 in. double amplitude (DA) $\pm$ 0.015 in. DA from 5 to 36 Hz, thru 3 g peak $\pm$ 0.5 g peak from 36 to 2000 Hz; and (3) a sweep rate - applied manually and sufficiently slow to identify the occurrence of resonances. The test sequence was then to apply pressure, measure the pillow height, and then perform a 3 g resonance search.

This test involved eight different panel configurations fabricated with 0.008-in. target sheets. The general test results from the 102 tests indicated that the pillow heights and cell geometry that created the stiffest test configuration also generated the highest peripheral dynamic loads. Therefore, these were not the most desirable configurations for the final design.

Full-size evaluation testing.- The primary objective of this testing was principally the same as the subsize evaluation, that of assessing the survival capability of the basic design and the fabrication processes used. This was accomplished on the complete family of detectors and included proof pressure, leak testing, and vibration and acoustic testing. In addition, other critical design parameters such as measurement of detector dynamic characteristics and transmissability, peripheral loading, bumper sheet deflection, and evaluation of bumper sheet mounting techniques were also investigated.

Design and process evaluation testing: This test series was designed to evaluate the ability of the various full-size design and fabrication processes to survive critical dynamic environments while at the same time measuring individual design resonance and transmission characteristics. In addition, the fabrication processes were evaluated to ensure that critical leak criteria were within the scope of the involved welding techniques. This test program included the following tests: proof pressure, helium leak test, residual gas analysis leak test, and out-of-plane sinusoidal vibration testing.

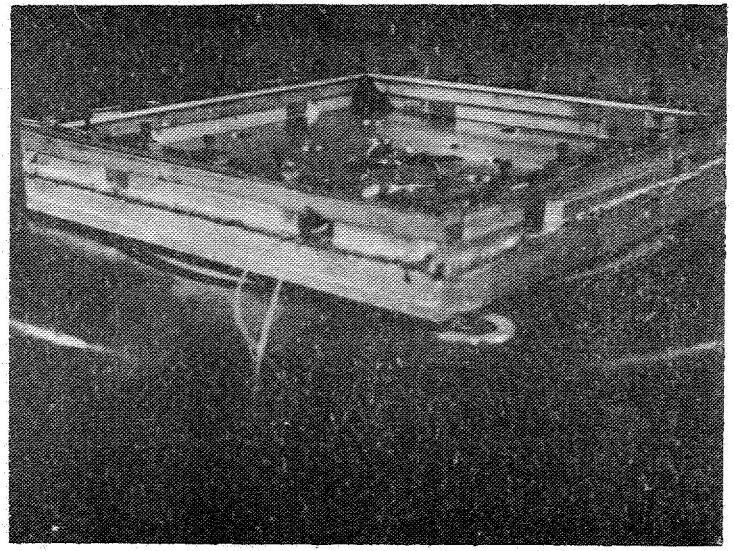

(a) Fixture, Unloaded

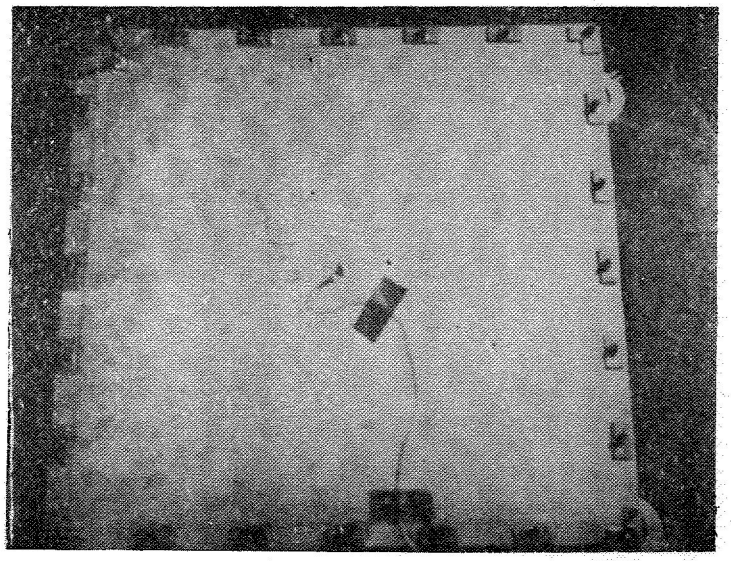

(b) Stiffness Panel Mounted

Figure 85.- Subsize Stiffness Evaluation Test Setup

The proof pressure evaluation test evaluated effects of overpressure conditions in the pressure switch region for assessment of the weld strength that bonded the simulated switch assembly to the detector. The test setup (fig. 86) applied approximately 55 psig or 25% greater than the nominal charge pressure corrected to the maximum temperature level expected in the thermal environment. The general results obtained are as follows:

1) The Type "B" configuration, Panels 8280-04001 (B1), S/N 0000001 and 8280-05001, S/N 0000001 successfully met the requirements of this test;

2) The Type "C" configuration, Panel 8280-07001, S/Ns 0000001 and 0000002 successfully met the requirements of this test. Panel 8280-07051, S/Ns 0000001 and 0000002 successfully met the requirements of this test. Panel 8280-08001, S/N 0000001 successfully met the requirements of this test;

3) The Type "D" configuration, Panel 8280-10001 (D1A), S/Ns 0000001 and 0000002 successfully met the requirements of this test. Panel 8280-14001, S/N 0000001 successfully met the requirements of this test. Panel 8280-16001, S/Ns 0000001 and 0000002 successfully met the requirements of this test;

4) The Type "E" configuration, Panel 8280-19001 (E1A), S/Ns 0000001 and 0000002 successfully met the requirements of this test. Panel 8280-24001, S/N 0000001, successfully met the requirements of this test;

5) The Type "F" configuration, Panel 8280-28000 (F1A), S/N 0000001, received no proof pressure or leak tests because several leaks were found in it during the pressure expansion phase of manufacture. Panel 8280-29000 (F1B), S/N 0000001, received no proof pressure or leak tests because the panel failed during the pressure expansion phase of manufacture.

The helium and residual gas analyzer (RGA) leak test was performed to verify that the fabrication processes used to manufacture the detectors did provide sufficient leaktight conditions to allow an unpunctured specimen to survive 100 years in space. Two types of leak tests were performed. The first was a standard helium leak test performed with a helium mass spectrometer. However, because of the extremely low leakage requirements to satisfy the long life in space, this test (fig. 87) was performed in vacuum

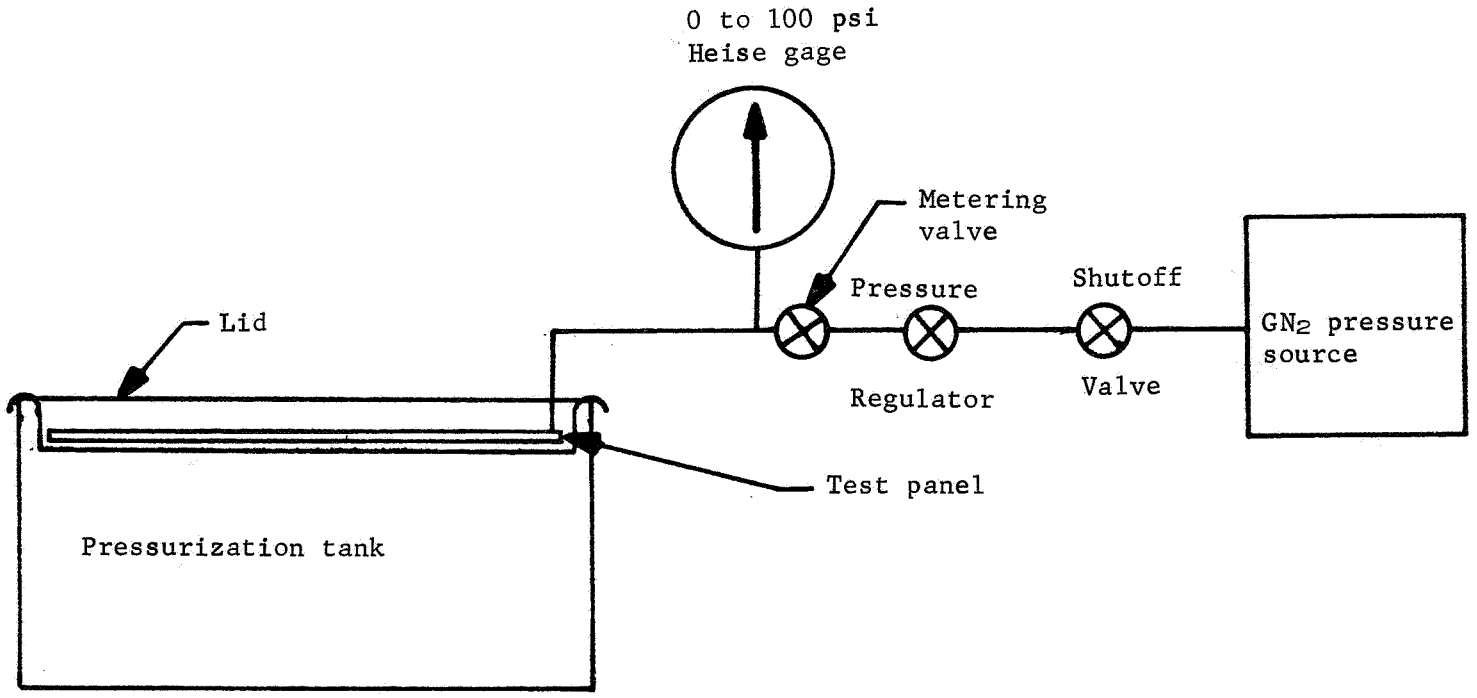


Figure 86.- Proof Pressure Test Setup

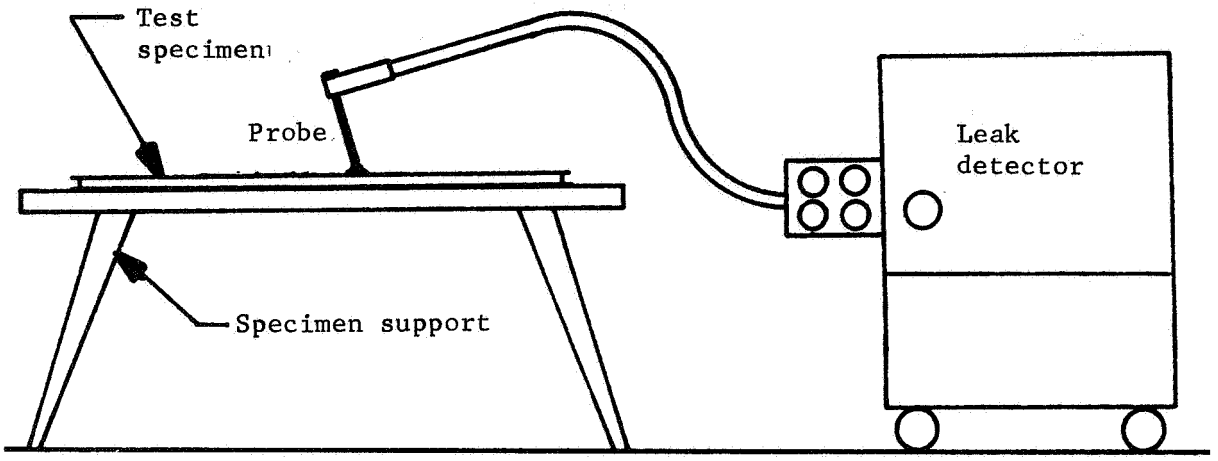


(a) Probe Test Setup

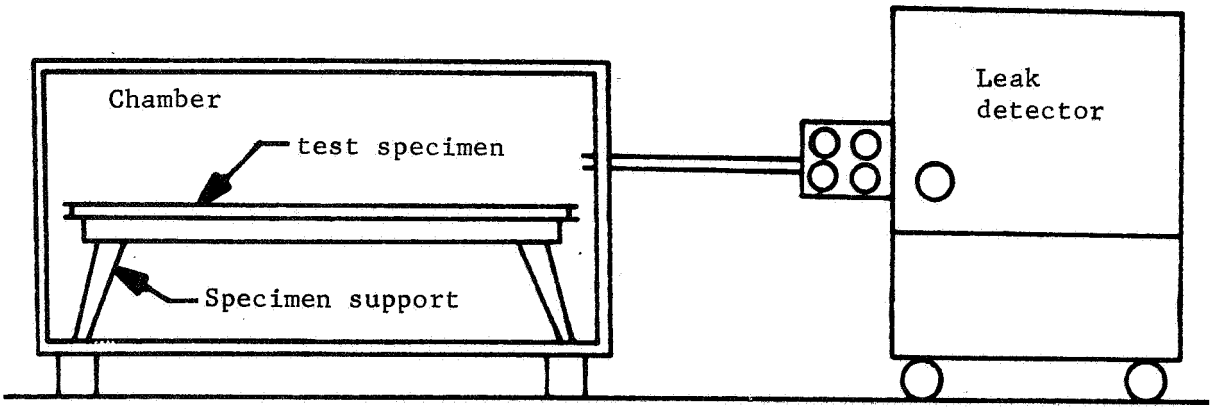


(b) Chamber Test Setup

Figure 87.- Leak Test Setup

chamber to increase accuracy of the mass spectrometer readings. The second type of leak test used a residual gas analyzer in lieu of a helium mass spectrometer. This test setup (fig. 88) was developed specifically for use on this program because of several configurations that required dual pressure chambers that shared a common seam weld or core sheet to separate the pressure chambers. Physically a seal was then contained internal to the detector that did not permit the use of a single tracer gas. Therefore, helium was injected on one side of the seam and Krypton on the other, and through special calibration of the RGA, leaks could be measured across the internal seam or core sheet. The initial test conditions required that no leak could exist that was greater than $1.0 \times 10^{-8}$ scc He/sec. The following is a summary of test results:

1) The Type "B" configuration Panel 8280-04001 (B1), S/N 0000001 successfully met the requirements of the helium leak test. The B1 detector received a mass spectrometer test. Panel 8280-04001, S/N 0000001, was leak tested after vibration and again met the helium leak test requirements. Panel 8280-05001, S/N 0000001, was RGA leak tested in the vacuum chamber and met the requirements of the test;

2) The Type "C" configuration Panel 8280-07001, S/Ns 0000001 and 0000002 both initially received helium leak tests. S/N 0000001 leaked at the fusion weld joint of the panel and pressure switch. It was subsequently repaired and retested. S/N 0000002 met the requirements of this test before and after vibration. Panel 8280-07051, S/Ns 0000001 and 0000002 met the requirements of the helium leak test. Panel 8280-08001, S/N 0000001 was RGA leak tested and found to leak;

3) The Type "D" configuration Panels 8280-10001 (D1A), S/Ns 0000001 and 0000002 successfully met the requirements of the helium leak test. Both detectors received mass spectrometer tests in the vacuum chamber. S/N 0000001 was leak tested after vibration and again met test requirements. Panel 8280-14001, S/N 0000001 initially received a helium leak test. It was found to leak. It was subsequently retested with the RGA system and found to leak. Panel 8280-16001, S/Ns 0000001 and 0000002, met the requirements of the helium leak test;

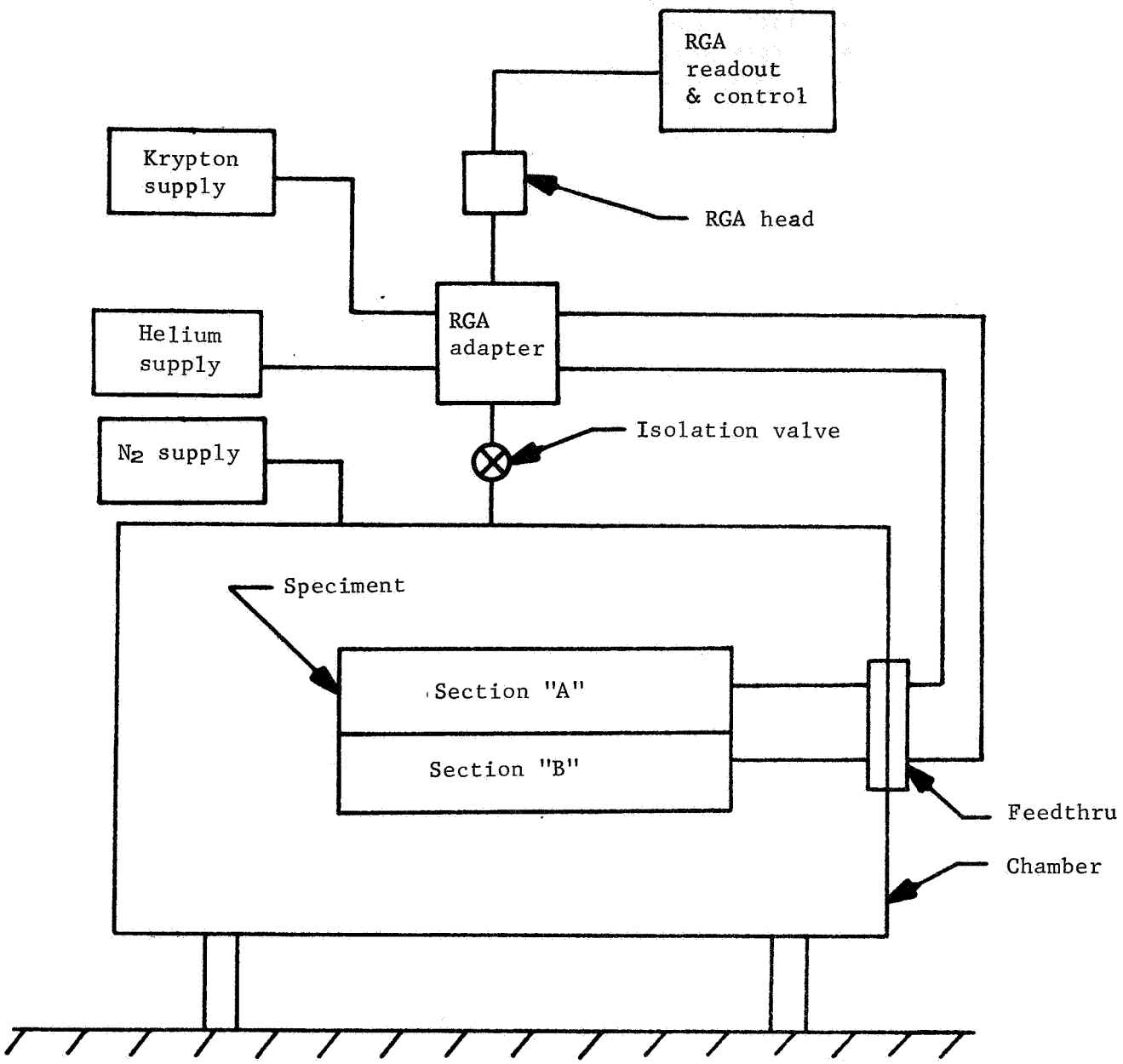


Figure 88.- Residual Gas Analysis Test Setup

4) The Type "E" configuration Panel 8280-19001, S/Ns 0000001 and 0000002, successfully met the requirements of the helium leak test. Both detectors received mass spectrometer tests in the vacuum chamber. S/N 0000001 was leak tested after vibration and again met test requirements. Panel 8280-24001, S/N 0000001, successfully met the requirements of the RGA leak test.

The dynamics evaluation testing consisted primarily of sinusoidal vibration testing to determine detector survival capability and to assess dynamic transmissability characteristic and resonance search of the designs. Other areas of vibration investigation accomplished at the same time were a confirmation of the subsize stiffness evaluation data on full size detectors, and investigation of several mounting designs. In addition tests were performed to evaluate "F" configuration bumper sheet mounting schemes and measurement on bumper sheet deflection when exposed to out-of-plane vibration excitation.

Acoustic effects on thin foils such as the 0.001-in. bumper sheets were also included in this series of evaluation testing.

The setup for the above mentioned test are shown in figures 89 thru 95, and the test conditions were as follows. The sinusoidal vibration test conditions are single axis out-of-plane, with a frequency range of 20 thru 2000 Hz, applied amplitude of 0.3 in. DA $\pm$ 0.015 in. DA from 20 to 36 Hz and $\pm$ 20 g peak $\pm$ 1.0 g peak from 36 to 2000 Hz, with a rate of 1 octave/minute.

The acoustics test conditions were random acoustic field with the following spectrum shape:

| Octave band SPL, dB (re: 0.0002 dynes/cm$^2$) | Midfrequencies of octave bands, Hz |
|---|---|
| 140.9 | 25.0 |
| 143.3 | 50.0 |
| 144.3 | 100.0 |
| 144.1 | 200.0 |
| 142.5 | 400.0 |
| 139.5 | 800.0 |
| 135.0 | 1600.0 |
| 129.2 | 3200.0 |
| 123.1 | 6400.0 |

The overall SPL was 151 dB, with a test exposure of 4 minutes.

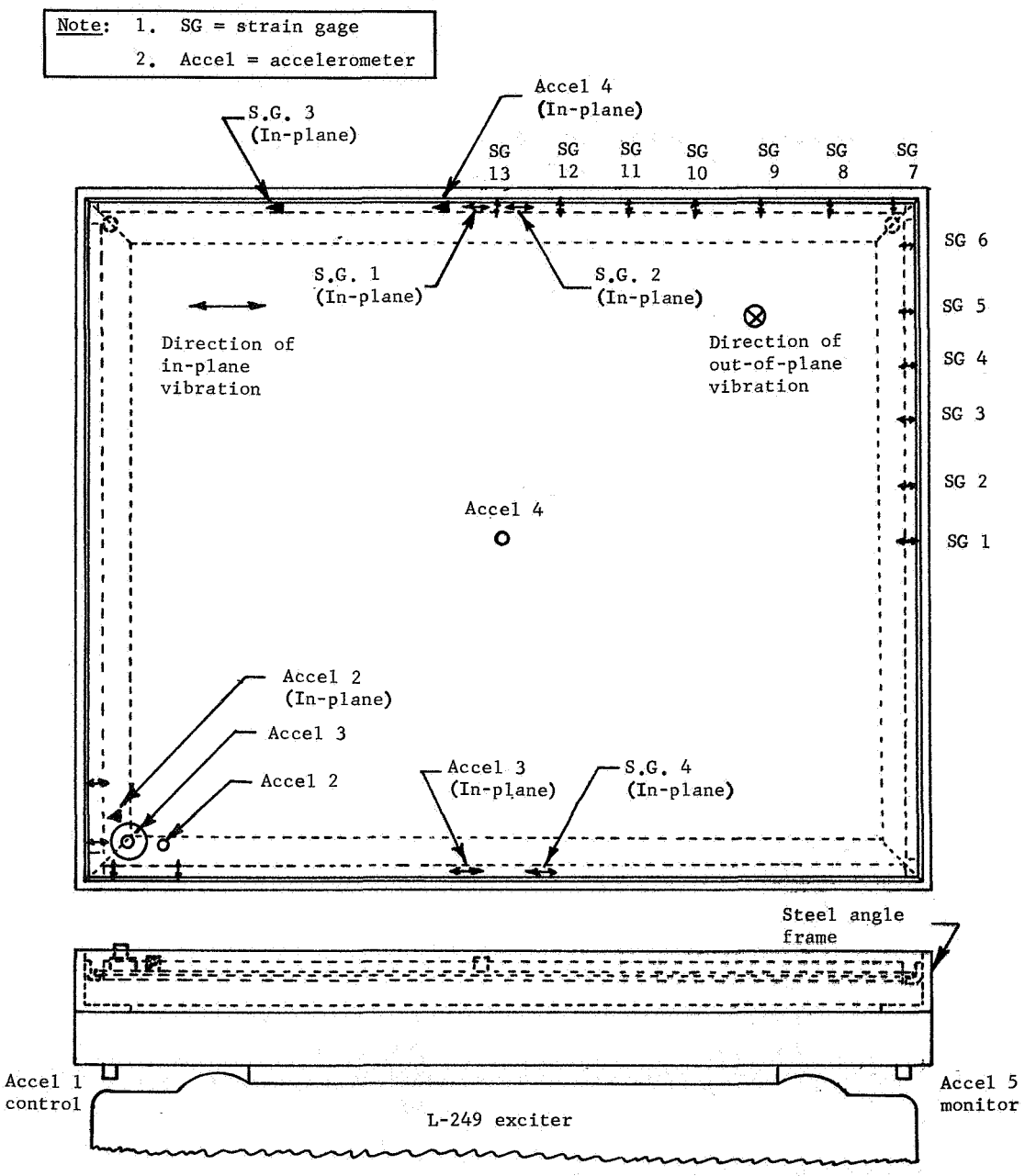


Figure 89.- Accelerometer and Strain Gage Locations, Stiffness Evaluation Test

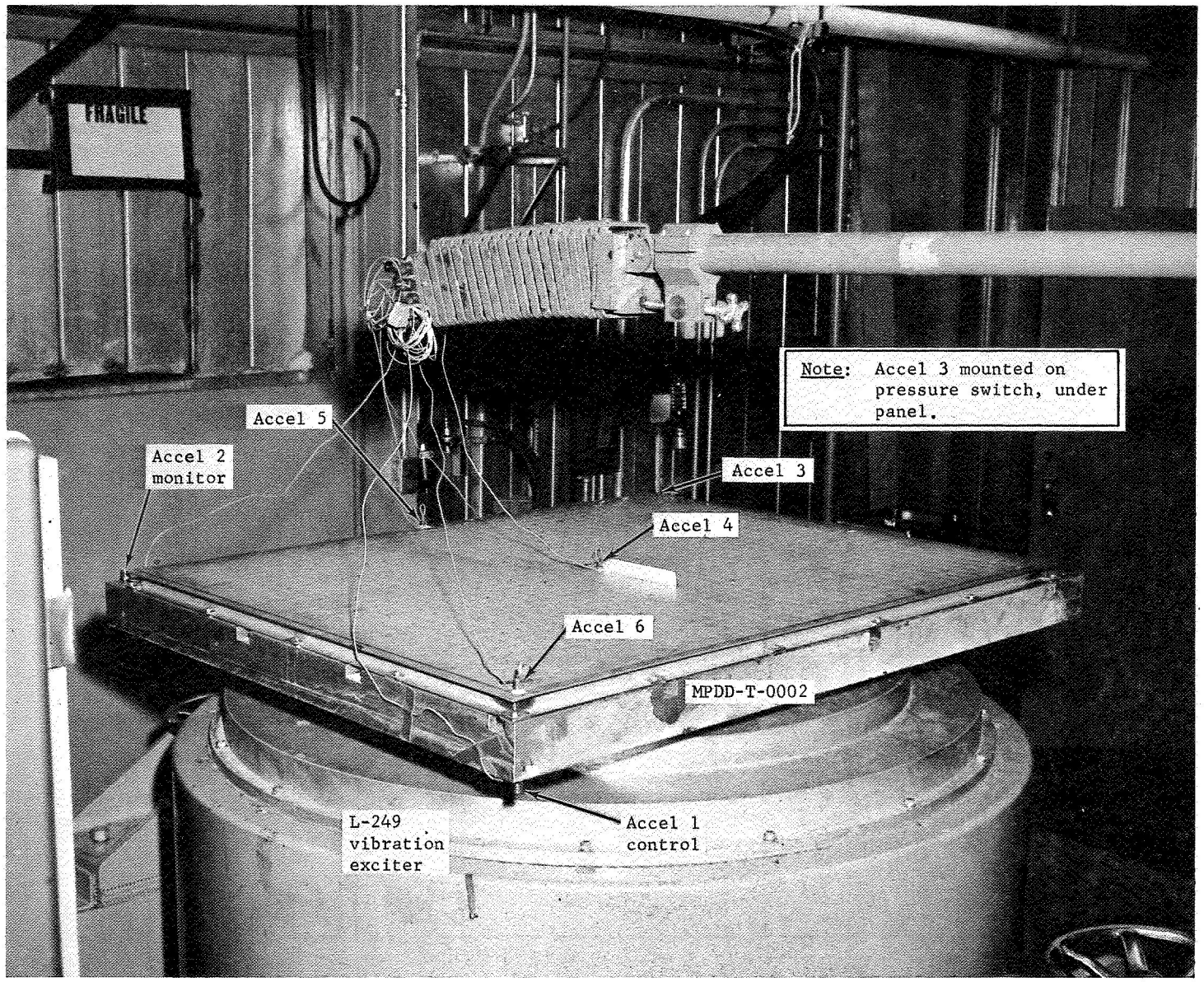


Figure 90.- Vibration Test Setup Photograph

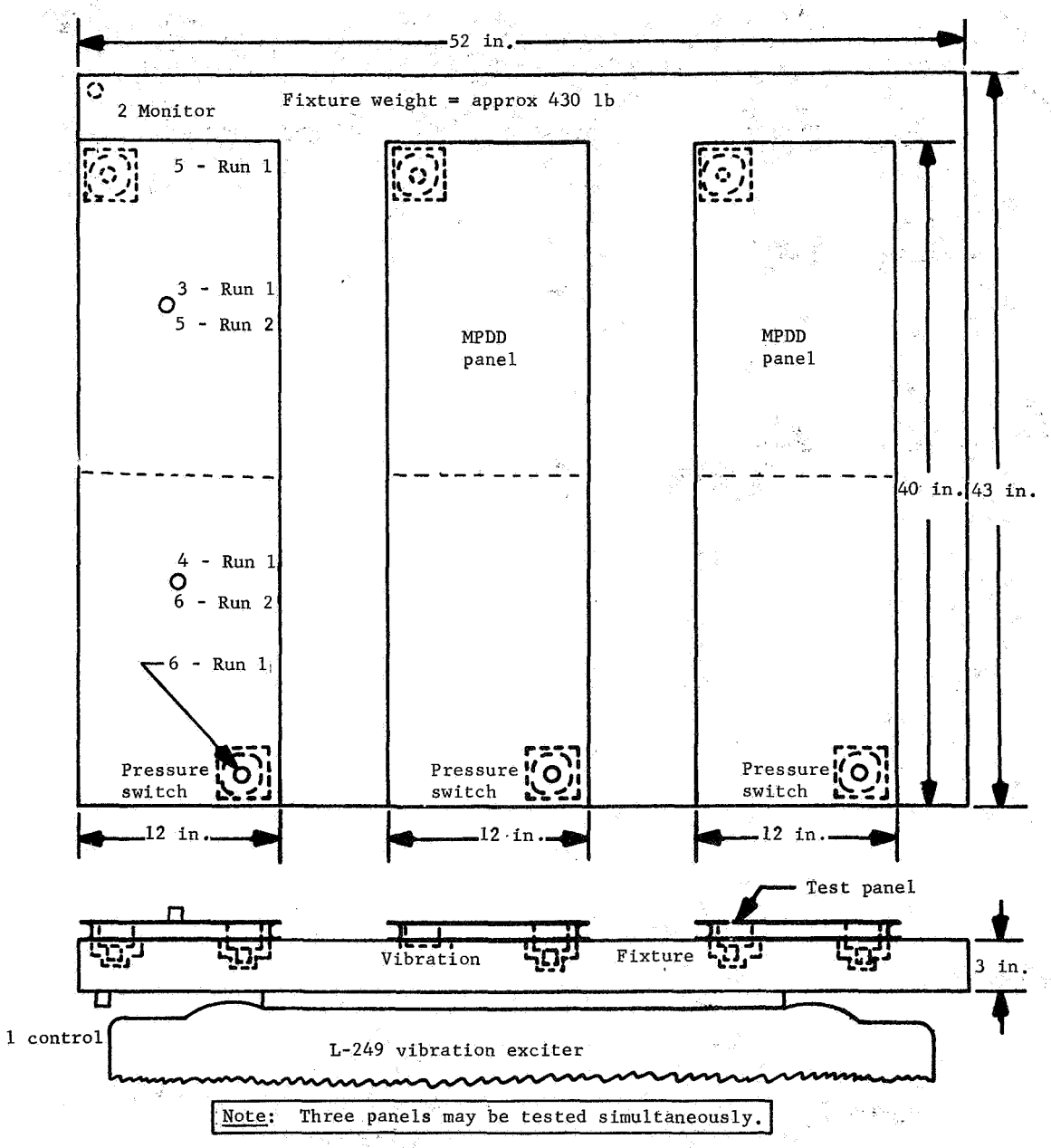


Figure 91.- Vibration Test Setup

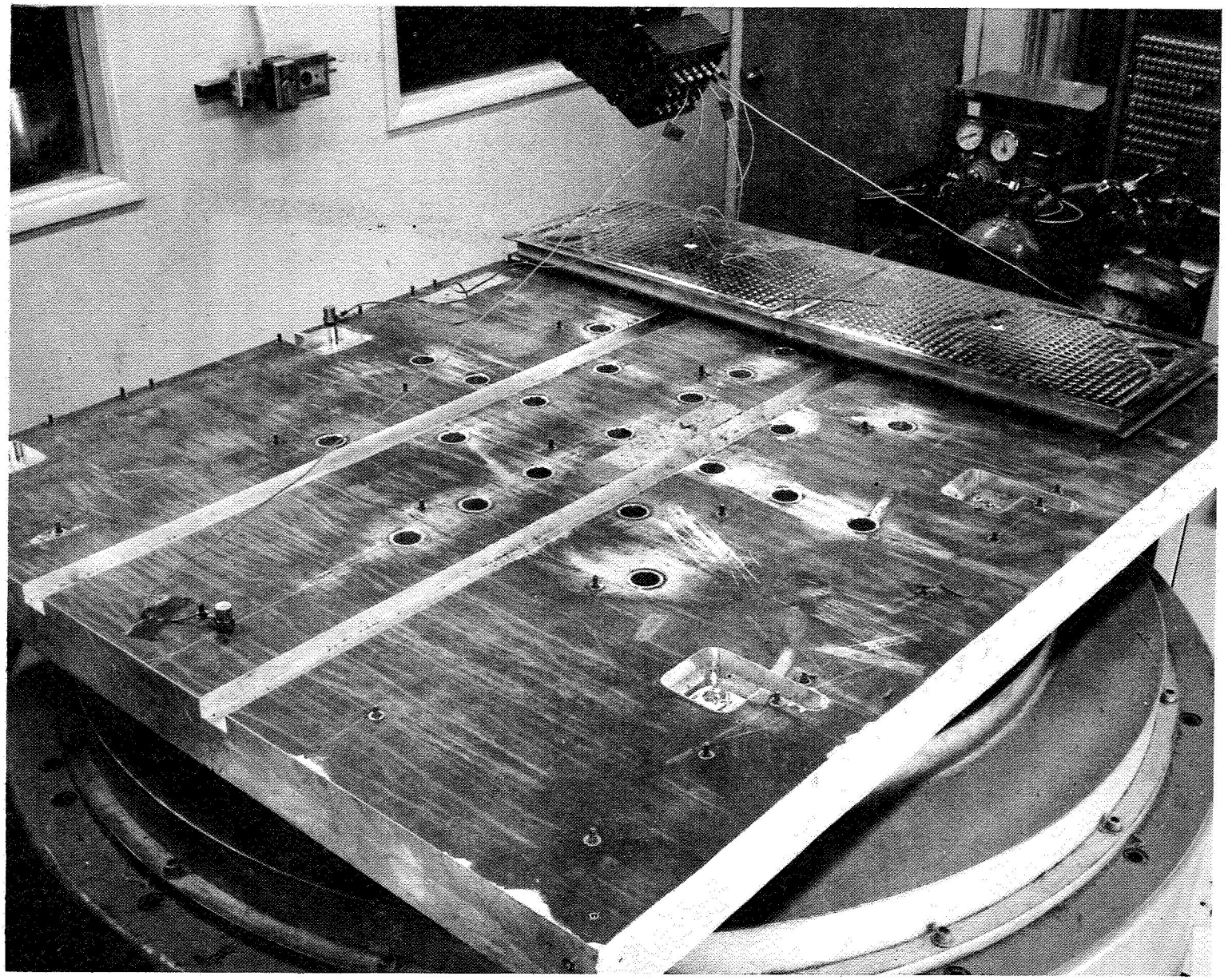

Figure 92.- Vibration Test Setup for F Configuration Panel

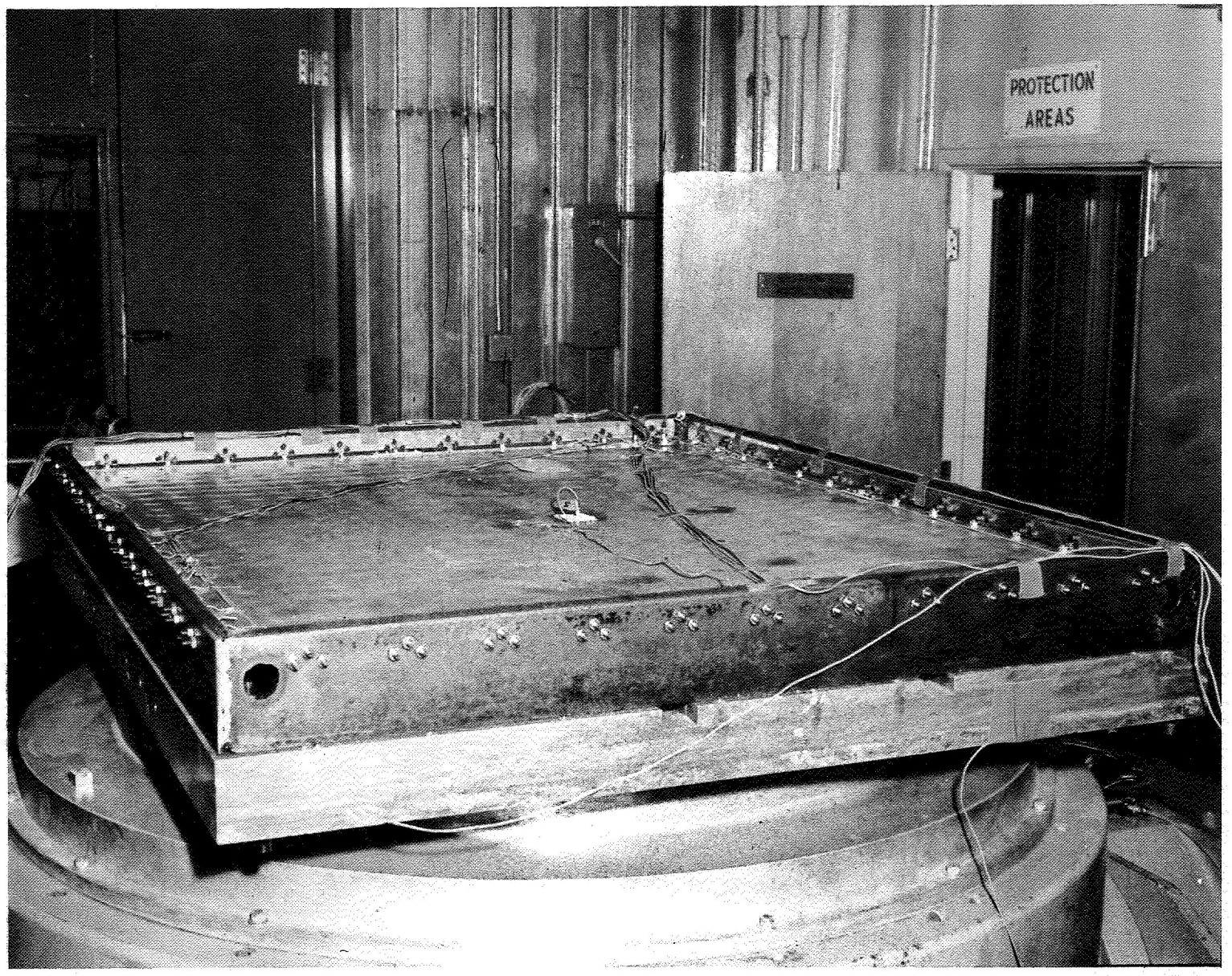


Figure 93.- Angle Mounting Evaluation Setup

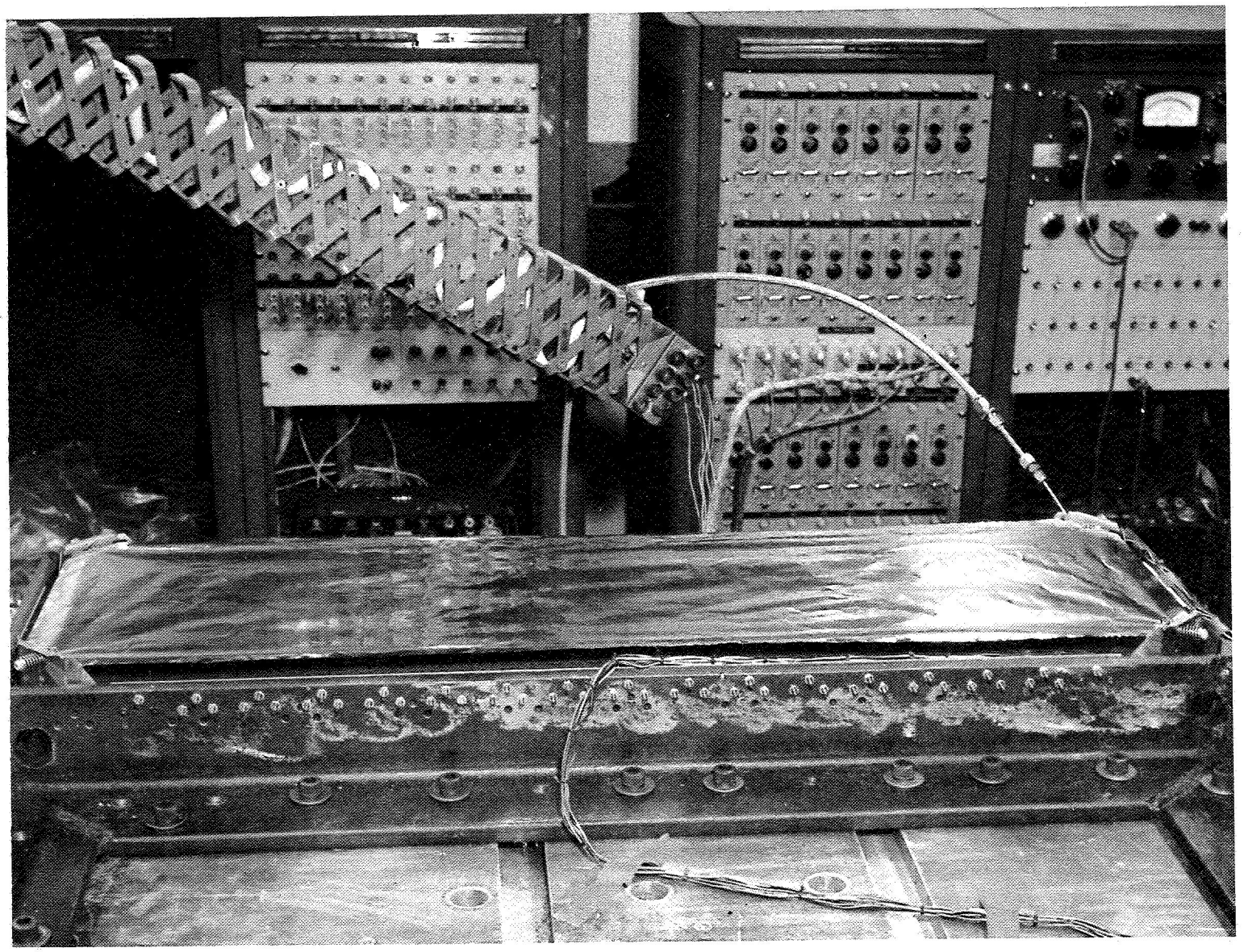

Figure 94.- Bumper Sheet Deflection Evaluation Test Setup

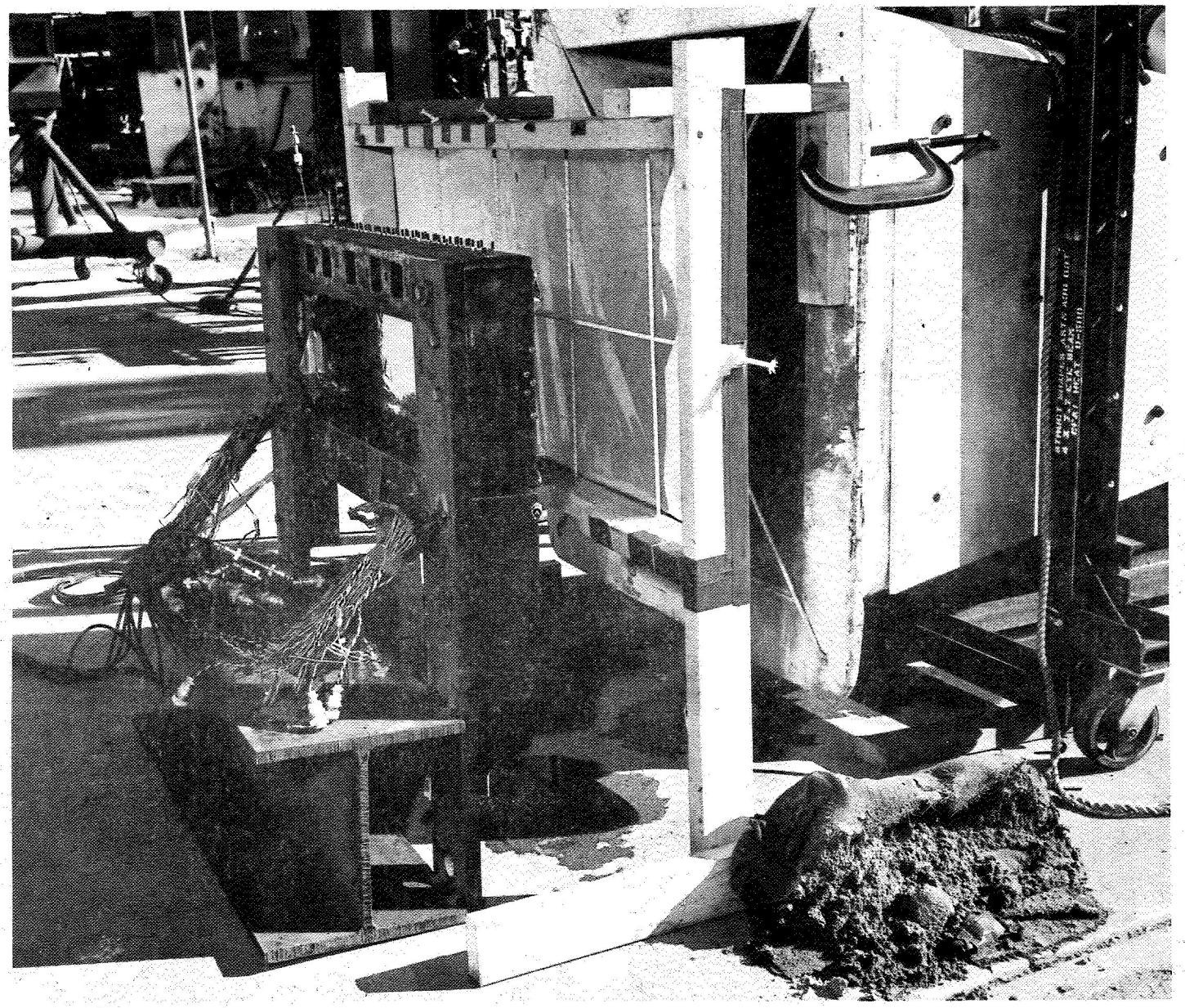

Figure 95.- Acoustic Test Setup, F Configuration

The following paragraphs summarize the test results obtained during the aforementioned testing:

1) The Type "B" configuration, vibration tests, Panel 8280-04001, S/N 0000001, was subjected to a 20 g peak sinewave vibration. Accelerometer data were obtained during this test. The detector met the requirements of this test.

2) The Type "C" configuration, vibration tests, Panel 8280-07001, S/N 0000002, was subjected to a 20 g peak sinewave vibration test. Accelerometer data were obtained during this test. The detector met the requirements of this test.

3) The Type "D" configuration, vibration tests, Detector 8280-10001 (D1A), S/N 0000001, was subjected to a 20 g peak sinewave vibration. Accelerometer data were obtained during this test. The detector met the requirements of this test.

4) The Type "E" configuration, Detector 8280-19001 (E1A), S/N 0000002, was subjected to a 20 g peak sinewave vibration. Accelerometer data were obtained during this test. The detector met the requirements of this test. This detector was also instrumented with strain gages to obtain load data. The detector was rerun a second time after it was pressurized to 280 psig to increase its stiffness. At the conclusion of all these tests, the detector did not leak, nor had it developed any metal fatigue. Detector 8280-19001 (E1A), S/N 0000001 was fitted with the aluminum angle mount system, instrumented with strain gages and accelerometers, and subjected to tests in the following sequence:

   Sinewave - 10 g peak, out-of-plane axis;

   Random - 11.1 grms, out-of-plane axis;

   Sinewave - 10 g peak, in-plane axis;

   Random - 11.1 grms, in-plane axis;

   Sinewave - 10 g peak, out-of-plane axis;

   Sinewave - 10 g peak, out-of-plane axis, increased pillow height;

Sinewave - 10 g peak, out-of-plane axis, further increased pillow height.

No physical damage was incurred during this testing.

5) The Type "F" configuration, vibration tests, Panel 8280-28000, S/N 0000001, was subjected to a 10 g peak sinewave vibration and an 11.1 grms random vibration. Accelerometer and strain gage data were obtained during this test. No mechanical damage was apparent at the completion of these tests.

The Acoustic Test on Panel 8280-28000, S/N 0000001, consisted of a 151 dB sound pressure level, random acoustic noise test. Microphone and strain gage data were obtained during this test. No mechanical damage was apparent at the completion of this test.

The bumper sheet deflection test determined which of two bumper sheet mount schemes would be most reliable in the operational conditions. The type of test performed was sine vibration with measurement of bumper sheet deflection during vibration excitation. Both methods proved to be satisfactory, however, performance of the spring mount appears to be superior to the rigid mount.

Additional mount evaluation testing was also accomplished during the full-size design evaluation testing to determine the effects of thermal expansion and contraction on the detector and its associated mounts when they are exposed to the extreme temperature conditions of outer space. This test was accomplished on an "E" type of detector, which was considered the worse-case condition. The test was performed as shown in figures 96 and 97. The following results were obtained.

Detector 8280-19001 (E1A), S/N 0000001 was subjected to radiant heat sufficient to obtain a minimum of +350°F, in the middle of the panel, with the panel vented to ambient pressure. It was next subjected to an $LN_2$ spray bath until the panel was at -320°F. The radiant heat portion was repeated with 11.5 psig in the panel. No physical damage was incurred during this testing.

Special design evaluation test.- Two special design evaluation tests were accomplished during the preliminary design evaluation testing. The first of these occurred before the mount evaluation testing of full-size detectors when it was thought

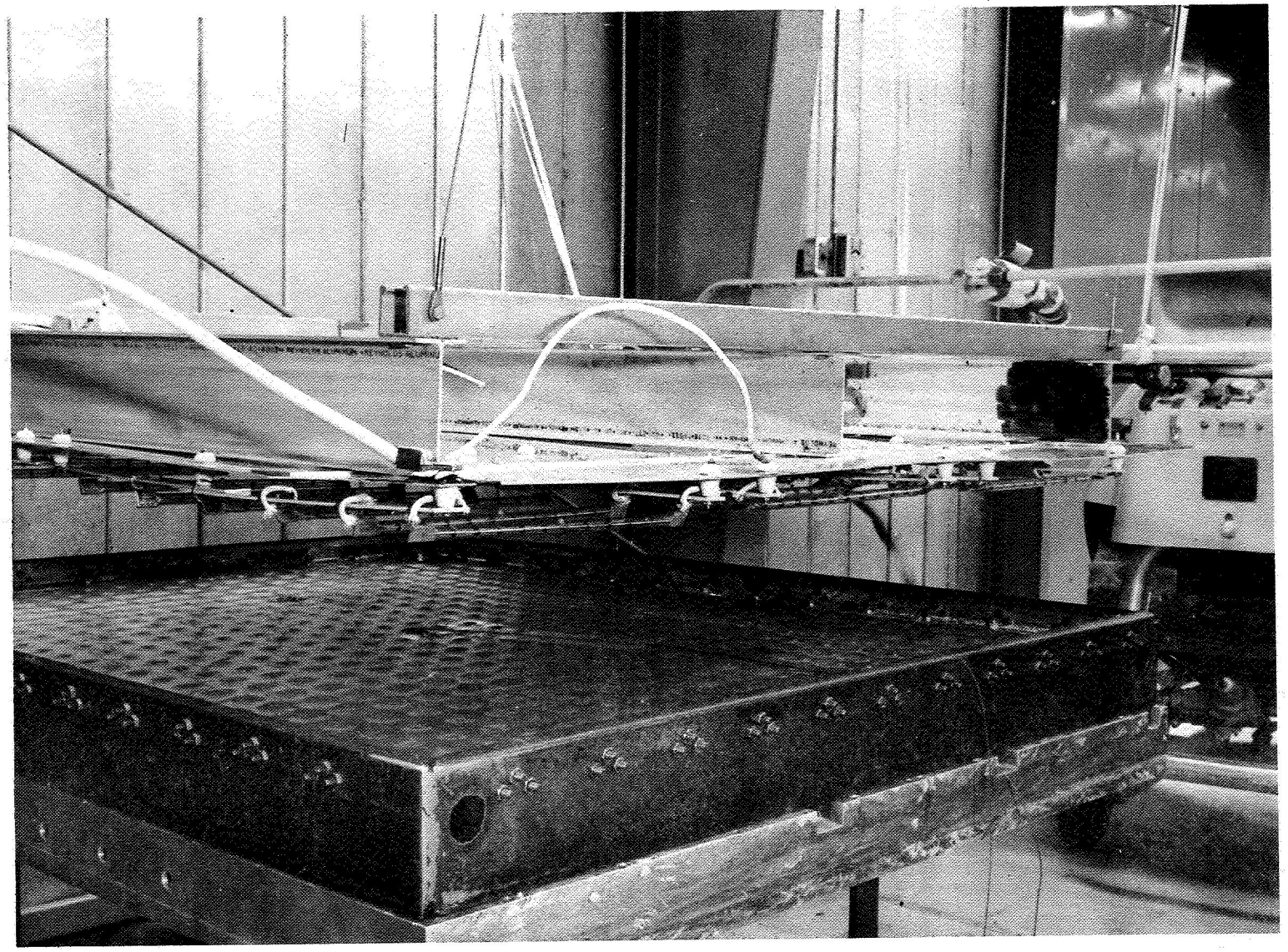

Figure 96.- Thermal Test, Radiant Heat, Mount Evaluation

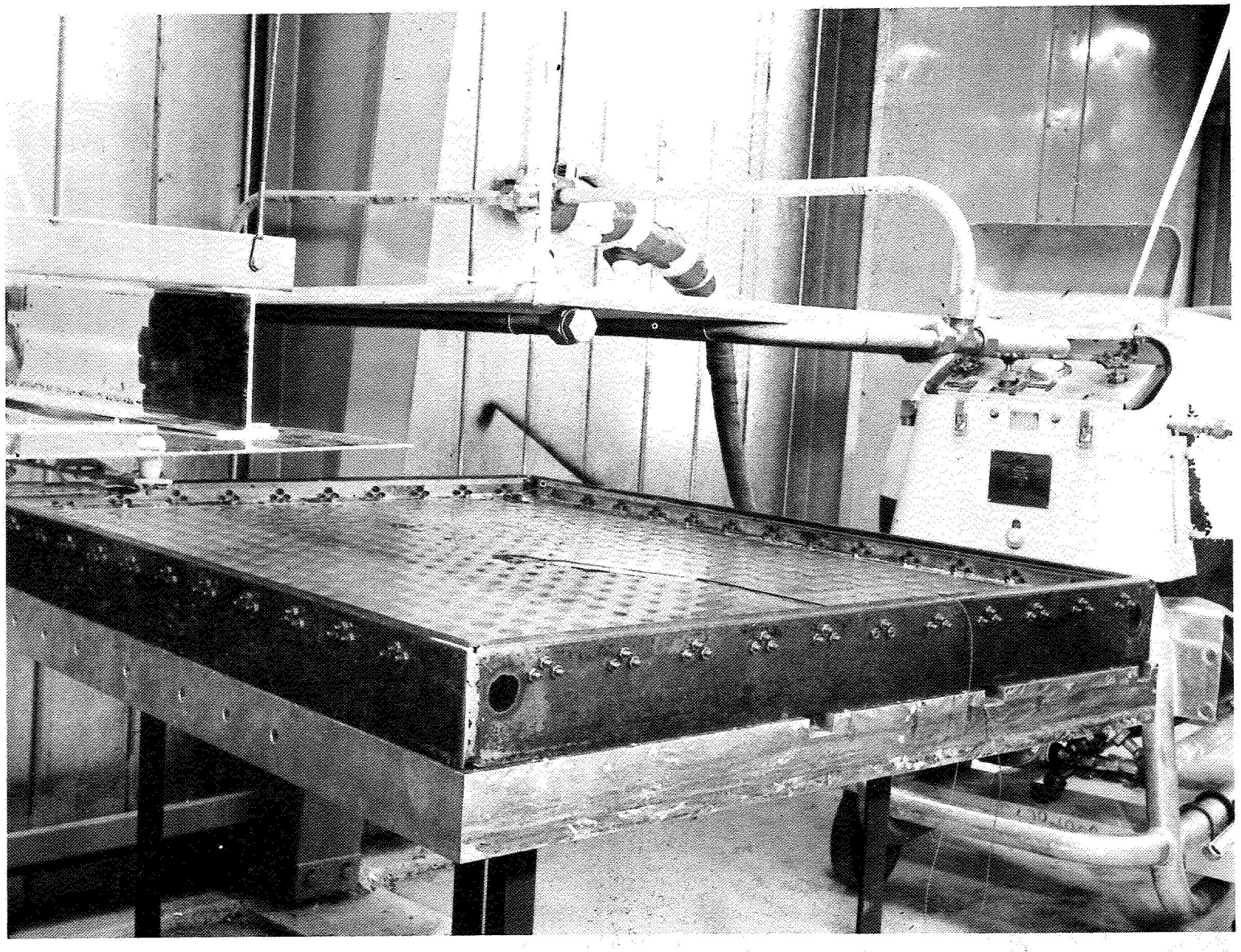

Figure 97.- Thermal Test, $LN_2$ Cooling, Mount Evaluation

that commercially available isolators could be incorporated into the detector design. The mounts considered most suitable were the Aeroflex ladder and helical isolators. Two isolators were selected from off-the-shelf items and were subjected to vibration evaluation. The second test was a high g vibration test of the pressure switch assembly that resulted from data gathered during vibration evaluation of full-size detectors. This test indicated a much higher detector amplification factor than the design had anticipated.

Commercial mounts evaluation: This test consisted of a complete vibration evaluation of the Aeroflex helical cable isolator C3-HBA10-12 and 6-strand ladder cable isolator.

The test setup is shown in figure 19. Two sets of isolators were loaded with metal weights of approximately 1, 2, and 3 lb isolators. A three-axis vibration test was planned. Each axis was subjected to a series of 5, 10, and 20 g at 0.3 double amplitude, and swept from 5 to 2000 Hz at a rate of 1 octave/minute.

The helical isolators failed during the first run at 5 g input and 18 cps with a load of 10 lb. The isolators were mounted in sheer with 1 g input along the axis of the helix. The forcing function was normal to the axis of the helix and normal to the plane of the load. At the time of failure the following levels were experienced: 30 g along the forcing vector axis, 48 g along a vector in the horizontal plane and normal to the forcing vector, and 62 g along a vector in a vertical plane and normal to the forcing vector. The isolators were permanently deformed as evidenced by static deflection along the shear axis of 2:1 over the before-test deflection. Also, the helic was permanently deformed radially.

The ladder isolator failed during the third run at 20 g input and 36 cps with a load of 1 lb. The single plane isolators were mounted in tension (upper isolator in tension; lower isolator unloaded). The forcing function was normal to the plane of the weight and normal to the cable strands. The isolators survived 5 and 10 g before failure. At the time of failure, levels of 38 g along the forcing vector, 20 g along a vector in the horizontal plane and normal to the forcing function, and 90 g along the vector in a vertical plane and normal to the forcing vector were experienced. Failure was indicated by strand breakage. A greater number of strands were broken at the center of the wire rope, indicating failure from excessive tensile force.

An investigation of instrumentation data indicated the motion of the weight was elliptical in all three planes. The highest g levels were experienced in a horizontal plane normal to the forcing vector.

Investigation of vendor data indicated the helical and ladder isolators have Q's of between 2 and 5 at input levels of 1/4 to 1/2 g. The input levels are an order of magnitude of 1/40 the inputs we are required to test to. Therefore, these isolators could not be used for panel isolation on the MPDD program. However, the isolators could be used where large loads are required to be isolated for low level inputs.

Pressure switch vibration evaluation: The objective of this test was to evaluate the pressure switches' capability to perform and survive in a high environment. The need for this evaluation was established during design and process evaluation testing when detector/panel dynamics characteristics indicated a considerably higher amplification factor than had been anticipated. This test was performed on one each of the Servonics and Carleton designs and is shown in figures 98 and 99. The test conditions were as follows: frequency range of 5 to 2000 Hz, with input levels of 0.4 in. DA from 5 to 70 Hz and 100 g peak from 70 to 2000 Hz.

The above levels were applied to each of the mutually perpendicular axes, and contact chatter was continuously monitored. Both switches survived the above environments with no apparent mechanical or functional degradation, however, both designs did experience contact chatter.

## Design Development Evaluation Testing

The Design Development evaluation test program was performed as a preliminary qualification test program for the detector/panel assemblies. The testing of the detectors included a complete environment evaluation except for thermal environments. Another area of development testing was the pressure switch subassemblies. These tests included total dynamic and thermal environmental evaluation.

As a result of the pressure switch development and fabrication techniques, untested materials were interjected into the program. This created a need for special material testing, which was also a portion of this testing phase. The following paragraphs define the testing operations and briefly summarize the test results.

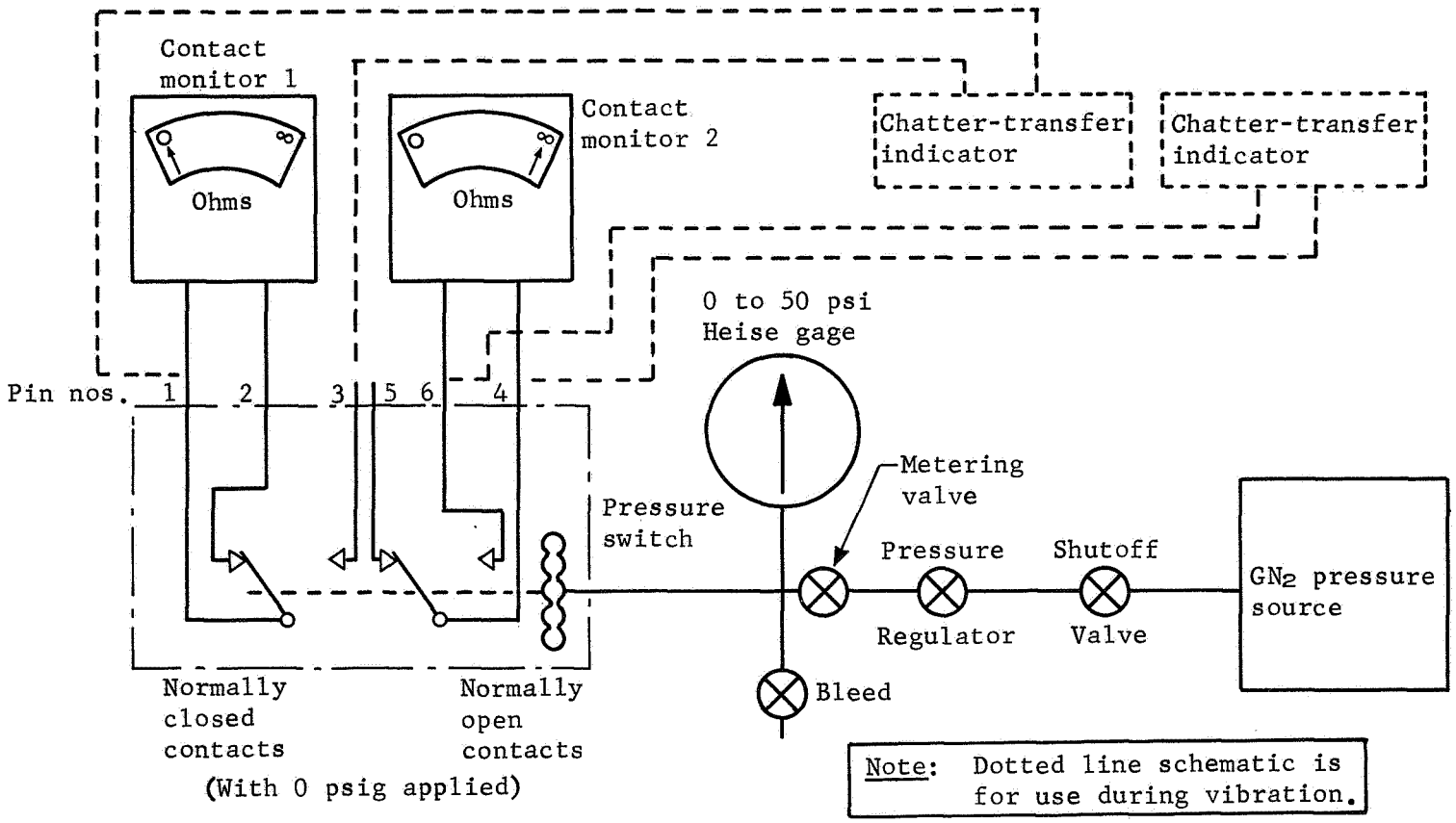


Figure 98.- Switch Monitoring Diagram

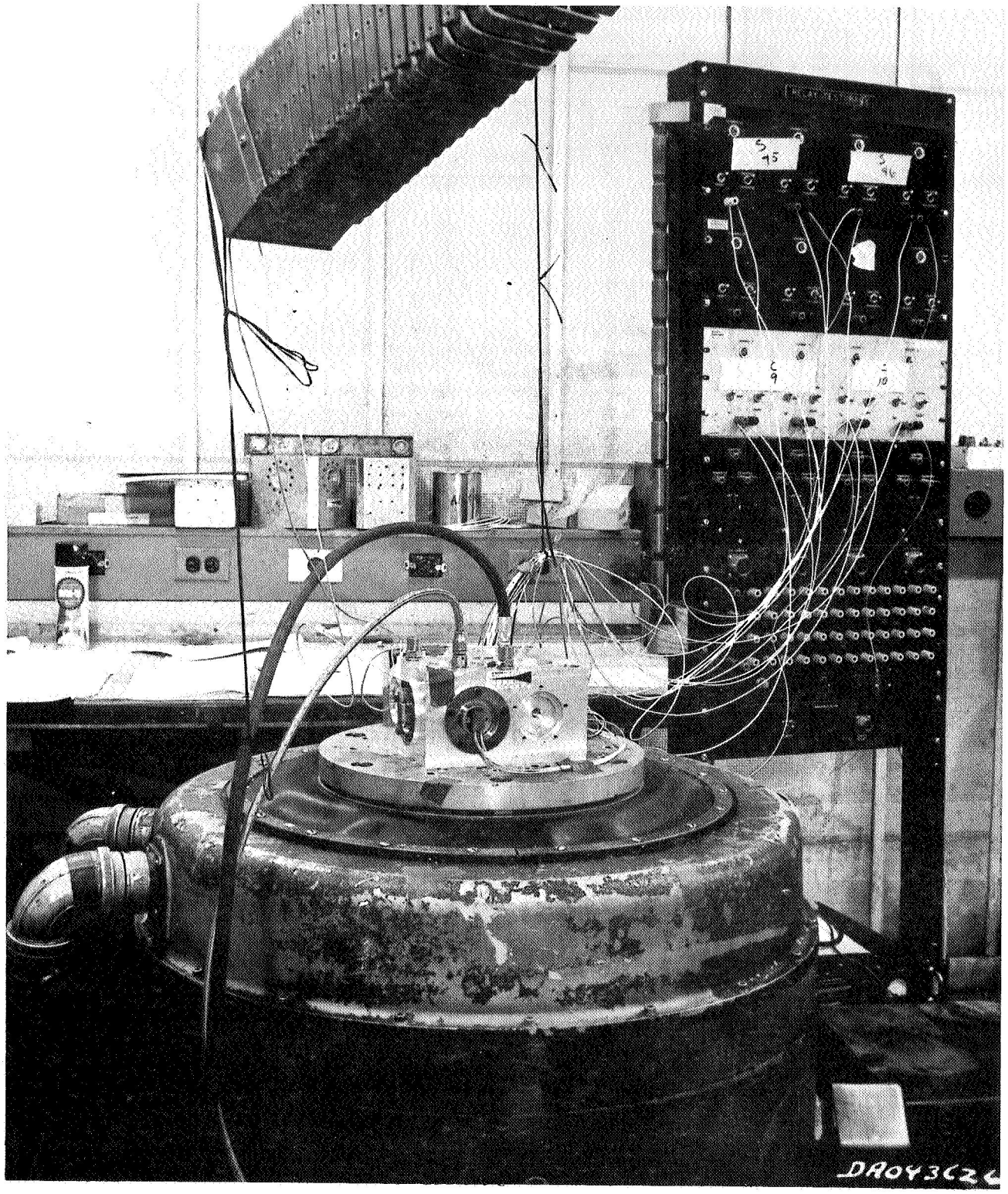


Figure 99.- Pressure Switch Vibration and Shock Test Setup

Pressure switch design evaluation test.- Two vendors were selected to develop pressure switch subassemblies for use on the MPDD detector/panels. Each vendor was responsible for conducting a series of development tests to ensure adequacy of his assembly to perform to the requirements of the Martin Marietta procurement specification. The test requirements were identified in drawing PD7100075 and included the following:

1) Functional operations;

2) Insulation resistance;

3) Proof pressure;

4) Helium leak;

5) Vibration (sine and random);

6) Shock;

7) Steady-state acceleration;

8) Thermal pressure cycling;

9) Acoustics;

10) Thermal vacuum soak;

11) Humidity;

12) Pressure burst.

The two vendors selected were Carleton Control Corporation and Servonic Instrument.

Servonic Instrument's pressure switch development testing summary: During the early part of the development testing, several problems were encountered. These problems, with their respective corrective actions, were documented on MARS tag numbers B-42959, B-35225, B-35226, B-35227, B-50673, B-50674, B-50674, and B50676.

The two major problems were insulation resistance breakdown and contamination of the electrical contacts. The insulation breakdown was solved by the elimination of the potting compound on the electrical terminations. The contact problem was solved by replacing the contacts with Ney ORO G material and

keeping moisture out of the contact area and by keeping the units backfilled with dry nitrogen throughout the test program.

At the start of the thermal pressure cycling test conducted by the Ogden Rototest Laboratories, the test units were connected to a shop air pressure supply. This caused icing and contamination of the contacts during the low temperature part of the test. This was in violation of the test procedure. All five samples were cleaned and dried, and testing was resumed using dry nitrogen as the pressurizing source in accordance with the procedure requirements. There were no more problems or out-of-tolerance conditions noted throughout the remainder of the test program. Due to instrumentation problems, both temperature and pressure were measured and recorded at convenient intervals instead of being continuously recorded during the thermal pressure cycling test and the thermal vacuum soak test.

There were some difficulties in scheduling the thermal pressure cycling test; therefore, upon agreement with the Martin Marietta, Denver representative, the testing sequence as outlined in Servonic Procedure, STP-3152-0101, was altered to allow continuance of the tests with a minimum of lost time.

Carleton Control's pressure switch development testing summary: Carleton did not perform a development test program. After design and fabrication this switch assembly was subjected directly to qualification testing (discussed later in this chapter).

Detector design development evaluation testing.- These tests evaluated operation of the detector in the area of all applicable functional and environmental criteria (excluding thermal environments) required for mission success. This program included the following tests: (1) switch assembly functional test; (2) leak test, both helium and RGA; (3) proof pressure test; (4) pressure cycling test; (5) vibration test, both sinewave and random; (6) shock test shaped pulse, and (7) acoustics test. To enhance the probability of success in the production test program all of the tests were performed using qualification test levels.

Functional test: The specific test performed included both switch point verification and contact resistance testing. The test setup used is shown in figures 100 and 101. The test criteria for switch point test required that switch contact transfer would occur when applying a differential overpressure of 6.0 $\pm$ 2.5 psig to the pressure port and verifying that the switch points reverse at the appropriate pressure levels. The contact resistance

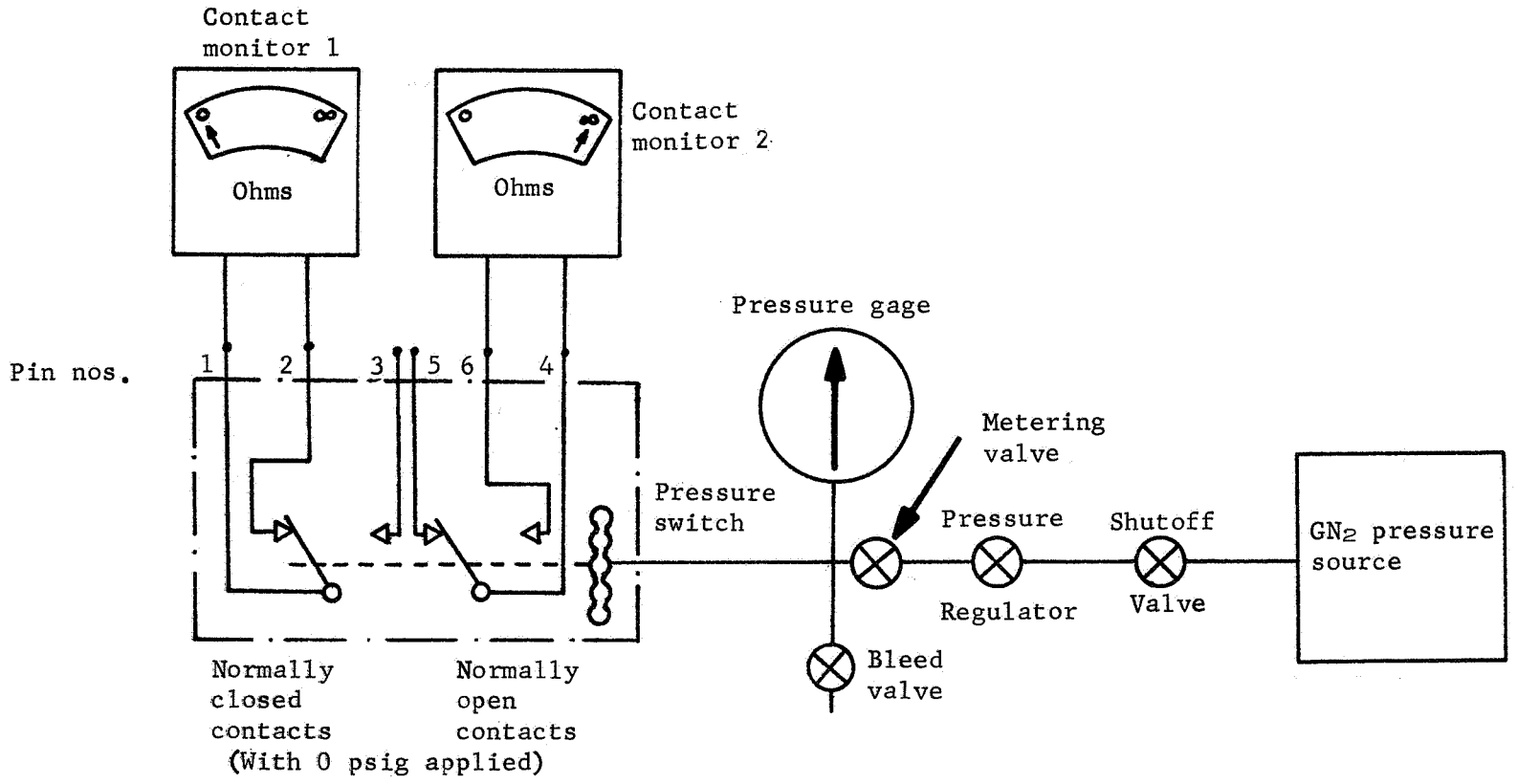


Figure 100.- Switch Monitoring Test Setup

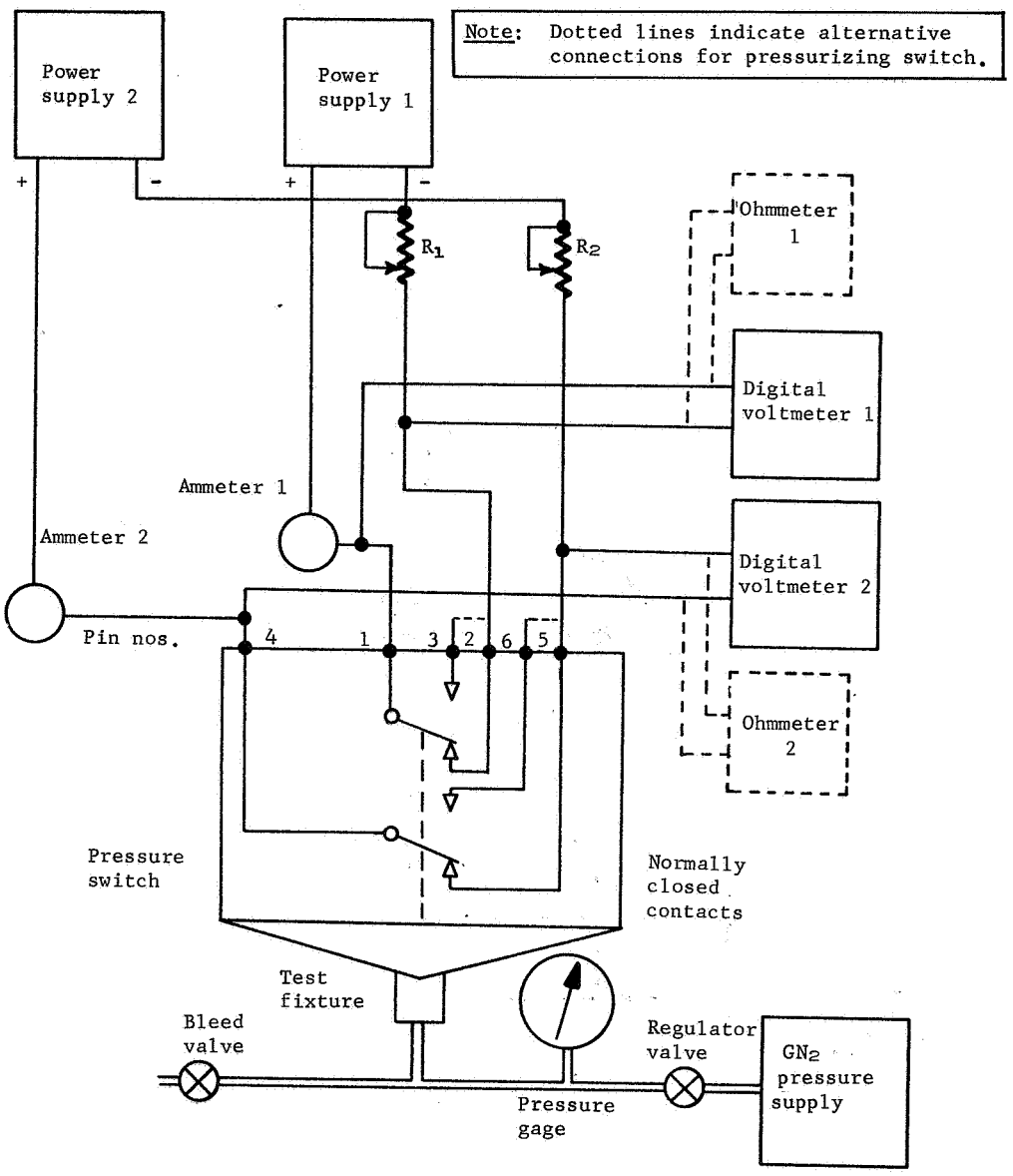


Figure 101.- Functional Test Setup, Contact Resistance

was measured as a voltage drop across the switch contact points and verifying that the resistances did not exceed 100 milliohms at 0.5 A nor 200 millohms at 100 uA.

Leak test: A helium leak test and residual gas analysis (RGA) was used on this program. Regardless of the test, all specimens were pressurized, subjected to a vacuum, and leakage sensed at the external surface of the specimen and/or between chambers on the dual detector.

The helium leak test (fig. 87) consisted of using gaseous helium in conjunction with a vacuum chamber and a helium mass spectrometer. The specimens were charged to 27.0 $\pm$ 0.5 psia at $70^{\circ} \pm 10^{\circ}$F and placed in a vacuum of $1 \times 10^{-5}$ torr. Verification that no leak exists greater than $3.0 \times 10^{-9}$ scc/sec was made using a helium mass spectrometer.

The RGA testing (fig. 88) required two inert gases (helium and krypton) and a residual gas analyzer in conjunction with a vacuum chamber. Specimens subjected to this test were charged to 27.0 $\pm$ 0.5 psia at $70^{\circ} \pm 10^{\circ}$F, with krypton gas on one side and helium gas on the other side. It was verified by use of a Ultek quad 250 RGA, that no intercore leakage greater than $3.0 \times 10^{-9}$ scc/sec exists between chambers or external to the panel.

Proof pressure test: This test (fig. 86) was performed on all detector/panel assemblies to determine if maximum overpressure has any harmful effect on the switch actuation pressure levels. This test was performed prior to any environmental tests.

The detector/panels were pressurized to a differential pressure 25% greater than the nominal charge pressure corrected to maximum temperature (55 psig minimum). Actuation and reactuation pressures were verified not to have changed from the required pressure of 6.0 $\pm$ 2.5 psig as a result of application of proof pressure.

Pressure cycling test: This test (figs. 82 and 83) was performed on selected specimens of all types of assemblies to assess structural fatigue levels.

This test consisted of connecting the detector/panel to a test tool capable of increasing and decreasing the applied pressure at a sufficiently slow rate to allow the pressure change to be sensed throughout the specimen volume. The pressure was cycled between 14 psig and 49.3 psig for a minimum of 21 344 cycles.

Actuation and reactuation pressures were verified not to have changed from the required pressure of 6.0 $\pm$ 2.5 psig.

Vibration test (figs. 102 and 103): The specified vibration environment was applied to the test specimens. All pertinent inputs and outputs were monitored during each part of the test. Any distortion of signal or information, or deviation of parameters that results from the vibration testing was recorded. A complete record of each vibration test was maintained, including a history of the sinewave survey showing all resonant frequencies detected and details regarding the operation of the specimen under test. All of the vibration tests were applied to the test specimen along each of the three mutually perpendicular axes.

The sinewave vibration test were performed on all detector assemblies using the following test conditions:

1) Frequency range: 5 to 2000 Hz;

2) Control amplitude: 0.4 in. DA from 5 to 10 Hz, $\pm$ 2 g peak from 10 to 44 Hz, 0.02 in. DA from 44 to 96 Hz, $\pm$ 10 g peak from 96 to 2000 Hz;

3) Sweep rate: 1 octave/minute (8.64 minutes nominal, 9.0 minutes maximum);

4) Type sweep: Unidirectional, constant octave.

The random vibration test was performed on all detector assemblies. The required spectrum consists of the following parameters:

1) Frequency range: 10 to 2000 Hz;

2) Spectrum shape: Flat 200 to 700 Hz at 0.12 $G^2$/Hz, rolloff below 200 Hz at 3 db/octave, rolloff above 700 Hz at 6 db/octave;

3) Test duration: 5 minutes/axis;

4) Overall level: 11.1 grms.

Shock test: The appropriate specified shock pulse was applied to each of the designated test units, once in each direction of the three mutually perpendicular axes for a total of six shock applications per unit. A shock pulse of 50 g peak was used for all detector/panel assemblies.

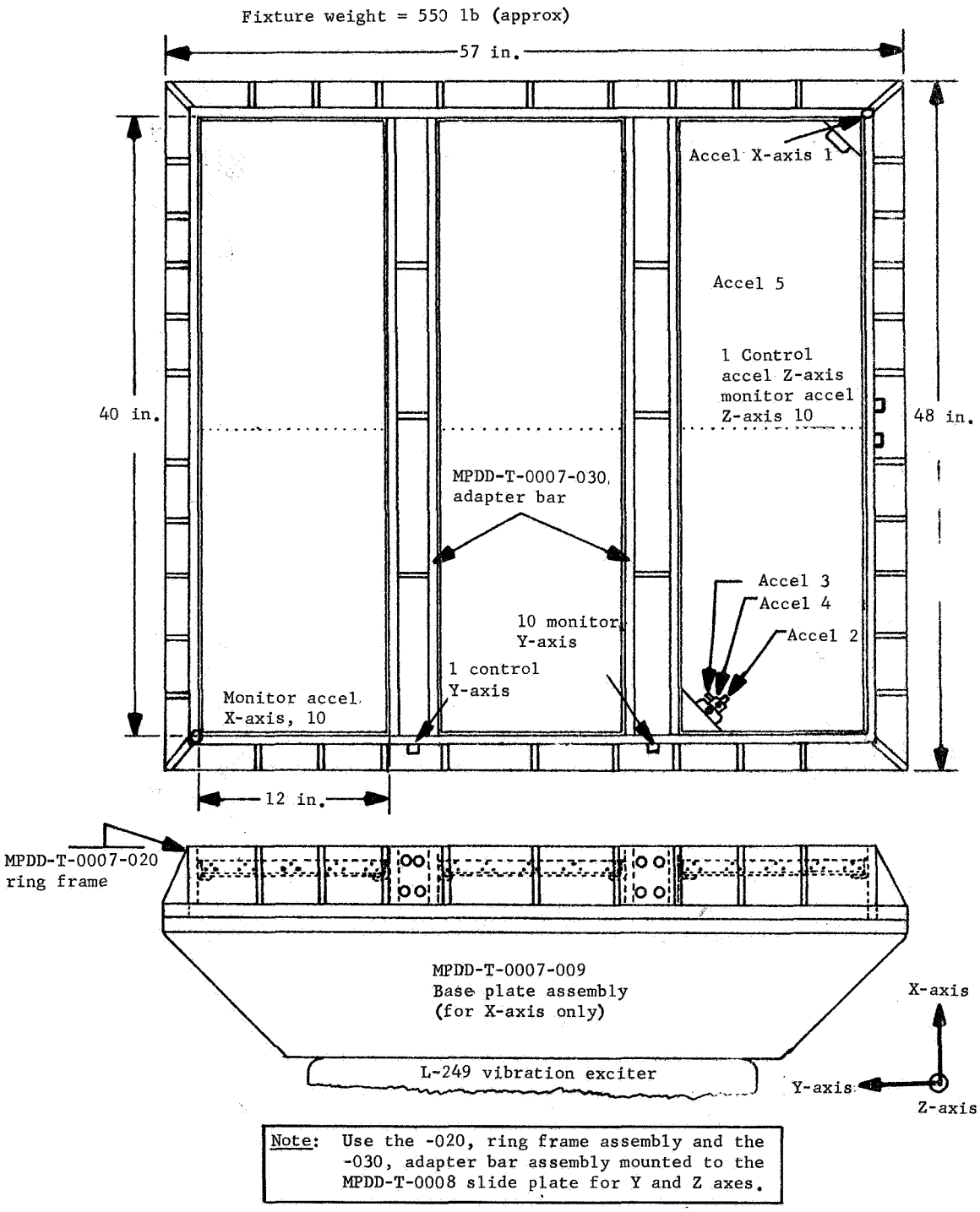


Figure 102.- 40x12-in. Panel Vibration Test Setup

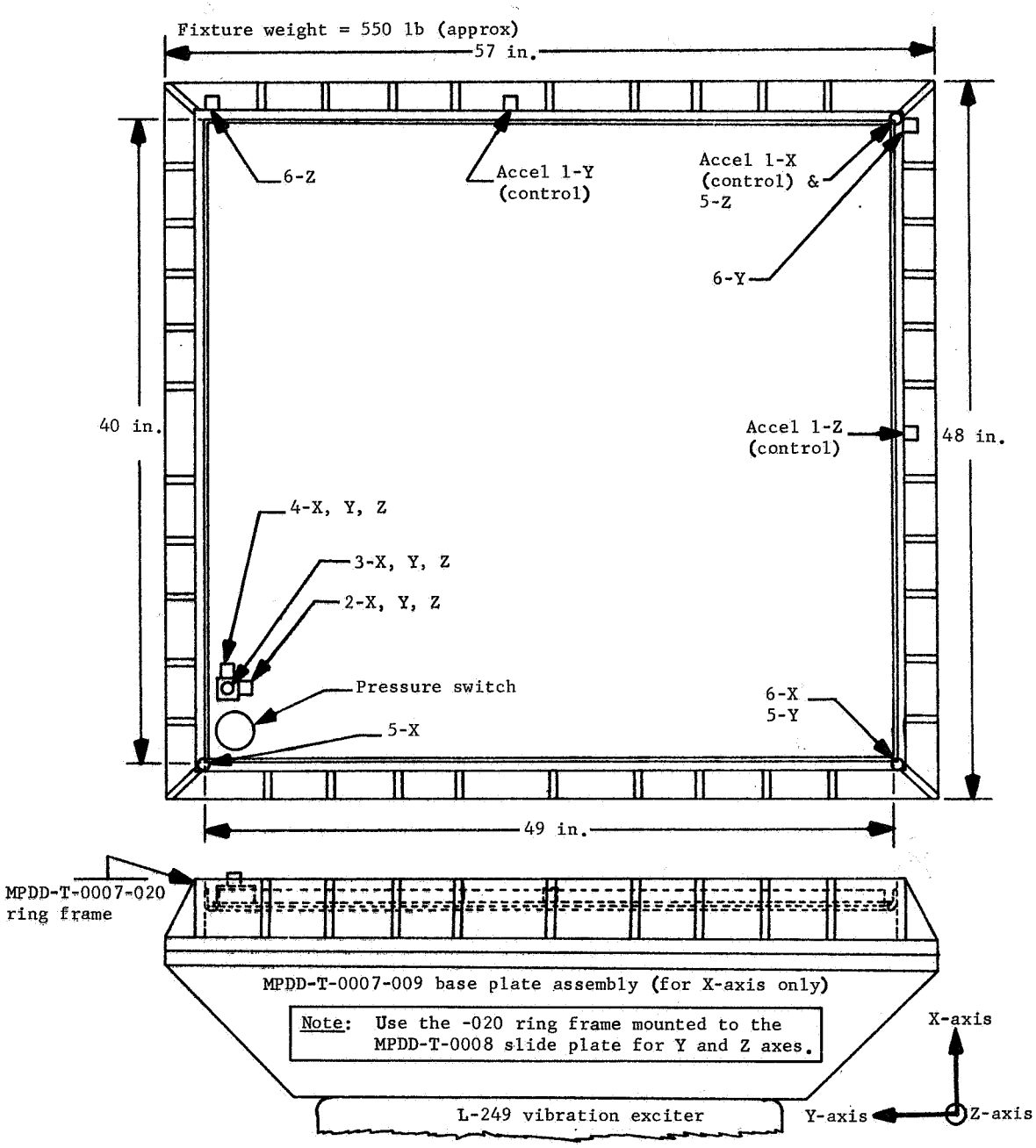


Figure 103. 40x49-in. Detector Vibration Test Setup

The same fixtures and setup (figs. 102 and 103) evaluated and approved for the vibration testing were used for mounting test units for the shock test. The fixture was capable of receiving the designated shock input and transmitting the shock to the test unit through the normal test unit mounting provisions.

Acoustics test (fig. 104): Each required test specimen was subjected to the random acoustic field defined here for the specified exposure duration. Pressure switches were tested using the reverberant-type chamber. Detector panels of all types were tested using plane wave application of the acoustic energy. The required spectrum shape for the acoustic test is comprised of the following octave band midfrequency dB levels.

| Octave band SPL, dB (re: 0.0002 dynes/cm$^2$) | Midfrequencies of octave bands, Hz |
|---|---|
| 140.9 | 25.0 |
| 143.3 | 50.0 |
| 144.3 | 100.0 |
| 144.1 | 200.0 |
| 142.5 | 400.0 |
| 139.5 | 800.0 |
| 135.0 | 1600.0 |
| 129.2 | 3200.0 |
| 123.1 | 6400.0 |

Overall level = 151 dB

Test duration for all acoustic tests was 4 minutes. The required acoustic field was produced by a source having random output with essentially Gaussian amplitude distribution over a bandwidth of 30 Hz to 10 Hz. Each test specimen was mounted in the acoustic field to a rigid static support using those mounting capabilities which were an integral part of the test specimen. The specimen was oriented to obtain an even distribution of the sound pressure level over the required specimen surface.

Detector design development test results.- The following paragraphs are a general summary of the results obtained during the design evaluation testing. The configuration summary will indicate only those areas of test in which problems were encountered:

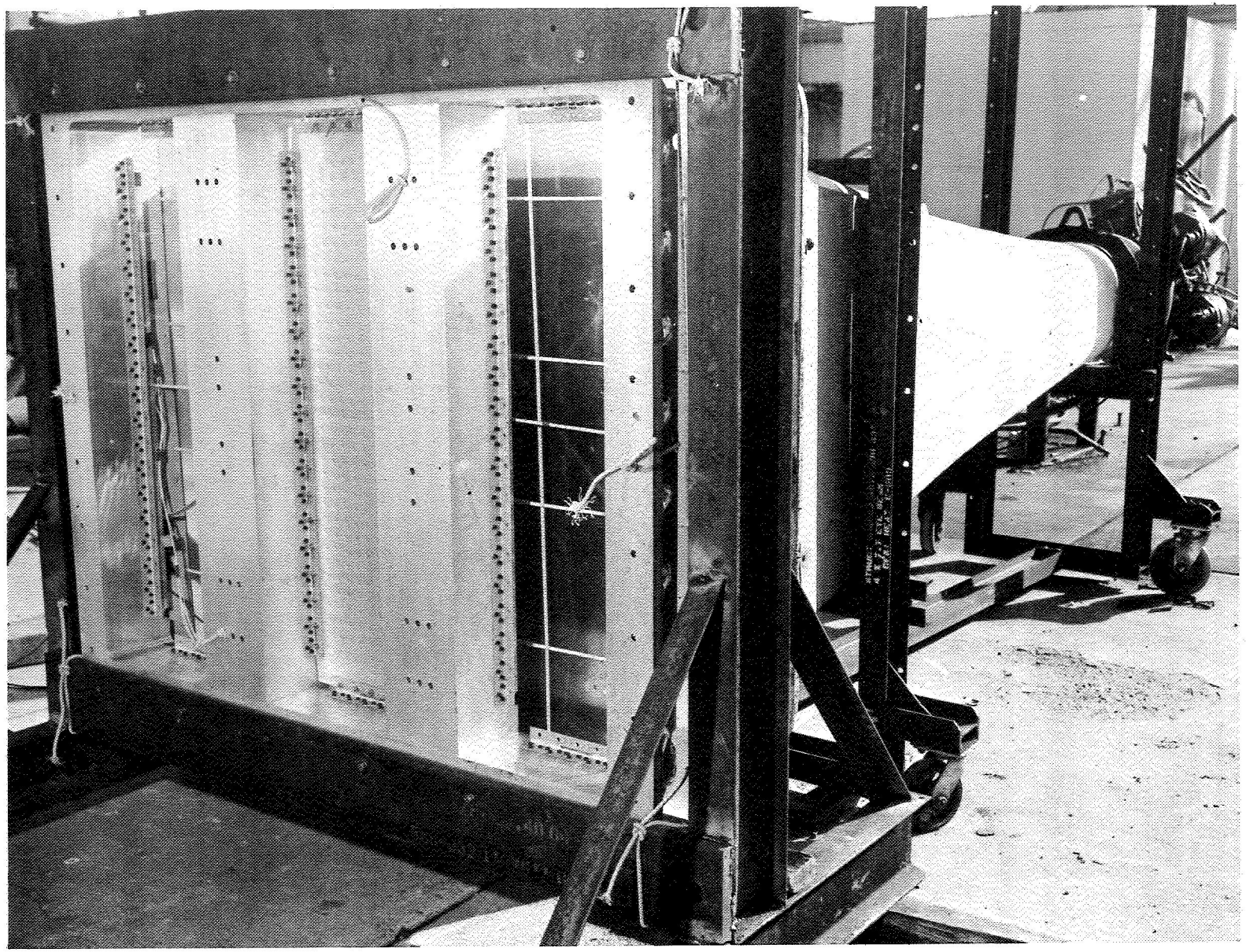

Figure 104.- Acoustic Test Setup, 40x12-in. Panel

1) 8280-04051, (D1A Panel) S/N 0000010 panel successfully completed all test requirements.

2) 8280-07061, (C1 Panel) S/N 0000001 and S/N 0000002. C1 Panel S/N 0000002 successfully completed all test requirements. C1 Panel S/N 0000001 failed to pass leak test requirements following vibration and shock testing. The panel indicated a leak rate of $2.8 \times 10^{-6}$ scc He/sec.

3) 8280-10051, (D1A Detector) S/N 0000001, detector successfully completed all test requirements.

4) 8280-13001, (D2A dual detector) S/N 0000002, detector successfully completed all test requirements.

5) After 8280-16051, (D3A Detector) completed shock testing, the specimen was transported to SSL for a leak test. During this test, a gross leak was found in the fill tube braze joint. The joint was rebrazed and the specimen was retested for leakage. No leakage was found during the retest. It was subsequently found that the panel had been dropped during transportation. Therefore, the above leak is <u>not</u> considered a test failure. Following acoustic testing the test specimen was pressurized with helium and sealed before its final leak test. It was found to have a gross leak. This leak was located at the seal off in the fill tube. The specimen was resealed and retested for leak. No leakage was found during this retest.

6) 8280-19051, (E1A Detector) S/N 0000001 and S/N 0000002. S/N 0000002 was found to be leaking after 21 344 cycles. The leak was located at the junction of the seam welds. The junction was spot welded and subjected to a second leak test. No measurable leakage was found during the retest. S/N 0000001 was found to be leaking after completion of sinewave and random vibration. A retest was performed to confirm the initial leakage measurement and the specimen was again found to leak. The location of the leak was thought to be at the ring weld of the fill tube. The area was brazed and the specimen subjected to a third leak. It was still found to leak but the leak was located at the seam weld intersection near the fill tube. All four seam weld intersections were spot welded and the specimen leak tested a fourth time. The specimen had no measurable leakage during this test. At this time, it was decided to discontinue testing on

S/N 0000001 and to perform all environmental testing on Specimen S/N 0000002, which had a similar leak after pressure cycling. This item was repaired in the same manner as S/N 0000001, i.e., the seam weld intersections were spot welded and the specimen was started through the environments. The specimen did not leak after being subjected to the required sinewave and random vibration and the shock test.

7) 8280-24051, (E2C dual detector) S/N 0000001 detector successfully completed all test requirements.

8) After 8280-25001, (E3A detector), S/N 0000001 completed of the acoustic test, the specimen was pressurized with helium and sealed. A subsequent leak test found leakage at the seal of the fill tube. Repair was attempted and leakage occurred a second time, at the fill tube seal. A second attempt at repair still resulted in leakage.

9) The 8280-28001, (F1A Panel) S/N 0000010 detector successfully completed all test requirements.

Special materials test.- The MPDD program requires the use of silastic materials in the final assembly of the meteoroid detectors. The silastic materials were a silicone potting compound (MMS-M138) used in the region of the pressure switch to provide support for the switch wiring, and a Teflon tape (MMSJ665) with an adhesive backing that provides a sliding surface on the perimeter of the detector to allow free movement during thermal expansion and/or contraction of the detector.

Outgassing characteristics of these silastic materials were unavailable from NASA/MSC or from the manufacturers. Therefore any knowledge concerning the contamination potential to solar cells was unknown. As a result a specific experiment was conducted to determine if any contamination hazard would be experienced. The subsequent paragraphs are a description of the test program that was accomplished.

The test was conducted in an environment that simulated an extreme condition for outgassing from the silastics and condensation on the solar cells. The primary objective was to measure any degradation in solar cell output as a result of outgassed materials from the silastic specimens.

The test setup is shown in figures 105 and 106. In general the fixture exposed six solar cells with an approximate area of

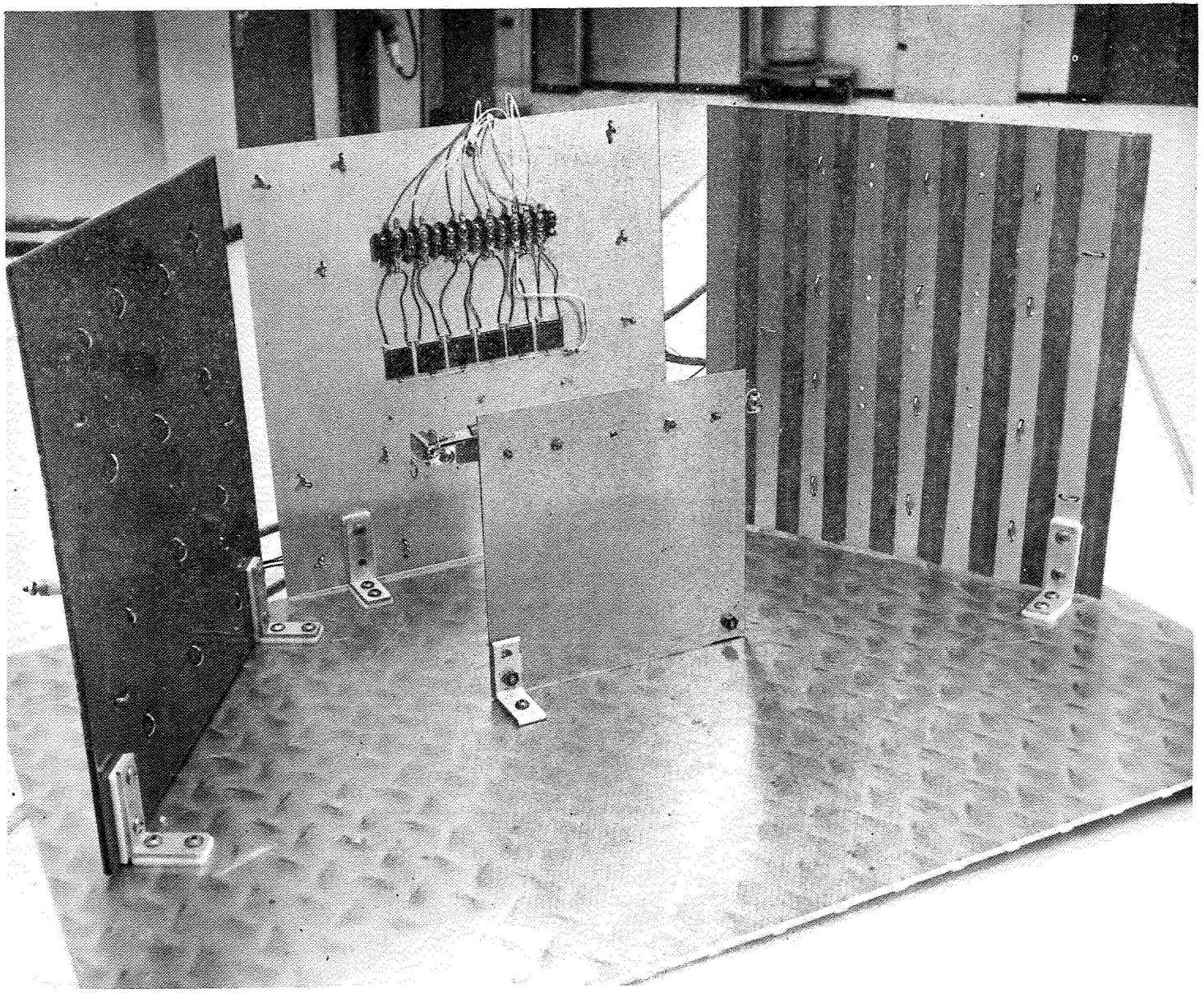

Figure 105.- Solar Cell Contamination Test Setup, Front View

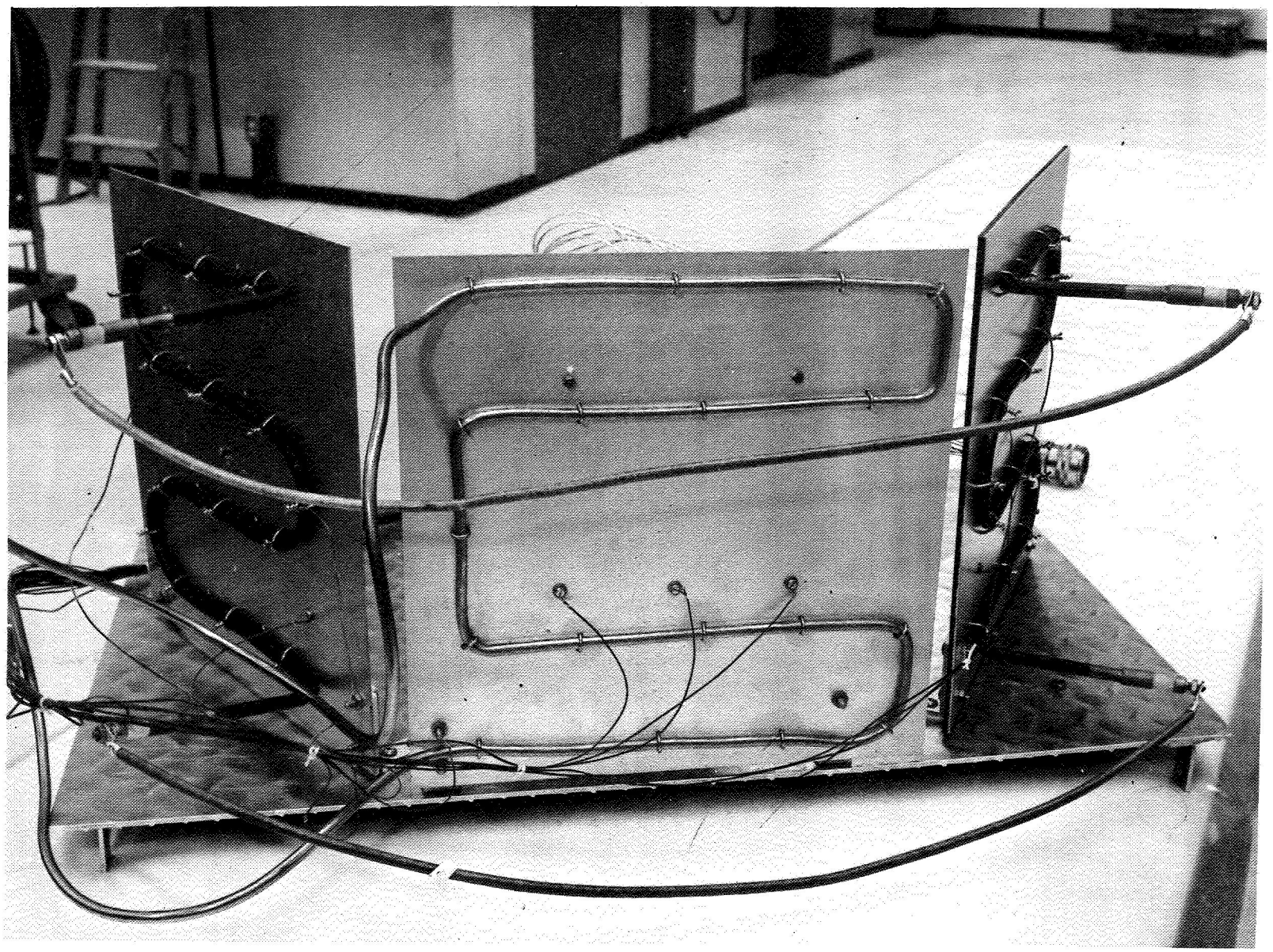

Figure 106.- Solar Cell Contamination Test Setup, Back View

6 sq in. to 144 sq in. of MMSM138 potting compound and 96 sq in. of MMSJ665 Teflon tape. The exposure was obtained in a thermal vacuum chamber in a vacuum of 3 to 5 x $10^{-7}$ torr, with the silastic materials heated to +350°F and the solar cell cooled to -100°F. The test sequence was as follows:

1) Check the output of the solar cells with the chamber at ambient pressure, and the test plates at ambient temperature. (All solar cell output are checked with IR lamps energized.);

2) Evacuate test chamber, and check solar cell outputs with test plates at ambient temperature;

3) Cool solar cells to -100° ± 15°F, and specimen plates at ambient temperature. Check output of solar cells;

4) Maintain solar cells at -100°F, and heat specimen plates to +350° ± 25°F. Check output of solar cells;

5) Maintain conditions of step 4), check output of solar cells after a 4-hr period;

6) Maintain conditions of step 4), check output of solar cells after an 8-hr period.

After completion of the above sequence there was no degradation in the output of the solar cells during the vacuum and thermal environmental exposure.

The outgassing characteristics of most materials are exponential functions, therefore, little or no contamination can be expected as a result of using these tested materials. If a contamination hazard existed it would have been detected early in the performance of this test.

## Production Testing

This phase of testing covers the pilot production of detector/panels and includes both component and subsystem levels that are composed of pressure switch (component) and a detector/panel (subsystem).

Pressure switches.-

Flight assurance testing: Two phases of flight assurance testing were conducted. The first was to obtain specimens for qualification testing and the second was to obtain specimens for production usage. Test parameters of both phases were identical, but were conducted at separate times. The flight assurance tests are described in the following paragraphs.

In the switch transfer pressure test the pressure switch was connected electrically and pneumatically to the functional test tool (see figs. 100 and 107). The specimen transfer and return pressures were checked to verify that the trip points were within 6 $\pm$ 2.5 psig. This test was conducted initially, at completion of dynamics, and after temperature cycling.

In the switch contact resistance test the electrical setup shown in figure 101 was used. The voltage drop across each set of contacts was measured with 5.0 $\pm$ 0.2 Vdc circuit voltage and 0.5 A and 100 uA circuit current. The maximum allowable voltage drops were 112 mV and 32 uV, respectively. This test was also conducted initially, after dynamics, and after temperature cycling.

In the helium leak test each specimen was clamped into a test fixture, placed in a vacuum chamber (see figs. 108 and 109) in which the pressure was reduced to 1 x $10^{-5}$ torr, or less, pressurized to 27.4 $\pm$ 0.5 psia, and leakage sensed at the normally exposed surface of the specimen. The maximum allowable leak rate was 1.0 x $10^{-9}$ scc He/sec. The test was conducted three times as with the functional tests.

In the random vibration test the specimens were installed, up to 12 units at a time (see figs. 99 and 110), pressurized to 27.4 $\pm$ 0.5 psig, and subjected to a random vibration spectrum. The spectrum was produced by an electrodynamic vibration exciter with a shape flat from 200 to 700 Hz at 0.381 $g^2$/Hz, rolled off at 3 dB/octave below 200 Hz and 6 dB/octave above 700 Hz. This shape yields an overall level of 20.0 grms and was applied for 5.0 minutes/axis (see fig. 111). Initially each specimen was monitored for chatter in excess of 10 usec because it was not a normally occurring event. However, when the pressure switches were reduced in weight, it became normal for them to chatter and monitoring for chatter was discontinued.

The sinewave vibration test setup was identical to that of the random vibration test. The sinewave spectrum was constant displacement of 0.25 in. double amplitude from 5 to 71 Hz, and 66.7 g peak from 71 to 2000 Hz (see fig. 112). The spectrum was swept from 5 to 2000 Hz in a maximum of 4.5 minutes/axis

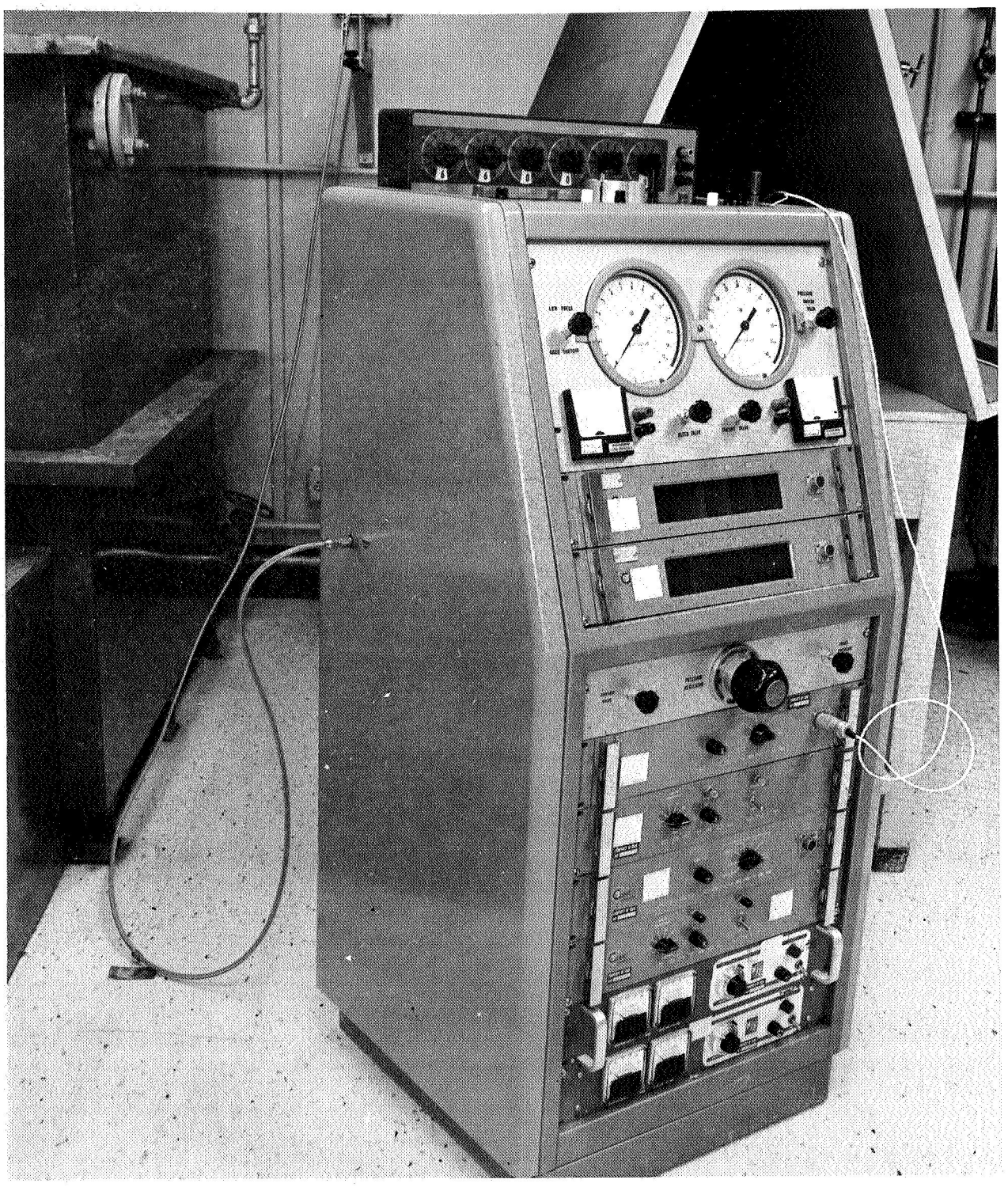

Figure 107.- Functional Test Tool for Pressure Switches and Panel/Detector

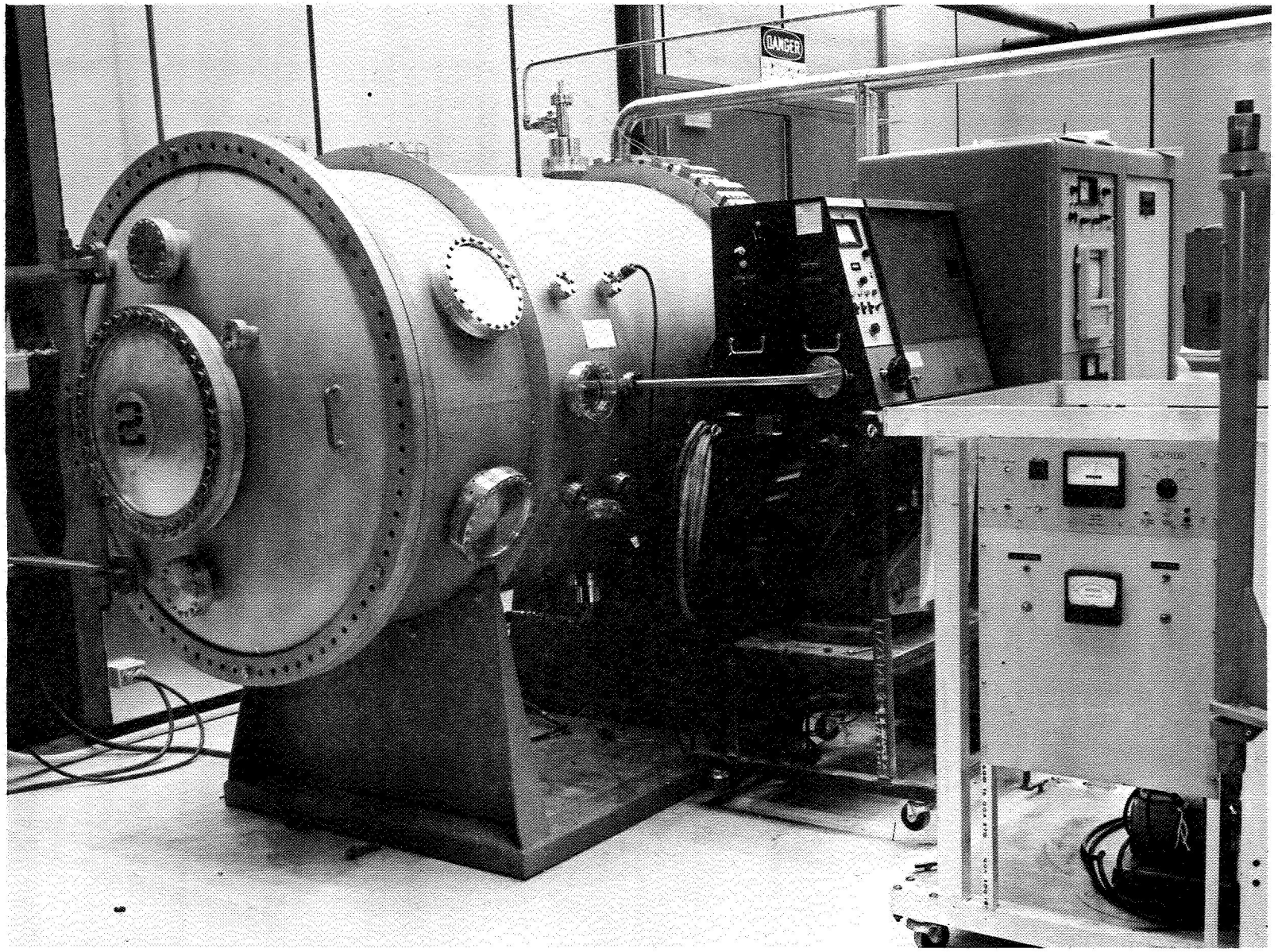


Figure 108.- Helium Leak Test Setup

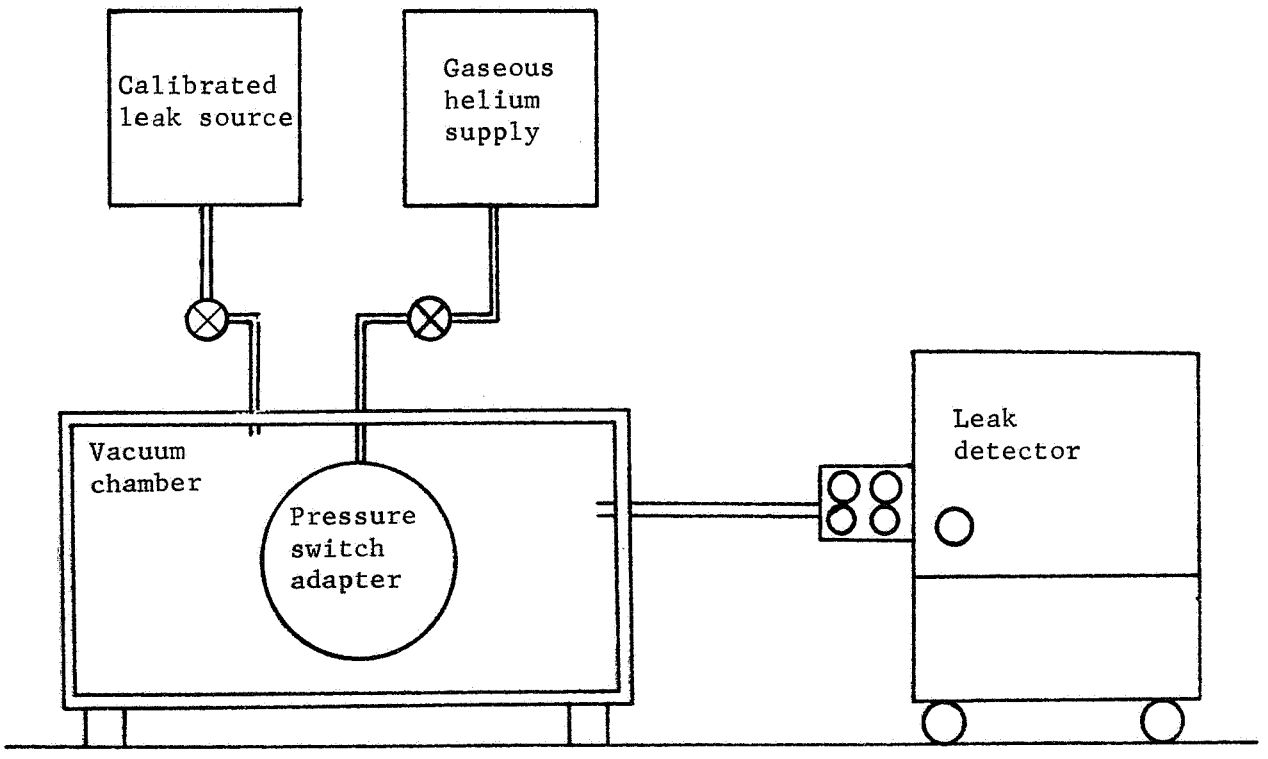


Figure 109.- Helium Leak Test Diagram

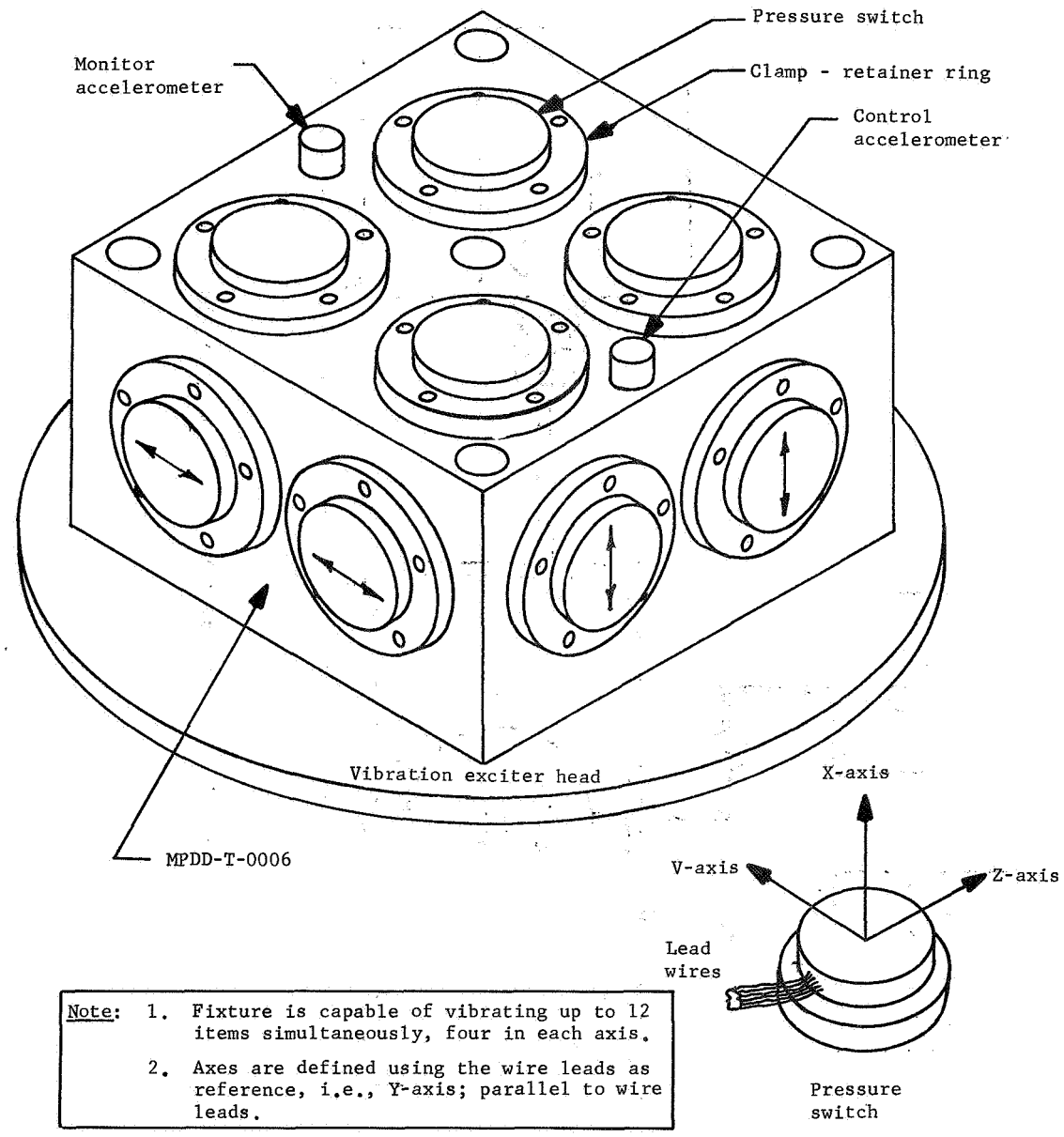


Figure 110.- Vibration Test Setup Sketch

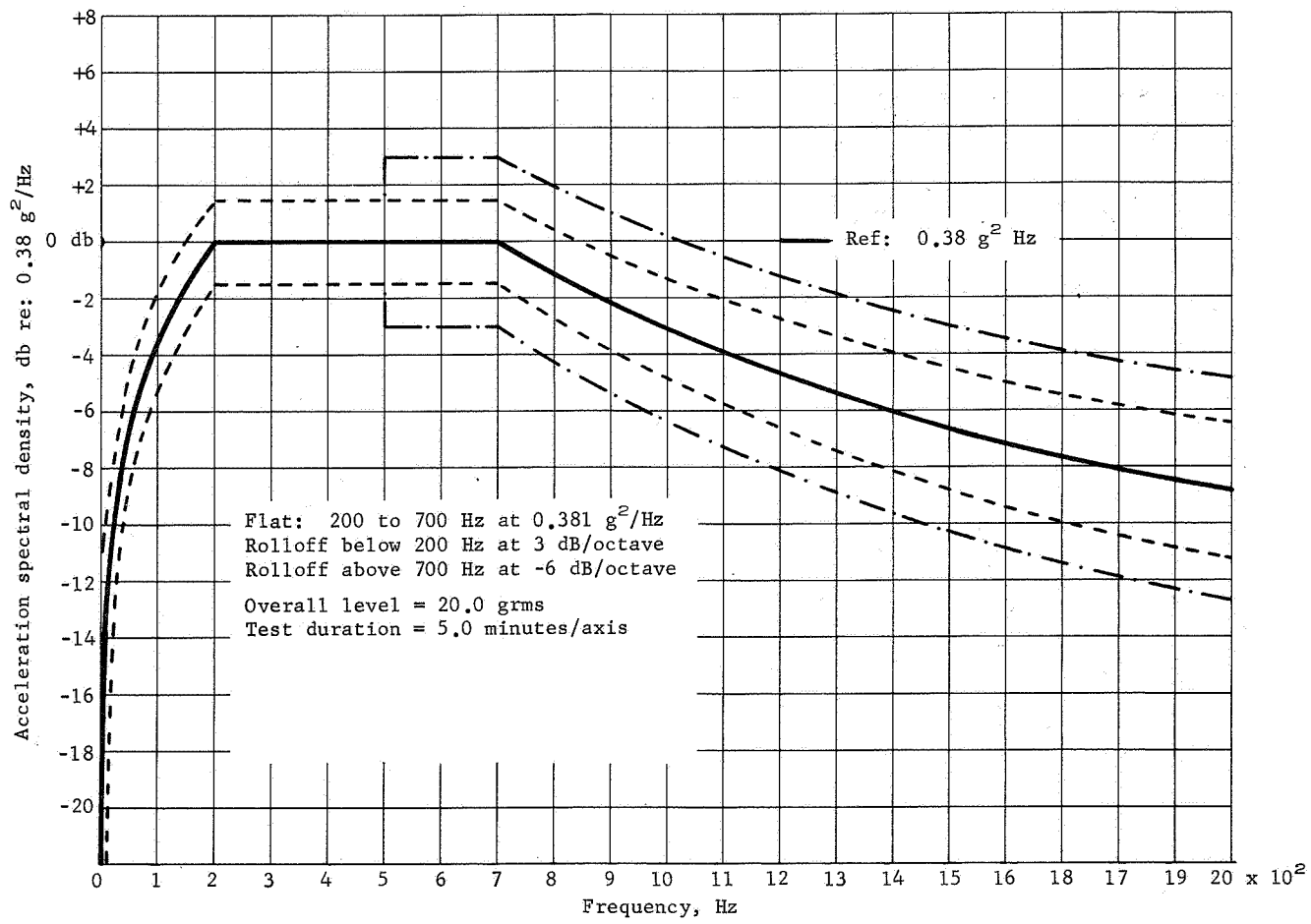


Figure 111.- Random Vibration Spectrum, Pressure Switch Fat

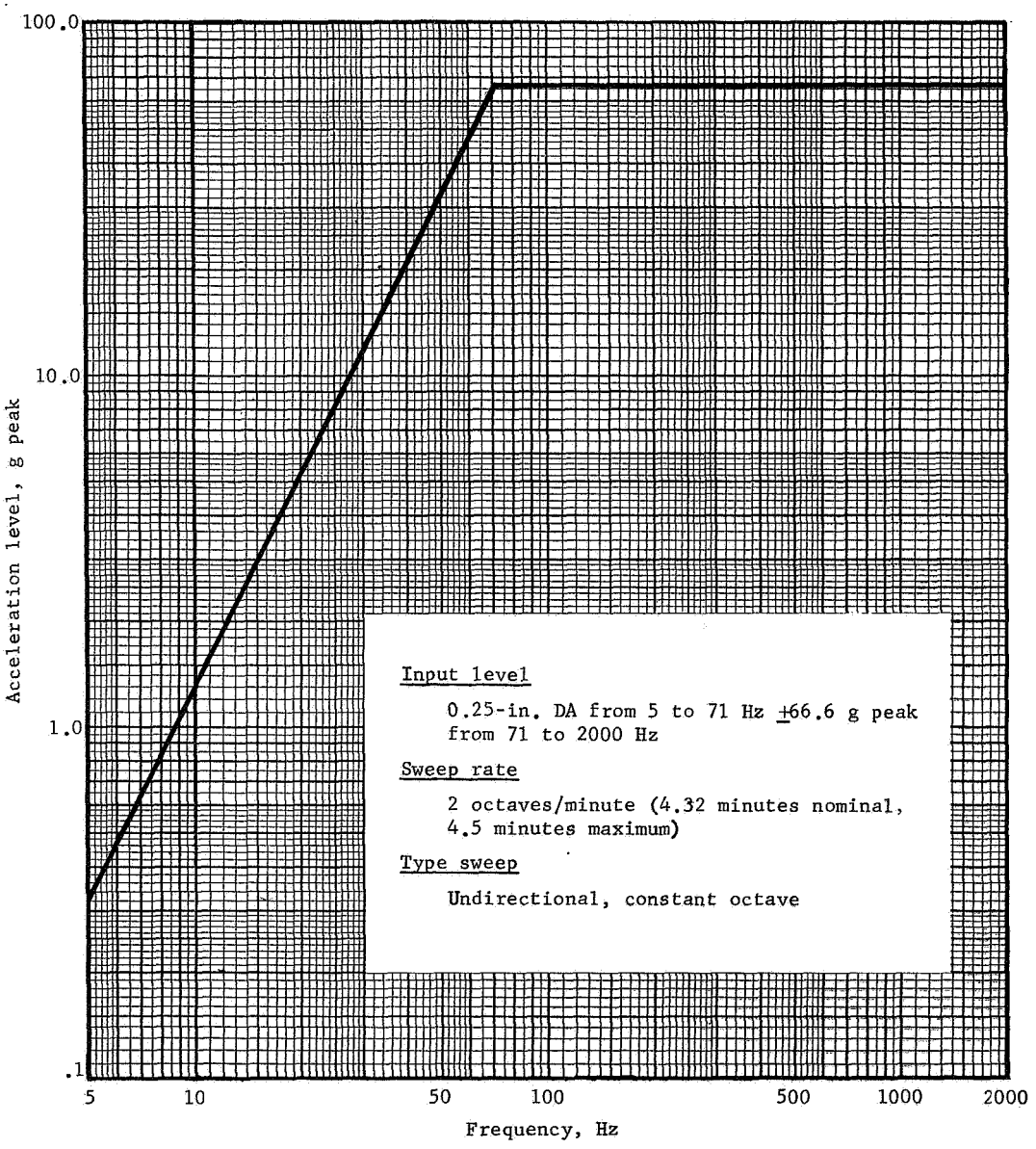


Figure 112.- Sinewave Vibration Specification, Pressure Switch FAT

using an electrodynamic vibration exciter. Chatter monitoring requirements were the same as described for random vibration.

For the shock test the same setup was used as in random and sinewave vibration. The spectrum response method was used to verify the shock input and an electrodynamic vibration exciter was programed as the shock source. The pulse requirement was 60 g peak, 7.0 $\pm$ 1.0 msec sawtooth as shown in figure 113. The equivalent response spectrum is shown in figure 114. Chatter monitoring was treated as described for the random vibration test. The test described in this paragraph and in the two preceding paragraphs are categorized together as "Dynamics" for the purpose of conducting functional and leak tests.

The temperature cycling test consisted of installing up to eight specimens into a special fixture in which resistive heating elements were imbedded and which also contained $LN_2$ passages in the body of the fixture. Thermocouples were attached to the body of the specimens and were first heated to $+350^{o}F \begin{smallmatrix} +15 \\ -0 \end{smallmatrix}$ $^{o}F$ and then cooled to $-250^{o}F \begin{smallmatrix} +0 \\ -15 \end{smallmatrix}$ $^{o}F$. The units were pressurized to 27.4 $\pm$ 0.5 psia throughout the test. Ten cycles as described above were conducted on the specimens.

The first phase of flight assurance testing consisted of two Servonics, Incorporated candidates (PD7100075-002, S/N 0000114, PD7100075-001, S/N 0000149) and two Carleton Controls candidates (PD7100075-003, S/N's 0000019 and 0000033). At that time in the flight assurance testing, the requirement existed, to monitor contact chatter during dynamics. The four candidates chattered during dynamics as follows:

| | |
|---|---|
| S/N 0000019 | Z-axis, sinewave vibration |
| S/N 0000033 | X & Y-axes, sinewave vibration |
| S/N 0000114 | X-axis, sinewave vibration |
| S/N 0000149 | X-axis, sinewave & random vibration |

No other anomalies occurred during flight assurance testing on the above items.

The second phase consisted of testing 78 pressure switches subjected to flight assurance testing. Of this number, 13 units were rejected for various reasons. Five of these units were repaired and later retested successfully. By the start of the second phase, only Carleton pressure switches had successfully completed qualification.

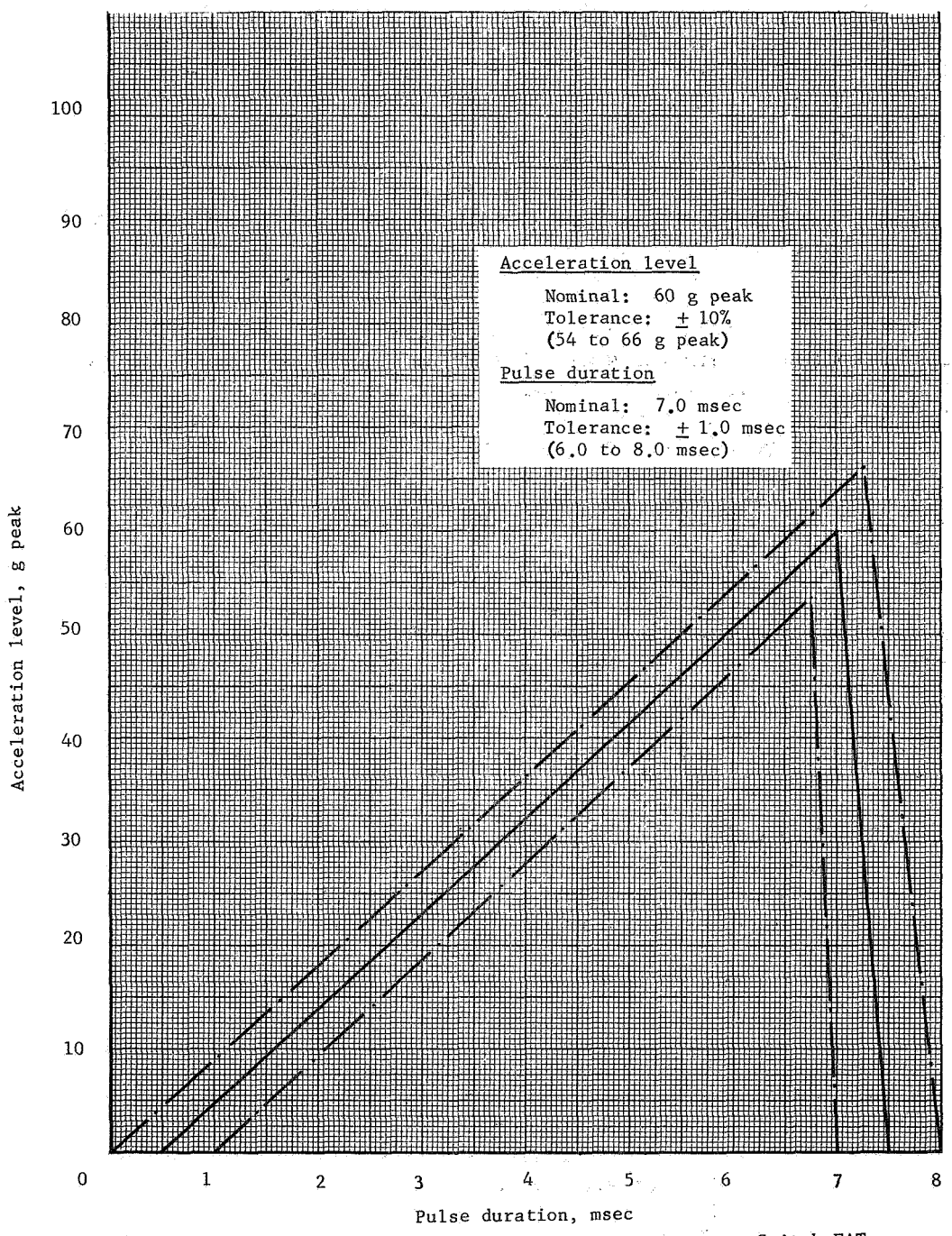


Figure 113.- Sawtooth Shock Pulse Specification. Pressure Switch FAT

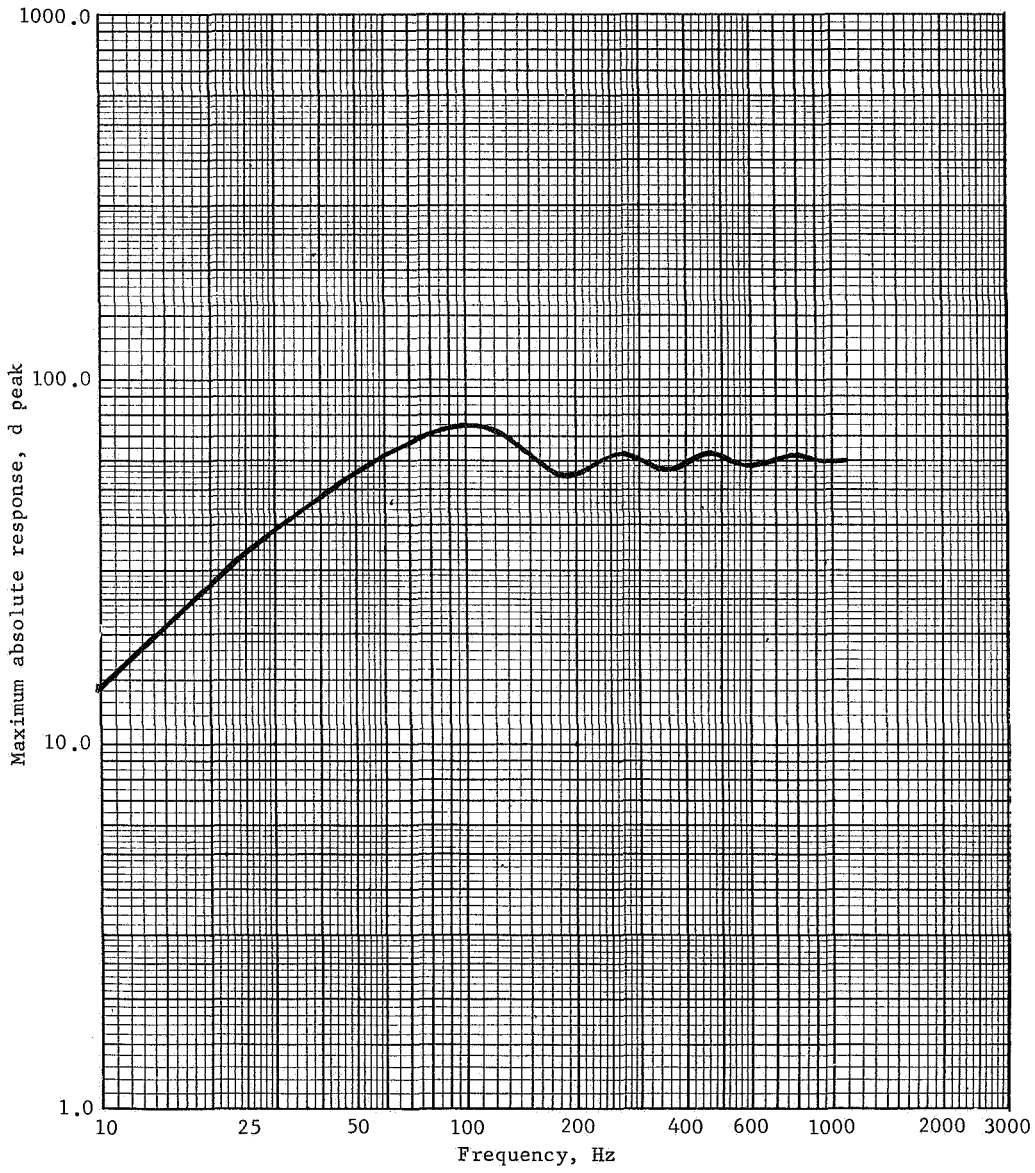


Figure 114.- Shock Response, Pressure Switch FAT

Qualification testing: Four candidates (two each of Servonics and Carleton Controls) were initiated into qualification testing. The qualification testing was performed on specimens that had previously been flight assurance tested and consisted of the tests described in the following paragraphs.

The switch transfer pressure test was identical to that of flight assurance testing. It was performed after contact burn-in, proof pressure, dynamics, sustained acceleration, acoustics, and thermal vacuum soak.

The switch contact resistance test was identical to that of flight assurance testing. It was performed after contact burn-in, proof pressure, dynamics, acoustics, and thermal vacuum soak.

In the contact burn-in test, using the circuitry shown in figure 101, 1 A was applied to each set of contacts for 1 hr. The object of this test was to determine if contact degradation occurred due to heating caused by higher than anticipated current. After this test, contact resistance was measured and compared against the measurements taken during the last flight assurance test. This test was performed twice, once at the start of qualification and once at the completion.

In the insulation resistance test, an insulation resistance tester was connected between each pin of the switch, and the switch case and between nonconducting pins. The applied voltage was 500 $^{+25}_{-0}$ Vdc rms and was applied for a minimum of 1 minute. The insulation resistance was measured and recorded. This test was performed twice; once at the beginning and once at the end of qualification testing.

The helium leak test was identical to that for flight assurance testing.

The proof pressure test setup was as shown in figure 86. A test specimen was subjected to a pressure of 53.4 $^{+1.6}_{-0.0}$ psig for 5 minutes. After the proof pressure the specimen received a functional and leak tests.

A sustained acceleration test was performed on qualification test specimens. The test consisted of 6 g in each of 3 mutually perpendicular axes for a duration of 3 minutes/axis. During the test, switch contacts were monitored for transfer, with the specimen pressurized to 27.4 $\pm$ 0.5 psia. The test setup is depicted in figure 115 and shown in figure 116.

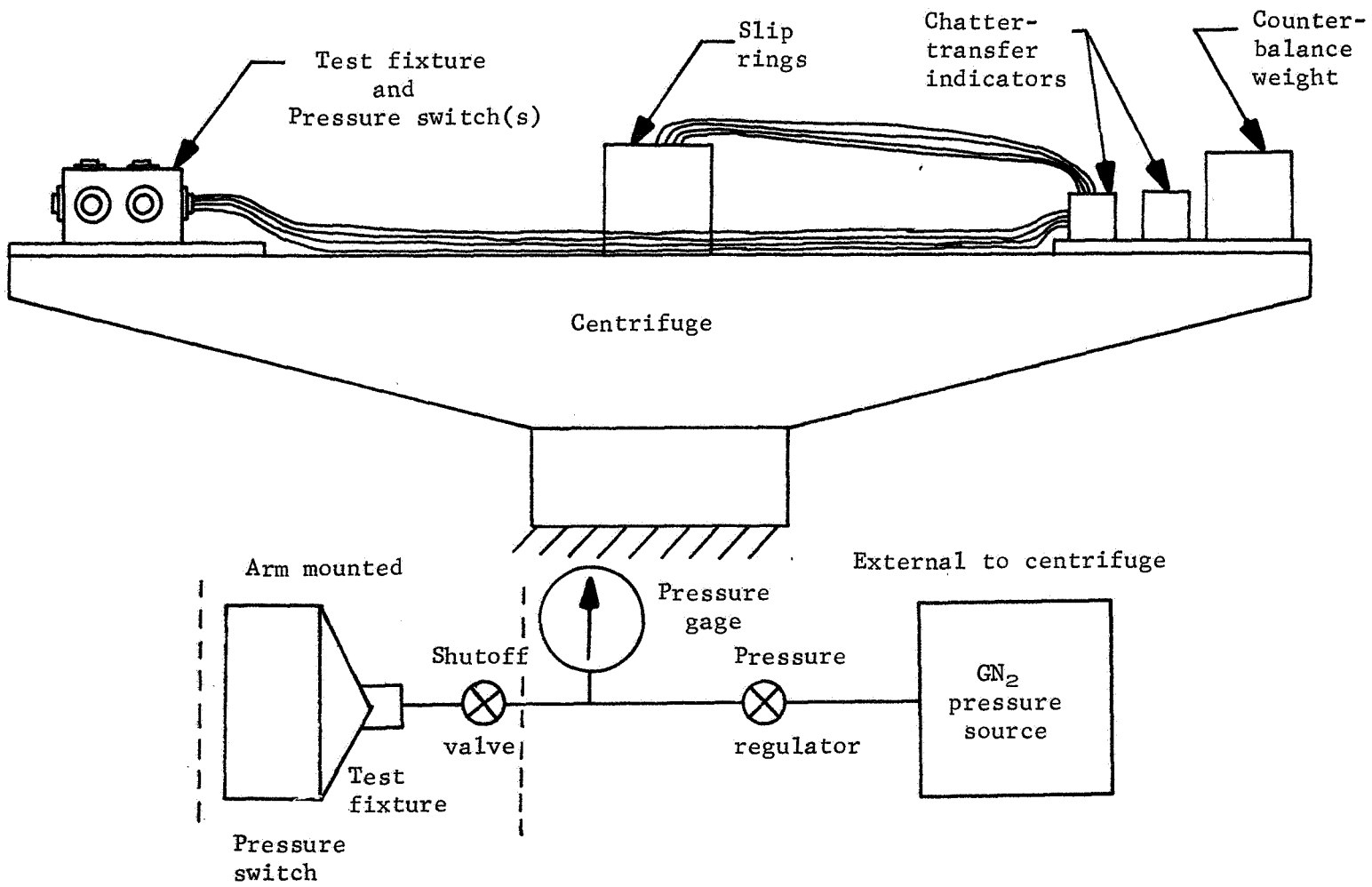


Figure 115.- Sustained Acceleration Test Setup Sketch

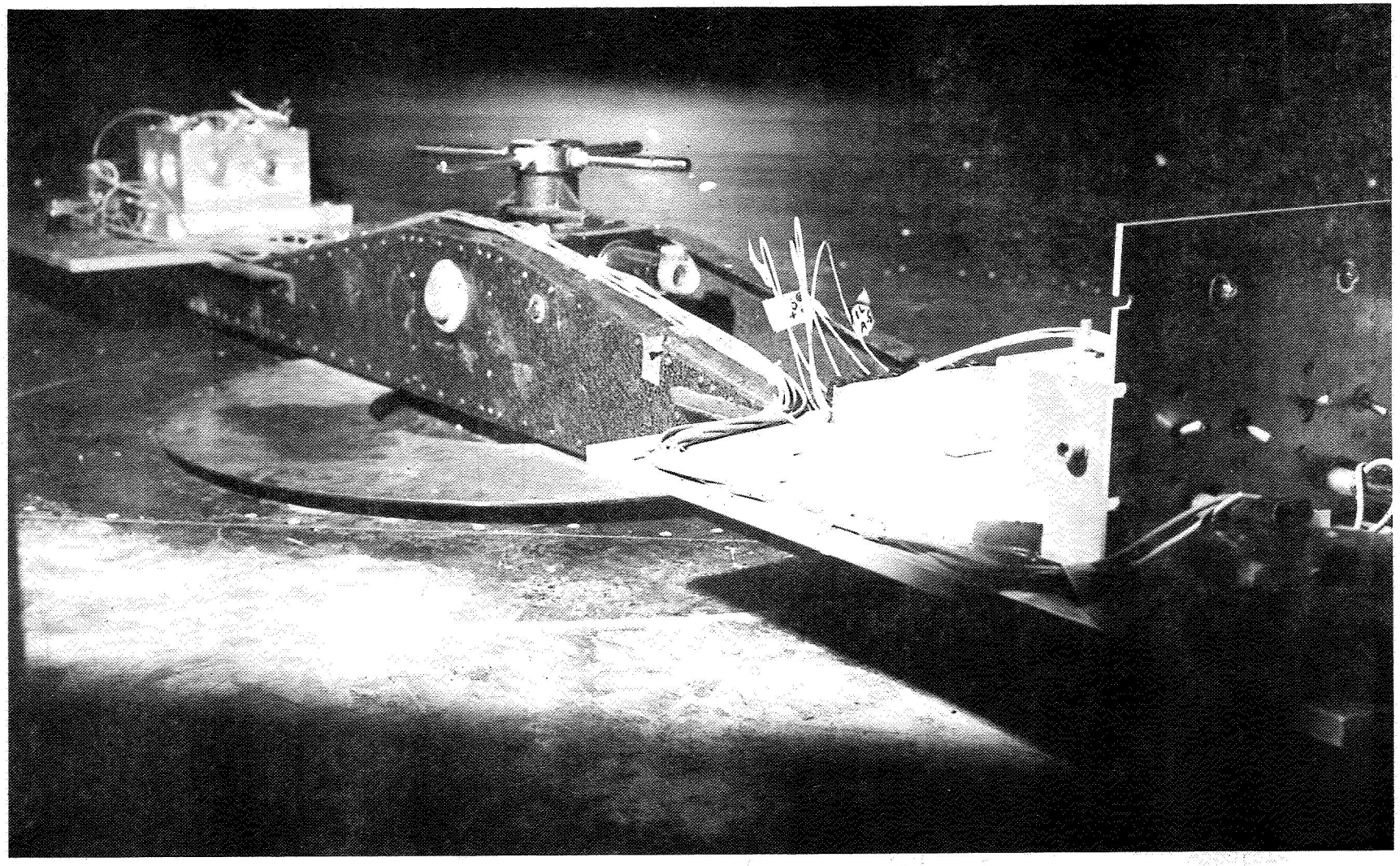

Figure 116.- Sustained Acceleration Test Setup

In the sinewave vibration test the specified environment to be applied to the pressure switches consisted of a unidirectional, constant octave sweep, from 5 to 89 Hz at 0.25 in. double amplitude, 89 to 2000 Hz at 100 g peak, for a duration of 9.0 minutes maximum (see fig. 117). All qualification specimens were monitored for contact chatter in excess of 10 usec while pressurized to 27.4 $\pm$ 0.5 psia. The input vibration was generated by an electrodynamic vibration exciter (see fig. 99) in each of three mutually perpendicular axes.

A random vibration environment was applied to the specimens which consisted of a 30 grms overall level for a period of 5 minutes/axis. The spectral shape was flat from 200 to 700 Hz at 0.88 $g^2$/Hz, rolled off above 700 Hz at 6 dB/octave to 2000 Hz, and rolled off below 200 Hz at 3 dB/octave to 10 Hz (see fig. 118). The excitation was applied in each of three mutually perpendicular axes. The test setup was essentially the same as for the sinewave test with switch contacts monitored for chatter in excess of 10 $\mu$sec.

A shock pulse, sufficient to obtain the shock response spectrum shown in figure 114, was generated and applied by an electrodynamic exciter to the same test setup employed during sinewave and random vibration. The spectrum shown above is the response spectrum resulting from application of a 60 g peak, 11 msec sawtooth pulse (fig. 113) with 10% damping employed in the analysis. As in other dynamic tests, switch chatter in excess of 10 $\mu$sec was monitored.

For the acoustics the test specimen was mounted in a freely suspended fixture. An overall sound pressure level of 151 dB and the spectral shape shown in figure 119, was applied to the qualification units. The test was conducted in a reverberant room facility for a test duration of 4 minutes.

The thermal vacuum soak was the final qualification test conducted on the pressure switches. It was a 30-day test, consisting of 15 days at 350°F and 15 days at -250°F. The total test duration was accomplished at a vacuum of $1 \times 10^{-7}$ torr or less. Figure 120 shows the test setup before the test specimen and bell jar installation. Figure 121 is an overall view of the test setup. The test specimens were required to hold 27.4 $\pm$ 0.5 psig and were monitored for contact transfer throughout the test period.

During qualification testing, the following significant events occurred.

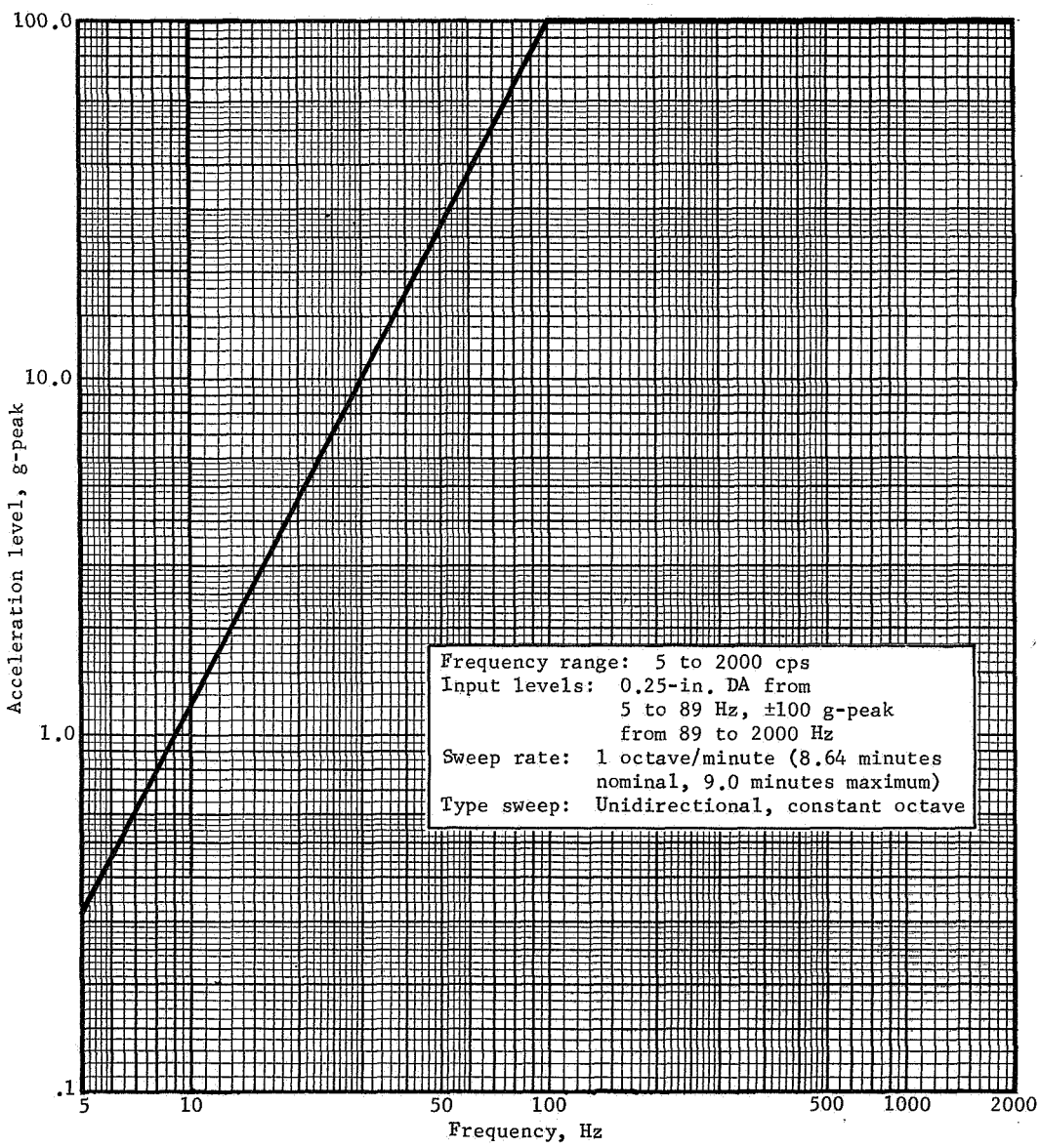


Figure 117.- Switch Qualification

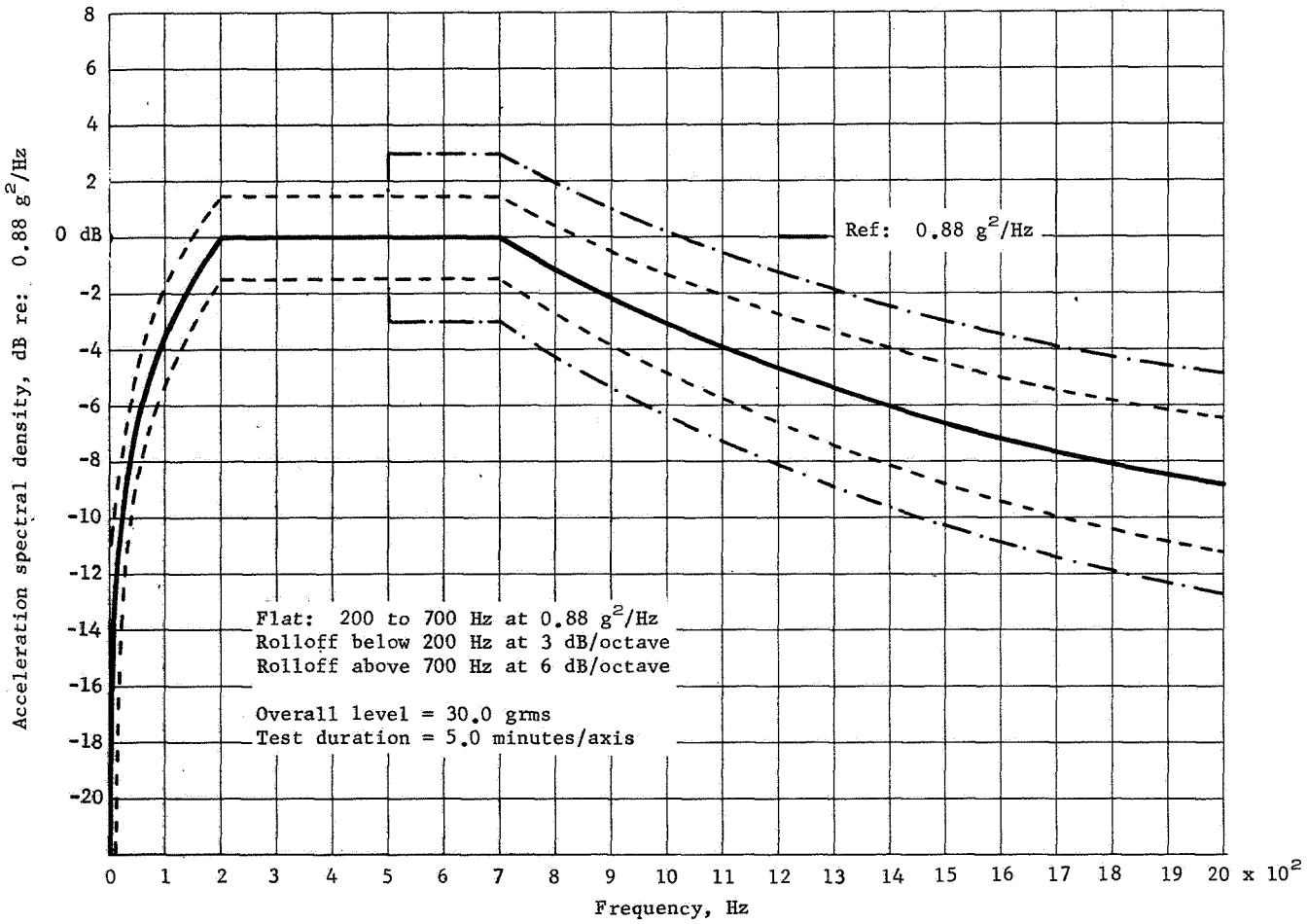


Figure 118.- Random Vibration Spectrum, Pressure Switch Qualification

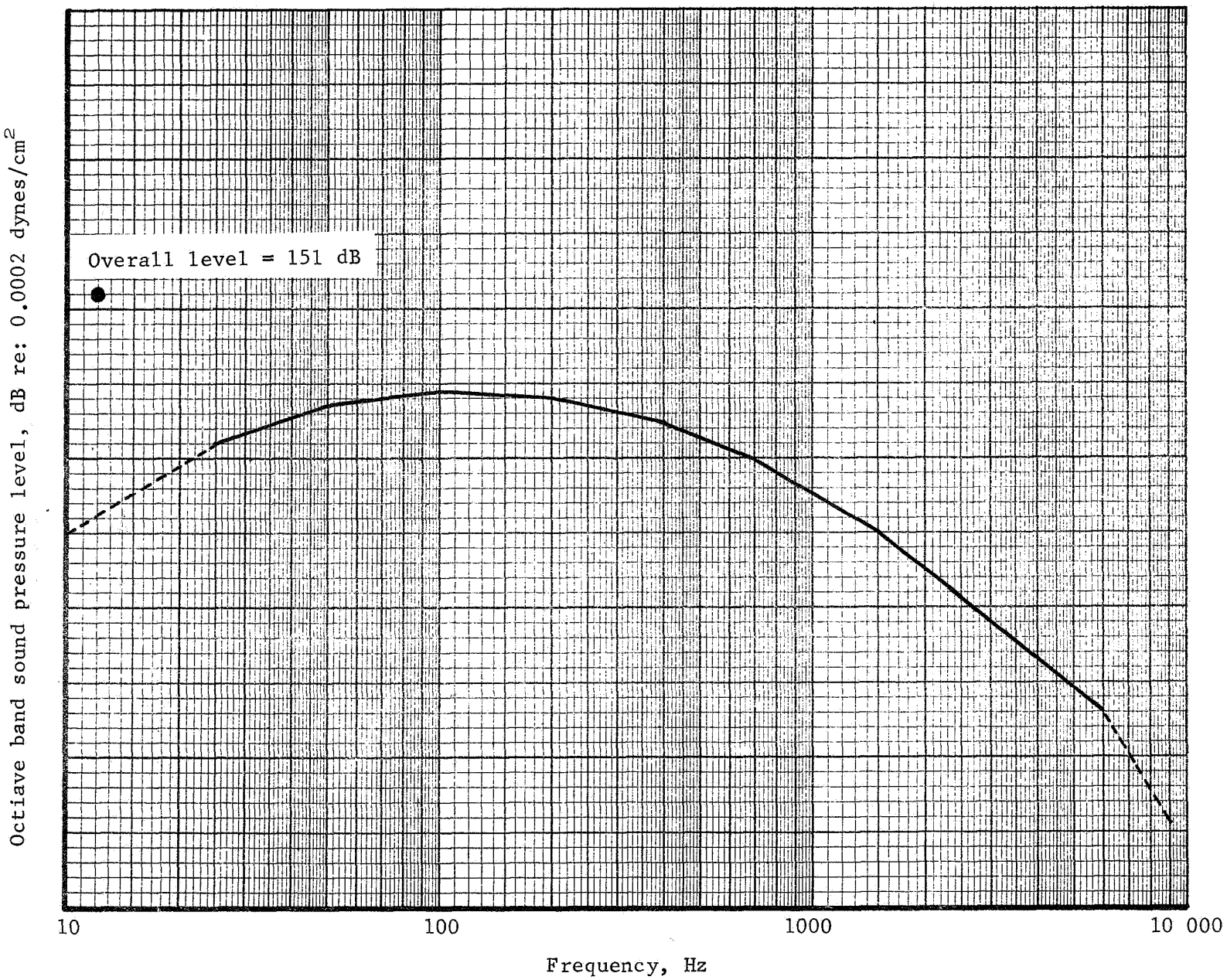


Figure 119.- Acoustic Test Spectrum, Pressure Switch Qualification

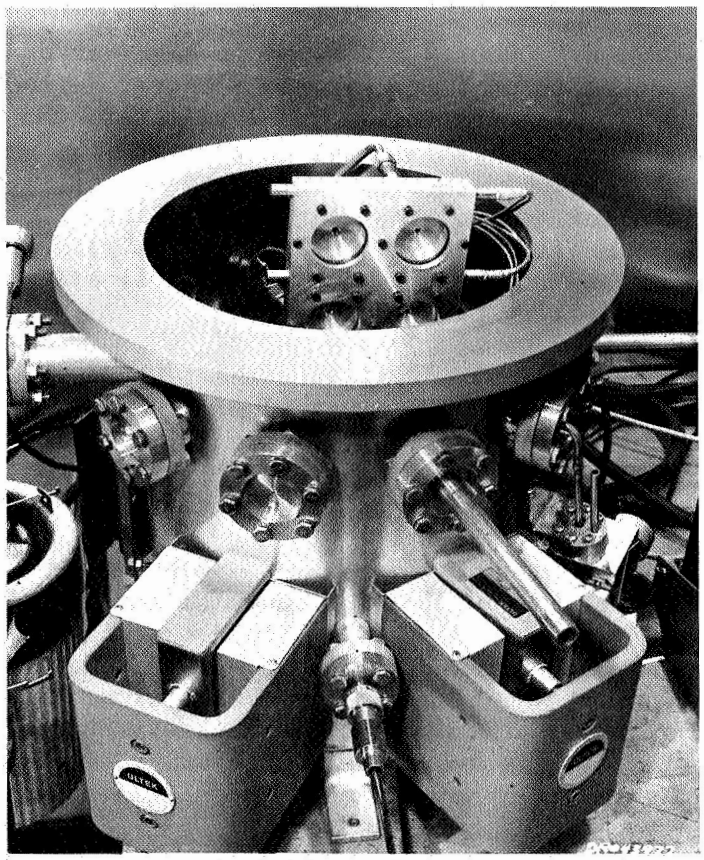

Figure 120.- Pressure Switch Thermal Vacuum Soak Test Setup before Switch Installation

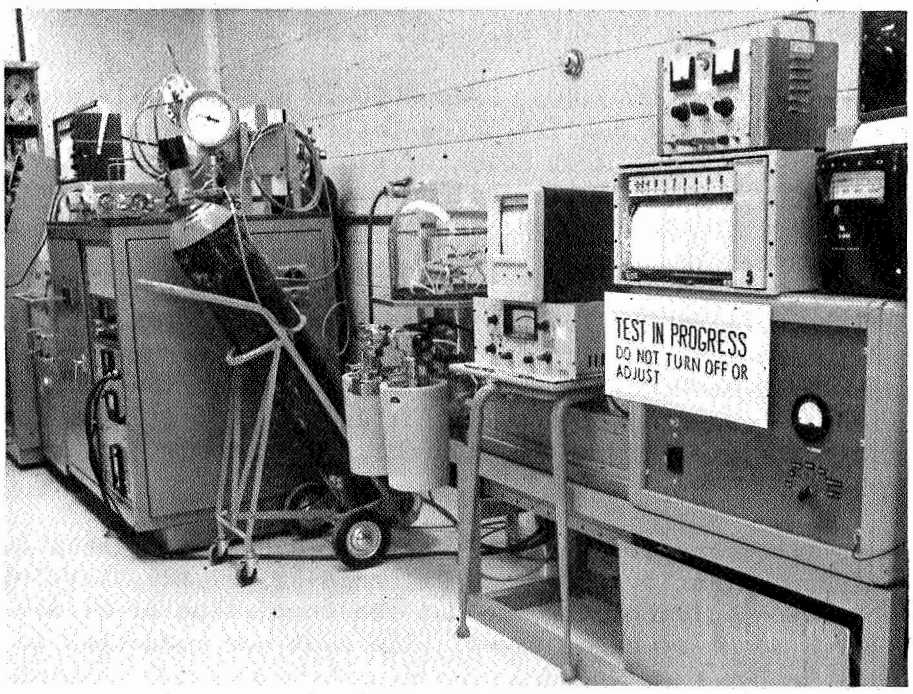


Figure 121.- Overall Test Setup, Pressure Switch Thermal Vacuum Soak

PD7100075-002, S/N 0000114 was found to have out-of-tolerance levels when subjected to contact resistance tests, following the 1 A, 1 hr current application test. Two days later, the unit was rechecked and found to be within required limits. The unit was continued through testing with no further evidence of this type of malfunction. After the out-of-tolerance readings first occurred, the DVM in question was rechecked by the Calibration Control Laboratory and found to be good. No explanation has been resolved for the initially bad readings.

After all four units were well into the test program, it was found that S/N 0000149 was a -001 instead of a -002 switch. The only difference was a mechanical biasing to alleviate chatter during vibration. Because the change was slight and chatter, by itself, had been eliminated as a failure criteria, it was decided to continue testing on this unit.

Both S/N 0000114 and 0000149 failed qualification testing. More specifically both units leaked, through the glass seal around the electrical terminals, at the required vacuum and temperature conditions of the high temperature portion of the thermal vacuum soak test. The failure occurred on the first day of the 15-day soak period. It is not known whether this environment caused the cracks initially or intensified existing cracks produced by preceding environmental tests.

A subsequent attempt to qualify the Servonics' design ended in failure when the test candidates leaked following the dynamics testing portion of the flight assurance test.

In summary, PD7100075-003, S/Ns 0000019 and 0000033, met all requirements of the qualification testing and are considered qualified for use on the MPDD detector/panels. PD7100075-001 and -002, S/Ns 0000149 and 0000114 failed to meet all requirements of the qualification testing and should not be considered for use on the MPDD detector/panels.

Accelerated life cycling testing: Three specimens were subjected to accelerated life cycling testing. They were Carleton Controls units S/Ns 0000182, 0000183, and 0000185. These units had previously been subjected to flight assurance testing. The ALC testing consisted of the tests described in the following paragraphs.

The switch transfer pressure test was identical to that for flight assurance testing. It was performed before the start of, after each 3000 cycles of ALC, and at the completion of 21 344 cycles, for a total of eight times. The test was conducted in a

special test fixture that applied pressure to the overpressure port of the switch and also maintained the applied pressure external to the switch.

The switch contact resistance test was identical to that of flight assurance testing. It was also performed before the start of, after each 3000 cycles of ALC, and at the completion of 21 344 cycles for a total of eight times.

In the helium leak test each specimen was welded into a switch cup, pressurized, and sealed with 35.4 $\pm$ 0.1 psia at 70°F. So that possible leak propagation phenomena would not be disturbed, each specimen was leak tested in a sealed condition. The leak test was conducted by installing the test specimen in a bell jar adapter to a helium mass spectrometer rather than the large 4x8-ft chamber used in flight assurance or qualification testing. A vacuum of $1.0 \times 10^{-5}$ torr, or less was obtained and leak rate, if any, measured. This test was conducted eight times as in the above tests. The maximum allowable leak rate was $1.0 \times 10^{-9}$ scc He/sec.

In accelerated life cycling the specimens were mechanically attached to a rotating arm and electrically connected to the monitoring circuits of the pressure switch ALC tool (see figs. 122, 123, and 124). They were then cycled 21 344 times between +325°F $\pm$ 10°F and -90°F $\pm$ 10°F. The high temperature was obtained by immersing the units into a bath of USP 98.5% pure glycerine that was maintained at the required temperature by a thermostatically controlled heater. The cold temperature was obtained by immersing the units into a bath of ethyl alcohol which was maintained at the required temperature by a thermostatically controlled liquid $CO_2$ injector. The cycle rate was initially controlled by the readout of a thermocouple imbedded into the center of mass of a "dummy" instrumented pressure switch (see fig. 125), which was also attached to the rotating arm. After sufficient data were obtained to firmly establish the cycle rate required to allow the test specimens to "see" the specified temperatures, cycle rate was then controlled by a synchronous motor-driven timer. The cycle time was established at 7.5 minutes/cycle. At 3000, 6000, 9000, 12 000, 15 000, 18 000, and 21 344 cycles, the test items were removed from the ALC test setup and functional and leak tests performed.

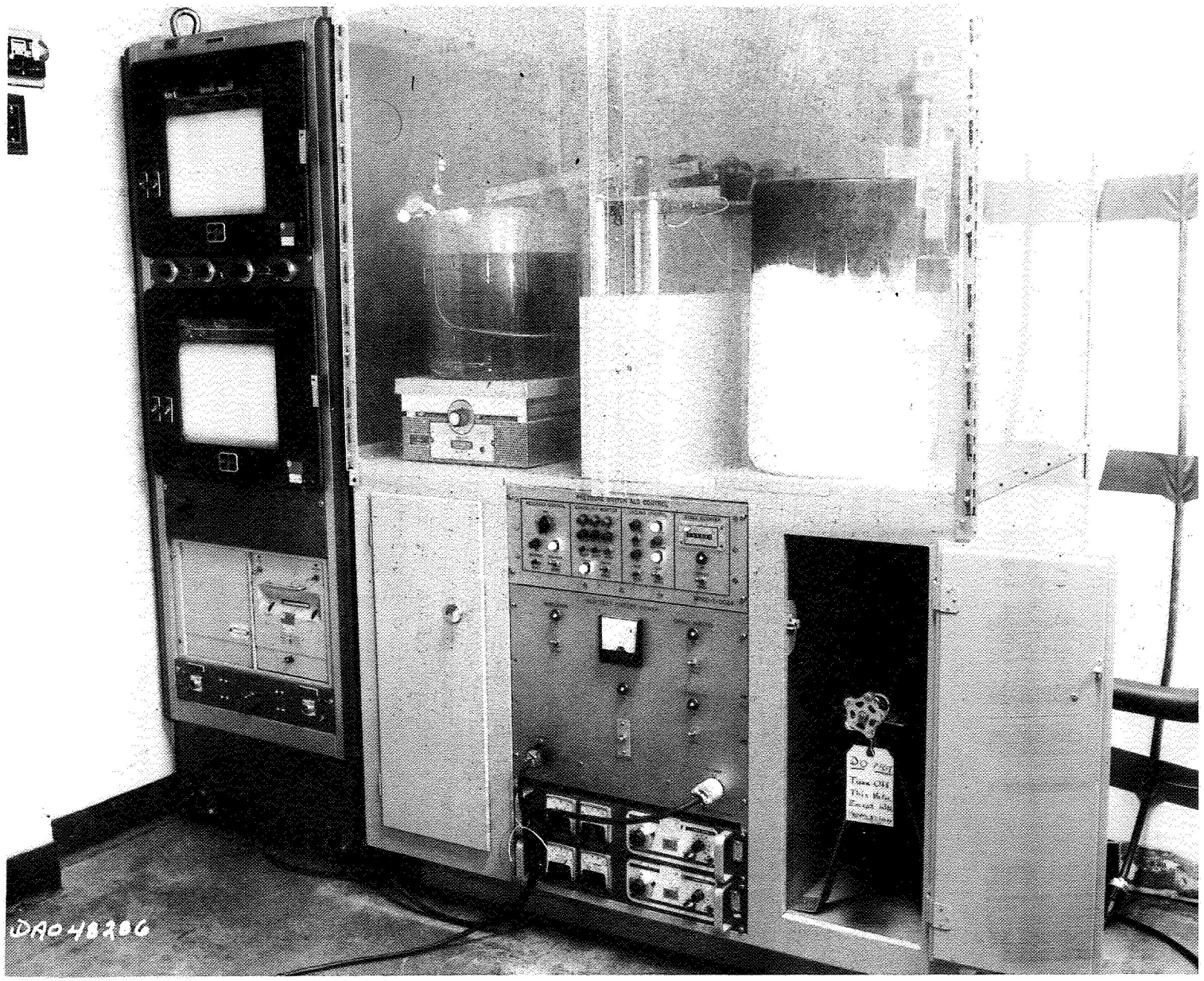


Figure 122.- Overall Test Setup, Pressure Switch ALC Test

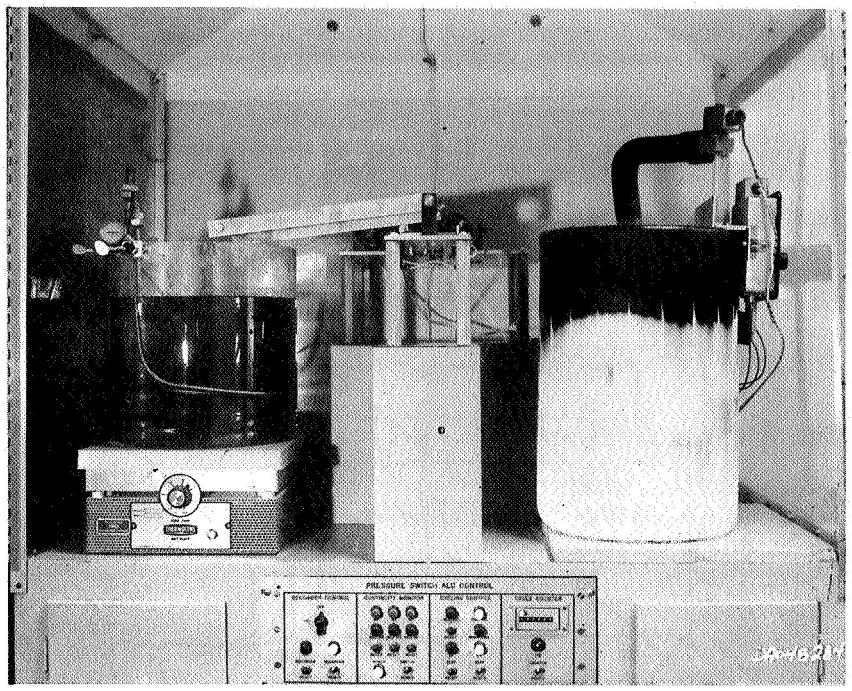

Figure 123.- Closeup of Hot and Cold Baths, Pressure Switch ALC Test

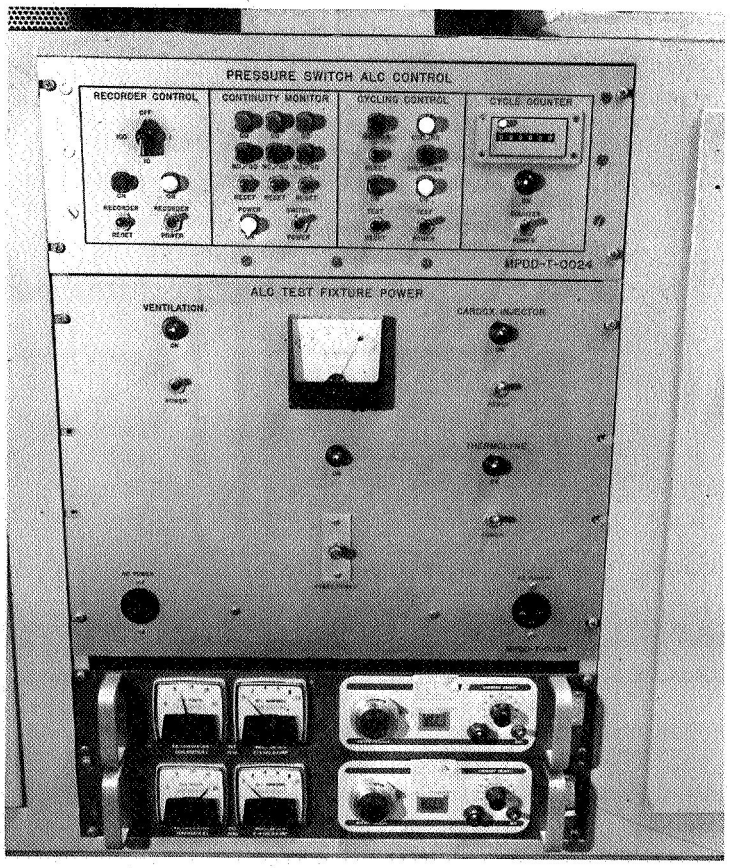


Figure 124.- Pressure Switch ALC Control and Power Rack

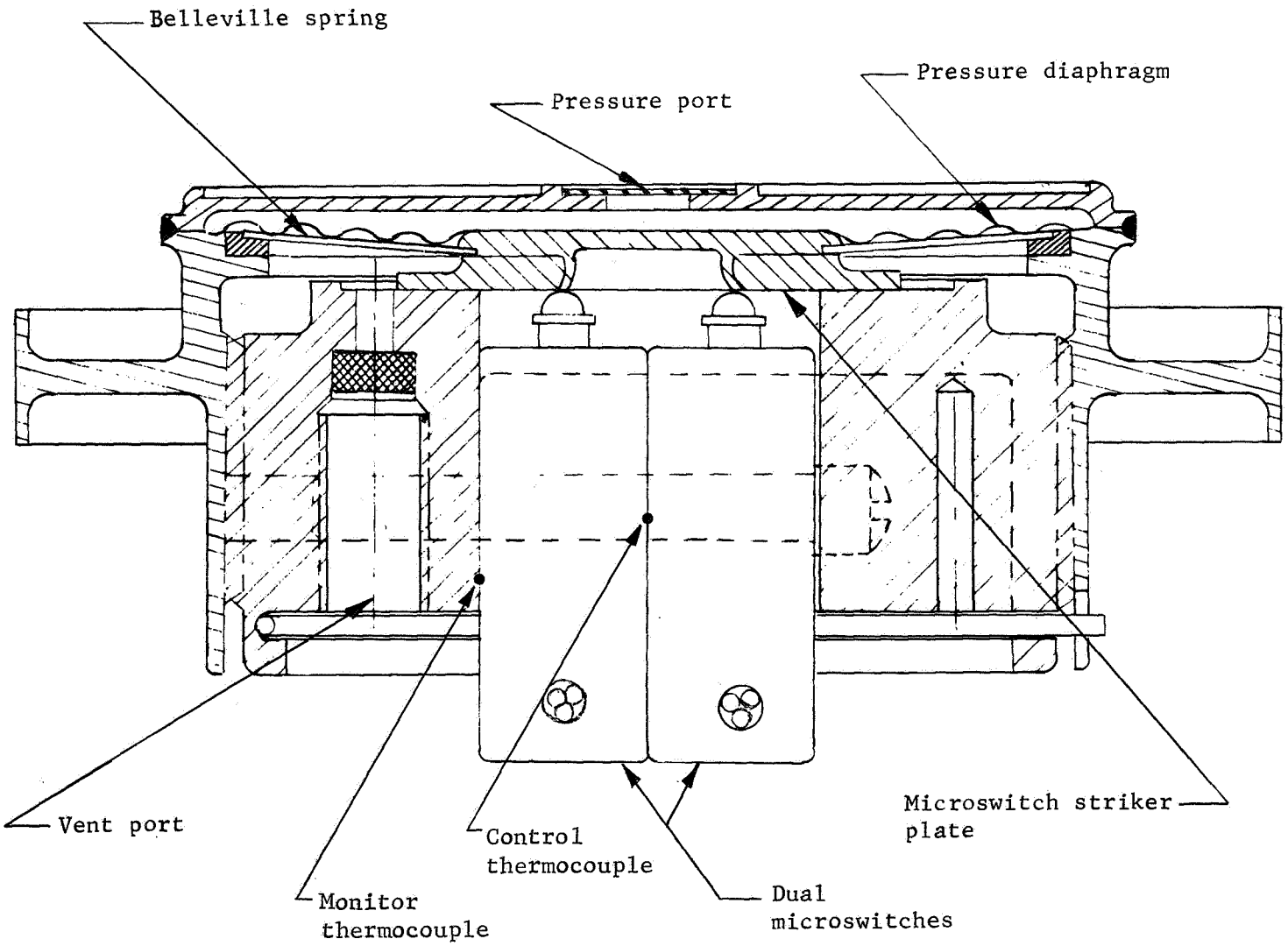


Figure 125.- Pressure Switch Instrumentation Sketch, ALC Test

The test results from the pressure switch ALC testing program were completed during the first part of September 1969. They are briefly summarized below.

Functional tests were performed as specified in the procedure, i.e., at the start of ALC at about 3000, 6000, 9000, 12 000, 15 000, 18 000, and 21 344 cycles of ALC. The data taken before start were taken at the completion of FAT, before welding the switches into switch cups for pressurization and seal. All data are presented in Appendixes A, B, and C.

Pressure transfer point: At the 3000-cycle shock, it was noticed that the pressure actuation points had shifted down. When the shift was first obtained, it was believed that it was caused by pressure leaking past the threads of the switch assembly. To preclude the "dynamic" pressure readings, a fixture was fabricated in which the pressure switch was installed. The purpose of the fixture was to provide an atmosphere around the pressure switch at the same pressure being applied to the overpressure port of the unit. This was done to eliminate the $\Delta P$ between the atmospheric side of the pressure switch and the surrounding external pressure that caused pressure to leak past the threads. At the 6000-cycle check, the shift continued down even though the pressure fixture was used. Examination of the switch structure showed that contaminants, between the Belleville actuation washer and the trip lever could cause the same effect, essentially the same as screwing the electrical portion of the switch into the body. It was decided to continue the test to completion and then examine the internal portion of the switch. After taking pressure measurements after 21 448 cycles, the switch was disassembled, cleaned, and reassembled. The pressure measurements obtained were much closer to the original readings, which verified, to a large extent, the action of contaminants in reducing the pressure actuation levels. Some change (approximately 1 psi) appears to have been a result of the test environment or duration. A summary of these pressure measurements is presented in table 19.

Contact resistance: In all specimens, resistance increased, but did not exceed specification limits.

Helium leak tests were performed as specified after approximately each 3000 cycles. No leak indications were observed during any tests performed.

TABLE 19.- PRESSURE SWITCH TRANSFER POINT SHIFT

| Test specimen serial number | Transfer pressures at start of ALC | | Transfer pressures after 3000 cycles | | Transfer pressures after 6000 cycles | | Transfer pressures after 9000 cycles | | Transfer pressures after 12 000 cycles | |
|---|---|---|---|---|---|---|---|---|---|---|
| | Increase | Decrease | Increase | Decrease | Increase | Decrease | Increase | Decrease | Increase | Decrease |
| 0000182 | | | | | | | | | | |
| Set no. 1 | 6.9 | 5.4 | 5.1 | 3.2 | 4.6 | 3.0 | 4.7 | 3.3 | 6.9 | 4.1 |
| Set no. 2 | 6.9 | 5.4 | 5.1 | 3.2 | 4.6 | 3.0 | 4.7 | 3.3 | 6.9 | 4.1 |
| 0000183 | | | | | | | | | | |
| Set no. 1 | 7.0 | 5.4 | 5.4 | 3.2 | 5.4 | 2.2 | 5.4 | 3.5 | 5.9 | 3.1 |
| Set no. 2 | 7.0 | 5.4 | 5.4 | 3.2 | 8.6 | 2.2 | 5.4 | 3.5 | 5.9 | 3.1 |
| 0000185 | | | | | | | | | | |
| Set no. 1 | 6.6 | 5.3 | 4.2 | 2.8 | 4.0 | 2.7 | 4.9 | 3.4 | 4.3 | 2.9 |
| Set no. 2 | 6.6 | 5.3 | 4.2 | 2.8 | 4.0 | 2.7 | 4.9 | 3.4 | 4.3 | 2.9 |

| Test specimen serial number | Transfer pressures after 15 000 cycles | | Transfer pressures after 18 000 cycles | | Transfer pressures after 21 448 cycles | | Transfer pressures after cleaning | |
|---|---|---|---|---|---|---|---|---|
| | Increase | Decrease | Increase | Decrease | Increase | Decrease | Increase | Decrease |
| 0000182 | | | | | | | | |
| Set no. 1 | 4.8 | 3.2 | 4.4 | 2.5 | 4.4 | 2.8 | 6.6 | 4.8 |
| Set no. 2 | 4.8 | 3.2 | 4.4 | 2.5 | 4.4 | 2.8 | 6.6 | 4.8 |
| 0000183 | | | | | | | | |
| Set no. 1 | 4.6 | 2.0 | 4.5 | 1.8 | 4.8 | 1.8 | 6.6 | 3.2 |
| Set no. 2 | 4.6 | 2.0 | 4.5 | 1.8 | 4.8 | 1.8 | 6.6 | 3.2 |
| 0000185 | | | | | | | | |
| Set no. 1 | 4.1 | 3.1 | 3.9 | 2.6 | 3.9 | 2.6 | 5.9 | 4.5 |
| Set no. 2 | 4.1 | 3.1 | 3.9 | 2.6 | 3.9 | 2.6 | 5.9 | 4.5 |

The ALC testing was performed as required by the test procedure. All three specimens completed 21 448 cycles at the specified test temperatures. At approximately each 3000 cycles, the specimens were removed from the test tool and the required functional and leak tests were performed. At no time during the cycling did a "NO/GO" light energize. Significant events or anomalies are discussed in the following paragraphs. A typical temperature cycle, of the recorded temperature of all three thermocouples, is shown in figure 126.

In determining which fluids to use for the two temperature baths, a check was made with the manufacturers to assure compatibility of materials between the switch and the bath fluids. After receiving positive results, glycerine and ethylene alcohol were selected. Almost immediately after starting the test, the RTV potting, on the microswitch posts began to swell. The potting progressively deteriorated until it was completely gone at the 9000-cycle shutdown. The loss of potting did not immediately affect the operation of the pressure switches. Two side effects of potting loss were: (1) the potting "form," or top half of the microswitch assembly was free to move once the potting was gone and shorted the microswitch posts to ground causing the "GO" light to flicker. The form was removed on each switch, which corrected the situation; and (2) repeated cycling after the loss of restraint afforded by the potting eventually caused wire breakage, from the microswitch posts on S/N 0000183 only. This occurred between 15 000 cycle and 18 000 cycle checks. The switch was continued in cycling without monitoring until completion. Functional checks were still made by using clip leads on the switch posts.

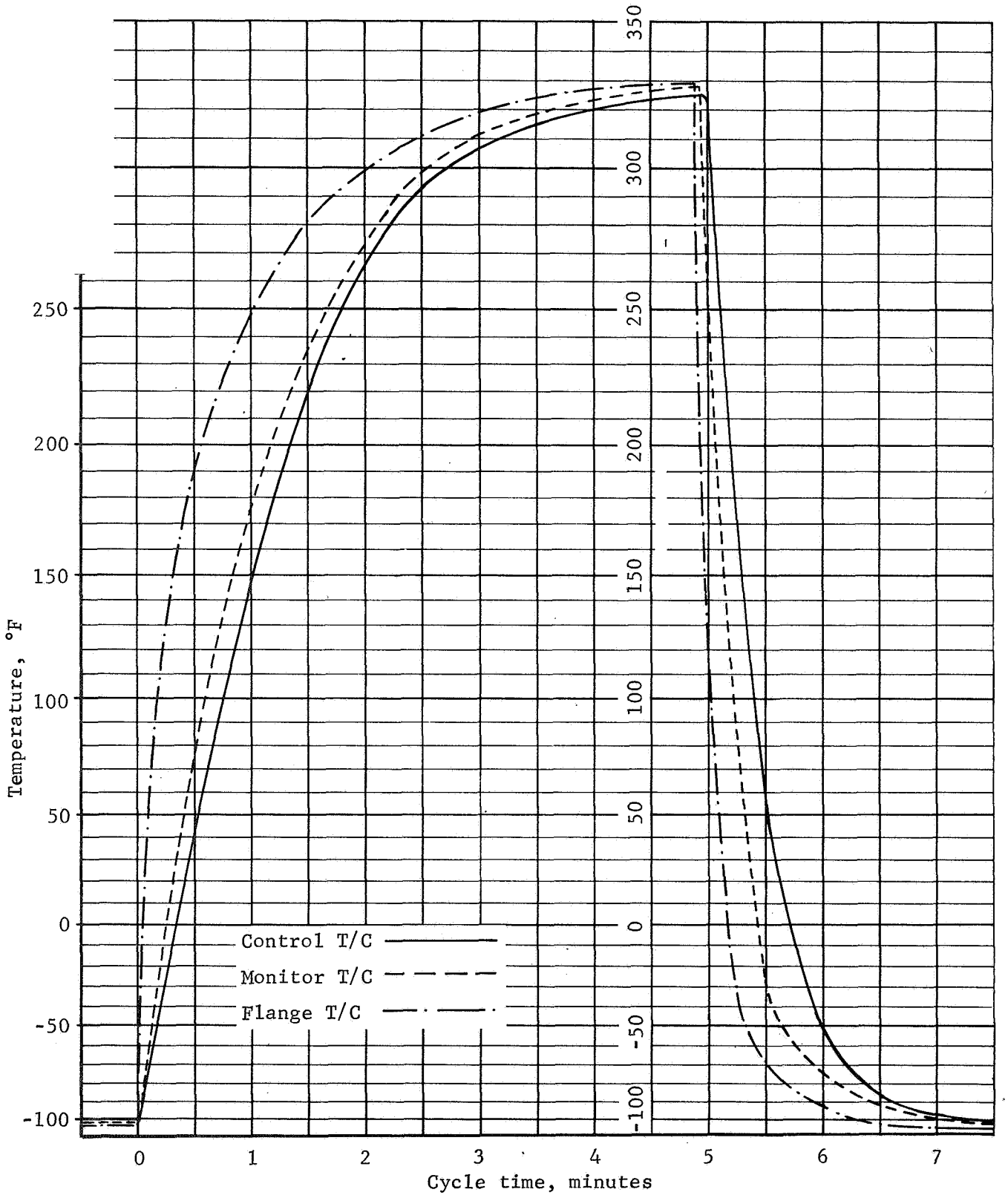


Figure 126.- Typical Temperature Cycle, Pressure Switch ALC

Detector/panels.-

Flight assurance testing: The flight assurance test program was conducted on those items selected from the Design and Development phase of the program. The candidate configurations were:

| | | |
|---|---|---|
| B1A Panel | 8280-04000 | 7 each |
| C1 Panel | 8280-07000 | 6 each |
| D2A Dual Detector | 8280-13000 | 3 each |
| D3A Detector | 8280-16000 | 4 each |
| E1A Detector | 8280-19000 | 4 each |
| E3A Detector | 8280-25000 | 6 each |
| F1A Panel with Bumper Sheet | 8280-28000 | 10 each |

The flight assurance testing consisted of the tests discussed in the following paragraphs.

The pressure switch was connected electrically and pneumatically to the functional test tool (see figs. 100 and 107). The specimen transfer and return pressures were checked to verify that the trip points were within 6 $\pm$ 2.5 psig. This test was conducted initially, after proof pressure, after dynamics (random vibration), and after thermal cycling.

To test switch contact resistance the electrical setup shown in figure 101 was used. The voltage drop across each set of contacts was measured with 5.0 $\pm$ .2 Vdc circuit voltage and 0.5 A and 100 uA circuit current. The maximum allowable voltage drops were 112 mV and 32 uV, respectively. This test was conducted initially, after proof pressure, after dynamics, and after thermal cycling.

For the helium leak test each specimen was placed in a vacuum chamber (see figs. 108 and 127) in which the pressure was reduced to 1 x $10^{-5}$ torr, or less, pressurized to 27.4 $\pm$ 0.5 psia, and leakage sensed at the normally exposed surface of the specimen. The maximum allowable leak rate was determined by the test specimen volume (see RGA leak). The test was conducted after proof pressure, after dynamics, and after thermal cycling on the D3A, E1A, E3A, and F1A specimens. For the B1A, C1, and D2A specimens, the test was conducted after dynamics and after thermal cycling. The initial leak test for the B1A, C1, and D2A items was an RGA leak test (see below).

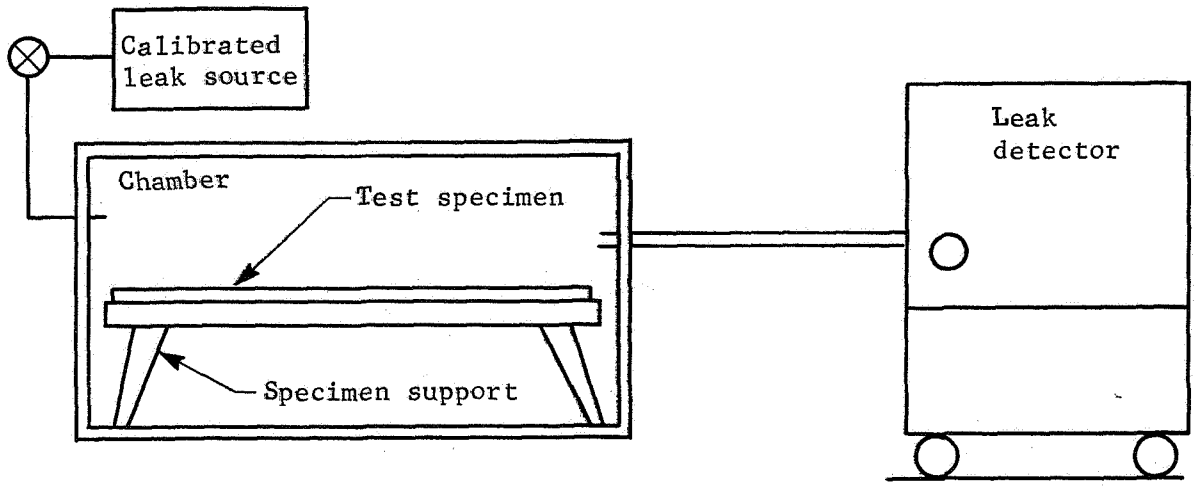


Figure 127.- Leak Test Setup, Helium

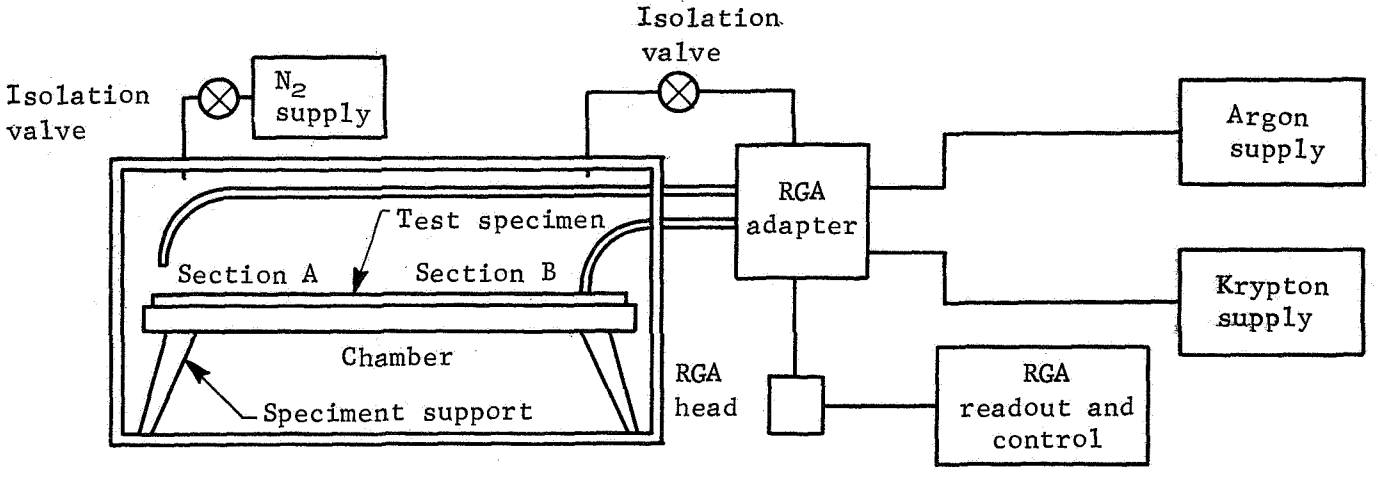


Figure 128.- Leak Test Setup, RGA

The residual gas analysis (RGA) leak test was conducted as the initial leak test on the B1A, C1, and D2A specimens. The purpose of this test was to determine if leakage between the separate halves of the specimens was occurring. It also verified that no external leakage occurred, as in the helium leak test. Each specimen was placed in the vacuum chamber and the pressure reduced to $1 \times 10^{-5}$ torr, or less. The first side of the specimen was pressurized to $27.4 \pm 0.5$ psia with Krypton and leakage sensed on the unpressurized side (see fig. 128). The second side was pressurized with helium while the first side was evacuated. This would allow sensing of leakage from the second side into the first side. External leakage was sensed in the same manner as in a helium leak test. The maximum allowable leak rates were:

| | | |
|---|---|---|
| B1A | 8280-04000 | $1.7 \times 10^{-8}$ scc/sec |
| C1 | 8280-07000 | $3.0 \times 10^{-8}$ scc/sec |
| D2A | 8280-13000 | $1.6 \times 10^{-7}$ scc/sec |
| D3A | 8280-16000 | $4.0 \times 10^{-8}$ scc/sec |
| E1A | 8280-19000 | $3.7 \times 10^{-7}$ scc/sec |
| E3A | 8280-25000 | $1.1 \times 10^{-7}$ scc/sec |
| F1A | 8280-28000 | $1.2 \times 10^{-7}$ scc/sec |

Figure 129 shows the RGA and chamber control consoles.

For the random vibration test the specimens were installed, either singly (D2A, D3A, E1A, and E3A) or up to three at a time (B1A, C1, and F1A) on the vibration test fixture (see figs. 130 and 131) and subjected to a random vibration input generated by an electrodynamic vibration exciter. The shape of the applied vibration spectrum was flat from 200 to 700 Hz at 0.052 $g^2$/Hz, rolled off from 200 to 20 Hz at 3 dB/octave and 6 dB/octave from 700 to 2000 Hz. This shape yields an overall level of 7.4 grms and was applied for 5.0 minutes/axis (see fig. 131). Figures 132 thru 135 show equipment used during vibration and three typical test setups.

For thermal cycling, each specimen was subjected to 100 thermal cycles between $325 \begin{smallmatrix}+50\\-0\end{smallmatrix}$ °F and -90, -60, -50 or $-20 \begin{smallmatrix}+10\\-30\end{smallmatrix}$ °F, depending on the specimen (see table 20). The test temperatures were obtained using resistive heating for the high temperature

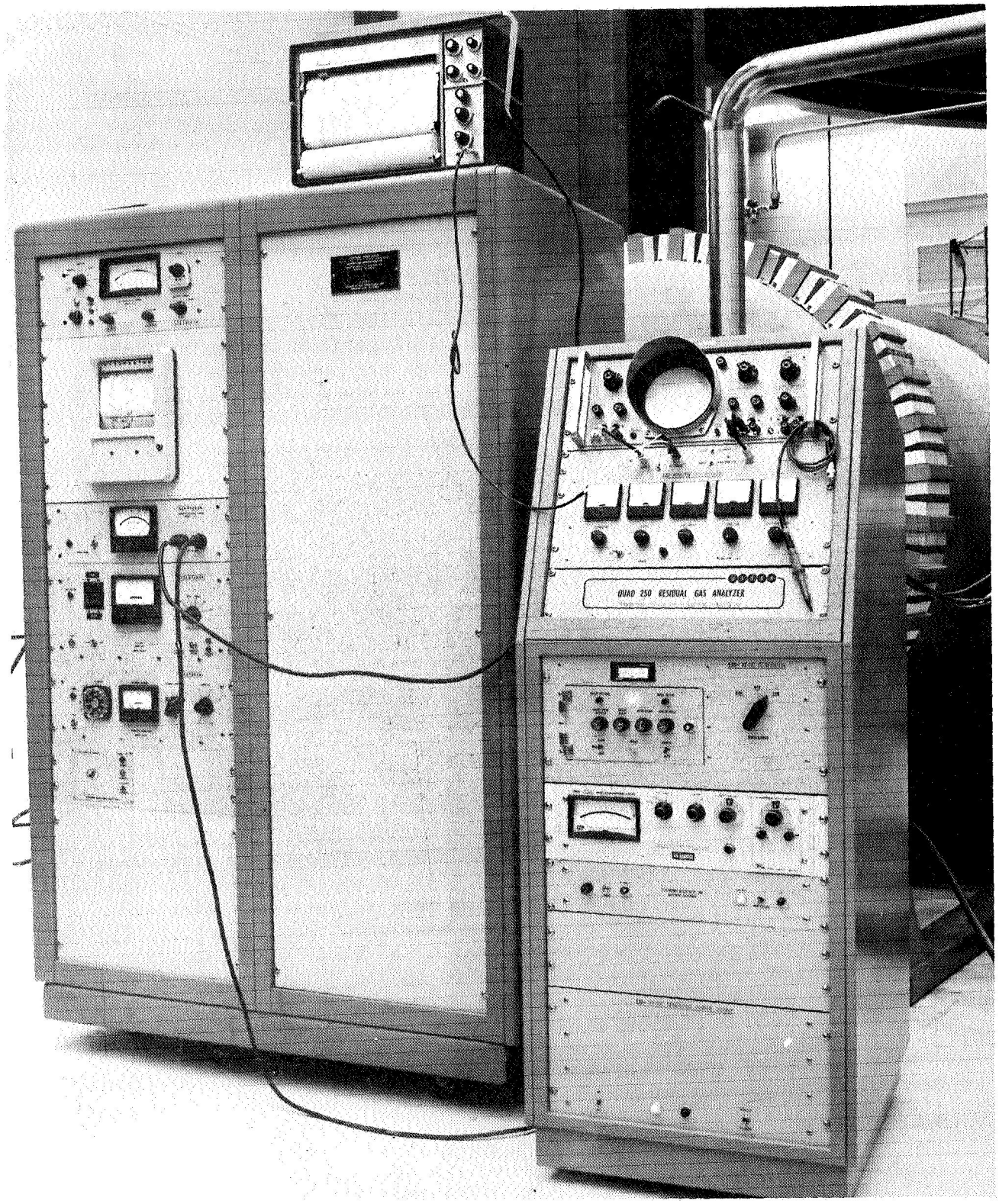


Figure 129.- Photo of RGA Leak Test Setup

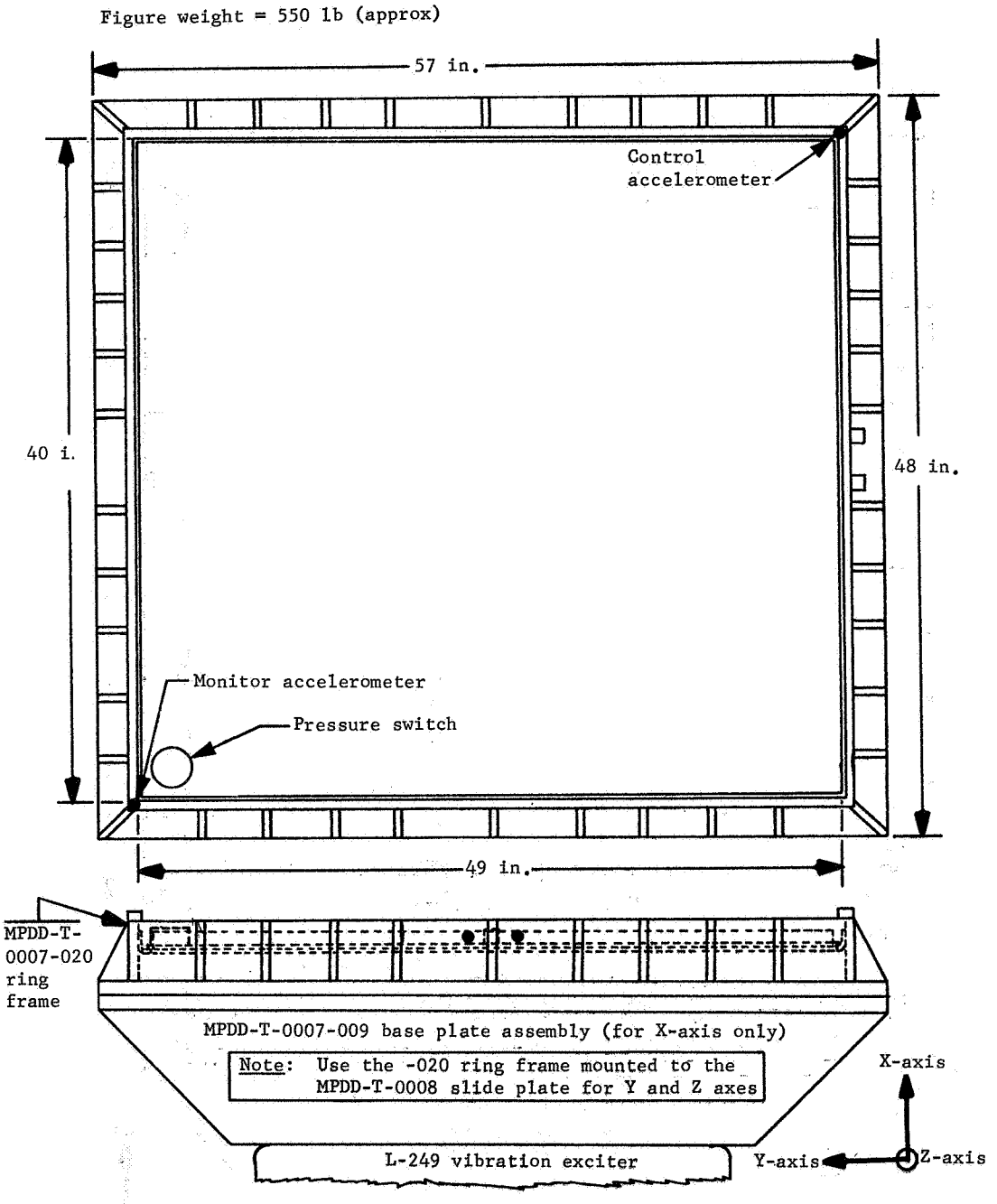


Figure 130.- Vibration Test Setup, 40x49-in. Detector, FAT

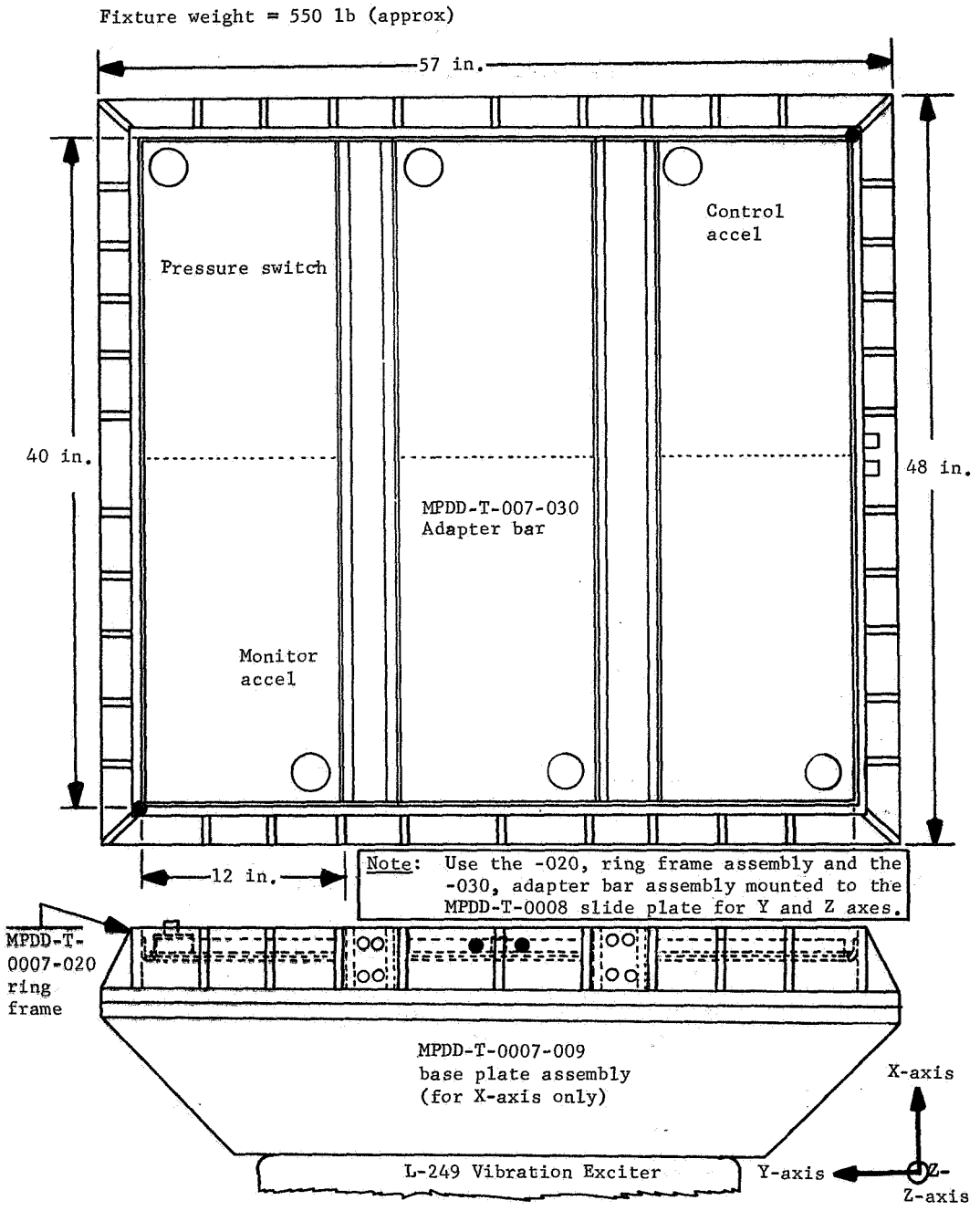


Figure 131.- Vibration Test Setup, 40x12-in. Panels, FAT

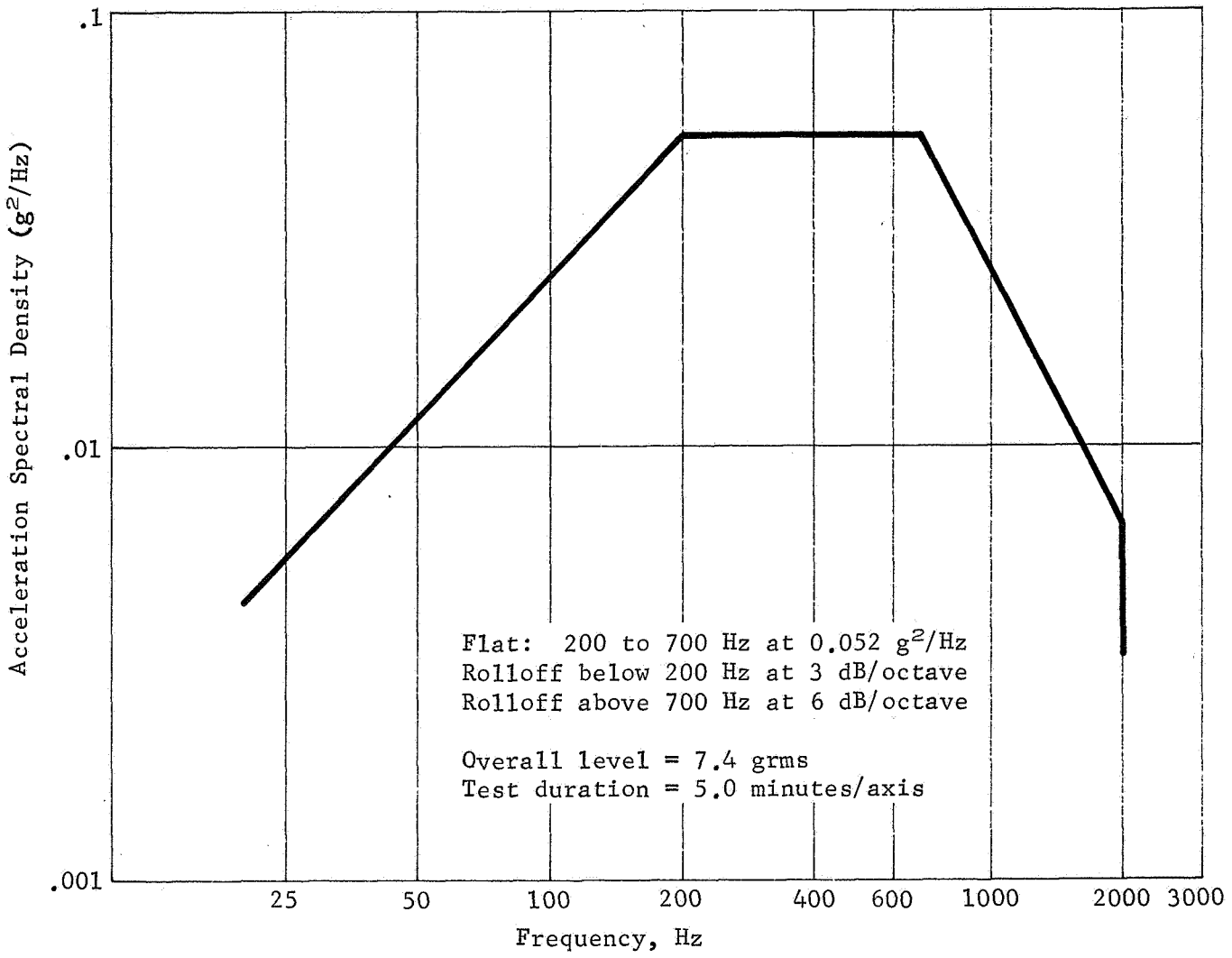


Figure 132.- Random Vibration Criteria, Detector/Panel FAT

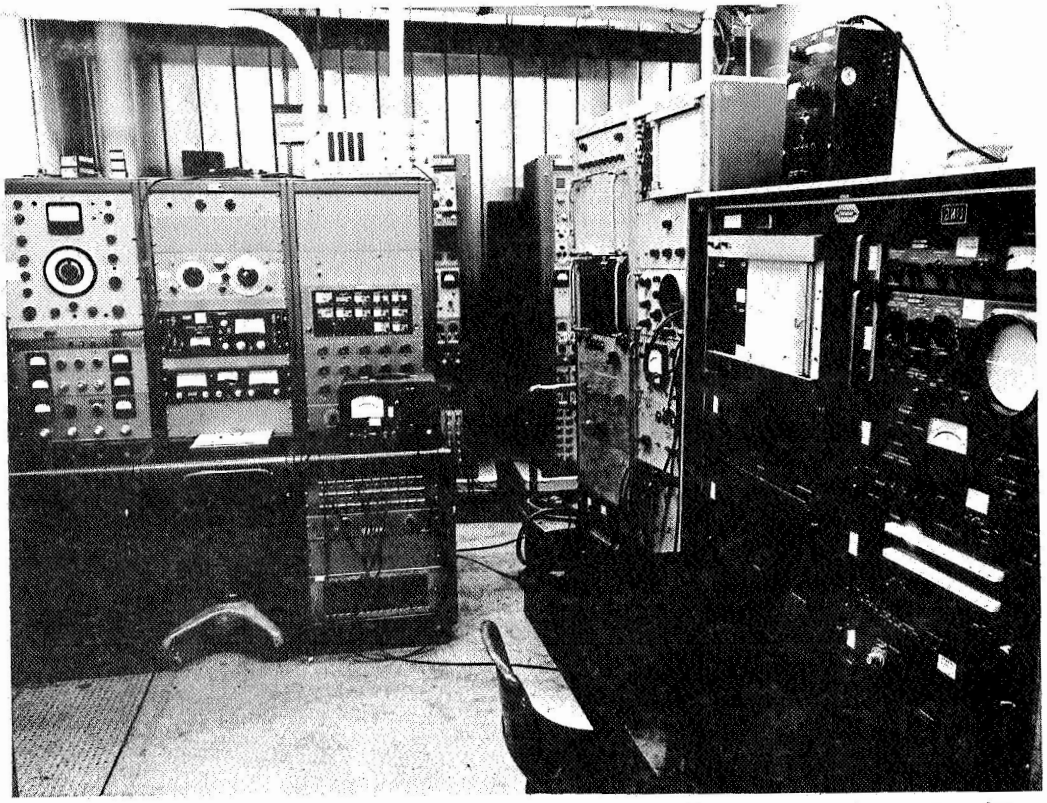

Figure 133.- Control Instrumentation Equipment, Dynamics, Detector/Panel FAT

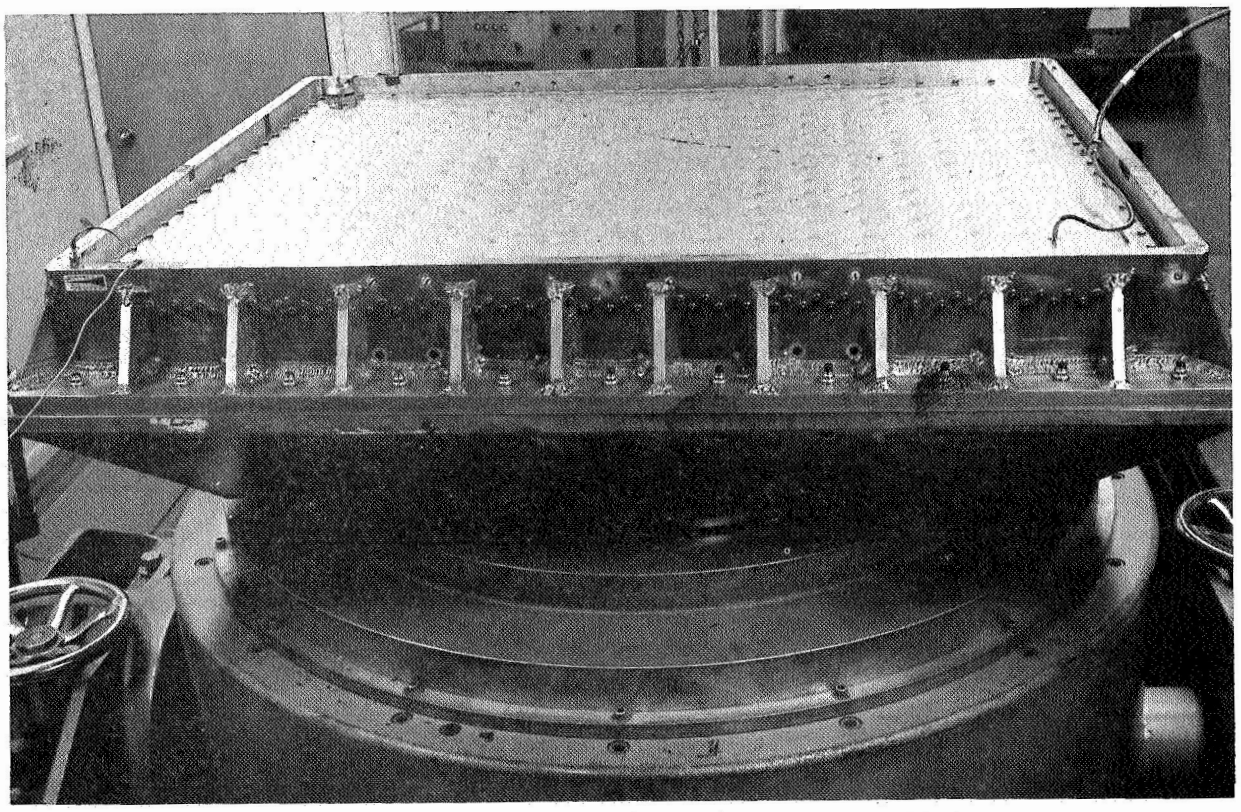

Figure 134.- X-Axis Vibration and Shock Test Setup, 40x49-in. Detector

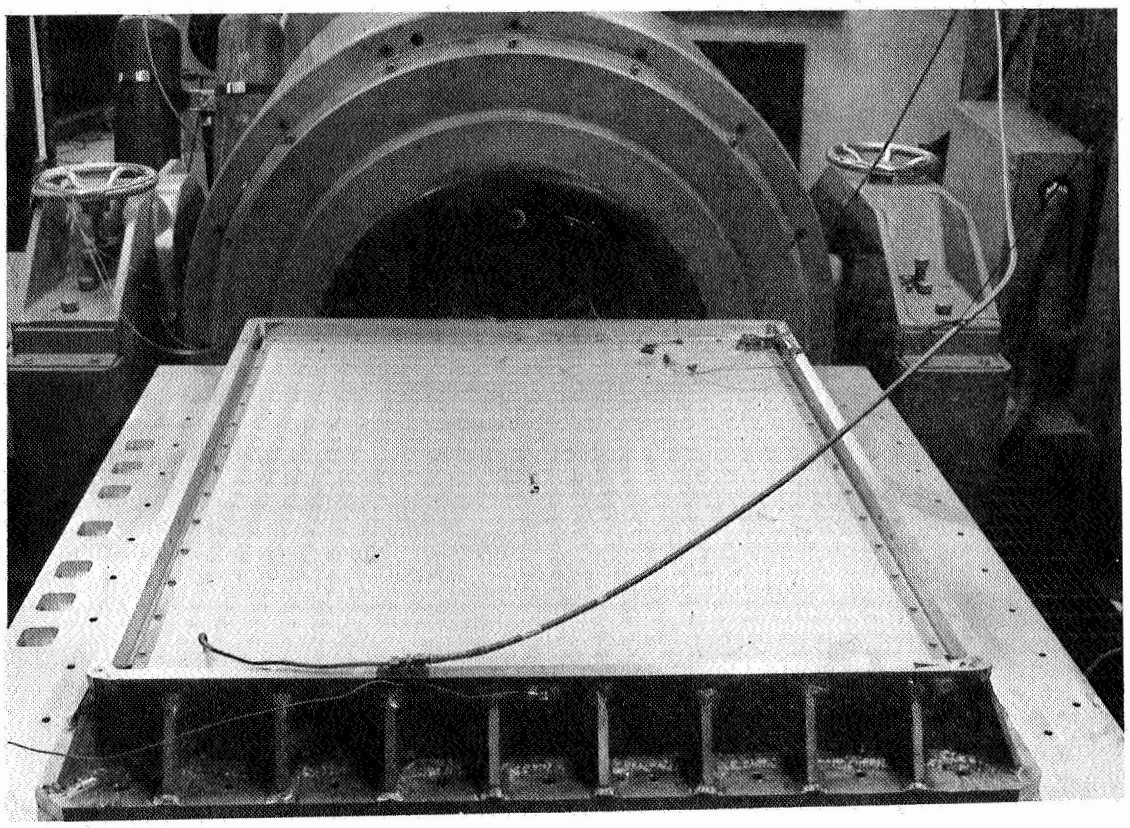

Figure 135.- Y-Axis Vibration and Shock Test Setup, 40x49-in. Detector

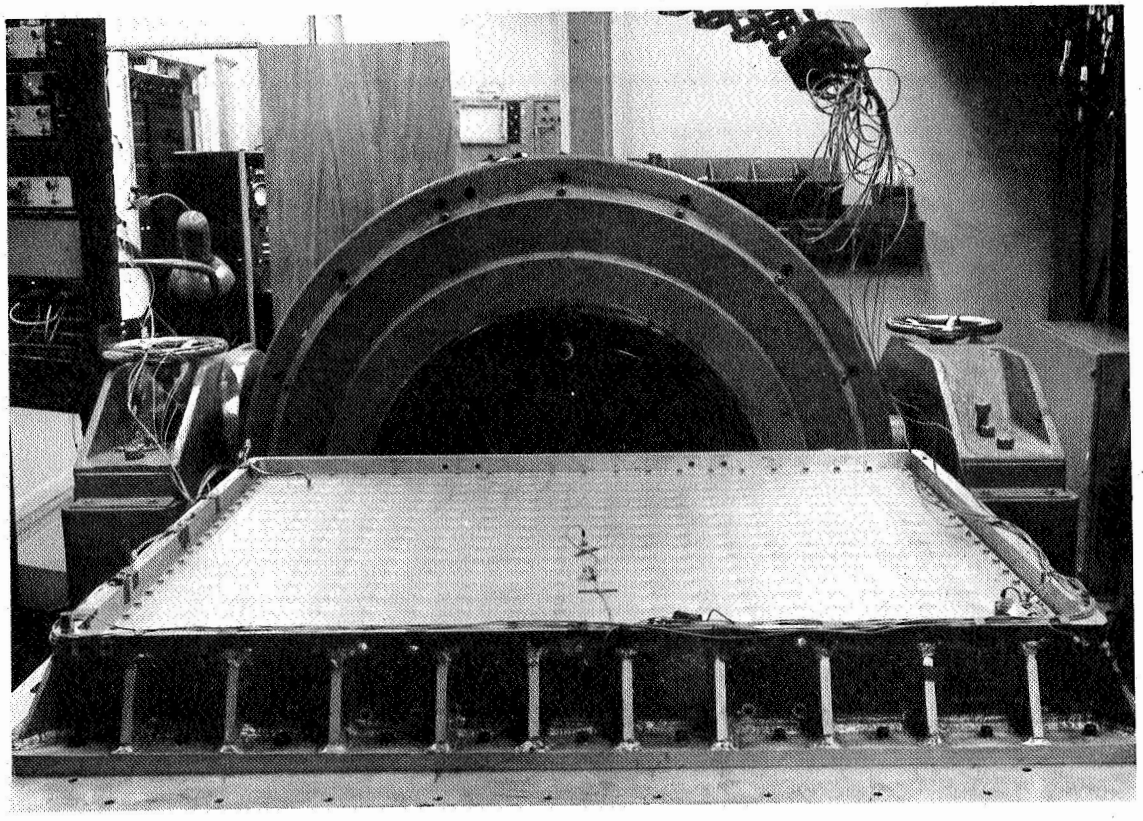

Figure 136.- Z-Axis Vibration and Shock Test Setup, 40x49-in. Detector

TABLE 20.- DETECTOR/PANEL THERMAL CYCLING TEMPERATURE LIMITS

| Detector/panel designation | Stainless steel thickness, in. (target) | Detector/panel skin temperature limits, °F | | |
|---|---|---|---|---|
| | | High limit (a) | Low limit (a) | Differential ($\Delta$ t) between heated side and other side (b) (c) |
| B1A | 0.008 | $325^{+50}_{-10}$ | $-90^{+10}_{-30}$ | $6^{+14}_{-0}$ |
| C1 | 0.016 | $325^{+50}_{-10}$ | $-60^{+10}_{-30}$ | $8^{+14}_{-0}$ |
| D3A | 0.027 | $325^{+50}_{-10}$ | $-50^{+10}_{-30}$ | $4^{+14}_{-0}$ |
| E1A & E3A | 0.042 | $325^{+50}_{-10}$ | $-20^{+10}_{-30}$ | $18^{+18}_{-0}$ |
| F1A (w/o bumper) | 0.002 | $325^{+50}_{-10}$ | $-20^{+10}_{-30}$ | N/A |

NOTE: The test shall be stopped within 100 thermal cycles of any switch transfer to verify detector pressure and switch functional characteristics. Each occurrence of switch transfer and subsequent verification of detector pressure and switch functional characteristics shall be reported on the test data sheets.

a) A survey shall be conducted on each representative configuration and fixture to establish the performance characteristics of the fixture and to provide data for location of control and monitor thermocouples. During the survey the fixture shall be adjusted so that the average high and low temperatures on both sides fall within the limits set in the table. A minimum of six thermocouples shall be installed on one side and two thermocouples on the other side of each configuration for use in determining the average temperature. One of these thermocouples shall be installed on a detector pillow center near each detector corner, and the remaining two thermocouples shall be installed on separate pillow centers near the detector center.

b) The differential ($\Delta$t) shall be obtained at least once during each cycle. Zero $\Delta$t may occur during the balance of the cycle.

c) Differential ($\Delta$t) does not apply to the FAT thermal cycle test on specimens to be subjected to qualification and ALC testing.

and an $LN_2$ spray for the cold temperature. Thermocouples were attached to the test specimens that were used to control the application of current or $LN_2$ spray by means of the ALC Control Console shown in figure 137. The pressure switches were monitored for pressure loss or decay as shown schematically in figure 138. Each specimen was pressurized and sealed with a helium pressure of 35.4 $\pm$ 0.1 psia. This overpressure was to simulate vacuum conditions.

The test history of the FAT program is presented in table 21. During the course of testing eight test failures occurred. The items affected were the B1A, S/N 0000105; C1, S/N 0000101; D2A, S/N 0000101; E1A, S/N 0000105; F1A, S/N 0000101; F1A, S/N 0000102; F1A, S/N 0000103; F1A, S/N 0000105; and F1A, S/N 0000108.

C1, S/N 0000101 had high contact resistance at 100 uA current and 4.999 Vdc (268.8 uv measured average versus 32 uv allowable maximum). The electrical portion of the switch was replaced (see MARS B50941) and the specimen subjected to dynamics a second time. The retest and the remaining flight assurance testing were successfully completed.

The D2A, 8280-13000, S/N 0000101 specimen failed the initial RGA test (see MARS B50966). The failure was a leak at the fusion weld that joins the fill tube to the ring weld fitting. The fusion weld was repaired and a helium leak test performed to verify the repair. The specimen was given an RGA test as its final FAT leak test and was successful.

The E1A, 8280-19000, S/N 0000105 specimen failed the post-dynamics helium leak test. The measured leak rate was $6.4 \times 10^{-7}$ scc He/sec and was isolated to the pressure switch diaphragm (see MARS B60712). The subject pressure switch was removed, a new switch welded in its place, and the specimen retested through dynamics. The remainder of the FAT sequence was successfully completed.

F1A, 8280-28000, S/Ns 0000101 and 0000102 items leaked after completion of the thermal cycling test (see MARS B65014 and MARS B42462). The S/N 0000101 was leaking at a rate of $1.0 \times 10^{-7}$ scc He/sec while the S/N 0000102 had a leak rate of $6.0 \times 10^{-7}$ scc He/sec. Both leaks occurred at the ring weld fitting. Each panel had one bad side and one good side. The bad sides were scrapped and the good sides were mated to produce S/N 0000101A.

The F1A, 8280-28000, S/N 0000103 specimen also leaked following thermal cycling. As with the above cases, the good side

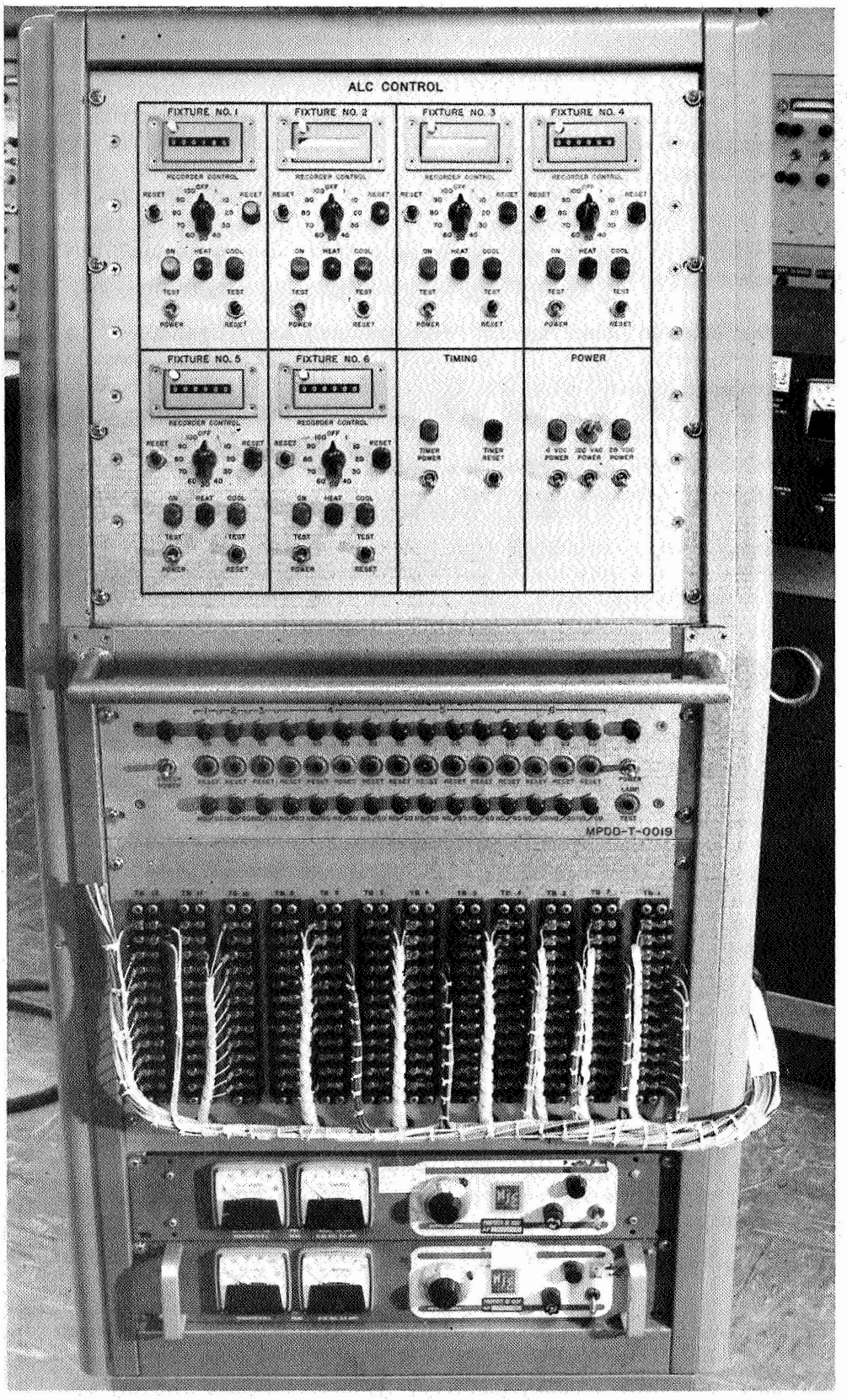


Figure 137.- Thermal Cycling and ALC Control Console

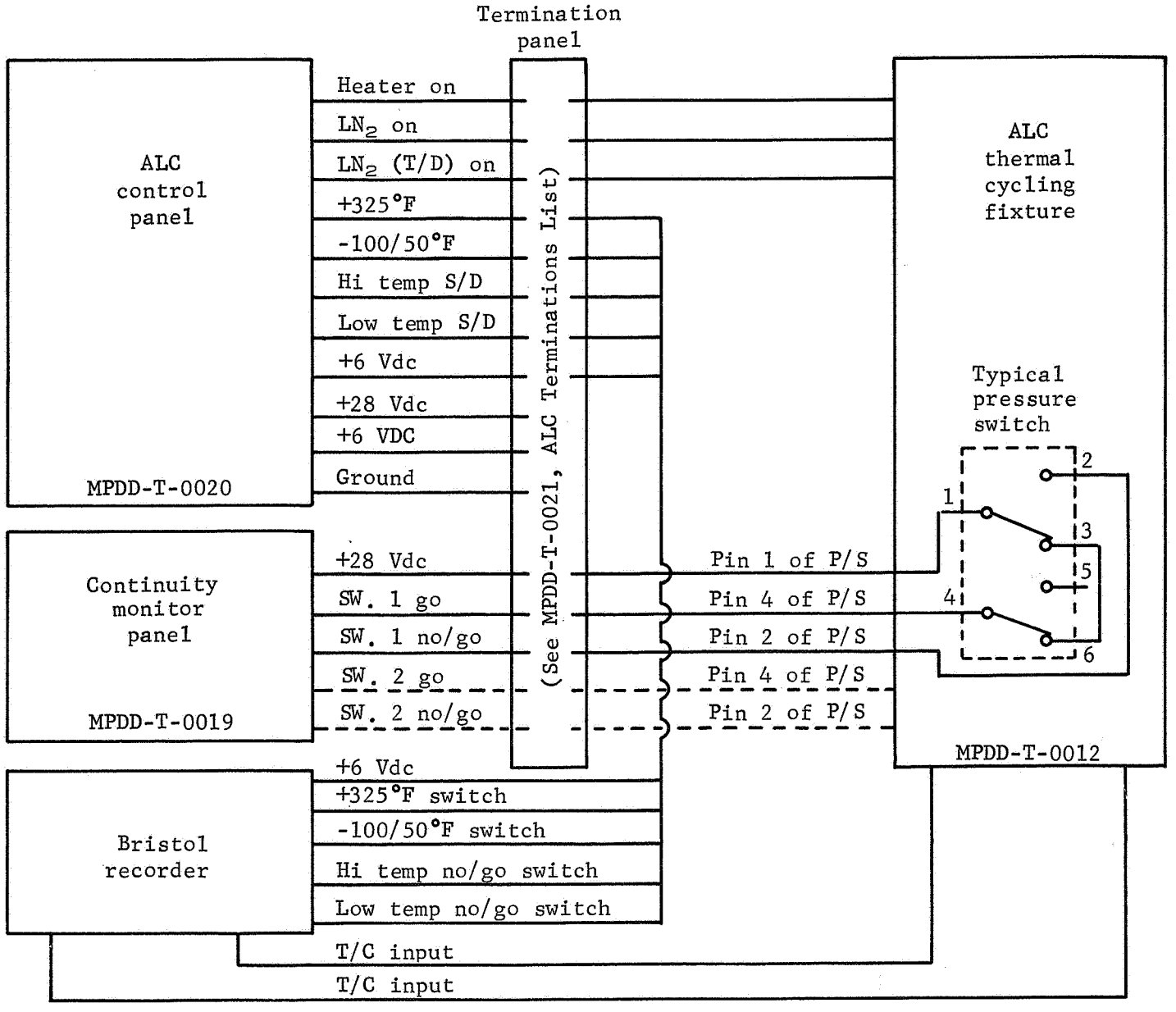


Figure 138.- Block Diagram, Thermal Cycling Test

TABLE 21.- TEST HISTORY, FLIGHT ASSURANCE TEST PROGRAM

| Item, part no., S/N | Initial function | Proof pressure | Post-proof function | Initial leak | Random vibration X-axis | Random vibration Y-axis | Random vibration Z-axis | Post function | Post He leak | Thermal cycling | Post-T/C function | Post-T/C He leak | Random Function retest | Random He leak retest | Random vibration retest | Random Post function | Random Post He leak | MARS no. |
|---|---|---|---|---|---|---|---|---|---|---|---|---|---|---|---|---|---|---|
| B1A, 8280-04000, 0000101 | 9 4 68 | 9 4 68 | 9 4 68 | 9 19 68 | 9 23 68 | 9 24 68 | 9 24 68 | 9 25 68 | 10 1 68 | 2 5 69 | 2 14 68 | 2 17 68 | | | | | | B42083 |
| B1A, 8280-04000, 0000102 | 9 4 68 | 9 4 68 | 9 4 68 | 9 17 68 | 9 20 68 | 9 20 68 | 9 20 68 | 9 23 68 | 10 2 68 | 3 5 69 | 3 7 69 | 3 11 69 | | | | | | B42082 |
| B1A, 8280-04000, 0000103 | 9 4 68 | 9 4 68 | 9 4 68 | 9 17 68 | 9 20 68 | 9 20 68 | 9 20 68 | 9 23 68 | 10 2 68 | 2 5 69 | 2 14 69 | 2 17 69 | | | | | | |
| B1A, 8280-04000, 0000104 | 9 4 68 | 9 4 68 | 9 4 68 | 9 20 68 | 9 23 68 | 9 24 68 | 9 24 68 | 9 25 68 | 10 1 68 | 3 5 69 | 3 7 69 | 3 7 69 | | | | | | B42085 |
| B1A, 8280-04000, 0000105 | 9 12/13 68 | 9 12/13 68 | 9 13 68 | 9 18 68 | 9 20 68 | 9 20 68 | 9 20 68 | 9 23 68 | 10 7 68 | 3 14 69 | 3 26 69 | 5 6 69 | | | | | | B42082<br>B42100 |
| B1A, 8280-04000, 0000106 | 9 13 68 | 9 13 68 | 9 13 68 | 9 19 68 | 9 23 68 | 9 24 68 | 9 24 68 | 9 25 68 | 10 1 68 | 3 14 69 | 3 19/20 69 | 3 26 69 | | | | | | |
| B1A, 8280-04000, 0000107 | 6 17 69 | | | 6 13 69 | 6 20 69 | 6 20 69 | 6 20 69 | 6 24 69<br>Failed | 6 24 69 | 7 11 69 | 7 11 69 | 7 14 69 | | | | | | |
| C1, 88280-07000, 0000101 | 6 3 68 | 6 3 68 | 6 3/4 68 | 6 20 68 | 7 12 68 | 7 11 68 | 7 11 68 | 7 15 68 | 8 21 68 | 2 7 69 | 2 17 69 | 2 18 69 | 8 13 68 | | 10 22 68 | 10 23 68 | 10 23 68 | B50941 |
| C1, 8280-07000, 0000102 | | | | Failed<br>7 24 68 | | | | | | | | | | | | | | B50970 |
| C1, 8280-07000, 0000103 | 5 28 68 | 5 28 68 | 5 29 68 | 6 20 68 | 7 12 68 | 7 11 68 | 7 11 68 | 7 15 68 | 7 24 68 | 2 7 69 | 2 19 69 | 2 20 69 | | | | | | |
| C1, 8280-07000, 0000104 | 5 29 68 | 6 3 68 | 6 4 68 | 6 21 68 | 7 12 68 | 7 15 68 | 7 12 68 | 7 15 68 | 7 24 68 | 1 30 69 | 2 14 69 | 2 28 69 | | | | | | |
| C1, 8280-07000, 0000105 | 6 3 68 | 6 3 68 | 6 4 68 | 6 21 68 | 7 12 68 | 7 15 68 | 7 12 68 | 7 15 68 | 7 25 68 | 2 11 69 | 2 17 69 | 2 27 69 | | | | | | |
| C1, 8280-07000, 0000106 | 6 3 68 | 6 3 68 | 6 4 68 | 6 21 68 | 7 12 68 | 7 15 68 | 7 12 68 | 7 15 68 | 7 24 68 | 2 11 69 | 2 17 69 | 2 24 69 | | | | | | |
| C1, 8280-07000, 0000107 | 9 18 68 | 9 18 68 | 9 18 68 | 10 14 68 | 10 22 68 | 10 22 68 | 10 22 68 | 10 23 68 | 10 23 68 | 1 30 69 | 2 14 69 | 2 18 69 | | | | | | |
| D2A, 8280-13000, 0000101 | 6 17 68 | 6 17 68 | 6 17 68 | Failed<br>6 25 68 | 7 30 68 | 7 30 68 | 7 30 68 | 8 1 68 | 8 12 68 | | | | | 7 22 68 | | | | B50966 |
| D2A, 8280-13000, 0000102 | 6 17 68 | 6 17 68 | 6 17 68 | 6 27 68 | 7 12 68 | 7 11 68 | 7 11 68 | 7 12 68 | 7 19 68 | | | | | | | | | |
| D2A, 8280-13000, 0000103 | 6 17 68 | 6 17 68 | 6 17 68 | 6 21 68 | 7 12 68 | 7 15 68 | 7 15 68 | 7 16 68 | 7 25 68 | | | | | | | | | |
| D3A, 8280-16000, 0000101 | 7 10 68 | 7 10 68 | 7 10 68 | 7 23 68 | 8 5 68 | 8 5 68 | 8 5 68 | 8 6 68 | 8 8 68 | 1 23 69 | 2 17 69 | 2 18 69 | | | | | | |
| D3A, 8280-16000, 0000102 | 7 9 68 | 7 10 68 | 7 10 68 | 7 23 68 | 8 2 68 | 8 2 68 | 8 2 68 | 8 6 68 | 8 8 68 | 1 24 69 | 2 17 69 | 2 19 69 | | | | | | |
| D3A, 8280-16000, 0000103 | 7 10 68 | 7 10 68 | 7 10 68 | 7 23 68 | 8 1 68 | 8 1 68 | 8 1 68 | 8 6 68 | 8 8 68 | 1 31 69 | 2 17/18 69 | 3 14 69 | | | | | | |
| D3A, 8280-16000, 0000104 | 7 9 68 | 7 9 68 | 7 9 68 | 7 23 68 | 8 2 68 | 8 2 68 | 8 2 68 | 8 6 68 | 8 8 68 | 2 3 69 | 2 18 69 | 3 14 69 | | | | | | |
| E1A, 8280-19000, 0000101 | 7 2 68 | 7 2 68 | 7 2 68 | 7 16 68 | 7 30 68 | 7 30 68 | 7 30 68 | 7 31 68 | 8 8 68 | 1 14 69 | 2 20 69 | 2 27 69 | | 1 3 69 | | | | |
| E1A, 8280-19000, 0000102 | 7 2 68 | 7 2 68 | 7 2 68 | 7 15 68 | 7 23 68 | 7 28 68 | 7 28 68 | 8 1 68 | 8 8 68 | 1 28 69 | 2 6 69 | 2 7 69 | | | | | | |
| E1A, 8280-19000, 0000103 | | | | Failed<br>7 18 68 | | | | | | | | | | | | | | B50969 |
| E1A, 8280-19000, 0000104 | 7 2 68 | 7 2 68 | 7 2 68 | 7 15 68 | 7 31 68 | 7 31 68 | 7 31 68 | 8 2 68 | 8 8 68 | 1 15 69 | 2 20 69 | 3 18 69 | | 1 3 69 | | | | |
| E1A, 8280-19000, 0000105 | 10 8 68 | 10 8 68 | 10 8 68 | 10 16 68 | 10 23 68 | 10 23 68 | 10 23 68 | 10 24 68 | Failed<br>10 24 68 | 1 27 69 | 2 17 69 | 2 18 69 | 11 13 69 | 11 14 69 | 12 3 68 | 12 7 68 | 12 4 68 | B60712 |
| E3A, 8280-25000, 0000101 | 7 31 68 | 7 31 68 | 7 31 68 | 8 7 68 | 9 3 68 | 9 3 68 | 9 3 68 | 9 5 68 | 9 11 68 | 1 22 69 | 2 17 69 | 2 18 69 | | | | | | |
| E3A, 8280-25000, 0000102 | 7 31 68 | 7 31 68 | 7 31 68 | 8 7 68 | 9 4 68 | 9 4 68 | 9 4 68 | 9 5 68 | 9 12 68 | 1 17 69 | 2 6 69 | 2 7 69 | | | | | | |
| E3A, 8280-25000, 0000103 | 7 31 68 | 7 31 68 | 7 31 68 | 8 7 68 | 8 12 68 | 8 12 68 | 8 12 68 | 8 13 68 | 8 20 68 | 1 30 69 | 2 17 69 | 3 19 69 | | | | | | |
| E3A, 8280-25000, 0000104 | 7 31 68 | 7 31 68 | 7 31 68 | 8 7 68 | 9 3 68 | 9 3 68 | 9 3 68 | 9 5 68 | 9 12 68 | 2 4 69 | 2 20 69 | 2 21 69 | | | | | | |
| E3A, 8280-25000, 0000105 | 5 8 69 | 5 8 69 | 5 8 69 | 5 6 69 | 5 21 69 | 5 21 69 | 5 21 69 | 5 26 69 | 5 28 69 | 6 10 69 | 6 16 69 | 6 17 69 | | | | | | |
| E3A, 8280-25000, 0000106 | 5 8 69 | 5 8 69 | 5 8 69 | 5 8 69 | 5 22 69 | 5 22 69 | 5 22 69 | 5 26 69 | 5 28 69 | 6 10 69 | 6 17 69 | 6 16 69 | | | | | | |
| F1A, 8280-28000, 0000101 | 10 4 68 | 10 4 68 | 10 4 68 | 10 10 68 | 10 16 68 | 10 16 68 | 10 16 68 | 10 18 68 | 10 18 68 | 2 12 69 | 2 14 69 | Failed<br>2 21 69 | | | | | | B65104 |
| F1A, 8280-28000, 0000101A | 10 4 68 | 10 4 68 | 10 4 68 | 10 4 68 | 10 16/18 68 | 10 16/18 68 | 10 16/18 68 | 10 18/22 68 | 10 18/22 68 | 2 12 69 | 2 14/17 69 | 4 2 69 | | | | | | |
| F1A, 8280-28000, 0000102 | 10 4 68 | 10 4 68 | 10 4 68 | 10 14 68 | 10 18 68 | 10 18 68 | 10 18 68 | 10 22 68 | 10 22 68 | 2 12 69 | 2 17 69 | Failed<br>2 21 69 | | | | | | B42462 |
| F1A, 8280-28000, 0000103 | 10 8 68 | 10 8 68 | 10 8 68 | 10 11 68 | 10 16 68 | 10 16 68 | 10 16 68 | 10 18 68 | 10 21 68 | 3 4 69 | 3 5 69 | Failed<br>3 12 69 | | | | | | B55774 |
| F1A, 8280-28000, 0000103A | 5 20 69 | | | 5 9 69 | 5 23 69 | 5 26 69 | 5 26 69 | 5 28 69 | 5 29 68 | 7 10 69 | 7 11 69 | 7 14 69 | | | | | | |
| F1A, 8280-28000, 0000104 | 10 10 68 | 10 10 68 | 10 10 68 | 10 14 68 | 10 18 68 | 10 18 68 | 10 21 68 | 10 22 68 | 10 23 68 | 3 28 69 | 4 1 69 | 4 3 69 | | | | | | B42097 |
| F1A, 8280-28000, 0000105 | 10 10 68 | 10 10 68 | 10 10 68 | 10 11 68 | 10 16 68 | 10 16 68 | 10 16 68 | 10 18 68 | 10 21 68 | Failed<br>2 6 69 | | | | | | | | B42091 |
| F1A, 8280-28000, 0000108 | 10 10 68 | 10 10 68 | 10 10 68 | 10 14 68 | 10 18 68 | 10 18 68 | 10 21 68 | 10 22 68 | 10 23 68 | 3 4 69<br>7 9 69 | 3 5 69<br>7 11 69 | 3 7 69<br>7 14 69 | 5 20 69<br>6 17 69 | 5 8 69<br>6 14 69 | 5 23 69<br>6 20 69 | 5 28 69<br>6 24 69 | Failed<br>5 29 69<br>6 24 69 | B66035 |
| F1A, 8280-28000, 0000109 | 10 15 68 | 10 15 68 | 10 15 68 | 10 15 68 | 10 22 68 | 10 22 68 | 10 22 68 | 10 23 68 | 10 23 68 | 3 28 69 | 4 1 69 | 4 2 69 | | | | | | B42092 |
| F1A, 8280-28000, 0000110 | | | | Failed<br>5 22 69 | | | | | | | | | | | | | | B66036 |
| F1A, 8280-28000, 0000111 | 6 17 69 | | | 6 14 69 | 6 20 69 | 6 20 69 | 6 20 69 | 6 24 69 | 6 23 69 | 7 9 69 | 7 11 69 | 7 15 69 | | | | | | |

was salvaged and later mated with a new build half to produce S/N 0000103A.

F1A, 8280-28000, S/N 0000105 is the only specimen to fail during test. The failure was directly contributable to an overheating condition that occurred at approximately the 80th cycle. The overheating occurred as a result of the high resistance created by the splice strip which joins the two halves of an F1A panel. Figures 139, 140, and 141 are photographs of the damage. The panel was severely damaged and was removed from further testing.

For B1A, S/N 0000105 detector, throughout the 100 cycle thermal cycling test, a "no-go" light was lighted on the pressure switch S/N 0000155 side (see MARS B42100). At the conclusion of the 100 cycles, the specimen was subjected to a verification of internal pressure by back pressuring the pressure switch. This could not be done because of what was subsequently found to be a blocked filter. The filter was blocked by potting during the switch potting operation that preceded thermal cycling. The filter was removed and the specimen successfully resubjected to 100 cycles of thermal cycling.

The F1A, S/N 0000108 panel originally passed FAT and went into qualification testing where it subsequently failed the post-acoustics helium leak test (see MARS B65065). The above MARS ordered repair and re-FAT as a deliverable item. The repair made was to install a serpentine fill tube. During the re-FAT, the item was found to leak at the braze connection made during installation of the serpentine tube (see MARS B66035). The braze was repaired and a third FAT was performed. The specimen was successful during this test. In summary, this specimen underwent complete FAT once, qualification testing through acoustics, re-FAT through dynamics, and the third FAT completely.

As a result of the leak failures incurred during the FAT program, the fill tube, between the switch cup and the target sheet, was redesigned on the B1A and F1A panels. The design change was to replace the rigid 1/8-in. O.D. fill tube with a serpentine tube 1/16-in. O.D.

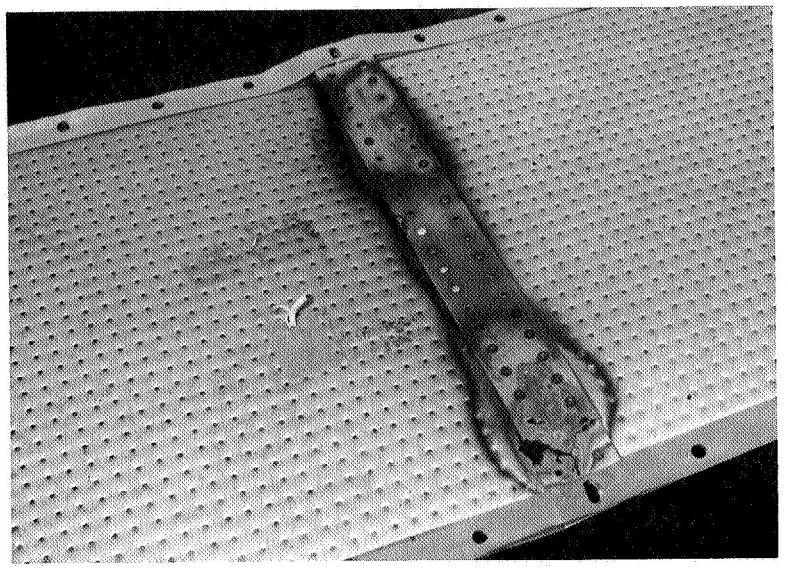

Figure 139.- Top View of Damage to F1A, S/N 0000105

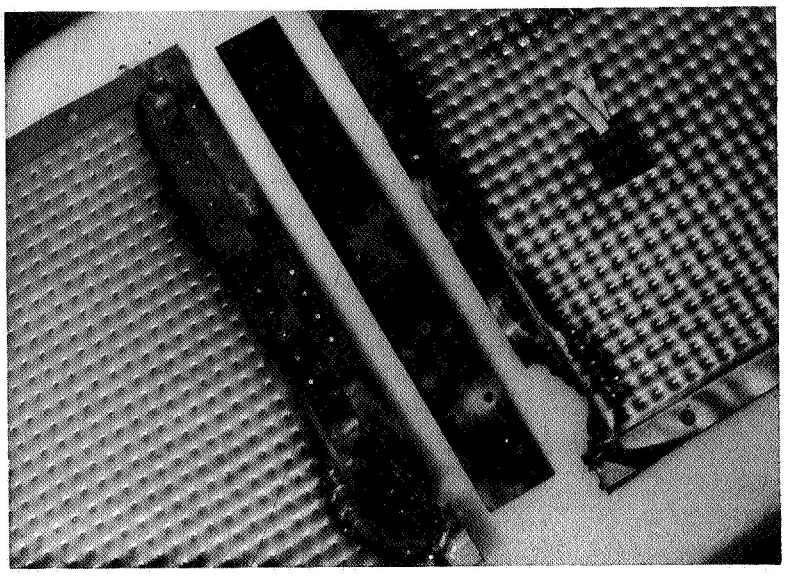

Figure 140.- Bottom View of Overall Splice Area, F1A, S/N 0000105

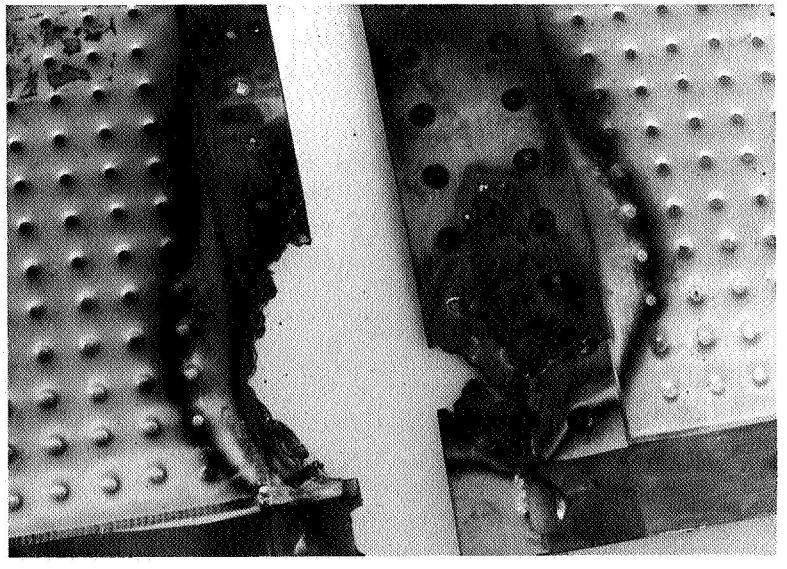

Figure 141.- Closeup of Top View of Damage to F1A, S/N 0000105

Qualification testing: The qualification test program was conducted on the following items:

| | | |
|---|---|---|
| B1A | 8280-04000 | S/N 0000101 |
| B1A | 8280-04000 | S/N 0000103 |
| B1A | 8280-04000 | S/N 0000103A |
| C1 | 8280-07000 | S/N 0000104 |
| C1 | 8280-07000 | S/N 0000107 |
| D2A | 8280-13000 | S/N 0000102 |
| D3A | 8280-16000 | S/N 0000101 |
| E1A | 8280-19000 | S/N 0000102 |
| E3A | 8280-25000 | S/N 0000101 |
| F1A | 8280-28000 | S/N 0000101A |
| F1A | 8280-28000 | S/N 0000108 |
| F1A | 8280-28000 | S/N 0000109 |

The qualification testing consisted of tests described in the following paragraphs.

Switch transfer pressure.- This test was identical to that described for FAT. It was performed before the start of testing, after dynamics, after acoustics, and after the 30-day thermal vacuum soak test.

The switch contact resistance test was identical to that described for FAT. It was performed before the start of testing, after dynamics, after acoustics, and after thermal vacuum soak.

The helium leak test was identical to that described for FAT and was performed before the start of, after dynamics, after acoustics, and after thermal-vacuum soak on the D3A, E1A, E3A, and F1A specimens. For the B1A, C1, and D2A specimens, the last test only (post-thermal-vacuum soak leak) was an RGA test. The maximum allowable leak rate was determined by the test specimen volume and was as delineated for FAT.

The residual gas analysis test was identical to that described for FAT. It was performed on the B1A, C1, and D2A specimens as the final leak test (post-thermal-vacuum soak).

For the sinewave vibration test the specified environment to be applied to the pressure switches consisted of an unidirectional, constant octave sweep, from 5 to 10 Hz at 0.4 in. double amplitude, 2 g peak from 10 to 44 Hz, 0.02 in. double amplitude from 44 to 96 Hz, and 10 g peak from 96 to 2000 Hz (see fig. 141). This two-step sweep was applied for a duration of 9.0 minutes maximum per axis. Each specimen was pressurized to 27.4 $\pm$ 0.5 psia. The input vibration was generated by an electrodynamic vibration exciter in each of three mutually perpendicular axes. The test setup was identical to flight assurance testing and is shown in figures 133 thru 136.

A random vibration environment was applied to the specimens. This environment consisted of an 11.1 grms overall level for a period of 5 minutes/axis. The spectral shape was flat from 200 to 700 Hz at 0.12 $g^2$/Hz, rolled off above 700 Hz at 6 dB/octave to 2000 Hz, and rolled off below 200 Hz at 3 dB/octave to 10 Hz (see fig. 143). The excitation was applied in each of three mutually perpendicular axes. The test setup was the same as for flight assurance testing.

A shock pulse, sufficient to obtain the shock response spectrum shown in figure 144 was generated and applied by a electrodynamic exciter to the same test setup employed during sinewave and random vibration. The spectrum shown is the response spectrum resulting from application of a 50 g peak, 11 msec sawtooth pulse (fig. 145) with 10% damping employed in the analysis.

For the acoustics test the test specimens were mounted in the ring frame fixture used for dynamics tests. This fixture was rigidly mounted to a support frame. An overall sound pressure level of 151 dB nominal, with the spectral shape shown in figure 146, was applied for a duration of four minutes. Figures 147, 148, and 149 show control and instrumentation equipment and typical test setups for the detector/panels. The plastic covering shown placed in front of the panels was to protect them from residual oil spray emanating from the random siren.

The thermal vacuum soak test was the final test scheduled to be performed. All test specimens were subjected to this environment simultaneously in the Space Simulation Laboratory's 29x45-ft vacuum chamber. The specified specimen temperatures were 350°F (plus 20°, minus 0°) for the hot soak and -250°F

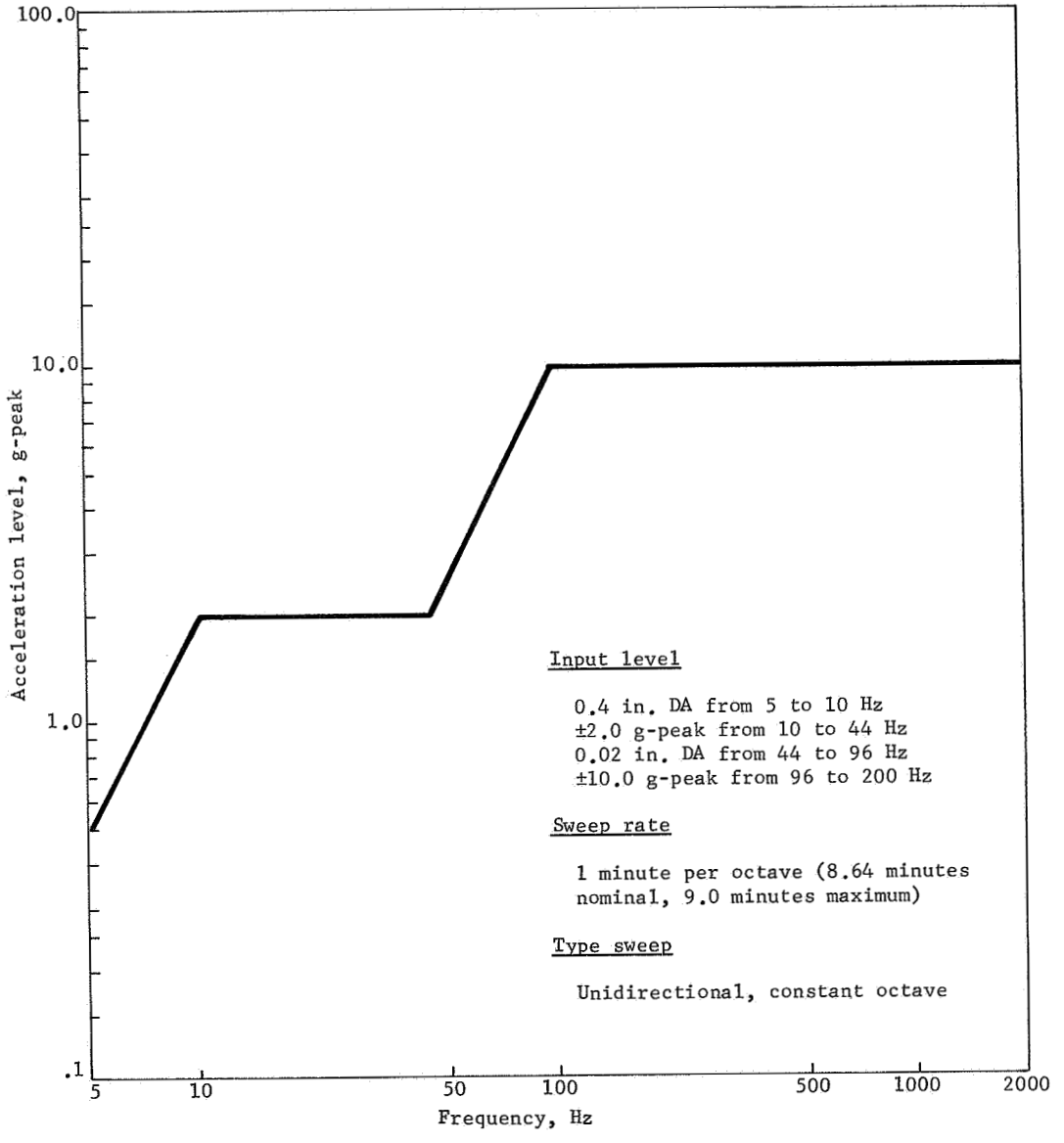


Figure 142.- Sinewave Vibration Specification, Detector/Panel Qual

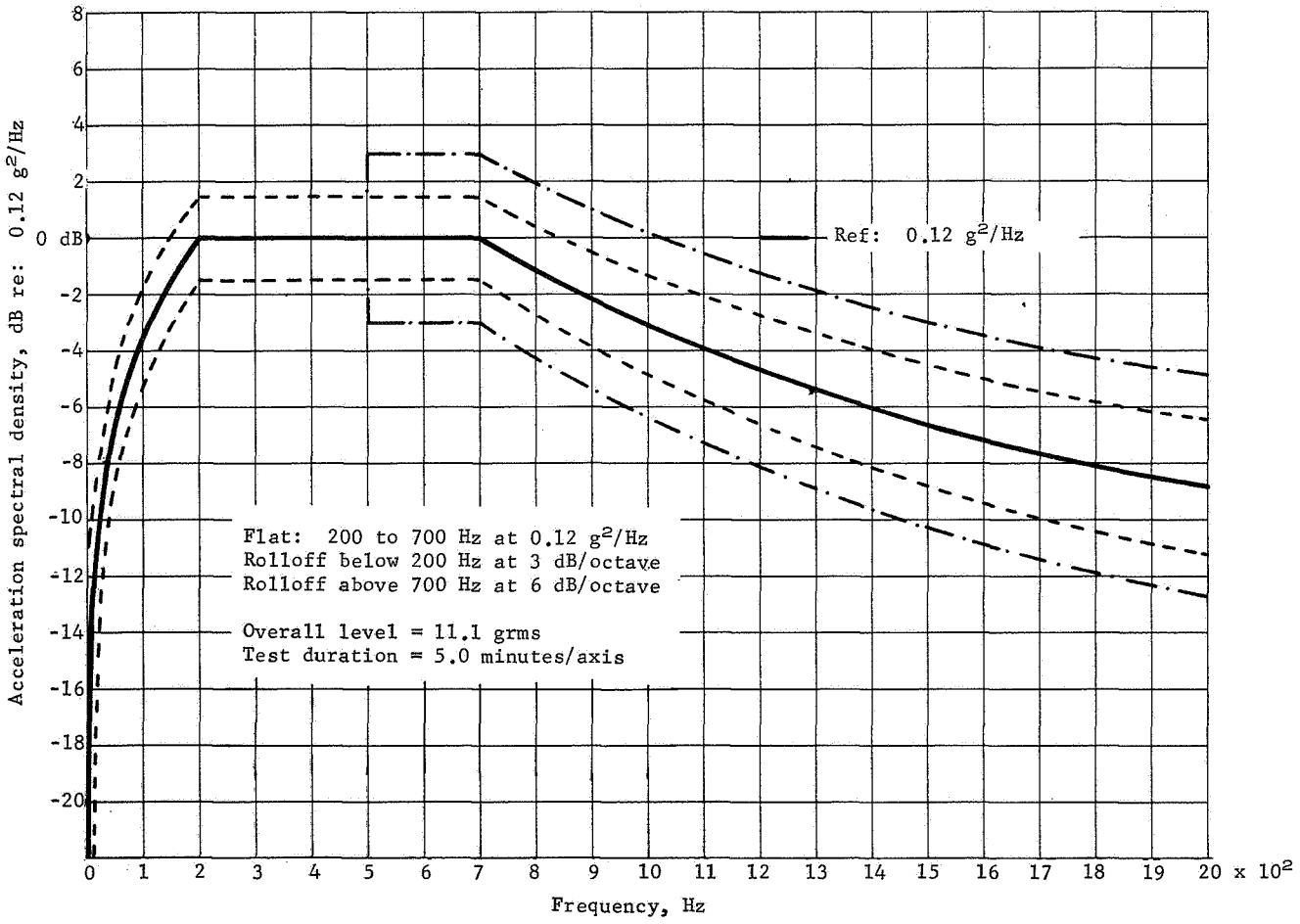


Figure 143.- Random Vibration Criteria, Detector/Panel Qual

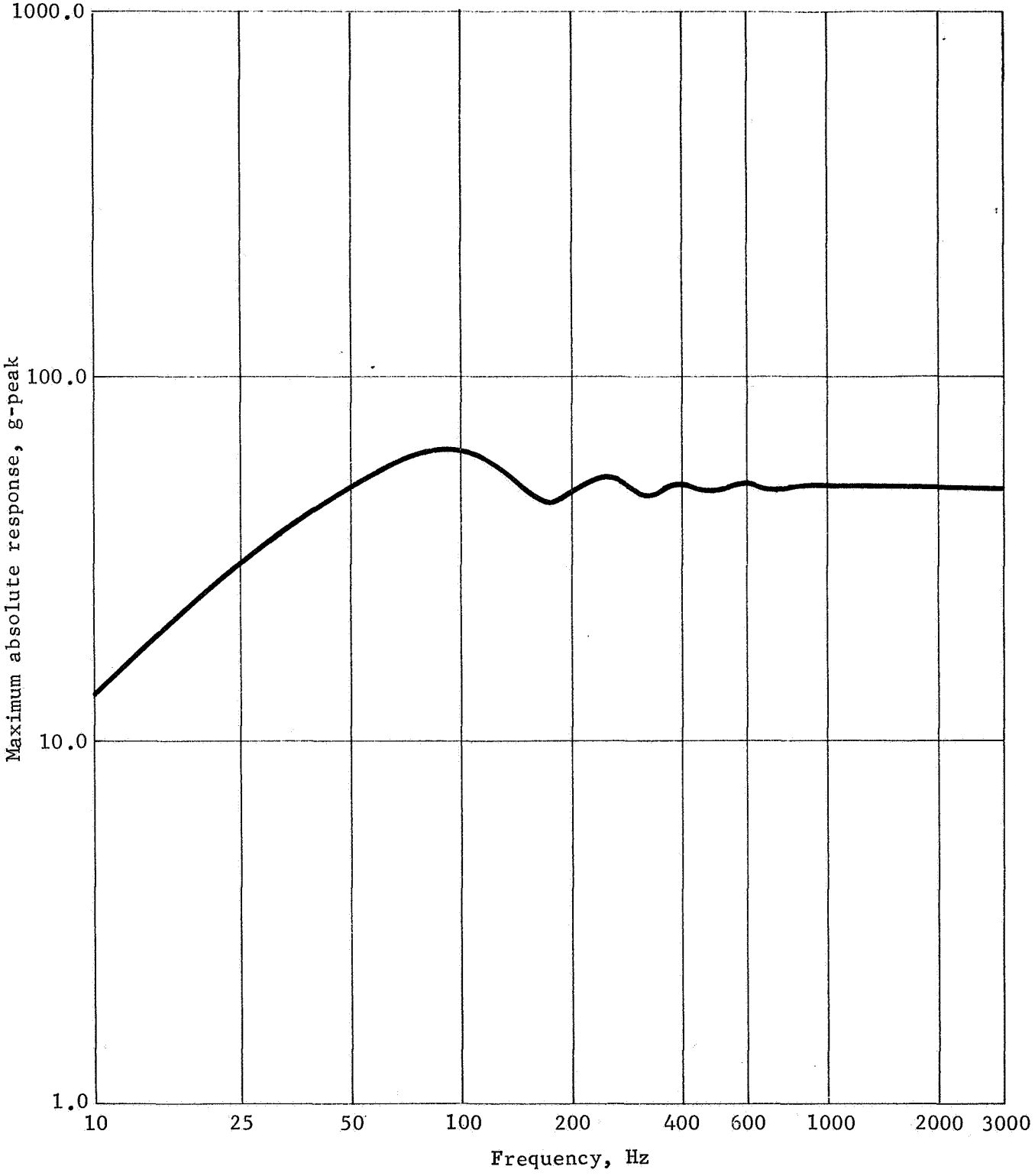


Figure 144.- Shock Response Spectrum, Detector/Panel Qual

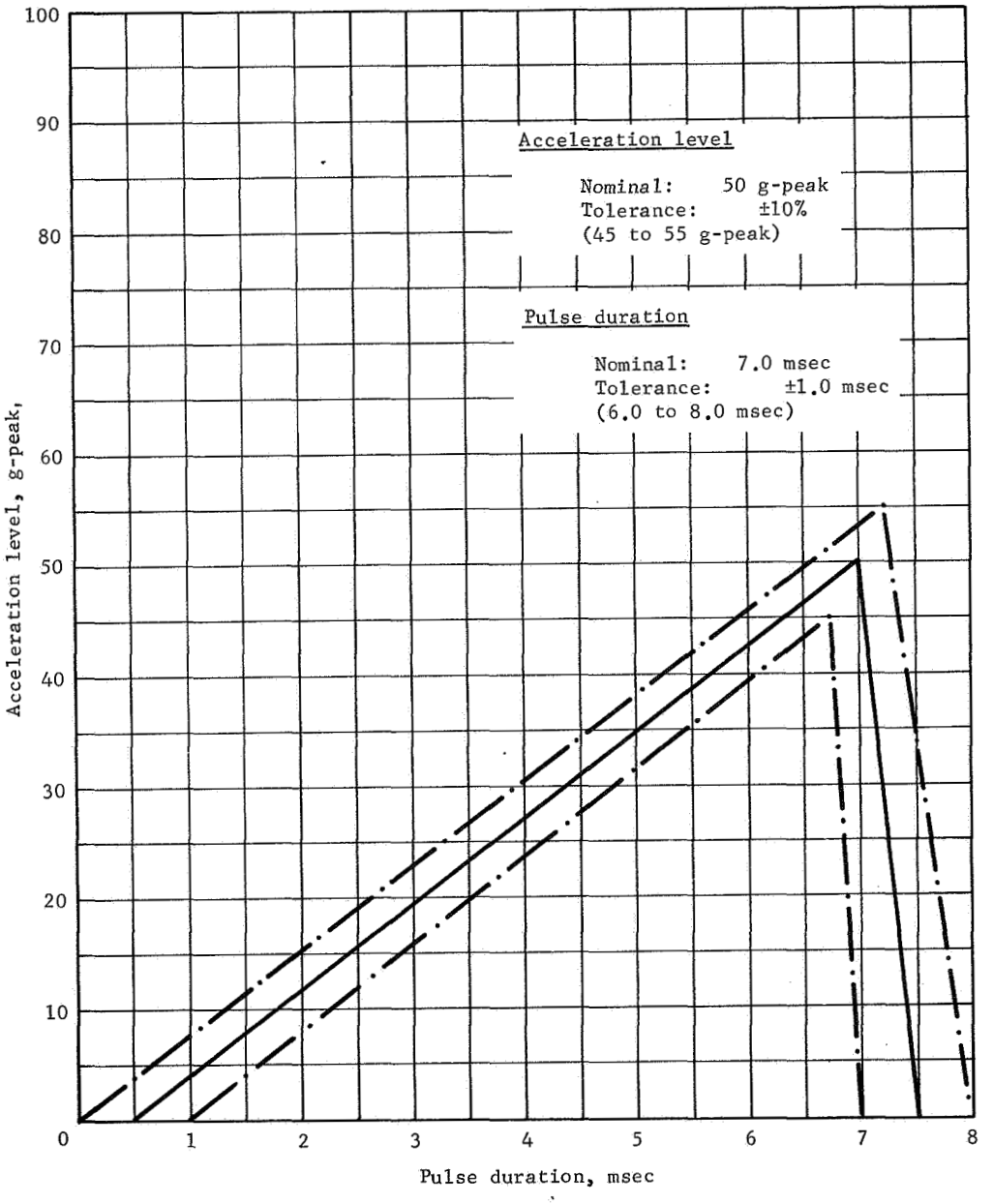


Figure 145.- Sawtooth Pulse Specification, Detector Panel Qual

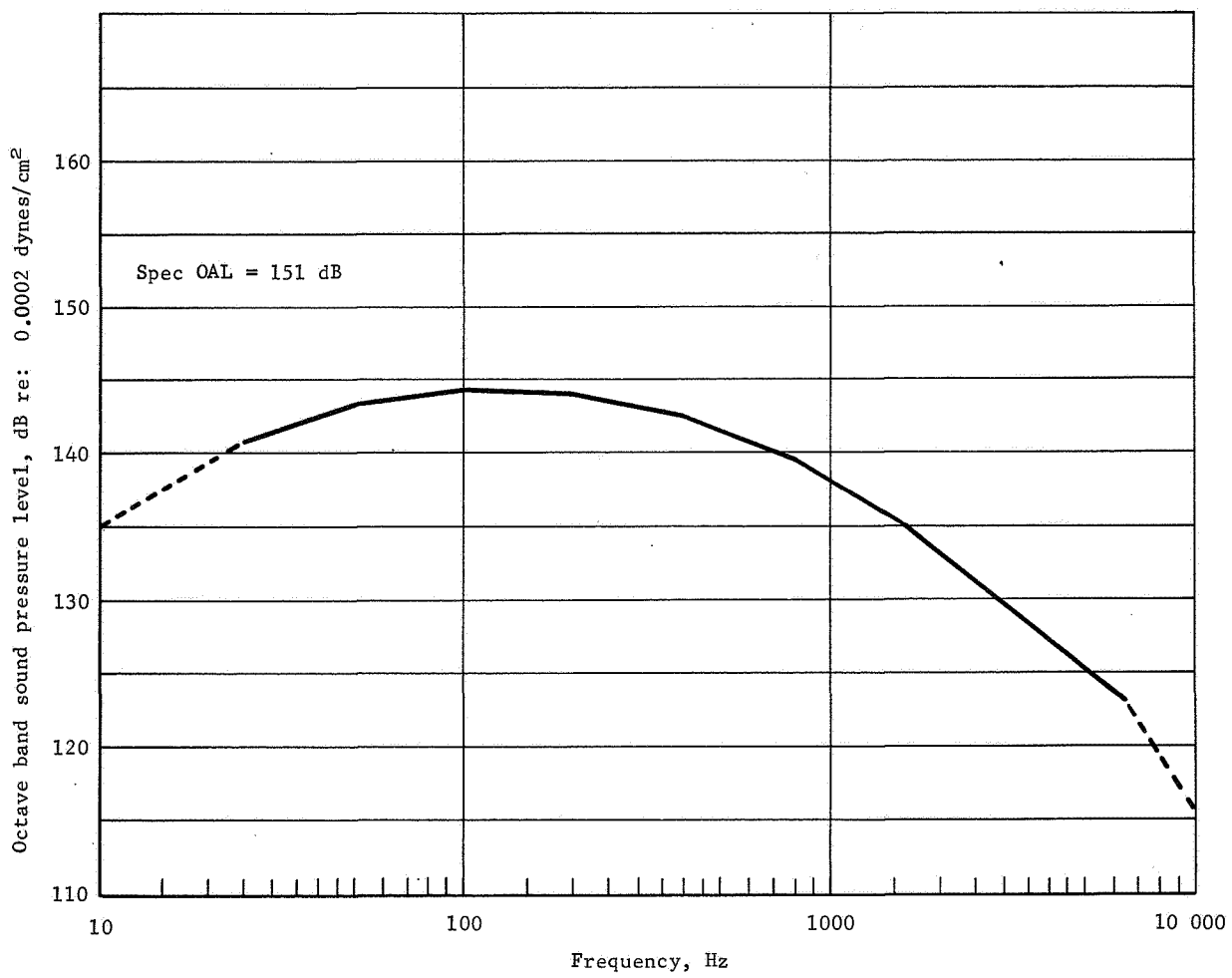


Figure 146.- Acoustic Spectrum, Detector/Panel Qual

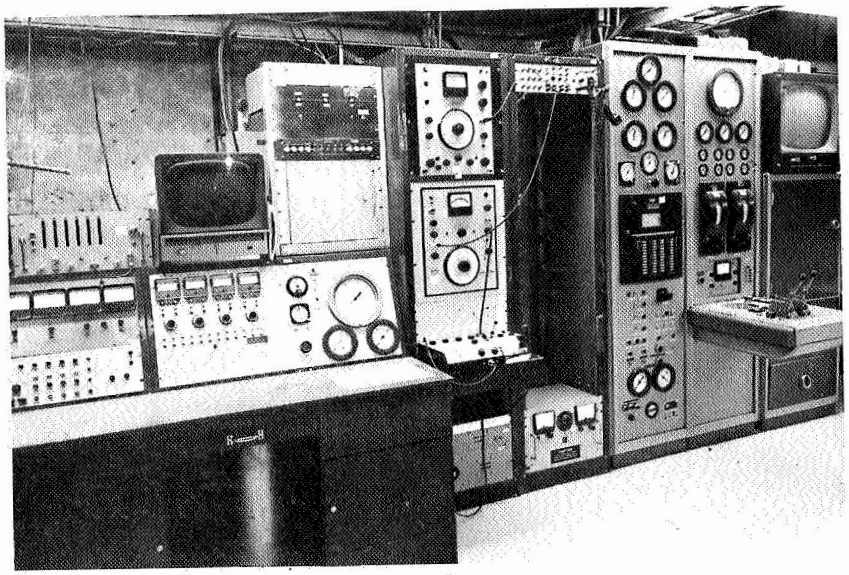

Figure 147.- Acoustic Facility Control and Analysis Consoles

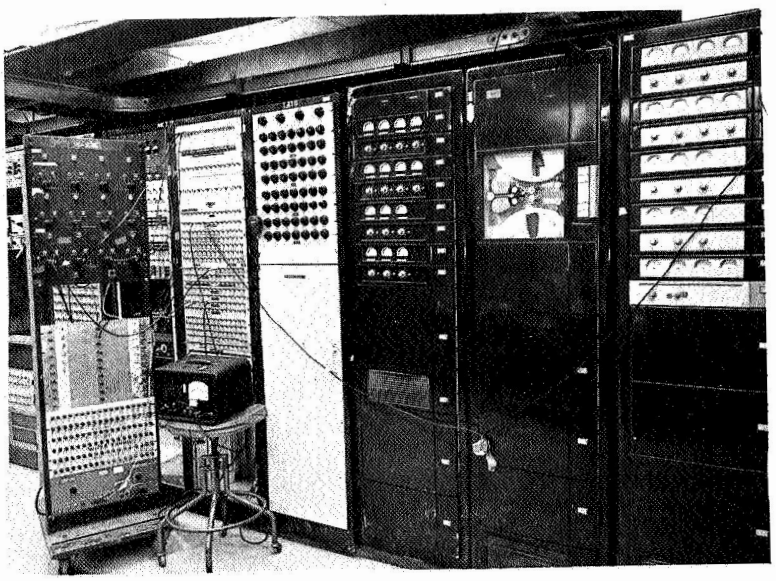

Figure 148.- Acoustic Facility Recording Consoles

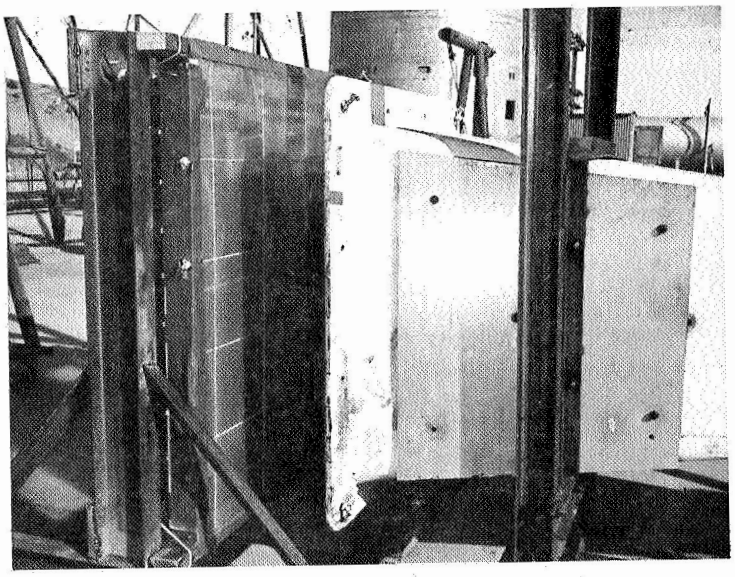

Figure 149.- Typical Test Setup

(plus $0^{o}$, minus $50^{o}$) for the cold soak. Chamber pressure was not to exceed $1 \times 10^{-5}$ torr during the test periods (two 15-day periods for a total of 30 days).

An aluminum fixture was designed and fabricated. This fixture supported the test panels facing each other, in pairs, with an array of infrared lamps between each pair. The unheated side of each panel had an unobstructed view of the chamber wall while the rest of the assembly was enshrouded with Alzac spectral finish aluminum. Figure 150 is a photograph of a portion of the fixture showing one of the IR arrays with both test panels removed. The MPDD panels were mounted on the fixture in the arrangement shown in figure 151. Each panel was attached to the structure using Teflon brackets that provided thermal/electrical isolation. Technicians are shown installing the D2A dual detector in figure 152. Two of the panels (C1, S/N 104 and E1A, S/N 102) were mounted using flight-type mounting hardware in order to qualify these components as well as the panels. The entire test setup was suspended from the chamber lid as shown in figure 153, and all power cabling, thermocouple wires, and switch leads were brought out of the chamber through the lid and spool-piece feedthroughs. This simplified pretest and posttest check-outs and eliminated the need for personnel to enter the chamber.

Two paste-on thermocouples were attached to each test panel near its center. Thermocouples were installed only on the unheated side in all cases. One of each pair of thermocouples was used to monitor the temperature of the panel while the other one was used as either an IR feedback control or as a backup for this control. A total of 17 pressure switches were mounted on the ten panels. The position of these switches was monitored on a go/no-go panel that displayed a green light for normally-open contacts OPEN and a red light if the contacts transferred to the CLOSED position. The monitor panel was wired so that if a red light came on it would stay on until reset.

Photographs of the loading operation are shown in figure 154.

A chronological summary of qualification testing is shown in table 22. During the course of qualification testing, the following significant events occurred.

The B1A, 8280-04000, S/N 0000103 specimen leaked during the helium leak test performed after the acoustics test. The leak was located on the switch cup at a circumferential crack in the forming radius. The switch assembly, S/N 0000058, was

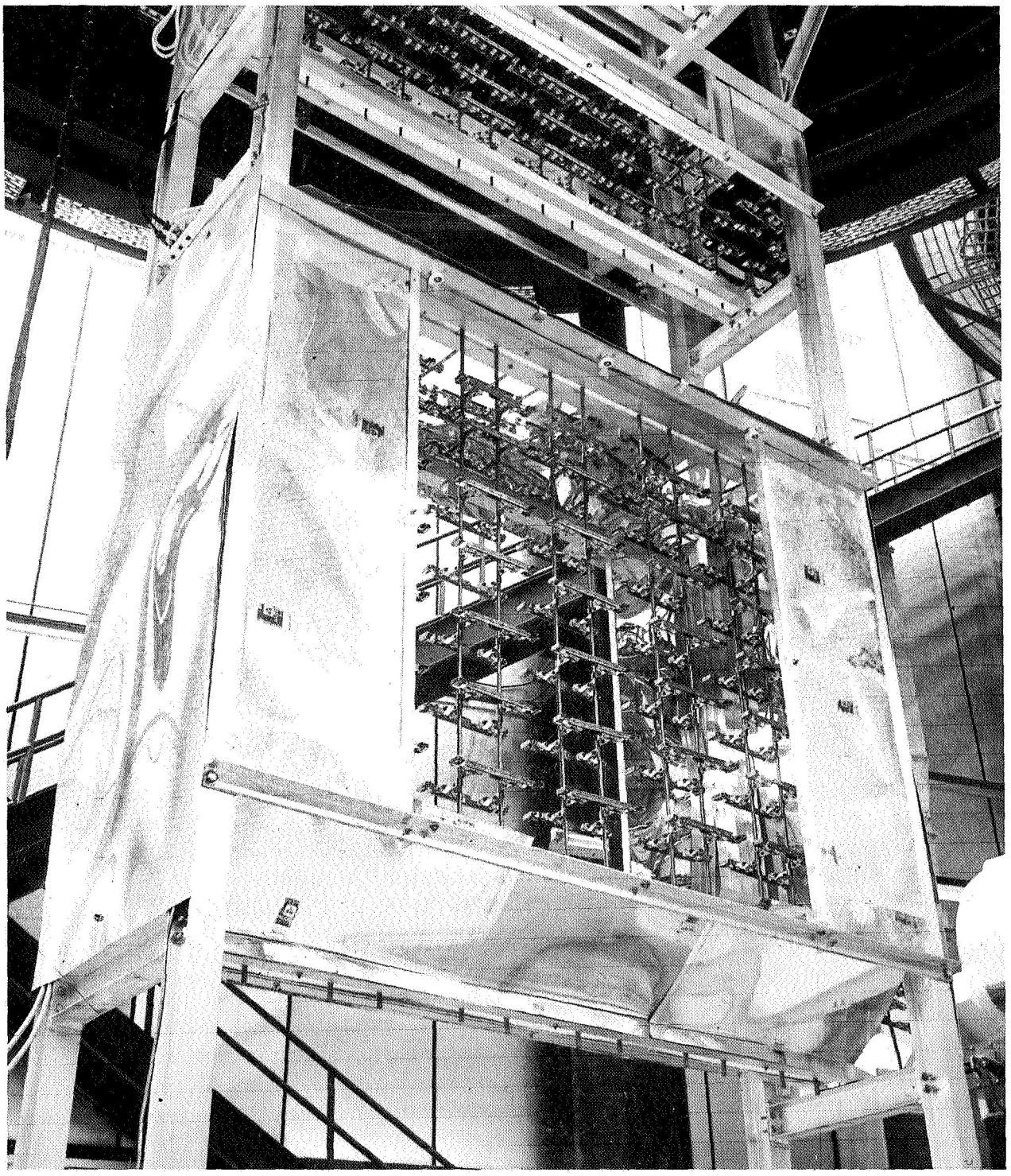

Figure 150.- Infrared Lamp Array for 40x49-in. Detector

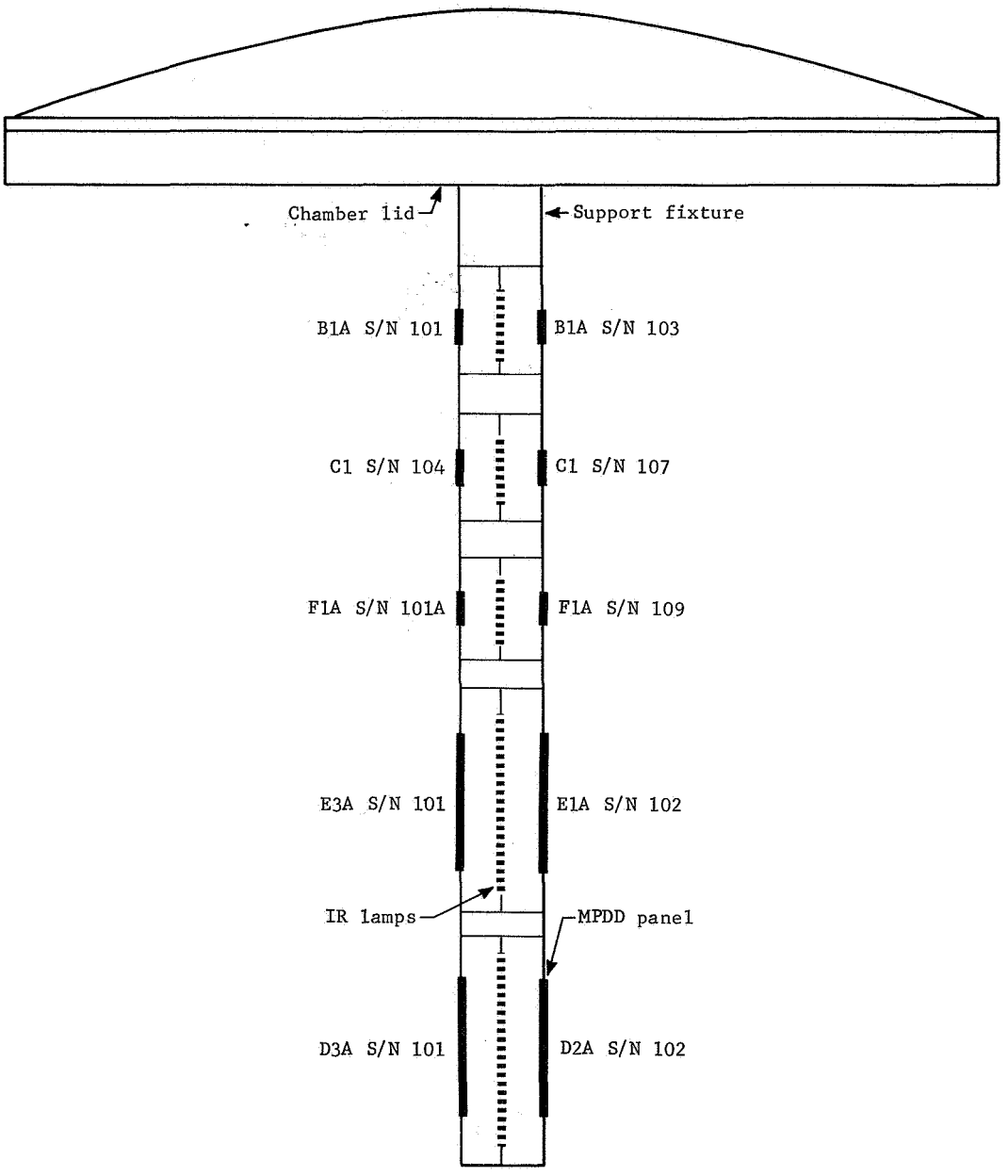


Figure 151.- Sketch of Test Setup, Thermal Vacuum Soak

Figure 152.- Installation of D2A Dual Detector

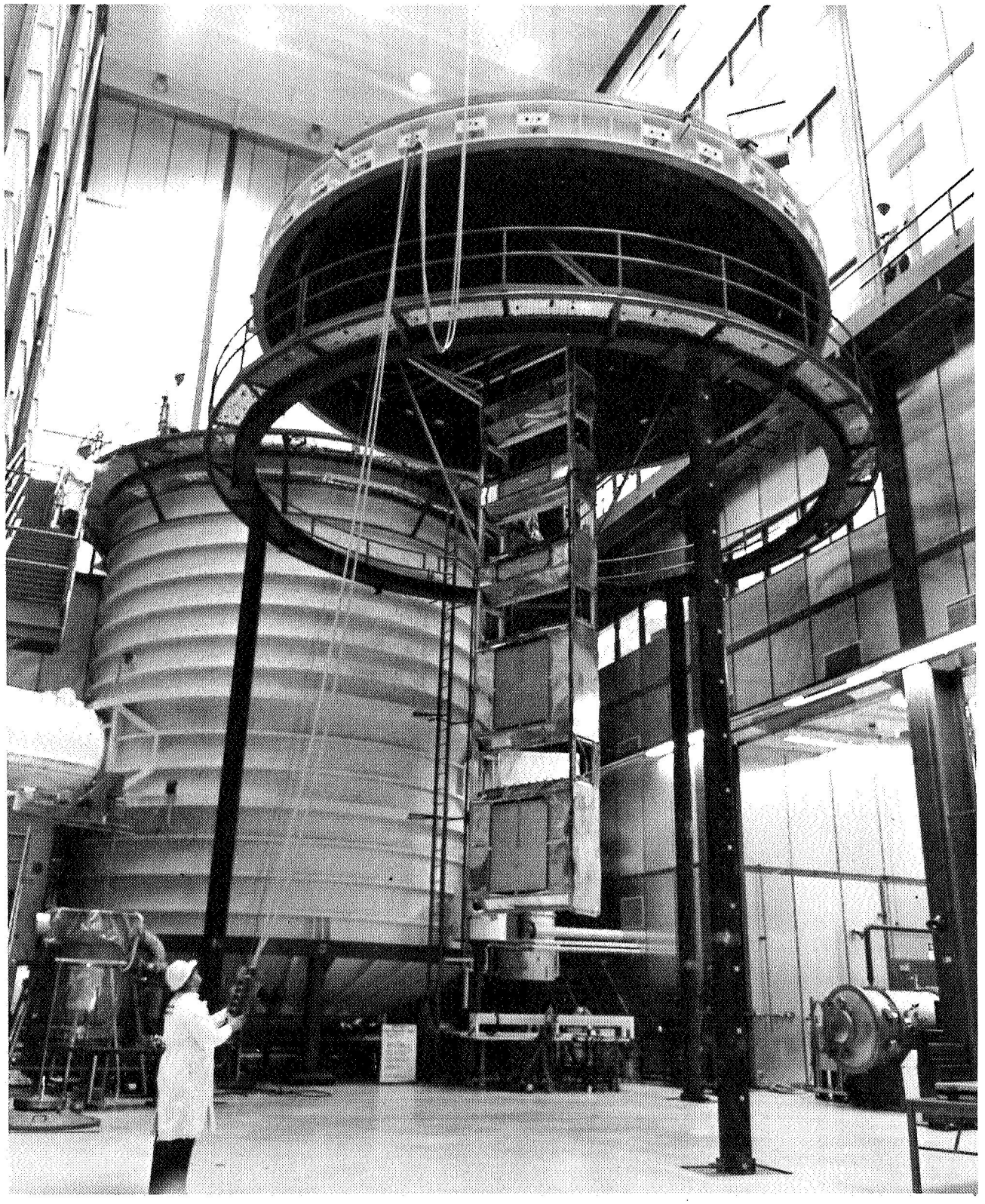

Figure 153.- Test Holding Fixture Shown Suspended from Chamber Lid

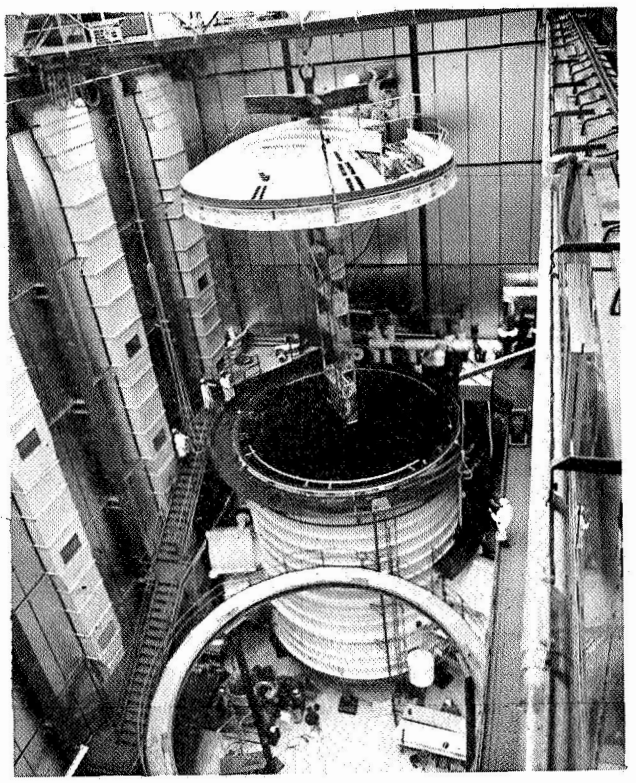

a

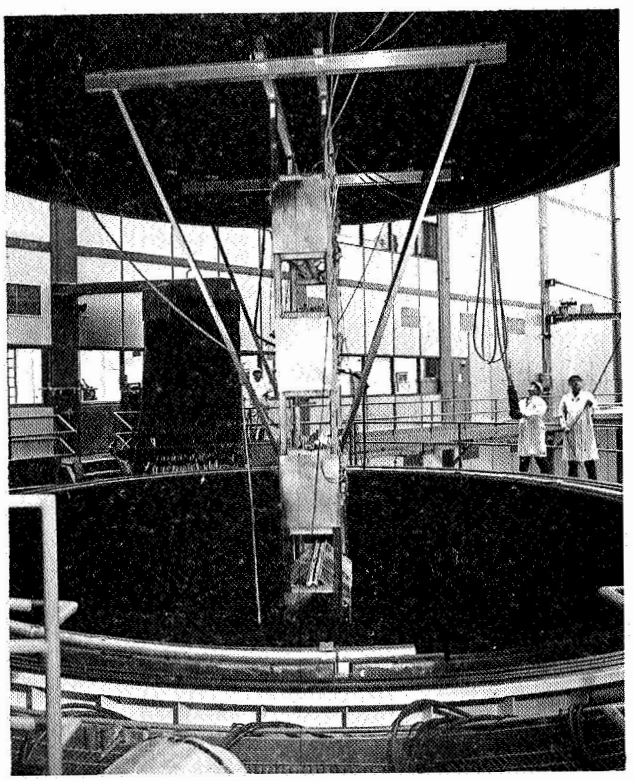

b

Figure 154.- Loading Operations

TABLE 22.- CHRONOLOGICAL SUMMARY
OF QUALIFICATION TESTING

| Date | Item nomenclature, part no., and serial no. | Event | Results |
|---|---|---|---|
| 07/12/68 | D2A, 8280-13000, 0000102 | Initial functional test | Passed |
| 07/18/68 | D2A, 8280-13000, 0000102 | Initial He leak test | Passed |
| 08/09/68 | D2A, 8280-13000, 0000102 | Sinewave, random, and shock tests | Completed |
| 08/14/68 | D2A, 8280-13000, 0000102 | Post-dynamics functional test | Passed |
| 08/20/68 | D2A, 8280-13000, 0000102 | Post-dynamics He leak test | Passed |
| 08/21/68 | D2A, 8280-13000, 0000102 | Acoustics test | Completed |
| 08/23/68 | D2A, 8280-13000, 0000102 | Post-acoustics functional test | Passed |
| 08/27/68 | D2A, 8280-13000, 0000102 | Post-acoustics He leak test | Passed |
| 02/06/69 | E1A, 8280-19000, 0000102 | Initial functional test | Passed |
| 02/07/69 | E1A, 8280-19000, 0000102 | Initial He leak test | Passed |
| 02/14/69 | B1A, 8280-04000, 0000101 | Initial functional test | Passed |
| 02/14/69 | B1A, 8280-04000, 0000103 | Initial functional test | Passed |
| 02/14/69 | B1A, 8280-04000, 0000103 | Initial He leak test | Passed |
| 02/14/69 | C1, 8280-07000, 0000104 | Initial function test | Passed |
| 02/14/69 | C1, 8280-07000, 0000107 | Initial functional test | Passed |
| 02/14/69 | F1A, 8280-28000, 0000101 | Initial functional test | Passed |
| 02/17/69 | B1A, 8280-04000, 0000103 | Initial He leak test | Passed |
| 02/17/69 | D3A, 8280-16000, 0000101 | Initial functional test | Passed |
| 02/17/69 | E3A, 8280-25000, 0000101 | Initial functional test | Passed |
| 02/17/69 | F1A, 8280-28000, 0000102 | Initial functional test | Passed |
| 02/18/69 | C1, 8280-07000, 0000107 | Initial He leak test | Passed |
| 02/18/69 | D3A, 8280-16000, 0000101 | Initial He leak test | Passed |
| 02/18/69 | E3A, 8280-25000, 0000101 | Initial He leak test | Passed |
| 02/27/69 | D3A, 8280-16000, 0000101 | Sinewave vibration, X-axis | Completed |
| 02/28/69 | D3A, 8280-16000, 0000101 | Random X, Y, & Z, Sine Y & Z, shock X & Z | Completed |

TABLE 22.- CHRONOLOGICAL SUMMARY
OF QUALIFICATION TESTING - Continued

| Date | Item nomenclature, part no., and serial no. | Event | Results |
|---|---|---|---|
| 02/28/69 | C1, 8280-07000, 0000104 | Initial He leak test | Passed |
| 03/03/69 | D3A, 8280-16000, 0000101 | Shock, Y-axis | Completed |
| 03/03/69 | E3A, 8280-25000, 0000101 | Sinewave, random, and shock | Completed |
| 03/05/69 | B1A, 8280-04000, 0000101 | Random vibration, X, Y, & Z-axes | Completed |
| 03/05/69 | B1A, 8280-04000, 0000103 | Random vibration, X, Y, & Z-axes | Completed |
| 03/05/69 | C1, 8280-07000, 0000107 | Random vibration, X, Y, & Z-axes | Completed |
| 03/05/69 | E3A, 8280-25000, 0000101 | Post-dynamics He leak | Passed |
| 03/05/69 | F1A, 8280-28000, 0000108 | Initial functional test | Passed |
| 03/06/69 | B1A, 8280-04000, 0000101 | Shock X, Y, & Z-axes | Completed |
| 03/06/69 | B1A, 8280-04000, 0000103 | Shock X, Y, & Z-axes | Completed |
| 03/06/69 | C1, 8280-04000, 0000107 | Shock X, Y, & Z-axes | Completed |
| 03/06/69 | D3A, 8280-16000, 0000101 | Post-dynamics functional test | Passed |
| 03/06/69 | D3A, 8280-16000, 0000101 | Post-dynamics He leak test | Passed |
| 03/06/69 | E3A, 8280-25000, 0000101 | Post-dynamics functional test | Passed |
| 03/07/69 | C1, 8280-25000, 0000107 | Sinewave vibration, X, Y, & Z-axes | Completed |
| 03/07/69 | B1A, 8280-04000, 0000101 | Sinewave vibration, X, Y, & Z-axes | Completed |
| 03/07/69 | B1A, 8280-04000, 0000101 | Sinewave vibration, X, Y, & Z-axes | Completed |
| 03/07/69 | F1A, 8280-28000, 0000108 | Initial He leak test | Passed |
| 03/12/69 | B1A, 8280-04000, 0000101 | Post-dynamics functional test | Passed |
| 03/12/69 | B1A, 8280-04000, 0000103 | Post-dynamics functional test | Passed |
| 03/12/69 | C1, 8280-07000, 0000107 | Post-dynamics functional test | Passed |
| 03/14/69 | B1A, 8280-04000, 0000101 | Post-dynamics He leak test | Passed |
| 03/14/69 | B1A, 8280-04000, 0000103 | Post-dynamics He leak test | Passed |
| 03/14/69 | C1, 8280-07000, 0000107 | Post-dynamics He leak test | Passed |

TABLE 22.- CHRONOLOGICAL SUMMARY
OF QUALIFICATION TESTING - Continued

| Date | Item nomenclature, part no., and serial no. | Event | Results |
|---|---|---|---|
| 03/14/69 | D3A, 8280-16000, 0000101 | Acoustics test | Completed |
| 03/14/69 | E1A, 8280-19000, 0000102 | Sinewave, random, shock, Z-axis | Completed |
| 03/14/69 | E3A, 8280-25000, 0000101 | Acoustics test | Completed |
| 03/17/69 | D3A, 8280-16000, 0000101 | Post-acoustics functional test | Passed |
| 03/17/69 | E1A, 8280-19000, 0000102 | Sinewave, random, shock, X & Y-axes | Completed |
| 03/17/69 | E3A, 8280-25000, 0000101 | Post-acoustics functional test | Passed |
| 03/18/69 | B1A, 8280-04000, 0000101 | Acoustics test | Completed |
| 03/18/69 | B1A, 8280-04000, 0000103 | Acoustics test | Completed |
| 03/18/69 | C1, 8280-07000, 0000107 | Acoustics test | Completed |
| 03/18/69 | B1A, 8280-04000, 0000101 | Post-acoustics functional test | Passed |
| 03/18/69 | B1A, 8280-04000, 0000103 | Post-acoustics functional test | Passed |
| 03/18/69 | B1A, 8280-04000, 0000103 | Post-acoustics functional test | Passed |
| 03/18/69 | C1, 8280-07000, 0000107 | Post-acoustics functional test | Passed |
| 03/18/69 | D2A, 8280-13000, 0000102 | He leak test (recheck) | Passed |
| 03/18/69 | E1A, 8280-19000, 0000102 | Post-dynamics functional test | Passed |
| 03/18/69 | E1A, 8280-19000, 0000102 | Post-dynamics He leak test | Passed |
| 03/19/69 | E1A, 8280-19000, 0000102 | Acoustics test | Completed |
| 03/20/69 | B1A, 8280-04000, 0000103 | Post-acoustics He leak test | One side leaking |
| 03/20/69 | C1, 8280-07000, 0000107 | Post-acoustics He leak test | Passed |
| 03/20/69 | D3A, 8280-16000, 0000101 | Post-acoustics He leak test | Passed |
| 03/20/69 | E3A, 8280-25000, 0000101 | Post-acoustics He leak test | Passed |
| 03/21/69 | B1A, 8280-04000, 0000101 | Post-acoustics He leak test | Passed |
| 03/21/69 | E1A, 8280-19000, 0000102 | Post-acoustics functional test | Passed |
| 03/25/69 | E1A, 8280-19000, 0000102 | Post-acoustics He leak test | Passed |
| 03/27/69 | C1, 8280-07000, 0000104 | Sinewave and random vibration, X-axis | Completed |

TABLE 22.- CHRONOLOGICAL SUMMARY
OF QUALIFICATION TESTING - Continued

| Date | Item nomenclature, part no., and serial no. | Event | Results |
|---|---|---|---|
| 03/27/69 | F1A, 8280-28000, 0000108 | Sinewave & random vibration, X-axis | Completed |
| 03/28/69 | C1, 8280-07000, 0000104 | Sinewave & random, Y & Z, shock, X, Y, & Z | Completed |
| 03/28/69 | F1A, 8280-28000, 0000108 | Sinewave & random, Y & Z, shock, X, Y, & Z | Completed |
| 03/31/69 | C1, 8280-07000, 0000104 | Post-dynamics functional test | Passed |
| 03/31/69 | F1A, 8280-28000, 0000108 | Post-dynamics functional test | Passed |
| 04/01/69 | C1, 8280-07000, 0000104 | Post-dynamics He leak test | Passed |
| 04/01/69 | F1A, 8280-28000, 0000103 | Post-dynamics He leak test | Passed |
| 04/01/69 | F1A, 8280-28000, 0000109 | Initial functional test | Passed |
| 04/02/69 | F1A, 8280-28000, 0000101A | Initial He leak test | Passed |
| 04/02/69 | F1A, 8280-28000, 0000109 | Initial He leak test | Passed |
| 04/03/69 | C1, 8280-07000, 0000104 | Acoustics test | Completed |
| 04/03/69 | C1, 8280-07000, 0000104 | Post-acoustics functional test | Passed |
| 04/03/69 | F1A, 8280-28000, 0000108 | Acoustics test | Completed |
| 04/03/69 | F1A, 8280-28000, 0000108 | Post-acoustics functional test | Passed |
| 04/06/69 | F1A, 8280-28000, 0000108 | Post-acoustics He leak test | Failed |
| 04/07/69 | B1A, 8280-04000, 0000103A | Post-acoustics He leak test | Passed |
| 04/07/69 | C1, 8280-07000, 0000104 | Post-acoustics He leak test | Passed |
| 04/09/69 thru 05/13/69 | B1A, 8280-04000, 0000101 and 0000103A; C1, 8280-07000, 0000104 and 0000107; D2A, 8280-13000, 0000102; D3A, 8280-16000, 0000101; E1A, 8280-19000, 0000102; E3A, 8280-25000, 0000101; & F1A, 8280-28000, 0000101A & 0000109 | Start of thermal vacuum soak test<br>End of thermal vacuum soak test | Completed |
| 05/14/69 | D3A, 8280-16000, 0000101 | Post-T/V soak He leak test | Passed |
| 05/14/69 | E1A, 8280-19000, 0000102 | Post-T/V soak functional test | Passed |

TABLE 22.- CHRONOLOGICAL SUMMARY
OF QUALIFICATION TESTING - Continued

| Date | Item nomenclature, part no., and serial no. | Event | Results |
|---|---|---|---|
| 05/14/69 | E3A, 8280-25000, 0000101 | Post-T/V soak functional test | Passed |
| 05/14/69 | F1A, 8280-28000, 0000109 | Post-T/V soak He leak test | Failed |
| 05/15/69 | B1A, 8280-04000, 0000101 | Post-T/V soak functional test | Passed |
| 05/15/69 | F1A, 8280-28000, 0000101A | Post-T/V soak He leak test | Passed |
| 05/16/69 | B1A, 8280-04000, 0000101 | Post-T/V soak He leak test | Passed |
| 05/16/69 | D3A, 8280-13000, 0000101 | Post-T/V soak functional test | Passed |
| 05/16/69 | E1A, 8280-19000, 0000102 | Post-T/V soak He leak test | Passed |
| 05/19/69 | B1A, 8280-04000, 0000101 | Post-T/V soak functional test | Passed |
| 05/19/69 | C1, 8280-07000, 0000104 | Post-T/V soak functional test | Passed |
| 05/19/69 | E3A, 8280-25000, 0000101 | Post-T/V soak functional test | Passed |
| 05/19/69 | F1A, 8280-28000, 0000101A | Post-T/V soak functional test | Passed |
| 05/20/69 | D2A, 8280-13000, 0000102 | Post-T/V soak functional test | Passed |
| 05/21/69 | C1, 8280-07000, 0000107 | Post-T/V soak RGA test | Passed |
| 05/22/69 | B1A, 8280-04000, 0000101 | Post-T/V soak RGA test | Passed |
| 05/22/69 | C1, 8280-07000, 0000104 | Post-T/V soak RGA test | Passed |
| 05/23/69 | D2A, 8280-13000, 0000102 | Post-T/V soak RGA test | Passed |
| 05/27/69 | F1A, 8280-28000, 0000109 | Post-T/V soak He leak test | Passed |
| 06/04/69 | B1A, 8280-04000, 0000103A | Random vibration, X, Y, & Z-axes | Completed |
| 06/04/69 | B1A, 8280-04000, 0000103A | Sinewave vibration, X, Y, & Z-axes | Completed |
| 06/04/69 | F1A, 8280-28000, 0000101A | Sinewave and random vibration X-axis | Completed |
| 06/04/69 | F1A, 8280-28000, 0000109 | Sinewave and random vibration X-axis | Completed |
| 06/09/69 | F1A, 8280-28000, 0000101A | Shock, X-axis | Completed |
| 06/09/69 | F1A, 8280-28000, 0000109 | Shock, X-axis | Completed |
| 06/10/69 | B1A, 8280-04000, 0000103A | Shock, X, Y & Z-axes | Completed |

TABLE 22.- CHRONOLOGICAL SUMMARY
OF QUALIFICATION TESTING - Continued

| Date | Item nomenclature, part no., and serial no. | Event | Results |
|---|---|---|---|
| 06/10/69 | F1A, 8280-28000, 0000101A | Shock, Y & Z-axes | Completed |
| 06/10/69 | F1A, 8280-28000, 0000109 | Shock, Y & Z-azes | Completed |
| 06/11/69 | F1A, 8280-28000, 0000101A | Sinewave and random vibration, Y & Z-axes | Completed |
| 06/11/69 | F1A, 8280-28000, 0000109 | Sinewave and random vibration, Y & Z-axes | Completed |
| 06/13/69 | B1A, 8280-04000, 0000103A | Post-dynamics He leak test | Passed |
| 06/14/69 | F1A, 8280-28000, 0000101A | Post-dynamics He leak test | Passed |
| 06/17/69 | B1A, 8280-04000, 0000103A | Post-dynamics functional test | Passed |
| 06/17/69 | F1A, 8280-28000, 0000101A | Post-dynamics functional test | Passed |
| 06/17/69 | F1A, 8280-28000, 0000109 | Post-dynamics functional test | Passed |
| 06/18/69 | B1A, 8280-04000, 0000103A | Acoustics test | Failed |
| 06/18/69 | F1A, 8280-28000, 0000101A | Acoustics test | Completed |
| 06/18/69 | F1A, 8280-28000, 0000109 | Acoustics test | Completed |
| 06/20/69 | F1A, 8280-28000, 0000101A | Post-acoustics He leak test | Passed |
| 06/23/69 | F1A, 8280-28000, 0000109 | Post-acoustics He leak test | Passed |
| 06/23/69 | F1A, 8280-28000, 0000109 | Post-acoustics functional test | Passed |
| 06/23/69 | F1A, 8280-28000, 0000101A | Post-acoustics functional test | Passed |
| 06/24/69 | B1A, 8280-04000, 0000103A | Post-acoustics He leak test on P/S 0000179 side only | Passed |
| 06/25/69 | B1A, 8280-04000, 0000103A | Post-acoustics functional test on P/S 0000179 side only | Passed |

replaced with a new assembly, S/N 0000179, and the specimen redesignated S/N 0000103A. More detailed information is presented in MARS B65064.

The F1A, 8280-28000, S/N 0000108 specimen leaked during the helium leak test following the acoustics test. The leak rate was $1.3 \times 10^{-8}$ scc He/sec. The leak was isolated to the top fusion weld of the interconnect tube splice sleeve. The failure is reported in MARS B65065.

The F1A, 8280-28000, S/N 0000109 specimen leaked during the helium leak test following the thermal vacuum soak. The leak was isolated to the braze joint at the switch cup forming the radius and interconnect tube. The specimen was rebrazed, a serpentine tube installed, and requalification dynamics and acoustics performed. The failure is reported in MARS B65068.

The B1A, 8280-04000, S/N 0000103A specimen failed the qualification acoustic test at the ringweld panel fitting on the P/S S/N 0000071 side. This was the second time this panel half and switch assembly had been subjected to all dynamic environments. This failure is reported in detail in MARS B66038.

At 1042 hr on April 30th, the "go" light went out on switch 2 of panel B1A, S/N 101. The switch evidently did not transfer since the "no-go" light did not come on. The circuitry from the switch-monitoring panel to the chamber feedthrough was checked out and no discrepancy was discovered. The panel temperature was -271°F at the time the "go" light went out. During the shroud warmup, the "go" light for switch 2 came back on. The panel temperature at that time was 58°F and the chamber pressure was 25 (0.025 torr). Once the chamber had been unloaded, the wiring between switch 2 and the lid feedthrough was checked out before anything else was done. Again, no discrepancies in the circuit were detected. Figure 155 shows this examination being made.

The following paragraphs summarize the various test results.

At no time during switch transfer pressure testing were measurements obtained that were beyond specification limits. The variation between switch point pressures, both with increasing and decreasing pressures, is between 0.1 and 1.2 psig. Generally, it is thought that much of this variation is caused by the operator caused, i.e., increasing pressure too rapidly (especially in the case of those specimens with a large volume) to allow the externally located pressure gage to respond to the true pressure within the specimen. Also, in the case of measurements taken on

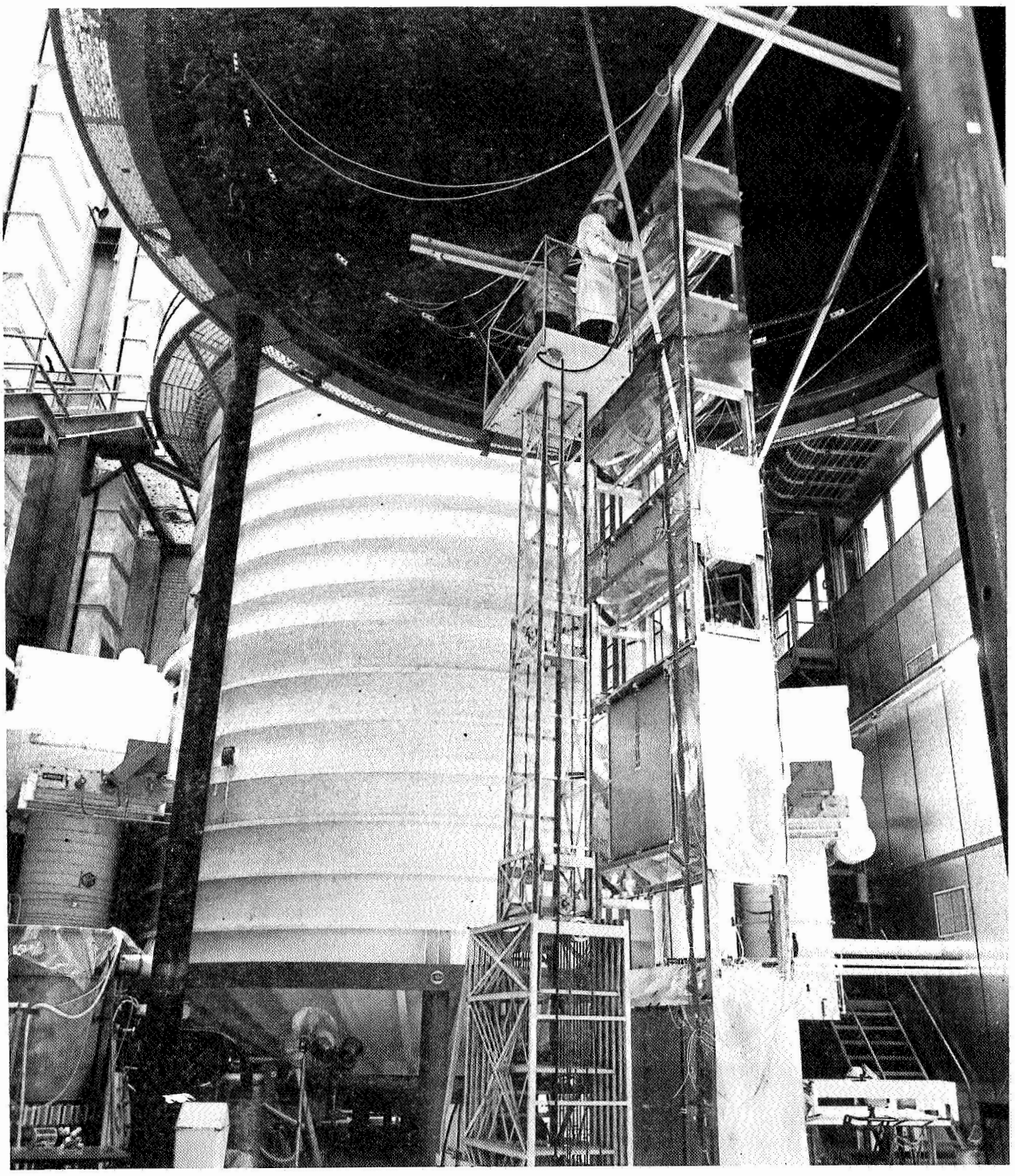

Figure 155.- Post-Thermal Vacuum Soak Test Examination of B1 A Panel, S/N 0000101

a sealed specimen, ambient conditions during the time of seal versus the time of reading enter into the pressure readings. Some evidence of switch point shift still remains, however, a rather thorough statistical analysis would be necessary to establish an actual trend, if any exists.

As with the switch point data, no contact resistance measurements were obtained that were beyond specification limits. The general trend is for the closed set (with pressure applied) of contacts to increase slightly or remain nearly constant throughout the testing.

Helium leak tests were performed as required by the procedure. Two failures occurred during the testing. The first failure was panel B1A, 8280-04000, S/N 0000103. The leak was found following acoustics testing and is reported in MARS B65064. The second failure occurred in F1A, 8280-28000, S/N 0000108. This leak also was found following the acoustics test. It is reported in MARS B65065.

No failures occurred during RGA test. These tests were always the last leak tests performed and were performed on the B1A, C1, and D2A configurations.

No visible structural failures were incurred on any test specimens subjected to the sinewave vibration environment. The reduced test input plots are included with the test data presented in the Qualification Test Report. Several plots show a variance of input versus specification requirements in the 5 to 10 Hz frequency range. This is due, in part, to difficulty in controlling the massive test fixture, but most of the variance arises when the control accelerometer output voltage (which is quite low between 5 to 10 Hz at 0.4 in. double amplitude) approaches the background noise level of the recording system. Those plots were plotted directly (as opposed to being recorded and then reduced, at later time) and show good control. (Refer to Z-axis plots of 03/07/69 versus 06/11/69 of B1A, 8280-04000, S/N 0000103A, Appendix B. Qualification Test Report, OP530).

No visible structural failures were incurred on any test specimens subjected to the random vibration environment. The input was well within specification limits in all cases except the last test performed (B1A-0000103A, F1A-0000101A, and F1A-0000109). During this test a total of three 25 Hz bandwidths were at or above the maximum limit for all three axes. Since they were all on the high limit of the spectrum and then less than +1 dB out, they were accepted.

There were no visible structural failures incurred on any test specimen subjected to the shock environment. The reduced test input plots are included with the test data. All data points were within specified limits (-3 dB, up to 3 1/3 octave band points). Three units (B1A, 8280-04000, S/N 0000101; B1A, 8280-04000, S/N 0000103; and C1, 8280-07000, S/N 0000107) are missing plots for the Y-axis shock. This occurred as a result of human error during data reduction when the data were inadvertently destroyed. The visual pulse data observed at the time of test was within limits.

Two specimens leaked following the acoustics test, as explained previously. During the requalification testing of B1A, S/N 0000103A, F1A, S/N 0000101A, and F1A, S/N 0000109 one octave plot point was 5 1/3 dB below the minimum tolerance (-3 dB) for a total of 8 1/2 dB below the desired spectrum. The overall SPL was 152 dB, which is within specification limits. The calibration run, prior to testing the line test specimens, was well shaped. A dummy panel was used during the calibration run. This could account for the spectrum shape variation. Since all test specimens had been previously subjected to the acoustic field, per agreement with NASA-LRC, the out-of-tolerance point was accepted. Also, during this test, B1A, S/N 0000103A, experienced a structural failure, as explained previously. All other specimens met the requirements of acoustic testing.

As previously discussed one specimen was leaking following the thermal vacuum soak test. Also, the "go" anomaly was discussed, previously. The chamber vacuum during the hot soak portion of the test was at $1.0 \times 10^{-5}$ torr, at the beginning of the test, and, within three days stabilized at about $2.2 \times 10^{-7}$ torr. During the cold soak period, the chamber vacuum was maintained at about $2.2 \times 10^{-6}$ torr except for one short period when the vacuum decreased to $4.5 \times 10^{-6}$ torr. This was the result of loss of coolant water to one of the diffusion pumps. The time versus temperature history for the entire qualification test is summarized in figure 156. The curves have been constructed by selecting the highest and lowest panel temperatures at 0000 hr each day during the hot soak and similar temperatures at 1200 hr each day during the cold soak. This type of presentation is realistic since hourly variations of a given temperature are only fractional. If all of the temperature data were to be plotted on this figure, the points would lie between the two curves shown. The temperature tolerance limits are also shown to demonstrate that all temperatures during each 15-day period were within the specified range. During the test, data were recorded each hour after temperature stabilization had been attained, and more frequently during the transition periods.

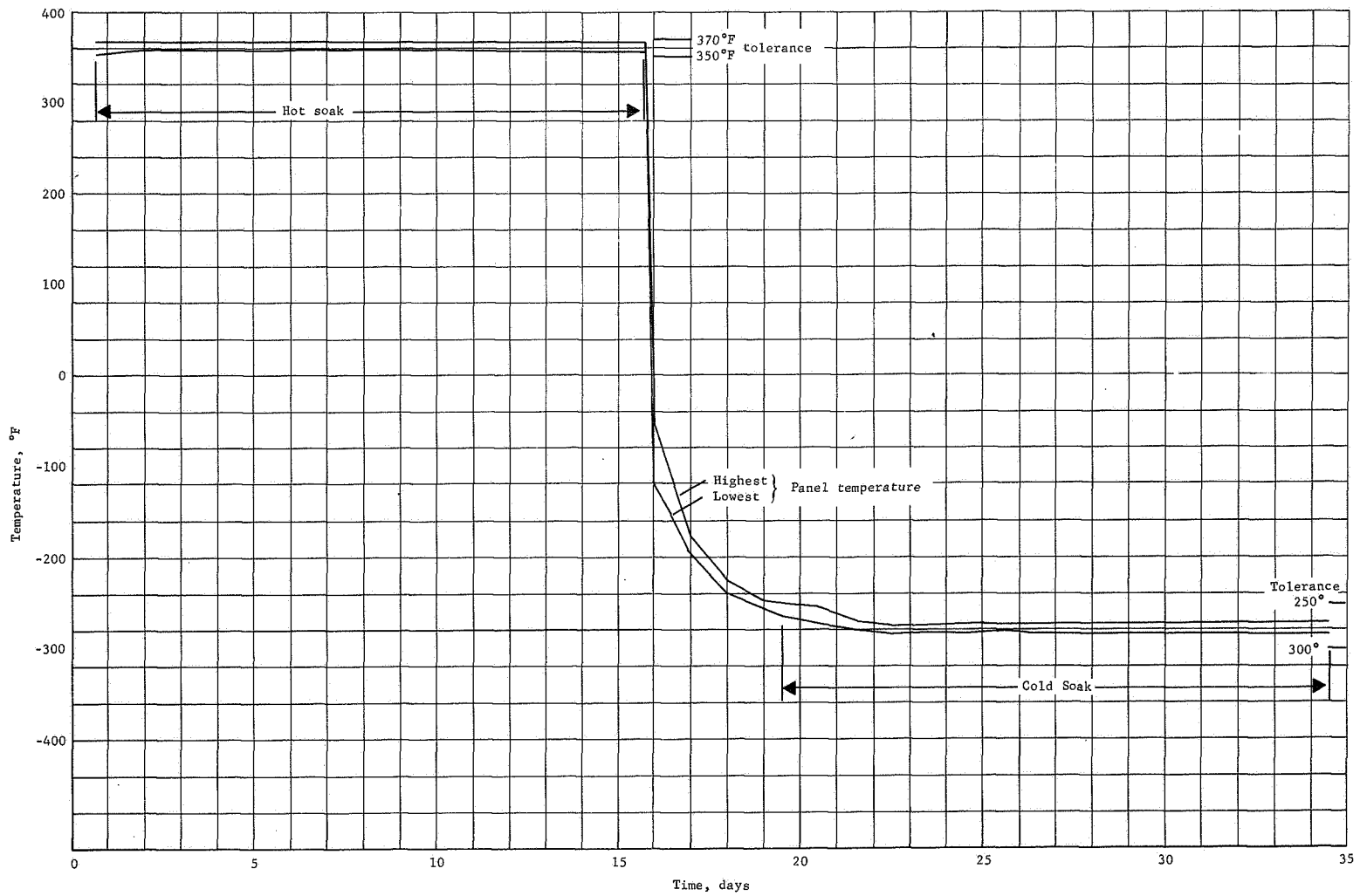


Figure 156.- Temperature History Summary

In order to qualify the angle mounting assemblies (8280-10072-01, bolt-hard point; 8280-10068-09, angle assembly; 8280-10068-10, angle assembly; 8280-28039-09, angle assembly; and 8280-28039-10, angle assembly) for use on MPDD detector/panels, one set of each configuration was subjected to all qualification tests. The vehicles for the assemblies were the E1A, S/N 0000102 and C1, S/N 0000104. The angle assemblies successfully met the requirements of the qualification testing.

Accelerated life cycling (ALC) testing: The accelerated life cycling test program was completed on the following items:

| | | |
|---|---|---|
| B1A | 8280-04000 | S/N 0000104 |
| B1A | 8280-04000 | S/N 0000105 |
| C1 | 8280-07000 | S/N 0000101 |
| C1 | 8280-07000 | S/N 0000103 |
| D3A | 8280-16000 | S/N 0000102 |
| E1A | 8280-19000 | S/N 0000105 |
| E3A | 8280-25000 | S/N 0000103 |
| F1A | 8280-28000 | S/N 0000103A |
| F1A | 8280-28000 | S/N 0000111 |

The ALC testing is described in the following paragraphs.

The switch transfer test was identical to the FAT. This test was performed before the start of, and after the completion of ALC.

The switch contact resistance test was identical to the FAT. It was performed before the start of, and after the completion of ALC.

The helium leak test was identical to the FAT and was performed before the start of the ALC on all specimens at various times during the course of the cycling (whenever a "no-go" light or other indication of malfunction occurred), and at the completion of ALC on the D3A, E1A, E3A, and F1A specimens.

The RGA leak test was identical to the FAT. It was performed on the B1A, C1, and D2A specimens as the final leak test following ALC.

The accelerated life cycling test consisted of subjecting the previously enumerated test specimens to a minimum of 21 344 temperature cycles, at ambient pressure (see figs. 157, 158, and 159). The upper temperature required was $325 \begin{smallmatrix}+50\\-10\end{smallmatrix}$ °F and the lower temperature was -90, -60, -50, or $-20 \begin{smallmatrix}+10\\-30\end{smallmatrix}$ °F, depending on the specimen being tested (see table 20). The test temperatures were obtained in the identical fashion explained in the FAT description. The mechanical attachment of the specimens to the power bus was different than that used during FAT in that permanent "fingers" were spot welded to the panels and these fingers attached to the power buses (see figs. 160 and 161). Thermocouples were attached to each specimen, as in FAT, to provide a temperature readout circuit to the ALC control console (see fig. 137) which, in turn, operated the switching circuits for both the $LN_2$ spray and the resistive heating systems. Pressure was monitored, on each specimen, by connecting pressure switch leads into the continuity monitor section of the ALC control console.

The test results from the accelerated life cycle testing program were completed during the first part of September 1969. They are briefly summarized below.

Functional tests were performed before the start of and at the completion of ALC. Switch pressure checks were made as necessary during the cycling portion of the test. All functional tests were successful with one exception; this was on the final functional test of B1A, 8280-04000, S/N 0000104. The failure was in the form of a no-transfer of pins 4, 5, and 6 (microswitch 2) of P/S 0000060. The switch was disassembled and inspected for blockage or contamination. None was found, therefore, the switch was reassembled and rechecked. The operation of the switch was normal and in spec. This activity is reported in MARS B69832 and discussed in FAR 8280-29.

The RGA leak test was performed after completion of cycling on B1A, S/N 0000102; B1A, S/N0000105; C1, S/N 0000101; and C1, S/N 0000103. All tests were successful.

The helium leak test was performed on all specimens before the start of ALC and on the D3A, S/N 0000102; E1A, S/N 0000105; and E3A, S/N 0000103 at the completion of ALC. The D3A specimen

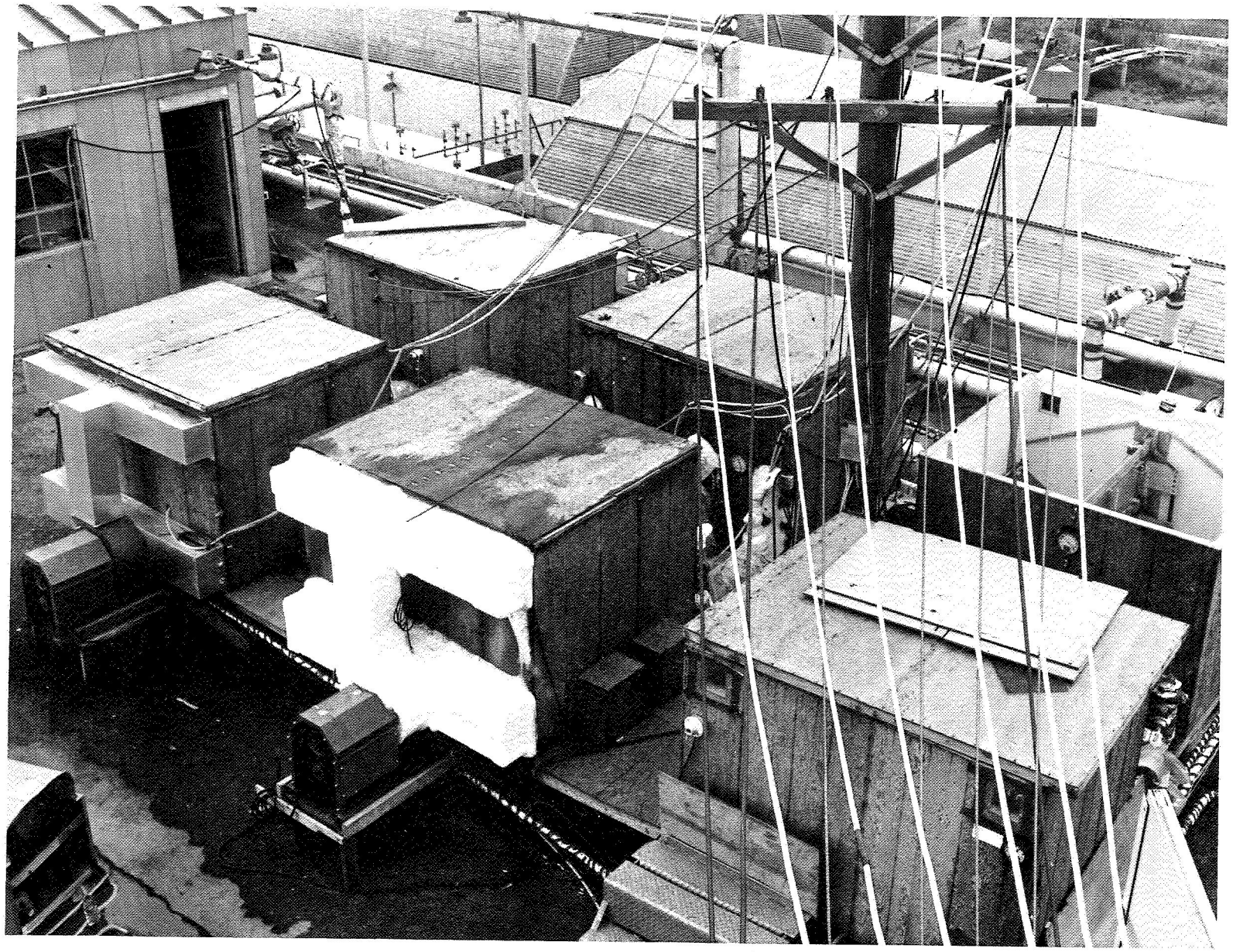

Figure 157.- Overall View, ALC Test Setup

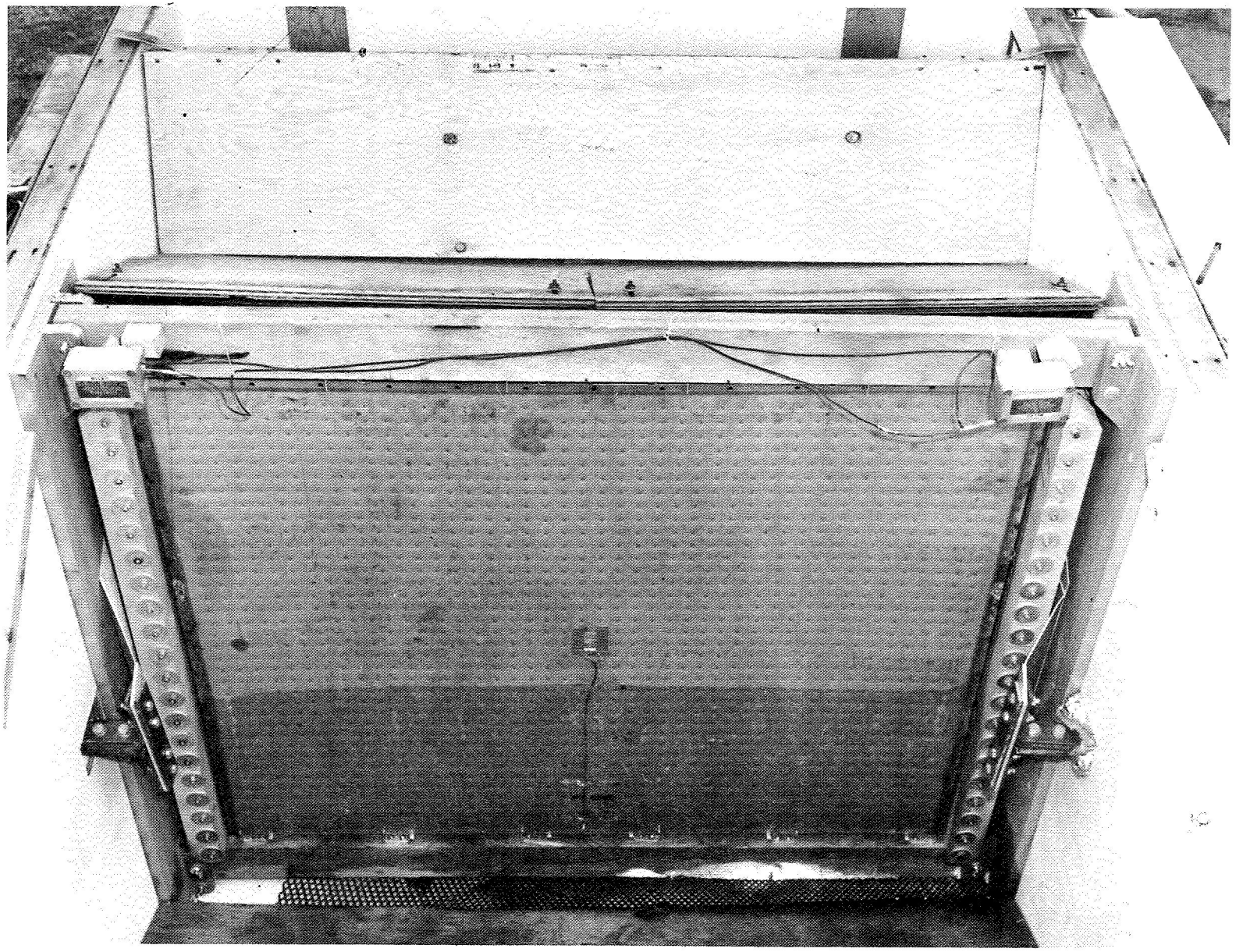

Figure 158.- Typical 40x40-in. Detector Setup

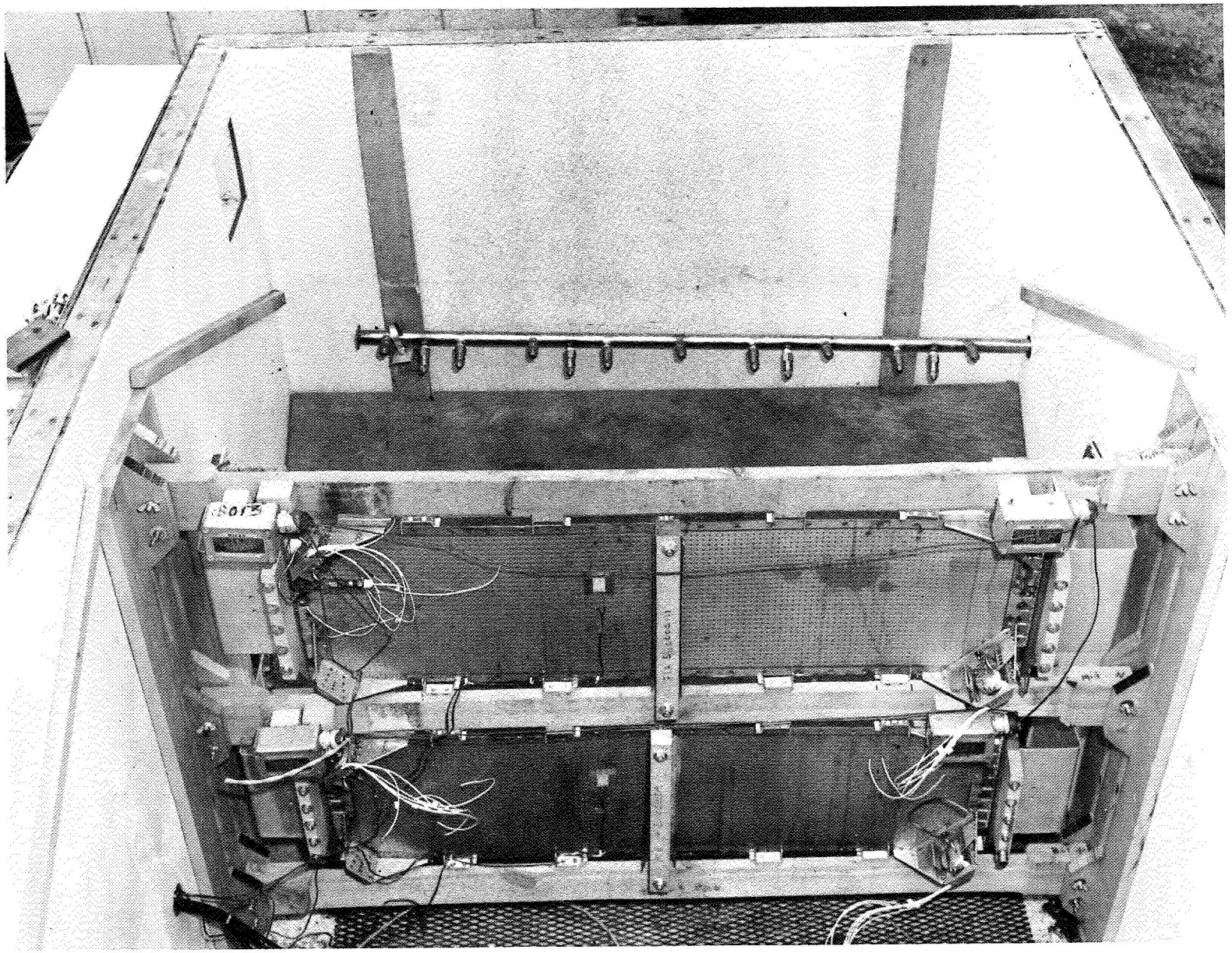

Figure 159.- Typical 12x40-in. Panel Setup

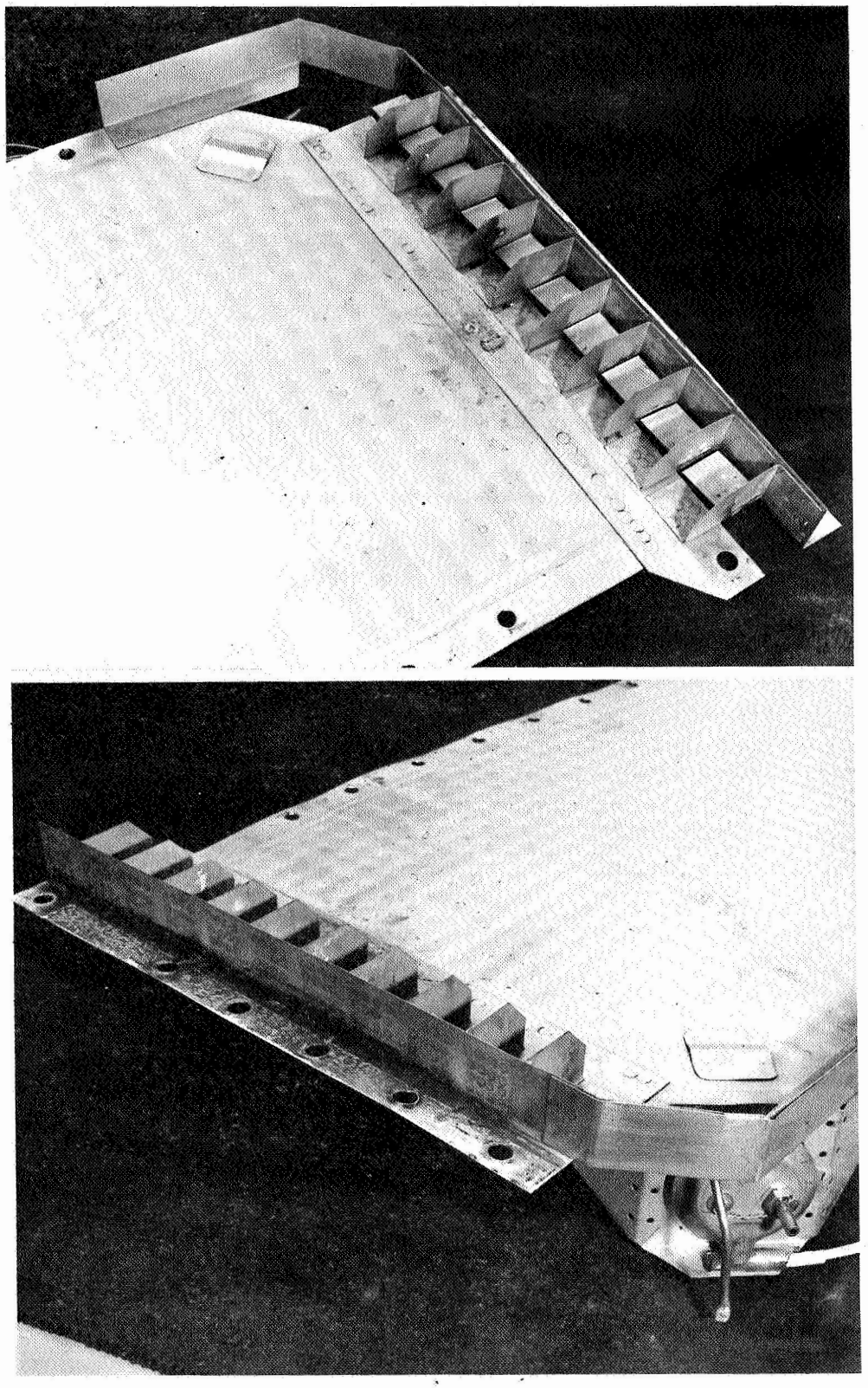

Figure 160.- Typical 12x40-in. Current Conduction Fingers

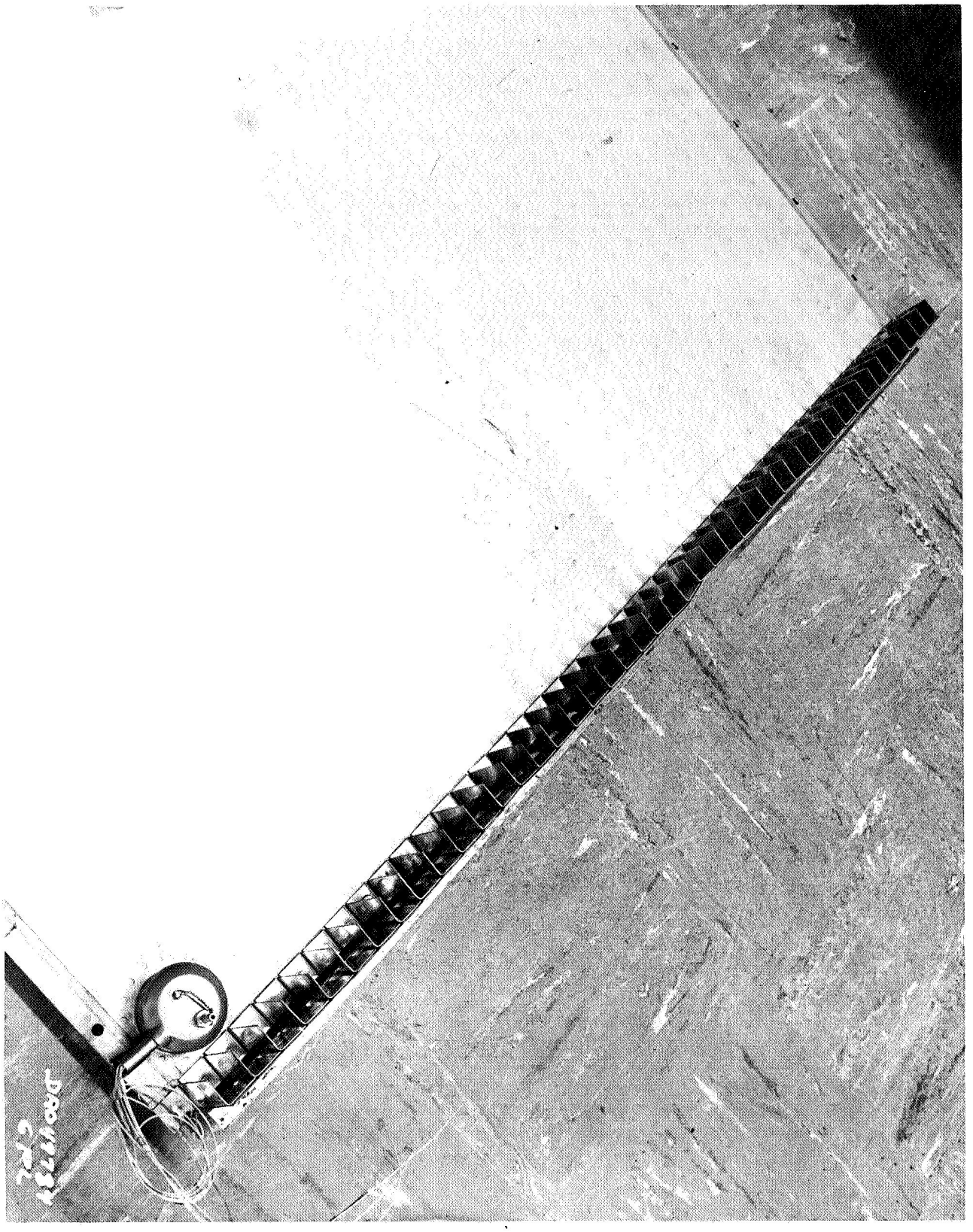

Figure 161.- Typical 40x49-in. Current Conduction Fingers

was found to leak (MARS B66037), first at 14 346 cycles due to thermal stresses created by the specimen mounting method then employed. The mounting was redesigned, the leak brazed shut, and testing continued. The specimen completed 21 370 cycles and was found to leak a second time. The leak was attributed to the initial thermal stresses created by earlier mounting method and which occurred early in test. The remaining ALC specimens never reached the final leak test stage due to test failure in ALC.

The ALC testing was performed as required by the test procedure. Figures 162, 163, and 164 show typical time vs. temperature cycles for the 350°F, -100°F; 350°F, -50°F or -60°F; and 350°F, -20°F cycle requirements.

All specimens received some quantity of cycles greater than 21 344 to be sure to have a sufficient number of good cycles. The actual count is summarized below by specimen.

The following specimens successfully completed ALC testing in its entirety:

B1A, 8280-04000, S/N 0000105 - 21 403 cycles within specification limits, passed post-functional and leak tests;

C1, 8280-07000, S/N 0000101 - 21 766 cycles within specification limits, passed post-functional and leak tests;

C1, 8280-07000, S/N 0000103 - 21 350 cycles within specification limits, passed post-functional and leak tests;

E1A, 8280-19000, S/N 0000105 - 21 450 cycles within specification limits, passed post-functional and leak tests;

E3A, 8280-25000, S/N 0000103 - 21 445 cycles within specification limits, passed post-functional and leak tests.

The following specimens completed the required number of cycles but were unsuccessful during the post-ALC functional leak tests:

B1A, 8280-04000, S/N 0000104 - 21 938 cycles within specification limits. This specimen failed during the post-ALC pressure transfer check as previously explained;

D3A, 8280-16000, S/N 0000102 - 21 370 cycles within specification limits. This specimen failed during the tests, was repaired, testing continued, and was found to be leaking again at completion as previously explained.

The following specimens were unsuccessful in completing the required number of accelerated life cycles.

B1A, 8280-04000, S/N 0000102 - At 4670 cycles, the specimen signaled loss-of-pressure. Subsequent examination disclosed a crack on the P/S 0000053 target sheet (reference: MARS B 65067). This failure was determined to have been caused by the bus bar clamping technique for detector mounting as in the previous cases. The mounting was redesigned and a new specimen initiated into ALC.

E3A, 8280-25000, S/N 0000102 - At 3357 cycles, the specimen was electrically burned along the bus bar edge. The cause was due to jamming of recording paper in the thermal recorder that caused the control circuit to continue calling for heat. The kill circuit actuated when the overtemperature was sensed but due to the erroneous use of a nonlatching relay, the circuit would not latch out. This was not a specimen failure, but a combination of instrumentation failure and human error.

E3A, 8280-25000, S/N 0000104 - At 1768 cycles, the specimen was overheated due to removal of power to the signal conditioning amplifiers providing data to the control mechanism. The specimen was distorted, precluding further testing. This was a case of human error rather than that of specimen malfunction.

F1A, 8280-28000, S/N 0000103A - At 7147 cycles, the NO/GO light was energized signaling loss of pressure. A leak was located on the P/S 0000164 side of the panel, on the same target side as the switch mounting, in the first row of spotwelds near the splice. The failure was determined as having been caused as a result of the mass discontinuity that exists between the splice and the target field. Large temperature gradients (about 200°F or 300°F) exist in this area. It is felt that if the temperature cycling rate were considerably longer (approaching actual space cycle times) the F1A specimens could survive the required number of cycles.

F1A, 8280-28000, S/N 0000111 - Same as above.

The areas of leakage and "crippling" caused by the situation discussed above are shown in figures 165 and 166.

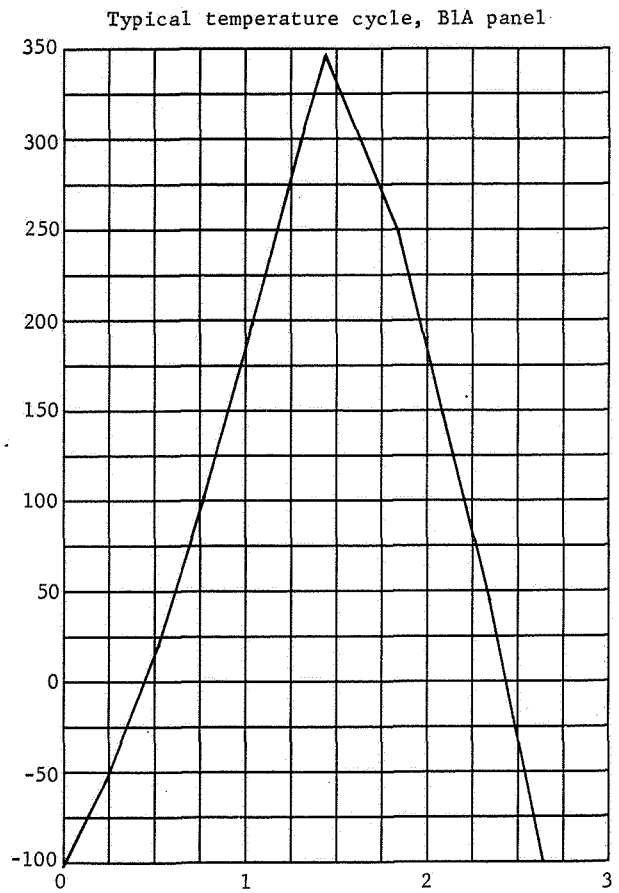


Figure 162.- Typical Temperature Cycle, 325°F, -100°F Requirement

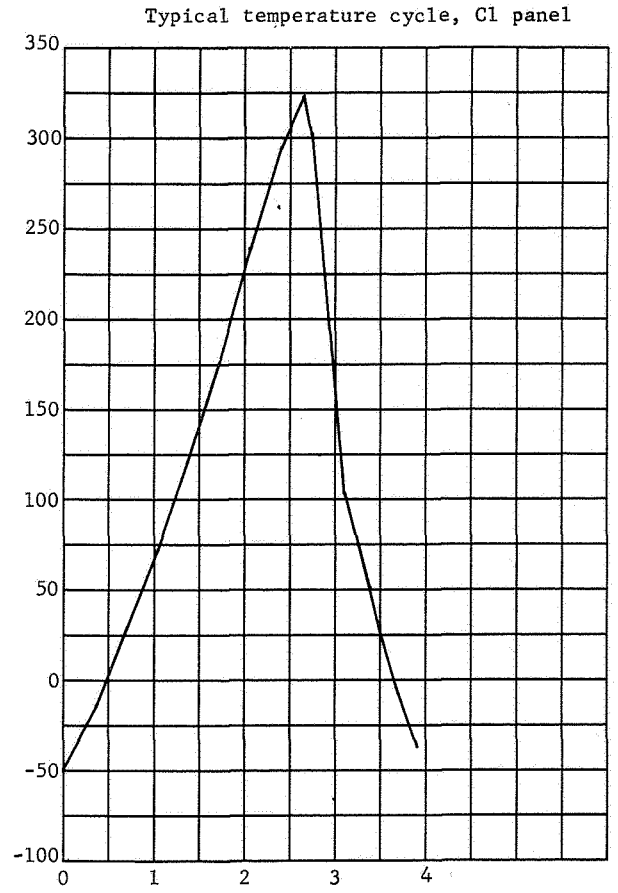


Figure 163.- Typical Temperature Cycle, 325°F, -50°F Requirement

Typical temperature cycle, E1A panel

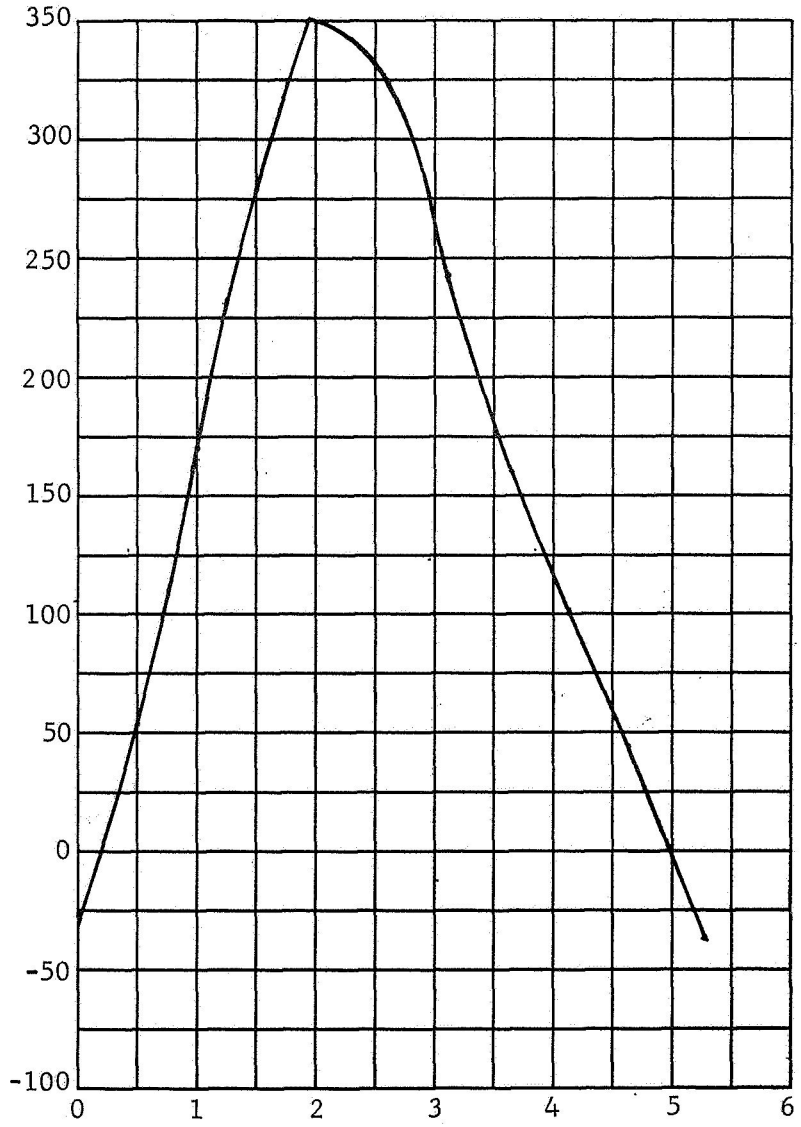


Figure 164.- Typical Temperature Cycle, 325°F, -20°F Requirement

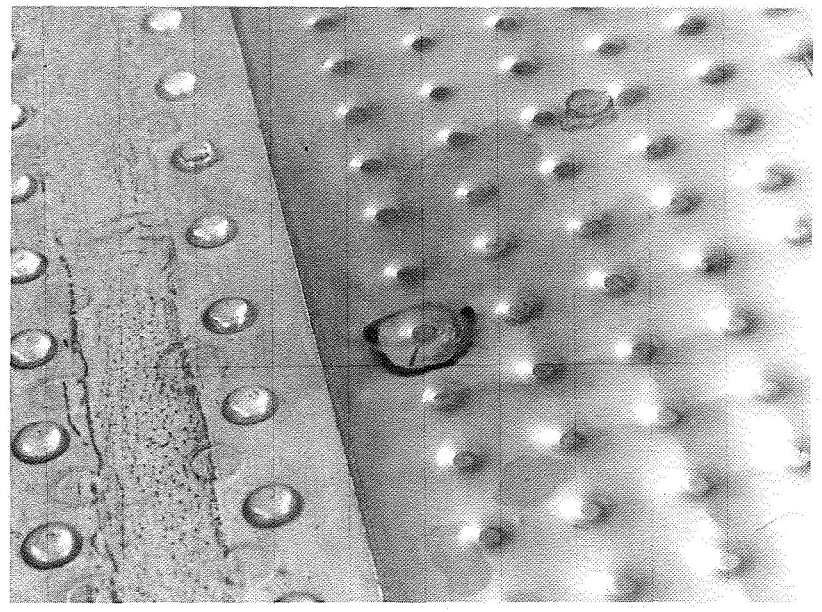

Figure 165.- Leak and Stress Area, F1A, S/N 0000103A

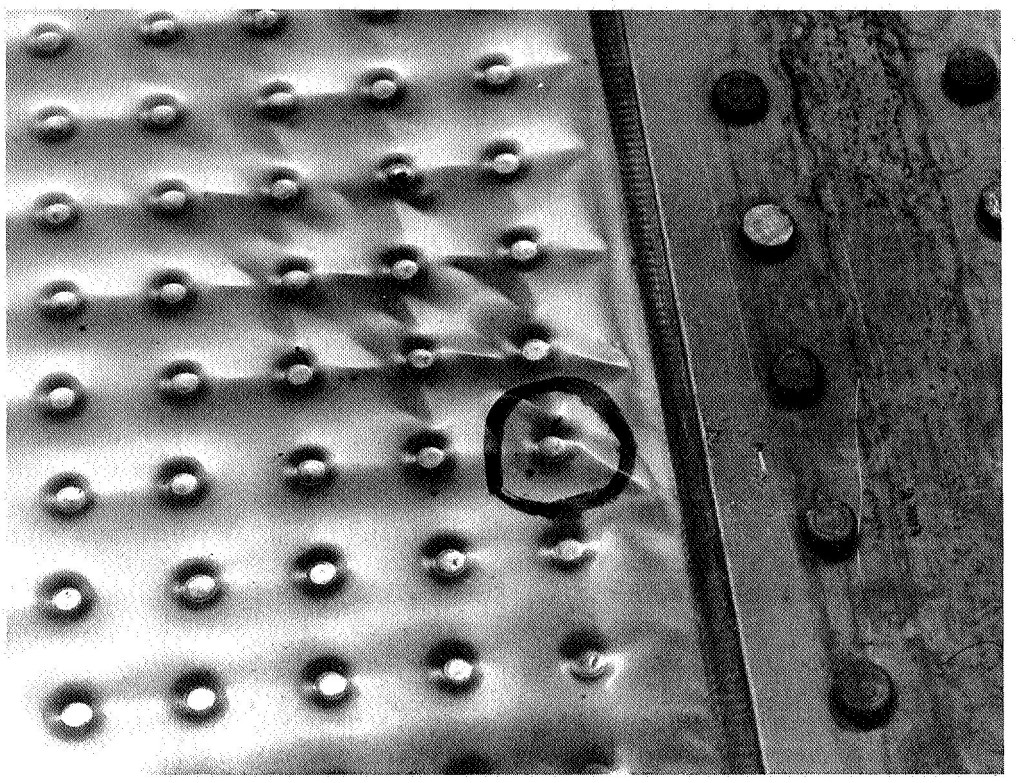

Figure 166.- Leak and Stress Area, F1A, S/N 0000111

## Test Program Evaluation

Test documentation.-

PD&D phase: In the PD&D phase of this program, the data were gathered using a test procedure, with semidetailed step-by-step methods. The data obtained were then entered onto separate, but included, data sheet(s) that followed each test section that required the taking of data. Technicians experienced some difficulty in following the procedure in one portion of the document, and then turning pages to enter the data taken. Each test specimen required a complete package consisting of procedure and data sheets. With 29 anticipated test configurations, the sheer volume of paperwork became oppressive. This fact evidenced itself even more clearly when the testing was completed and test reports were being prepared. The format of the test reports was the same as the procedure. As a result the test report was bulky and lacked continuity. The data were not in order and reading of the report required the turning of pages to compare test data with written test results and explanations. Also, considerable editorial and typing effort was expended. For these reasons this type of documentation was discontinued for the following phase.

D&D phase: The D&D phase required the preparation of a Development Test Plan to delineate responsibilities, applicable documents, test controls, test conditions and requirements, and implementation. The plan specified documentation format, environmental controls and tolerances, and specific tests to be performed. The final, approved version accomplished the original objectives.

The format for Test Procedures for this phase was changed to a type where the data are entered where the operator was instructed to take data. The only exception were those tests that had to be repeated several times (functional and leak). The data for a postenvironment functional and/or leak test were entered immediately following the environmental data, i.e., "Perform sinewave vibration" - data entered; "perform a functional test per paragraph 3.0 herein" - data entered; "Perform a leak test per paragraph 4.0 herein" - data entered. This format eliminated the continuity problem encountered during the previous phase but still necessitated a copy of the procedure for each specimen tested.

Test Reports for any given test specimen were created by entering a summary sheet(s), general statements as to report format, and retyping pages with data entered. The creation of the test report was simplified considerably over that of the previous phase. Editorial time was reduced but typing effort remained nearly the same. The readability of the report was more continuous, moving from one test environment (complete with postenvironment checks) to the next test environment without unnecessary to thumb through several pages of text to find a particular piece of data.

M&T phase: This phase of the program required the preparation of an Integrated Test Plan (ITP) covering FA and qualification of both components (pressure switches) and subassemblies. The final Integrated Test Plan was issued on 20 January 1968. Subsequently two Plan Change Notices (PCNs) were issued against the plan. PCN 1 was issued on 24 April 1968 and PCN 2 was issued on 6 March 1969. As with the DTP, the ITP delineated responsibilities, applicable documents, test controls, test conditions and requirements, test documentation, and program implementation. The ITP went into considerably more detail in the environmental criteria and functional test requirements area. Also, vibration test

fixture requirements were specified. The ITP changes made were due to test criteria changes, not to any inherent lack in the document.

As a result of the difficulties experienced in the data recording areas of the previous two phases, a new Test Procedure approach was made for this phase. Procedures were written for each type of testing, i.e., Flight Assurance Test, Qualification Test, and Accelerated Life Cycling Test, and, on a component (pressure switch) and subsystem (detector/panel) for a total of six "Master" procedures. The procedures for pressure switches only covered one configuration because the differences between switches from the two vendors in mounting requirements and operation were minimal. The procedures for the detector/panels covered all configurations to be tested in this phase; hence the nomenclature of "Master Procedure". Data were entered in a separate, bound book entitled "Data Sheet Package". These packages contained data sheets in the order and requirements for each configuration. The main variation was that some specimens required more functional data sheets since they used two pressure switches. Also, some specimens required an RGA leak data sheet at least once in the testing in place of a helium leak data sheet. The first advantage of this method is that it allowed the operator to follow the procedure required to obtain data without turning several pages to enter data. A second advantage was that, as retest became necessary, extra data sheets could be inserted into the data sheet package as required. A third advantage was the availability of a small, concise book to accompany the items under test, from introduction into test through delivery to the customer. Other advantages are described in the following paragraphs on test reports.

With the exception of the pressure switch qualification report (which used the D&D Phase types of documentation) Test Reports were created in an expeditious manner.

For FA testing, the Data Sheet Packages were reproduced in their original and manually recorded data form and transmitted to the customer as soon as all data had been reviewed and approved. These data packages also included any MARS and Failure Reports. At the completion of detector/panel FA testing a general report was written. This report consisted of all procedural steps with a general discussion of the results of any given test on all items tested included immediately following the procedural section relating to the test. For additional clarity and information, a chronological summary of testing and a summary discussion of test failures was included in the front of the report.

The Qualification and Accelerated Life Cycling test reports were created by writing a general report, as was done for Flight Assurance Testing, with the Data Sheet Packages included as appendices. It was possible to do this with qualification and ALC reports since there were fewer items under test. With this type of presentation, editing and typing were reduced to a minimum consistent with the desired legibility and accuracy.

Based on the experience gained during the three phases of this program, the test documentation method used in the M&T phase offers the greatest versatility and mobility. Data are easily recorded and transmitted to the necessary area(s). A complete data history of a completed subassembly, including component data, is not more than 60 pages, on an average. For the reasons discussed here, it is recommended that the M&T Phase data documentation method, or one similar to it be employed in any future programs.

Test criteria.-

Pressure switch FA tests: The following tests were performed during FA testing on the pressure switch. They are discussed as to the usable function they performed in screening out potentially troublesome components.

The transfer pressure (switch point) test, as a functional test, is the vehicle by which environmental effects, if any, are brought to light. It serves as a "fingerprinting" test and establishes the basis for comparison, as well as eliminating any items with manufacturing or shipping damage. This test should be retained in any future programs whether small (under 100) or large procurement is anticipated, and then only as an initial and final test.

As with the transfer pressure, the contact resistance test is a means of assessing damage or environmental effect. It is a better indicator of potential malfunction than the pressure transfer test. It should be retained in any future programs and be performed initially and finally.

During this program, more items were rejected, due to leakage during the helium leak test, than from either of the two functional tests. Any defect that is not picked up by the functional tests will be detected during leak testing. The leak test should be retained in any future use of pressure switches, but it should only performed initially and finally.

The sinewave vibration test did not produce any detectable malfunctions. It has certain value as an investigative or "information only" test and should be used if significant design changes are made. It is not a realistic environment for components intended for use on a rocket boosted payloads. It is recommended that this test be deleted in future programs.

The level of random vibration applied to pressure switches was derived as being 2/3 of the level measured at the pressure switch mounting during full-level tests of several detector/panels. The shape was likewise obtained. Of the dynamic tests performed during FAT, the random vibration test is the most realistic. It is, therefore, recommended that, if any dynamic environment is retained in FA testing, random vibration should be retained.

The shock test, as specified for this program, does not accomplish its intended function. Shock, as generated in most boosters, is a result of ordnance devices and is normally of much shorter (0.1 to 0.4 msec compared to the present duration of 7 msec) duration and considerable higher levels (dependent on distance from shock source, but generally greater than 100 g as compared to 60 g). No malfunction or damage occurred that is attributable to shock. The recommendation is that shock tests be deleted in future programs.

Functional and leak tests following the temperature cycling environment did detect some failures and malfunctions. Based on the results of this program this test has worth and should be retained.

Pressure switch qualification tests: The following tests are those which were performed during Qualification testing of the pressure switch. Only the environmental tests are discussed since the contact transfer, contact resistance, and helium leak have already been discussed and should be retained during qualification.

During pressure switch qualification, contacts were monitored for chatter and all specimens chattered at the high level of 100 g. Functional tests performed after sinewave vibration did not indicate any degradation of the item. As with the FA sinewave test, this test has value as an information-only test and should be used if a new development program is required. It should not be made part of a qualification program.

The random vibration test is a realistic simulation of an expected launch/boost environment. Although this test did not degrade the pressure switch during this program, it still remains one of the best test environments to prove the flight worthiness of the component. Random vibration should be retained in future qualification programs.

In its present form (60 g peak, 7 msec pulse), the shock test does not simulate the normally expected booster shock environment. It should either be deleted in future test programs, or be revised to a shorter duration, higher level pulse (0.1 to 0.4 msec half-sinewave, 100 g peak). Even at the revised level, experience has indicated that this type of component does not show any evidence of permanent susceptibility.

As with random vibration, acoustics is a realistic simulation of an expected booster environment. The level and shape presently specified are to be expected if a large booster is used (i.e., external level of 165 dB, most probable during max q, with 15 dB attenuation afforded by the payload shroud). Although no malfunctions were detected following this test, it is capable of pinpointing design weaknesses and should, therefore, be retained in any future qualification program.

There were no discernable results from the performance of the sustained acceleration test on the pressure switch. The test setup and performance of this test are extensive and time consuming. The effect of this test on a given component can be derived analytically at less cost and time. In general, sustained acceleration is no longer being performed in most test programs. For these reasons, it is recommended that this test be deleted in any future test programs.

The thermal vacuum soak test produced the disqualifying failures of the Servonic Instrument, Inc. test candidates. The switches leaked through cracks in the glass seal beads around the electrical feedthroughs. As previously explained, it is not known whether this environment caused the cracks initially or intensified existing cracks produced by preceding environmental tests. It is felt that properly designed and fabricated items would not respond to this test environment. However, at a component level, the test is not prohibitive from a cost and schedule viewpoint. Program cost and schedule requirements should dictate the inclusion or deletion of this test in any future programs.

Detector/panel FA tests: The detector/panel FA program, currently required, consists of the tests described in the following paragraphs.

The switch transfer pressure test is identical to that described previously under Pressure Switch FA Tests and should be retained for the same reasons. Program experience indicates that only two tests need be performed, one initially and one at the completion of FAT.

Switch contact resistance.- This test is identical to the pressure switch tests and should be retained for the same reasons. Based on this program's empirical data, one out of 40 items to receive FA failed this test. It is recommended that only two tests be performed, one initially and one at the completion of FA, even though this could allow 1 to 2% of the total build to proceed through FA in a failed condition. Considering that it takes 2 hr per item functional, this would save 60 manhours (80 manhours saved on functional - 20 manhours on unnecessary thermal cycling test) for each 40 items tested.

The helium leak test produced results similar to pressure switch tests and should be retained. In addition, it should be performed after each environment for a total of three times.

The RGA leak test is required for dual detectors with a common boundary. It is necessary to retain this test if dual detector design is part of any future programs. This test should be performed as an initial leak test only since the RGA tests performed after all other testing have not resulted in failure.

The level applied during the random vibration test was 2/3 of the qualification level. The shape was obtained by enveloping sinewave response data obtained during the D&D phase. This proved to be a reasonable test in that it was able to detect flaws. This test should be retained for future programs.

The thermal cycling test produced the most malfunctions and failures of the FA program. The test levels and duration are sufficient to point up correctable weaknesses. This fact is indicative of the necessity of retaining the test in any future FA programs.

Detector/panel qualification test: Functional and leak tests should be retained as they presently exist, with one exception. The RGA test should now be the final leak test performed. This closes the loop, having performed RGA as an initial FA leak test and now, as a final qualification leak test.

For reasons already stated the sinewave vibration test should not be retained in any future qualification programs.

There does not seem to be any reason to either change or delete the random vibration test, as it is presently specified. It is, therefore, recommended that it be retained in any future qualification program.

For reasons already discussed the shock test should either be revised or deleted in future qualification programs.

Considering the large surface area of the detector/panels, the acoustics test is a valid test, in its present form, does produce test results by amplifying weaknesses, and should be retained.

The thermal vacuum soak test was successfully performed as specified. The temperatures were realistic as was the vacuum requirements. The net results were a "go" light that went out during the cold portion for an undetermined reason, and one item leaking after test because of impurities in the braze. The test was quite expensive and time consuming. On static performing items, such as panels, the effect can be readily obtained by mathematical analysis. Since the weak spot in these items would most likely be the pressure switch diaphragm, a test of the pressure switch (already recommended) is a much less costly way of verifying operation in this environment. It is recommended that this test not be performed in future programs.

Accelerated life cycling: This test was performed on both components (pressure switches) and subassemblies (panel/detectors). The test criteria were the same for both, but testing was accomplished in a different manner in that hot and cold temperature media were different. In both cases the specimens received an initial functional and helium leak test after completing FA tests. They were then cycled through 21 344 cycles (minimum) of the required hot and cold temperatures. The test criteria seem well founded, but discounting test setup induced problems, no environmental effect was detected. The test setup and operation (at least on panels) is expensive and time consuming. Since the basic designs tested seem capable of surviving the simulated environment it is recommended that this test be excluded in future programs.

Summary of recommendations: The pressure switch FAT testing should be performed in the following sequence:

Initial functional (switch point and contact resistance);

Helium leak;

Random vibration;

Temperature cycling;

Functional;

Helium leak.

The recommended pressure switch qualification tests and sequence are as follows:

Initial functional (same as final FAT functional);

Helium leak (same as final FAT leak);

Random vibration;

Higher level, shorter duration shock;

Functional;

Leak;

Acoustics;

Functional;

Leak;

Thermal-vacuum soak;

Functional;

Leak.

The recommended detector/panel FAT and sequence are as follows:

Initial functional (switch point and contact resistance);

Helium or RGA leak;

Random vibration;

Thermal cycling;

Final functional;

Final helium leak.

The recommended detector/panel qualification tests and sequence are as follows:

Initial functional (same as final FAT);

Initial helium leak (same as final FAT);

Random vibration;

Higher level, shorter duration shock;

Functional;

Helium leak;

Acoustics;

Final functional;

Final helium or RGA leak.

Test tooling development.- During the various phases of this test program several test tools were undergoing development because of a contract requirement beyond state-of-the art techniques, and also because of the unique configurations of some of the detectors. Generally, all other tooling was routine in nature and will not be covered in this section. The area discussed in subsequent paragraphs describes the features of the dynamics fixture, and detector and switch accelerated life cycle fixturing.

Dynamics fixture: Several design concepts were considered in development of the dynamics fixture. The initial design considerations were the limitation of the vibration exciter table size and the worse-case detector size. These conditions, in

conjunction with the weight and force limitation of the vibration exciter, ultimately led to the fixture design used on the MPDD program.

The initial design considered was a forced cone configuration that would have extended the shaker table size to be compatible with detector physical dimensions with maximum rigidity. This fixture would have been a magnesium casting. However, during design analyses it was discovered that if the cone was extended to accommodate the 40x49-in. detector at an optimum angle, the weight of the fixture would exceed the shaker limitations.

The second design considered was a truncated pyramid with I-beam cross-section construction of machined weldments (figs. 167 thru 171). This fixture was so designed that it could be assembled into several configurations that would satisfy all dynamic test conditions allowing all or part of the fixture to constitute the tool needed to perform vibration, shock, and acoustics test required by the program. Further the fixture was designed to accommodate all detector configurations, eliminating the need for more than one fixture.

The fixture consists of several assemblies: (1) truncated pyramid base assembly; (2) ring frame assembly with cross bars; (3) slide plate assembly; and (4) acoustics rigid support assembly. The fixture configurations used during performance of the dynamics testing were as follows:

1) Vibration and shock (out-of-plane axis) used the base assembly, and the ring frame with/without cross bars depending on detector configuration being tested;

2) Vibration and shock (in-plane axes) used the slide plate assembly and the ring frame with/without cross bars depending on detector configuration being tested;

3) Acoustics used the rigid support assembly, and the ring frame with/without cross bars depending on detector configuration being tested.

Detector accelerated life cycle fixture: This fixture was designed to simulate the thermal environment experienced by the detector during the near-earth orbital mission. The design goal was to accomplish the thermal cycle in a 4-minute period. This type of test had not been previously performed. Therefore, design of this fixture went through several development iterations

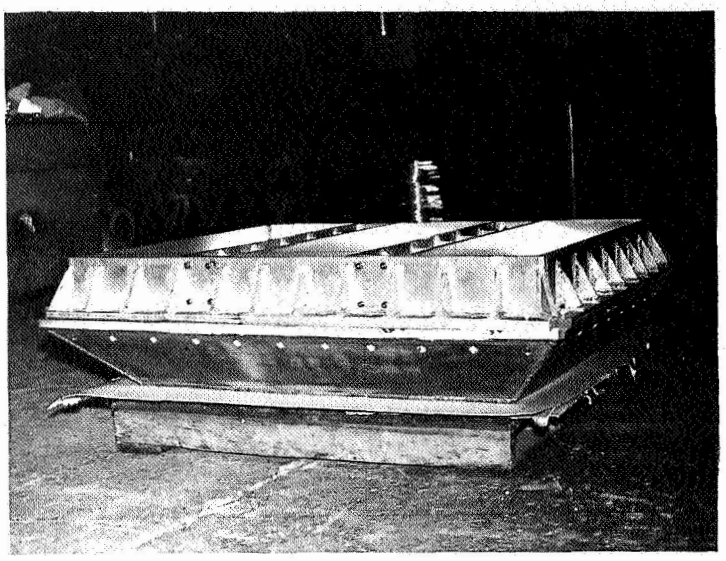

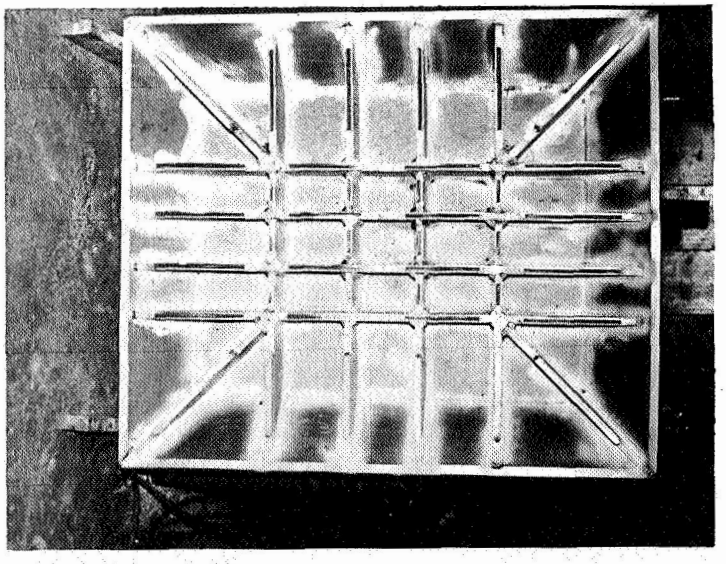

Figure 167.- Machined Weldment Vibration Fixture

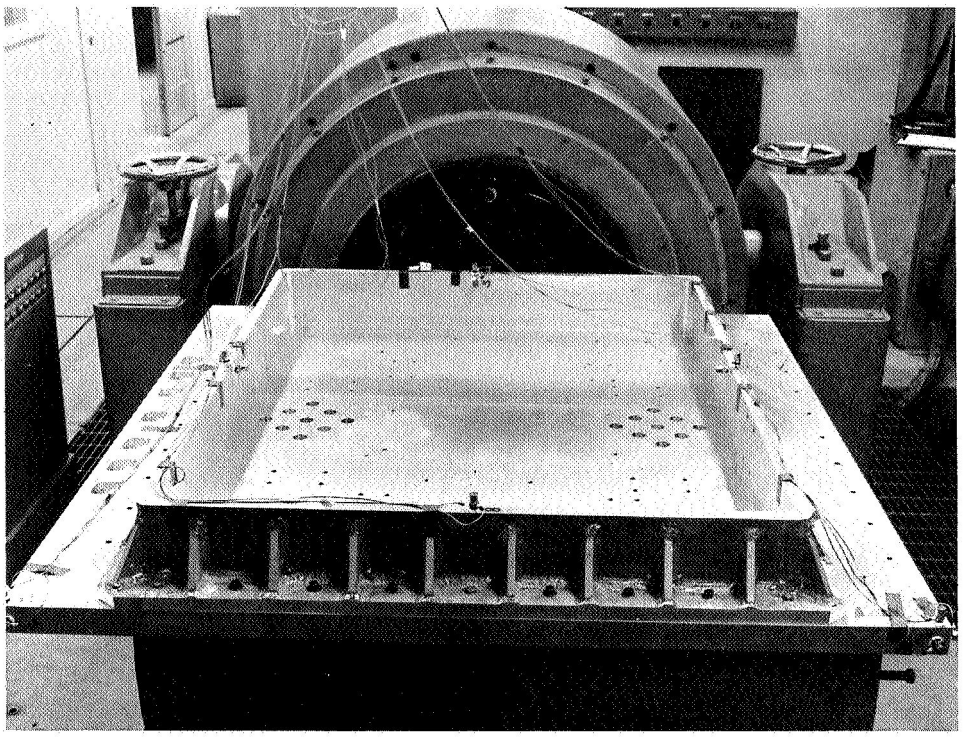

Figure 168.- 40x49-in. Configuration, In-Plane Axis

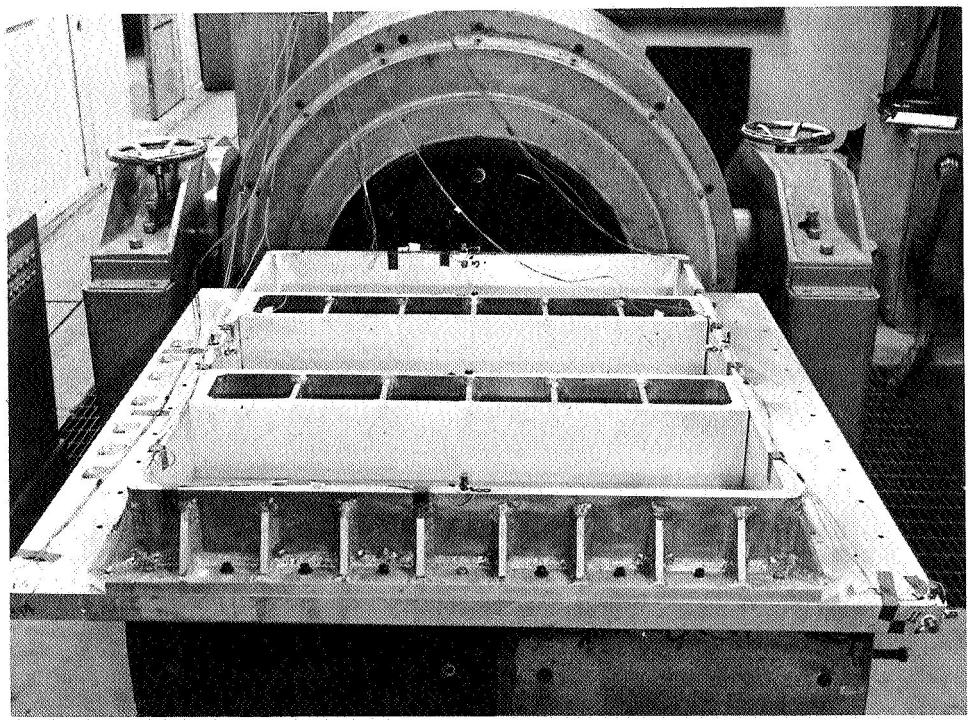

Figure 169.- 12x40-in. Configuration, In-Plane Axis

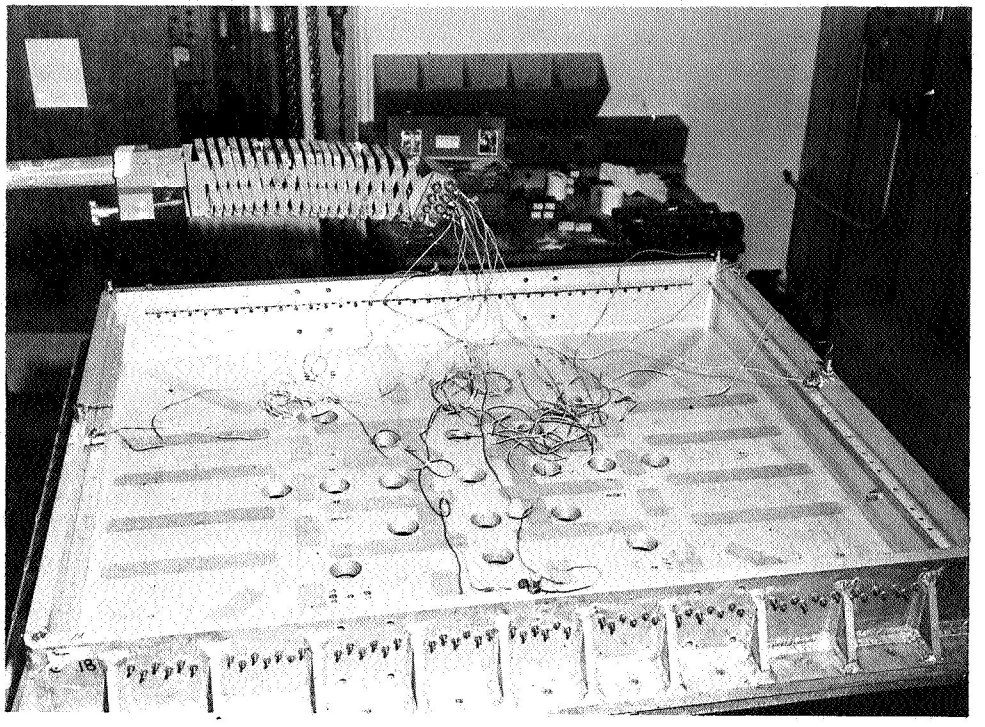

Figure 170.- 40x49-in. Configuration, Out-of-Plane Axis

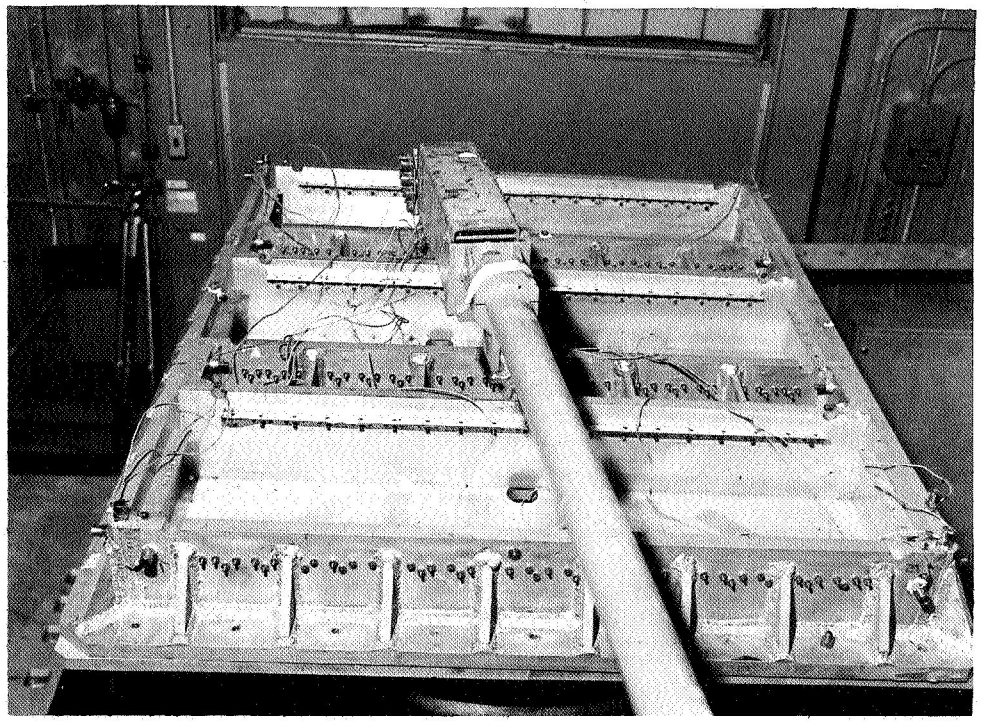

Figure 171.- 12x40-in. Configuration, Out-of-Plane Axis

before an adequate system was developed to meet the required test conditions. The first system considered was one that used a combination of a cold liquid bath and radiant heating. The initial problem was the requirement to perform the test in a vacuum condition of 1 torr. After research of many liquids that could be chilled to -160°F and still remained stable at pressures of 1 torr, only the hydnocarbon pentane appeared to be feasible for the application. At this point a subsize prototype fixture (fig. 172) was fabricated to evaluate pentane behavior at the required test conditions. The results of this test were encouraging enough to proceed with a full-size prototype fixture (fig. 173). However, during the full-size evaluation several problems in functional and thermal control areas were encountered. The most serious problems was in providing sufficient heat exchange to properly cool the pentane to the required level. To correct this situation, the fixture would have required extensive modification. Therefore, pentane was abandoned as a cooling media and was replaced by use of $LN_2$. This scheme, however, proved to be unsatisfactory, also because of excessive thermal gradient created across the surface of the test specimens.

During fixture development a series of thermal analyses were performed, resulting in changes to the test requirements. The primary changes were that of removing the 1 torr pressure requirements and relieving all-low temperature requirements. These changes coupled with the previously encountered design problems led to the third system which used an inductive heating system and a $LN_2$ spray cooling system. This system adequately satisfied the test requirements and was the system used to perform the detector ALC test. The control system used with this fixture was a relay logic system that will respond to either one of two control modes. These modes are cycle control as a function of temperature or a particular selected time base.

Pressure switch accelerated life cycle fixture (figs. 122 thru 124): This fixture was designed using the experience gained during development of the detector fixture. The principal difference is in the method of heating and cooling. This design uses the initial immersion concept with different fluids. It also uses an immersion bath for the heating. The fluids are glycerin and alcohol. The glycerin is heated with a thermostatic controlled hot plate and the alcohol is cooled using a liquid $CO_2$ injector. The control system used is identical to that used on the detector ALC test.

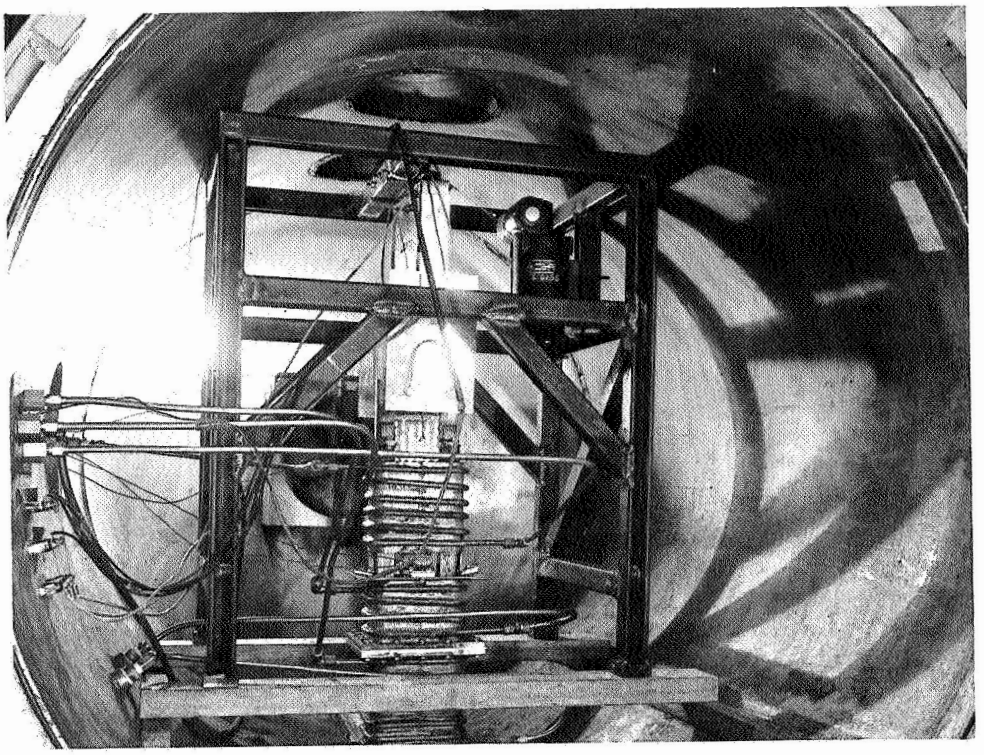

Figure 172.- Pentane Evaluation Fixture

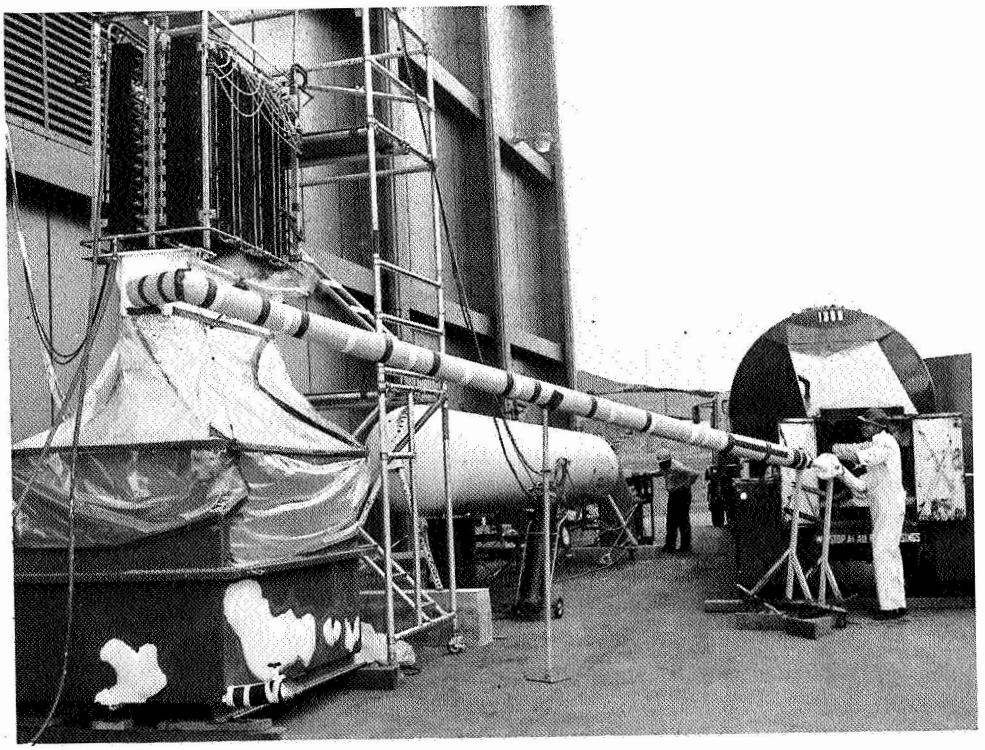

Figure 173.- Full-Size Pentane Fixture

## RELIABILITY AND QUALITY

Throughout the MPDD program, Reliability and Quality maintained a complete chronological history of the fabrication and test operations of each detector/panel configuration selected by NASA-LRC for M&T Operations. A system for periodic reporting of failures and Material Review Board (MRB) Actions was established and maintained. Appendix C summarizes the individual MRB actions and failures that were reported on the MPDD hardware.

Source data documents such as the initial Failure Report, Martin Automatic Reporting System (MARS Form), and Failure Analysis Reports are referenced in Appendix C for the convenience of the reader. Copies of these documents were forwarded to NASA-LRC concurrent with the hardware failure. Appendix C presents the MRB actions and failure history for the pressure actuated switch. Following the switch histories the final detector/panel configurations B1A, C1, D2A, D3A, E1A, E3A, and F1A are grouped together to relate a composite failure history picture for a given configuration.

Most of the pressure switch and completed detector failures were random failures and exhibited no particular trends. Some detector failures did occur, however; in the pressure tube of the B1A and F1A detectors. This tube joins the remotely mounted pressure switch to the detector target sheet; and these failures were attributed to a possible design deficiency. The problem was corrected by redesign of this pressure tube.

Failures in ALC test were almost entirely attributable to test fixture problems, and not to inability of the detectors to survive the ALC test environment. A detailed summary of failures is included in Appendix C.

### Summary of Deliverable Contract End Items for the MPDD Program

Two each of contract end items representative of the seven configurations selected by NASA-LRC are deliverable in accordance with Exhibit A, NASA Statement of Work L-7138A dated March 1, 1967, reference paragraph 4.1.3 thereof.

The following tabulation summarizes the hardware deliveries:

| Configuration & P/N | Serial No. | Delivery helium pressurization levels |
|---|---|---|
| B1A, 8280-04000-29 | S/N 0000106 | 27.7 psia @ 76°F |
| -39 | S/N 0000107 | 27.7 psia @ 75°F |
| C1 , 8280-07000-29 | S/N 0000105 | 27.9 psia @ 79°F |
| | S/N 0000106 | 27.9 psia @ 79°F |
| D2A, 8280-13000-29 | S/N 0000101 | 27.7 psia @ 76°F |
| | S/N 0000103 | 27.6 psia @ 72°F |
| D3A, 8280-16000-29 | S/N 0000103 | 27.6 psia @ 74°F |
| | S/N 0000104 | 27.6 psia @ 74°F |
| E1A, 8280-19000-30 | S/N 0000101 | 27.7 psia @ 75°F |
| | S/N 0000104 | 27.7 psia @ 76°F |
| E3A, 8280-25000-29 | S/N 0000105 | 27.6 psia @ 72°F |
| | S/N 0000106 | 27.6 psia @ 72°F |
| F1A, 8280-28000-20 | S/N 0000104 | 27.6 psia @ 74°F |
| -39 | S/N 0000108 | 27.7 psia @ 76°F |

Each unit of deliverable hardware was accompanied by an Acceptance Data Package consisting of the following data items:

1) Form DD250;

2) Final recap certification on shortages;

3) Copy of applicable MRB actions;

4) Copy of each installed pressure switch FAT data and a copy of the detector/panel FAT data;

5) Copy of the configuration log (baseline definition and all applicable changes effective on the end item).

## Corrosion Resistant Steel Sheet Selection

The material initially chosen for the MPDD program was 304L stainless steel. The reason for this choice was that preproposal work performed by Martin Marietta indicated that any weldable 300 series stainless steel could suffice for this application. Therefore, the criteria for selecting a material included:

1) Existence of a standard specification covering the raw material;

2) Availability of the material;

3) Metallurgical "cleanliness" of the material.

Stainless steel 304L appeared to be the best material to fit these criteria. In addition specification QQ-S-766 covered the raw material, it was readily available in sheet and foil gages, and Titan experience showed it to be one of the "cleanest"

materials (metallurgically) of any of the common 300 stainless steels. Consequently, 304L material was ordered for the MPDD program.

When the 304L material was received, it was found to be metallurgically less clean than what was considered typical. For example, seven of the nine shipments received were rejected for not meeting specification requirements. This rejection rate was completely unacceptable and it was necessary to determine if the quality of material desired was unavailable from industry or if there were omissions in the quality requirements placed on the purchase orders by Martin Marietta. Consultation with the vendors verified that the 304L material was not typical of the majority of 304L produced, but that it would be difficult and time consuming, if not uneconomical, to segregate 304L rolling stock to produce foil thicknesses with the desired microstructure. Aside from this problem it was also determined that 304L annealed material did not have a high enough yield strength for the "A" configurations of the program and a decision was made to use Armco produced alloy, 21-6-9 instead of 304L.

Martin Marietta Specification (STM 1216) was prepared and released as the governing specification for procurement and control of 21-6-9 corrosion resistant steel sheet. Two sources were used in the procurement of 21-6-9 material on the MPDD program. They were:

1) Rodney Metals, Incorporated
   New Bedford, Massachusetts

2) Esco Corporation
   Denver, Colorado

## Nondestructive Testing Methods

During the PDD phase of the program several nondestructive inspection testing techniques showed promise for use on MPDD hardware. A program to evaluate ultrasonic, infrared, and radiographic inspection techniques with relation to spotweld integrity was established and carried out by the Quality Laboratory. By the time specimen testing was completed, it was concluded that only the radiographic method was acceptable for use on MPDD hardware. Radiographic inspection parameters were established and incorporated into the MPDD welding specification. A summary of each method follows.

Ultrasonic inspection technique.- The equipment employed throughout the ultrasonic evaluation phase was a Model UM715 Reflectoscope, manufactured by Automation Industries Inc. It was a pulse-type instrument with an ultrasonic test frequency range of 2.25 MHz to 15 MHz. It was used in conjunction with a Budd Bridge Scanner and an Aldin "C" Scan Recorder that provided a permanent recorded output. Figures 174, 175, and 176 show the ultrasonic inspection equipment.

A set of specimens were fabricated using 0.016-in. to 0.016-in. thick 21-6-9 stainless steel sheet material. This combination was selected because the material was available at the time of the evaluation program and weld schedules had been established for this combination of material. Several specimens were welded using the established weld schedule, thus, producing good spot-welds. Using low current and pressure settings, low penetration specimens were produced, and finally high current and pressure settings produced specimens with excessive penetration. None of the later test specimens used current settings high enough to produce weld expulsions or spits. Two ultrasonic techniques were investigated.

Pulse-echo immersion: This method involves passing the sound wave pulse into the material, reflecting it from the back surface of the material after passing through the weld nugget and monitoring this reflected sound. Frequencies of 2.25 MHz, 5 MHz, 10 MHz and 15 MHz were used on each of the nondestructive specimens fabricated. Resolution of the front and back surfaces was found to be very difficult with this techniques and equipment, thus, the technique was discontinued.

Through transmission (modified) immersion: With this technique the sound pulse passes completely through the test pieces where they are welded and is reflected from a reflection plate placed under the weld. Using this method at 15 MHz it was possible in some, but not in all cases to distinguish between the lack of penetration samples and the excessive penetration samples. On completion of ultrasonic testing, all of the ultrasonic data were correlated with destructive tests. These tests included shear, peel, and tension. The correlation for distinguishing good welds from substandard quality was found to be about 60%. It was concluded that lack of 100% assurance in the prediction of weld quality through ultrasonic inspection was sufficient cause for disqualification of its use on MPDD hardware. Ultrasonic methods were abandoned on the basis of insufficient reliability.

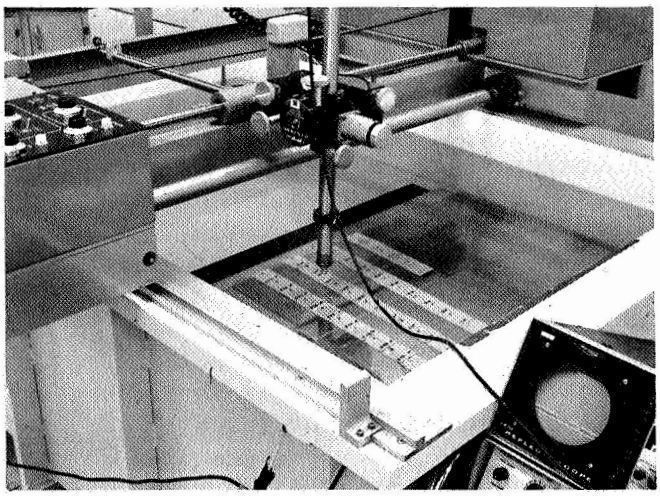

Figure 174.- Ultrasonic Inspection of .016-in. Welding Samples

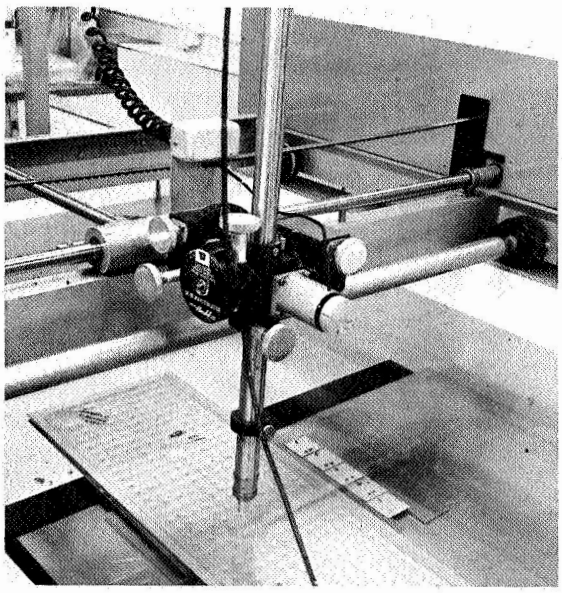

Figure 175.- Ultrasonic Inspection of Welds on Full-Size Panel, Transducer Assembly

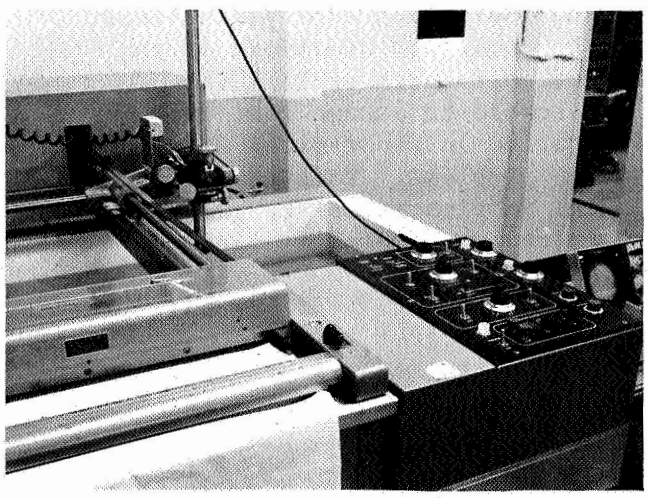

Figure 176.- Chart Recorder Used for Ultrasonic Inspection of Welds on Full-Size Panel

Infrared inspection technique.- This method of inspection used a Spectratherm (Liquid Crystal) B793-10, range 37°C to 40°C, produced by Westinghouse Electric Corporation. Sample spotweld specimens identical to those used in ultrasonic evaluation were subjected to the infrared technique. Liquid crystal material was used to evaluate the differences in thermal conductivity in the parent material and in the spot nugget. In the liquid crystal method, the mixture is painted on the test surface, the specimen is warmed by an infrared lamp and then air-cooled. Transient differences in temperature are indicated by color changes in the liquid coating. Discrimination of the spot nugget was readily apparent from the parent metal. However, the color changes from differences in spotweld quality with regard to penetration could not be correlated. The color changes were too subtle, and in some instances spots that were forged only via pressure application and no current were not discernable from a spotweld nugget. This method was discontinued because of a total lack of confidence in its results.

Radiographic inspection techniques.- This inspection method used a General Electric Resotron 300 (300 kV) X-ray tube. The results of X-ray on MPDD hardware was successful. The characteristics of lack of fusion, weld spits, porosity, and cracks were readily apparent with radiographic inspection. Spotweld peeling as a result of pressure expanding was also not a problem and was readily inspected visually. Radiographic inspection was incorporated in all MPDD fabrication process plans. Requirements for radiographic inspection quality were set forth in the 8280-00005, Weld and Braze Process Control Specification, MPDD Program.

## CONCLUSIONS

The MPDD program has demonstrated that large flat pressurized meteoroid penetration detectors can be built and qualified in the specified configurations and sizes for near-earth orbital and deep-space missions. It is also reasonable to assume that the configurations chosen for MPDD fabrication in other sizes and thickness combinations will present no problems. This conclusion is further supported by the successful fabrication of curved detectors in a number of different thickness combinations and sizes other than those originally specified for MPDD.

From specific experiences during the program it may be concluded that mill finishes are a poorly controlled measure of the optical and surface resistance properties of stainless steels.

Finishes vary between mills and between different types of stainless steels. For the MPDD application the fabrication should provide the processes to obtain desired optical and surface resistance properties.

Resistance spot welding is capable of producing joints of higher strength, uniformity, and repeatability than indicated by handbook data. Correspondingly in a specific high quality controlled application, the use of handbook data for spot welds in design will probably result in an overdesign. The significance of material surface resistance to weldability was noted during the program. In welding thick foils of approximately equivalent thickness, uniformity of resistance is most important. The absolute value of resistance is less important because it may be compensated for by parameter changes on the welding machine. When plies of very unequal thicknesses are welded, not only is the uniformity important but the absolute value of surface resistance should be low to help locate the weld nugget more in the thicker ply and prevent melting completely through the thin ply. The use of a "peel" sheet to aid in spot and seam welding 0.002-in. foils to 0.016-in. foils was verified during the program. In our experience consistently strong leak-free welds in this combination could be obtained much more consistently with the use of a 0.001-in. peel sheet for spot welds and a 0.008-in. peel sheet for seam welds.

Early in the program it was concluded that chem-milling to preform the cavity in target sheets was unacceptable because the required thickness tolerances of the target sheet could not be maintained.

Experiments during the program verified and provided some quantitative data on the positive relation between pressure formed detectors and their ability to survive pressure cycling.

Another empirically derived conclusion was that the simple square joint pattern structurally had the highest increase in stiffness with increasing cavity and the most consistent relation between cavity and forming pressure of all the patterns considered.

It was also concluded that preforming does not produce stiffer panels nor does stiffness affect the load carried by the detector mounts.

It was well established during the program that spot welded detector joint arrays were superior to seam welded arrays. This superiority was demonstrated in target area efficiency, stiffness

and structural stability, consistency of the relation between cavity formation and forming pressure and success of the specimens in pressure cycle testing.

The superiority of resistance welding as the primary joining process over fluxless brazing or diffusion bonding was never clearly established. Rather the selection of resistance welding was forced by its great success relative to the success in brazing and bonding. The lack of success in these two processes was initially attributed to equipment and contamination problems. More recent work in a new high-vacuum, high-temperature furnace did not, however, produce test specimens to challenge those obtained by resistance welding with a machine costing 4% the cost of the furnace. Thus, resistance welding proved itself an adequate process for MPDD. Also it was concluded that even if the ultimate in brazed joint strengths had been consistently reached, brazed joints would not have been strong enough to be used in pressure formed detectors. With regard to diffusion bonding where the joint strength is theoretically as good as the parent metal, our experiments produced specimens that had extremely poor success in pressure cycling tests because of some degradation of the metal during the high temperature bonding process.

Explosive preforming of detector cavities was a successful process. The high cost of the forming die precludes the use of this technique to configurations where pressure forming is not practical.

The extensive use of large numbers of relatively inexpensive subsize specimens provided quick conclusive evaluations of many facets of design early in the program, and in a number of cases, provided evaluations where the problem did not yield to analysis. The subsize specimens were simplified versions of the full-size configurations. They did not have sealed-off fill tubes or simulated pressure switches. No problem was expected with tubes and the switches were not evolved until well after the subsize detector program was concluded. Unfortunately, as indicated in Appendix C these two areas gave the most trouble during the final phase of the program. It is a reasonable conclusion that if these items had been adequately considered in the early experimental program the problems in the last phase would not have occurred.

Martin Marietta Corporation
Denver, Colorado, October 20, 1969

# APPENDIX A

## DOCUMENTATION

A significant amount of data and documentation has been prepared and published during the Meteoroid Penetration Detector Development Program. This appendix is a compilation of the contractual data prepared by Martin Marietta Corporation and submitted to NASA-LRC during the conduct of contract NAS1-7043.

MPDD Documentation Summary

| Item no. | Title | Document no. | Dated | Summary of contents |
|---|---|---|---|---|
| 1. | Preliminary Design Review Material | | | The following material was prepared and submitted to NASA-LRC in support of the Preliminary Design Review |
| | Design Review Reports on Pressure Switch Designs | None | | Subcontractor meeting minutes |
| | | | 17 July 67 | Servonic Design Review 1 |
| | | | 17 July 67 | Carleton Design Review 1 |
| | | | 24 July 67 | Servonic Design Review 2 |
| | | | 17 Oct. 67 | Carleton Design Review 2 |
| | Preliminary Design Review Report for Meteoroid Penetration Detectors | None | | Contractor/NASA-LRC design review meeting minutes: |
| | | | 21 June 67 | Initial Design Review Meeting |
| | | | 23 Oct. 67 | Incremental Review Report |
| | | | 23 Oct. 67 | D1 - E1 Configuration Report |
| | | | 10 Nov. 67 | Submittal of Agenda -- Discussion material, and vuegraphs for PDR |
| | | | 6 Dec. 67 | Preliminary Design Review Report |
| 2 | Design Development Review Material | | | The following material was prepared and submitted to NASA-LRC in support of the Development Design Review |
| | | None | 13 Feb. 68 | Submittal of agenda, discussion material and vuegraphs |
| | | | 26 Feb. 68 | Design Development Review Report |
| | | | 4 Apr. 68 | MPDD Design Baseline and Drawings for C1 Panel 8280-07000-019, -020 |
| | | | 29 Mar. 68 | MPDD Design Baseline and Drawings for D2A Detector - 8280-13000-019, -020 |
| | | | 29 Mar. 68 | MPDD Design Baseline and Drawings for D3A Detector - 8280-16000-019, -020 |

MPDD Documentation Summary

| Item no. | Title | Document no. | Dated | Summary of contents |
|---|---|---|---|---|
| 2 | Continued | | 29 Mar. 68 | MPDD Design Baseline and Drawings for E1A Detector - 8280-19000-020, -029 |
| | | | 29 Mar. 68 | MPDD Design Baseline and Drawings for E3A Detector - 8280-25000-019, -020 |
| | | | 7 Aug. 68 | MPDD Design Baseline and Drawings for B1A Panel - 8280-04000-019 |
| | | | 7 Aug. 68 | MPDD Design Baseline and Drawings for F1A Panel - 8280-28000-019 |
| 3 | Final Review Presentation and Agenda | None | 15 Sep. 69 | Final Review Vuegraphs and discussion material |
| 4 | Development Test Plan | MDS-10001 | 26 Oct. 69 | MPDD test plan for the development test period of the program |
| 5 | Design Development Inspection and Test Procedures | OP510 | 28 Nov. 67 | Detailed step-by-step inspection and test procedures used by QC, Engineering, and Test during the Design Development Test Phase for the development model testing. |
| | B1A Detector | 8280-04051 | | |
| | B4 Detector | 8280-06051 | | |
| | C1 Detector | 8280-07061 | | |
| | C1B Detector | 8280-07071 | | |
| | D1A Detector | 8280-10051 | | |
| | D2A Detector | 8280-13001 | | |
| | D3A Detector | 8280-16051 | | |
| | E1A Detector | 8280-19051 | | |
| | E2C Detector | 8280-24051 | | |
| | E3A Detector | 8280-25001 | | |
| | F1A Detector | 8280-28001 | | |
| | F1B Detector | 8280-29001 | | |

MPDD Documentation Summary

| Item no. | Title | Document no. | Dated | Summary of contents |
|---|---|---|---|---|
| 6 | Design Development Test Reports | | | Completed test reports of the development model testing using the Inspection and Test Procedures with the compiled test data for each detector completing the development test program |
| | B1A Detector, S/N 0000010 | 8280-04051 | 15 Aug. 68 | |
| | C1 Detector, S/N 0000001 and S/N 0000002 | 8280-07061 | 13 Mar. 68 | |
| | D1A Detector, S/N 0000001 | 8280-10051 | 20 Feb. 68 | |
| | D2A Detector, S/N 0000002 | 8280-13001 | 16 Mar. 68 | |
| | D3A Detector, S/N 0000001 | 8280-16051 | 21 Feb. 68 | |
| | E1A Detector, S/N 0000001 and S/N 0000002 | 8280-19051 | 29 Feb. 68 | |
| | E2C Detector, S/N 0000001 | 8280-24051 | 23 Feb. 68 | |
| | E3A Detector, S/N 0000001 | 8280-25001 | 22 Feb. 68 | |
| | F1A Detector, S/N 0000010 | 8280-28001 | 22 Aug. 68 | |
| 7 | Integrated Test Plan | MDS-10003 with Change Notice 2 | Preliminary 20 Nov. 67<br>Final 29 Jan. 68<br>30 June 69 | This Test Plan establishes the requirements, test methods and procedures to be used in the Flight Assurance Test, Qualification Test, and Accelerated Life Cycle Test on the MPDD Program |
| 8 | Integrated Test Specifications and Procedures | | | Master step-by-step Inspection and Test Procedures to be used by QC, Engineering, and Test during the Qualification and Factory acceptance and Accelerated Life testing of the production models of the detectors and pressure switches |
| | Pressure Switch-Qualification Test Procedure | PD7100075 -003 -OP530 thru Change Notice 4 | 5 Feb. 68 | |
| | Pressure Switch-Flight Assurance Test Procedure | PD7100075 -003 -OP520 with Change Notice 3 | 13 Mar. 68 | |

MPDD Documentation Summary

| Item no. | Title | Document no. | Dated | Summary of contents |
|---|---|---|---|---|
| 8 | Continued | | | |
| | Meteoroid Detector/Panel Qualification Test Master Procedure | OP530 with Change Notice 2 | 24 May 68 | |
| | Meteoroid Detector/Panel Flight Assurance Test Master Procedure | OP520 with Change Notice 2 | 7 May 68 | |
| | Accelerated Life Cycle Test - Meteoroid Detector Panel Master Procedure | OP540 with Change Notice 1 | 10 Feb. 69 | |
| | Accelerated Life Cycle Test - Pressure Switch Master Procedure | OP550 with Change Notice None | 15 Mar. 69 | |
| 9 | Test Reports for Flight Assurance Tests Qualification Tests Accelerated Life Cycle Tests on the Production model of the Meteoroid Detector/ Panels and Pressure Switches | PD7100075 -003 -OP520 PD710007 -003 -OP530 -OP520 -OP530 -OP540 -OP550 | Various | Individual Test Reports and data packages have been submitted to NASA-LRC on each component and end item that has completed the applicable test cycle. The data format uses the completed data sheets set up in the Master Test procedures listed in Item 8. The reports are identified by part number and serial number. |
| 10 | Production Plan | MDS-10002 Books 1 thru 5 | Preliminary 22 Jan. 68 Final 27 Apr. 69 | This Production Plan provides the detail methods and processes to be used in the procurement, receiving, fabrication, testing, and handling of meteoroid penetration detectors in sufficient detail to enable capable contractors to undertake and complete all steps in the fabrication, testing, and delivery of flight qualified meteoroid penetration detectors of the configurations designed, developed, and tested for NASA-LRC under this contract. |

MPDD Documentation Summary

| Item no. | Title | Document no. | Dated | Summary of contents |
|---|---|---|---|---|
| 11 | Procurement Specification for Pressure Actuated Switch | NASA-LRC Drawing No. LA412417<br>MMC Drawing No. PD7100075 | Latest Change "J" 20 Jan. 69 | Detailed procurement specification for the pressure-actuated switch used on the meteoroid detectors. |
| 12 | Special Handling and Storage Requirements Specification-MPDD Program | NASA-LRC Drawing No.<br>MMC Drawing No. 8280-00002 | Latest Change "A" 4 Apr. 68 | Establishes the requirements for handling and processing of MPDD hardware. |
| 13 | Leakage Control Specification - MPDD Program | NASA-LRC Drawing No. LA412301<br>MMC Drawing No. 8280-00003 | Latest Change "A" 18 Apr. 68 | Establishes the criteria for allowable leakage requirements during the fabrication and testing of MPDD hardware. |
| 14 | Cleaning, Contamination, and Material Surface Treatment Specification - MPDD Program | NASA-LRC Drawing No. LA412302<br>MMC Drawing No. 8280-00004 | Latest Change "B" 9 Aug. 68 | Establishes the requirements and procedures to be used in establishing and maintaining the cleanliness of detail parts, components, and assemblies for the MPDD hardware. |
| 15 | Weld and Braze Process Control Specification - MPDD Program | NASA-LRC Drawing No. LA412303<br>MMC Drawing No. 8280-00005 | Latest Change "F" 10 Mar. 69 | Establishes the requirements for resistance spot and seam welding, and fusion welding of MPDD hardware. |

MPDD Documentation Summary

| Item no. | Title | Document no. | Dated | Summary of contents |
|---|---|---|---|---|
| 16 | Parts List and Instructions, Pack and Ship - MPDD Program | NASA-LRC Drawing No. LA412304 MMC Drawing No. 8280-00009 | Latest Change "C" 18 Jul. 69 | Establishes the requirements, instructions and parts lists for the packaging and shipping of MPDD hardware. |
| 17 | Helium Fill and Fill Tube Pinch Off Specification - MPDD Program | NASA-LRC Drawing No. LA412305 MMC Drawing No. 8280-00010 | Latest Change "B" 10 May 68 | Establishes the requirements for filling the MPDD detectors and panels with helium gas and for sealing the helium within the MPDD hardware. |
| 18 | Pressure Expansion Criteria Specification - MPDD Program | NASA-LRC Drawing No. LA412306 MMC Drawing No. 8280-00011 | Latest Change "A" 3 May 68 | Establishes the requirements for the gas expansion of the meteoroid penetration detectors and panels. |
| 19 | Material Specification - Lightweight Unshielded Electrical Wire, 600 V | MMS-E078 Rev 3 | 10 Feb. 69 | Specification for electrical wire used for pressure switch interconnection on the MPDD hardware. |
| 20 | Material Specification - Sheet, Strip, and Foil 21-6-9 Corrosion and Heat Resistant Sheet Steel - Restricted Cleanliness | STM 1216 Rev 3 | 3 Nov. 67 | Specification for the stainless steel used in fabrication of the MPDD hardware. |
| 21 | Surface Preparation and Inspection Procedure | None | 20 Feb. 68 | Engineering report on the techniques and data used in the analysis and evaluation of the surface finish required for the MPDD hardware and the applicable range of absorptivity and emissivity ratios. |

MPDD Documentation Summary

| Item no. | Title | Document no. | Dated | Summary of contents |
|---|---|---|---|---|
| 22 | Surface Finish Report | MDS-10010 | 21 Nov. 67 | Engineering report on the development of surface finishing techniques to be used on the MPDD hardware for a proper absorptivity and emissivity ratio. |
| 23 | Material Selection Analyses Report | MDS-10027 | 18 Sep. 67 | Establishes the requirements and analyses required in the selection of the stainless steel alloy for detector target application. |
| 24 | Environmental and Design Criteria Specification | MDS-10012 Rev 1 | 4 Apr. 67 June 67 | Establishes the environmental and design criteria for the design, construction, performance and testing requirements for the meteoroid penetration detectors and pressure switch. |
| 25 | Detector Interchangeability Study Report | MDS-10030 | 27 Oct. 67 | Documents on analyses conducted to determine the best meteoroid detector mounting approach to achieve detector interchange ability in the spacecraft mounting. |
| 26 | Solar Cell Contamination Test Report | MDS-10015 | 23 Sep. 68 | Engineering report of a test on the outgassing characteristics of the silicone potting compound, and Teflon tape used in the MPDD hardware and its possible effects on contamination of the detector surface. |
| 27 | Strain Evaluation Analysis Report | MDS-10029 | 23 Oct. 67 | Engineering report of test program conducted on the internal pressure, and stainless steel material -- strain relationship at various locations on the surface of pressure formed detectors. |
| 28 | Pressurization Media Analysis Report | MDS-10028 Plus Addendum | 20 Sep. 67 4 Oct. 68 | Engineering report on an analysis to determine the pressure test media (gas) to be used on the MPDD hardware to determine the leak areas and leak rate |

MPDD Documentation Summary

| Item no. | Title | Document no. | Dated | Summary of contents |
|---|---|---|---|---|
| 29 | Feasibility Study for Attaching Meteoroid Penetration Detectors to the Exterior of the S-IVB Propulsion Stage | None | 9 Oct. 68 | Engineering report and stress analysis of a study conducted in cooperation with NASA-LRC Contract NAS1-8157 to establish a possible design criteria for attachment of MPDD-type detectors on the exterior of a S-IVB. |
| 30 | Materials Reports | | | These reports were submitted to NASA in accordance with the requirements of the General Contract Clause requiring material test reports each 6 months. |
| | Technical Resolution of MPDD Finish Welding Problems | MDS-10016 | 9 Oct. 68 | Engineering report on the resolution of the weld "spit" problem found during the resistance welding of the MPDD stainless detectors and the surface finish influence in this phenomenon. |
| | Resistance Welding Technology Developments for the MPDD F1A Configuration Meteoroid Detector | MDS-10018 | 24 Mar. 69 | Engineering report on the resolution of the weld "spit" problem found when resistance welding 0.002/0.016/0.002-in. stainless detectors. |
| 31 | New Technology Reports | Martin Marietta Corporation Denver, Colo. | | These reports were submitted to NASA in accordance with the requirements of the General Contract Clause requiring reports on new technology |
| | Resistance Welding with Peel Sheet | Report 12 | 18 Sep. 67 | Use a strippable 0.002-in. peel sheet when spot welding 0.002/0.016/0.002-in. stainless steel material. |
| | Technique for Tensile Testing Thin Foil Specimens (0.005" - 0.0005") | Report 18 | 9 Nov. 67 | Special procedures and test fixture for tensile testing thin gage materials. |

MPDD Documentation Summary

| Item no. | Title | Document no. | Dated | Summary of contents |
|---|---|---|---|---|
| 31 | Continued | | | |
| | Accelerated Life Cycling Fixture | Report 23 | 3 June 68 | Testing system for accelerated life cycle testing of MPDD detectors. |
| | Hole Cutting Technique for Thin Metals | Report 25 | 3 Jan 68 | Special drill design for cutting holes in thin metals. |
| | Technique to Locate Small Helium Leaks in MPDD Detectors | Report 39 | 23 Sep. 68 | Uses a nitrogen filled tent to provide a proper background for location of helium leaks. |
| 32 | Pressure Switch Accelerated Life Cycle Test Report | N/A | - - - | To be prepared at completion of ALC switch testing. |
| 33 | Thermal Control Coating Technical Report | N/A | - - - | To be prepared at completion of engineering study. |
| 34. | Failure Mode, Effects and Criticality Analysis (FMECA) | N/A | - - - | These analyses are included in the applicable monthly and quarterly reports. |
| 35 | Reliability and Quality Program Plan | MDS-10005 | Preliminary 21 Apr. 67 | Reliability and Quality Program Plan prepared for the MPDD program in accordance with the applicable requirements of NPC 200-2 and NPC 250-1. |
| 36 | Reliability Evaluation Plan | MDS-10008 | 20 Nov. 67 | Establishes the method of evaluating the reliability of the MPDD hardware and designates the program milestones and phases that will require re-evaluation to confirm the reliability predictions. |

MPDD Documentation Summary

| Item no. | Title | Document no. | Dated | Summary of contents |
|---|---|---|---|---|
| 37 | Reliability Evaluation Program Review Reports | MDS-10009 | 2 Aug. 68<br>Aug. 69<br>Oct. 69 | Engineering reports on the formal reliability reviews conducted on the MPDD program and the results of the subsequent review and coordination with NASA-LRC |
| 38 | Failure Malfunction Reports and Follow up Corrective Action and Failure Analysis Reports | None | Various | The individual failure reports are reported each week to the NASA representative three copies of the applicable Martin Reporting System format. Subsequent Corrective Action and Failure Analysis reports are transmitted to the NASA representative when available. |
| 39 | Approved Parts and Materials Lists | MDS-10019 | 5 Feb. 69 | Parts and Materials Lists for the MPDD hardware in accordance with the requirements of NPC-250-1. |
| 40 | Parts and Materials Qualification Status List | MDS-10017 | 22 June 68 | Current status of the Qualification program for parts and materials to be used in the MPDD hardware. This status has been included in the monthly and quarterly reports since Aug. 1968. |
| 41 | Acceptance Data Package and Equipment Logs | None | Various | The individual Acceptance Data Package and Equipment Log records are prepared in accordance with NPC 200-2 and NPC 250-1 and shipped with the hardware to NASA-LRC. |
| 42 | Documentation Plan | MDS-10006 | 23 May 67 updated quarterly | Compilation of all of the deliverable data required for delivery to NASA-LRC under the MPDD Contract. This data list updated and included as part of the quarterly report to provide NASA-LRC with a current list of all program data. |
| 43 | Photography Plan | MDS-10007 | 16 May 67 | Establishes the requirements for photographing the MPDD hardware during the development, fabrication and test phases. The photos are submitted in the monthly and quarterly reports. |

MPDD Documentation Summary

| Item no. | Title | Document no. | Dated | Summary of contents |
|---|---|---|---|---|
| 44 | Program Manager's Biweekly Schedule Status Report | MDS-10038 Issue 1 thru Issue XX | 5 Apr. 67 Oct. 69 | Biweekly report to NASA-LRC by the Contractor's Program Manager on the MPDD program status and current problems. |
| 45 | Monthly Technical Progress Report | MDS-10039 Issue 1 thru Issue 18 | 11 May 67 5 June 69 | Monthly report to NASA-LRC by the Contractor's Program Manager on the summary of work accomplished during the past month, current problems, and schedule status. Includes monthly reports on Engineering Design and Development, Testing, Manufacturing, Reliability and Quality, FMECA, and Qualification status. |
| 46 | Quarterly Technical Progress Report | MDS-10040 Issue 1 thru Issue 9 | 7 Jul. 67 11 Jul. 69 | Quarterly report to NASA-LRC by the Contractor's Program Manager on the summary of work accomplished during the past quarter. Supersedes the monthly report for the 3rd month of each quarter. Content similar to the monthly report except that the report also includes the current documentation status and program schedule status. |
| 47 | Financial Management Report - Monthly | MCR-67-195 Issue 1 thru Issue 30 | 25 Apr. 67 Oct. 69 | Contractor's monthly report of the financial status of the MPDD program on NASA Form 533a. |
| 48 | Financial Management Report - Quarterly | MCR-68-235 Issue 1 thru Issue 11 | 21 Jul. 67 5 Oct. 69 | Contractor's quarterly report of the financial status of the MPDD program on NASA Form 533. |
| 49 | Configuration Management Plan | MDS-10042 | 15 Apr. 68 | Establishes the requirements for identification and control of the data and engineering design and subsequent changes to the NASA approved baseline. |

MPDD Documentation Summary

| Item no. | Title | Document no. | Dated | Summary of contents |
|---|---|---|---|---|
| 50 | Drawings for Meteoroid Penetration Detectors and Panels | - - - - - | Various | The design drawings have been cross-referenced with NASA-LRC and Contractor drawing numbers. Sepia copies (2) will be submitted at the completion of the contract. |

This page left blank intentionally.

# APPENDIX B

## ENGINEERING DRAWING IDENTIFICATION
## AND
## NUMERICAL DRAWING INDEX

DETECTOR PANEL DESIGNATION B1A

| | |
|---|---|
| LE412307-19 | Panel Installation B1A |
| LF412308-20 | Panel Assembly B1A |
| LF412309-20 | |
| LF412308-30 | Panel Subassembly B1A |
| LF412309-30 | |
| LF412311-01 | Target Sheet |
| LC412313-01 | Backup Plate |
| LC412356-09 | Fill Tube Assembly |
| LC412356-01 | Tube |
| LF412310-10 | Target Sheet Assembly |
| LF412312-01 | Target Sheet |
| LC412325-01 | Fitting, Filler Tube |
| LB412316-01 | Reinforcing Plate, Filler Tube |
| LF412314-19 | Switch Support Assembly |
| LC412411-39 | Switch Cup Assembly |
| LA412417-003 | Switch, Pressure Actuated |
| LC412411-30 | Switch Cup Subassembly |
| LC412390-01 | Cup, Switch |
| LB412409-02 | Clip, Switch Support |
| LC412379-01 | Tube, Interconnect |
| LB412408-01 | Fill Tube |
| LD412406-01 | Bracket, Switch Support |
| LB412402-01 | Tube, Wire Cover |
| LB412405-01 | Tube, Protective Sleeve |
| LC412324-01 | Switch Cover |
| LC412329-02 | Adapter, Pressure Switch |
| LB412330-01 | Spacer, Switch Cover |
| LC412315-01 | Sleeve, Pressure Tube |
| LF412399 | Mounting Hole Pattern |
| LC412398-09 | Angle Assembly |
| LD412397-01 | Panel Support Angles |
| LC412323-02 | Doubler |
| LC412398-10 | Angle Assembly |
| LD412397-02 | Panel Support Angles |
| LC412323-01 | Doubler |
| LC412336-01 | Bolt - Hard Point |
| LF412399 | Mounting Hole Pattern |

DETECTOR PANEL DESIGNATION C1

| | |
|---|---|
| LE412317-19 | Panel Installation |
| LF412318-29 | Panel Assembly C1 |
| LF412319-29 | |
| LF412318-20 | Panel Subassembly C1 |
| LF412319-20 | |
| LF412321-01 | Target Sheet |
| LC412356-09 | Fill Tube Assembly |
| LC412356-01 | Tube |
| LD412322-09 | Target Sheet Assembly C1 |
| LF412320-01 | Target Sheet C1 |
| LC412325-01 | Fitting, Filler Tube |
| LA412417-003 | Switch, Pressure Actuated |
| LC412326-01 | Sleeve, Protective |
| LC412327-01 | Clip, Wire Cover |
| LC412324-01 | Cover, Pressure Switch |
| LB412330-01 | Spacer, Switch Cover |
| LC412329-02 | Adapter, Pressure Switch |
| LB412331-01 | Cover, Fill Tube |
| LC412332-01 | Cap, Wire Cover |
| LF412399 | Mounting Hole Pattern |
| LC412398-09 | Angle Assembly |
| LC412397-01 | Panel Support Angle |
| LC412323-02 | Doubler |
| LC412398-10 | Angle Assembly |
| LC412397-02 | Panel Support Angle |
| LC412323-01 | Doubler |
| LC412336-01 | Bolt, Hard Point |

DETECTOR DESIGNATION D2A

| | |
|---|---|
| LE412337-19 | Detector Installation D2A |
| LE412338-19 | |
| LF412339-20 | |
| LF412340-20 | Detector Assembly D2A |
| LF412341-20 | |
| LF412339-19 | |
| LF412340-19 | Detector Subassembly |
| LF412341-19 | |
| LF412351-01 | Core/Backup Sheet |
| LC412356-09 | Fill Tube Assembly |
| LC412356-01 | Tube |
| LC412344-09 | Target Sheet Assembly |
| LF412342-01 | Target Sheet |
| LC412325-01 | Filler Tube Fitting |
| LC412345-09 | Target Sheet Assembly |
| LF412343-01 | Target Sheet |
| LC412325-01 | Filler Tube Fitting |
| LA412417-003 | Switch, Pressure Actuated |
| LC412326-01 | Sleeve, Protective |
| LC412327-02 | Clip, Wire Cover |
| LC412324-02 | Cover, Pressure Switch |
| LC412329-02 | Adapter, Pressure Switch |
| LB412331-01 | Cover, Fill Tube |
| LB412330-01 | Spacer, Switch Cover |
| LC412332-02 | Cap, Wire Cover |
| LC412332-04 | Cap, Wire Cover |
| LF412335 | Mounting Hole Pattern |
| LC412334-09 | Angle Assembly |
| LD412333-01 | Angle, Detector Support |
| LC412328-03 | Doubler |
| LC412334-10 | Angle Assembly |
| LD412333-02 | Angle, Detector Support |
| LC412328-03 | Doubler |
| LC412336-01 | Bolt, Hard Point |
| LF412335 | Mounting Hole Pattern |

DETECTOR DESIGNATION D3A

| | |
|---|---|
| LE412346-19<br>LE412347-19 | Detector Installation D3A |
| LF412348-29<br>LF412349-29<br>LF412350-29 | Detector Assembly D3A |
| LF412348-20<br>LF412349-20<br>LF412350-20 | Detector Subassembly D3A |
| LF412351-01 | Core/Backup Sheet |
| LC412356-09 | Fill Tube Assembly |
| LC412356-01 | Tube |
| LC412353-09 | Target Sheet Assembly |
| LF412352-01 | Target Sheet |
| LC412325-01 | Fitting Filler Tube |
| LC412327-02 | Clip, Wire Cover |
| LC412326-01 | Sleeve, Protective |
| LA412417-003 | Switch, Pressure Actuated |
| LC412324-02 | Cover, Pressure Switch |
| LC412329-02 | Adapter, Pressure Switch |
| LB412330-01 | Spacer, Switch Cover |
| LC412332-02 | Cap, Wire Cover |
| LB412331-01 | Cover, Fill Tube |
| LF412335 | Mounting Hole Pattern |
| LC412334-09 | Angle Assembly |
| LD412333-01 | Angle, Detector Support |
| LC412328-03 | Doubler |
| LC412334-10 | Angle Assembly |
| LD412333-02 | Angle, Detector Support |
| LC412328-03 | Doubler |
| LC412336-01 | Bolt - Hard Point |
| LF412335 | Mounting Hole Pattern |

DETECTOR DESIGNATION E1A

| | |
|---|---|
| LE412354-20 | Detector Installation E1A |
| LE412355-20 | |
| LF412357-20 | Detector Assembly E1A |
| LF412358-20 | |
| LF412359-20 | |
| LF412357-39 | Detector Subassembly E1A |
| LF412358-39 | |
| LF412359-39 | |
| LF412361-01 | Target Sheet |
| LC412356-09 | Fill Tube Assembly |
| LC412356-01 | Tube |
| LC412362-09 | Target Sheet Assembly |
| LF412360-01 | Target Sheet |
| LC412325-01 | Fitting, Filler Tube |
| LA412417-003 | Switch, Pressure Actuated |
| LC412326-01 | Sleeve, Protective |
| LC412327-03 | Clip, Wire Cover |
| LC412324-03 | Cover, Pressure Switch |
| LC412329-02 | Adapter, Pressure Switch |
| LB412330-01 | Spacer, Switch Cover |
| LB412331-01 | Cover, Fill Tube |
| LC412332-03 | Cap, Wire Cover |
| LF412335 | Mounting Hole Pattern |
| LC412334-09 | Angle Assembly |
| LD412333-01 | Angle, Detector Support |
| LC412328-03 | Doubler |
| LC412334-10 | Angle Assembly |
| LD412333-02 | Angle, Detector Support |
| LC412328-03 | Doubler |
| LC412336-01 | Bolt, Hard Point |
| LF412335 | Mounting Hole Pattern |

DETECTOR DESIGNATION E3A

| | |
|---|---|
| LE412363-19<br>LE412364-19 | Detector Installation E3A |
| LF412365-39<br>LF412366-39<br>LF412367-39 | Detector Assembly E3A |
| LF412365-30<br>LF412366-30<br>LF412367-30 | Detector Subassembly E3A |
| LF412369-01 | Backup Sheet |
| LC412356-09 | Fill Tube Assembly |
| LC412356-01 | Tube |
| LC412370-09 | Target Sheet Assembly E3A |
| LF412368-01 | Target Sheet |
| LC412325-01 | Fitting, Filler Tube |
| LA412417-003 | Switch, Pressure Actuated |
| LC412326-01 | Sleeve, Protective |
| LC412324-03 | Cover, Pressure Switch |
| LC412329-02 | Adapter, Pressure Switch |
| LB412330-01 | Spacer, Switch Cover |
| LC412327-03 | Clip, Wire Cover |
| LC412332-03 | Cap, Wire Cover |
| LB412331-01 | Cover, Fill Tube |
| LF412335 | Mounting Hole Pattern |
| LC412334-09 | Angle Assembly |
| LD412333-01 | Angle, Detector Support |
| LC412328-03 | Doubler |
| LC412334-10 | Angle Assembly |
| LD412333-02 | Angle, Detector Support |
| LC412328-03 | Doubler |
| LC412336-01 | Bolt - Hard Point |
| LF412335 | Mounting Hole Pattern |

BUMPER PANEL DESIGNATION F1A

| | |
|---|---|
| LE412371-19 | Panel Installation F1A |
| LF412372-40<br>LF412373-40<br>LF412374-40 | Panel Assembly F1A |
| LF412372-30<br>LF412373-30<br>LF412374-30 | Panel Subassembly F1A |
| LD412389-10 | Target Sheet Assembly F1A |
| LD412375-02 | Core Sheet |
| LD412377-02 | Target Sheet |
| LC412325-01 | Fitting, Filler Tube |
| LD412376-02 | Target Sheet |
| LC412378-01 | Backup Plate |
| LC412356-09 | Fill Tube Assembly |
| LC412356-01 | Tube |
| LB412316-01 | Reinforcing Plate, Filler Tube |
| LC412395-09 | Bumper Support Assembly |
| LC412393-01 | Angle Support - Bumper |
| LC412393-02 | Angle Support - Bumper |
| LC412394-01 | Plate - Bumper Support |
| LC412401-09 | Bumper Support Assembly |
| LD412385-02 | Bracket, Bumper Support |
| LC412400-01 | Bumper, Support Channel |
| LF412314-19 | Switch Support Assembly |
| LC412411-39 | Switch Cup Assembly |
| LA412417-003 | Switch, Pressure Actuated |
| LC412411-30 | Switch Cup Subassembly |
| LC412390-01 | Cup, Switch |
| LB412409-02 | Clip, Switch Support |
| LC412379-01 | Tube, Interconnect |
| LB412408-01 | Fill Tube |
| LD412406-01 | Bracket, Switch Support |
| LB412402-01 | Tube, Wire Cover |
| LB412405-01 | Tube, Protective Sleeve |
| LC412396-01 | Support, Bumper |
| LC412396-02 | Support, Bumper |
| LC412329-02 | Adapter, Pressure Switch |

BUMPER PANEL DESIGNATION F1A CONT'D.

| | | | | |
|---|---|---|---|---|
| | | | LB412330-01 | Spacer, Switch Cover |
| | | | LC412407-01 | Target Sheet Shield |
| | | | LC412392-03 | Cover, Pressure Switch |
| | | | LC412324-01 | Cover, Pressure Switch (M/F) |
| | | | LC412315-01 | Sleeve, Pressure Tube |
| | | | LC412415-01 | Splice Strap |
| | | | LC412415-02 | Splice Strap |
| | | LF412399 | | Mounting Hole Pattern |
| | LF412404-09 | | | Bumper Installation |
| | | LD412380-10 | | Bumper Sheet Assembly |
| | | | LD412383-02 | Bumper Sheet |
| | | | LB412410-01 | Stiffener |
| | | | LB412414-01 | Stiffener |
| | | LD412381-20 | | Bumper Sheet Assembly |
| | | | LD412382-02 | Bumper Sheet |
| | | | LB412384-01 | Stiffener |
| | | | LB412403-01 | Stiffener |
| | | | LB412388-01 | Spring Retainer - Bumper |
| | | | LB412388-02 | Spring Retainer - Bumper |
| | | | LB412387-01 | Spring - Bumper |
| | | | LB412387-02 | Spring - Bumper |
| | | LB412391-09 | | Clevis Assembly |
| | | | LB412386-01 | Clevis, Bumper |
| | | LB412391-10 | | Clevis Assembly |
| | | | LB412386-02 | Clevis, Bumper |
| | LC412398-09 | | | Angle Assembly |
| | | | LD412397-01 | Panel Support Angles |
| | | | LC412323-02 | Doubler |
| | LC412398-10 | | | Angle Assembly |
| | | | LD412397-02 | Panel Support Angles |
| | | | LC412323-01 | Doubler |
| | | | LC412412-01 | Bolt - Hard Point |
| | | | LC412413-01 | Bolt - Special |
| | | | LC412416-01 | Bolt - Hard Point |
| | LF412399 | | | Mounting Hole Pattern |

APPENDIX B

| | | |
|---|---|---|
| 8280-00002 | Special Handling and Storage Requirements Specification - MPDD Program | LA412300 |
| 8280-00003 | Leakage Control Specification - MPDD Program | LA412301 |
| 8280-00004 | Cleaning, Contamination, and Material Surface Treatment Specification - MPDD Program | LA412302 |
| 8280-00005 | Weld and Braze Process Control Specification - MPDD Program | LA412303 |
| 8280-00009 | Parts List and Instructions, Pack and Ship - MPDD Program | LA412304 |
| 8280-00010 | Helium Fill and Fill Tube Pinch Off Specification - MPDD Program | LA412305 |
| 8280-00011 | Pressure Expansion Criteria Specification - MPDD Program | LA412306 |

APPENDIX B

| | | |
|---|---|---|
| 8280-04000, Sh 1 | Panel Installation - B1A | LE412307 |
| 8280-04051, Sh 1 | Detector Panel Assembly - B1A | LF412308 |
| 8280-04051, Sh 2 | Panel Subassembly - B1A | LF412309 |
| 8280-04052, Sh 1 | Target Sheet Assembly - B1A | LF412310 |
| 8280-04053, Sh 1 | Target Sheet - B1A | LF412311 |
| 8280-04054, Sh 1 | Target Sheet - B1A | LF412312 |
| 8280-04055, Sh 1 | Backup Plate - B1A | LF412313 |
| 8280-04060, Sh 1 | Switch Support Assembly | LF412314 |
| 8280-04061, Sh 1 | Sleeve, Pressure Tube | LC412315 |
| 8280-04062, Sh 1 | Reinforcing Plate, Filler Tube | LB412316 |
| 8280-07000 | Panel Installation - C1 | LE412317 |
| 8280-07061, Sh 1 | Subassembly, Welded - C1 | LF412318 |
| 8280-07061, Sh 2 | Detector Panel Assembly - C1 | LF412319 |
| 8280-07062 | Target Sheet - C1 | LF412320 |
| 8280-07063 | Target Sheet - C1 | LF412321 |
| 8280-07064 | Target Sheet Assembly - C1 | LD412322 |
| 8280-07074 | Doubler | LC412323 |
| 8280-10054 | Cover, Pressure Switch | LC412324 |
| 8280-10056 | Fitting, Filler Tube | LC412325 |
| 8280-10057 | Sleeve, Protective | LC412326 |
| 8280-10059 | Clip, Wire Cover | LC412327 |
| 8280-10061 | Doubler | LC412328 |
| 8280-10063 | Adapter, Pressure Switch | LC412329 |
| 8280-10064 | Spacer - Switch Cover | LB412330 |
| 8280-10065 | Cover, Fill Tube | LB412331 |
| 8280-10066 | Cap, Wire Cover | LC412332 |
| 8280-10067 | Angle, Detector Support | LD412333 |
| 8280-10068 | Angle Assembly | LC412334 |
| 8280-10069 | Mounting Hole Pattern, Large Detector | LF412335 |
| 8280-10072 | Bold - Hard Point | LC412336 |
| 8280-13000, Sh 1 | Detector Installation - D2A | LE412337 |
| 8280-13000, Sh 2 | | LE412338 |
| 8280-13001, Sh 1 | Detector Assembly - D2A | LF412339 |
| 8280-13001, Sh 2 | Subassembly, Welded - D2A | LF412340 |
| 8280-13001, Sh 3 | | LF412341 |
| 8280-13002, Sh 1 | Target Sheet - D2A | LF412342 |
| 8280-13003, Sh 1 | Target Sheet - D2A | LF412343 |
| 8280-13004, Sh 1 | Target Sheet Assembly - D2A | LB412344 |
| 8280-13006, Sh 1 | Target Sheet Assembly - D2A | LB412345 |

| | | |
|---|---|---|
| 8280-16000, Sh 1 | Detector Installation - D3A | LE412346 |
| 8280-16000, Sh 2 | | LE412347 |
| 8280-16051, Sh 1 | Detector Assembly - D3A | LF412348 |
| 8280-16051, Sh 2 | Subassembly, Welded - D3A | LF412349 |
| 8280-16051, Sh 3 | | LF412350 |
| 8280-16052, Sh 1 | Core/Backup Sheet | LF412351 |
| 8280-16054, Sh 1 | Target Sheet - D3A | LF412352 |
| 8280-16055, Sh 1 | Target Sheet Assembly - D3A | LC412353 |
| 8280-19000, Sh 1 | Detector Installation - E1A | LE412354 |
| 8280-19000, Sh 2 | | LE412355 |
| 8280-19005, Sh 1 | Fill Tube Assembly | LC412356 |
| 8280-19051, Sh 1 | Detector Assembly - E1A | LF412357 |
| 8280-19051, Sh 2 | Subassembly, Welded - E1A | LF412358 |
| 8280-19051, Sh 3 | | LF412359 |
| 8280-19052, Sh 1 | Target Sheet - E1A | LF412360 |
| 8280-19053, Sh 1 | Target Sheet - E1A | LF412361 |
| 8280-19054, Sh 1 | Target Sheet Assembly - E1A | LC412362 |
| 8280-25000, Sh 1 | Detector Installation - E3A | LE412363 |
| 8280-25000, Sh 2 | | LE412364 |
| 8280-25001, Sh 1 | Detector Assembly - E3A | LF412365 |
| 8280-25001, Sh 2 | Detector Subassembly - E3A | LF412366 |
| 8280-25001, Sh 3 | | LF412367 |
| 8280-25002, Sh 1 | Target Sheet - E3A | LF412368 |
| 8280-25003, Sh 1 | Backup Sheet - E3A | LF412369 |
| 8280-25006, Sh 1 | Target Sheet Assembly - E3A | LC412370 |
| 8280-28000, Sh 1 | Panel Installation - F1A | LE412371 |
| 8280-28002, Sh 1 | Detector Panel Assembly - F1A | LF412372 |
| 8280-28002, Sh 3 | Detector Assembly - F1A | LF412373 |
| 8280-28002, Sh 5 | | LF412374 |
| 8280-28003, Sh 1 | Core Sheet - F1A | LD412375 |
| 8280-28004, Sh 1 | Target Sheet - F1A | LD412376 |
| 8280-28005, Sh 1 | Target Sheet - F1A | LD412377 |
| 8280-28007 | Backup Plate - F1A | LC412378 |
| 8280-28008 | Tube, Interconnect | LC412379 |
| 8280-28009 | Bumper Sheet Assembly - F1A | LD412380 |
| 8280-28010 | Bumper Sheet Assembly - F1A | LD412381 |
| 8280-28011 | Bumper Sheet Detail - F1A | LD412382 |
| 8280-28012 | Bumper Sheet Detail - F1A | LD412383 |
| 8280-28014 | Stiffener - Bumper - F1A | LB412384 |
| 8280-28017 | Bracket, Bumper Support - F1A | LD412385 |

| | | |
|---|---|---|
| 8280-28019 | Clevis - Bumper - F1A | LB412386 |
| 8280-28020 | Spring - Bumper - F1A | LB412387 |
| 8280-28021 | Spring Retainer - Bumper - F1A | LB412388 |
| 8280-28022 | Target Sheet Assembly - F1A | LD412389 |
| 8280-28024 | Cup, Switch | LC412390 |
| 8280-28025 | Clevis Assembly - F1A | LB412391 |
| 8280-28030 | Cover, Pressure Switch - F1A | LC412392 |
| 8280-28033 | Angle Support - Bumper - F1A | LC412393 |
| 8280-28034 | Plate - Bumper Support - F1A | LC412394 |
| 8280-28035 | Bumper Support Assembly - F1A | LC412395 |
| 8280-28037 | Support - Bumper - F1A | LC412396 |
| 8280-28038 | Panel Support Angles | LD412397 |
| 8280-28039 | Angle Assembly - Small Panel Mount | LC412398 |
| 8280-28040 | Mounting Hole Pattern, Small Detector Panel | LF412399 |
| 8280-28041 | Bumper Support Channel - F1A | LC412400 |
| 8280-28042 | Bumper Support Assembly - F1A | LC412401 |
| 8280-28045 | Tube, Wire Cover | LB412402 |
| 8280-28047 | Stiffener - Bumper - F1A | LB412403 |
| 8280-28049 | Bumper Installation | LF412404 |
| 8280-28050 | Tube, Protective Sleeve | LB412405 |
| 8280-28051 | Bracket, Switch Support | LD412406 |
| 8280-28052 | Target Sheet Shield - F1A | LC412407 |
| 8280-28053 | Fill Tube | LB412408 |
| 8280-28055 | Clip, Switch Support | LB412409 |
| 8280-28056 | Stiffener - Bumper - F1A | LB412410 |
| 8280-28057 | Switch Cup Assembly | LC412411 |
| 8280-28058 | Bolt - Hard Point - F1A | LC412412 |
| 8280-28059 | Bolt - Special - F1A | LC412413 |
| 8280-28060 | Stiffener - Bumper - F1A | LB412414 |
| 8280-28061 | Splice Strap - F1A Detector | LC412415 |
| 8280-28062 | Bolt - Hard Point - F1A | LC412416 |
| PD7100075 | Switch, Pressure Actuated | LA412417 |

This page left blank intentionally.

# APPENDIX C

## FAILURE HISTORIES

APPENDIX C

Pressure Actuated Switch MRB and Failure History

At the onset of the program two procurement sources were selected for supplying the pressure-actuated switch:

1) Servonic Instrument Incorporated
   Costa Mesa, California
   Part Number PD7100075-002

2) Carleton Controls Corporation
   East Aurora, New York
   Part Number PD7100075-003

PD7100075-002; S/N 0000114 and S/N 0000149.-
Failure Report B50936
Failure Analysis Report 8280-1
History: During thermal vacuum soak of Qualification Tests both units leaked helium in excess of $1.0 \times 10^{-9}$ scc/sec. The failure occurred on the third day of the 15-day soak period while at -250°F. The leakage was isolated by mass spectrometer and microscopic examination of the test specimens. In both units the glass seals at the switch terminal posts exhibited multiple fractures determined to be the leakage source. The supplier, Servonic Instrument Incorporated, was disqualified as a result of this failure in Qualification. All Servonic hardware was rejected. Engineering changes were issued that cancelled and deleted the Servonic pressure-actuated switch on all MPDD build requirements.

PD7100075-003; S/N 0000039.-
Failure Report B50947
Failure Analysis Report 8280-2
History: Unit failed helium leak test following dynamics test of the FAT sequence. The leakage exceeded $1.0 \times 10^{-9}$ scc/sec and was isolated, following dissection, to a 3/8-in. diameter section in the center of the switch diaphragm. A defect in the diaphragm parent metal was the cause of failure. Carleton Controls was notified of the failure and closer inspection by the supplier was initiated to arrest such defects at the source. The leaking unit, S/N 0000039, was scrapped.

PD7100075-003; S/N 0000044.-
Failure Report B50960
Failure Analysis Report 8280-3
History: During dynamics testing in the FAT sequence, this unit was accidentally dropped approximately 27 in. onto a concrete floor. In its next functional test the unit exhibited intermittent electrical readout on switch point number one, at zero pressure. The

damage to the switch case resulting from the fall was obvious. Internal damage to the microswitch was apparent from the results of the electrical checkout. The unit was scrapped. The cause of failure was attributed to mishandling in test.

PD7100075-003; S/N 0000028.-
Failure Report B50962
Failure Analysis Report 8280-4
History: During temperature cycle test of the FAT sequence the microswitch contacts failed to transfer on increasing pressure from -250°F. This unit was dissected to determine the cause of failure. A pumping action was created through the back pressure port in the switch when cycling from hot to cold temperatures. This permitted moisture in ambient air to condense out and freeze behind the switch diaphragm. The ice buildup after several cycles was sufficient to prevent microswitch transfer operation. The fixture was redesigned to insulate the specimens from ambient air. No subsequent failures have ever been experienced following the modification.

PD7100075-003; S/N 000029.-
Failure Report B50963
Failure Analysis Report 8280-4
History: This unit was in test and in the fixture with S/N 0000028. The cause of failure was identical; therefore the unit was returned to the vendor, reinspected, retested successfully, and returned for FAT at Martin Marietta, Denver. FAT at Martin Marietta was completed successfully. The above rework and retest was directed by MRB action on MARS B50963.

PD7100075-003; S/N 0000050.-
Failure Report B50964
Failure Analysis Report 8280-4
History: This unit accompanied S/N 0000028 in test and its failure was the same as S/N 0000028. A MRB disposition was directed via MARS B50964 identical to that referenced for S/N 0000029. The unit passed all retest and FAT successfully.

PD7100075-003; S/N 0000065.-
Failure Report B50938
Failure Analysis Report 8280-5
History: During FAT temperature cycling test, at the eighth cycle, this unit failed. Failure was due to potting material around the microswitch disintegrating during dynamics testing and becoming lodged between the actuation arms of the microswitch when subjected to temperature cycling. Carleton Controls acknowledged responsibility for this unit failure and instituted additional in-process control to preclude a recurrence of failure. The microswitch and housing were salvageable; therefore, a MRB disposition directed this unit to be returned to Carleton Controls. Following rework it was retested through vendor acceptance tests and FAT at Martin Marietta. Denver.

PD7100075-003; S/N 0000022.-
Failure Report T10061
Failure Analysis Report 8280-6
History: This unit failed the contact resistance part of the functional test. A reading of 240 milliohms was evident at a current of 100 micro-amps compared to the allowable of 200 milliohms at 100 micro-amps current. The failure could not be duplicated on several recheck attempts. An MRB disposition was processed to remove the microswitches and salvage the switch body. The switch body was mated with the microswitch and microswitch housing from pressure actuated switch S/N 0000065. The rebuilt unit was retested as switch S/N 0000022A, which successfull completed all retests and FAT.

The initial failure of S/N 0000022 was recorded as an unverified failure with the malfunction attributed to a malfunction of the digital voltmeter rather than a true switch electrical failure. The microswitch portion of S/N 0000022 was scrapped for reliability considerations.

PD7100075-003; S/N 0000159.-
Failure Report B50957
Failure Analysis Report 8280-8
History: This unit failed its initial functional test on receipt from the vendor. Failure was determined to be the result of misidentified wire leads. The microswitch wiring was retraced and the leads properly identified. The switch was repotted and reinstated in FAT.

PD7100075-003; S/N 0000066.-
Failure Report B50956
Failure Analysis Report - Not applicable
History: This unit successfully completed FAT but was found to have a damaged housing before installation in a detector. Via MRB disposition, a functional recheck was performed on the switch and checked against its original FAT data. There was no degradation in the switch. The microswitch section was removed from the damaged housing and used to refurbish pressure actuated switch S/N 0000027 installed in detector C1, S/N 0000101. The detector after the above rework passed FAT retest.

PD7100075-003; S/N 0000069.-
Failure Report B50953
Failure Analysis - Not applicable
History: Unit failed contact resistance portion of functional test following FAT temperature cycle test. Ten readings were

taken with a resultant average contact resistance equivalent of 96.3 microvolts at 100 microamps current. The maximum allowable was 32 microvolts. NASA-LRC requested a special test be run on a scrapped E1A detector S/N 0000103 to evaluate the thermal lag of the switch body in accelerated life cycle test. The microswitch section of pressure actuated switch S/N 0000069 was removed and the body housing welded into the E1A test specimen. Thermocouples were attached to the switch and engineering personnel performed the thermal lag test on the E1A test specimen.

PD7100075-003; S/N 0000059.-
Failure Report B50951
Failure Analysis - Not applicable
History: This unit exhibited high contact resistance following temperature cycling test. An average over ten readings was 55.5 microvolts drop at 100 microamps current. The maximum allowable is 32 microvolts. No failure analysis was performed on this unit because it was released, as is, to Mr. B. B. Brown, Jr. on November 5, 1968. Mr. Brown had requested this unit for a NASA-LRC test specimen.

PD7100075-003; S/N 0000164.-
Failure Report B50950
Failure Analysis Report - Not applicable
History: While mounting this switch in the dynamics fixture the number five wire lead was damaged. The insulation was nicked and several wire strands sheared. A technician's wrench slipped causing the wire damage. Via MRB disposition, the damaged section of wire was cut off (approximately a 7-in. section) and the unit was reinstated in FAT.

PD7100075-003; S/N 0000169; S/N 0000172; S/N 0000174.-
Failure Report B50696
Failure Analysis Report - Not applicable
History: Vendor did not provide proper identification on wire leads per procurement specification. Via MRB disposition a wrap-around plastic marker was permitted for wire identification. Also, a heat shrinkable plastic sleeve was added to cover nicked wire insulation.

PD7100075-003; S/N 0000169; S/N 0000172; S/N 0000174.-
Failure Report B50949
Failure Analysis Report - Not applicable
History: This failure report was cancelled. The Martin Marietta inspector overlooked vendor MRB request stated in the previous paragraph and therefore rejected the subject switches for the same reason stated there. (Failure Report B50949 was cancelled.)

PD7100075-003; S/N 0000151 thru S/N 0000162.-
Failure Report B50694
Failure Analysis Report - Not applicable
History: Vendor could not procure proper wire lead marker identification material. MRB disposition permitted single plastic wire leak marker for the subject units.

PD7100075-003; S/N 0000179; S/N 0000180; S/N 0000182; S/N 0000183.-
Failure Report B55668
Failure Analysis Report - Not applicable
History: Vendor could not procure proper wire lead marker identification material. MRB disposition permitted single plastic wire lead marker for the subject units.

PD7100075-003; S/N 0000175.-
Failure Report B55669
Failure Analysis Report - Not applicable
History: Vendor requested MRB disposition for same condition stated in two previous paragraphs. This was the final unit purchased under the initial purchase agreement.

PD7100075-003; S/N 0000183.-
Failure Report B66496
Failure Analysis Report 8280-30
History: During ALC Testing at the 3000th cycle check point, the switch failed to transfer when backpressure was applied to verify switch trip points. Upon visual examination the switch vent-port filter was found to be blocked. The switch was removed from its holder, the blocked vent filter was removed and the switch was reassembled. In subsequent backpressure checks at 3000-cycle intervals, the low-pressure setting was below specification minimum of 3.5 psig. A glycerin film contamination coupled with possible marginal reassembly (adjustment screw-in depth) was suspected as the cause for the below specification readout on pressure set points. After 21 344 cycles, the switch was cleaned to remove all glycerin contaminates and reassembled. The readings were improved; however, the low point was still 0.3 psig below specification. At this point, experimentation on the screw-in depth was accomplished. The pressure settings were brought to within specification requirements by adjustment of the screw-in depth. Misadjustment on reinstallation of the switch following its initial disassembly and after cleaning at the 21 344 cycle point was determined as the cause of low pressure readout during functional checks.

APPENDIX C

## Summary of Switch Functional Parameters

To obtain a trend of switch functional parameters response to the induced environments, statistical analyses were made. In both cases (pressure transfer point and contact resistance) the mean does not change as much as the standard deviation, and then this change only occurs on the normally closed (open with pressure applied) sets of contacts. The most notable change occurred after the thermal vacuum soak test. Without a thorough examination of the switch contacts, no positive reason can be set forth. However, the measurements of contact resistance react in much the same manner as previous cases where the contacts were dirty. The most probable cause is assumed to be foreign matter on the open set of contacts. The only source of this matter must be the inert fill gas used to seal the microswitches. The shift in pressure point measurements can also be blamed on contamination of the biasing mechanism from foreign material entering the upper switch body through the vent port. It could also be caused by temporary (several days) or permanent change in the Belleville spring characteristics. This analysis was brief in an attempt to ascertain if the induced environments produced any trend in functional parameters. The conclusions are suppositional and would require a thorough test and analysis program to verify them.

Pressure transfer point.- Using the pressure switch data gathered during qualification testing of the MPDD detectors/panels, a statistical study was made to determine if any change in the switch point pressures occurred between initial readings and readings after thermal vacuum soak. Based on the 20 units tested there were no significant differences in the measurements of the means and standard deviations. The results are shown in the following tabulation.

| | Initial readings | | After T/V soak | |
|---|---|---|---|---|
| | Increasing pressure, psig | Decreasing pressure, psig | Increasing pressure, psig | Decreasing pressure, psig |
| $\overline{X}$ Mean | 6.9 | 5.4 | 6.7 | 5.1 |
| S Std Dev | .6 | .5 | .6 | .98 |

# APPENDIX C

Contact resistance.- Using the summary of switch contact resistance measurements, a statistical study was made to determine if any change in the contact resistance occurred between the initial readings and readings after thermal vacuum soak. Based on the data from the 20 units tested (table 23) there were changes in the open contact set means and standard deviations. No significant difference was noticed in the means and standard deviations of the closed contact sets. The results are shown in the following tabulation.

| | Initial readings | | | | After T/V soak | | | |
|---|---|---|---|---|---|---|---|---|
| | at 0 psi + 0.5 A | at 0 psi + 100 uA | at 10 psi + 0.5 A | at 10 psi + 100 uA | at 0 psi + 0.5 A | at 0 psi + 100 uA | at 10 psi + 0.5 A | at 10 psi + 100 uA |
| $\overline{X}$ (Mean) | 43.0 mv | 8.3 uv | 42.5 mv | 8.2 uv | 52.8 mv | 11.2 uV | 42.1 mv | 8.9 uv |
| S Std Dev | 2.3 mv | 2.2 uv | 1.9 mv | 1.9 uv | 18.7 mv | 5.0 uv | 2.4 mv | 1.3 uv |

TABLE 23.- SUMMARY OF SWITCH CONTACT RESISTANCE MEASUREMENTS OBTAINED DURING QUALIFICATION TESTING

| Item | Part no. | Serial no. | Pressure switch serial no. | Initial measurements | | | | After dynamics | | | | After acoustics | | | | After thermal vacuum soak | | | |
|---|---|---|---|---|---|---|---|---|---|---|---|---|---|---|---|---|---|---|---|
| | | | | At 0 psi & 0.5 A, mV | At 0 psi & 100 μA, μV | At 10 psi & 0.5 A, mV | At 10 psi & 100 μA, μV | At 0 psi & 0.5 A, mV | At 0 psi & 100 μA, μV | At 10 psi & 0.5 A, mV | At 10 psi & 100 μA, μV | At 0 psi & 0.5 A, mV | At 0 psi & 100 μA, μV | At 10 psi & 0.5 A, mV | At 10 psi & 100 μA, μV | At 0 psi & 0.5 A, mV | At 0 psi & 100 μA, μV | At 10 psi & 0.5 A, mV | At 10 psi & 100 μA, μV |
| B1A | 8280-04000 | 0000101 | 0000075 | 93.1 | 9.9 | 39.8 | 7.8 | 41.5 | 11.1 | 38.8 | 8.0 | 41.9 | 11.2 | 40.2 | 9.0 | 40.3 | 12.3 | 40.0 | 11.8 |
| | | | | 43.7 | 6.9 | 44.1 | 7.5 | 43.1 | 8.3 | 43.1 | 7.0 | 44.3 | 7.2 | 44.3 | 8.1 | 43.2 | 9.5 | 43.3 | 10.3 |
| | | | 0000037 | 41.0 | 10.6 | 40.1 | 10.9 | 39.8 | 11.0 | 38.9 | 9.7 | 41.3 | 10.3 | 40.1 | 9.1 | 45.7 | 8.8 | 40.1 | 7.8 |
| | | | | 47.1 | 9.1 | 43.0 | 9.7 | 43.3 | 9.7 | 41.2 | 9.3 | 42.6 | 7.3 | 42.9 | 8.3 | 44.3 | 11.9 | 43.8 | 11.0 |
| B1A | 8280-04000 | 0000103A | 0000058 | 40.6 | 6.2 | 40.8 | 7.2 | 39.1 | 8.8 | 40.2 | 7.1 | 40.5 | 11.3 | 40.5 | 8.3 | | | | |
| | | | | 44.5 | 8.2 | 44.1 | 9.1 | 43.4 | 8.2 | 42.9 | 7.8 | 43.7 | 4.2 | 43.6 | 6.2 | | | | |
| | | | 0000071 | 39.8 | 8.1 | 39.8 | 7.8 | 38.0 39.1 | 10.2 10.6 | 38.8 39.4 | 9.2 11.0 | 39.2 | 12.2 | 39.5 | 9.6 | 38.7 | 7.0 | 38.4 | 7.7 |
| | | | | 44.0 | 8.3 | 45.1 | 8.3 | 43.8 47.8 | 8.8 9.9 | 43.5 43.2 | 9.0 9.9 | 44.0 | 1.4 | 44.3 | 4.5 | 48.8 | 11.5 | 44.6 | 9.2 |
| | | | 0000179 | | | | | 41.9 | 9.1 | 40.1 | 9.3 | 41.4 | 4.7 | 39.6 | 6.4 | 42.1 | 8.2 | 40.7 | 7.0 |
| | | | | | | | | 44.9 | 10.8 | 44.8 | 11.1 | 44.5 | 6.6 | 44.3 | 7.7 | 45.3 | 9.6 | 45.9 | 9.5 |
| C1 | 8280-07000 | 0000104 | 0000048 | 43.0 | 12.0 | 40.8 | 11.4 | 43.0 | 12.6 | 41.5 | 9.4 | 42.1 | 11.3 | 40.9 | 9.7 | 78.6 | 13.9 | 39.4 | 8.6 |
| | | | | 41.2 | 12.3 | 44.9 | 11.6 | 46.2 | 9.2 | 45.1 | 8.6 | 44.2 | 9.6 | 43.6 | 9.7 | 101.9 | 31.5 | 46.0 | 8.9 |
| | | | 0000049 | 45.2 | 9.6 | 44.5 | 8.8 | 44.5 | 14.1 | 43.7 | 13.1 | 44.8 | 12.3 | 43.7 | 11.0 | 48.3 | 12.3 | 40.5 | 10.0 |
| | | | | 46.1 | 7.7 | 45.1 | 8.3 | 45.1 | 10.4 | 44.8 | 11.1 | 48.8 | 9.5 | 48.7 | 9.8 | 92.3 | 19.0 | 45.9 | 10.3 |
| C1 | 8280-07000 | 0000107 | 0000158 | 40.6 | 8.5 | 40.9 | 7.2 | 39.3 | 6.4 | 39.9 | 5.8 | 39.7 | 9.6 | 40.1 | 8.1 | 39.5 | 7.2 | 39.4 | 9.0 |
| | | | | 43.3 | 8.3 | 43.4 | 8.5 | 42.0 | 6.9 | 42.5 | 7.0 | 42.5 | 4.3 | 42.6 | 3.9 | 43.6 | 9.5 | 43.8 | 10.2 |
| | | | 0000160 | 40.8 | 6.4 | 40.5 | 6.6 | 39.1 | 9.8 | 39.0 | 9.2 | 40.4 | 5.4 | 40.3 | 6.4 | 40.9 | 9.6 | 39.1 | 8.4 |
| | | | | 43.8 | 8.0 | 44.1 | 8.0 | 42.0 | 9.9 | 42.5 | 8.7 | 43.2 | 3.0 | 43.4 | 4.6 | 46.6 | 10.7 | 44.0 | 10.2 |
| D2A | 8280-13000 | 0000102 | 0000042 | 40.9 | 8.4 | 41.2 | 8.8 | 41.2 | 9.2 | 41.5 | 9.8 | 41.4 | 10.3 | 40.6 | 11.8 | 56.0 | 9.7 | 41.1 | 7.1 |
| | | | | 44.9 | 8.5 | 44.7 | 9.5 | 45.6 | 10.1 | 45.2 | 10.7 | 44.9 | 9.0 | 44.3 | 11.4 | 93.8 | 13.5 | 44.6 | 8.4 |
| | | | 0000041 | 42.0 | 8.7 | 41.0 | 8.8 | 42.9 | 9.4 | 41.4 | 10.7 | 42.2 | 12.4 | 42.0 | 12.8 | 40.6 | 8.5 | 40.7 | 9.0 |
| | | | | 44.6 | 8.7 | 44.9 | 9.7 | 45.1 | 9.8 | 45.4 | 11.1 | 45.0 | 10.3 | 45.8 | 12.4 | 45.9 | 11.6 | 44.2 | 10.8 |
| D3A | 8280-16000 | 0000101 | 0000054 | 40.9 | 8.8 | 39.9 | 6.3 | 40.2 | 2.9 | 39.5 | 4.7 | 40.3 | 11.3 | 39.6 | 9.7 | 94.1 | 20.6 | 39.5 | 8.3 |
| | | | | 44.2 | 2.2 | 44.1 | 3.3 | 43.4 | 7.6 | 43.6 | 8.6 | 43.8 | 7.6 | 43.6 | 8.1 | 47.2 | 9.2 | 43.9 | 8.7 |
| E1A | 8280-19000 | 0000102 | 0000062 | 41.4 | 6.4 | 40.5 | 5.9 | 40.7 | 10.4 | 40.5 | 7.9 | 40.5 | 8.6 | 40.1 | 9.6 | 44.6 | 8.3 | 40.1 | 5.7 |
| | | | | 44.9 | 5.7 | 44.5 | 6.4 | 45.4 | 3.6 | 44.4 | 6.7 | 44.9 | 6.4 | 44.1 | 8.5 | 44.8 | 10.5 | 44.6 | 9.3 |
| E3A | 8280-25000 | 0000101 | 0000072 | 41.9 | 10.4 | 41.1 | 7.2 | 40.9 | 10.5 | 40.2 | 10.1 | 41.6 | 14.2 | 40.8 | 10.9 | 41.8 | 6.9 | 38.8 | 7.6 |
| | | | | 51.1 | 4.0 | 44.5 | 3.9 | 46.3 | 12.6 | 43.6 | 12.6 | 46.0 | 4.6 | 44.2 | 7.5 | 56.5 | 13.6 | 43.5 | 9.6 |
| F1A | 8280-28000 | 0000101A | 0000166 | 42.1 | 10.4 | 41.0 | 7.1 | 39.3 | 9.4 | 39.3 | 10.2 | 39.4 | 7.8 | 38.9 | 7.0 | 39.8 | 7.8 | 39.6 | 7.0 |
| | | | | 44.8 | 4.9 | 43.8 | 7.3 | 42.8 | 9.3 | 42.8 | 11.4 | 42.6 | 6.5 | 42.5 | 6.9 | 43.3 | 8.3 | 43.2 | 8.5 |
| | | | 0000154 | 40.5 | 7.4 | 40.3 | 7.0 | 39.8 | 12.0 | 39.1 | 9.2 | 39.4 | 8.5 | 38.8 | 8.3 | 40.0 | 8.7 | 39.0 | 10.5 |
| | | | | 43.3 | 6.4 | 43.4 | 6.3 | 42.7 | 12.4 | 42.9 | 11.9 | 42.4 | 7.4 | 42.4 | 8.0 | 43.5 | 7.5 | 42.9 | 10.1 |
| F1A | 8280-28000 | 0000108 | 0000022A | 41.0 | 7.0 | 39.8 | 9.6 | 40.9 | 8.4 | 39.4 | 8.4 | 41.7 | 10.4 | 41.2 | 8.4 | No measurements, unit failed prior to this test | | | |
| | | | | 44.9 | 13.1 | 42.5 | 11.4 | 45.0 | 10.5 | 43.7 | 9.9 | 44.7 | 6.7 | 44.6 | 6.6 | | | | |
| | | | 0000173 | 41.5 | 9.7 | 40.7 | 9.5 | 41.7 | 9.4 | 40.7 | 9.6 | 40.7 | 12.2 | 40.4 | 10.1 | | | | |
| | | | | 43.8 | 11.2 | 44.0 | 11.0 | 44.5 | 10.1 | 44.1 | 10.5 | 45.4 | 10.5 | 43.8 | 9.8 | | | | |
| F1A | 8280-28000 | 0000109 | 0000174 | 41.2 | 9.3 | 40.4 | 8.3 | 43.4 | 14.9 | 40.5 | 13.6 | 42.8 | 8.6 | 40.6 | 8.5 | No readings taken | | | |
| | | | | 43.9 | 9.6 | 44.4 | 9.4 | 45.5 | 5.9 | 44.2 | 9.0 | 44.8 | 7.9 | 44.5 | 8.0 | | | | |
| | | | 0000170 | 40.5 | 9.1 | 40.5 | 9.3 | 39.7 | 15.3 | 39.6 | 13.4 | 40.3 | 9.3 | 39.4 | 8.7 | | | | |
| | | | | 43.7 | 7.3 | 44.2 | 7.9 | 44.2 | 5.7 | 44.9 | 9.1 | 44.6 | 7.9 | 44.9 | 9.5 | | | | |

APPENDIX C

B1A Detector Panel Failure Reports

8280-04000; S/N 0000105.-
Failure Report B42082
Failure Analysis Report 8280-13
History: During FAT thermal cycling test a no-go signal was received on the console for switch S/N 0000155 while at -20°F to -40°F. A go condition was indicated throughout the warming cycle. Initially, an incorrect wiring condition led to the no-go signals and was corrected. The no-go signals again were received at various points in the cold cycle. The failure was caused by low helium pressurization in the specimen brought about by insufficient soak time to allow the pressure to stabilize before pinch off. The helium fill procedure was changed to allow the panel pressure to stabilize and testing was resumed via MRB disposition action. The same condition occurred for B1A, S/N 0000101, S/N 0000102 and S/N 0000104. The failure investigation was performed to cover all four units since S/N 0000105 and S/N 0000102 ran together in the fixture and S/N 0000101 and S/N 0000104 were together in the fixture.

8280-04000; S/N 0000102.-
Failure Report B42084
Failure Analysis Report 8280-13
History: No-go signal during cold cycle side at -20°F to -40°F on switch S/N 0000053. Refer to S/N 0000105 above for failure analysis information and MRB disposition.

8280-04000; S/N 0000101.-
Failure Report B42083
Failure Analysis Report 8280-13
History: No-go signal during cold cycle on switch S/N 0000075. Refer to S/N 0000105 above for failure analysis information and MRB disposition.

8280-04000; S/N 0000104.-
Failure Report B42085
Failure Analysis Report 8280-13
History: No-go signal during cold cycle on switch S/N 0000060. Refer to S/N 0000105 above for failure analysis information and MRB disposition.

8280-04000; S/N 0000105.-
Failure Report B42100
Failure Analysis Report 8280-15
History: No-go signal occurred during FAT temperature cycle test on switch S/N 0000155. The switch vent port was clogged with potting compound that prevented a back pressure check of the panel

pressurization level. Via MRB disposition the vent port was carefully reamed out to clear the obstruction; the unit was repressurized and rechecked via the vent port and reinstated in FAT temperature cycle test.

8280-04000; S/N 0000102.-
Failure Report B65067
Failure Analysis Report 8280-21
History: During ALC testing at cycle 4670 the panel signalled a loss of pressure on switch S/N 0000053 side of the detector. Failure analysis determined the cause of failure as a cyclic fatigue resulting in a crack in the target area parent metal (8280-04053-01). The crack was 0.10-in. long, oriented parallel to the length of the panel. It was 6.25-in. up from the 45° corner cutoff. A high bending stress was induced in the panel as a result of the clamping technique employed to mount the panel in the ALC fixture. The mounts were redesigned. Via MRB action both switch assemblies in this unit were salvaged and used in a new build effort to replace S/N 0000102. B1A, S/N 0000107 (new build) used the switch assemblies S/N 0000053 and S/N 0000056 from the scrapped B1A, S/N 0000102. B1A, S/N 0000105 replaced B1A, S/N 0000102 as ALC test specimen.

8280-04000; S/N 0000103.-
Failure Report B65064
Failure Analysis Report 8280-19
History: This unit leaked following the acoustic qualification test at switch S/N 0000058. The failure analysis determined the leak source to be a circumferential crack in the parent metal of the switch cup. The crack began at the brazed joint of the switch cup and gas tube. It was approximately 0.20-in. long and directly in the switch cup forming radius. The panel was salvaged via MRB action coordinated between NASA-LRC and Martin Marietta Engineering. The defective switch assembly S/N 0000058 was removed and replaced with switch assembly S/N 0000179, which in turn was modified to incorporate a soft, serpentine design gas transfer tube. This modification was directed by design and fabrication parameters set up on MRB MARS supplemental data sheets 1 thru 4. This modification has been referred to as Modification 1 in all liaison contact with NASA-LRC and Martin Marietta Engineering.
NOTE: The modification survived all qualification retests directed as a result of the MRB action. Refer to the next paragraph for the final action on this panel. Following the incorporation of Modification 1 on switch S/N 0000179 this panel assembly was assigned S/N 0000103A.

8280-04000; S/N 0000103A.-
Failure Report B66038
Failure Analysis Report 8280-25
History: During Qualification acoustics retest directed as a result of Modification 1 (Refer to preceding paragraph), a loss of pressure was experienced on switch S/N 0000071 side of the panel. The leak was pinpointed under the base of fill tube fitting (8280-10056-01). Failure analysis revealed the pressure loss to be caused by fracture extending along the periphery of the ringweld in the fitting to target sheet. Excessive fatigue bending was evident from the discoloration of the metal along the fracture, induced by frictional heat. Oxidation was only evident on the outside surface of the metal. The inner surface, blanketed by helium, was not discolored; therefore, it was concluded that frictional heat in acoustics testing induced the failure. This switch, S/N 0000071 had the original configuration gas transfer tube and had seen two complete Qualification Test sequences, except for a final leak and functional test. The switch, S/N 0000071 detector half was considered qualified after the first test sequence. The switch with the modified tube, S/N 0000179, survived all Qualification testing.

8280-04000; S/N 0000104.-
Failure Report B69832
Failure Analysis Report 8280-29
History: Upon completion of 21 344 cycles in ALC the no. 2 set of contacts (wire leads 4, 5, and 6) on which S/N 0000060 failed to transfer on both increase and decrease pressure applications. Because there are dual microswitch installations in the pressure-actuated switch, this phenomenon represented a partial failure of switch S/N 0000060. Under visual inspection the switch failed to disclose any evidence of damage. The microswitch holder was removed and examined visually. Again, no damage was evident, either in the switch or in the Belleville spring assembly. Upon reinstallation, the switch functioned properly when subjected to a complete functional (electrical and mechanical recheck) test. The microswitches were removed, cut open and examined under a microscope. They appeared in good condition and nothing was evident inside the switch capable of causing a malfunction. It was concluded that the initial malfunction was attributed to possible marginal installation on the screw-in depth of the microswitch holder. As stated, upon reinstallation, the switch functioned properly. This failure, therefore, is considered a random, unverified failure.

APPENDIX C

## C1 Detector Panel Failure Reports

8280-07061-29; S/N 0000101.-
Failure Report B50941
Failure Analysis Report 8280-7
History: Following FAT dynamics testing, switch S/N 0000027 exhibited a contact resistance equivalent to voltage drop of 268.8 microvolts at 100 microamps current. Specification maximum is 32 microvolts. Failure analyses disclosed a misaligned warped actuation arm in the microswitch section of the switch assembly. Poor contact on the normally closed set of switch points caused the high contact resistance. Via MRB action the electrical section of switch S/N 0000066 was salvaged following a retest for integrity and was installed in C1, S/N 0000101. Following the rework of switch S/N 0000027 the unit was designated S/N 0000027A and the C1, S/N 0000101 was reinstated in FAT. The unit passed all FAT testing.

8280-07061-20; S/N 0000102.-
Failure Report B50970
Failure Analysis Report 8280-9
History: Panel leaked at a rate of $3.3 \times 10^{-7}$ scc/sec in vacuum. Failure analysis disclosed leakage at both fill tube fitting ringwelds on the panel. Defective ringwelds are not reparable once the spotwelds have been made. This unit was scrapped. A replacement panel S/N 0000107 was fabricated to replace the scrapped unit. Poor workmanship was attributed as cause of ringweld failure.

## D2A Detector Failure Reports

8280-13000; S/N 0000101.-
Failure Report B50966
Failure Analysis - Not applicable
History: This unit exhibited an excessive leak at a test condition of $6.9 \times 10^{-6}$ torr during RGA test of FAT. The unit was removed from the chamber and the leak located in the fusion weld at the end of the fill tube fitting. Via MRB action the weld was ground and rewelded. The unit was reinstated in RGA and successfully completed the FAT sequence.

8280-13000; S/N 0000103.-
Failure Report B66040
Failure Analysis - Not applicable
History: After completion of FAT, following the final helium pressurization, this unit was found to be leaking at the fill tube end. Several attempts were made at rewelding but the leak persisted. Via MRB action the fill tube fitting was cut off approximately 1/32-in. below the fusion weld; a .083-in. diameter tube was brazed into the existing fill tube; the unit was repressurized, pinched-off, and end brazed in lieu of welding. The repair was successful. The final leak rate was $2.09 \times 10^{-8}$ scc/sec in a vacuum of $4.5 \times 10^{-6}$ torr. The leakage permissable per specification is $1.6 \times 10^{-7}$ scc/sec at a vacuum of $1 \times 10^{-5}$ torr or more. The unit was prepared for delivery following this MRB action.

## D3A Detector Failure Reports

8280-16000; S/N 0000102.-
Failure Report B66037
Failure Analysis Report 8280-22
History: During ALC testing at cycle 14 346 a loss of pressure signal was received at the test console. Failure analysis of the test specimen disclosed a cracked spotweld in the 0.016-in. backup sheet (8280-16052-01). The crack was found to have terminations at the intersection of crease in the backup sheet and the spotweld boundary. Several other slightly creased (crippled) areas were evident in the panel. Failure was caused by bending stress induced crippling along the 40.0-in. dimension. This crippling was attributed to the clamping technique employed to mount the detector on the ALC fixture. A redesign was made and incorporated into all fixtures housing the 40.0x49.0-in. detectors. Via MRB disposition the crack was brazed to prevent growth and the specimen reinstated in ALC testing. This MRB action was coordinated with NASA-LRC before implementation on the specimen.

8280-16000; S/N 0000102.-
Failure Report B66833
Failure Analysis Report 8280-28
History: Upon completion of 21 344 cycles of ALC test, the detector exhibited a low pressure during the routine backpressure check. The detector internal pressure indicated slightly less than 8 psi lower than its ambient 35.5 psia pressurization level. The point of failure was isolated to a single spotweld located roughly near the center of the first row of spotwelds adjacent to the electric bus bar. The failure was virtually at the same

location as the previous failure on this detector (reference preceding failure analysis report 8280-22), but on its opposite edge. This specimen had previously been rigidly clamped, and as stated in the preceding failure report, several crippled areas were evident at the 14 346th cycle point in ALC. At this point, the clamping technique was redesigned. It is concluded that the failure was caused via the initial clamping method and its contribution to crippling the detector. The subsequent cycling from 14 346 to 21 344 induced the fatigue failure. The spotweld leak isolation was determined by vacuum chamber check to confirm the presence of a leak and was then isolated by CEC mass spectrometer to the aforenoted spotweld.

## E1A Detector Failure Reports

8280-19000; S/N 0000101.-
Failure Report B50939
Failure Analysis - Not applicable
History: At completion of welding operations radiographic inspection disclosed a crack in the overspot at a seamweld junction. The unit was permitted to go into FAT and was required to be X-rayed again in the area of the crack following FAT. This action was authorized via MRB disposition. The unit successfully completed all FAT and was re-X-rayed. There was no change in the cracked area following test.

8280-19051-20; S/N 0000103.-
Failure Report B50969
Failure Analysis Report 8280-10
History: During initial leak test of FAT this unit leaked at a rate of $8.2 \times 10^{7}$ scc/sec. Permissable leakage shall not exceed $1.0 \times 10^{-8}$ scc/sec. The leak was isolated to the switch assembly S/N 0000064. Failure analysis pinpointed the leak source to the switch diaphragm. Under microscopic examination the point of failure was determined to be diaphragm fatigue caused by a deep scratch in the parent metal. This detector was scrapped. Latent defect notice was forwarded to the switch vendor. At the time of failure, two other switch assemblies (scrapped units) were investigated for similar defects, but none was found. E1A, S/N 0000105 was built to replace this scrapped unit.

8280-19000; S/N 0000105.-
Failure Report B60712
Failure Analysis Report 8280-11
History: Following FAT dynamics, this unit leaked at a rate of $6.4 \times 10^{7}$ scc/sec. The leak was pinpointed to switch S/N 0000029. Failure analysis disclosed the leak source to be several spots in the weld of the switch diaphragm to the upper switch shell and lower switch case. The leak was confined to the interior side of the switch only. Weld porosity and/or minute burnthrough of the diaphragm were the suspected cause of the leakage. Via MRB

action switch S/N 0000162 was installed to replace the failed switch S/N 0000029. The unit, E1A, S/N 0000105 was reinstated in FAT and successfully completed all tests.

8280-19052-01; target sheet detail.-
Failure Report B60693
Failure Analysis Report - Not applicable
History: The height of the volcano was trimmed out of plane with the base of the target sheet. Height measured 0.406 to 0.455 in. This flange should have been $0.44 \begin{smallmatrix} +0.030 \\ -0.000 \end{smallmatrix}$ in. Via MRB disposition this detail was used as is in the new build of E1A, S/N 0000105. Special care was taken when installing the switch assembly. This unit completed all testing successfully.

## E3A Detector Failure Reports

8280-25000; S/N 0000102.-
Failure Report B55773
Failure Analysis Report 8280-14
History: During ALC testing, at about 3300 test cycles, the control thermocouple recorder malfunctioned and called for continuous heat input to the test specimen. The overheating condition caused the wood clamp bars to relax pressure and in turn loosened the aluminum bus bars. Arcing resulted and partially melted the test specimen. The unit was burned beyond recovery and was scrapped. The cause of failure was evident on the fixture and several fixes were incorporated to preclude as recurrence of this problem. Proper kill circuit latching relay was installed to replace an existing nonlatching relay in the circuit. Maple bars replaced the fir wood bars in the fixture and the Bristol recorder was rechecked to ensure smooth operation. E3A, S/N 0000104 replaced the failed unit in ALC.

8280-25000; S/N 0000104.-
Failure Report B65063
Failure Analysis Report 8280-16
History: During ALC testing on automatic operation, personnel working in another area of the test facility inadvertently shut off partial power to the E3A test setup. The circuit shutdown was providing power to the signal conditioning amplifier supplying temperature data to the E3A detector Bristol temperature recorder. Hence, the recorders for both control and monitor ceased to function, resulting in overheating the specimen. The specimen was burned and warped beyond recovery. This was classified as a facility failure rather than specimen failure, thus S/N 0000103 was introduced into ALC testing to replace E3A, S/N 0000104.

Replacement E3A detectors, S/N 0000105 and S/N 0000106 were fabricated to replace scrapped S/N 0000102 and S/N 0000104. Both of these units successfully met all FAT test requirements and were subsequently delivered to NASA-LRC.

## F1A Detector Panel Failure Reports

8280-28000; S/N 0000101 and S/N 0000102
Failure Report B50965
Failure Analysis Report - Not applicable
History: In the process of splicing the F1A half panels, the monel rivets were too hard for the thin gages of panel material and the splice straps. The rivets swelled in driving causing the target sheets and core sheets to buckle and become distorted. Acceptable riveting quality could not be achieved. This event was classified as a design deficiency and engineering changes were processed to change from monel to aluminum riveting on all subsequent fabrication. Via MRB action both F1A, S/N 0000101 and S/N 0000102 were dispositioned "use as is" with monel riveting and were directed to be assigned to ALC use only.

8280-28000; S/N 0000101.-
Failure Report B60691
Failure Analysis - Not applicable
History: During the fabrication splice operation this unit was damaged by the drill tool chaffing against the target area of the panel. The interference caused a slight abrasion in the target area. Via MRB disposition the panel was accepted as is and designated for ALC usage.

8280-28000; S/N 0000101.-
Failure Report B65014
Failure Analysis Report 8280-18
History: This unit failed its final leak test of FAT following temperature cycling. A leak rate of $1.0 \times 10^{-7}$ scc/sec was recorded while in a test condition of $4.8 \times 10^{-6}$ torr. Via failure analysis the unit was found to be leaking in the parent metal of the fill tube fitting. The pore was too small to be picked up with any equipment other than the Veeco MS-12A Mass Spectrometer. The leak was confined to the switch S/N 0000167 side of the detector panel. An MRB disposition was rendered to salvage the switch S/N 0000166 half of the panel and splice it to the switch S/N 0000154 half of F1A, S/N 0000102. After splicing the unit was designated F1A, S/N 0000101A. This new unit, S/N 0000101A was assigned as a Qualification specimen. The unit survived all Qualification testing. (Refer to S/N 0000102 for data concerning the assignment of switch S/N 0000154 from F1A, S/N 0000102 into F1A, S/N 0000101A.

8280-28000; S/N 0000102.-
Failure Report B60692
Failure Analysis Report - Not applicable
History: Switch mounting bracket, 8280-28017-02, was not to the latest engineering change. The part was fabricated to Change C, but should have been to Change E. The changes concerned material thickness revision from 0.027 in. (Change C configuration) to 0.020 (Change E configuration). MRB disposition authorized a "use as is" decision since the bracket was functionally and physically interchangeable except for the material thickness and assigned it to ALC usage.

8280-28000; S/N 0000102.-
Failure Report B42462
Failure Analysis Report 8280-18
History: This unit failed its final leak test of FAT following temperature cycling. A leak rate of $6.0 \times 10^{-7}$ scc/sec was recorded while in a test condition of $5.0 \times 10^{-6}$ torr. Via failure analysis the unit was found to be leaking severe enough to pinpoint its source to the fill tube fitting at the ringweld. The leak was caused by a pore in the parent metal of the fitting. The leak was confined to the switch S/N 0000153 detector half. An MRB disposition was rendered to salvage the switch S/N 0000154 half of the panel and splice it to the salvaged switch S/N 0000166 half of F1A, S/N 0000101. The newly spliced unit was assigned to Qualification testing as F1A, S/N 0000101A following successful completion of a recheck of the individual panel halves. This unit (S/N 0000101A) successfully completed all Qualification testing. NOTE: S/N 0000101A was the F1A qualification specimen representative of the original configuration of a straight interconnection of the gas transfer tube from the fill tube fitting to the switch cup.

8280-28000; S/N 0000103.-
Failure Report B55774
Failure Analysis Report 8280-17
History: This detector panel failed its final leak test in FAT following temperature cycling. The leak was too great to obtain a leak rate since the roughing cart for the vacuum chamber could not be valved out of the test setup. Failure analysis was performed using microscopic examination to evaluate the leak point. The leak source was the result of a crack in the switch-to-switch cup weld bead. The weld was accomplished in two passes with an apparent cold shut between the two weld passes. The leak path was apparently opened up as a result of thermal cycling. The leak was isolated to switch S/N 0000163 half only. Via MRB action the switch S/N 0000168 half of this panel was salvaged

and respliced to a newly built half panel to complete an F1A configuration. The new half section used a salvaged switch assembly from F1A, S/N 0000105. Following the rework in accordance with MRB instructions the unit was identified F1A, S/N 0000103A. This panel (S/N 0000103A) was rerouted back through a complete FAT retest successfully and was then assigned to ALC. It went to ALC with the switch S/N 0000168 half of the panel exhibiting the original design on the gas interconnect tube. The switch S/N 0000164 half of the panel was worked in accordance with the disposition of MRB instructions defined on MARS B65065 supplemental data sheets number 1 thru 4. This document contained all the fabrication details and parameters referred to as Modification 2 in Martin Marietta and NASA-LRC liaison concerning the F1A detector panels.

8280-28000; S/N 0000105.-
Failure Report B42091
Failure Analysis Report 8280-12
History: During temperature cycling of FAT at 73rd to the 81st cycle the panel burned. Failure analysis disclosed that the failure was the result of the splice having a higher electrical resistance than the remainder of the panel. This resulted in hot spots when passing current through the detector panel. Differential expansion caused loosening of rivets, followed by arcing to the point of ruining the panel. Severe burning occurred at the splice. The panel was scrapped. Switch assembly S/N 0000164 was salvaged from the scrapped F1A, S/N 0000105 and used in the new build of a half panel section of F1A, S/N 0000103A. (Refer to the previous paragraph for the details of F1A, S/N 0000103A.)

8280-28000; S/N 0000109.-
Failure Report B42092
Failure Analysis Report - Not applicable
History: The interconnect tube between the fill tube fitting and the interconnect splice was blocked with weld on switch S/N 0000174 side of the panel. This was not known when the panel was subjected to dynamics FAT. The blockage was discovered when the panel was being repressurized for the temperature cycling test of FAT. Via MRB disposition the blockage was corrected, the unit was leak checked and reinstated in FAT for the temperature cycle test. In the interim F1A, S/N 0000108 failed following acoustics test in Qualification. NASA-LRC along with Martin Marietta directed F1A, S/N 0000109 to be reassigned from an ALC specimen to a Qualification specimen. In addition, following the thermal vacuum soak test of Qualification, the F1A, S/N 0000109 was to be modified at both switch assemblies to a Modification 2 configuration (flexible serpentine interconnect tube).

8280-28000; S/N 0000109.-
Failure Report B65068
Failure Analysis Report 8280-26
History: Following thermal vacuum soak of Qualification testing, this unit was found to be leaking at the switch S/N 0000174 half. The leak was discovered at a $4.0 \times 10^{-4}$ torr vacuum chamber pressure. Mass spectrometry later isolated the leak at the brazed joint of the gas transfer tube at the switch cup forming radius. Flux contaminate had disintegrated during thermal vacuum soak opening the leak path. The brazed joint was repaired per MRB disposition and the serpentine gas transfer tube (Modification 2) was made to both switch assemblies (S/N 0000170 and S/N 0000174) of this detector panel. The panel, following this action, successfully completed all assigned Qualification testing.

8280-28000; S/N 0000104.-
Failure Report B42097
Failure Analysis Report 8280-12
History: This unit was accompanying F1A, S/N 0000105 in FAT temperature cycle test when damaged by electrical arcing. Only minor overheating occurred on this unit causing a slight discoloration of the panel at the splice. In accordance with MRB disposition, the splice was removed, the area at the splice was cleaned up and the panel reassembled and reinstated in FAT. It thereafter completed temperature cycle, leak and functional tests in FAT as directed by NASA-LRC.

8280-28000; S/N 0000108.-
Failure Report B65065
Failure Analysis Report 8280-20
History: This detector panel was found to be leaking after acoustics testing in Qualification. The leak was located by means of MS-12A Mass Spectrometer in the upper fusion weld which joins the interconnect tube (8280-28008-01) and the sleeve (8280-04061-01) on the switch S/N 0000173 half of the panel. The cause of failure was a void in the weld created by contraction of the metal at the point of weld taper-off. Project engineering and NASA-LRC coordinated a MRB disposition for this panel as follows. Rework both switch assemblies (S/N 0000022A and S/N 0000173) in accordance with MRB B65065 supplemental data sheets 1 thru 4. These data sheets define the fabrication and design parameters that is referred to as Modification 2. Following the incorporation of Modification 2, reassign this panel for delivery following a complete run of FAT. See the next paragraph for continuation of this panel's history.

8280-28000; S/N 0000108.-
Failure Report B66035
Failure Analysis Report 8280-24
History: In the re-FAT sequence directed in the preceding paragraph this unit was found to be leaking following the dynamics test. Failure analysis isolated the leak to switch S/N 0000173 half of the panel. Mass spectrometry determined the source of leakage to be at the top serpentine brazed joint. Solidified braze flux entrapped in the braze joints caused the leakage when it disintegrated as a result of dynamics testing. An MRB disposition directed a rework of the defective brazed joint and recycling back through FAT. The unit completed FAT successfully following the rework.

8280-28000; S/N 0000110.-
Failure Report B66036
Failure Analysis Report 8280-23
History: This panel was built late in the program as a replacement for F1A losses in test. The switch assemblies for this unit (S/N 0000167 and S/N 0000153) were salvaged from F1A, S/N 0000101 and S/N 0000102 panels, respectively. F1A, S/N 0000110 failed its initial leak test of FAT. The failure was isolated to the seamweld. Microscopic examination for failure concluded the failure to be the result of contamination brought about by improper handling following the cleaning process. Contamination of the surface impaired the welding and created cracking which is attributed as the leak path. This unit was scrapped and the switch assemblies S/N 0000167 and S/N 0000153 were salvaged per MRB and used in the fabrication of F1A, S/N 0000111. The F1A, S/N 0000111 completed FAT testing satisfactorily.

8280-28000; S/N 0000103A and S/N 0000111.-
Failure Report B66041
Failure Analysis Report 8280-27
History: In the course of ALC testing at the 7147th cycle, both of the aforenoted F1A specimens signalled a pressure loss at the test control console. On F1A, S/N 0000103A, the leak was isolated to the switch S/N 0000164 half of the detector panel. On F1A, S/N 0000111, the leak was isolated to the switch S/N 0000153 half of the detector panel. Via VEECO mass spectrometer, the failures were pinpointed to a single spotweld failure in each of the detector panels. In both cases the failed spotweld was adjacent to the center splice, in the first row of spotwelds outboard of the splice. On F1A, S/N 0000103A, the failure occurred at the 10th spotweld down from the longitudinal direction of the panel. On F1A, S/N 0000111, the failure was at the 13th spotweld. In both cases, the failures were typical fatigue

failures brought about by mass discontinuities associated with the attachment of the electrical bus-bar and thermal stresses induced by the clamping method employed at the splice. Large temperature gradients of the order of 200 to 300°F were experienced at the splice area owing to the clamp shielding. In 2 mil target sheets, the F1A apparently cannot stand pressure cycle stresses combined with unrealistically high (test) thermal stresses; thus, the failures were induced. No further testing was accomplished on the F1A. Given fixture modification coupled with realistic spaceflight thermal simulation, the F1A configuration could successfully withstand the rigors of ALC testing.

## Failure Report Trend Analysis

To establish a trend relationship with respect to all failure reports on the MPDD program, all Martin Marietta Automatic Reporting System (MARS forms) were reviewed. The MARS form was used exclusively as a single point failure report and/or Material Review Board disposition form. All discrepancies, regardless of their origin (vendor or Martin Marietta Corporation) were reported; were summarized in Appendix C; and are hereinafter accountable except as noted for Servonics Instruments Incorporated. The Servonics pressure-activated switch (first entry in Appendix C) failed to qualify for MPDD use. It, therefore, was not used in any final MPDD hardware and was removed by engineering change from all reference on the M&T production drawings.

The analysis is presented in two sections as follows:

1) Carleton Controls pressure activated switch component [vendor and Martin Marietta Corporation failure reports (MARS) through FAT];

2) MPDD assemblies [Martin Marietta Corporation failure reports (MARS) throughout M&T, FAT, Qual, ALC].

Summary of pressure-activated switch component.- A total of 18 reports were processed against the Carleton Control Incorporated pressure-activated switch (table 24) during its course of fabrication and test at the supplier, through FAT at Martin Marietta Corporation. In the table, items A, B, C, and I are typical MRB requests. They are not test failures and do not present any trend significance contributing to an out of control situation. Item F, although reported during FAT in one case and after FAT in the other, both are rejections resulting from mishandling. Two damaged units over the total procurement is not considered significant.

TABLE 24.- CARLETON CONTROLS PRESSURE ACTUATED SWITCH COMPONENT
[VENDOR AND MARTIN MARIETTA CORPORATION FAILURE REPORTS (MARS) THROUGH FAT]

| Item identifier | Failure reports | | Failure report condition | Summary |
|---|---|---|---|---|
| | Qty | Identification | | |
| A | 4 | B50696<br>B50694<br>B55668<br>B55669 | Request for MRB approval for substitute wire lead identification sleeves | Vendor could not procure proper identification sleeves in time for schedule commitment of detectors; MRB |
| B | 1 | B50949 | Duplication of MARS B50696 | Martin Marietta Corporation inspector inadvertently duplicated the conditions stated on B50696; B50949 was therefore canceled |
| C | 1 | B50950 | Damaged wire insulation | No failure, vendor request for MRB; wire lead insulation was nicked; no wire damage |
| D | 3 | T-10061<br>B50953<br>B50951 | High contact resistance | One condition was malfunction of measuring equipment; the remaining two were valid test failures |
| E | 1 | B50947 | Leak | Pore in parent metal of diaphragm; valid test failure |
| F | 2 | B50960<br>B50956 | Mishandling | Physical damage due to dropping and mishandling; not a true test failure |
| G | 3 | B50962<br>B50963<br>B50964 | Test fixture induced icing | Design deficiency in fixture caused icing and specimen malfunction; fixture was modified and all units except the one used in failure analysis were reinstated and passed all tests |
| H | 2 | B50938<br>B-66496 (ALC) | Improper assembly | Potting installation was too thin and disintegrated during dynamics testing; in the second unit, the switch installation was installed marginal on its pressure setting screw-in depth |
| I | 1 | B50957 | Misidentified wiring | Vendor misidentified wires; Martin Marietta Corporation retraced wires, correctly identified same, and unit passed all tests |

Item G, likewise, was a failure reported during FAT. The icing condition that resulted in the three failures was induced by a deficient fixture design. The fixture was modified and no further failures were experienced over the entire test program.

Items D, E, and H are valid test failures; however, neither the failure characteristic nor the quantity involved are suggestive of an undesirable design or fabrication deficiency trend.

Summary of MPDD assemblies.- A total of 35 reports were processed against the MPDD assemblies during their assembly, FAT, Qual, and ALC processing (table 25). In item A, a revision of the fill and punch-off specification requiring additional temperature stabilization time corrected the problem. In item B, the failures were caused by the clamping technique employed in mounting the specimens. Several modifications were made in the clamping technique to elminate the problem. In items C thru H, the quantity of hardware involved in each classification of failure is not significant to establish a trend relationship. An interesting point worthy of note lies in the relationship of item H to item I. In all of the welding performed on the MPDD hardware under the automatic mode or machine welding, only two deficient conditions were reported. In the manual mode, however, seven failures were reported. The human element generally is the variable that cannot be predicted and repeatability of 100% good welds and/or brazed joints cannot be expected on the first pass as was demonstrated on the machine or automatic weld. Although all of the manual welds and brazed joints were of the type where rework to achieve acceptable welds/brazing was possible, and was accomplished, a failure report was nonetheless necessary, since the failures could not be detected until the unit was in FAT. On future production, the area of manual welding should be minimized. In line testing to verify manual welds should be permitted and repairs allowed without penalty of being classed as "failures." The production test to screen and repair welds should be accomplished as a separate item to FAT. Once in FAT, the unit if failure occurs should be categorized a "failure."

TABLE 25.- MPPD ASSEMBLIES
[MARTIN MARIETTA CORPORATION FAILURE REPORTS (MARS) THROUGHOUT M&T, FAT, QUAC, AND ALC]

| Item identifier | Failure reports | | Failure report condition | Summary |
|---|---|---|---|---|
| | Qty | Identification | | |
| A | 5 | B42082<br>B42083<br>B42084<br>B42085<br>B50965 | Engineering | Insufficient soak time to allow pressure stabilization; specification was revised to allow additional time for temperature stabilization; no further problems. Monel rivets could not be driven in 0.002 and 0.016 material without tearing material; engineering changed to aluminum riveting |
| B | 6 | B65067<br>B66037<br>B66833<br>B42091<br>B42097<br>B66041 | Tool design | All of these failures concern either a cracked spotweld or specimens burned; in all cases, the cause of failure was due to the clamping method employed in the fixture |
| C | 2 | B55773<br>B65063 | Test equipment malfunction/test personnel error | One failure on each condition resulted in destroying of specimen by burning |
| D | 1 | B66038 | Overtest | Specimen cycled twice through qualification |
| E | 2 | B60693<br>B60692 | Detail part error | Detail part volcano flange undersize; detail part 0.027 material used in lieu of 0.020; both were requests for MRB |
| F | 3 | B50941<br>B50969<br>B60712 | Switch/vendor deficiencies | Workmanship items but not repetitive; rejections represent one warped contacts, one scratched diaphragm, one weld burnthrough in diaphragm |
| G | 4 | B50970<br>B65014<br>B42462<br>B66036 | Leakage | One defective ringweld, two parent metal pore, one contamination, caused by improper handling following cleaning |
| H | 2 | B50939<br>B55774 | Automatic weld deficiencies | One crack at seamweld corner; this was re-X-rayed after FAT and no growth delivered with MRB. One cold shut between weld passes. Only one item in entire contract |
| I | 10 | B42100<br>B65064<br>B69832<br>B50966<br>B66040<br>B60691<br>B42092<br>B65068<br>B65065<br>B66035 | Workmanship manual weld/brazing | Except for B42100 (a clogged vent port), B69832 (marginal switch installation, and B60691 (drill chaffing damage, all of the remaining failures (7) were Manual welding and/or manual brazing failures. The points of failures were common to the fusion weld at the gas interconnect tube and/or brazed joint at the gas tube to switch cup. or serpentine brazed joints |

## REFERENCES


1. Seely, Fred B.; and Smith, James D.: Advanced Mechanics of Materials. John Wiley & Sons, October 1957.

2. Martin Marietta Procurement Drawing PD7100075 (NASA-LRC Number LA 412417).

3. Anon.: Pressurization Media Analysis Report. MDS-10028 Martin Marietta Corporation, Denver, Colorado, 20 September 1967. (Addendum, October 1968).